FUSE

Volume 8, December 2021

Fungal Systematics and Evolution

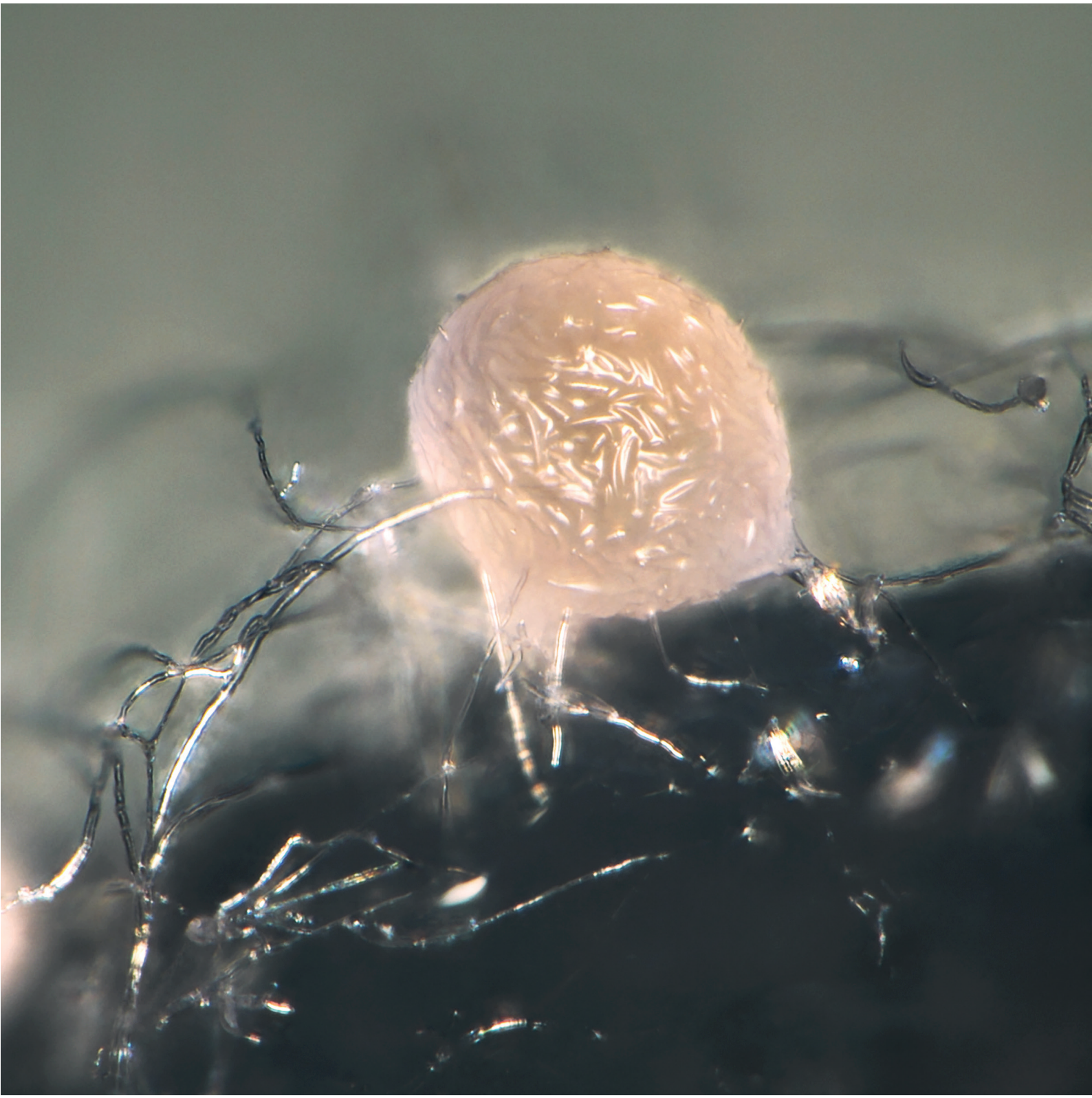

WESTERDIJK FUNGALBIODIVERSITY INSTITUTE

EDITORIAL BOARD

Editor-in-Chief

Prof. dr P.W. Crous, Westerdijk Fungal Biodiversity Institute, P.O. Box 85167, 3508 AD Utrecht, The Netherlands. E-mail: p.crous@wi.knaw.nl

Senior Editors

Prof. dr U. Braun, Martin-Luther-Universität, Institut für Biologie, Geobotanik und Botanischer Garten, Herbarium, Neuwerk 21, D-06099 Halle, Germany; e-mail: uwe.braun@botanik.uni-halle.de

Dr J.Z. Groenewald, Westerdijk Fungal Biodiversity Institute, P.O. Box 85167, 3508 AD Utrecht, The Netherlands; e-mail: e.groenewald@wi.knaw.nl

Prof. dr M. Thines, Goethe University Frankfurt am Main, Faculty of Biosciences, Institute of Ecology, Evolution and Diversity, Max-von-Laue-Str. 9, D-60438 Frankfurt am Main, Germany; e-mail: Marco.Thines@senckenberg.de

Layout Editor

M.J. van den Hoeven-Verweij, Westerdijk Fungal Biodiversity Institute, P.O. Box 85167, 3508 AD Utrecht, The Netherlands; e-mail: m.verweij@wi.knaw.nl

Graphic Design Editor

M. Vermaas, Westerdijk Fungal Biodiversity Institute, P.O. Box 85167, 3508 AD Utrecht, The Netherlands; e-mail: m.vermaas@wi.knaw.nl

Associate Editors

Prof. dr A.M. Al-Sadi, Department of Crop Sciences, College of Agricultural and Marine Sciences, Sultan Qaboos University, P.O. Box 34, Al-Khod 123, Sultanate of Oman; e-mail: alsadiam@gmail.com

Prof. dr M. Arzanlou, Plant Protection Department, Agriculture Faculty, University of Tabriz, P.O. Box: 5166614766, Tabriz, Iran; e-mail: arzanlou@hotmail.com

Prof. dr T.I. Burgess, School of Biological Sciences and Biotechnology, Murdoch University, Perth, 6150, Australia; e-mail: tburgess@murdoch.edu.au

Prof. dr L. Cai, State Key Laboratory of Mycology, Institute of Microbiology, Chinese Academy of Sciences, No. 3 Park 1, Beichen West Road, Chaoyang District, Beijing, 100101, China; e-mail: cail@im.ac.cn

Prof. dr L. Carris, Associate Professor, Department of Plant Pathology, Washington State University, Pullman, WA 99164-6340, USA; e-mail: carris@mail.wsu.edu

Dr C. Decock, MUCL, Croix du Sud 2 bte L7.05.06, B-1348 Louvain-la-Neuve, Belgium; e-mail: cony.decock@uclouvain.be

Dr X.L. Fan, The Key Laboratory for Silviculture and Conservation of Ministry of Education, Beijing Forestry University, Beijing 100083, China; e-mail: xinleifan@bjfu.edu.cn

Dr D. Gramaje, Instituto de Ciencias de la Vid y del Vino (ICVV), Consejo Superior de Investigaciones Científicas - Universidad de la Rioja - Gobierno de La Rioja, Ctra. Mendavia-Logroño NA 134, Km. 90, 26071 Logroño, Spain; e-mail: david.gramaje@icvv.es

Dr V. Guarnaccia, Department of Agriculture, Forestry and Food Sciences (DiSAFA), University of Torino, via Paolo Braccini 2, 10095 Grugliasco, TO, Italy., Italy; e-mail: vladimiro.guarnaccia@unito.it

Dr J. Houbraken, Westerdijk Fungal Biodiversity Institute, P.O. Box 85167, 3508 AD Utrecht, The Netherlands; e-mail: j.houbraken@wi.knaw.nl

Dr R. Jeewon, Department of Health Sciences, Faculty of Science, University of Mauritius, Reduit, Mauritius; e-mail: r.jeewon@uom.ac.mu

Dr F. Liu, State Key Laboratory of Mycology, Institute of Microbiology, Chinese Academy of Sciences, No. 3 Park 1, Beichen West Road, Chaoyang District, Beijing, 100101, China; liufang@im.ac.cn

Dr L. Mostert, Department of Plant Pathology, University of Stellenbosch, P. Bag X1, Matieland 7602, South Africa; e-mail: lmost@sun.ac.za

Prof. dr A.J.L. Phillips, University of Lisbon, Faculty of Sciences, Biosystems and Integrative Sciences Institute (BioISI), Campo Grande, 1749-016 Lisbon, Portugal; e-mail: alan.jl.phillips@gmail.com

Dr H.D.T. Nguyen, Agriculture and Agri-Food Canada, K.W. Neatby Building, 960 Carling Ave., Ottawa, ON, Canada, K1A 0C9; e-mail: Hai.Nguyen@agr.gc.ca

Dr M. Piątek, Department of Mycology, W. Szafer Institute of Botany, Polish Academy of Sciences, Lubicz 46, PL-31-512 Kraków, Poland; e-mail: m.piatek@botany.pl

Prof. dr H.-D. Shin, Division of Environmental Science and Ecological Engineering, Korea University, Seoul 02841, Korea; e-mail: hdshin@korea.ac.kr

Prof. dr B. Summerell, Royal Botanic Gardens and Domain Trust, Mrs. Macquaries Road, Sydney, NSW 2000, Australia; e-mail: Brett.Summerell@rbgsyd.nsw.gov.au

Dr J.B. Tanney, Pacific Forestry Centre, Canadian Forest Service, Natural Resources Canada, 506 Burnside Rd W, Victoria, BC V8Z 1MS, Canada; e-mail jtanney@lakeheadu.ca

Prof. dr P. Taylor, Faculty of Veterinary and Agricultural Sciences, University of Melbourne, VIC, 3010, Australia; e-mail: paulwjt@unimelb.edu.au

Dr A.D. van Diepeningen, Business Unit Biointeractions and Plant Health, Wageningen University and Research, Wageningen, the Netherlands; e-mail: anne.vandiepeningen@wur.nl

Prof. dr C.M. Visagie, Forestry and Agricultural Research Institute (FABI), University of Pretoria, Pretoria 0002, South Africa; e-mail: cobus.visagie@up.ac.za

Prof. dr M.J. Wingfield, Forestry and Agricultural Research Institute (FABI), University of Pretoria, Pretoria 0002, South Africa; e-mail: mike.wingfield@up.ac.za

Prof. dr R. Zare, Agricultural Research, Education and Extension Organization, Tehrãn, Iran; e-mail: simplicillium@yahoo.com

Cover: Sporodochium of *Fusarium wereldwijsianum* on carnation-leaf agar

© 2021 Westerdijk Fungal Biodiversity Institute

SCOPE AND AIMS

SCOPE

All aspects of systematics and evolution of fungi.

AIMS

Fungal Systematics and Evolution is an international, peer-reviewed, open-access, full colour, fast-track journal. Papers will include reviews, research articles, methodology papers, taxonomic monographs, and the description of fungi. The journal strongly supports good practice policies, and requires voucher specimens to be deposited in a fungarium, cultures in long-term genetic resource collection, sequences in GenBank, alignments in TreeBASE, and taxonomic novelties in MycoBank.

ABOUT FUNGAL SYSTEMATICS AND EVOLUTION

Fungal Systematics and Evolution has an OPEN ACCESS publishing policy. All manuscripts will undergo peer review before acceptance, and will be published as quickly as possible following acceptance. There are no page charges or length restrictions, or fees for colour plates. The official journal language is English. All content submitted to Fungal Systematics and Evolution is checked for plagiarism.

Fungal Systematics and Evolution is licensed under a Creative Commons Attribution-NonCommercial-ShareAlike 4.0 International License.

PUBLISHED BY

Westerdijk Fungal Biodiversity Institute, P.O. Box 85167, 3508 AD Utrecht, The Netherlands.

WESTERDIJK FUNGALBIO DIVERSITY INSTITUTE

All articles are copyright of Westerdijk Fungal Biodiversity Institute.

FREQUENCY

Twice per year (June and December).

ISSN: 2589-3823
E-ISSN: 2589-3831

CONTENTS

Research papers

Looney BP, Buyck B, Menolli Jr. N, Randrianjohany E, Hibbett D. *Lentinula madagasikarensis sp. nov.*, a relative of shiitake mushrooms from Madagascar 1

Lebel T, Cooper JA, Castellano MA, Nuytinck J. Three independent evolutionary events of sequestrate *Lactifluus* species in Australasia 9

Mongkolsamrit S, Noisripoom W, Thanakitpipattana D, Khonsanit A, Lamlertthon S, Luangsa-ard JJ. New species in *Aciculosporium*, *Shimizuomyces* and a new genus *Morakotia* associated with plants in *Clavicipitaceae* from Thailand 27

Alqurashi AS, Kerrigan J, Savchenko KG. Morphological and molecular characterization of *Langdonia walkerae sp. nov.* infecting *Aristida stricta* and *A. beyrichiana* in longleaf pine-grassland ecosystems in the southeastern USA 39

Millar AN, Réblová M. Phylogenetic placement of *Iodosphaeriaceae* (*Xylariales*, *Ascomycota*), designation of an epitype for the type species of *Iodosphaeria*, *I. phyllophila*, and description of *I. foliicola sp. nov.* 49

Davoodian N, Lebel T, Castellano MA, Hosaka K. *Hysterangiales* revisited: expanded phylogeny reveals new genera and two new suborders 65

Visagie CM, Goodwell M, Nkwe DO. *Aspergillus* diversity from the Gcwihaba Cave in Botswana and description of one new species 81

Karlsen-Ayala E, Gazis R, Smith ME. *Asperosporus subterraneus*, a new genus and species of sequestrate *Agaricaceae* found in Florida nursery production 91

Crous PW, Hernández-Restrepo M, van Iperen AL, Starink-Willemse M, Sandoval-Denis M, Groenewald JZ. Citizen science project reveals novel fusarioid fungi (*Nectriaceae*, *Sordariomycetes*) from urban soils 101

Ribes MA, Escobia V, Negrín, R, Baral HO, Pfister DH, Quijada L. Wanted on *Agave americana*! *Hymenobolus agaves*, an overlooked introduced pathogen in the western palearctic region 129

Svantesson S, Kõljalg U, Wurzbacher C, Saar I, Larsson K-H, Larsson E. *Polyozellus vs. Pseudotomentella*: generic delimitation with a multi-gene dataset 143

Chang R, Wingfield MJ, Marincowitz S, de Beer ZW, Zhou X, Duong TA. Ophiostomatoid fungi including a new species associated with Asian larch bark beetle *Ips subelongatus*, in Heilongjiang (Northeast China) 155

Viner I, Bortnikov F, Ryvarden L, Miettinen O. On six African species of *Lyomyces* and *Xylodon* 163

Walker C, Schüßler A, Vincent B, Cranenbrouck S, Declerck S. Anchoring the species *Rhizophagus intraradices* (formerly *Glomus intraradices*) 179

© 2021 Westerdijk Fungal Biodiversity Institute

© 2021 Westerdijk Fungal Biodiversity Institute

FUSE

Fungal Systematics and Evolution

VOLUME 8
DECEMBER 2021
PAGES 1–8

doi.org/10.3114/fuse.2021.08.01

Lentinula madagasikarensis sp. nov., a relative of shiitake mushrooms from Madagascar

B.P. Looney[1], B. Buyck[2], N. Menolli Jr.[3,4], E. Randrianjohany[5], D. Hibbett[1*]

[1]Clark University, Department of Biology, Worcester, MA 01610, USA
[2]Muséum national d'Histoire naturelle, CNRS, Sorbonne Université, Institut de Systématique, Écologie, Biodiversité (ISYEB), EPHE, 57 rue Cuvier, CP 39, F-75005, Paris, France
[3]Instituto Federal de Educação, Ciência e Tecnologia de São Paulo (IFSP), Departamento de Ciências da Natureza e Matemática (DCM), Subárea de Biologia (SAB), Câmpus São Paulo, Rua Pedro Vicente 625, São Paulo, SP, 01109-010, Brazil
[4]Instituto de Botânica (IBt), Núcleo de Pesquisa em Micologia (NPM), Av. Miguel Stefano 3687, Água Funda, São Paulo, SP, 04301-012, Brazil
[5]Centre National de Recherche sur l'Environnement (CNRE), BP 1739, Lab. de Microbiologie de l'Environnement (LME), Antananarivo, Madagascar

*Corresponding author: dhibbett@clarku.edu

Key words:
Africa
biogeography
edible mushrooms
Omphalotaceae
systematics
1 new taxon

Abstract: We describe the first species of *Lentinula* from Africa, *Lentinula madagasikarensis sp. nov*. The new taxon, which was collected from central Madagascar, is strikingly similar to *L. edodes*, the shiitake mushroom. A BLAST search using ITS sequences from *L. madagasikarensis* as the query retrieves a mix of *Lentinula, Gymnopus*, *Marasmiellus*, and other members of *Omphalotaceae* as the top hits. A 28S phylogeny of the *Omphalotaceae* confirms placement of *L. madagasikarensis* within *Lentinula*. An ITS phylogeny places *L. madagasikarensis* as the sister group of *L. aciculospora*, which is a neotropical species. *Lentinula madagasikarensis* is characterized by robust basidiomata with vinaceous pilei, prominent floccose scales near the pileus margin, florets of sphaeropedunculate cheilocystidia, and subcylindrical basidiospores. This report constitutes a 4 000-mile, trans-oceanic range extension for *Lentinula*.

Citation: Looney BP, Buyck B, Menolli Jr N, Randrianjohany E, Hibbett D (2021). *Lentinula madagasikarensis sp. nov.*, a relative of shiitake mushrooms from Madagascar. *Fungal Systematics and Evolution* **8**: 1–8. doi: 10.3114/fuse.2021.08.01
Received: 14 April 2021; **Accepted:** 3 May 2021; **Effectively published online:** 1 June 2021
Corresponding editor: P.W. Crous

INTRODUCTION

Lentinula is a group of lignicolous agarics that includes the shiitake mushroom, *L. edodes*. Shiitake is a traditional food in East Asia and it has reportedly been cultivated in China for *ca*. 1 000 years (Chang & Miles 1987). However, the genus *Lentinula* has a broad distribution that spans much of South Asia, Australasia, and tropical and subtropical regions of the Americas (Pegler 1983). *Lentinula* has been resolved as a monophyletic group within the *Omphalotaceae* (*Agaricales*), which also contains *Gymnopus*, *Rhodocollybia*, and other collybioid mushrooms (Wilson & Desjardin 2005, Matheny *et al.* 2006, He *et al.* 2019, Oliviera *et al.* 2019).

Seven species have been formally described in *Lentinula*. Pegler (1983) included five species in his monograph of *Lentinula*: *L. edodes* in eastern Asia; *L. lateritia* in southeast Asia and Australasia; *L. novae-zelandiae* in New Zealand; *L. boryana* from the Gulf Coast of North America to South America; and *L. guarapiensis* from Paraguay. The latter is known only from the type collection (Spegazzini 1883). Using a combination of morphology, mating compatibility, and ITS sequences, Mata & Petersen (2000) described a new species from Costa Rica, *L. aciculospora*. Mata *et al.* (2001) then segregated a previous synonym, *Armillaria raphanica*, as *L. raphanica* from Pegler's broad concept of *L. boryana*. *Lentinula raphanica* is reported by Mata *et al.* (2001) from Florida, Louisiana, Puerto Rico, Costa Rica, Venezuela, and Brazil (*i.e.*, overlapping with *L. boryana s. str.*). Phylogenetic analyses of ITS sequences suggest that *L. lateritia* and *L. edodes* may each contain multiple species-level lineages, but these have not been formally described (Hibbett *et al.* 1998).

Most species of *Lentinula* grow on wood of *Fagales*, specifically *Fagaceae* or *Nothofagaceae* (Pegler 1983). The absence of *Lentinula* from Europe and most of North America (where oaks and their relatives abound, and outdoor log cultivation of shiitake is successful) is puzzling. Historical biogeographic analyses have suggested that the present distribution of *Lentinula* could reflect an ancient trans-Beringian distribution, which would require local extinction in North America (Hibbett 2001), but alternative dispersal routes via the southern hemisphere cannot be rejected.

During a study of the wild edible mushrooms of Madagascar, Buyck (2008) made two collections of a fungus that closely resembled *L. edodes*. Here, we present morphological and molecular analyses of the Malagasy material, which we describe as *L. madagasikarensis*.

MATERIALS AND METHODS

Sampling and phylogenetic inference

Two collections were made by Buyck (2008) in native forests of central Madagascar with endemic *Uapaca densifolia*

Fungal Systematics and Evolution is licensed under a Creative Commons Attribution-NonCommercial-ShareAlike 4.0 International License

© 2021 Westerdijk Fungal Biodiversity Institute

(*Phyllanthaceae*) and *Sarcolaenaceae*, and introduced *Eucalyptus robusta* in 2006 and 2008. Both collections have been deposited at the fungarium (PC) of the Muséum National d'Histoire Naturelle, Paris. Genomic DNA was extracted from both collections in 2020 using the Extraction Solution-based method of Looney *et al.* (2020).

Two nuclear loci were amplified and sequenced with standard primer sets: ITS1F-ITS4 (White *et al.* 1990) for ITS, and LROR-LR5 (Vilgalys & Hester 1990) for 28S. Both strands were sequenced using the Sanger method, by Psomagen, New York, NY, and sequences have been deposited into GenBank (accession Nos. MW810299–MW810302).

Two datasets were used to infer relationships at different scales, Dataset 1 was used to assess the placement within the *Omphalotaceae* and Dataset 2 was used to infer placement within *Lentinula*. Dataset 1 used the 28S *Omphalotaceae* matrix from Oliveira *et al.* (2019) as a starting alignment. Dataset 2 included 60 ITS sequences, representing all known lineages of *Lentinula*, which were downloaded using *emerencia* (Nilsson *et al*. 2005), and six sequences of *Gymnopus* spp. as the outgroup.

Sequences of the Madagascar material were manually aligned with the two datasets in AliView v. 1.27 (Larsson 2014). Phylogenetic inference under Maximum Likelihood was performed in RAxML-VI-HPC using raxmlGUI v. 2.0 with autoMRE bootstopping criteria (Stamatakis 2006, Edler *et al*. 2020). Bayesian analysis was performed in MrBayes v. 3.2.7a using Metropolis coupled MCMC under a GTR +G model through the CIPRES Science gateway (Ronquist *et al.* 2012). The analysis consisted of 3 runs of 50 M generations and four chains sampled every 5 000 generations. Finally, a distance matrix of nine representative sequences of different taxa was generated from the final ITS alignment in R using the dist.dna function of the 'ape' package. Alignments and resulting trees have been deposited in TreeBASE (https://treebase.org/) under study number 28094.

Morphological analysis

Morphological field notes were taken on fresh basidiomata using color standards given in parentheses (Kornerup & Wanscher 1978). Microscopic observations were made on a Nikon Eclipse e600 compound microscope with a mounted SPOT RT Slider digital camera. Dried specimens were rehydrated in 3 % KOH and observed in phase contrast or stained with phloxine and by bright field microscopy. Melzer's reagent was used for testing amyloidity. At least 20 observations were made for each feature. Microscopic feature measurements are given as lower limit–[arithmetic mean]–upper limit with *n* = total number of observations and Q-value for basidiospores calculated as arithmetic mean of the lengths divided by arithmetic mean of the widths for the lower limit–[arithmetic mean]–upper limit.

RESULTS

Molecular systematics

BLAST searches using ITS sequences from *L. madagasikarensis* as the queries retrieved sequences of *Lentinula, Gymnopus*, *Marasmiellus*, and other members of *Omphalotaceae* as the top hits (results not shown). Phylogenetic analyses of Dataset 1 recovered all of the major clades of *Omphalotaceae* identified by Oliveira *et al.* (2019), but often with weak bootstrap support (BS) (Fig. 1). *Lentinula* was strongly supported as monophyletic (BS 91 %). The sister group of *Lentinula* was not resolved with confidence, but a clade containing *Lentinula* and Clades A–J of Oliveira *et al.* (2019) was strongly supported (BS 99 %).

The *Lentinula*-focused ITS analyses of Dataset 2 placed *L. madagasikarensis* as sister to *L. aciculospora* with moderate BS (84 %) (Fig. 2). Two major groups were resolved in *Lentinula*, one weakly-supported group containing all Asian-Australasian species (BS 56 %) and one strongly-supported clade containing all American species, plus *L. madagasikarensis* (BS 98 %). There are three major groups in the Americas, *L. aciculospora* (BS 100 %), *L. boryana* (BS 86 %), and *L. raphanica* (BS 100 %).

The Asian-Australasian clade contains five lineages that have previously been termed Groups 1–5 based on ITS data (Hibbett *et al.* 1998). Each of the ITS-based groups are moderately to strongly supported as monophyletic, but relationships among them are not well resolved (Fig. 2). Groups 1 and 5 correspond to *L. edodes sensu lato*, including cultivated shiitake mushrooms. Based on sampling in the present study and that of Hibbett *et al.* (1998), Group 1 includes isolates from China, Japan, South Korea, Philippines, India, and the Russian Far East, whereas Group 5 includes isolates from China, Nepal and India. Group 2 and Group 4 both include collections from Papua New Guinea; Group 2 also includes collections from Australia. Group 3 is equivalent to *L. novae-zelandieae*, from New Zealand.

Pairwise distances of ITS sequences of *L. madagasikarensis* to other species of *Lentinula* ranged from 11 % *vs*. *L. edodes* (Group 5), *L. lateritia* (Group 2), *L. novae-zelandiae*, and *L. aciculospora*, to 20 % *vs. L. raphanica* (Fig. 3). Pairwise sequence distances among three isolates from the Americas are 11–20 %, whereas those among five Asian-Australasian isolates are 1–4 % (Fig. 3).

Taxonomy

Lentinula madagasikarensis Buyck, Randrianjohany & Looney, ***sp. nov.*** MycoBank MB 839129. Fig. 4A–G.

Etymology: The specific epithet is derived from Madagasikara, which is the Malagasy name for Madagascar. To our knowledge, there is no Malagasy name for this species.

Diagnosis: Robust basidiomata with vinaceous pileus color and large, tufted scales near pileus margin merging into an appendiculate margin. Fibrous, ivory-colored stipe with squamules. Small and narrow basidiospores. Sphaeropedunculate cheilocystidia forming scattered florets.

Typus: **Madagascar**, Moramanga district, Alaotra-Mangoro region, Andasibe, 18°56'S 48°25'E, on *E. robusta* log, 20 Jan. 2006, *B. Buyck & V. Hofstetter* 06.007 (holotype PC0142531).

Description: *Pileus* convex to hemisphaerical when young, soon umbonate to applanate or broadly depressed, firm and fleshy, up to 6–7 cm diam.; surface smooth, sometimes scurfy or with minute scales or granules and almost greasy at the touch in the central portion, toward the margin rapidly becoming covered with a paler, hairy-fibrillose scurf, building more or less concentrically arranged, thick, floccose deposits with fibrillose extremities pointing downward; dark reddish brown (9EF6-8) to vinaceous or purplish brown (14EF5-8) at center when young, at maturity becoming paler, pale reddish brown to ochraceous brown (3A5-6, 4B5-8, 5C5-7) but retaining locally some darker

© 2021 Westerdijk Fungal Biodiversity Institute

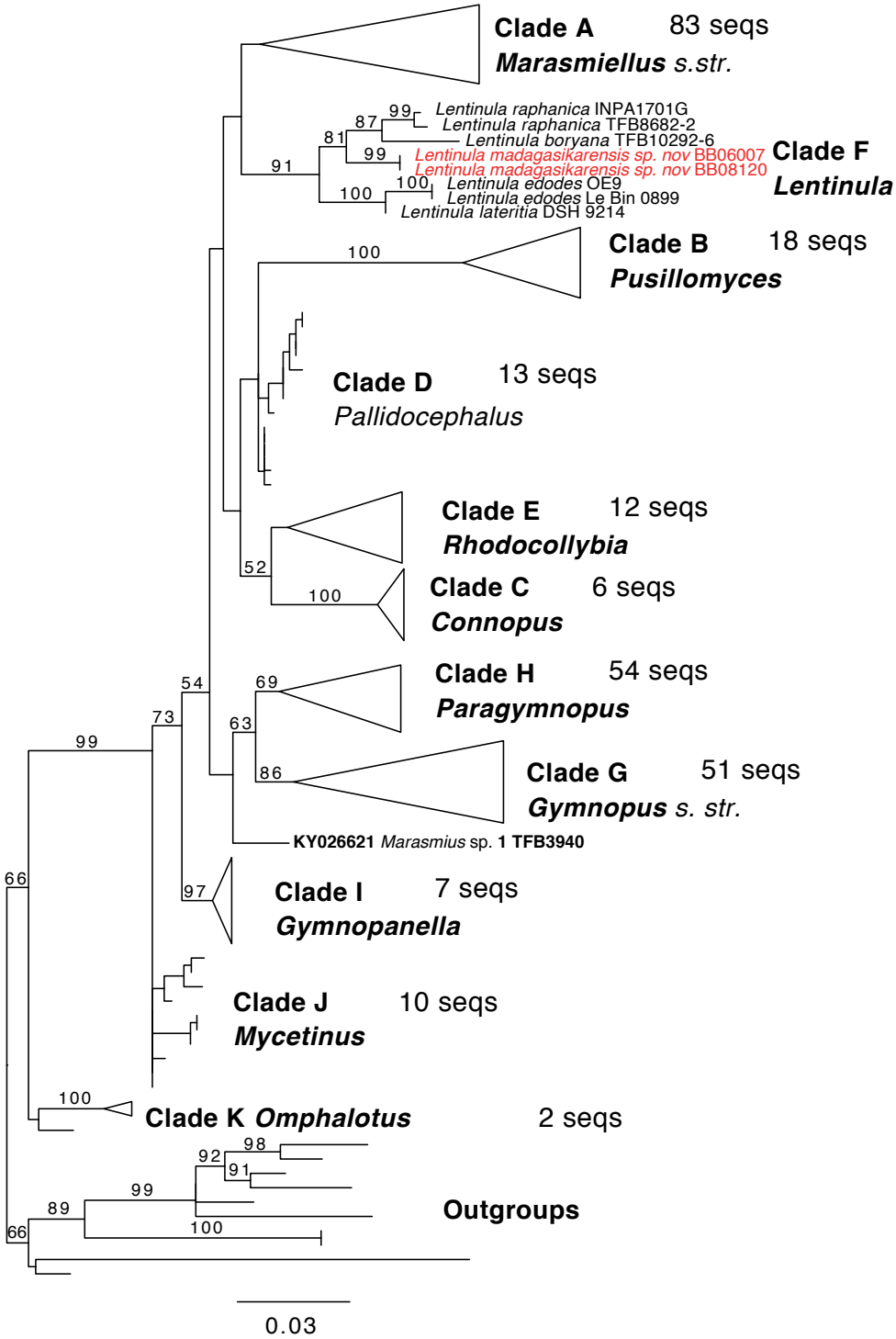

Fig. 1. Maximum-likelihood phylogeny of *Omphalotaceae* based on the 28S sequence dataset of Oliveira *et al.* (2019) with 788 bootstrap replicates according to autoMRE bootstopping criteria. Major clades from the original study are labeled and collapsed with number of samples included in each clade. BS values ≥ 50 % are included with the branches.

shades. *Lamellae* adnato- or adnexo-sinuate with a decurrent tooth, later frequently subfree, unequal with up to 4–5 series of lamellulae of different lengths, whitish to ivory, discolouring brownish after injury, crowded; edge concolorous, entire or irregularly serrulate. *Stipe* up to 4 × 2.5 cm; stout and firm, always shorter than the pileus diameter, central to mostly eccentric, cylindrical or a little widening to almost bulbous near the base, strongly fibrillose-squamose over the entire surface from thick fibrils or squamae pointing out- or upward, solid. *Partial veil* a thick cottony tissue, strongly fibrillose-squamose on the lower surface from fibrils pointing downward, fugacious, soon breaking up and limited to remnants on the pileal margin or sometimes leaving a (partial) ring on upper part of the stipe. *Context* firm-fleshy, pale coloured, not discolouring but often colored yellowish in the stipe near the attachment to the woody host surface. *Spore print* white. *Basidiospores* oblong to subcylindrical, 5.0–[6.0]–7.0 × 2.0–[3.0]–3.5 µm; Q = 1.7–[2.1]–2.4 (*n* = 30), hyaline, inamyloid, thin-walled, smooth; hilar appendage conspicuous; contents heterogenous or homogeneous. *Hymenium* composed mostly of basidia and basidioles. *Basidia* 11.0–[19.0]–26 ×

© 2021 Westerdijk Fungal Biodiversity Institute

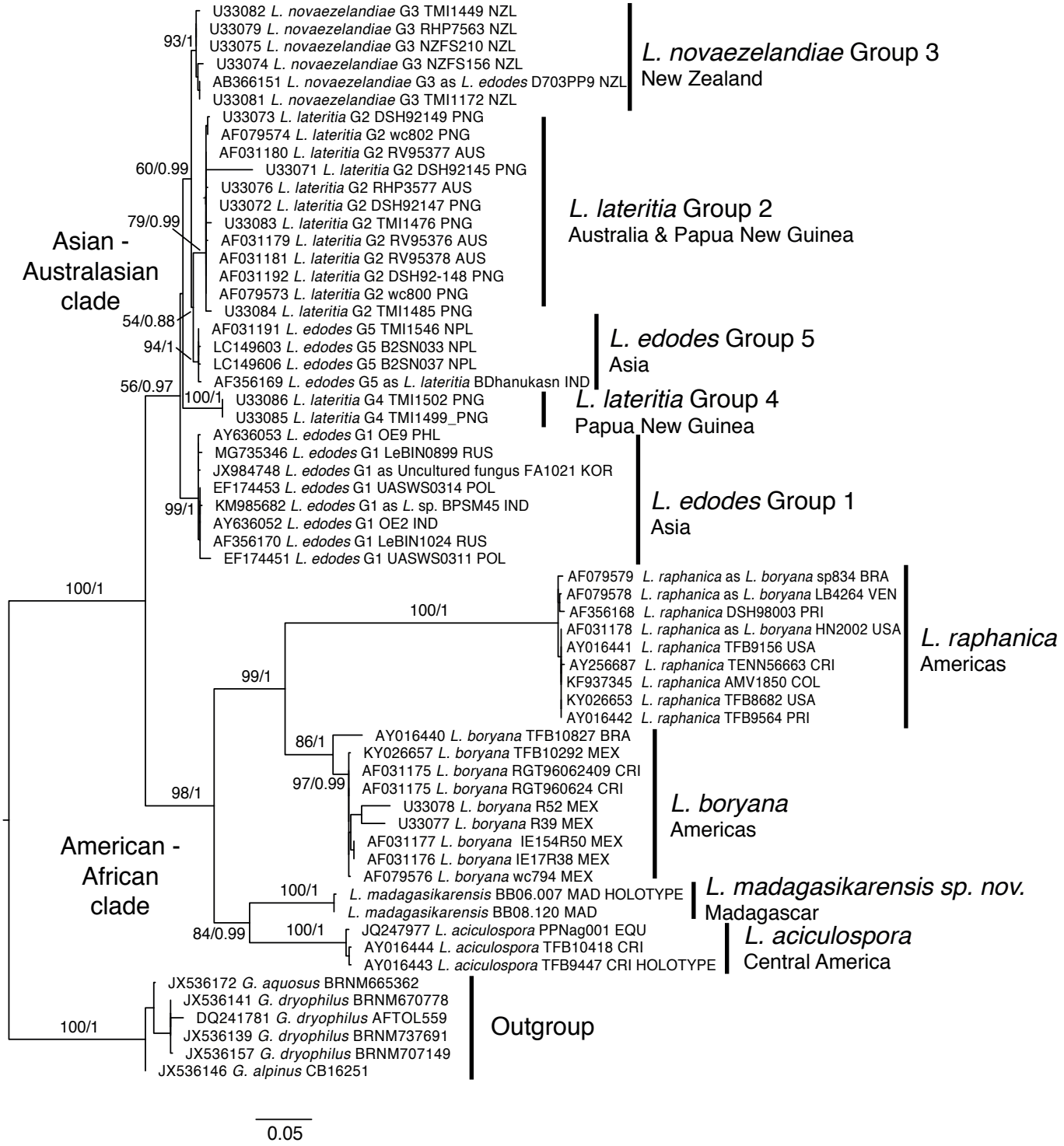

Fig. 2. Maximum-likelihood phylogeny of *Lentinula* based on Dataset 2 of ITS. BS values ≥ 50 % / Bayesian PP values ≥ 0.80 are included with the branches. Sequence labels include GenBank accession numbers and collection numbers. G1–G5 in the Asian-Australasian clade correspond to ITS-based groups from Hibbett *et al.* (1998). Country codes: AUS = Australia, BRA = Brazil, COL = Colombia, CRI = Costa Rica, IND = India, KOR = South Korea, MEX = Mexico, NPL = Nepal, NZL = New Zealand, PHL = Philippines, PNG = Papua New Guinea, POL = Poland (possible cultivar), PRI = Puerto Rico, RUS = Russia, USA = continental USA, VEN = Venezuela.

4.0–[5.0]–5.5 µm (*n* = 40), oblong to cylindrical, clavate with a median constriction, with a clamp connection at the base, four-sterigmate; sterigmata slender, up to 3 µm long. *Pleurocystidia* absent. *Cheilocystidia* 15.0–[28]–46 × 7.0–[11.0]–16.0 µm (*n* = 20), clavate to sphaeropedunculate, inflated apically without lobes, thin-walled, smooth, forming dense clusters or florets, infrequent. *Lamellar trama* regular to subregular; hyphae 4.0–15.0 µm diam., thin- to thick-walled. Subhymenium rudimentary. *Epicutis* 30–50 µm thick; hyphae 3.0–7.0 µm diam, brown in mass, hyaline singly, repent, interwoven and subregular cutis; hyphae in scales erumpent, ending in eroded hyphal fragments. *Subpellis* composed of frequently branching, irregular hyphae 5.0–11.0 µm diam, hyaline, thick-walled. *Stipitipellis* composed of interwoven hyphae 3.0–7.0 µm diam, branching, with floccons formed of obtuse terminal end cells. *Caulocystidia* absent.

© 2021 Westerdijk Fungal Biodiversity Institute

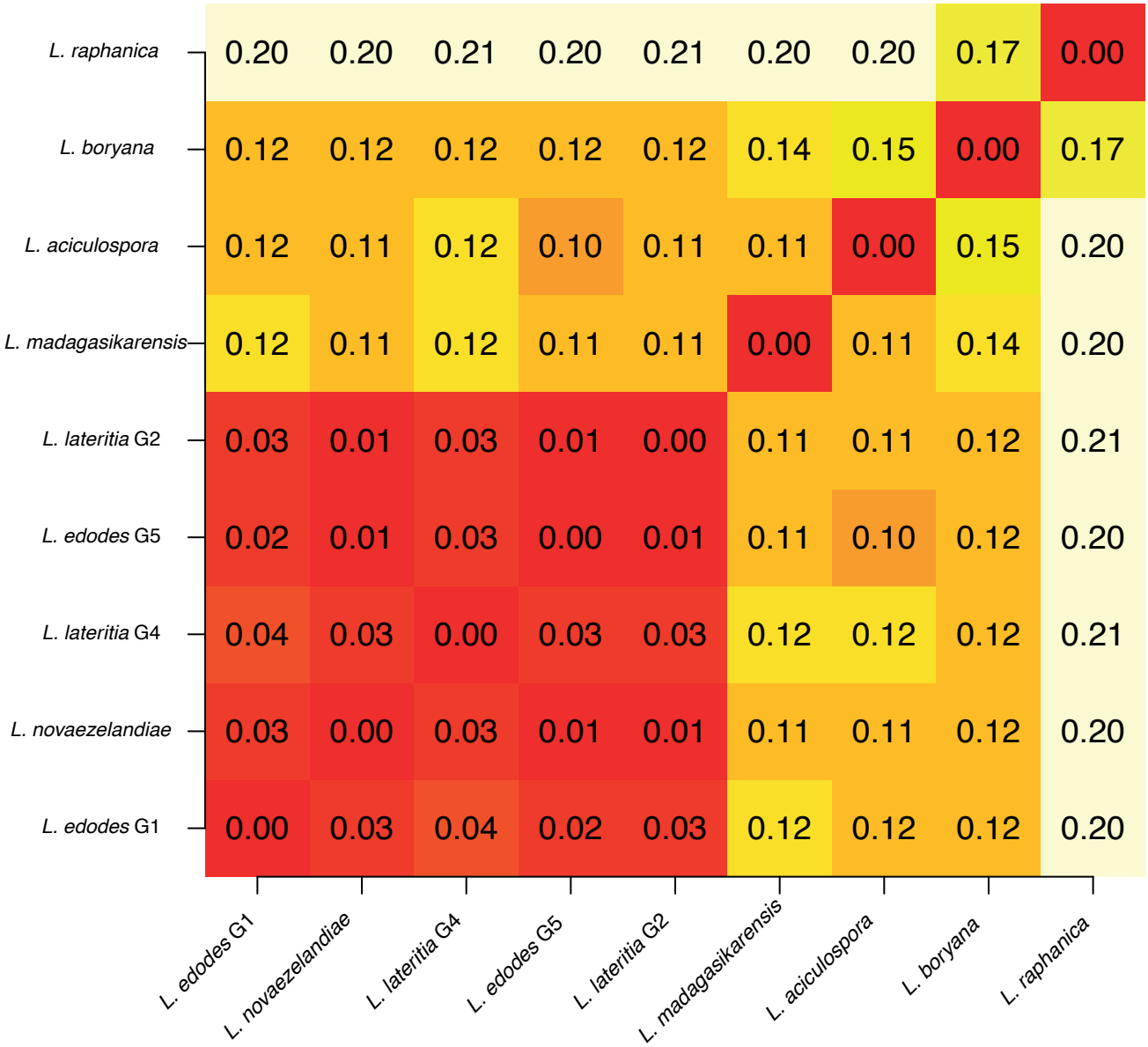

Fig. 3. Distance-matrix heat map of representative sequences of species of *Lentinula* based on pairwise distances from the ITS multi-sequence alignment given as proportion of divergence.

Habit and habitat: Gregarious to scattered on corticate logs of *E. robusta* and unidentified hardwood in humid, mixed mountain forests at higher elevations of the central plateau and eastern escarpment of Madagascar.

Additional specimen examined: **Madagascar**, Ankazobe district, Analamanga region, Ambohitantely Special Reserve, 18.161°S 47.302°E, in primary forest dominated by *U. densifolia* and *Sarcolaenaceae*, 22 Jan. 2008, *B. Buyck & V. Hofstetter* no. 08.120 (paratype PC0142532).

Notes: *Lentinula madagasikarensis* can readily be distinguished from its apparent sister species, *L. aciculospora*, by gross morphological characters including a darker, vinaceous pileus color in *L. madagasikarensis* and larger tufted scales concentrated near the pileus margin forming a distinctive appendiculate margin as well as microscopic differences in basidiospore size, which is smaller in *L. aciculospora* (5.6–8.8 × 1.6–2.8 µm), and shape of cheilocystidia that are gnarled and bluntly lobed in *L. aciculospora* (Mata & Petersen 2000). *Lentinula madagasikarensis* closely resembles *L. boryana* (Mata *et al.* 2001) but differs microscopically because the first never has appendages on cheilocystidia and caulocystidia are absent. Macroscopically, *L. madagasikarensis* differs from *L. boryana* in size, color, and robustness of the pilei, which are smaller (1.8–2.5 cm) and paler (light brown to golden brown or grayish orange) in *L. boryana* (Mata *et al.* 2001). Morphologically, *L. madagasikarensis* closely resembles *L. edodes* in pileus color and the robust aspect of the basidiomata, which also has a dark vinaceous brown and > 5 cm diam pileus (Pegler 1983). Microscopic characters are similar between the two species with similar size of the basidiospores, 5–6.5(–7) × 3–3.7 µm in *L. edodes* and general shape of cheilocystidia, also clavate without any apical appendages in *L. edodes* (Pegler 1983). However, basidiospores of *L. edodes* are slightly more ovoid (Q = 1.78) as reported by Pegler (1983) and cheilocystidia are not reported as sphaeropedunculate or forming florets as is typically found in *L. madagasikarensis*. The geographic distribution also separates *L. edodes* from *L. madagasikarensis* with the first broadly distributed in Asia and the latter known only from Madagascar.

© 2021 Westerdijk Fungal Biodiversity Institute

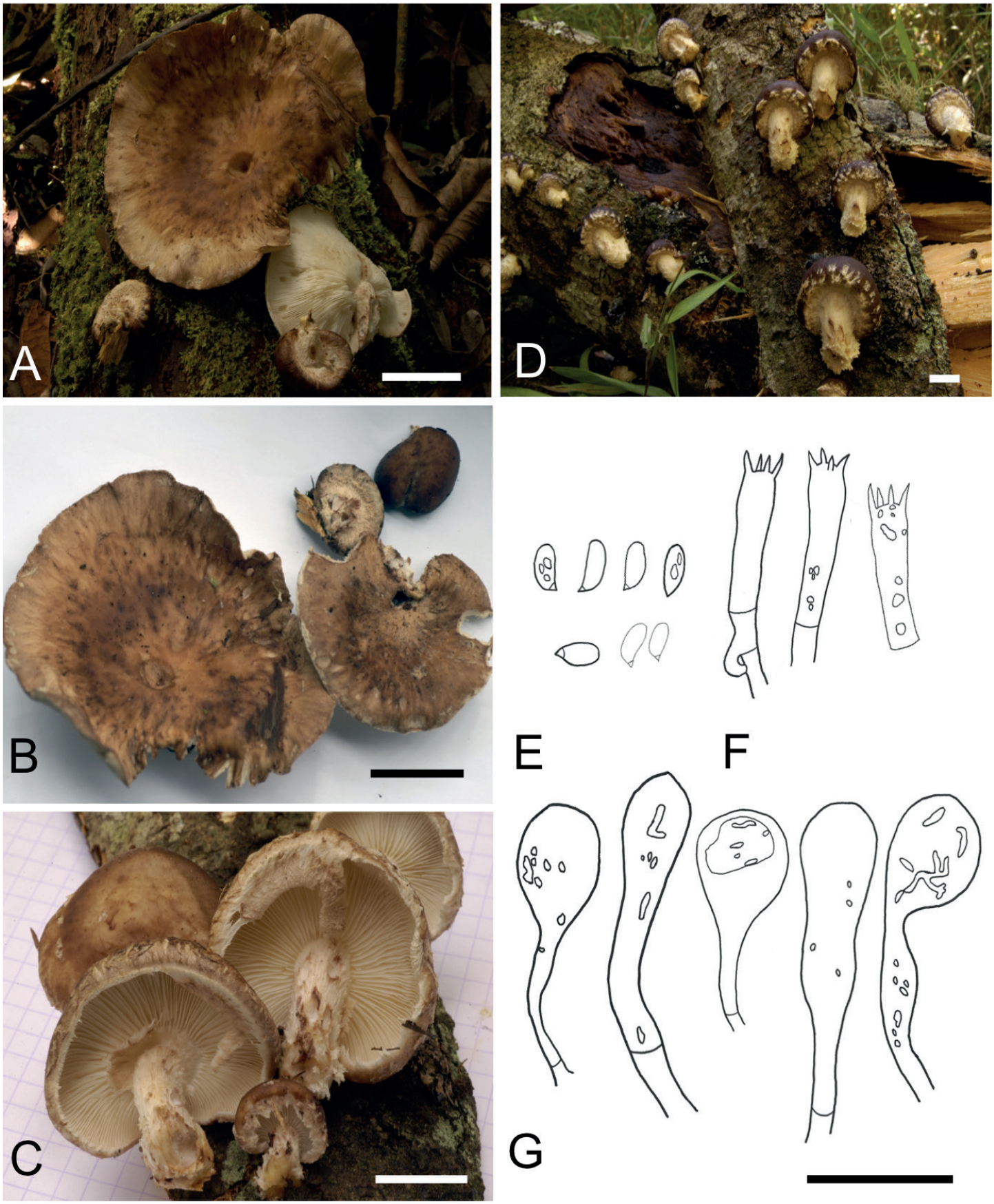

Fig. 4. A, B. Field photograph of *Lentinula madagasikarensis* (type specimen, PC coll. BB06.007). **C, D.** Field photographs of *Lentinula madagasikarensis* (paratype specimen, PC coll. BB08.120). **E.** Basidiospores. **F.** Basidia. **G.** Cheilocystidia. Scale bars: A–D = 2 cm, E–G = 20 µm.

© 2021 Westerdijk Fungal Biodiversity Institute

DISCUSSION

Buyck (2008: 516) described the Malagasy *Lentinula* as a "shiitake look-alike." Our analyses confirm that his collections, from two different localities in Madagascar, represent a new species of *Lentinula*. *Lentinula madagasikarensis* was discovered 4 000 miles from the nearest well-documented wild populations of *Lentinula*, which are those of *L. edodes* Group 5 in India and Nepal. Its apparent sister group, *L. aciculospora*, occurs 9 000 miles away, in Costa Rica (Mata & Petersen 2000), Ecuador (Andrade *et al.* 2012), Panama (Piepenbring 2008), and Nicaragua (Gómez 2018). However, several collections identified as *L. edodes* or "*L. edodes*-like" have been reported from the Democratic Republic of the Congo (DRC), which is less than 2 000 miles from Madagascar (Global Biodiversity Information Facility [www.gbif.org] occurrence records 1836956264, 1840736410, 1840736444). As of this writing, we have not been able to study the material from the DRC.

At its narrowest point, the Mozambique Channel separates Madagascar and mainland Africa by less than 300 miles. Based on their geographic proximity, one would expect a *Lentinula* species from the DRC and *L. madagasikarensis* to be closely related. Even if they are, the presence of *Lentinula* in Madagascar is probably due to long-distance dispersal; Madagascar began to separate from continental Africa during the Late Jurassic Period, about 150-M-yr ago (de Wit 2003), whereas *Lentinula* is about 50-M-yr-old, according to a molecular clock analysis by Varga *et al.* (2019).

Both collections of *L. madagasikarensis* were found in similar habitats in the highlands of the Central Plateau at 1 500–2 000 m alt. One collection was found growing on wood of *E. robusta* and the other was on a fallen log of an "unidentified native tree" (Buyck 2008: 516), but both were in dense forests largely dominated by *U. densifolia* and various species of *Sarcolaenaceae*. All other species or species complexes of *Lentinula* are reported to occur on *Fagales*, particularly *Fagaceae* or *Nothofagaceae*, but some are also capable of growing on other hardwood substrates (Pegler 1983, Mata & Petersen 2000, McKenzie *et al.* 2000, Mata *et al.* 2001, Piepenbring 2008). There are no native *Fagaceae* or *Nothofagaceae* in Madagascar or Sub-Saharan Africa (Manos & Stanford 2001, Knapp *et al.* 2005). A recent discovery of 52-M-yr-old *Castanopsis* fossils from Patagonia shows that *Fagaceae* was present in the southern hemisphere in the early Eocene (Wilf *et al.* 2019), but that was late in the breakup of Gondwana, long after the opening of the South Atlantic Ocean. *Nothofagus* has an 80-M-yr fossil record, but there is no evidence of this group having existed in Africa or Madagascar (Knapp *et al.* 2005).

The phylogenetic placement of *L. madagasikarensis* is important for understanding host shifts and historical biogeography of *Lentinula*. The distribution of host ranges in *Lentinula* suggests that the ancestor of the genus decayed *Fagales*. If so, then *L. madagasikarensis* would represent an expansion onto hosts that are indigenous to Madagascar, as well as introduced eucalypts. Based on the ITS phylogeny, *L. madagasikarensis* is closely related to *L. aciculospora* within the American-African clade (Fig. 2), suggesting that it (and possibly the entire genus) is derived from an ancestor in the neotropics. However, many branches in the ITS phylogeny of *Lentinula* are not strongly resolved (Fig. 2). We defer formal analyses of historical biogeography and evolution of substrate ranges until we have a genome sequence for *L. madagasikarensis*, which we are currently pursuing.

ACKNOWLEDGEMENTS

BB expresses sincere thanks to the Committee for Research and Exploration of the National Geographic Society for funding part of the fieldwork through grant #7921-05. Colleagues of the CNRE at Antananarivo are acknowledged for excellent field assistance. Jadson J. S. Oliveira kindly provided the starting alignment for Dataset 1. Research at Clark University was supported by National Science Foundation award DEB-1456588 (DSH, PI).

Conflict of interest: The authors declare that there is no conflict of interest.

REFERENCES

Andrade JM, Malagón O, Piepenbring M, *et al.* (2012). Etnomicología y valor nutricional de macrohongos silvestres de la comunidad indígena Saraguro en el Sur del Ecuador. *Boletín de la Sociedad Micologíca de Madrid* **36**: 193–201.

Bazzicalupo AL, Buyck B, Saar I, *et al.* (2017). Troubles with mycorrhizal mushroom identification where morphological differentiation lags behind barcode sequence divergence. *Taxon* **66**: 791–810.

Berkeley MJ (1877). Contribution to the botany of H.M.S. 'Challenger.' XXXVIII. Enumeration of the fungi during the expedition of H.M.S. 'Challenger,' 1874–75. *Journal of the Linnean Society, Botany* **16**: 38–54.

Berkeley MJ, Curtis MA (1869). Fungi Cubenses (*Hymenomycetes*). *Journal of the Linnean Society, Botany* **10**: 280–342.

Buyck B (2008). The edible mushrooms of Madagascar: an evolving enigma. *Economic Botany* **62**: 509–520.

Chang ST, Miles PG (1987). Historical record of the early cultivation of *Lentinus* in China. *The Mushroom Journal for the Tropics* **7**: 31–37.

Edler D, Klein J, Antonelli A, *et al.* (2020). raxmlGUI 2.0: a graphical interface and toolkit for phylogenetic analyses using RAxML. *Methods in Ecology and Evolution* **12**: 373–377.

Gómez ILS (2018). Hongos del Caribe nicaragüense. Resumen de especies de dos estudios hechos en la Reserva Biológica Indio Maíz. *Wani* **73**: 44–54.

Harrower E, Ammirati JF, Cappuccino AA, *et al.* (2011) *Cortinarius* species diversity in British Columbia and molecular phylogenetic comparison with European specimen sequences. *Botany* **89**: 799–810.

He MQ, Zhao RL, Hyde KD, *et al*. (2019). Notes, outline and divergence times of *Basidiomycota*. *Fungal Diversity* **99**: 105–367.

Hibbett DS (2001). Shiitake mushrooms and molecular clocks: historical biogeography of *Lentinula*. *Journal of Biogeography* **28**: 231–241.

Hibbett DS, Hansen K, Donoghue MJ (1998). Phylogeny and biogeography of *Lentinula* inferred from an expanded rDNA dataset. *Mycological Research* **102**: 1041–1049.

Hughes KW, Petersen RH, Lickey EB (2009). Using heterozygosity to estimate a percentage DNA sequence similarity for environmental species' delimitation across basidiomycete fungi. *The New Phytologist* **182**: 795–798.

Knapp M, Stöckler K, Havell D, *et al.* (2005). Relaxed molecular clock provides evidence for long-distance dispersal of *Nothofagus* (southern beech). *PLoS Biology* **3**: e14.

Kornerup A, Wanscher JH (1978). *Methuen Handbook of Colour*. 3rd ed., Methuen Co., London.

Larsson A (2014). AliView: a fast and lightweight alignment viewer and editor for large datasets. *Bioinformatics* **30**: 3276–3278.

Looney BP, Adamčík S, Matheny PB (2020). Coalescent-based delimitation and species-tree estimations reveal Appalachian

origin and Neogene diversification in *Russula* subsection *Roseinae*. *Molecular Phylogenetics and Evolution* **147**: 106787.

Manos PS, Standofr AM (2001). The historical biogeography of *Fagaceae*: tracking the tertiary history of temperate and subtropical forests of the northern hemisphere. *International Journal of Plant Sciences* **162**: S77–S93.

Mata JL, Petersen RH (2000). A new species of *Lentinula* (*Agaricales*) from Central America. *Mycoscience* **41**: 351–355.

Mata JL, Petersen RH, Hughes KW (2001). The genus *Lentinula* in the Americas. *Mycologia* **93**: 1102–1112.

McKenzie EHC, Buchanan PK, Johnston PR (2000). Checklist of fungi on *Nothofagus* species in New Zealand. *New Zealand Journal of Botany* **38**: 635–720.

McLoughlin S (2001). The breakup history of Gondwana and its impact on pre-Cenozoic floristic provincialism. *Australian Journal of Botany* **49**: 271–300.

Nilsson RH, Kristiansson E, Ryberg M, *et al.* (2005). Approaching the taxonomic affiliation of unidentified sequences in public databases–an example from the mycorrhizal fungi. *BMC Bioinformatics* **6**: 1–7.

Oliveira JJ, Vargas-Isla R, Cabral TS, *et al.* (2019). Progress on the phylogeny of the *Omphalotaceae*: *Gymnopus s. str*., *Marasmiellus s. str*., *Paragymnopus gen. nov*. and *Pusillomyces gen. nov*. *Mycological Progress* **18**: 713–739.

Pegler DN (1984). The genus *Lentinula* (*Tricholomataceae* tribe *Collybieae*). *Sydowia* **36**: 227–239.

Piepenbring M (2008). Reportes nuevos de *Agaricales* para Panamá. *Acta Biologica Panamensis* **1**: 22–38.

Rehner SA, Buckley E (2005). A *Beauveria* phylogeny inferred from nuclear ITS and *EF1-α* sequences: evidence for cryptic diversification and links to *Cordyceps* teleomorphs. *Mycologia* **97**: 84–98.

Ronquist F, Teslenko M, Van Der Mark P, *et al.* (2012). MrBayes 3.2: efficient Bayesian phylogenetic inference and model choice across a large model space. *Systematic Biology* **61**: 539–542.

Spegazzini C (1883). Fungi guarantici. *Anales de la Sociedad Científica Argentina* **16**: 242–248.

Stamatakis A (2006). RAxML-VI-HPC: maximum likelihood-based phylogenetic analyses with thousands of taxa and mixed models. *Bioinformatics* **22**: 2688–2690.

Varga T, Krizsán K, Földi C, *et al.* (2019). Megaphylogeny resolves global patterns of mushroom evolution. *Nature Ecology & Evolution* **3**: 668–678.

Vilgalys R, Hester M (1990). Rapid genetic identification and mapping of enzymatically amplified ribosomal DNA from several *Cryptococcus* species. *Journal of Bacteriology* **172**: 4238–4246.

White TJ, Bruns T, Lee SB, *et al.* (1990). Amplification and direct sequencing of fungal ribosomal RNA genes for phylogenetics. In: *PCR protocols: a guide to methods and applications* (Innis MA, Gelfand DH, Sninsky JJ, *et al*., eds). Academic Press, Inc., New York: 315–322.

Wilf P, Nixon KC, Gandolfo MA, *et al.* (2019). Eocene *Fagaceae* from Patagonia and Gondwanan legacy in Asian rainforests. *Science* **364**: eaaw5139.

Wilson AW, Desjardin DE (2005) Phylogenetic relationships in the gymnopoid and marasmioid fungi (*Basidiomycetes*, euagarics clade). *Mycologia* **97**: 667–679.

Wilson DS, Pollard D, DeConto RM, *et al.* (2013). Initiation of the West Antarctic Ice Sheet and estimates of total Antarctic ice volume in the earliest Oligocene. *Geophysical Research Letters* **40**: 4305–4309.

Wit MJD (2003). Madagascar: heads it's a continent, tails it's an island. *Annual Review of Earth and Planetary Sciences* **31**: 213–248.

© 2021 Westerdijk Fungal Biodiversity Institute

FUSE

Fungal Systematics and Evolution

VOLUME 8
DECEMBER 2021
PAGES 9–25

doi.org/10.3114/fuse.2021.08.02

Three independent evolutionary events of sequestrate *Lactifluus* species in Australasia

T. Lebel[1,2,3*], J.A. Cooper[3], M.A. Castellano[4], J. Nuytinck[5]

[1]Botanic Gardens and State Herbarium of South Australia, Hackney Rd, Adelaide, SA 5000, Australia
[2]Royal Botanic Gardens Victoria, Birdwood Avenue, South Yarra, Victoria, 3141 Australia
[3]Mannaki Whenua - Landcare Research, P.O. Box 69040, Lincoln 7640, New Zealand
[4]USDA Forest Service, Northern Research Station, 3200 Jefferson Way, Corvallis, Oregon, USA
[5]Naturalis Biodiversity Center, Darwinweg 2, 2333 CR Leiden, The Netherlands

*Corresponding author: Teresa.Lebel@sa.gov.au

Key words:
lactarioid
new taxa
ruffle-like
systematics
taxonomy

Abstract: Three Australian species with sequestrate basidiome forms are recorded for the first time in the genus *Lactifluus* based on nuclear ITS-LSU and morphological data. These species represent three rare independent evolutionary events resulting in sequestrate basidiomes arising from agaricoid species in three different sections in two subgenera. All three species have highly reduced basidiome forms, and no species with intermediate forms have been found. *Lactifluus dendriticus* is unique in the genus in having highly branched, dendritic terminal elements in the pileipellis. We provide full descriptions of two species: *Zelleromyces dendriticus* (= *Lactifluus dendriticus comb. nov*.) in *Lactifluus* subg. *Lactifluus* sect. *Gerardii*, and *Lactifluus geoprofluens sp. nov*. in *Lf.* subg. *Lactifluus* sect. *Lactifluus*. A reduced description is provided for the third, *Lactifluus sp. prov.* KV181 in *Lf.* subg. *Pseudogymnocarpi* sect. *Pseudogymnocarpi*, as it is currently known from a single sequence.

Citation: Lebel T, Cooper JA, Castellano MA, Nuytinck J (2021). Three independent evolutionary events of sequestrate *Lactifluus* species in Australasi. *Fungal Systematics and Evolution* **8**: 9–25. doi: 10.3114/fuse.2021.08.02
Received: 15 January 2021; **Accepted:** 15 April 2021; **Effectively published online:** 2 June 2021
Corresponding editor: P.W. Crous

INTRODUCTION

Distinguishing species of *Lactarius* and *Lactifluus* is difficult enough, but the loss or reduction of macroscopic features in sequestrate species makes them equally problematic to distinguish between genera. In *Lactarius*, sequestrate basidiome forms are known from three main subgenera: subg. *Plinthogalus*, subg. *Russularia*, and subg. *Lactarius* (Dring & Pegler 1978, Beaton *et al.*1984, Desjardin 2003, Nuytinck *et al.* 2003, Eberhardt & Verbeken 2004, Verbeken & Walleyn 2010, Wang *et al.* 2012, Verbeken *et al.* 2014a, b, Sang *et al.*2016, Beenken *et al.* 2016, De Crop *et al.* 2017, Vidal *et al.* 2019). All of the Australasian lactarioid sequestrate forms were historically described in the genera *Zelleromyces*, *Arcangeliella* or *Gastrolactarius*, based on morphology, following Northern Hemisphere circumscriptions of genera. Apart from a regional treatment of species of *Zelleromyces* by Beaton *et al*. (1984) for Victoria, in which the descriptions and illustrations to six species were provided, Australian species have been little studied. Bougher & Syme (1998) provided a further description of *Z. daucinus* from Western Australia, Grgurinovic (1997) short descriptions and a key to three South Australian species, and Trappe & Claridge (2003, 2008) descriptions of two more species. However, the diversification of sequestrate basidiome forms in *Lactarius* in Australasia is known to be high, with eight species currently described and a further 20–25 species remaining to be described (Beaton *et al.*1984, Bougher & Lebel 2001, Lebel 2002b, Trappe & Claridge 2003, 2008, Lebel *et al.* unpub. data). However, no phylogenetic analyses of subgenus or sectional placement has as yet been completed for these taxa or the related epigeal taxa, and species circumscription remains based on morphology.

While conducting research on Australasian sequestrate lactarioid taxa and the *Lactifluus clarkeae* species complex, DNA sequencing revealed species with affinities to *Lactifluus* rather than *Lactarius*. This unexpected finding led us to study their morphological characters in detail, test species delimitation and further examine the phylogenetic relationships between agaricoid and sequestrate *Lactifluus* species, to determine whether sequestrate forms in *Lactifluus* are the result of independent evolutionary events, similar to the pattern seen in *Lactarius* (Verbeken *et al*. 2014a, Sheedy *et al*. 2016). Here we provide descriptions where possible and confirm placement of the taxa in different subgenera within *Lactifluus*.

MATERIALS AND METHODS

Morphology

Several hundred collections from Australasian herbaria and fungaria (MEL, PERTH, BRI, AD, HO, CANB, PDD) and material held at Oregon State Herbarium (OSC) were examined from diverse geographic regions and habitat types across Australia. Detailed coordinate and elevation data for collections mentioned here are available online through the Atlas of Living Australia

Fungal Systematics and Evolution is licensed under a Creative Commons Attribution-NonCommercial-ShareAlike 4.0 International License

© 2021 Westerdijk Fungal Biodiversity Institute

(https://www.ala.org.au/). Collections matching morphological characters of the known *Lactifluus* related taxa, or with typical *Lactifluus* pileipellis structure and cystidia form (approximately 35 collections), were examined in greater detail and sampled for DNA sequencing. Macroscopic characters are described and measured from fresh material, field notes of other collectors, or dried herbarium collections. Measurements taken using dried fungarium material are listed as such and are estimated to be approximately 30 % smaller than measurements taken from fresh specimens. This estimate is based on fresh and dry weights of 30 recent collections of lactarioid sequestrate basidiomes. Colours are described in general terms from field observations in daylight conditions. Habitat, associated plant communities, sporulating season, presence and nature of latex, fresh odour, and taste are based on field notes.

Microscopic characters are described from examination of dried fungarium material. Hand-cut sections were rehydrated in 5 % KOH solution then mounted in congo red to observe the hymenium, trama, and pileipellis. Spore size, shape, ornamentation and amyloidity were observed in lamellae tissue mounted in Melzer's reagent. Measurements of microscopic characters were taken on an Olympus BX-52 microscope at ×400 or ×1 000 using an Olympus DP-73 camera attachment and measurement tools in cellSens standard (v. 1.16). Microscopic measurements are given as a raw range of length × width with mean ± standard deviation (SD) of *n* measurements in parentheses. The length/width quotient (Q) of individual spores is presented as the raw range of Q values with mean ± standard deviation (SD) of *n* measurements in parentheses. Basidia, basidioles, and cystidia measurements are given as length (not including sterigmata) × width at widest point, and width at base or apex. Pseudocystidia, laticiferous hyphae, and hyaline hyphae measurements are given as a raw range of diameters. In highly reduced sequestrate basidiomes there is some difficulty in determining position of cystidial elements, thus in descriptions provided here they are referred to as hymenial cystidia.

Scanning electron microscopy (SEM) of gold-sputtered basidiospores mounted on carbon tape was performed using a Thermo Fisher Scientific XL30 FEG microscope (Waltham, USA) at the University of Melbourne Biosciences Microscopy Unit.

All photographs are based on the type collections unless otherwise stated. Names of fungaria are abbreviated according to Thiers (2011) (http://sweetgum.nybg.org/ih/ — continuously updated). We use the abbreviation '*Lf.*' to distinguish *Lactifluus* from *Lactarius* ('*L.*') when discussing species in these genera.

Molecular studies

Protocols for DNA extraction (Qiagen Plant DNeasy kit, Germantown, USA or the EZNA forensic kit, Omega Bio-tek, Norcross USA, for samples older than 1995), PCR, and sequencing followed those in Lebel & Syme (2012) and Lebel *et al.* (2015) and the references therein. Assembly, manual editing, and preliminary alignment of sequences were performed within Geneious v. 9.1.7 (Biomatters Ltd). Individual alignments for the ITS and LSU were then manually trimmed in BioEdit v. 7.1.3 (Hall 2011) and some final manual editing done in Geneious v. 9.1.7. The concatenated alignment and phylogenetic trees are available from the Landcare Research datastore https://doi.org/10.7931/n4fc-4z93.

Sequences of the ITS and LSU from similar species (based on blast searches), and representative taxa to cover subgenera and sections within *Lactifluus* were retrieved from GenBank and UNITE (Kõljalg *et al.* 2013), to generate a concatenated alignment. This was done with the on-line version of MAFFT v. 7 (Katoh *et al.* 2019). Three species of *Multifurca* were utilised as outgroup. Novel sequences representing collections from Australasia and other regions generated for this study are listed in Table 1 with relevant GenBank accession numbers, and all sequences utilised in analyses. Sequences labelled as provisional taxa "*Lf.* sp. 1–13" are numbered according to a broader analysis of Australasian species of *Lactifluus* which will be published elsewhere; we have retained the numbering convention for consistency.

Phylogenetic analyses of the concatenated ITS+LSU alignment was performed with Maximum Likelihood (ML) in RAxML v. 8.2.12 (Stamatakis *et al.* 2014) using the CIPRES Science Gateway v. 3.3 (Miller *et al.* 2010). The final alignment comprised 211 specimens (195 ITS and 146 LSU sequences), consisting of 2 087 bp including gaps. Gaps in alignments were treated as missing data. The tree was visualised in FigTree v. 1.4.2 (Rambaut 2009).

RESULTS

Sequestrate forms arose independently in at least three sections in two subgenera of *Lactifluus*: subg. *Lactifluus* sect. *Gerardii* (*Lf. dendriticus comb. nov*.) and sect. *Lactifluus* (*Lf. geoprofluens sp. nov*.), and subg. *Pseudogymnocarpi* sect. *Pseudogymnocarpi* (*Lf. sp. prov.* KV181). *Lactifluus dendriticus comb. nov*. appears to be a wide-spread species from eastern Australia, ectomycorrhizal with *Eucalyptus* and *Acacia*. It is in a strongly supported clade, sister to *Lf. wirrabara,* three provisional Australian species with agaricoid basidiomes (*Lf*. *sp. prov.* 10–12), an environmental sequence with unknown basidiome form *Lf. sp. prov*. 13 from Australia, *Lf. limbatus* from Malaysia, *Lf. sinensis* from China, *Lf. coniculus* from Sri Lanka, and *Lf. midnapurensis* from India in section *Gerardii* (Fig. 1). All of these Asian taxa are associated with lowland tropical rainforest dominated by Dipterocarp taxa (Stubbe *et al.* 2012, Song *et al.* 2017, Phookamsak *et al.* 2019).

Lactifluus geoprofluens sp. nov. is in a weakly supported clade with two agaricoid species *Lf. jetiae nom. prov*. (Fig. 3C) and *Lf. rugulostipitatus nom. prov*. (in press; these provisional species will be published elsewhere), a third provisional species known only from environmental sequences (*Lf. sp. prov.* 8), several undescribed taxa with agaricoid basidiomes from Thailand and Japan, and *Lf. distantifolius* and *Lf. Longipilus* (Fig. 2). More data are required to reliably recognise sister relationships as branch support values are low in this mixed clade of mostly undescribed taxa.

A single sequence of the sequestrate *Lactifluus sp. prov.* KV181 is in a clade with a mix of species from diverse geographic locations, *Lf. pseudoluteopus* from Thailand, *Lf. hygrophoroides* from North America, *Lf. rugatus* from Southern Europe, and *Lf. holophyllus* and *Lf. luteolamellatus* from South Korea in sect. *Pseudogymnocarpi*. While we did take a small sample for DNA in the field, unfortunately, the single collection of *Lf. sp. prov*. KV181 was destroyed by mould contamination after drying and discarded, and no further collections of this sequestrate taxon were found while looking through abundant material of sequestrate lactarioid taxa in herbaria. Thus while a full description cannot be provided at this time, we do provide a photo of basidiomes, and a partial description, in the hope that further material will be found.

© 2021 Westerdijk Fungal Biodiversity Institute

Table 1. Specimens used in the phylogenetic analysis, including infrageneric taxon, species (as originally identified in the field or as labelled in GenBank), herbarium numbers and typification, country of origin, and ITS/LSU GenBank accession numbers. New sequences generated for this study are indicated in bold. Abbreviations used: AU - Australia, NZ - New Zealand, NCal - New Caledonia, WA - Western Australia, VIC - Victoria, TAS - Tasmania, SA - South Australia, NT - Northern Territory, NSW - New South Wales, QLD - Queensland, FrIsland - Fraser Island.

(Infrageneric) taxon	Species	Herbarium or collection number	Country	GenBank accession numbers	
				ITS	LSU
Multifurca	*Multifurca ochricompacta*	BB02107	n/a	DQ421984	DQ421984
	Multifurca sp.	MEL238568	AU	MW134734	MW128106
	Multifurca stenophylla	CWD584	AU	JX266628	JX266633
	Multifurca zonaria	FH12-009	Thailand	KR364083	KR364212
subg. *Gymnocarpi* sect. *Gymnocarpi*	*Lactifluus foetens*	ADK3688 BR	Benin	KR364022	KR364149
	Lactifluus gymnocarpus	EDC12-047 GENT	Cameroon	KR364065	KR364194
	Lactifluus tanzanicus	TS1277	Tanzania	KR364037	n/a
subg. *Gymnocarpi* sect. *Luteoli*	*Lactifluus brunneoviolascens*	AV13-038 GENT	Italy	KR364123	KR364246
	Lactifluus caliendrifer	KW378 GENT Holotype	Thailand	MK517655	n/a
	Lactifluus luteolus	AV05-253 GENT	USA	KR364016	KR364142
	Lactifluus russulisporus	REH9398 NY Holotype	AU	KR364097	KR364229
subg. *Gymnocarpi* sect. *Nebulosi*	*Lactifluus chiapanensis*	V.M.Bandala 4374A GENT	Mexico	GU258297	GU265580
	Lactifluus guadeloupensis	RC_Guad11-023 LIP Holotype	Guadeloupe	KP691412	KP691421
subg. *Gymnocarpi* sect. *Panuoidei*	*Lactifluus panuoides*	G128	Guyana	KJ786647	KJ786551
subg. *Gymnocarpi* sect. *Phlebonemi*	*Lactifluus* aff. *phlebonemus*	EDC12-023 GENT	Cameroon	KR364062	KR364191
subg. *Gymnocarpi* sect. *Tomentosi*	*Lactifluus albens*	MEL2231695 Type	AU_WA	MW134740	MW128112
	Lactifluus aurantioruber	MEL2257827	AU_TAS	MW134745	MW128115
	Lactifluus clarkeae	MEL2101947 Epitype	AU_SA	MW134754	MW128120
	Lactifluus clarkeae	PDD102596	NZ	MW134770	MW128130
	Lactifluus flocktonae	MEL2238290 Epitype	AU_VIC	JX266621	JX266637
	Lactifluus psammophilus	MEL2238407 Type	AU_VIC	MW134791	MW128144
	Lactifluus pseudoflocktonae	MEL2238269 Holotype	AU_VIC	MW134801	MW128151
	Lactifluus sp. 1	environmental sample CMMy30M1	New Caledonia	KY774240	n/a
	Lactifluus sp. 5	PGK13-130 Nothofagus	New Caledonia	KP691436	KR605507
	Lactifluus sp. 6	environmental sample KT-26 Tristaniopsis	New Caledonia	LC271308	n/a
subg. *Lactariopsis* sect. *Albati*	*Lactifluus vellereus*	UE20.09.2004-22 UPS	n/a	DQ422034	DQ422034
subg. *Lactariopsis* sect. *Edules*	*Lactifluus edulis*	FN05-628 GENT	Malawi	KR364020	KR364147
subg. *Lactariopsis* sect. *Lactariopsis*	*Lactifluus annulatoangustifolius*	BB00-1518 PC	Madagascar	AY606981	KR364253
	Lactifluus velutissimus	JD886	Congo	KR364075	KR364204
subg. *Lactariopsis* sect. *Neotropicus*	*Lactifluus venezuelanus*	RC_Gaud11-017 LIP	Guadeloupe	KP691411	KP691420
subg. *Lactifluus* sect. *Allardii*	*Lactifluus allardii*	AV05-286 GENT	USA	KF220015	KF220124
subg. *Lactifluus* sect. *Ambicystidiati*	*Lactifluus ambicystidiatus*	KUN_F88179	China	KR908670	KR908672
subg. *Lactifluus* sect. *Gerardii*	*Lactifluus auriculiformis*	AV12-050 GENT Holotype	Thailand	KR364086	KR364216

© 2021 Westerdijk Fungal Biodiversity Institute

Table 1. (Continued).

(Infrageneric) taxon	Species	Herbarium or collection number	Country	GenBank accession numbers	
				ITS	LSU
	Lactifluus bhandaryi	TENN 051830 Holotype	Nepal	KR364111	n/a
	Lactifluus conchatulus	LTH457 GENT Isotype	Thailand	GU258296	GU265659
	Lactifluus coniculus	DS07-496 GENT Holotype	Sri Lanka	GU258236	GU265594
	Lactifluus coniculus	DS07-497 GENT	Sri Lanka	GU258237	GU265595
subg. *Lactifluus* sect. *Gerardii*	***Lactifluus dendriticus comb. nov.***	**MEL2063377**	**AU_VIC**	**MW471118**	**MW471115**
	Lactifluus dendriticus comb. nov.	**MEL2292167_CANB748620**	**AU_VIC**	**MW471119**	**MW471116**
	Lactifluus dendriticus comb. nov.	**MEL2326248**	**AU_VIC**	**MW471120**	n/a
	Lactifluus dendriticus comb. nov.	**MEL2126553**	**AU_VIC**	**MW471121**	n/a
	Lactifluus dendriticus comb. nov.	**MEL2061947**	**AU_NSW**	**MW471122**	n/a
	Lactifluus fuscomarginatus	GO2010-144	Mexico	KC152157	n/a
	Lactifluus genevievae	G.Gates_D.Ratkowsky 17-2-2005	AU	GU258294	GU265657
	Lactifluus gerardiellus	KW386 GENT Holotype	Thailand	KX889845	KX889844
	Lactifluus gerardii	AV05-375 GENT	USA	GU258254	GU265616
	Lactifluus gerardii	Desjardin3630	USA	GU258220	n/a
	Lactifluus igniculus	LE262983 Type	Vietnam	JX442759	n/a
	Lactifluus indicus	CAL 1282 Holotype	India	KU145119	KU145121
	Lactifluus leae	AV-RW04-90 GENT	Thailand	GU258244	
	Lactifluus leae	FH12-13 GENT	Thailand	KF432957	
	Lactifluus leonardii	P.Leonard 35607	AU	GU258295	GU265658
	Lactifluus leonardii	G.Gates 29-1-2002	AU	GU258304	GU265664
	Lactifluus limbatus	DS06-230 GENT	Malaysia	GU258222	GU265578
	Lactifluus limbatus	DS06-247 GENT	Malaysia	GU258223	GU265579
	Lactifluus midnapurensis	CAL 1516 Holotype	India	KY785175	KY785177
	Lactifluus ochrogalactus	E.Nagasawa 80-102 TMI Type	Japan	GU258280	
	Lactifluus parvigerardii	KUN_F61367 Holotype	China	JF975641	JF975642
	Lactifluus petersenii	AV05-267 GENT	USA	GU258282	GU265643
	Lactifluus pulchrellus	KW304_FH12-037 GENT Holotype	Thailand	KR364092	KR364223
	Lactifluus raspei	EDC14-517 Holotype	Thailand	KX889849	n/a
	Lactifluus reticulatovenosus	Horak 6472 GENT Holotype	Indonesia	GU258286	GU265649
	Lactifluus robustus	K16053113	China	KY353803	KY353806
	Lactifluus robustus	K15052822	China	KY353802	KY353805
	Lactifluus sepiaceus	MEL2300727	AU	GU258293	GU265656
	Lactifluus sepiaceus	MEL1054958	AU_VIC	MW134808	n/a
	Lactifluus sepiaceus	P.Leonard 40509	NZ	GU258287	GU265650
	Lactifluus sinensis	K15060710 Holotype	China	KT900208	n/a
	Lactifluus sinensis	K15070203	China	KT900209	n/a
	Lactifluus sinensis	environmental sample HIB12	China	JX457047	n/a
	Lactifluus sp.	DS06-003 GENT	Malaysia	GU258231	GU265588
	Lactifluus sp.	AV05-283 GENT	USA	GU258259	n/a
	Lactifluus sp.	DPLewis6983	USA	GU258272	n/a
	Lactifluus sp.	Desjardin3564	n/a	GU258273	n/a
	Lactifluus sp. 10	P.Leonard 10409	AU	JF731001	JF731003
	Lactifluus sp. 10	MEL2305122	AU_QLD	MW134809	n/a
	Lactifluus sp. 10	MEL2332066	AU_QLD	MW134810	n/a
	Lactifluus sp. 11	PL26078	AU	n/a	MW128157

© 2021 Westerdijk Fungal Biodiversity Institute

Table 1. (Continued).

(Infrageneric) taxon	Species	Herbarium or collection number	Country	GenBank accession numbers	
				ITS	LSU
	Lactifluus sp. 12	R.E.Halling 6800	AU	JF731000	JF731002
	Lactifluus sp. 13	environmental sample RFLP61	AU	DQ388868	n/a
	Lactifluus sp. 13	environmental sample Toosoil16	AU	KC222796	n/a
	Lactifluus sp. 13	environmental sample Toosoil56	AU	KC222836	n/a
	Lactifluus subgerardii	AV05-389 GENT	USA	GU258271	n/a
	Lactifluus wirrabara	G.Gates_D.Ratkowsky 12-07-2003	AU	GU258306	GU265666
	Lactifluus wirrabara	G.Gates_D.Ratkowsky 17-01-2002	AU	GU258305	GU265665
	Lactifluus wirrabara	G.Gates_D.Ratkowsky 24-01-2004	AU	GU258307	n/a
	Lactifluus wirrabara	JET943 MEL	AU	GU258291	n/a
subg. *Lactifluus* sect. *Lactifluus*	*Lactifluus acicularis*	DS07-456 GENT	Thailand	HQ318224	HQ318125
	Lactifluus acicularis	KVP08-033 GENT	Thailand	HQ318242	HQ318150
	Lactifluus corrugis	JN2004-015 GENT	USA	JQ753820	JQ348262
	Lactifluus corrugis	AV05-291 GENT	USA	JQ753823	JQ348266
	Lactifluus crocatus	LTH268 GENT	Thailand	HQ318266	HQ318181
	Lactifluus crocatus	LTH202 GENT	Thailand	HQ318248	HQ318157
	Lactifluus dissitus	AV-KD-KVP09-082 GENT	India	n/a	JN389035
	Lactifluus distantifolius	DS07-461 GENT Isotype	Thailand	HQ318223	HQ318124
	Lactifluus distantifolius	LTH288 GENT	Thailand	HQ318274	HQ318193
	Lactifluus geoprofluens sp. nov.	**MEL2145804 Holotype**	**AU_VIC**	**MW471123**	**MW471117**
	Lactifluus jetiae	MEL2238281 Holotype	AU_VIC	MW134811	MW128158
	Lactifluus jetiae	MEL2341759	AU_VIC	MW134813	n/a
	Lactifluus leptomerus	AV-KD-KVP09-130 GENT	India	JN388971	JN389022
	Lactifluus leptomerus	AV-KD-KVP09-131 GENT Holotype	India	JN388972	JN389023
	Lactifluus longipilus	LTH273 GENT	Thailand	HQ318276	HQ318195
	Lactifluus longipilus	LTH168 GENT	Thailand	HQ318235	HQ318143
	Lactifluus maenamensis	KD 16-008	India	MF928075	n/a
	Lactifluus mexicanus	Montoya5276 Holotype	Mexico	MK211181	MK211190
	Lactifluus oedematopus	AV07-079 GENT	Belgium	JQ753835	JQ348270
	Lactifluus oedematopus	RW1228 GENT	France	HQ318216	HQ318116
	Lactifluus oedematopus	KVP12-001 GENT Neotype	Germany	KR364100	KR364232
	Lactifluus pagodicystidiatus	MEL2121979	AU_VIC	MW134815	MW128161
	Lactifluus pagodicystidiatus	MEL2150777 Holotype	AU_VIC	MW134816	MW128162
	Lactifluus pallidilamellatus	Leticia Montoya 4716	Mexico	JQ753824	JQ348268
	Lactifluus pinguis	LTH117 GENT Holotype	Thailand	HQ318211	HQ318111
	Lactifluus pinguis	LTH169 GENT	Thailand	HQ318221	HQ318121
	Lactifluus rugulostipitatus	MEL2329677 Holotype	AU_NT	MW134817	MW128163
	Lactifluus rugulostipitatus	MEL2329673	AU_NT	MW134819	n/a
	Lactifluus sp.	KIINA158 GENT	China	HQ318225	HQ318126
	Lactifluus sp.	AV-KD-KVP09-134 GENT	India	JN388978	JN389026
	Lactifluus sp.	AV-KD-KVP09-128	India	n/a	JN389020
	Lactifluus sp.	AV-KD-KVP09-137	India	n/a	JN389027
	Lactifluus sp.	AV-KD-KVP09-129	India	n/a	JN389021
	Lactifluus sp.	OSA-My-3993	Japan	n/a	AB238645
	Lactifluus sp.	OSA-My-3998	Japan	n/a	AB238650
	Lactifluus sp.	OSA-My-4003	Japan	n/a	AB238655

© 2021 Westerdijk Fungal Biodiversity Institute

Table 1. (Continued).

(Infrageneric) taxon	Species	Herbarium or collection number	Country	GenBank accession numbers	
				ITS	LSU
	Lactifluus sp.	OSA-My-3994	Japan	n/a	AB238646
	Lactifluus sp.	OSA-My-4014	Japan	n/a	AB238666
	Lactifluus sp.	OSA-My-4015	Japan	n/a	AB238667
	Lactifluus sp.	OSA-My-3999	Japan	n/a	AB238651
	Lactifluus sp.	LTH313 GENT	Thailand	HQ318272	HQ318190
	Lactifluus sp.	LTH133 GENT	Thailand	HQ318212	HQ318112
	Lactifluus sp.	KVP08-006 GENT	Thailand	HQ318229	HQ318136
	Lactifluus sp.	LTH231 GENT	Thailand	HQ318278	HQ318197
	Lactifluus sp.	LTH123 GENT	Thailand	HQ318222	HQ318122
	Lactifluus sp.	LTH294 GENT	Thailand	HQ318273	HQ318191
	Lactifluus sp.	KVP08-021 GENT	Thailand	HQ318233	HQ318140
	Lactifluus sp.	LTH170 GENT	Thailand	HQ318252	HQ318165
	Lactifluus sp.	LTH264 GENT	Thailand	HQ318264	HQ318179
	Lactifluus sp.	KVP08-008 GENT	Thailand	HQ318231	HQ318138
	Lactifluus sp.	LTH249 GENT	Thailand	n/a	HQ318176
	Lactifluus sp.	LTH284 GENT	Thailand	HQ318253	HQ318166
	Lactifluus sp.	KVP08-026 GENT	Thailand	HQ318238	HQ318146
	Lactifluus sp.	DED7577	USA	n/a	HQ318188
	Lactifluus sp.	AV05-394 GENT	USA	GU258300	GU265660
	Lactifluus sp.	EIU-ASM10990	USA	JQ358921	JN940236
	Lactifluus sp.	AV04-209 GENT	USA	JN388977	JN388998
	Lactifluus sp.	EIU-ASM11130	USA	JQ358938	JN940223
	Lactifluus sp.	SAM310809-02 TENN	USA	MF773609	n/a
	Lactifluus sp.	MycoMap10398	USA	MH975019	n/a
	Lactifluus sp.	AV05-337 GENT	USA	JQ753821	n/a
	Lactifluus sp.	AV04-167 GENT	n/a	JQ753827	JQ348273
	Lactifluus sp. 8	environmental sample RFLP38	AU_QLD	DQ388845	n/a
	Lactifluus sp. 8	environmental sample RFLP39	AU_QLD	DQ388846	n/a
	Lactifluus sp. 8	environmental sample RFLP5	AU_QLD	DQ388812	n/a
	Lactifluus sp. 9	REH9320 NY	AU	KR364096	KR364228
	Lactifluus sp. 9	environmental sample Toosoil58	AU_QLD	KC222838	n/a
	Lactifluus subvolemus	KVP08-048 GENT	Slovenia	JQ753927	JQ348379
	Lactifluus subvolemus	LAS75_092-A	Sweden	n/a	JQ348348
	Lactifluus versiformis	AV-KD-KVP09-047 GENT	India	JN388964	JN389032
	Lactifluus versiformis	AV-KD-KVP09-014 GENT Holotype	India	JN388963	JN389029
	Lactifluus vitellinus	LTH348 GENT	Thailand	HQ318251	HQ318164
	Lactifluus vitellinus	KVP08-024 GENT Holotype	Thailand	HQ318236	HQ318144
	Lactifluus volemus	UE09.08.2004-5 UPS	n/a	DQ422008	DQ422008
subg. *Lactifluus* sect. *Piperati*	*Lactifluus albopicri*	MDB_F12_18	AU_NT	MN598888	MN598864
	Lactifluus albopicrus	MEL2297391 Type	AU_VIC	MN598874	MN598855
	Lactifluus austropiperatus	PERTH07550324 Type	AU_QLD	MN614115	MN614111
	Lactifluus austropiperatus	MEL2150778	AU_VIC	MN614116	MN614112
	Lactifluus dwaliensis	LTH67 GENT	Thailand	KF220108	KF220203
	Lactifluus glaucescens	M.Lecomte_2002-20-9-3	France	KF220031	KF220134
	Lactifluus leucophaeus	AV97-382 GENT	Papua New Guinea	GU258299	GU265640

© 2021 Westerdijk Fungal Biodiversity Institute

Table 1. (Continued).

(Infrageneric) taxon	Species	Herbarium or collection number	Country	GenBank accession numbers	
				ITS	LSU
	Lactifluus piperatus	M.Lecomte_2001-8-19-23	France	KF220120	KF220212
subg. *Lactifluus* sect. *Tenuicystidiati*	*Lactifluus subpruinosus*	KUN_F76034	China	KC154110	KC154136
	Lactifluus tropicosinicus	KUN_F59626	China	KC154120	KC154146
subg. *Pseudogymnocarpi*	*Lactifluus armeniacus*	EDC14-501 GENT Holotype	Thailand	KR364127	n/a
	Lactifluus sp.	TENN065929	USA	KR364102	KR364233
	Lactifluus sp.	JN2011-012 GENT	Vietnam	KR364045	KR364171
	Lactifluus sp. 7	AQ797939	AU_QLD	n/a	MW128164
	Lactifluus sp. 7	FG2018031	AU_QLD	MW134820	MW128165
	Lactifluus sp. 7	AQ794627	AU_QLD	MW134821	MW128166
	Lactifluus volemoides	TS0705 Holotype	Tanzania	KR364038	KR364165
subg. *Pseudogymnocarpi* sect. *Pseudogymnocarpi*	*Lactifluus* cf. *pseudogymnocarpus*	AV05-085 GENT	Malawi	KR364012	n/a
	Lactifluus cf. *pumilus*	EDC12-066 GENT	Cameroon	KR364067	n/a
	Lactifluus flavellus	MD393 Holotype	Togo	LK392594	n/a
	Lactifluus gymnocarpoides	JD885	DR Congo	KR364074	n/a
	Lactifluus holophyllus	ASIS19960	South Korea	MF611684	MF611659
	Lactifluus holophyllus	ASIS22632	South Korea	MF611685	n/a
	Lactifluus holophyllus	SFC20150812-63 Holotype	South Korea	MF611683	n/a
	Lactifluus hygrophoroides	AV05-251 GENT	USA	HQ318285	HQ318208
	Lactifluus hygrophoroides	EIU-ASM10004 clone c4	USA	JQ358911	n/a
	Lactifluus longisporus	AV94-557 GENT	Burundi	KR364118	KR364244
	Lactifluus longisporus	AV11-025 GENT	Tanzania	KR364054	n/a
	Lactifluus luteolamellatus	MHHNU8297	China	MK167429	n/a
	Lactifluus luteolamellatus	SFC20150818-39	South Korea	MF611680	n/a
	Lactifluus luteopus	AV94-463 GENT Type	Burundi	KR364119	n/a
	Lactifluus luteopus	EDC11-087 GENT	Tanzania	KR364049	KR364176
	Lactifluus medusae	EDC12-152 GENT	Cameroon	KR364069	n/a
	Lactifluus pseudohygrophoroides	SFC20140821-45 Holotype	South Korea	MF611682	MF611657
	Lactifluus pseudohygrophoroides	SFC20150813-71	South Korea	MF611681	n/a
	Lactifluus pseudoluteopus	LTH155 GENT	Thailand	HQ318286	HQ318210
	Lactifluus pseudoluteopus	FH12-026 GENT	Thailand	KR364084	n/a
	Lactifluus pseudoluteopus	environmental sample CD15	Thailand	FJ644702	n/a
	Lactifluus rugatus	EP 1212_7 LGAM-AUA	Greece	KR364104	KR364235
	Lactifluus rugatus	PA2010R	Greece	MH125243	n/a
	Lactifluus rugatus	4_01_2015	Italy	KU885436	n/a
	Lactifluus sp.	environmental sample L7524_ Russ MAD37	Madagascar	FR731264	n/a
	Lactifluus sp.	environmental sample T071b	Thailand	JN969388	n/a
	Lactifluus sp.	MycoMap6251	USA	MK560130	n/a
	Lactifluus sp.	MycoMap6284	USA	MK560131	n/a
	Lactifluus sp.	FLAS-F-61011	USA	MH016945	n/a
	Lactifluus sp.	KUNF58696	n/a	KC154100	n/a
	***Lactifluus* sp.**	**KV181**	**AU_NSW**	**MW471124**	n/a
	Lactifluus sudanicus	AV11-174 MD105	Togo	HG426469	KR364186
	Lactifluus sudanicus	MD148	Togo	HG426476	n/a

© 2021 Westerdijk Fungal Biodiversity Institute

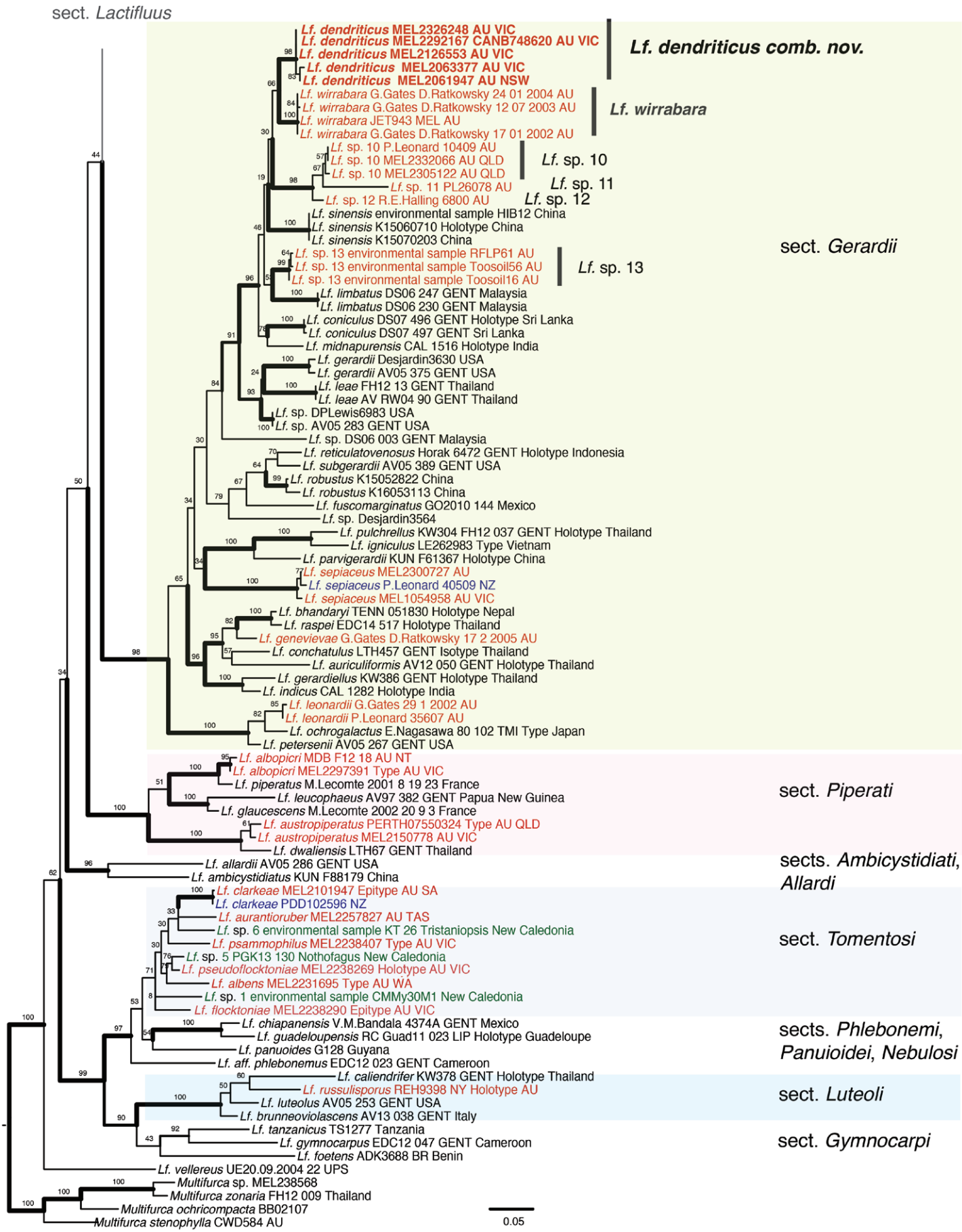

Fig. 1. Maximum Likelihood tree based on ITS and LSU sequences for subgenus *Lactifluus* sections *Gerardii*, *Piperati*, *Ambicystidiati*, and *Allardi*; subgenus *Gymnocarpi* sections *Tomentosi*, *Phlebonemi*, *Panuioidei*, *Nebulosi*, *Luteoli*, *Gymnocarpi*, and *Lf. vellereus* from *Lf.* sect. *Albati*, subg. *Lactariopsis*, with outgroup *Multifurca*. Bold lines indicate ML support ≥ 90 %. Bold text sequences of sequestrate taxa generated for this study. Red text: Australian specimens or sequences, blue text: New Zealand specimens, green text: New Caledonia specimens or sequences.

© 2021 Westerdijk Fungal Biodiversity Institute

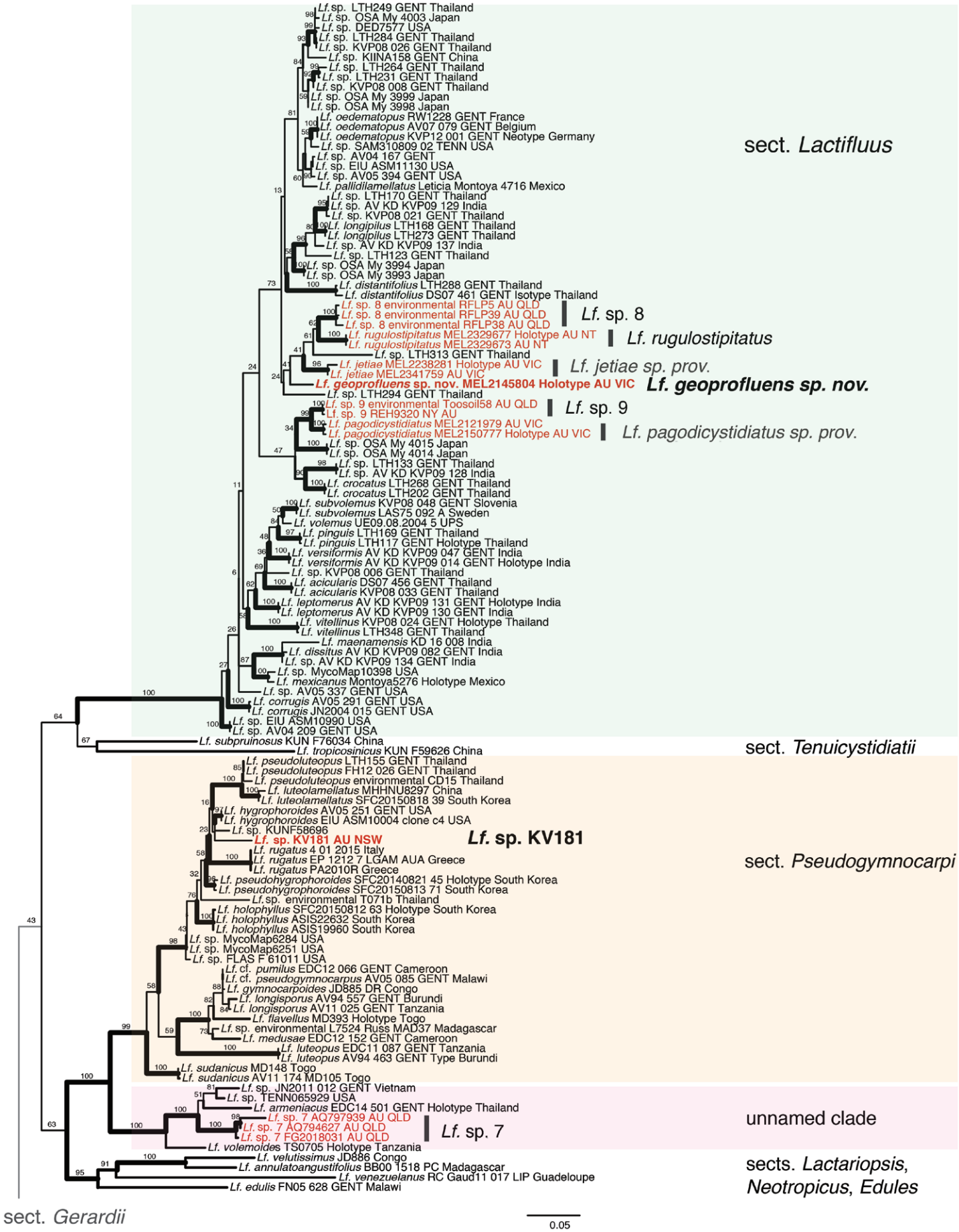

Fig. 2. Maximum Likelihood tree based on ITS and LSU sequences for subgenus *Lactifluus* sections *Lactifluus* and *Tenuicystidiati*; and subgenus *Pseudogymnocarpi* section *Pseudogymnocarpi* and an unnamed clade, and exemplars from sections *Lactariopsis*, *Neotropicus* and *Edules*. Bold lines ML ≥ 90 %. Bold text sequences generated for this study. Red text: Australian specimens or sequences.

Taxonomy

Section *Gerardii*

Lactifluus dendriticus (T. Lebel) T. Lebel, J. Cooper & Nuytinck, *comb. nov*. MycoBank MB 838127. Figs 3B, 4A–F.
Basionym: *Zelleromyces dendriticus* T. Lebel, *Australasian Mycologist* **21**: 4. 2002. figs 1–4. MB 373383.

Etymology: The specific epithet, "*dendriticus*" (L), refers to the dendritic terminal element of the pileipellis.

Diagnosis: This species can be distinguished by the pale sequestrate basidiomes, unique dendritic terminal elements forming a short turf in the pileipellis, and globose spores.

Typus: **Australia**, Victoria, Errinundra National Park, The Gap Scenic Reserve, Gunmark Road, 1.3 km southeast of Survey

Fig. 3. Basidiomata of new sequestrate species and representative agaricoid species. **A.** *Lactifluus wirrabara* (JET 943; photo J.E. Tonkin). **B.** *Lf. dendriticus* (photo T. Lebel). **C.** *Lf. jetiae* (photo J.E. Tonkin). **D.** *Lf. geoprofluens* (photo L. Vaughan). **E.** *Lf. rugatus* (photo U. Pero). **F.** *Lf. sp. prov.* KV181 (photo T. Lebel). Scale bars = 10 mm

© 2021 Westerdijk Fungal Biodiversity Institute

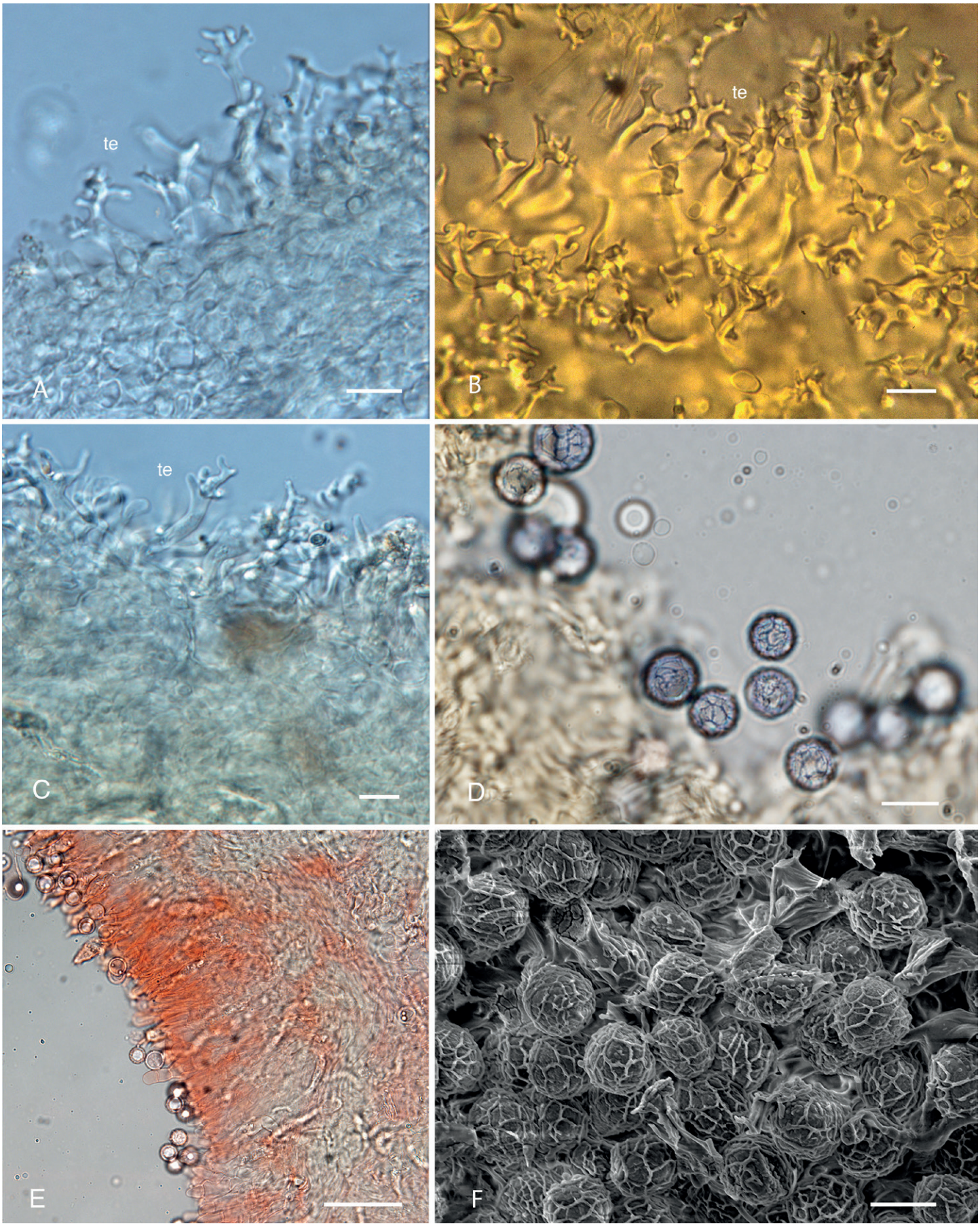

Fig. 4. *Lactifluus dendriticus.* **A.** Cross-section of pileipellis with dendritic terminal elements. **B.** Scalp section showing dendritic terminal elements. **C.** Dendritic terminal elements. **D.** Basidiospores. **E.** Hymenial trama with pseudocystidia. **F.** Scanning Electron Microscopy photo micrograph of basidiospores. Scale bars: A–D, F = 10 µm, E = 50 µm.

© 2021 Westerdijk Fungal Biodiversity Institute

Road, Claridge site 124, 28 May 1996, *A. Jumpponen & J. Trappe* 18478 (holotype MEL 2063482, isotype OSC 80519).

Basidiomes hypogeal, sequestrate, 5–25 × 5–20 mm, globose to subglobose, slightly irregular or furrowed near point of attachment; locules exposed at point of attachment in some basidiomata as pileus is incomplete, surface dry, smooth to minutely fibrillose or verrucose, white with a faint yellowish tinge and often with small darker yellow-brown patches, pileipellis thin, off-white in cross-section. *Hymenophore* loculate, locules large 0.5–2 mm diam, somewhat irregular, white when young, becoming pale yellow to pale brown-yellow with maturity, pale tan when dried. *Stipe-columella* absent. *Latex* scant to abundant, white, unchanging. *Taste* mild. *Odour* mildly sweet, pleasant. *Basidiospores* 9.0–10.8 × 8.5–10.6 µm ($\bar{x}$ =9.8 ± 0.53 × 9.69 ± 0.64, n = 50), globose [Q=1.0–1.05 ($\bar{x}$ = 1.01 ± 0.02, *n* = 50)], walls weakly amyloid, ornamentation a fine, complete to almost complete regular mesh reticulum ± 0.5–0.7 µm high, with few scattered, isolated warts also present; hilar appendix small, central, plage absent. *Basidia* 33–65 × 7–13 µm, elongated clavate to cylindrical or rarely narrowly ventricose, hyaline, thin-walled, with 2 or 4 robust, slightly curved sterigmata 4–10 × 2–3.5 µm. *Hymenophoral trama* 14–22 µm wide, a narrow central strand of crowded, hyaline hyphae 2–4 µm diam, with slightly thickened walls intermixed with scattered sinuous laticiferous hyphae 3–7.5 µm diam, sphaerocytes absent; subhymenium 15–35 µm wide, with two or three tiers of ± isodiametric cells 8–15 µm diam. *Pseudocystidia* absent or when present, 5–11 µm diam, thin-walled, cylindrical to narrowly clavate, scattered, with oily refractive contents; arising in trama from laticiferous hyphae extending up through the subhymenium. *Pileipellis* 18–45 µm wide, composed of a very narrow cutis with an almost complete turf of thick-walled (throughout length) dendritic terminal elements and scattered rare laticiferous hyphae when young, this turf becoming patchy as basidiomata expands; no gelatinous matter or very little in some basidiomes apparent amongst terminal elements dendritic terminal elements less branched and intricate when young, variously and often elaborately branched when older, coralloid to irregularly repeatedly branched with coralloid tips, 18–32 µm high, 4–25 µm wide, 3–6 µm at base, walls thick. *Pileus trama* 32–60 µm wide, of tightly interwoven, subgelatinous, hyaline hyphae 2–4 µm diam, more crowded towards the surface than within, with scattered to common, sinuous laticiferous hyphae 3–8 µm diam, refractive in KOH; sphaerocytes absent.

Ecology and Distribution: Sporulating in April–July in small to large groups, at mid to higher elevations in the mountains of south eastern Australia in Victoria, Tasmania, and New South Wales. Hypogeal in mixed forests of *Eucalyptus fastigata, E. cypellocarpa, E. radiata, E. dalrympleana, E. globoidea, E. obliqua, E. pauciflora, E. stellulata, E. regnans, Acacia dealbata, A. melanoxylon, A. aculeatissima, A. cognata,* or *A. mearnsii*.

Additional specimens examined: **Australia**, Victoria, Kinglake National Park, 120 m down Mountain Creek Track, 8 Jul. 1993, *M.A. Castellano* OSC 80520 (MEL 2063479); East Gippsland, Errinundra National Park, The Gap Scenic Reserve, Gunmark Road, 1.3 km SE of Survey Road, Claridge Site 124, 30 May 2003, *A.W. Claridge, W. Colgan III, A. Jumpponen, I. Kratzer* AWC5079 (CANB 748631); *ibid*., Gap Road, 50 m E of Bonang River Bridge, Claridge Site 117, 9 May 2003, *A.W. Claridge* AWC4731 (CANB 65451); *ibid*. Claridge Site 117, 27 May 1999, *J.M. Trappe* AWC2589 (MEL 2105044); *ibid*., 27 May 1999, *J.M. Trappe* AWC2588 (MEL 2105043); *ibid*., Gap Road, 3.9 km E of Bonang Highway, Claridge site 118, 28 May 1996, *J.M. Trappe* 18434 (MEL 2063477); *ibid*., Gap Road, 2.1 km west of track to Result Creek Falls, Claridge Site 138, 11 Jun. 1996, *J.M. Trappe* 19022 (MEL 2063472); *ibid*., Gap Road, 5.2 km E of Junction with Bonang Highway, Claridge Site 119, 9 May 2003, *J.M. Trappe & A.W. Claridge* AWC4741 (DAR 76661, CANB 748620, MEL 2292167) (also in K, NY, BPI, FH); *ibid*., Claridge Site 119, 26 May 2001, *T. Lebel* AWC3994 (CANB 736252); *ibid*., Gap Road, 2.1 km west of track to Result Creek Falls, Claridge Site 138, 11 Jun. 1996, *A.M. Jumpponen* JMT19021 (MEL 2063473); Rich Forest Management Block, Jack Road, 0.7 km N of Winter Road, Claridge Retrospective Study Site R19, 27 Apr. 1996, *A.W. Claridge* AWC352 (CANB 669623); Lind National Park, Euchre Valley Road, 0.2 km W of Junction with Lind Park Road, Claridge Site 74, 29 May 1999, *A.W. Claridge* AWC2746B (MEL 210507); Murrungowar Forest Management Block, Princes Highway, 0.4 km E of Junction with Bendoc Ridge Road, Claridge Site 64, 26 May 1999, *T. Lebel* AWC2556 (MEL 2105041); 2.4 km N of Baw Baw National Park,16 Jun. 1994, *J.M. Trappe* H6792 (PERTH 7593031); 20 km west of Mansfield near Mt Buller, 9 Jul. 1993, *T. Lebel* JMT14063 (MEL 2063478); Alpine National Park, Black Mountain Road, Rams Horn Track. Claridge Site No. 78, 11 Nov. 2008, *A.W. Claridge* JMT18089 (MEL 2326248); Noojee State Park, *ca*. 1 km from Tooronga Road, along Link Road in small carpark area, 25 Feb. 2002, *S.H. Lewis* 791 (MEL 2061947); North east of Marysville on Lady Talbot Drive, wishing Well Track, 19 Apr. 1999, *T. Lebel* TL5 (MEL 2063377); New South Wales, Bombala, Bondi Gulf Nature Reserve, Bondi Gulf Road, 4 km E of Cann Valley Highway, Claridge Site 53, 15 Jun. 1999, *J.M. Trappe* AWC2972 (CANB 748185); Tasmania, Break O'Day, Elephant Pass, 16 kms southeast of St Marys, 2 May 1990, *N. Malajczuk* MEL 2063481; Elephant Pass, 2 May 1990, *J.M. Trappe* H1373 (PERTH 7673167).

Notes: A revised description of *Lactifluus dendriticus* is provided here to enable better comparisons to other taxa, and to incorporate more data from fresh collections. Detailed illustrations of spores, pileipellis and hymenophore structure and constituent elements were provided as part of the original description (Lebel 2002). *Lactifluus dendriticus* is widespread in eucalypt forests occurring in regions with relatively higher rainfall. Its basidiomata do not always produce a latex when cut or bruised. Microscopically, *Lactifluus dendriticus* is unique, with distinct highly branched pileal terminal elements (Fig. 4A–C) that have not been observed in any other species of sequestrate or currently known agaricoid *Russulales* taxa.

Taxa in the larger clade, *Lactifluus wirrabara*, *Lf. limbatus*, *Lf. coniculus*, *Lf. sinensis*, and *Lf. midnapurensis* all have brownish agaricoid basidiocarps (Fig. 3A), and spores with a low almost complete to complete reticulum; however these species have smaller, subglobose to broadly ellipsoid spores, and very different pileicystidia or pileal terminal elements.

Section *Lactifluus*

Lactifluus geoprofluens T. Lebel, Castellano, Claridge & Trappe, *sp. nov.* MycoBank MB 838126. Figs 3D, 5A–F.

Etymology: The species epithet, "*profluens*", from Latin, meaning "freely flowing" referring to the abundantly flowing latex in cut basidiomes of this species, and "geo" in reference to the hypogeal basidiomes.

Diagnosis: Differs from other currently known lactarioid sequestrate taxa by the faint fishy odour, abundant white latex, globose to occasionally barely subglobose basidiospores, up to

© 2021 Westerdijk Fungal Biodiversity Institute

10.5 × 10.0 µm, ornamented with a robust amyloid reticulum, and presence of dendritic pileal terminal elements

Typus: **Australia**, Victoria, East Gippsland, Rich Forest Management Block, near Jack Road 0.7 km N of junction with Winter Road, Claridge site R19, 29 Feb. 1996, *A.W. Claridge* AWC201 (holotype MEL 2145804).

Basidiomes hypogeal, sequestrate, 5–15 mm broad, globose to subglobose or irregular, surface dry, smooth to rugulose and irregularly folded radially particularly around the point of attachment to substrate, minutely pruinose and velutinous, pale orange-ochre to almost reddish-brown in folds; pileus in cross-section thin (≤ 0.5 mm), pale orange becoming orange-brown in dried specimens. *Hymenophore* loculate, locules

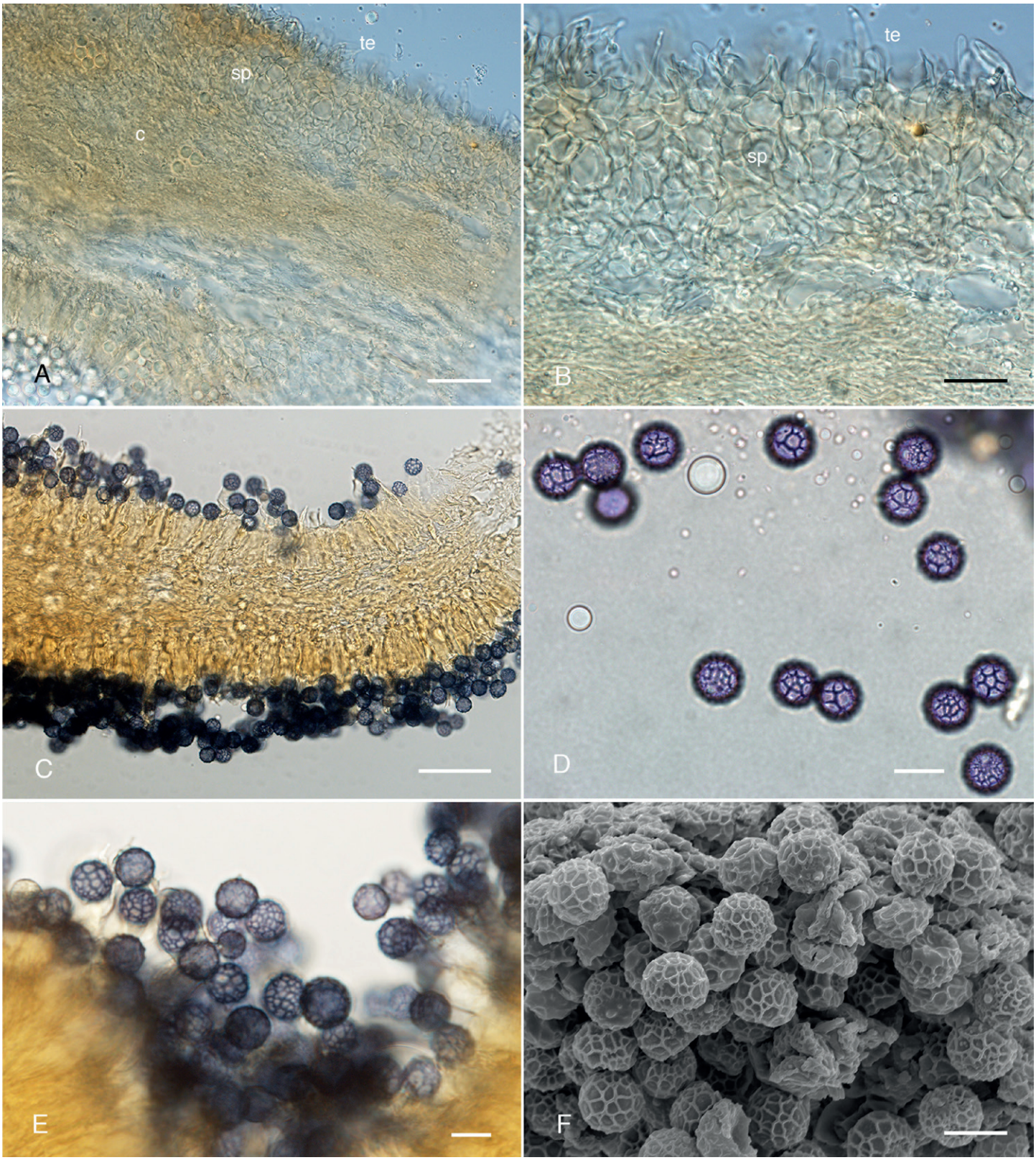

Fig. 5. *Lactifluus geoprofluens* **A.** Lampropallisade pileipellis terminal elements (te), subpellis (sp) and context (c). **B.** Pileipellis terminal elements (te) and subpellis (sp). **C.** Hymenial trama. **D–E.** Basidiospores. **F.** Scanning Electron Microscopy photo micrograph of basidiospores. Scale bars: A, C = 50 µm; B = 20 µm; D–F =10 µm.

© 2021 Westerdijk Fungal Biodiversity Institute

0.5–2 mm, labyrinthine and vaguely radial from columella attachment, pale orange-ochre to reddish orange-brown. *Stipe-columella* present or absent, much reduced if present and variable, 0.5–3 mm long × 0.5–2 mm wide, irregularly cylindrical, slightly tapering towards the base, orange-ochre to reddish-brown in patches, minutely pruinose and finely rugulose; context golden to reddish-brown. *Latex* white, unchanging, abundant along the pileipellis edges and the interior of the hymenophore. *Taste* mild. *Odour* not obvious or slightly fishy when fresh. *Basidiospores* 8.0–10.5 × 8.0–10.0 µm ($\bar{x}$ = 9.85 ± 0.43 × 9.79 ± 0.35, *n* = 40), globose to occasionally barely subglobose [Q = 1.00–1.05 ($\bar{x}$ = 1.02 ± 0.02, *n* = 40)], walls amyloid between ridges and plage distally to completely amyloid, ornamentation reticulate with ridge apices to 1 µm tall. *Basidia* 31–52 × 8–14 µm ($\bar{x}$ = 44.18 ± 5.33 × 11.25 ± 1.08, *n* = 19), 3–6 µm wide at base ($\bar{x}$ = 3.87 ± 0.54, *n* = 16), clavate, mostly 4-spored but occasionally 3-spored; sterigmata 3–10 × 1–2.5 µm, ($\bar{x}$ = 7.18 ± 2.20 × 2.00 ± 0.51, *n* = 12); basidioles 30–51 × 6–11 µm ($\bar{x}$ = 39.89 ± 4.46 × 9.14 ± 1.41, *n* = 14), 2–5 µm wide at base ($\bar{x}$ = 3.36 ± 0.74, *n* = 14), cylindrical to barely clavate. *Hymenophoral trama* comprised of interwoven and parallel tightly packed hyphae 2–3 µm diam, interspersed with sinuous laticiferous hyphae 5–7 µm diam ($\bar{x}$ = 5.64 ± 0.31, *n* = 8) and occasional sphaerocytes 30–45 × 17–38 µm; *subhymenium* composed of chains of 3–4 inflated cells 8–21 × 6–17 µm ($\bar{x}$ = 11.30 ± 6.70 × 10.40 ± 5.72, *n* = 18), laticiferous hyphae present and occasionally extending into pseudocystidia 3–8 µm diam., thin-walled, cylindrical to slightly tortuous, with oily refractive contents. *Hymenial cystidia* scarce, when present not well differentiated, 31–52 × 7–11 µm ($\bar{x}$ = 46.34 ± 4.78 × 9.56 ± 1.16, *n* = 12), subcylindrical tapering to apex, apex mucronate or obtuse, rarely emergent above hymenium, hyaline, thin-walled, contents scattered when present. *Pileipellis* a lampropalisade; subpellis composed of 3–6 layers of thin-walled polygonal cells 8–19 × 7–17 ($\bar{x}$ = 15.02 ± 3.28 × 13.20 ± 2.06, *n* = 12) µm; lamprocystidia 18–27 × 2–5 µm ($\bar{x}$ = 24.32 ± 4.12 × 3.73 ± 1.02, *n* = 15), elongate cylindrical and slightly sinuate, tapering toward apex, apex mucronate or capitate or obtuse, thick-walled, basal width 2–5 µm ($\bar{x}$ = 3.73 ± 1.02, *n* = 15), and apical width 1–3 µm ($\bar{x}$ = 1.59 ± 0.35, *n* = 15); *pileus trama* similar to hymenophoral trama, heteromerous, hyphae tightly compressed and interwoven, sphaerocytes not abundant.

Ecology and distribution: Sporulating in February–June in cool temperate forests in NE Victoria. Hypogeal in mixed forests of *Eucalyptus maculata, E. muellerana, E. paniculata, E. obliqua*, *E. cypellocarpa, E. delegatensis*, *Angophora floribunda, E. longifolia, E. muellerana, E. sieberi*, *E. baxteri, E. botryoides*, with an *Acacia cognata, A. verticillata, A. melanoxylon, A. mucronata, A. longifolia, A. mearnsii*, *A. implexa* understorey.

Additional specimens examined: **Australia**, Victoria, East Gippsland, Mimosa Rocks National Park, Tanja-Tathra Road, 0.5 km N of junction with track Leading to 'Gillards', Claridge Site 40, 7 Jun. 2003, *J.M. Trappe, A.W. Claridge, A. Jumpponen* AWC5539 (OSC 148637); *ibid*., Murrangowar Forest Management Block, Bendoc Ridge Road, 0.4 km from Princes Hwy, Claridge Site 66, 2 Jun. 2003, *M. Vavrek* AWC5306 (OSC 148635); *ibid*., Cape Conran-Sydenham Inlet Coastal Park, Swampy Creek trail, Crossing of Swampy Creek, Claridge site 128, 31 May 2003, *A. Jumpponen* AWC5204 (OSC 148634); *ibid*., East Gippsland, Rich Forest Management Block, junction of Mills Road and Jack Rich Divide Track, Claridge Retrospective study site R8, 18 Jul. 1996, *B. Gunn* JMT19613 and AWC452 (OSC 159173); *ibid*., Nunniong Forest Management Block, off Nunniong Road, Claridge site 106 (relocated 1999), 18 May 2001, *T. Lebel* AWC3614 (OSC 148633); Ben Boyd National Park, Bittangabee Picnic Area, Bittangabee Creek, Crossing of Walking Track leading N from Picnic Area, Claridge Site 52, 4 Jun. 2003, *A. Jumpponen* AWC5415 (OSC 148636); Lind National Park, Euchre Valley Road, 0.2 km W of Junction with Lind Park Road, Claridge site 13 (1999 relocation), 29 May 2001, *W. Colgan III* AWC4223 (OSC 148632).

Notes: This hypogeous, sequestrate fungus is known from cool-temperate mixed species *Eucalyptus* forest in East Gippsland, Victoria. It differs from the other two sequestrate taxa in often having a distinct columella, radial-locular hymenophore and abundant white latex in all tissues. *Lactifluus geoprofluens* shares with other species in *Lactifluus* section *Lactifluus* the fishy odour, velutinous orange-brown pileus and a lampropalisade pileipellis structure. The basidiospores in *Lf. geoprofluens* are large (up to 10.5 × 10 µm) and globose (Q = 1–1.05), unique among the Australian section *Lactifluus* species.

Section *Pseudogymnocarpi*

***Lactifluus sp. prov.* KV181** Fig. 3F.

Basidiomes sequestrate, up to 19 mm broad, globose to subglobose, surface dry, smooth to minutely pruinose and velutinous, pale creamy yellow-tan with some minor slightly darker bruising; pileipellis in section thin (≤ 0.5 mm), pale tan. *Hymenophore* loculate, empty locules 0.5–2 mm, labyrinthine, orange-ochre. *Stipe* absent; *columella* present, percurrent central strand, 0.5–2 mm wide, white to pale cream. *Latex* white turning slightly yellowish, abundant, particularly along the pileipellis edges and the interior of the hymenophore near columella. *Taste* mild. *Odour* faint, fungal.

Distribution and habitat: Sporulating in June in cool temperate open woodland in the eastern tablelands of New South Wales. Hypogeal in mixed *Eucalyptus* forest.

Sequence data: **Australia**, New South Wales, Gibraltar Range National Park, Mulligans Dr., 16 Jun. 2006, *K. Vernes, T. Lebel & A. O'Malley* KV181.

Notes: We provide the image of the basidiome and general notes in the hope that further material will be found. Our analyses show that this taxon is in a strongly supported section *Pseudogymnocarpi*, however support values within the clade are low (Fig. 2). The majority of agaricoid species currently known within this clade (*e.g. Lf. rugatus, Lf. pseudoluteopus, Lf. hygrophoroides*) have pale orange to orange-red pilei and stipe, pale coloured lamellae, abundant white latex (Fig. 3E), and an association with *Fagaceae* or *Pinaceae*. The lack of microscopic detail, and additional data for Australasian agaricoid taxa or environmental sequences, precludes any statements regarding how well this sequestrate taxon fits in this clade generally.

DISCUSSION

Both agaricoid and pleurotoid basidiome forms have been found in *Lactifluus.* In this predominantly agaricoid genus, the

© 2021 Westerdijk Fungal Biodiversity Institute

pleurotoid habit has at least seven different origins in three subgenera: subg. *Lactifluus* section *Gerardii*, subg. *Lactariopsis* and subg. *Gymnocarpi* (De Crop *et al.* 2017). No pleurotoid forms are thus far known in *Lactarius*, but they have been found in *Russula* (Buyck & Horak 1999, Henkel *et al.* 2000). Before the present study, sequestrate forms were not known from *Lactifluus,* but have evolved many times over in *Lactarius*; the evolution of a sequestrate basidiome form thus appears to be a rare event in *Lactifluus*.

All three sequestrate *Lactifluus* species have a phylogenetic affinity with Southeast Asian taxa. Some, like *Lf. geoprofluens* and *Lf. dendriticus*, probably evolved in Australia from local ancestors (that have a SE Asian descent - or other way around; cannot be determined at this point). However, the isolated position of *Lf. sp. prov.* KV181 is intriguing, as apart from Asian relatives, a European and a North American species are also closely related. This could be due to under sampling of the Australian and Malesian taxa in particular. However, placement within section *Pseudogymnocarpi* is well supported (BS 98 %).

While the number of species in *Lactarius* with sequestrate basidiome forms is much greater (in the order of 25–30 undescribed and nine named species known for Australasia; and a further 22 spp. worldwide) than in *Lactifluus*, all sequestrate taxa also appear to have evolved as independent and isolated incidents within the genus (Trappe *et al*. 2002, Desjardin 2003, Verbeken *et al.* 2014a, Sheedy *et al*. 2016). None of the sequestrate taxa have evolved into a clade containing a large diversity of species with similar basidiome forms, all indicative of relatively recent origin of this basidiome form in *Lactarius* (Verbeken *et al.* 2014a) and *Lactifluus.* The recent description of several sequestrate *Lactarius* from tropical forests (Verbeken *et al.* 2014a, b, Buyck *et al.* 2017), and discovery of hidden diversity of Australasian *Lactifluus* species lend support to the theory that sequestrate basidiome forms are essentially an excellent way to maintain a fairly constant relative humidity in the enclosed hymenophore, allowing full development of spores to ensue, regardless of arid, seasonally dry or tropical, seasonally waterlogged conditions (Beever & Lebel 2014).

Unsurprisingly, given the trouble with morphological differentiation of *Lactifluus* and *Lactarius* agaricoid species, it is also difficult to distinguish taxa with sequestrate basidiomes. As a broad generalisation, in Australia, the majority of sequestrate *Lactarius* have yellow to orange to red tinged basidiomes, whereas two of the three *Lactifluus* taxa described in this study have white to pale cream basidiomes. Pale basidiome colouring is more common in Australasian sequestrate russuloid taxa (Beaton *et al.* 1984, Lebel & Trappe 2000, Lebel & Castellano 2002, Lebel 2002a, b, 2003a, b, Lebel & Tonkin 2007). General trends in microscopic differentiation between *Lactarius* and *Lactifluus* were formulated by Verbeken & Nuytinck (2013) and can be summarised as: (i) thick-walled elements in the pileipellis and stipitipellis, as well as lamprocystidia, are generally present in *Lactifluus* and very rarely observed in *Lactarius*, and (ii) a hymenophoral trama composed of sphaerocytes (as in *Russula*) is common in *Lactifluus* but is rarely observed in *Lactarius*. Both trends don't seem to hold up for the sequestrate *Lactifluus* species. The loss of thick-walled elements in pileus and hymenium in sequestrate forms could be due to increased folding and loculisation of the hymenophoral trama in combination with loss of ballistospory (*i.e.* no longer require spacing to allow for spore drop). As the basidiomes are submersed in the soil, dispersal of spores by vectors such as marsupial mammals or insects, is highly likely; by having thin walls the ripe basidiomes would be easier to break open or eat. The highly branched, angular pileal dendritic terminal elements of *Lf. dendriticus* are unique. The presence of distinctively shaped pileicystidia or terminal elements is more typical of species of *Russula* but rarely seen in milkcaps (Verbeken 1996a, Verbeken & Walleyn 2010). Initially thought to be a contaminant, perhaps a mycenoid mycoparasite or virus, but these terminal elements are found consistently in multiple basidiomes from geographically distant collections, and no DNA sequences for mycenoid taxa were ever recovered as contaminants.

In *Lactifluus* section *Gerardii* the majority of species have a brown stipe and pileus contrasting with white mostly distant lamellae, reticulate spore ornamentation < 2 µm high, a palisade pileipellis structure, and are generally lacking in macrocystidia (Stubbe *et al.* 2010, De Crop *et al.* 2017, 2018). The basidiomes can also be small, white and pleurotoid, with thick-walled terminal elements in the pileipellis (Stubbe *et al.* 2012, Latha *et al.* 2016, De Crop *et al.* 2018). Several of the agaricoid and pleurotoid taxa have latex that changes colour on exposure, however this is not the case for *Lf. dendriticus.* While the pale sequestrate basidiomes of *Lf. dendriticus* can be easily mistaken for sequestrate russuloid taxa as latex production is variable, the more open form of locules in the hymenophoral tissue tend to suggest a lactarioid taxon. However, it is the unique dendritic pileal terminal elements of *Lf. dendriticus* that are intriguing. How does a cystidium evolve from a simple filamentous, perhaps irregularly capitate form, to a highly branched, sharp angled form?

Lactifluus geoprofluens is readily distinguished from Australian and international species in *Lf.* section *Lactifluus* by lacking lamprocystidia, having large globose basidiospores and a sequestrate basidiome form. It is the first known sequestrate member of *Lf.* section *Lactifluus* (De Crop *et al.* 2017). Unfortunately, we do not have an image of the fresh basidiomes of *Lf. geoprofluens*, however the field notes all state pale orange-ochre to reddish brown in colour, with slightly paler hymenophoral tissue.

We currently lack data to describe *Lf. sp. prov*. KV181 as a new species, but we do provide a picture and a description of field characteristics. It is the first time a non-agaricoid representative of *Lf.* subg. *Pseudogymnocarpi* is documented, and the first Australasian representative in section *Pseudogymnocarpi*. We look forward to obtaining new material for further examination.

ACKNOWLEDGEMENTS

We gratefully acknowledge the curation staff at MEL, BRI, and OSC who facilitated access to material for study. The molecular work conducted by James Douch, Luke Vaughan, and Lachlan Tegart was supported by the Jim Willis Studentship program hosted by the Royal Botanic Gardens Victoria, and by some external funding through the 'Fungal Barcode Project' Bioplatforms and the Australian Genome Research Facility. Travel by Jorinde Nuyinck to MEL was supported by Australian Biological Resources grant (RFL217-63). J.A. Cooper is supported by the Strategic Investment Fund of the New Zealand Ministry for Business, Innovation and Employment (MBIE). We also thank J.M. Trappe and A.W. Claridge for providing additional material of *Lf. geoprofluens*.

Conflict of interest: The authors declare that there is no conflict of interest.

© 2021 Westerdijk Fungal Biodiversity Institute

REFERENCES

Beaton G, Pegler DN, Young TWK (1984). Gasteroid basidiomycota of Victoria state, Australia. 2. *Russulales*. *Kew Bulletin* **39**: 669–698.

Beenken L, Sainge MN, Kocyan A (2016). *Lactarius megalopterus*, a new angiocarpous species from a tropical rainforest in Central Africa, shows adaptations to endozoochorous spore dispersal. *Mycological Progress* **15**: 58.

Beever RE, Lebel T (2014). Truffles of New Zealand: a discussion of bird dispersal characteristics of fruit bodies. *Auckland Botanical Society* **69**: 170–178.

Bougher NL, Lebel T (2001). Sequestrate (truffle-like) fungi of Australia and New Zealand. *Australian Systematic Botany* **14**: 439–484.

Buyck B, Horak E (1999). New taxa of pleurotoid *Russulaceae*. *Mycologia* **91**: 532–537

Buyck B, Duhem B, Das K, *et al*. (2017). Fungal Biodiversity Profiles 21–30. *Cryptogamie, Mycologie* **38**: 101–146.

De Crop E, Hampe F, Wisitrassameewong K, *et al*. (2018). Novel diversity in *Lactifluus* section *Gerardii* from Asia: five new species with pleurotoid or small agaricoid basidiocarps. *Mycologia* **110**: 962–984.

De Crop E, Nuytinck J, Van de Putte K, *et al*. (2017). A multi-gene phylogeny of *Lactifluus* (*Basidiomycota*, *Russulales*) translated into a new infrageneric classification of the genus. *Persoonia* **38**: 58–80.

Desjardin DE (2003). A unique ballistosporic hypogeous sequestrate *Lactarius* from California. *Mycologia* **95**: 148–155.

Dring DM, Pegler DN (1978). New and noteworthy gasteroid relatives of the *Agaricales* from tropical Africa. *Kew Bulletin* **32**: 563–569.

Eberhardt U, Verbeken A (2004). Sequestrate *Lactarius* species from tropical Africa: *L. angiocarpus nov. sp*. and *L. dolichocaulis comb. nov*. *Mycological Research* **108**: 1042–1052.

Hall T (2011). *Bioedit v7.1.3.* http://www.mbio.ncsu.edu/bioedit/bioedit.html.

Heenan PB, Smissen RD (2013). Revised circumscription of *Nothofagus* and recognition of the segregate genera *Fuscospora*, *Lophozonia*, and *Trisyngyne* (*Nothofagaceae*). *Phytotaxa* **146**: 1–31.

Henkel TW, Aime MC, Miller SL (2000). Systematics of pleurotoid *Russulaceae* from Guyana and Japan, with notes on their ectomycorrhizal status. *Mycologia* **92**: 1119–1132

Katoh K, Rozewicki J, Yamada KD (2019). MAFFT online service: multiple sequence alignment, interactive sequence choice and visualization. *Briefings in Bioinformatics* **20**: 1160–1166.

Kõljalg U, Nilsson RH, Abarenkov K, *et al*. (2013). Towards a unified paradigm for sequence-based identification of fungi. *Molecular Ecology* **22**: 5271–5277.

Latha KPD, Raj KNA, Farook VA, *et al*. (2016). Three new species of *Russulaceae* from India based on morphology and molecular phylogeny. *Phytotaxa* **246**: 61–77.

Lebel T (2002a). The sequestrate *Russulales* of New Zealand. *New Zealand Journal of Botany* **40**: 489–509.

Lebel T (2002b). *Zelleromyces dendriticus* a new species from Australia. *Australasian Mycologist* **20**: 4–8.

Lebel T (2003a). Australasian Truffle-like Fungi XV. *Cystangium*. *Australian Systematic Botany* **16**: 371–400.

Lebel T (2003b). Australasian Truffle-like Fungi XVI. *Gymnomyces. Australian Systematic Botany* **16**: 401–426.

Lebel T, Castellano MA (2002). Type studies of sequestrate *Russulales*. Part II. Species related to *Russula* from Australia and New Zealand. *Mycologia.* **94**: 327–354.

Lebel T, Castellano MA, Beever RE (2015). Cryptic diversity in the sequestrate genus *Stephanospora* (*Stephanosporaceae: Agaricales*) in Australasia. *Fungal Biology* **119**: 201–228.

Lebel T, Syme A (2012.) Sequestrate species of *Agaricus* and *Macrolepiota* from Australia: new species and combinations and their position in a calibrated phylogeny. *Mycologia* **104**: 496–520.

Lebel T, Tonkin JE (2007). Australasian species of *Macowanites* are sequestrate species of *Russula* (*Russulaceae, Basidiomycota*). *Australian Systematic Botany* **20**: 355–381.

Lebel T, Trappe JM (2000). Type studies of sequestrate *Russulales*. Part I. Generic type species. *Mycologia* **92**: 1188–1205.

Miller MA, Pfeiffer W, Schwartz T (2010). Creating the CIPRES Science Gateway for inference of large phylogenetic trees. In: *Proceedings of the Gateway Computing Environments Workshop (GCE)*, 14 Nov. 2010, New Orleans, LA: 1–8.

Nuytinck J, Verbeken A, Delarue S, Walleyn R (2003). Systematics of European sequestrate lactarioid *Russulaceae* with spiny spore ornamentation. *Belgian Journal of Botany* **136**: 145–153.

Phookamsak R, Hyde KD, Jeewon R, *et al.* (2019). Fungal diversity notes 929–1035: taxonomic and phylogenetic contributions on genera and species of fungi. *Fungal Diversity* **95**: 1–273.

Rambaut A (2009). *FigTree.* http://tree.bio.ed.ac.uk/software/figtree/.

Sang X-Y, Li X-D, Wang Y-W, *et al.* (2016). Four new sequestrate species of *Russulaceae* found in China. *Phytotaxa* **289**: 101–117.

Sheedy EM, Martin AF, Ryberg M, *et al*. (2016). Dating the emergence of truffle-like fungi in Australia, by using an augmented meta-analysis. *Australian Systematic Botany* **29**: 284–302.

Song Y, Zhang JB, Li JW, *et al*. (2017). *Lactifluus sinensis sp. nov.* and *L. sinensis var. reticulatus var. nov*. (*Russulaceae*) from southern China. *Nova Hedwigia*. **107**: 91–103.

Stamatakis A (2014). RAxML Version 8: A tool for Phylogenetic Analysis and Post-Analysis of Large Phylogenies. *Bioinformatics* **30**: 1312–1313.

Stubbe D, Le HT, Wang XH, *et al.* (2012). The Australasian species of *Lactarius* subgenus *Gerardii* (*Russulales*). *Fungal Diversity* **52**: 141–167.

Stubbe D, Nuytinck J, Verbeken A (2010). Critical assessment of the *Lactarius gerardii* species complex (*Russulales*). *Fungal Biology* **114**: 271–283.

Thiers B (2011) (continuously updated). Index Herbariorum: a global directory of public herbaria and associated staff. New York Botanical Garden's Virtual Herbarium. http://sweetgum.nybg.org/ih/.

Trappe JM, Claridge AW (2003). Australasian sequestrate (truffle-like) fungi 15. New species from tree line in the Australian Alps. *Australasian Mycologist* **22**: 27–38.

Trappe JM, Claridge AW (2008). *Arcangeliella claridgei comb. nov*. and *A. corkii comb. nov.* transferred from the genus *Zelleromyces*. *Australasian Mycologist* **27**: 117.

Trappe JM, Lebel T, Castellano MA (2002). Nomenclatural revisions in the sequestrate russuloid genera. *Mycotaxon* **81**: 195–214.

Verbeken A (1996). *Biodiversity of the genus Lactarius Pers. in tropical Africa*. Part 1, text. Part 2, plates and maps. Ph.D. dissertation. Biology Department, Ghent University, Belgium.

Verbeken A, Hampe F, Wissitrassameewong K, *et al*. (2014b). A new angiocarpous *Lactarius* species from Thailand. *Phytotaxa* **181**: 163–170.

Verbeken A, Nuytinck J (2013). Not every milkcap is a *Lactarius*. *Scripta Botanica Belgica* **51**: 162–168.

Verbeken A, Stubbe D, Van de Putte K, *et al.* (2014a). Tales of the unexpected: angiocarpous representatives of the *Russulaceae* in tropical South East Asia. *Persoonia* **32**: 13–24.

Verbeken A, Walleyn R (2010). *Fungus Flora of Tropical Africa, volume 2. Monograph of Lactarius in Tropical Africa*. Nationale Plantentuin België, Meise.

Vidal JM, Alvarado P, Loizides M, *et al*. (2019). A phylogenetic and taxonomic revision of sequestrate *Russulaceae* in Mediterranean and temperate Europe. *Persoonia* **42**: 127–185.

© 2021 Westerdijk Fungal Biodiversity Institute

Wang XH, Stubbe D, Verbeken A (2012). *Lactifluus parvigerardii sp. nov*., a new link towards the pleurotoid habit in *Lactifluus* subgen. *Gerardii* (*Russulaceae, Russulales*). *Cryptogamie, Mycologie* **33**: 181–190.

© 2021 Westerdijk Fungal Biodiversity Institute

© 2021 Westerdijk Fungal Biodiversity Institute

FUSE

Fungal Systematics and Evolution

VOLUME 8
DECEMBER 2021
PAGES 27–37

doi.org/10.3114/fuse.2021.08.03

New species in *Aciculosporium*, *Shimizuomyces* and a new genus *Morakotia* associated with plants in *Clavicipitaceae* from Thailand

S. Mongkolsamrit[1], W. Noisripoom[1], D. Thanakitpipattana[1], A. Khonsanit[1], S. Lamlertthon[2], J.J. Luangsa-ard[1]*

[1]Plant Microbe Interaction Research Team, National Center for Genetic Engineering and Biotechnology (BIOTEC), 113 Thailand Science Park, Phahonyothin Road, Khlong Nueng, Khlong Luang, Pathum Thani, 12120, Thailand
[2]Center of Excellence in Fungal Research, Faculty of Medical Science, Naresuan University, Phitsanulok, 65000, Thailand

*Corresponding author: jajen@biotec.or.th

Key words:
new taxa
phylogeny
taxonomy

Abstract: Three new fungal species in the *Clavicipitaceae* (*Hypocreales*, *Ascomycota*) associated with plants were collected in Thailand. Morphological characterisation and phylogenetic analyses based on multi-locus sequences of LSU, *RPB1* and *TEF1* showed that two species belong to *Aciculosporium* and *Shimizuomyces. Morakotia* occupies a unique clade and is proposed as a novel genus in *Clavicipitaceae*. *Shimizuomyces cinereus* and *Morakotia fusca* share the morphological characteristic of having cylindrical to clavate stromata arising from seeds. *Aciculosporium siamense* produces perithecial plates and occurs on a leaf sheath of an unknown panicoid grass.

Citation: Mongkolsamrit S, Noisripoom W, Thanakitpipattana D, Khonsanit A, Lamlertthon S, Luangsa-ard JJ (2021). New species in *Aciculosporium, Shimizuomyces* and a new genus *Morakotia* associated with plants in *Clavicipitaceae* from Thailand. *Fungal Systematics and Evolution* **8**: 27–37. doi: 10.3114/fuse.2021.08.03
Received: 10 January 2021; **Accepted:** 14 April 2021; **Effectively published online:** 2 June 2021
Corresponding editor: P.W. Crous

INTRODUCTION

Clavicipitaceae is one of the most heterogeneous fungal families in the order *Hypocreales* (*Ascomycota*) that is associated with insects, plants, fungi and invertebrates (Gams & Zare 2003, Spatafora *et al*. 2007, Sung *et al*. 2007, Steiner *et al*. 2011, Kepler *et al*. 2012b). For instance, *Metarhizium* species are well-known entomopathogens in the *Clavicipitaceae* and are associated with both insects and plants. Furthermore, they play roles as endophytes and rhizosphere-inhabiting fungi (Greenfield *et al*. 2016, Nishi & Sato 2019, Mongkolsamrit *et al.* 2020). *Tyrannicordyceps* was proposed as a new genus associated with fungi, producing yellow or bright red stromata attacking the sclerotia of *Claviceps* (Kepler *et al*. 2012b). Clavicipitaceous fungi associated with plants have been described for species in *Aciculosporium*, *Atkinsonella*, *Balansia*, *Claviceps*, *Epichloë*, *Heteroepichloë*, *Myriogenospora*, *Periglandula*, *Shimizuomyces* and *Ustilaginoidea.* Species in *Aciculosporium*, *Atkinsonella*, *Balansia*, *Epichloë, Myriogenospora* and *Parepichloë* have been documented as fungal endophytes of grasses, and in their life cycle they can form ascomata (sexual morph) on these host plants (Cheplick & Faeth 2009, Torres & White 2009). Macro-morphology and habitats of several species associated with plants within these genera are epibiotic and produce ascomata on stems, leaves or culms, and inflorescences of plants. Most species of these genera produce pale brown to black coloured stromata such as *B. aristidae, C. purpurea*, *M. atramentosa*, *P. cinerea,* except for *Epichloë typhina* which produces white to yellow stromata (Bischoff & White 2003, Górzyńska *et al*. 2017).

The genus *Aciculosporium* was established by Miyake (1908) with *A. take* as type species. Almost a century later, a second species, *A. sasicola,* was reported from Japan (Oguchi 2001). *Aciculosporium take* and *A. sasicola* were documented as causative agents of the economically important witches' broom disease of bamboo in Japan, China, and Taiwan (Tsuda *et al*. 1997, Oguchi 2001, Tanaka *et al*. 2003). Recently, Píchová *et al*. (2018) combined *Cepsiclava phalaridis* and *Neoclaviceps monostipa* in *Aciculosporium.* To date, this genus comprises only four fungal species *viz*. *A. take, A. monostipum, A. phalaridis,* and *A. sasicola*. *Aciculosporium phalaridis* (= *Cepsiclava phalaridis*) produces stromata on sclerotia of commercial phalaris (*Phalaris aquatica*) seeds in southern New South Wales and Victoria (Walker 2004). *Neoclaviceps monostipum* was discovered in Costa Rica from unknown panicoid grasses (Sullivan *et al*. 2001).

Kobayasi (1981) established the genus *Shimizuomyces* from Japanese collections, comprising two species, namely *S. paradoxus* (type species) growing on *Smilax sieboldii* fruits and *S. kibianus* growing on *Smilax china* seeds (Kobayasi 1984). Besides Japan, *S. paradoxus* was also reported from Korea by Sung *et al.* (2010). Based on the morphological characters in the natural specimens, *Shimizuomyces* resembles *Cordyceps* in possessing brightly coloured, fleshy stromata with cylindrical stipes and enlarged apical heads (Sung *et al*. 2007).

During field surveys for arthropod-pathogenic fungi in central and western regions of Thailand, we collected two unidentified species producing brown cylindrical to clavate stromata and another species with grey stromata occurring on seeds. Based on the macro- and micro-morphological characteristics of all

Fungal Systematics and Evolution is licensed under a Creative Commons Attribution-NonCommercial-ShareAlike 4.0 International License

© 2021 Westerdijk Fungal Biodiversity Institute

collected strains, they were preliminarily identified as members of *Shimizuomyces.* Additionally, we also found one species that morphologically resembles *Aciculosporium* by producing brown ascomata on the leaf sheath of an unknown panicoid grass. The aims of this study were to clarify the placement and name these collections through molecular phylogenetic studies combined with observations of diagnostic micro-morphological characters.

MATERIALS AND METHODS

Collection and isolation

Fungal specimens occurring on seeds of dicot plants and the leaf sheath of an unknown panicoid grass were collected from Ban Phaothai community forest and Khao Yai National Park, Thailand. The specimens were collected carefully so as not to damage either host or stipe, and were placed in small plastic boxes before returning to the laboratory for isolation. The protocol for the isolation from stromata containing mature perithecia followed previous studies (Luangsa-ard *et al*. 2018, Mongkolsamrit *et al*. 2018). Ascospores were discharged on potato dextrose agar (PDA; freshly diced potato 200 g, dextrose 20 g, agar 15 g, in 1 L distilled water) and placed in a plastic box with moist tissue paper overnight to create a humid chamber with 99 % humidity at 25 °C. The following morning, plates were examined with an Olympus SZ61 dissecting microscope to observe discharged ascospores that were then transferred to fresh PDA plates. Pure cultures were deposited at the BIOTEC Culture Collection (BCC), National Center for Genetic Engineering and Biotechnology, Thailand. Specimens were dried in an electric food dryer (50–55 °C) overnight and stored in plastic boxes before storage at the BIOTEC Bangkok Fungarium (BBH), National Biobank of Thailand.

Morphological study

Fungal structures, such as perithecia, asci and ascospores were mounted in lactophenol cotton blue solution and measured using a compound microscope. Twenty to fifty perithecia, asci, ascospores, phialides and conidia were measured and the range and standard deviation calculated. Morphological characters of these structures were photographed using an Olympus DP70 Digital Camera mounted on an Olympus BX51 compound microscope and SZX12 (Olympus) dissecting microscope. Colour changes of stromata were monitored in 3 % potassium hydroxide (KOH). For detailed morphological comparisons of conidia, phialides and colony colours, cultures were grown on PDA agar plates and 2 % malt extract agar (2 % MEA Difco; malt extract, 20 g; agar, 15 g in 1 L distilled water) at 25 °C under a zeitgeber 14:10 light : dark cycle for 21 to 30 d, depending on fungal sporulation. Protocols for culture observations and comparisons followed Mongkolsamrit *et al*. (2018). Colours of fresh specimens and cultures incubated on PDA and MEA were described following the Sixth Royal Horticultural Society (R.H.S.) Colour Chart.

DNA extraction, sequencing and phylogenetic analysis

Genomic DNA was harvested from mycelia on PDA plates and small pieces of fresh stromatal tissue using a modified cetyltrimethyl-ammonium bromide (CTAB) method as described previously (Mongkolsamrit *et al*. 2009). Nuclear loci, including nuc 28 rDNA (Large Subunit Ribosomal DNA: LSU), the partial gene regions of the RNA polymerase II largest subunit (*RPB1*) and the translation elongation factor-1α gene (*TEF1*), were sequenced. The primer pairs and thermocycler conditions for PCR amplifications used in this study followed the method described in Mongkolsamrit *et al*. (2019). The purified PCR products were sequenced with PCR amplification primers for Sanger dideoxy sequencing. The PCR amplicon sequences were examined for ambiguous base calls using BioEdit v. 7.2.5 (Hall 2004). Verified sequences were submitted to GenBank. Multi-locus sequences of closely-related taxa for analyses were taken from previous studies as shown in Table 1. The final alignment was deposited in TreeBASE (www.treebase.org) under accession number ID 26949. Phylogenetic analysis was performed using RAxML-VI-HPC2 v. 8.2.12 (Stamatakis 2014) on XSEDE (http://www.phylo.org/), with 1 000 bootstrap iterations. Bayesian inference (BI) analysis was performed in MrBayes v. 3.2.7a (Ronquist *et al*. 2012) on XSEDE, with the GTR + I + G model (General Time Reversible model with a proportion of invariable sites and a gamma-shaped distribution of rates across sites). Markov chain Monte Carlo (MCMC) simulations were run for 5 000 000 generations, sampling every 1 000, and discarding the first 10 % as burn-in. RAxML output was imported into TreeView v. 1.6.6 to view the phylogenetic tree (Page 1996; http://taxonomy.zoology.gla.ac.uk/rod/treeview.html).

RESULTS

Molecular phylogeny

We generated seven LSU, five *RPB1* and six *TEF1* sequences in this study from living cultures and fresh stromata (Table 1). The combined dataset of 55 taxa with multi-locus sequences had a total alignment length of 2 286 characters. Sequences of *Simplicillium lanosoniveum* CBS 704.86 and *Simplicillium lanosoniveum* CBS 101267 in the *Cordycipitaceae* were used as outgroups. The RAxML analysis resulted in a single tree which is shown in Fig. 1. The phylogenetic tree strongly supports *Aciculosporium, Morakotia* and *Shimizuomyces* as monophyletic clades. The descriptions based on morphological characters of two new species belong to *Aciculosporium* and *Shimizuomyces*, and a new genus *Morakotia* are provided below.

Taxonomy

Aciculosporium siamense Mongkolsamrit, Noisripoom & Luangsa-ard, ***sp. nov.*** MycoBank MB 838347. Fig. 2A–S.

Etymology: The specific epithet refers to the old name of the Kingdom of Thailand*, Siam*.

Typus: **Thailand**, Saraburi Province, Chet Kot Waterfall, Khao Yai National Park**,** on leaf sheath (*Poaceae*), 8 Jan. 2017, *U. Pinruan (UP)*, *S. Mongkolsamrit (SM)* & *P. Srikitikulchai (PS)*, SM 2081 (holotype BBH 43077, ex-type culture BCC 85382).

Ascomata hemispherical perithecial plates, singly or composed of multiple perithecial plates, pale brownish orange (N167A), 2–8 mm in diam, 2–3 mm high. *Perithecia* immersed, obovate, 420–550(–600) × (160–)180–220(–230) µm, with dark brown ostioles. *Asci* cylindrical, (165–)203–347(–400) × 4–(4.5–5) µm with caps 4–5 µm thick. *Ascospores* hyaline, filiform with one end blunt and

© 2021 Westerdijk Fungal Biodiversity Institute

Table 1. List of species and GenBank accession numbers of sequences used in this study. The novelties described here are in bold font.

Species	Strain	Host/Substratum	GenBank Accession no.			References
			LSU	*RPB1*	*TEF1*	
Aciculosporium monostipum	INBio 6 141[T]	*Poaceae*	AF245293	DQ000353	AY986983	Sullivan *et al.* (2001), Chaverri *et al*. (2005b)
Aciculosporium phalaridis	CCC 293	*Poaceae*	–	–	LT216524	Píchová *et al*. (2018)
Aciculosporium siamense	**BCC 85382[T]**	***Poaceae***	**MT743002**	–	**MT762147**	This study
	BCC 85384	***Poaceae***	**MT743003**	**MT762149**	**MT762148**	This study
Aciculosporium take	MAFF 241224	Plants	–	KC113319	KP689550	Schardl *et al*. (2013)
Aschersonia samoensis	BCC 2097	*Hemiptera*	AF327381	DQ000346	AY986945	Artjariyasripong *et al*. (2001), Chaverri *et al*. (2005b)
Atkinsonella hypoxylon	B4728	Plants	–	–	KP689546	Young *et al.* (2015)
Balansia henningsiana	GAM 16112	*Poaceae*	AY545727	AY489643	AY489610	Castlebury *et al*. (2004)
Balansia pilulaeformis	A.E.G. 94-2	*Poaceae*	AF543788	DQ522365	DQ522319	Currie *et al*. (2003), Spatafora *et al*. (2007)
Claviceps purpurea	GAM 12885	*Poaceae*	AF543789	AY489648	AF543778	Currie *et al.* (2003), Castlebury *et al*. (2004)
	S.A. cp11	*Poaceae*	EF469075	EF469087	EF469058	Sung *et al*. (2007)
Conoideocrella luteorostrata	NHJ 12516	*Hemiptera*	EF468849	EF468905	EF468800	Sung *et al*. (2007)
	NHJ 11343	*Hemiptera*	EF468850	EF468906	EF468801	Sung *et al*. (2007)
Conoideocrella tenuis	NHJ 6293	*Hemiptera*	EU369044	EU369068	EU369029	Johnson *et al*. (2009)
	NHJ 6791	*Hemiptera*	EU369046	EU369069	EU369028	Johnson *et al*. (2009)
Corallocytostroma ornithocopreoides	WAC 8705	Plants	–	–	LT216546	Píchová *et al*. (2018)
Dussiella tuberiformis	J.F. White	*Hemiptera*	–	JQ257015	JQ257027	Kepler *et al*. (2012b)
Epichloë elymi	C. Schardl760	–	AY986924	DQ000352	AY986951	Chaverri *et al*. (2005b)
Epichloë typhina	ATCC 56429	*Poaceae*	U17396	AY489653	AF543777	Rehner & Samuels (1995), Currie *et al*. (2003), Castlebury *et al.* (2004)
Helicocollum surathaniense	BCC 34463	*Hemiptera*	KT222328	–	KT222336	Luangsa-ard *et al*. (2017a)
	BCC 34464[T]	*Hemiptera*	KT222329	–	KT222337	Luangsa-ard *et al*. (2017a)
Hypocrella discoidea	I93-901D	*Hemiptera*	EU392567	EU392700	EU392646	Chaverri *et al*. (2008)
Metapochonia goniodes	CBS 891.72[T]	*Nematoda*	AF339550	DQ522401	DQ522354	Sung *et al*. (2001), Spatafora *et al*. (2007)
Metarhizium anisopliae	CBS 130.71[T]	*Avena sativa*	MT078853	MT07886	MT078845	Mongkolsamrit *et al*. (2020)
Metarhizium minus	ARSEF 1099	*Hemiptera*	–	KJ398608	KJ398799	Kepler *et al*. (2014)
	ARSEF 2037[T]	*Hemiptera*	AF339531	DQ522400	DQ522353	Spatafora *et al*. (2007)
Morakotia fusca	**BCC 64125**	**Plant**	**KY794862**	–	**KY794857**	This study
	BCC 79272[T]	**Plant**	**KY794861**	**KY794865**	**KY794856**	This study
	BCC 79273	**Plant**	**KY794860**	**KY794866**	–	This study
Moelleriella phyllogena	P.C.555	*Hemiptera*	EU392610	EU392726	EU392674	Chaverri *et al*. (2008)

© 2021 Westerdijk Fungal Biodiversity Institute

Table 1. (Continued).

Species	Strain	Host/Substratum	GenBank Accession no.			References
			LSU	*RPB1*	*TEF1*	
	J.B.130	*Hemiptera*	EU392610	EU392726	EU392674	Chaverri *et al*. (2008)
Myriogenospora atramentosa	A.E.G.96-32	*Poaceae*	AY489733	AY489665	AY489628	Castlebury *et al*. (2004)
Nigelia aurantiaca	BCC 37621	*Lepidoptera*	GU979946	GU979964	GU979955	Luangsa-ard *et al*. (2017b)
	BCC 37627	*Lepidoptera*	GU979947	GU979965	GU979956	Luangsa-ard *et al*. (2017b)
Orbiocrella petchii	NHJ 6240	*Hemiptera*	EU369038	EU369060	EU369022	Johnson *et al.* (2009)
	NHJ 6209	*Hemiptera*	EU369039	EU369061	EU369023	Johnson *et al.* (2009)
Periglandula ipomoeae	IasaF 13	Plant	–	JN587270	–	Schardl *et al.* (2013)
Purpureomyces khaoyaiensis	BCC 1376[T]	*Lepidoptera*	KX983462	–	KX983457	Luangsa-ard *et al*. (2017b)
	BCC 14290	*Lepidoptera*	JF415970	JN049888	JF416012	Kepler *et al.* (2012a)
Regiocrella camerunensis	CUP 67512[T]	*Hemiptera*	DQ118735	DQ127234	DQ118743	Chaverri *et al*. (2005a)
Regiocrella sinensis	CUP CH-2640[T]	*Hemiptera*	DQ118736	DQ127235	DQ118744	Chaverri *et al*. (2005a)
Rotiferophthora angustispora	CBS 101437	*Rotifera*	AF339535	DQ522402	AF543776	Chaverri *et al*. (2005a), Currie *et al*. (2003), Spatafora *et al*. (2007)
Samuelsia chalalensis	P.C. 560	*Hemiptera*	EU392637	EU392743	EU392691	Chaverri *et al*. (2008)
Samuelsia rufobrunnea	P.C. 613	*Hemiptera*	AY986918	DQ000345	AY986944	Chaverri *et al*. (2005b)
Shimizuomyces cinereus	**BBH 41714[T]**	***Smilacaceae* (Plant)**	**KY794864**	**KY794867**	**KY794859**	This study
	BBH 41715	***Smilacaceae* (Plant)**	**KY794863**	**KY794868**	**KY794858**	This study
Shimizuomyces paradoxus	EFCC 6279	*Smilacaceae* (Plant)	EF469084	EF469100	EF469071	Sung *et al*. (2007)
	EFCC 6564	*Smilacaceae* (Plant)	EF469083	EF469101	EF469072	Sung *et al*. (2007)
Simplicillium lanosoniveum	CBS 704.86	*Hemileia vastatrix* (*Uredinales*)	AF339553	DQ522406	DQ522358	Sung *et al.* 2001, Spatafora *et al*. (2007)
	CBS 101267	*Hemileia vastatrix* (*Uredinales*)	–	DQ522405	DQ522357	Spatafora *et al*. (2007)
Tyrannicordyceps fratricida	TNS 19011	Fungi	JQ257023	JQ257016	JQ257028	Kepler *et al*. (2012b)
Ustilaginoidea virens	ATCC 16180	Plant	–	JQ257014	JQ257026	Kepler *et al*. (2012b)
	MAFF 240421	Plant	JQ257011	–	JQ257024	Kepler *et al*. (2012b)
Verticillium epiphytum	CBS 154.61[T]	*Hemileia vastatrix* (*Uredinales*)	AF339548	–	EF468802	Sung *et al*. (2001), Sung *et al*. (2007)
	CBS 384.81	*Hemileia vastatrix* (*Uredinales*)	AF339547	DQ522409	DQ522361	Sung *et al*. (2001), Spatafora *et al.* (2007)

[T] = Type species.

narrow at the other end, 3-septate, (60–)71.5–95.5(–125) × (1–)1.5–2 µm. Colour change of stromata in 3 % KOH not observed.

Culture characteristics: Colonies on PDA attaining 8–10 mm diam in 14 d, yellowish white (N158C), reverse uncoloured. Dimorphic with mass of conidia, yeast-like and vegetative hyphae smooth, wet, 3–4 µm diam. *Conidia* holoblastic, hyaline, cylindrical to filiform, narrower at one end than the other, 1–3-septate, (22–)33–57.5(–70) × 1.5–2 µm, with dichotomously branched appendages, usually appearing at the narrow end of conidia, 1–5 × 0.5 µm.

Colonies on 2 % MEA attaining 4–5 mm diam in 14 d, light yellow (163D), reverse uncoloured. Colonies dimorphic, producing a cerebriform yeast-like mass of conidia at the centre

© 2021 Westerdijk Fungal Biodiversity Institute

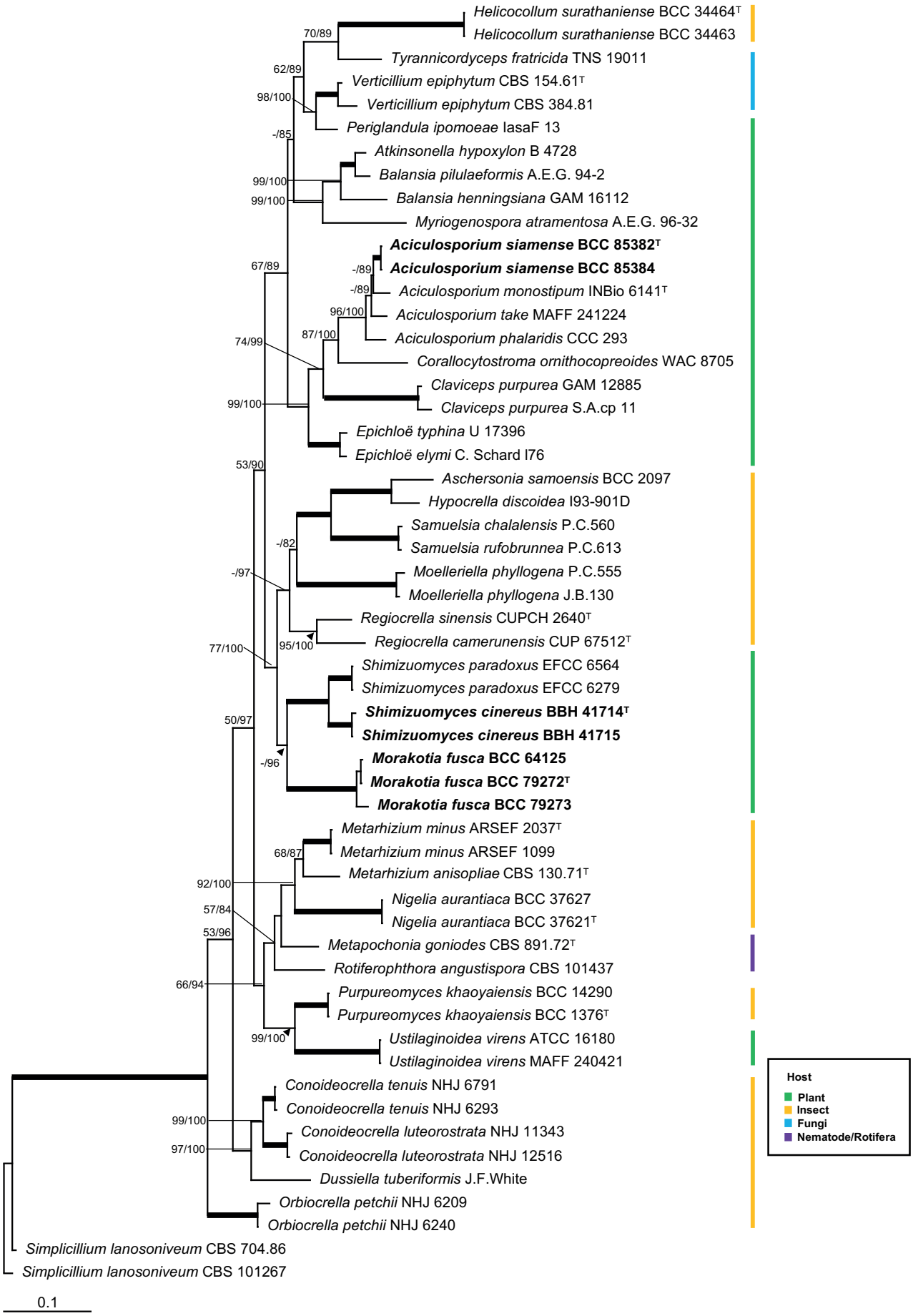

Fig. 1. RAxML tree of *Aciculosporium siamense*, *Morakotia fusca* and *Shimizuomyces cinereus* with other genera in the *Clavicipitaceae* from a combined LSU, *RPB1* and *TEF1* dataset. Numbers at the major nodes represent maximum likelihood bootstrap values (MLBP) and Bayesian posterior probabilities (BPP) multiplied by 100. Fully-supported (MLBP/BPP = 100/100) branches are thickened.

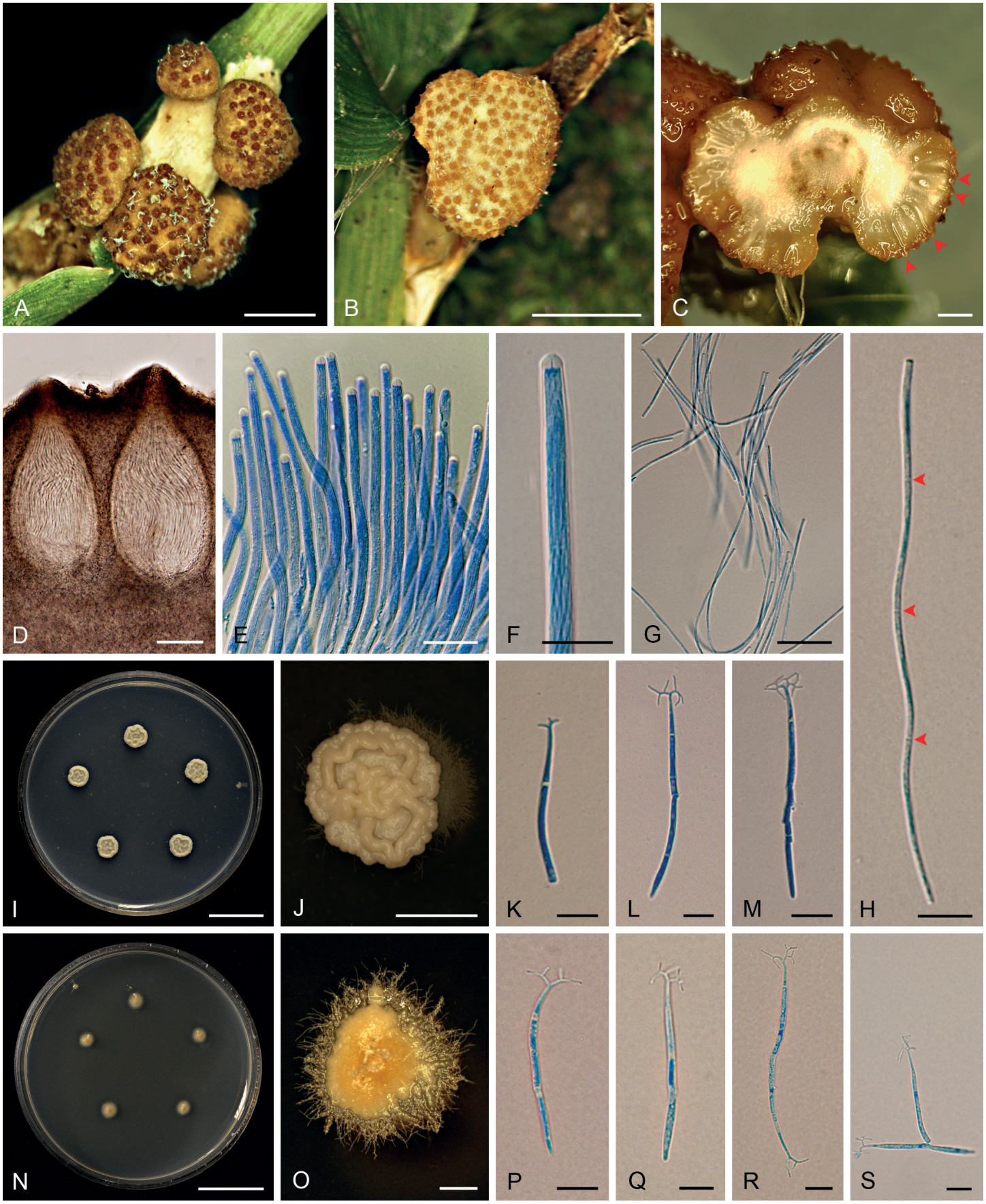

Fig. 2. *Aciculosporium siamense* (BBH 43077, BCC 85382). **A–C.** Ascomata on leaf sheaths of grass. **D.** Perithecia. **E.** Asci. **F.** Ascus tip. **G.** Whole ascospores. **H.** Whole ascospore with septations. **I, J.** Colonies on PDA. **K–M.** Holoblastic conidia on PDA. **N, O.** Colonies on 2 % MEA. **P–S.** Holoblastic conidia on 2 % MEA. Scale bars: I, N = 20 mm; A, J = 5 mm; B, C, O = 1 mm; D = 100 µm; E, G = 20 µm; F, H, P–S = 10 µm; K–M = 5 µm.

© 2021 Westerdijk Fungal Biodiversity Institute

and smooth vegetative hyphae on the edges of the colony, wet, 3–4 µm diam. *Conidia* holoblastic, hyaline, cylindrical to filiform, narrower at one end than the other, 1–2-septate, (24–)30–50(–60) × 1.5–2 µm, with dichotomously branched appendages, usually appearing at the narrow end of conidia, 1–6 × 0.5 µm.

Distribution: Found in the central and western regions of Thailand.

Additional materials examined: **Thailand**, Chet Kot Waterfall, Khao Yai National Park**,** on leaf sheath (*Poaceae*), 8 Jan. 2017, *UP*, *SM & PS*, SM 2080 (BBH 43076 paratype), ex-paratype culture BCC 85381, SM 2082 (BBH 43078), culture BCC 85383, SM 2083 (BBH 43079), culture BCC 85384; Pi Tu Kro Waterfall, Umphang Wildlife Sanctuary, on leaf sheath (*Poaceae*), 26 Jun. 2008, *SM*, *K. Tasanathai (KT)*, *B. Thongnuch (BT)*, *PS*, *AK & J.J. Luangsa-ard (JJL)*, SM 517 (BBH 24722), culture BCC 32351.

Notes: *Aciculosporium siamense* is a rare species in Thailand, found only in Chet Kot Waterfall and Pi Tu Kro Waterfall. This species produces single to multiple hemispherical perithecial plates similar to the sexual morph of *Aschersonia luteola* and *A. badia* by producing crowded perithecia immersed in stromata (Mongkolsamrit *et al.* 2009). However, *Aciculosporium siamense* differs from *Aschersonia luteola* and *A. badia* on the basis of their hosts. *Aciculosporium siamense* occurs on leaf sheaths (*Poaceae*), while *Aschersonia luteola* and *A. badia* occur on scale insects (*Hemiptera*) and are found on the underside of leaves.

Morakotia Mongkolsamrit, Noisripoom, Khonsanit, Thanakitpipattana & Luangsa-ard, ***gen. nov.*** MycoBank MB 838348.

Etymology: In honour of Prof. Dr Morakot Tanticharoen, for her support of invertebrate-pathogenic fungi research in BIOTEC, Thailand.

Stromata solitary or multiple, unbranched, tough, arising from seed plant, cylindrical to clavate, moderate orange yellow to brown orange (164A–164B). *Fertile part* clavate. *Perithecia* crowded, densely packed, ovoid to long ovoid, ordinal in arrangement, completely immersed, with a reddish brown ostioles. *Asci* cylindrical. *Ascospores* hyaline, whole, filiform, elongate clavate with septations.

Type species: *Morakotia fusca* Mongkolsamrit, Noisripoom, Khonsanit, Thanakitpipattana & Luangsa-ard

Morakotia fusca Mongkolsamrit, Noisripoom, Khonsanit, Thanakitpipattana & Luangsa-ard, ***sp. nov.*** MycoBank MB 838349. Fig. 3A–P.

Etymology: The specific epithet is from the Latin "*fuscus*", referring to brown colour of fresh stromata.

Typus: **Thailand**, Phitsanulok Province, Ban Phaothai community forest, on seed (*Smilacaceae*), in leaf litter, 10 Oct. 2015, *A. Khonsanit (AK)*, *D. Thanakitpipattana (DT)*, *S. Lamlertthon (SL)*, *SM* & *W. Noisripoom (WN)*, MY 10972 (holotype BBH 41710, ex-type culture BCC 79272).

Stromata solitary or multiple, unbranched, tough, 20–75 mm long, 0.5–2 mm broad, cylindrical to enlarging apically, arising from the seed buried approximately 5–10 mm underground. *Fertile part* moderate orange yellow to brown orange (164A–164B), cylindrical to clavate, 5–20 mm long, 1.5–2.5 mm broad. *Perithecia* completely immersed, ordinal in arrangement, narrow flask-shaped, (320–)380–510(–570) × (120–)130–165(–180) µm, ostioles darker reddish orange (175B). *Asci* cylindrical, 8-spored, (105–)160–240(–245) × (7–)8–9(–10) µm with caps 4–5 µm thick. *Ascospores* hyaline, whole, filiform, 7–8-septate, (70–)80–95(–105) × 2–4 µm. Colour change of stromata in 3 % KOH not observed.

Culture characteristics: Colonies on PDA attaining 30–35 mm diam in 30 d, cottony with high mycelial density, pale yellow (11C–D) to strong orange yellow (163B), reverse pale brown. *Synnemata* deep orange yellow (163A), 5–20 × 2–2.5 mm. *Conidiogenous* structures consisting of erect conidiophores arising from the vegetative hyphae. *Conidiophores* consist of verticillate phialides, singly or in whorls of two. *Phialides* awl-shaped, (20–)22–35(–40) × 1.5–2.5 µm. *Conidia* hyaline, globose, not in chains, (4–)4.5–5.5(–6) µm diam. *Chlamydospores* not observed.

Colonies on 2 % MEA attaining 20–25 mm diam in 30 d, cottony, white, scarce mycelial density, reverse brownish orange (N167B). *Conidiogenous* structures consisting of erect conidiophores arising from the vegetative hyphae or monophialidic arising along the hyphae. *Conidiophores* consist of verticillate phialides, singly or in whorls of two. *Phialides* awl-shaped, (20–)25–35(–40) × (1–)1.5–2(–2.5) µm. *Conidia* hyaline, globose, singly not in chains, (4–)4.5–6 µm diam. *Chlamydospores* not observed.

Distribution: Found in the central and northeastern regions of Thailand.

Additional materials examined: **Thailand**, Phitsanulok Province, Ban Phaothai community forest, on seed (*Smilacaceae*), in the leaf litter, 10 Oct. 2015, *AK*, *DT*, *SL*, *SM & W. Noisripoom (WN)*; MY 10973 (BBH 41711 paratype), ex-paratype culture BCC 79273, MY 10974 (BBH 41712), culture BCC 79274; *idem.,* 4 Sep. 2016, *SM*, *WN*, *R. Somnuk* (*RS*), *PS*, *KT*, *DT*, *S. Wongkanoun* (*SW*), MY 11425 (BBH 41790), culture BCC 82798; Nakhon Ratchasima, Khao Yai National Park, on seed (*Palmae*), in the leaf litter, 24 Jun. 2012, *AK*, *SM*, *WN*, *RS*, *PS & KT*, MY 8554 (BBH 37585), culture BCC 64124, MY 8555 (BBH 37740) culture BCC 64125, *idem.,* 26 Jun. 2012, *AK*, *SM*, *WN*, *RS*, *PS & KT*, MY 8624 (BBH 37745), culture BCC 64172.

Notes: Based on the natural specimen*, Morakotia fusca* is similar to *Tolypocladium ophioglossoides* in the colour and shape of its stromata. Both *Morakotia fusca* and *T. ophioglossoides* have brown orange and cylindrical stromata. However, *Morakotia fusca* differs from *T. ophioglossoides* on the basis of their hosts. *Morakotia fusca* occurs on seeds, whereas *T. ophioglossoides* occurs on truffles.

Shimizuomyces cinereus Mongkolsamrit, Noisripoom, Khonsanit, Thanakitpipattana & Luangsa-ard, ***sp. nov.*** MycoBank MB 838350. Fig. 4A–H.

Etymology: The specific epithet is from the Latin "*cinereus*", referring to the grey colour of the stroma.

Typus: **Thailand,** Phitsanulok Province, Ban Phaothai community forest, on seed (*Smilacaceae*), in the leaf litter, 10 Oct. 2015, *AK*, *DT*, *SL*, *SM* & *WN*, MY 10976 (holotype BBH 41714).

© 2021 Westerdijk Fungal Biodiversity Institute

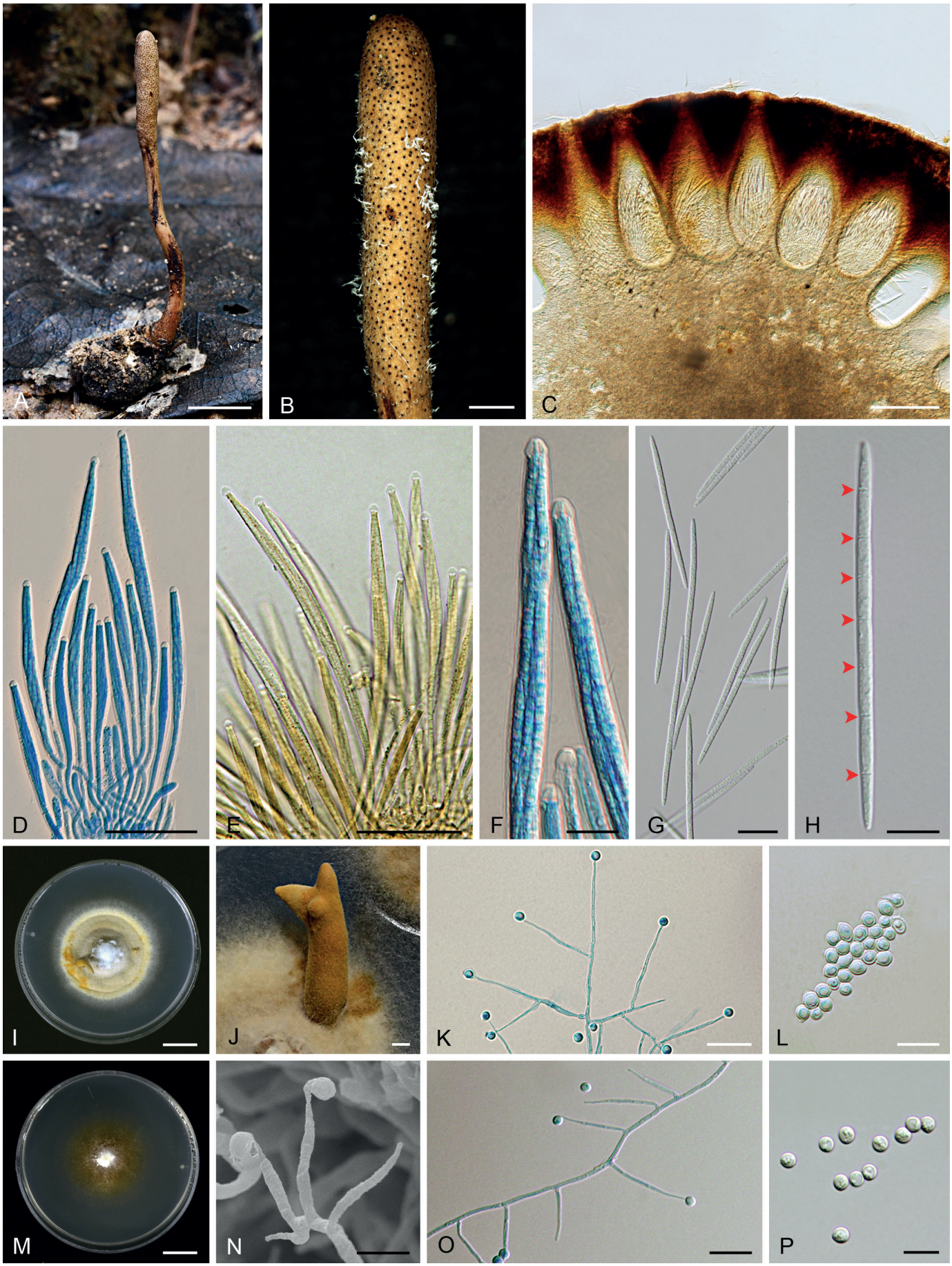

Fig. 3. *Morakotia fusca* (BBH 41710, BCC 79272). **A.** Stroma on seed. **B.** Fertile part of stroma. **C.** Immersed perithecia. **D–F.** Asci with asci caps. **G, H.** Whole ascospores with septations (arrows). **I, J.** Colony with synnema on PDA. **K.** Conidiophores consisting of verticillate phialides on PDA. **L.** Conidia on PDA. **M.** Colony on 2 % MEA. **N, O.** Conidiophores consisting of verticillate phialides on 2 % MEA. **P.** Conidia on 2 % MEA. Scale bars: I, M = 10 mm; A = 5 mm; B, J = 1 mm; C = 200 µm; D, E = 50 µm; G, K, O = 20 µm; F, H, L, N, P = 10 µm.

© 2021 Westerdijk Fungal Biodiversity Institute

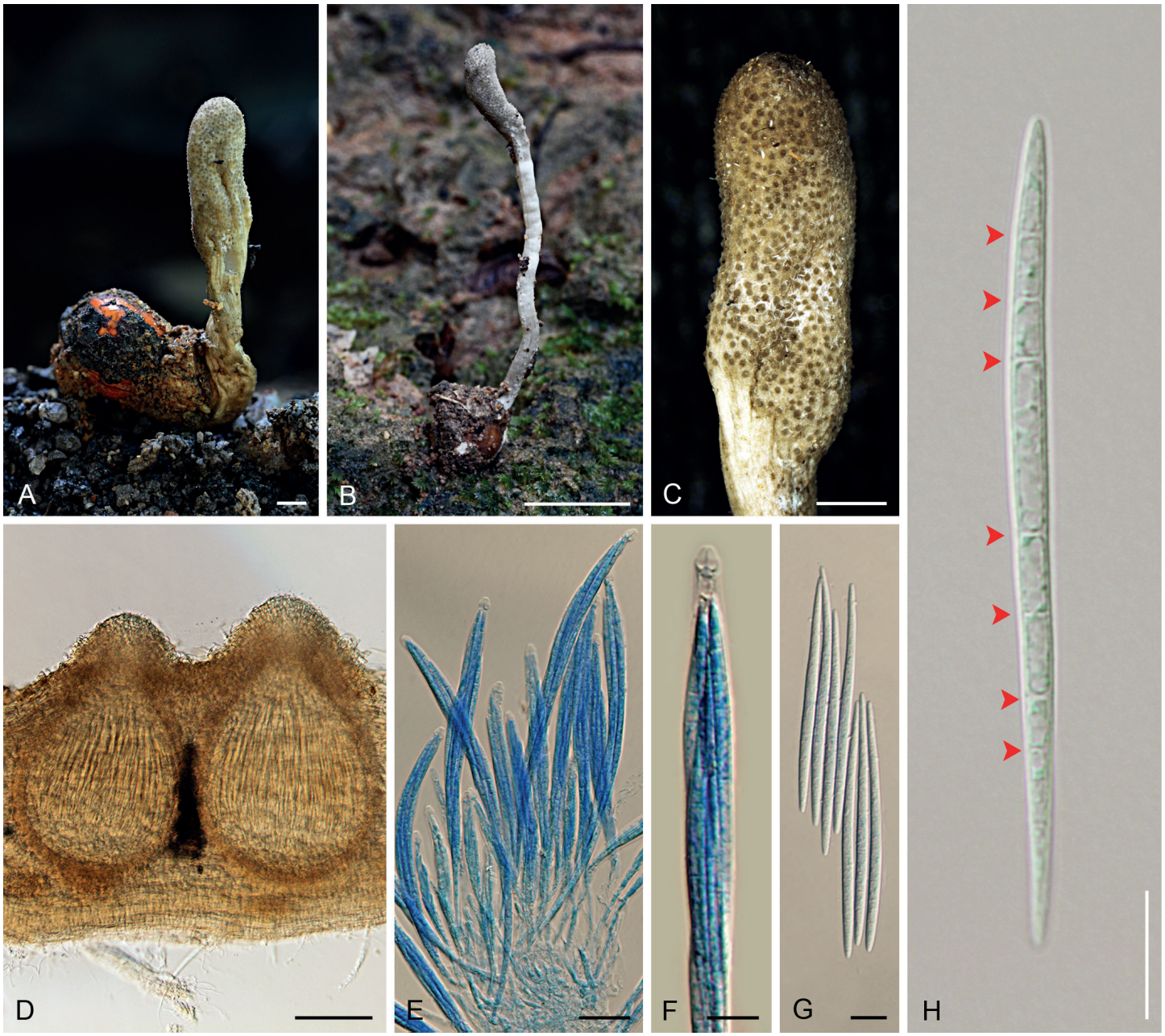

Fig. 4. *Shimizuomyces cinereus* (BBH 41714). **A, B.** Stroma on seed. **C.** Fertile part of stroma. **D.** Perithecia. **E, F.** Asci and asci caps. **G, H.** Whole ascospores with septations (arrows). Scale bars: B = 5 mm; A, C = 1 mm; D = 100 µm; E = 20 µm; F–H = 10 µm.

Stroma solitary, unbranched, 10–28 mm in long and 0.5–2 mm broad, cylindrical to enlarging apically, arising from the seed buried approximately 5–10 mm in the leaf litter. *Fertile part* yellowish grey (A–B), 3–8 × 1.5–3 mm, cylindrical to clavate. *Perithecia* immersed, with ostioles slightly projecting, ordinal in arrangement, pyriform, (310–)320–370(–380) × (150–)190–250 µm, ostioles greyish yellow green (197D), *ca*. 100 µm diam. *Asci* cylindrical, 8-spored, (125–)160–235(–250) × (8–)7–9(–10) µm, with caps 4–5 µm thick. *Ascospores* hyaline, whole, filiform, 7–8 septate, (65–)70–85 × (3–)3.5–4 µm. Colour change of stromata in 3 % KOH not observed.

Distribution: Found in the central region of Thailand.

Additional materials examined: **Thailand**, Phitsanulok Province, Ban Phaothai community forest, on seed (*Smilacaceae*), in the leaf litter, 10 Oct. 2015, *AK*, *DT*, *SL*, *SM*, *WN*, MY 10979 (**paratype** BBH 41715), MY 10959 (BBH 41709), MY 10975 (BBH 41713).

Notes: *Shimizuomyces cinereus* is only recorded from Ban Phaothai community forest in Phitsanulok Province. This species is easy to find in the leaf litter or on the ground due to the abundance of natural specimens located around the area producing bright grey stromata. *Shimizuomyces cinereus* and *Morakotia fusca* occur on seeds (*Smilacaceae*) and these two species can be found at the same site in Ban Phaothai community forest. *Shimizuomyces cinereus* differs from *Morakotia fusca* in having pale grey stromata meanwhile *M. fusca* has an orange and tough stroma.

DISCUSSION

Phylogenetic analyses combined with morphology classified Thai specimens associated with plants as new species in *Aciculosporium* and *Shimizuomyces,* and a novel genus,

© 2021 Westerdijk Fungal Biodiversity Institute

Table 2. Morphological comparisons of *Morakotia fusca* and species in *Shimizuomyces.*

Species	Stroma (mm)	Fertile part (mm)	Perithecia (µm)	Asci (µm)	Ascospores (µm)	References
Morakotia fusca	20–75 × 0.5–2	5–20 × 1.5–2.5	narrow flask-shaped, 320–570 × 120–180	105–245 × 7–10	70–105 × 2–4, with septation	This study
Shimizuomyces cinereus	10–28 × 0.5–2	3–8 × 1.5–3	pyriform, 310–380 × 150–250	125–250 × 8–10	65–85 × 3–4, with septation	This study
S. kibianus	15–18 mm long	2.5 × 2	pyriform, 300–320 × 230–240	140–160 × 6	30–80 × 1.5, with septation	Kobayasi (1984), Shimizu (1994)
S. paradoxus	10–30 × 0.5–1.2	5–15 × 1–2	pyriform, 350–400 × 200–250	100–130 × 6–7	60–75 × 2–2.5, with septation	Kobayasi (1981)

Morakotia. This study has contributed to our knowledge on the taxonomy, morphology and geographical distribution of fungi in *Clavicipitaceae* (*Hypocreales*).

Aciculosporium siamense from Thailand can be easily recognised by its host – an unknown panicoid grass found in the rainforest that was also reported for *A. monostipum* from Costa Rica (South America) and *A. phalaridis* from *Phalaris aquatica* in Australia and New Zealand. *Aciculosporium take* and *A. sasicola* can be found on several genera of bambusoid grasses in Japan (Tsuda *et al*. 1997). We compared the morphological characters of *A. siamense* with known species in *Aciculosporium* and found that *A. siamense* is morphologically similar to *A. take* and *A. sasicola* in the formation of astipitate ascomatal stromata (Tsuda *et al*. 1997). *Aciculosporium monostipum* produces stipitate ascomatal stromata arising directly from parasitised plant ovaries (Sullivan *et al*. 2001), whereas *A. phalaridis* produces a discrete sclerotium with stalked ascostromata (Walker 2004) on seeds. Although the asexual morph of *Aciculosporium siamense* was not seen in the natural habitat, cream-coloured, yeast-like masses of conidia were produced on PDA and 2 % MEA. From our microscopic observation of the conidia on cultures, we found that *Aciculosporium siamense* produces holoblastic appendaged conidia on both media. Our results reveal that species in *Aciculosporium* share this unique character (apomorphies) in having a holoblastic appendaged conidia, which was also reported from *A. monostipum, A. phalaridis, A. take* and *A. sasicola* (Oguchi 2001, Sullivan *et al*. 2001, Walker 2004, Píchová *et al*. 2018).

Multi-gene phylogenetic analyses presented in Fig. 1 fully support (MLBP/BPP = 100/100) *Morakotia* as a distinct clade from *Shimizuomyces.* So far, only one species, *Morakotia fusca*, has been proposed in *Morakotia*. Considering the morphology of natural specimens and ecology, these two genera share similarity of having cylindrical stroma arising directly from seeds, the fertile parts are cylindrical to clavate, and can be found on the ground. Microscopic observation between species in the two genera showed the synapomorphic character of producing filiform ascospores with distinct septations. However, *Morakotia fusca* differs from *Shimizuomyces* spp. (Table 2) in that the perithecia in *M. fusca* are completely immersed and narrow flask-shaped, whereas the perithecia in all species of *Shimizuomyces* are immersed with slightly projecting ostioles and are pyriform in shape. The *Shimizuomyces* clade itself is fully supported (MLBP/BPP = 100/100) with the Thai specimens as a new member in *Shimizuomyces. Shimizuomyces cinereus* differs from *S. paradoxus* in having grey stroma, whereas stroma in *S. paradoxus* is bright yellow. *Shimizuomyces kibianus* was not included in the phylogenetic analysis because no sequence data was available for this taxon. According to the description and illustration given by Kobayasi (1984) and Shimizu (1994), *S. kibianus* also has grey stroma similar to *S. cinereus.* However, *S. cinereus* possesses a larger fertile part and perithecia, and longer asci than reported for *S. kibianus*. *Shimizuomyces* is thus distributed in Japan, Korea and Thailand.

ACKNOWLEDGEMENTS

This study was supported by the Platform Technology Management Section, National Center for Genetic Engineering and Biotechnology (BIOTEC), Grant No. P19-50231 and the Cluster and Program Management Office, NSTDA Grant No. P15-51452. We thank Mr. Witthaya Sangsawang and Ms. Wimonrat Guntang for assistance in collecting specimens. We are indebted to the Department of National Parks, Wildlife and Plant Conservation for their cooperation and support of our research project. We would like to thank Dr Philip James Shaw for thoughtful editing of the manuscript.

Conflict of interest: The authors declare that there is no conflict of interest.

REFERENCES

Artjariyasripong, S, Mitchell, JI, Hywel-Jones NL, *et al*. (2001). Relationship of the genus *Cordyceps* and related genera, based on parsimony and spectral analysis of partial 18S and 28S ribosomal gene sequences. *Mycoscience* **42**: 503–517.

Bischoff JF, White JF (2003). The plant-infecting clavicipitaleans. In: *Clavicipitalean fungi, evolutionary biology, chemistry, biocontrol and cultural impacts* (White JF Jr, Bacon CW, Hywel-Jones NL, *et al.*, eds). Marcel Decker, Inc., New York: 125–149.

Castlebury LA, Rossman AY, Sung GH, *et al.* (2004). Multigene phylogeny reveals new lineage for *Stachybotrys chartarum,* the indoor air fungus. *Mycological Research* **108**: 864–872.

Chaverri P, Bischoff JF, Evans HC, *et al.* (2005a). *Regiocrella*, a new entomopathogenic genus with a pycnidial anamorph and its phylogenetic placement in the *Clavicipitaceae*. *Mycologia* **97**: 1225–1237.

Chaverri P, Bischoff JF, Liu M, *et al*. (2005b). A new species of *Hypocrella*, *H. macrostroma*, and its phylogenetic relationships to other species with large stromata. *Mycological Research* **109**: 1268–1275.

Chaverri P, Liu M, Hodge KT (2008). A monograph of the entomopathogenic genera *Hypocrella*, *Moelleriella,* and *Samuelsia gen. nov.* (*Ascomycota, Hypocreales, Clavicipitaceae*), and their

© 2021 Westerdijk Fungal Biodiversity Institute

aschersonia-like anamorphs in the Neotropics. *Studies in Mycology* **60**: 1–66.

Cheplick GP, Faeth S (2009). *Ecology and evolution of the grass endophyte symbiosis*. Oxford University Press, New York.

Currie CR, Wong B, Stuart AE, *et al*. (2003). Ancient tripartite coevolution in the attine ant-microbe symbiosis. *Science* **299**: 386–388.

Gams W, Zare R (2003). A taxonomic review of the clavicipitaceous anamorphs parasitizing nematodes and other microinvertebrates. In: *Clavicipitalean fungi, evolutionary biology, chemistry, biocontrol and cultural impacts* (White JF Jr, Bacon CW, Hywel-Jones NL, *et al.*, eds). Marcel Decker, Inc., New York: 17–73.

Górzyńska K, Ryszka P, Anielska T, *et al.* (2017). Effect of *Epichloë typhina* fungal endophyte on the diversity and incidence of other fungi in *Puccinellia distans* wild grass seeds. *Flora* **228**: 60–64.

Greenfield M, Gómez-Jiménez MI, Ortiz V, *et al.* (2016). *Beauveria bassiana* and *Metarhizium anisopliae* endophytically colonize cassava roots following soil drench inoculation. *Biological Control* **95**: 40–48.

Hall T (2004). *BioEdit version 6.0.7*. Department of Microbiology, North Carolina State University. Raleigh, NC, USA.

Johnson D, Sung GH, Hywel-Jones NL, *et al*. (2009). Systematics and evolution of the genus *Torrubiella* (*Hypocreales*, *Ascomycota*). *Mycological Research* **113**: 279–289.

Kepler RM, Humber RA, Bischoff JF, *et al.* (2014). Clarification of generic and species boundaries for *Metarhizium* and related fungi through multigene phylogenetics. *Mycologia* **106**: 811–829.

Kepler RM, Sung GH, Ban S, *et al*. (2012a). New teleomorph combinations in the entomopathogenic genus *Metacordyceps. Mycologia* **104**: 182–197.

Kepler RM, Sung GH, Harada Y, *et al.* (2012b). Host jumping onto close relatives and across kingdoms by *Tyrannicordyceps* (*Clavicipitaceae*) *gen. nov*. and *Ustilaginoidea* (*Clavicipitaceae*). *American Journal of Botany* **99**: 552–561.

Kobayasi Y (1981). Revision of the genus *Cordyceps* and its allies 1. *Bulletin of the National Museum of Nature and Science*. Series B **7**: 1–13.

Kobayasi Y (1984). Miscellaneous notes of fungi (4). *Journal of Japanese Botany* **59**: 31–32.

Luangsa-ard J, Mongkolsamrit S, Noisripoom W, *et al.* (2017a). *Helicocollum*, a new clavicipitalean genus pathogenic to scale insects (*Hemiptera*) in Thailand. *Mycological Progress* **16**: 419–431.

Luangsa-ard JJ, Mongkolsamrit S, Thanakitpipattana D, *et al.* (2017b). Clavicipitaceous entomopathogens: new species in *Metarhizium* and a new genus *Nigelia. Mycological Progress* **16**: 369–391.

Luangsa-ard J, Tasanathai K, Thanakitpipattana D, *et al*. (2018). Novel and interesting *Ophiocordyceps* spp. (*Ophiocordycipitaceae*, *Hypocreales*) with superficial perithecia from Thailand. *Studies in Mycology* **89**: 125–142.

Miyake I (1908). Witches' broom disease of bamboo (Preliminary report). *Botanical Magazine Tokyo* **22**: 305– 307 (in Japanese).

Mongkolsamrit S, Khonsanit A, Thanakitpipattana D, *et al.* (2020). Revisiting *Metarhizium* and the description of new species from Thailand. *Studies in Mycology* **95**: 171–251.

Mongkolsamrit S, Luangsa-ard JJ, Spatafora JW, *et al*. (2009). A combined ITS rDNA and beta-tubulin phylogeny of Thai species of *Hypocrella* with non-fragmenting ascospores. *Mycological Research* **113**: 684–699.

Mongkolsamrit S, Noisripoom W, Arnamnart N, *et al.* (2019). Resurrection of *Paraisaria* in the *Ophiocordycipitaceae* with three new species from Thailand. *Mycological Progress* **18**: 1213–1230.

Mongkolsamrit S, Noisripoom W, Thanakitpipattana D, *et al*. (2018). Disentangling cryptic species with isaria-like morphs in *Cordycipitaceae*. *Mycologia* **110**: 230–257.

Nishi O, Sato H (2019). Isolation of *Metarhizium* spp. from rhizosphere soils of wild plants reflects fungal diversity in soil but not plant specificity. *Mycology* **10**: 22–31.

Oguchi T (2001). *Aciculosporium sasicola sp. nov.* on witches' broom of *Sasa senanensis*. *Mycoscience* **42**: 217–221.

Page RD (1996). TreeView: an application to display phylogenetic trees on personal computers. *Computer Applications in the Biosciences* **12**: 357–358.

Píchová K, Pažoutová S, Kostovčík M, *et al.* (2018). Evolutionary history of ergot with a new infrageneric classification (*Hypocreales*: *Clavicipitaceae*: *Claviceps*). *Molecular Phylogenetics and Evolution* **123**: 73–87.

Rehner SA, Samuels GJ (1995). Molecular systematics of the *Hypocreales*: a teleomorph gene phylogeny and the status of their anamorphs. *Canadian Journal of Botany* **73**: 816–823.

Ronquist F, Teslenko M, Mark P, *et al.* (2012). MrBayes 3.2: efficient Bayesian phylogenetic inference and model choice across a large model space. *Systematic Biology* **61**: 539–542.

Schardl CL, Young CA, Hesse U, *et al.* (2013). Plant-symbiotic fungi as chemical engineers: multi-genome analysis of the *Clavicipitaceae* reveals dynamics of alkaloid loci. *PLoS Genetics* **9**: e1003323.

Shimizu D (1994). Color iconography of vegetable wasps and plant worms (in Japanese). Seibundo Shinkosha, Tokyo.

Spatafora JW, Sung GH, Sung JM, *et al.* (2007). Phylogenetic evidence for an animal pathogen origin of ergot and the grass endophytes. *Molecular Ecology* **16**: 1701–1711.

Stamatakis A (2014). RAxML version 8: a tool for phylogenetic analysis and post-analysis of large phylogenies. *Bioinformatics* **30**: 1312–1313.

Steiner U, Leibner S, Schardl CL, *et al.* (2011). *Periglandula,* a new fungal genus within the *Clavicipitaceae* and its association with *Convolvulaceae*. *Mycologia* **103**: 1133–1145.

Sullivan R, Bergen MS, Patel R, *et al.* (2001). Features and phylogenetic status of an enigmatic clavicipitalean fungus *Neoclaviceps monostipa gen. et sp. nov. Mycologia* **93**: 90–99.

Sung GH, Hywel-Jones NL, Sung JM, *et al*. (2007). Phylogenetic classification of *Cordyceps* and the clavicipitaceous fungi. *Studies in Mycology* **57**: 5–59.

Sung GH, Shrestha B, Park KB, *et al.* (2010). Cultural characteristics of *Shimizuomyces paradoxus* collected from Korea. *Mycobiology* **38**: 189–194.

Sung GH, Spatafora JW, Zare R, *et al*. (2001) A revision of *Verticillium* sect. *Prostrata*. II. Phylogenetic analyses of SSU and LSU nuclear rDNA sequences from anamorphs and teleomorphs of the *Clavicipitaceae*. *Nova Hedwigia* **72**: 311–328.

Tanaka E, Tanaka C, Ishihara A, *et al*. (2003). Indole-3-acetic acid biosynthesis in *Aciculosporium take*, a causal agent of witches' broom of bamboo. *Journal of General Plant Pathology* **69**: 1–6.

Torres MS, White JF Jr (2009). Free-living and saprotrophs to plant endophytes. In: *Encyclopedia of Microbiology* 3rd edition. Moselio Schaechter, Ed., Elsevier: 422–430.

Tsuda M, Shimizu K, Matsumura K, *et al*. (1997). Host range of *Aciculosporium take*, the causal agent of witches' broom of bamboo plants. *Bulletin of the National Science Museum, Series B* **23**: 25–34.

Walker J (2004). *Claviceps phalaridis* in Australia: biology, pathology and taxonomy with a description of the new genus *Cepsiclava* (*Hypocreales, Clavicipitaceae*). *Australasian Plant Pathology* **33**: 211–239.

Young CA, Schardl CL, Panaccione DG, *et al.* (2015). Genetics, genomics and evolution of ergot alkaloid diversity. *Toxins* **7**: 1273–1302.

© 2021 Westerdijk Fungal Biodiversity Institute

© 2021 Westerdijk Fungal Biodiversity Institute

FUSE

Fungal Systematics and Evolution

VOLUME 8
DECEMBER 2021
PAGES 39–47

doi.org/10.3114/fuse.2021.08.04

Morphological and molecular characterization of *Langdonia walkerae sp. nov*. infecting *Aristida stricta* and *A. beyrichiana* in longleaf pine-grassland ecosystems in the southeastern USA

A.S. Alqurashi[1*], J. Kerrigan[1], K.G. Savchenko[2]

[1]Department of Plant and Environmental Sciences, Clemson University, Clemson, SC 29634, USA
[2]Department of Biological Sciences, Butler University, Indianapolis, IN 46208, USA

*Corresponding author: aalqura@g.clemson.edu

Key words:
new taxa
plant pathogens
smut fungi
spore balls
Ustilaginaceae

Abstract: A smut fungus that hinders wiregrass restoration efforts in longleaf pine-grassland ecosystems was collected from *Aristida stricta* and *A. beyrichiana* (*Poaceae*) in three states in the southeastern USA. Morphological and phylogenetic characteristics of this fungus were examined. These data show that the specimens from both plant species were infected by the same fungus and represent a new species of *Langdonia*. The new species differs morphologically from other species of *Langdonia* by teliospores being solitary and not compacted into spore balls. Spore wall ornamentation and teliospore size also differ from other *Langdonia* species. Phylogenetic analyses of DNA sequences of the ITS, LSU, and *EF-1α* supported separation of the species from *A. stricta* and *A. beyrichiana* from other *Langdonia* species. Based on these results, a new species, *Langdonia walkerae*, is proposed.

Citation: Alqurashi AS, Kerrigan J, Savchenko KG (2021). Morphological and molecular characterization of *Langdonia walkerae sp. nov.* infecting *Aristida stricta* and *A. beyrichiana* in longleaf pine-grassland ecosystems in the southeastern USA. *Fungal Systematics and Evolution* **8**: 39–47. doi: 10.3114/fuse.2021.08.04
Received: 8 December 2020; **Accepted:** 14 April 2021; **Effectively published online:** 15 June 2021
Corresponding editor: P.W. Crous

INTRODUCTION

Aristida, a member of the *Poaceae* and the *Aristidoideae* (Barkworth 2003, Cerros-Tlatilpa *et al.* 2011), is distributed worldwide with approximately 300 species (Barkworth 2003) primarily located in Central, North and South America, Australia, and Africa (Cerros-Tlatilpa *et al*. 2011). This genus is distinct from other grass genera by its three-awned lemma (Clewell 1989, Barkworth 2003). In the southeastern United States, two *Aristida* species, *A. stricta* and *A. beyrichiana*, are common grasses found in the ground layer of longleaf pine, *Pinus palustris*, forests (Peet 1993), which extend from the border of Texas and Louisiana eastward to the Atlantic Ocean and from the middle of Florida northward into Virginia (Brockway *et al*. 1998, Frost 2006). *Aristida stricta,* called Carolina wiregrass or the pineland threeawn, occurs in North Carolina and the northern part of South Carolina, and is distinguished morphologically by having hairs along the length of the blades, wider culms, and shorter ligules (Peet 1993, Van Eerden 1997). *Aristida beyrichiana,* called southern wiregrass or Beyrich threeawn, grows in the southern part of South Carolina into Florida and west to Mississippi, and is distinguished morphologically by its soft, short hairs at the base of the blades and the glumes are more unequal in length (Peet 1993, Van Eerden 1997).

These perennial bunchgrasses are adapted to fire, enabling them to persist and reproduce despite frequently recurring fires (Platt 1999, Means 2007) as well as to survive for decades without burning (Shearman *et al*. 2019). Flowers and seed production are most abundant within a year of burning; without fire, few, if any, are produced each subsequent year (Clewell 1989, Van Eerden 1997, Fill *et al*. 2012). These native wiregrasses are considered keystone species in the longleaf pine-grass ecosystem as they produce the fine fuels needed for frequent burning, a requirement for sustained ecosystem structure and function (Clewell 1989, Duever 1989, Noss 1989). Thus, the seed viability of wiregrasses is important for ecosystem restoration efforts (Van Eerden 1997) in projects that focus on wiregrass as a primary understory species.

The production of *A. stricta* and *A. beyrichiana* seeds has been observed to be affected by a smut fungus that replaces the developing ovaries with teliospores (Van Eerden 1997). Smut fungi are pathogens that primarily infect grasses and occur world-wide. They produce sori, sporocarps in which teliospores are produced, in different organs of their host (Vánky 2013). Previously, many grass-infecting smut fungi, including *Sporisorium*, were united into the genus *Ustilago* that has proved to be polyphyletic after the introduction of molecular phylogenetic studies (Begerow *et al*. 1997, 2006). In the taxonomy of smut fungi, the host plant is one of the criteria usually used to classify groups (Bauer *et al*. 2001, Begerow *et al*. 2004). Consequently, McTaggart *et al*. (2012b) emended the description of the genus *Sporisorium* and separated all species that occur on *Aristida* into a new genus, *Langdonia,* based on the host plant and morphological and phylogenetic differences.

Fungal Systematics and Evolution is licensed under a Creative Commons Attribution-NonCommercial-ShareAlike 4.0 International License

© 2021 Westerdijk Fungal Biodiversity Institute

Langdonia is a monophyletic group within the *Ustilaginaceae* (McTaggart *et al*. 2012b). Currently, eight species have been described on other *Aristida* species from various countries - including Argentina, Australia, Bolivia, Madagascar, Mexico, Thailand, and the USA (Durán 1987, McTaggart *et al*. 2012b, Vánky 2012, Denchev *et al*. 2015). The defining morphological characteristics of the genus *Langdonia* are sori that can be found in some or all ovaries of the panicle, lack of columella and sterile cells, teliospores compacted into spore balls, and *Ustilago*-type germination (McTaggart *et al*. 2012b, Vánky 2013). Based on these criteria, the tentative identification of the fungus causing smut on *A. stricta* and *A. beyrichiana* was a species of *Langdonia*. Therefore, the objectives of this study were to identify the fungus that infects *A. stricta* and *A. beyrichiana* and to determine if the same fungus species infects both *A. stricta* and *A. beyrichiana*.

MATERIALS AND METHODS

Sample collection and documentation

Naturally infected plants were collected from seven locations in North Carolina, South Carolina, and Florida during the seed production stage (Table 1). In 2017, samples were collected from two locations - one in South Carolina and one in Florida, and in 2018 samples were collected from six locations in all three states, with only one location being common to both years. All sampled sites had been burned by prescription within the year. The locations and the wiregrass species from which each sample was obtained are included in the "specimens examined" section and in Table 1. For collection, samples of infected wiregrass culms, erect stems bearing inflorescences, were cut at ground level, placed in paper bags, and returned to the laboratory where the specimens were kept at room temperature for subsequent use. Plant voucher specimens were deposited in the Clemson University Herbarium (CLEMS), and fungus specimens were deposited in the Washington State University Mycological Herbarium (WSP) and the U.S. National Fungus Collections - Herbarium (BPI) and kept as voucher specimens.

Morphological examination

The characteristics of the sori and teliospores were examined on infected plants. Pictures of sori were taken using a Nikon D5100 camera. Teliospore characteristics were studied using a compound microscope (LM; BX60F; Olympus optical Co. Ltd., Japan) equipped with ProgRes C5 camera (JENOPTIK, Germany) and CapturePro software; and a scanning electron microscope (SEM; Hitachi SU6600) at 5.0 kV at the Clemson University Electron Microscopy Facility. For LM, teliospores were mounted in lactic acid (85–90 %, VWR, International, LLC) (Savchenko *et al*. 2014) and examined at 1 000 × magnification. The diameters of 30 teliospores, oriented in plane view so that they appeared globose, were measured from each sample collection. The colors of the sori and the teliospores were described according to Rayner (1970). For SEM examination, teliospores were dusted on double-sided adhesive carbon tape, mounted on aluminum stubs, and sputter-coated with platinum using a Cressington sputter-coater (*ca*. 30 nm in 6 min).

Table 1. Smut samples on *Aristida beyrichiana* and *A. stricta* collected and examined for this study**.**

Site	Voucher	Isolate	State	City/County	*Aristida* spp.	Date
Silver Bluff Audubon Center	CLEMS0080381	JK 5017	SC	Jackson/Aiken	*A. beyrichiana*	10 Nov. 2017
	Holotype: WSP74240					
	Isotype: BPI911222					
	CLEMS0080382	JK 6017				
	CLEMS0080383 CLEMS0080384	SB 1218				6 Dec. 2018
Aiken Gopher Tortoise Heritage Preserve	CLEMS0080385	AGT 1218	SC	Aiken/Aiken	*A. beyrichiana*	6 Dec. 2018
Savannah River Site	CLEMS0080388 WSP74241	SRS 1218	SC	Barnwell/Barnwell	*A. beyrichiana*	4 Dec. 2018
	BPI 911220					
Apalachicola Bluffs and Ravines Preserve	CLEMS0080387	FLW 1017	FL	Bristol/Liberty	*A. beyrichiana*	31 Oct. 2017
Austin Cary Forest	CLEMS0080386	FL 1218	FL	Gainesville/Alachua	*A. beyrichiana*	3 Dec. 2018
Carolina Sandhills National Wildlife Refuge	CLEMS0080389	CSN 1118	SC	Hoffman/Richmond	*A. stricta*	27 Nov. 2018
	WSP74242					
	BPI 911221					
North Carolina Sandhills Game Land	CLEMS0080390	NC 1018	NC	Chesterfield/Chesterfield	*A. stricta*	29 Nov. 2018
	WSP74243	NC 2018				
	BPI 911219	NC 3018				
		NC 5018				

© 2021 Westerdijk Fungal Biodiversity Institute

Growth on artificial medium

Sori were carefully removed from infected plants and surface-sterilized by immersing in 70 % ethanol for 30 s, rinsing with sterile distilled water, immersing in 3 % sodium hypochlorite for 10 s, and rinsing twice with sterile distilled water. Each sorus was handled individually using aseptic techniques; one sorus was placed in a 2.0 mL centrifuge tube and gently ground with a tissue grinder pestle to release the teliospores. To make a spore suspension, 500 µL sterile distilled water was added to a tube, the contents were thoroughly mixed, 100 µL was pipetted onto a petri dish containing Difco™ malt extract agar (MEA; Becton, Dickinson and Co., Sparks, MD) and the suspension was spread with a L-shaped cell spreader over the agar surface. The MEA was made according to the manufacturer's instruction and amended with streptomycin (MEA+S; 200 ppm = 200 mg/L). Plates were placed at 28 °C for 2–3 d; and then individual colonies were aseptically subcultured onto MEA+S and incubated for 10 d at 28 °C. The morphological characteristics of shape, color, and diameter of the colony were recorded. The color of the colony was defined according to Rayner (1970).

DNA Extraction, Polymerase chain reaction (PCR), and sequencing

DNA was extracted from 10-d-old cultures using a DNeasy Plant Mini Kit (QIAGEN GmbH, Hilden, Germany) according to the manufacturer's instructions. DNA concentration was determined using a Thermo Scientific Nanodrop 2000 /2000c spectrophotometer. All DNA samples were stored at -20 °C until used for amplification. Genomic DNA was amplified using an Eppendorf Mastercycler Gradient thermocycler with Thermo Scientific Phusion High-Fidelity DNA Polymerase following the manufacturer's cycling and reaction conditions. Two nuclear ribosomal DNA regions and one gene locus were amplified and sequenced: the internal transcribed spacer (ITS) region, the large subunit region (LSU), and translation elongation factor-1α locus (*EF-1α*). The ITS region was amplified with primers M-ITS1 (Stoll *et al*. 2003) and ITS4 (White *et al*. 1990) and annealed at 58 °C (McTaggart *et al*. 2012a); the LSU region was amplified with primers LROR and LR5 (Vilgalys & Hester 1990) at 60 °C; and the *EF-1α* locus was amplified with primers EF-1αF and EF-1αR (McTaggart *et al*. 2012a) at 64 °C. The PCR products were analyzed using gel electrophoresis on a 1.0 % agarose gel and sent to Arizona State University Core Laboratories for purification and sequencing using the same forward and reverse PCR primers. AB1 sequence trace files were assembled using Geneious Prime® v. 2020.0.5 software, and a BLAST search was conducted for all resulting sequences to confirm accurate species identification. The sequences were deposited in GenBank and their accession numbers are shown in Table 2.

Phylogenetic analysis

The phylogenetic analysis was conducted using Geneious Prime® v. 2020.0.5 software. The relationships among the isolates of *Langdonia* species sequenced in this study and other taxa in the *Ustilaginaceae* were inferred from a phylogenetic tree based on the ITS, LSU, and *EF-1α* data sets. The sequences for all taxa were first concatenated for each taxon and then aligned using the MUSCLE algorithm. The final data set contained sequences from 12 isolates collected in this study and 43 reference sequences obtained from GenBank (Table 2). Alignments were uploaded to NGphylogeny.fr (https://ngphylogeny.fr; Lemoine *et al*. 2019) and curated using BMGE (Criscuolo & Gribaldo 2010) to remove poorly aligned positions. The final super matrix contained 1 465 characters, including gaps.

The phylogenetic analysis was conducted using Bayesian inference and maximum likelihood; a GTR model with GAMMA distribution (Nylander 2004) was selected for both analyses. For Bayesian inference, MrBayes v. 3.2.6 was used to conduct a Markov Chain Monte Carlo (MCMC) (Huelsenbeck & Ronquist 2001). Four runs, each consisting of four chains, were conducted for 1 000 000 generations, and the cold chain was heated at a temperature of 0.25. Trees were sampled every 1 000 generations. The standard deviation of split frequencies was 0.01. RAxML v. 8 (Stamatakis 2014) was used for the maximum likelihood using a bootstrapping analysis. RAxML analyses were run with a rapid bootstrap analysis to search for the best-scoring likelihood tree using a random starting tree and 1 000 maximum likelihood bootstrap replicates. Trees were rooted using *Melanotaenium euphorbiae* (HUV17733). The final alignment and trees were deposited in TreeBASE 23819.

RESULTS

Growth on artificial medium

When teliospores were cultured on MEA+S, germ-tube formation occurred after 6 h incubation at 28 °C, and the germination rate increased steadily over a period of 2–3 d. Spore germination was the *Ustilago*-type, making a phragmobasisium on which ovoid sporidia (*i.e*., basidiospores) were produced. Colonies grew slowly; most colonies were visible after 3–5 d, and when subcultured, a colony reached 3–4 cm diam after 14 d. However, more than 50 % of the teliospores remained dormant throughout the incubation period. Young colonies first appeared pale luteous but later became ochreous with age. Colony shape was convex and irregular with undulate edges. At a later stage of growth, the colony surface in some isolates became wrinkled and formed cerebriform sectors (Ulloa & Hanlin 2000).

Phylogenetic analysis

A total of 12 isolates from the culture were sequenced for two nuclear ribosomal DNA regions, ITS and LSU and one gene locus, *EF-1α*, and included in the final data set with 43 reference sequences obtained from GenBank. The list of taxa, their host plants and geographic sources, and the GenBank accession numbers for these sequences are shown in Table 2. The phylogenetic relationships between the isolates from *A. stricta* and *A. beyrichiana* exhibited full support to recognize them as one species based on the MrBayes and RAxML analyses, with values of 1.0 and 100, respectively. The topology of the MrBayes and RAxML trees (Figs 1, 2) indicate that the new species described below forms a highly supported sister group to other species of *Langdonia* as found from ITS+LSU+*EF-1α* analyses. Estimates for posteriori probabilities are indicated on branches of the tree (Fig. 1). In both analyses, isolates collected in this study clustered with values of 1.0 and 100 for MrBayes and RAxML, respectively (Figs 1, 2). The ITS+LSU+*EF-1α* dataset showed that the monophyly of these isolates within the *Ustilaginaceae* was fully supported. All taxa of *Langdonia*

© 2021 Westerdijk Fungal Biodiversity Institute

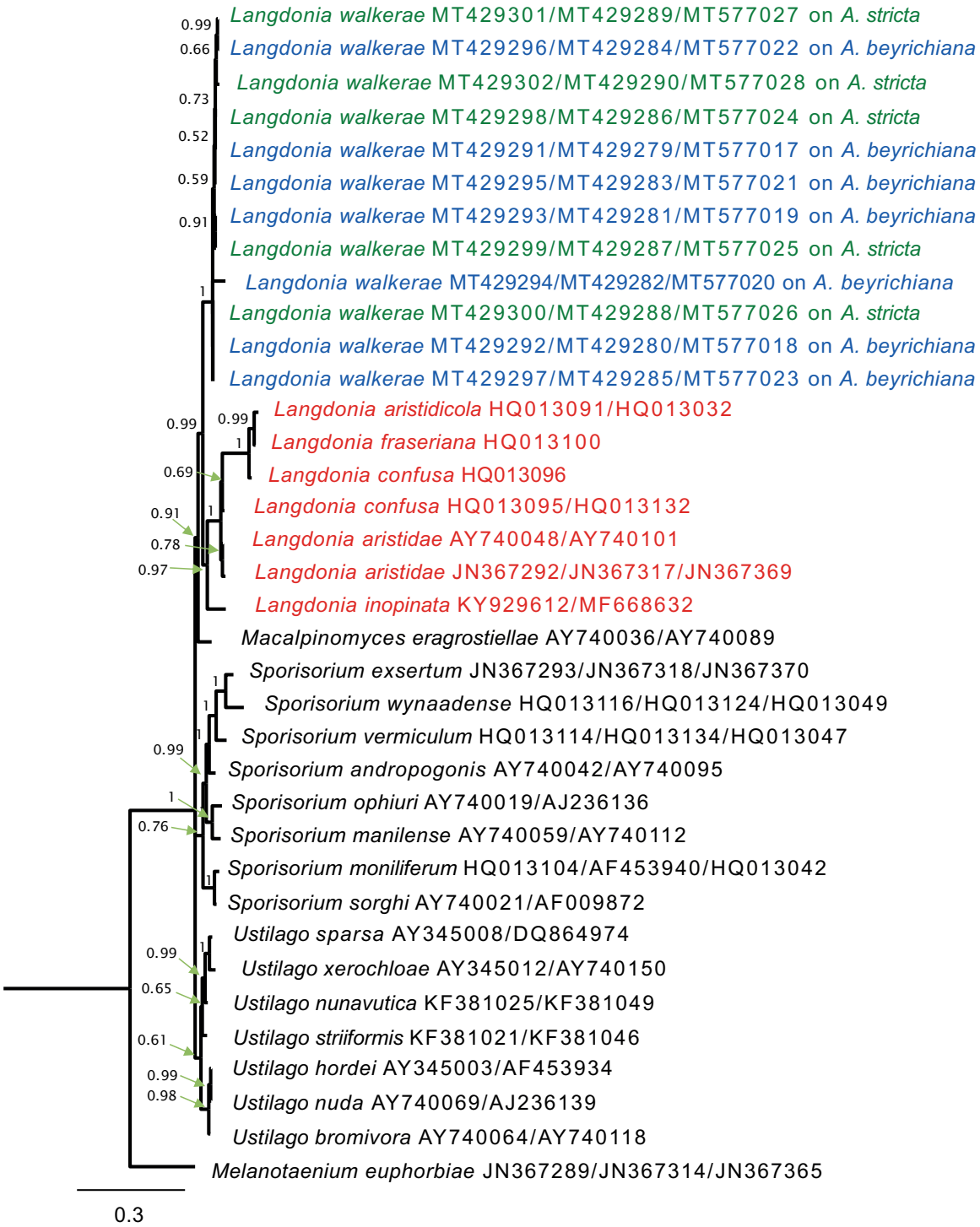

Fig. 1. Bayesian inference of phylogenetic relationships resulting from the analysis of ITS, LSU and *EF-1α* sequences. Numbers on the branches are estimates for Posterior Probability from Bayesian inference. The tree was rooted using *Melanotaenium euphorbiae.*

on *Aristida* spp. formed a well-supported monophyletic clade in the *Ustilaginaceae* and were well separated from the representatives of species in other genera of this family. Within this clade of *Langdonia* species, all isolates from both *Aristida* species clustered with strong support. In MrBayes and RAxML analyses of the alignment, *Macalpinomyces eragrostiellae* was sister to the clade of *Langdonia* species (Fig. 2).

Taxonomy

Langdonia walkerae Alqurashi, J. Kerrigan & K. G. Savchenko, ***sp. nov.*** MycoBank MB 839451. Fig. 3A–F.

Etymology: Named after Dr. Joan L. Walker (USDA-Forest Service), a plant ecologist and conservationist who observed and contemplated the ecological significance of the sori in *A. stricta* and *A. beyrichiana* inflorescences as early as 1979 and brought that to our attention for study.

© 2021 Westerdijk Fungal Biodiversity Institute

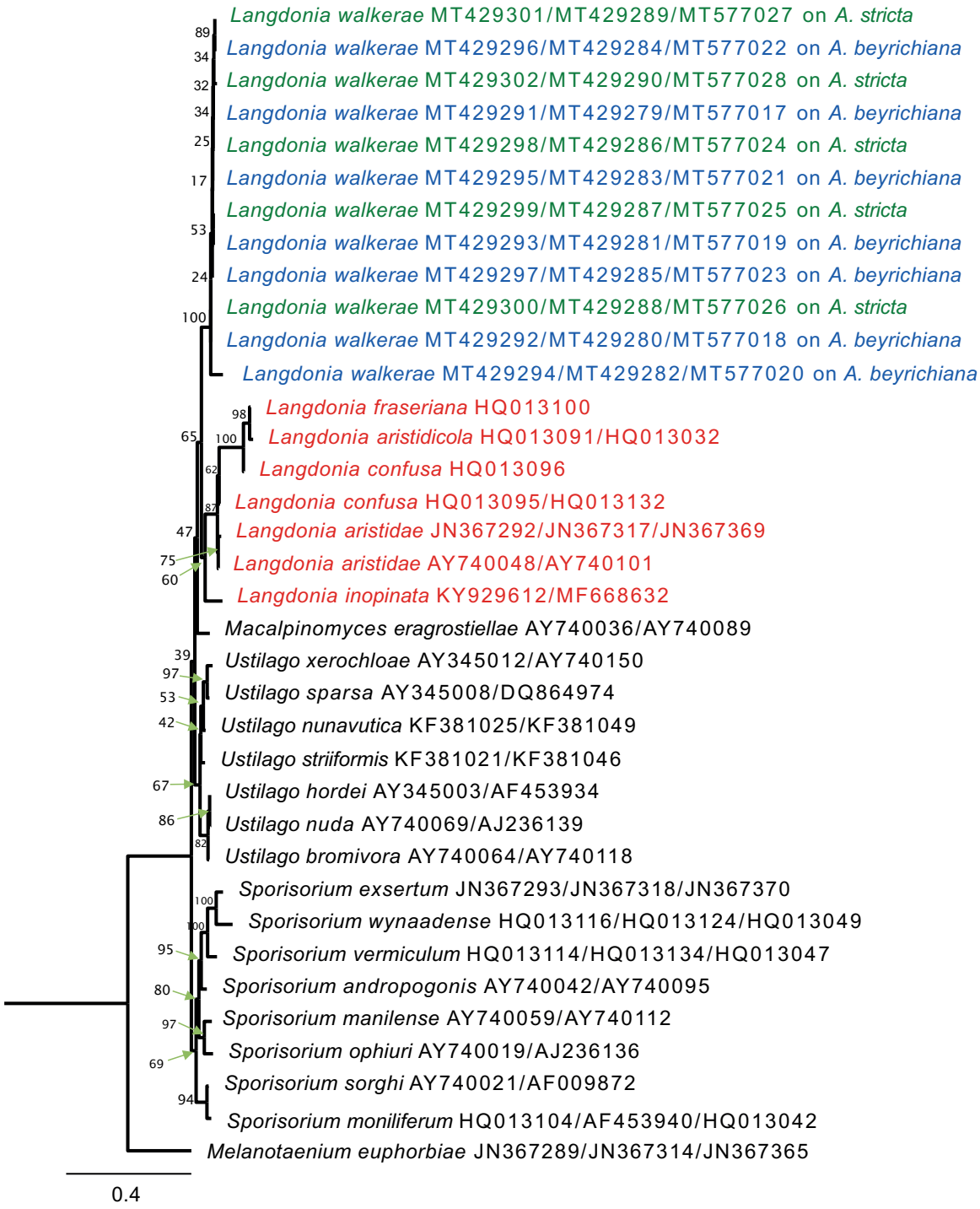

Fig. 2. Maximum likelihood of phylogenetic relationships resulting from the analysis of ITS, LSU and *EF-1α* sequences. Numbers on the branches are estimates of bootstrap support values. The tree was rooted using *Melanotaenium euphorbiae.*

Typus: **USA**, South Carolina, Silver Bluff Audubon Center, on *Aristida beyrichiana*, 10 Nov. 2017, *J. Kerrigan* & *A.S. Alqurashi*, CLEMS 0080381, CLEMS 0080382 (holotype WSP 74240; isotype BPI 911222).

Sori in some ovaries, covered at first by a dark herbage green and later by a dark brick peridium. *Sori* are conspicuous, ovoid or symmetrically fusiform with an acute tip and sized between 1–1.5 × 2.5–7 mm. *Teliospores* are solitary, not compacted into spore balls, dark sienna in color. In the plane view, teliospores are globose, subglobose, or ellipsoidal and sized 8–13 µm diam. In the side view, teliospores are slightly flattened tangentially. *Spore walls* are uniformly thick, aculeate, and have dense conical spines (Ulloa & Hanlin 2000). *Columella*, *spore balls,* and *sterile cells* are lacking.

Host: *Aristida beyrichiana* (*Poaceae*).

Distribution: USA, southern part of South Carolina to southern Florida.

Additional specimens examined: On *Aristida beyrichiana*. **USA**, South Carolina, Silver Bluff Audubon Center, 6 Dec. 2018, *A.S. Alqurashi* & *A.H. Alqurashi*, CLEMS 0080383 & CLEMS 0080384; South Carolina,

Table 2. Species of fungi used in phylogenetic analyses for this study, including host plant and country of origin.

Species	Voucher/Isolate	Host	Country	GenBank accession no.		
				ITS	LSU	*EF-1α*
Langdonia aristidae	H.U.V.19145	*Aristida urugayensis*	Germany	AY740048	AY740101	n/a
	HUV19145	*Aristida urugayensis*	Argentina	JN367292	JN367317	JN367369
Langdonia aristidicola	BRIP 26930	*Aristida jerichoensis*	Australia	HQ013091	n/a	HQ013032
Langdonia confusa	BRIP 42670	*Aristida queenslandica*	Australia	HQ013095	HQ013132	n/a
	BRIP 52755	*Aristida sp.*	Australia	HQ013096	n/a	n/a
Langdonia fraseriana	BRIP 49668	*Aristida nitidula*	Australia	HQ013100	n/a	n/a
Langdonia inopinata	M-0215944	*Aristida adscensionis*	Zambia	KY929612	MF668632	n/a
Langdonia walkerae	JK 5017	*Aristida beyrichiana*	USA, SC	**MT429291**	**MT429279**	**MT577017**
	JK 6017	*Aristida beyrichiana*	USA, SC	**MT429292**	**MT429280**	**MT577018**
	SB 1218	*Aristida beyrichiana*	USA, SC	**MT429293**	**MT429281**	**MT577019**
	AGT 1218	*Aristida beyrichiana*	USA, SC	**MT429294**	**MT429282**	**MT577020**
	SRS 1218	*Aristida beyrichiana*	USA, SC	**MT429295**	**MT429283**	**MT577021**
	FLW 1017	*Aristida beyrichiana*	USA, FL	**MT429296**	**MT429284**	**MT577022**
	FL 1218	*Aristida beyrichiana*	USA, FL	**MT429297**	**MT429285**	**MT577023**
	CSN 1118	*Aristida stricta*	USA, SC	**MT429298**	**MT429286**	**MT577024**
	NC 1018	*Aristida stricta*	USA, NC	**MT429299**	**MT429287**	**MT577025**
	NC 2018	*Aristida stricta*	USA, NC	**MT429300**	**MT429288**	**MT577026**
	NC 3018	*Aristida stricta*	USA, NC	**MT429301**	**MT429289**	**MT577027**
	NC 5018	*Aristida stricta*	USA, NC	**MT429302**	**MT429290**	**MT577028**
Macalpinomyces eragrostiellae	Ust. Exs. 960	*Eragrostiella bifaria*	India	AY740036	AY740089	n/a
Melanotaenium euphorbiae	HUV17733	*Euphorbia heterophylla*	Papua New Guinea	JN367289	JN367314	JN367365
Sporisorium andropogonis	56588 (M)	*Bothriochloa saccharoides*	Ecuador	AY740042	AY740095	n/a
Sporisorium exsertum	KVU965	*Themeda triandra*	Australia	JN367293	JN367318	JN367370
Sporisorium manilense	Ust.Exs.854 (M)	*Sacciolepis indica*	India	AY740059	AY740112	n/a
Sporisorium moniliferum	BRIP 52504	*Heteropogon contortus*	Australia	HQ013104	n/a	HQ01302
Sporisorium ophiuri	HB 20	*Rottboellia cochinchinensis*	Unknown	AY740019	AJ236136	n/a
Sporisorium sorghi	MP 2036a	*Sorghum bicolor*	Nicaragua	AY740021	AF009872	n/a
Sporisorium vermiculum	BRIP 49748	*Sorghum plumosum*	Australia	HQ013114	HQ013134	HQ01307
Sporisorium wynaadense	BRIP 27640	*Sarga leiocladum*	Australia	HQ013116	HQ013124	HQ01309
Ustilago bromivora	H.U.V.19322	*Bromus catharticus*	Argentina	AY740064	AY740118	n/a
Ustilago hordei	Ust.exs.784	*Hordeum vulgare*	Iran	AY345003	AF453934	n/a
Ustilago nuda	H.U.V.17782	*Hordeum leporinum*	Greece	AY740069	AJ236139	n/a
Ustilago nunavutica	DAOM 91211	*Puccinellia angustata*	Canada	KF381025	KF381049	n/a
Ustilago sparsa	Ust.exs.892	*Dactyloctenium aegyptium*	India	AY345008	DQ864974	n/a
Ustilago striiformis	HAI 4610	*Milium effusum*	Ukraine	KF381021	KF381046	n/a
Ustilago xerochloae	Ust. Exs. 1000	*Xerochloa imberbis*	Australia	AY345012	AY740150	n/a

Note: Species and accession numbers in bold are new sequences from this study.

Aiken Gopher Tortoise Heritage Preserve, 6 Dec. 2018, *A.S. Alqurashi* & *A.H. Alqurashi*, CLEMS 0080385; South Carolina, Savannah River Site, 4 Dec. 2018, *L. Lee,* CLEMS 0080388, WSP 74241, BPI 911220; Florida, Apalachicola Bluffs and Ravines Preserve, 31 Oct. 2017, *J. Walker*, CLEMS 0080387; Florida, Austin Cary Forest, 3 Dec. 2018, *J. Hong*, CLEMS 0080386. On *Aristida stricta*. **USA**, North Carolina, North Carolina Sandhills Game Land, 27 Nov. 2018, *A.S. Alqurashi, A.H. Alqurashi* & *B. Beck*, CLEMS 0080389, WSP 74242, BPI 911221;

© 2021 Westerdijk Fungal Biodiversity Institute

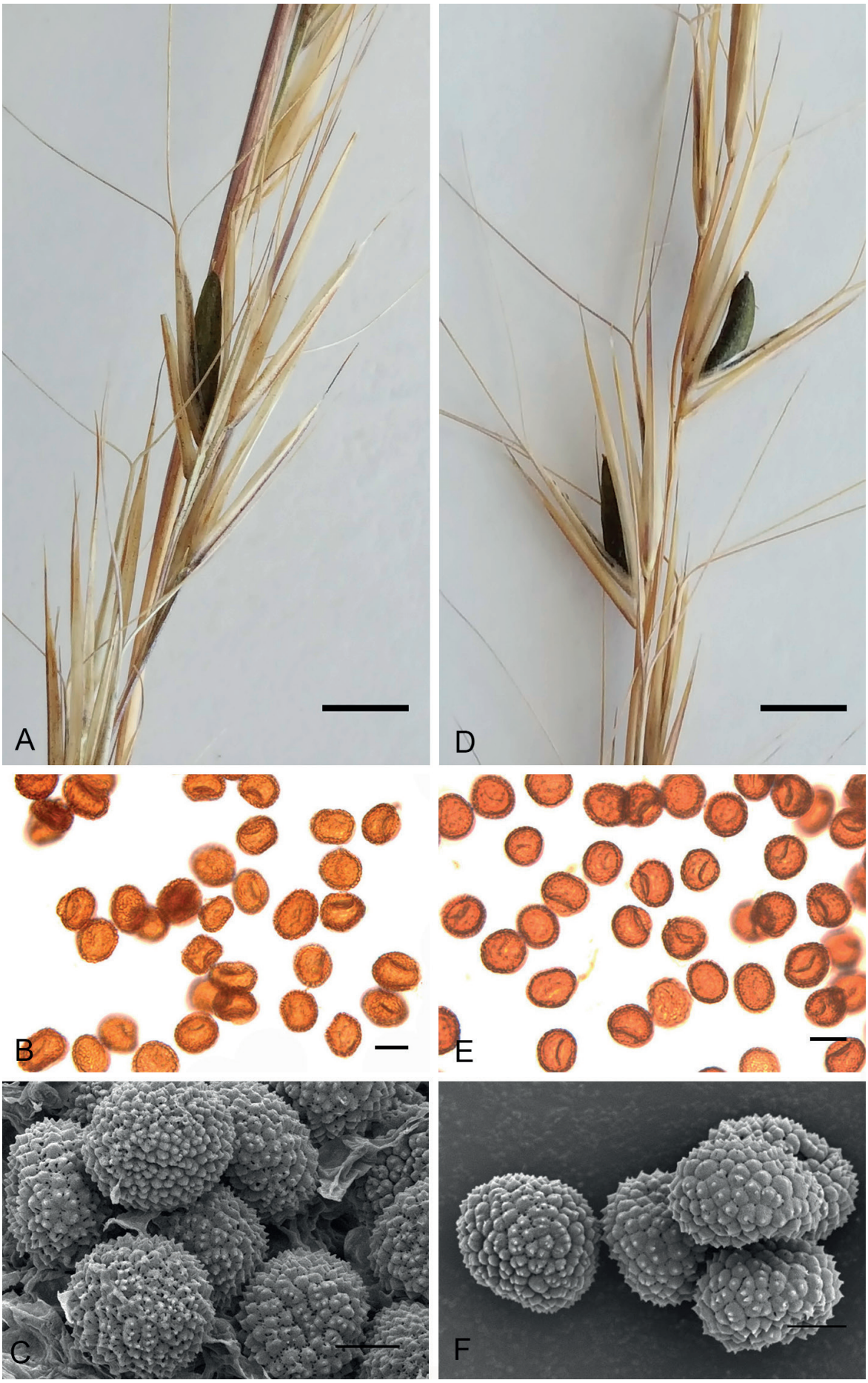

Fig. 3. Sori and teliospores of *Langdonia walkerae sp. nov.* on *Aristida beyrichiana* (A–C) and on *Aristida stricta* (D–F). **A.** Sori (WSU 74240). **B.** Teliospores viewed with transmitted light. **C.** Scanning electron micrograph (SEM) of teliospores. **D.** Sori. **E.** Teliospores viewed with transmitted light. **F.** SEM of teliospores. Scale bars: A, D = 2 mm; B, E = 10 µm; C, F = 5 µm.

© 2021 Westerdijk Fungal Biodiversity Institute

South Carolina, Carolina Sandhills National Wildlife Refuge, 29 Nov. 2018, *A.S. Alqurashi* & *A.H. Alqurashi*, CLEMS 0080390, WSP 74243, BPI 911219.

Notes: Morphologically, *Langdonia walkerae* is distinguished from other species of *Langdonia* by teliospores that are not compacted into spore balls (McTaggart *et al*. 2012a, b). Phylogenetically, there is a strong support to recognize *L. walkerae* as a separate species.

DISCUSSION

Smut specimens from two species of wiregrass, *A. stricta* and *A. beyrichiana*, collected from longleaf pine ecosystems in three southeastern states — South Carolina, North Carolina, and Florida — were examined and compared in terms of morphology and DNA sequence data. Our findings determined both *Aristida* species were infected by the same pathogen, which was identified as a new species. *Langdonia walkerae* is designated as a new species based on its morphological and phylogenetic differences from the other described species of *Langdonia*. Only eight other species of *Langdonia* have been erected, including *L. aristidae*, *L. aristidaria, L. aristidicola*, *L. clandestina, L. confusa, L. fraseriana, L. goniospora,* and *L. inopinata*. All of these species have been reported from two or more *Aristida* species. For example, *L. confusa,* originally named *Sporisorium confusum,* was reported from several species of *Aristida* including *A. dichotoma*, *A. fendleriana*, *A. spiciformis*, and *A. wrightii* from several US states (Farr & Rossman 2020). In contrast, one host has been reported to be infected by different *Langdonia* species. For example, *Aristida adscensionis* is infected by *Sporisorium aristidicola* ≡ *Langdonia aristidicola*, *S. consanguineum* ≡ *L. aristidae*, and *S. inopinatum* ≡ *L. inopinata* in Zambia, India, and Zimbabwe, respectively (Farr & Rossman 2020). In the present study, sori were found in a proportion of the ovaries of *A. stricta* and *A. beyrichiana*. This is similar to four species of *Langdonia*, namely *L. aristidaria* (Durán 1987), *L. aristidicola, L. clandestina* and *L. inopinata* (Vánky 2012). In the other four species of *Langdonia*, namely *L. confusa*, *L. aristidae*, *L. fraseriana* and *L. goniospora,* the sori are produced in all ovaries of an inflorescence on a culm of the host plants (Vánky 2012).

Langdonia walkerae teliospores were solitary in all specimens examined on *A. stricta* and *A. beyrichiana*, and no spore balls were observed. This finding conflicts with that from McTaggart *et al*. (2012b), who considered this an apomorphic characteristic among the species of *Langdonia*. Based on our data, the genus *Langdonia* seems to be sharing the recent common ancestor with *Macalpinomyces eragrostiellae*, another species with well-defined spore balls. It is possible that the ancestors of *L. walkerae* have had spore balls, but they were lost in the process of species evolution.

The absence of spore balls leads us to infer that this fungus is a new species of *Langdonia*, and the genus description, which states that teliospores are compacted into spore balls (McTaggart *et al*. 2012b), needs to be emended. The size of teliospores is distinct from *L. confusa* and *L. aristidae*, both of which have larger teliospore diameters, and from *L. aristidaria, L. aristidicola*, *L. clandestina, L. fraseriana, L. goniospora,* and *L. inopinata,* all of which have smaller teliospore diameters (Durán 1987, Vánky 2012, Denchev *et al*. 2015). Furthermore, the teliospore wall ornamentation of *L. walkerae* is distinguishable from other described species by having dense conical spines whereas the teliospore wall ornamentation in other species of *Langdonia* varies from smooth to verruculose (Vánky 2012). For example, the wall ornamentation in *Sporisorium confusum* ≡ *L. confusa* on *A. dichotoma* was densely verrucose-echinulate and in *S. consanguineum* ≡ *L. aristidae* on *A. arizonica*, the teliospores wall were almost smooth to finely verruculose (Vánky 2012). Teliospore germination of *L. walkerae* is *Ustilago*-type, and columella and sterile cells are absent, fitting the description of the genus *Langdonia*. No data are available from previous studies to compare the culture growth of *L. walkerae* with other species of *Langdonia*.

Phylogenetic analysis demonstrated that all 12 isolates included in this study, five on *A. stricta* and seven on *A. beyrichiana,* form a highly supported monophylum, clustering in one separate phylogenetic clade within the *Ustilaginaceae*. These isolates were sister to other species of *Langdonia* and together formed a monophyletic group supporting the results of McTaggart *et al*. (2012b).

Although many species of *Langdonia* were reported on different species of *Aristida* in different regions around the world, only limited molecular data are available in GenBank for some of these species. Thus, additional sequences are needed for a more complete understanding of the phylogenetic relationships within this genus. The current study shows that *L. walkerae* on *A. stricta* and *A. beyrichiana* is clearly distinguishable morphologically and phylogenetically from other species of *Langdonia* on *Aristida* spp. More material from additional locations in longleaf pine ecosystems should be collected and analyzed to determine if *L. walkerae* occurs throughout the natural range of longleaf pine.

ACKNOWLEDGEMENTS

Research was supported by the USDA–FS. Technical Contribution No. 6910 of the Clemson University Experiment Station. This material is based upon work supported by NIFA/USDA, under project number SC-1700560. We thank the curators of Aiken Gopher Tortoise Heritage Preserve, Carolina Sandhills National Wildlife Refuge, North Carolina Sandhills Game Land, and Silver Bluff Audubon Center for permissions to sample. Special thanks to Brady Beck, the southern piedmont management biologist, for his extreme field assistance in collecting the samples. Also, thanks to Dr. Joan Walker, Jessica Hong and Linda Lee for providing samples from Apalachicola Bluffs and Ravines Preserve, Austin Cary Forest, and Savannah River Site, respectively. We thank Dayton Cash and George Wetzel at Clemson University electron microscopy facility. We also thank Karen Bryson, Andrew Gitto and Linus Schmitz for technical assistance and Xinyuan Ma for his assistance in molecular data analysis. Also, thanks to the curators of CLEMSON, BPI and WSP herbaria for their help in depositing the samples. We thank Drs Steven Jeffers, Guido Schnabel, and Joan Walker for their valuable reviews and suggestions for the manuscript.

Conflict of interest: The authors declare that there is no conflict of interest.

REFERENCES

Barkworth ME, Capels KM, Long S, Michael B (2003). *Flora of North America, North of Mexico*: **25**, Part 2. *Magnoliophyta: Commelinidae* (in Part): *Poaceae*. Oxford University Press, NY, USA.

© 2021 Westerdijk Fungal Biodiversity Institute

Bauer R, Begerow D, Oberwinkler E, *et al*. (2001). *Ustilaginomycetes*. In: *Systematic and Evolution* (McLaughlin DJ, McLaughlin EG, Lemke PA, eds). *The Mycota* **7**: Part B. Springer, Berlin, Heidelberg: 57–83.

Begerow D, Bauer R, Oberwinkler F (1997). Phylogenetic studies on nuclear large subunit ribosomal DNA sequences of smut fungi and related taxa. *Canadian Journal of Botany* **75**: 2045–2056.

Begerow D, John B, Oberwinkler F (2004). Evolutionary relationships among β-tubulin gene sequences of basidiomycetous fungi. Part 222 of the series 'Studies in *Heterobasidiomycetes'*. *Mycological research* **108**: 1257–1263.

Begerow D, Stoll M, Bauer R (2006). A phylogenetic hypothesis of *Ustilaginomycotina* based on multiple gene analyses and morphological data. *Mycologia* **98**: 906–916.

Brockway DG, Outcalt KW, Wilkins RN (1998). Restoring longleaf pine wiregrass ecosystems: plant cover, diversity and biomass following low-rate hexazinone application on Florida sandhills. *Forest Ecology and Management* **103**: 159–175.

Cerros-Tlatilpa R, Columbus JT, Barker NP (2011). Phylogenetic relationships of *Aristida* and relatives (*Poaceae*, *Aristidoideae*) based on noncoding chloroplast (trnL-F, rpl16) and nuclear (ITS) DNA sequences. *American Journal of Botany* **98**: 1868–1886.

Clewell AF (1989). Natural history of wiregrass (*Aristida strida* Michx., *Gramineae*). *Natural Areas Journal* **1**: 223–233.

Criscuolo A, Gribaldo S (2010). BMGE (Block Mapping and Gathering with Entropy): a new software for selection of phylogenetic informative regions from multiple sequence alignments. *BMC Evolutionary Biology* **10**: 1–21.

Denchev TT, Vorontsova MS, Denchev CM (2015). First record of *Langdonia aristidae* (*Ustilaginales*) from Madagascar. *Mycobiota* **5**: 15–20.

Duever LC (1989). Research priorities for the preservation, management, and restoration of wiregrass ecosystems. *Natural Areas Journal* **9**: 214–218.

Durán R (1987). *Ustilaginales of Mexico: Taxonomy, symptomatology, spore germination, and basidial cytology*. Washington State University Press, Pullman, WA, USA.

Farr DF, Rossman AY (2020). Fungal Databases, systemic mycology and microbiology laboratory, ARS, USDA. Retrieved June 30, 2020, from https://nt.arsgrin.gov/fungaldatabases/

Fill JM, Welch SM, Waldron JL, *et al*. (2012). The reproductive response of an endemic bunchgrass indicates historical timing of a keystone process. *Ecosphere* **3**: 1–12.

Frost C (2007). History and future of the longleaf pine ecosystem. In: *The longleaf pine ecosystem* (Jose S, Jokela EJ, Miller DL, eds). Springer, NY, USA: 9–48.

Huelsenbeck JP, Ronquist F (2001). MRBAYES: Bayesian inference of phylogenetic trees. *Bioinformatics* **17**: 754–755.

Lemoine F, Correia D, Lefort V, *et al*. (2019). NGPhylogeny.fr: new generation phylogenetic services for non-specialists. *Nucleic Acids Research* **47**: W260–W265.

McTaggart AR, Shivas RG, Geering A, *et al*. (2012a). Soral synapomorphies are significant for the systematics of the *Ustilago-Sporisorium-Macalpinomyces* complex (*Ustilaginaceae*). *Persoonia* **29**: 63–77.

McTaggart AR, Shivas RG, Geering ADW, *et al*. (2012b). Taxonomic revision of *Ustilago, Sporisorium and Macalpinomyces*. *Persoonia* **29**: 116–132.

Means DB (2007). Vertebrate faunal diversity of longleaf pine ecosystems. In: *The longleaf pine ecosystem* (Jose S, Jokela EJ, Miller DL, eds). Springer, NY, USA: 157–213.

Noss RF (1989). Longleaf pine and wiregrass: keystone components of an endangered ecosystem. *Natural Areas Journal* **9**: 211–213.

Nylander JAA (2004). *MrModeltest v2.* (Programme distributed by the author). Evolutionary Biology Centre, Uppsala University, Sweden.

Peet RK (1993). A taxonomic study of *Aristida stricta* and *A. beyrichiana*. *Rhodora* **1**: 25–37.

Platt WJ (1999). Southeastern pine savannas. In: *Savannas, barrens, and rock outcrop plant communities of North America* (Anderson RC, Fralish JS, Basking JM, eds). Cambridge University Press, Cambridge, UK: 23–51.

Rayner RW (1970). *A mycological colour chart*. British Mycological Society Press, UK.

Savchenko KG, Carris LM, Castlebury LA, *et al*. (2014). Stripe smuts of grasses: one lineage or high levels of polyphyly? *Persoonia* **33**: 169–181.

Shearman TM, Varner JM, Kreye JK (2019). Pyrogenic flowering of *Aristida beyrichiana* following 50 years of fire exclusion. *Ecosphere* **10**: e02541.

Stamatakis A (2014). RAxML version 8: a tool for phylogenetic analysis and post-analysis of large phylogenies. *Bioinformatics* **30**: 1312–1313.

Stoll M, Piepenbring M, Begerow D, Oberwinkler F (2003). Molecular phylogeny of *Ustilago* and *Sporisorium* species (*Basidiomycota*, *Ustilaginales*) based on internal transcribed spacer (ITS) sequences. *Canadian Journal of Botany* **81**: 976–984.

Ulloa M, Hanlin RT (2000). *Illustrated dictionary of mycology*. American Phytopathological Society. APS Press, St. Paul, MN, USA.

Van Eerden BP (1997). *Studies on the reproductive biology of wiregrass (Aristida stricta Michx.) in the Carolina sandhills*. M.S. thesis. University of Georgia, Athens, USA.

Vánky K (2012). *Smut fungi of the world*. The American Phytopathological Society. APS Press, St. Paul, MN, USA.

Vánky K (2013). *Illustrated genera of smut fungi*. The American Phytopathological Society. APS Press, St. Paul, MN, USA.

Vilgalys R, Hester M (1990). Rapid genetic identification and mapping of enzymatically amplified ribosomal DNA from several *Cryptococcus* species. *Journal of Bacteriology* **172**: 4238–4246.

White TJ, Bruns T, Lee S, *et al*. (1990). Amplification and direct sequencing of fungal ribosomal RNA genes for phylogenetics. In: *PCR protocols*: *A guide to methods and applications* (Innis MA, Gelfand DH, Sninsky JJ, *et al*., eds). Academic Press, NY, USA: 315–322.

© 2021 Westerdijk Fungal Biodiversity Institute

© 2021 Westerdijk Fungal Biodiversity Institute

FUSE

Fungal Systematics and Evolution

VOLUME 8
DECEMBER 2021
PAGES 49–64

doi.org/10.3114/fuse.2021.08.05

Phylogenetic placement of *Iodosphaeriaceae* (*Xylariales, Ascomycota*), designation of an epitype for the type species of *Iodosphaeria*, *I. phyllophila*, and description of *I. foliicola sp. nov.*

A.N. Miller[1*], M. Réblová[2]

[1]Illinois Natural History Survey, University of Illinois Urbana-Champaign, Champaign, IL, USA
[2]Czech Academy of Sciences, Institute of Botany, 252 43 Průhonice, Czech Republic

*Corresponding author: amiller7@illinois.edu

Key words:
1 new taxon
epitypification
phylogeny
systematics
taxonomy

Abstract: The *Iodosphaeriaceae* is represented by the single genus, *Iodosphaeria*, which is composed of nine species with superficial, black, globose ascomata covered with long, flexuous, brown hairs projecting from the ascomata in a stellate fashion, unitunicate asci with an amyloid apical ring or ring lacking and ellipsoidal, ellipsoidal-fusiform or allantoid, hyaline, aseptate ascospores. Members of *Iodosphaeria* are infrequently found worldwide as saprobes on various hosts and a wide range of substrates. Only three species have been sequenced and included in phylogenetic analyses, but the type species, *I. phyllophila*, lacks sequence data. In order to stabilize the placement of the genus and family, an epitype for the type species was designated after obtaining ITS sequence data and conducting maximum likelihood and Bayesian phylogenetic analyses. *Iodosphaeria foliicola* occurring on overwintered *Alnus* sp. leaves is described as new. Five species in the genus form a well-supported monophyletic group, sister to the *Pseudosporidesmiaceae* in the *Xylariales*. Selenosporella-like and/or ceratosporium-like synasexual morphs were experimentally verified or found associated with ascomata of seven of the nine accepted species in the genus. Taxa included and excluded from *Iodosphaeria* are discussed.

Citation: Miller AN, Réblová M (2021). Phylogenetic placement of *Iodosphaeriaceae* (*Xylariales*, *Ascomycota*), designation of an epitype for the type species of *Iodosphaeria*, *I. phyllophila*, and description of *I. foliicola sp. nov. Fungal Systematics and Evolution* **8**: 49–64. doi: 10.3114/fuse.2021.08.05
Received: 28 May 2021; **Accepted:** 10 July 2021; **Effectively published online:** 19 July 2021
Corresponding editor: P.W. Crous

INTRODUCTION

Iodosphaeria was introduced by Samuels *et al.* (1987) to accommodate the type species, *I. phyllophila* based on *Lasiosphaeria phyllophila* (Mouton 1900), and a second species, *I. ripogoni*. Seven additional species have been added to the genus: *I. aquatica*, *I. arundinariae*, *I. honghensis*, *I. hongkongensis*, *I. podocarpi*, *I. polygoni*, and *I. tongrenensis* (MycoBank, www.mycobank.org, accessed on 7 Apr. 2021). Morphological and molecular analyses of *I. aquatica* have led to uncertainty in its taxonomic placement (Hsieh *et al.* 1997, Kang *et al.* 1999, Taylor & Hyde 1999). Jeewon *et al.* (2003) showed the genus to be paraphyletic when they included *I. aquatica* and another *Iodosphaeria* sp. in their molecular analyses. A key to all known species of *Iodosphaeria* was presented in Marasinghe *et al.* (2019).

Sexual morphs are comprised of superficial, black, globose to subglobose, non-stromatic ascomata with flat apices and covered with long, brown, flexuous hairs, a two-layered ascomal wall, cylindrical, 8-spored asci sometimes with an amyloid apical ring or ring is lacking, and ellipsoidal, allantoid or fusiform, hyaline, aseptate ascospores with or without a gelatinous sheath. Selenosporella- and ceratosporium-like synasexual morphs have been reported on the surface of ascomata in *I. tongrenensis* (Li *et al.* 2015), on field-collected material of *I. phyllophila* (Bell & Mahoney 2016) and *I. ripogoni* (Samuels *et al.* 1987, Bell & Mahoney 2016) and in cultures of *I. phyllophila* (Samuels *et al.* 1987). Ceratosporium-like conidia were observed on the host surface in *I. honghensis* (Marasinghe *et al.* 2019). Members of *Iodosphaeria* are infrequently found worldwide as saprobes on a variety of hosts and a wide range of substrates including dead branches, stems, vines, leaves and petioles.

Iodosphaeria was initially placed in the *Amphisphaeriaceae* (Samuels *et al.* 1987) based on its synasexual morphs and amyloid ascal ring, but Barr (1990) later transferred it to the *Lasiosphaeriaceae* based on ascomal wall anatomy and centrum similarities. It was placed in the *Trichosphaeriaceae* by Réblová (1999). Hilber & Hilber (2002) created a new family, *Iodosphaeriaceae*, for the genus. The family, represented by *I. honghensis* and *I. tongrenensis*, is placed in the *Xylariales* based on morphology and phylogeny (Marasinghe *et al.* 2019).

Only three species, *I. aquatica*, *I. honghensis* and *I. tongrenensis*, have been sequenced and included in phylogenetic analyses. Because the type species has never been sequenced, ambiguity surrounds the placement of the genus and family. The type material of *I. phyllophila*, described from decaying leaves of *Betula alba* and *Corylus* from Belgium, is sparse and over 120 years old, so attempts to obtain molecular data from this material would be futile. The goals of this study were to designate an epitype of *I. phyllophila* from the

Fungal Systematics and Evolution is licensed under a Creative Commons Attribution-NonCommercial-ShareAlike 4.0 International License

© 2021 Westerdijk Fungal Biodiversity Institute

country of origin, obtain sequence data from the epitype and provide a stable phylogenetic placement for *Iodosphaeria* and *Iodosphaeriaceae*. During our investigation, two specimens of unknown *Iodosphaeria* from Canada were discovered and compared with the known species.

MATERIALS AND METHODS

Taxon sampling and morphological examination

Fresh specimens were collected in the field, dried and stored in paper packets. No attempts were made to obtain these specimens in culture. All specimens are deposited in Meise Botanic Garden (BR, Meise, Belgium), the Fungarium of the Illinois Natural History Survey (ILLS, Champaign, Illinois, USA) and the New Zealand Fungarium (PDD, Auckland, New Zealand). Other specimens were obtained from the Plant Pathology Herbarium, Cornell University (CUP, Ithaca, New York, USA), New Brunswick Museum (NBM, Saint John, Canada), and Staatliche Naturwissenschaftliche Sammlungen Bayerns (M, Munich, Germany).

Ascomata were squash-mounted in distilled water and micromorphological structures were examined on an Olympus BX51 compound microscope using differential interference or phase contrast microscopy. Images were processed using Adobe Photoshop 2021 (Adobe Systems Inc., Mountain View, California). A minimum of 30 measurements was taken for all morphological structures using Olympus cellSens Standard v. 1.14 image analysis software after digital capture with an Olympus DP70 or a XC50 5.0 megapixel digital camera using Olympus Imaging Software Cell^D. Sections of the ascomal wall were prepared at 25 µm thickness using a Physitemp BSF-3 freezing stage mounted on a Leica SM2000 sliding microtome.

Molecular data

DNA was extracted directly from ascomata using an E.Z.N.A.® Microelute Genomic DNA kit (Omega Bio-tek, Norcross, Georgia, USA) following the manufacturer's instructions. The entire internal transcribed spacer (ITS) region and the first 600 bp of the 5' end of 28S nuclear large subunit (LSU) were PCR amplified using known primers (Vilgalys & Hester 1990, White *et al.* 1990, Rehner & Samuels 1995). PCR reactions contained 12.5 µL GoTaq® Green Master Mix (Promega, Madison, Wisconsin, USA), 2.5 µL of BSA (bovine serum albumin, New England Biolabs, Ipswich, MA), 2.5 µL of DMSO (dimethyl sulfoxide, Fisher Scientific, Pittsburgh, PA), 1.5 µl of each 10 mM primer, and 3–5 µl genomic DNA. PCR amplification of ITS and LSU was performed on a Bio-Rad C1000 thermal cycler under the following conditions: initial denaturation at 94 °C for 2 min, followed by 40 cycles of 94 °C for 30 s, 41 °C for 45 s, and 72 °C for 1 min with a final extension step of 72 °C for 10 min. After verification on an ethidium bromide-stained 1 % TBE agarose gel, PCR products were purified with a Wizard® SV Gel and PCR Clean-Up System (Promega, Madison, Wisconsin, USA). Purified PCR products were used in 11 µL sequencing reactions to sequence both strands with BigDye Terminators v. 3.1 (Applied Biosystems, Foster City, CA) in combination with the following ITS primers: ITS1F, ITS2, ITS3, ITS4, and LSU primers: LR0R, LR3. Sequences were generated on an Applied Biosystems 3730XL high throughput capillary sequencer at the Roy J. Carver Biotechnology Center at the University of Illinois Urbana-Champaign (Champaign, Illinois, USA). Consensus sequences for each gene were assembled with Sequencher v. 5.4 (Gene Codes Corp., Ann Arbor, Michigan, USA) and each sequence was subjected to an individual BLASTn analysis to verify its identity. PCR amplifications of *rpb2* and *tef1-α* were unsuccessful.

Phylogenetic analyses

The ITS-LSU for newly sequenced taxa was added to the combined ITS-LSU-*rpb2-tef1-α* alignment from Réblová *et al.* (2021). The two protein-coding genes were kept in the analyses to provide backbone support for higher level taxa. Portions of the 5' and 3' ends of each gene were excluded from all analyses due to missing data in most taxa and aligned using MUSCLE (Edgar 2004). PartitionFinder2 (Lanfear *et al.* 2016) was used to determine the best-fit model for each dataset, which was the SYM+I+G model for ITS, and the GTR+I+G model for LSU, *rpb2* and *tef1-α*. A maximum likelihood (ML) analysis with 1 000 bootstrap replicates was performed using RAxML-HPC2 v. 8.2.12 (Stamatakis 2014) with a GTRCAT approximation using the CIPRES Science Gateway v. 3.3 portal (Miller *et al.* 2010). Bootstrap replicates were performed 1 000 times under the GTR model employing a GAMMA model of rate heterogeneity and the rapid bootstrapping option (Stamatakis *et al.* 2008). Clades with bootstrap support (BS) values ≥ 70 % were considered significant and strongly supported (Hillis & Bull 1993). Bayesian Inference (BI) analysis was performed using MrBayes v. 3.2.7 (Huelsenbeck & Ronquist 2001, 2005) under the GTR model on the CIPRES v. 3.3 portal. Constant characters were included and 10 M generations with trees sampled every 1 000th generation were run, resulting in 10 000 total trees. The first 2 500 trees were discarded as burn-in, and Bayesian posterior probabilities (PP) were determined from a consensus tree generated from the remaining 7 500 trees using PAUP v. 4.0b10 (Swofford 2002). Clades with PP ≥ 95 % were considered significant and strongly supported (Larget & Simon 1999, Alfaro *et al.* 2003).

RESULTS

Phylogenetic analysis

The ITS-LSU region was sequenced for *I. phyllophila*, *I. ripogoni* and the new species (Table 1) and ML and BI analyses were performed on ITS-LSU and ITS-LSU-*rpb2-tef1-α* datasets of 90 representatives of the *Xylariales* modified from Réblová *et al.* (2021). Outgroup taxa were *Bactrodesmium abruptum* and *B. diversum* (*Savoryellaceae*) and *Helicoascotaiwania lacustris* and *Pleurotheciella erumpens* (*Pleurotheciaceae*). Initially, we performed an ITS-LSU analysis (results not shown) to assess the placement of *Iodosphaeria* and the new species in the *Xylariales*. The backbone of the ML tree was largely unresolved and familial relationships were not supported. *Iodosphaeria*, consisting of six strains representing four species, *i.e. I. honghensis*, *I. phyllophila*, *I. ripogoni* and *I. tongrenensis*, formed a well-supported monophyletic group. However, the new species was placed outside this clade. The next analysis was based on the combined ITS-LSU-*rpb2-tef1-α* sequences in order to study phylogenetic relationships of *Iodosphaeria* with other members of the *Xylariales*. The alignment had 4 002 characters including gaps (ITS = 871 characters, LSU = 766,

© 2021 Westerdijk Fungal Biodiversity Institute

Table 1. Specimens used in this study including specimen/strain, type status, GenBank accession numbers and source of sequences; T, E, I, N and P denote ex-type, ex-epitype, ex-neotype and ex-paratype strains.

			GenBank accession numbers				
Taxon	**Specimen/Strain**	**Type Status**	**ITS**	**LSU**	***tef1-α***	***rpb2***	**Reference**
Acrocordiella occulta	CBS 140500	E	KT949893	KT949893	—	—	Jaklitsch *et al.* (2016)
Amphibambusa bambusicola	MFLUCC 11-0617	T	KP744433	KP744474	—	—	Liu *et al.* (2015)
Amphisphaeria flava	MFLUCC 18-0361	T	MH971224	MH971234	—	—	Samarakoon *et al.* (2019)
Amphisphaeria fuckelii	CBS 140409	T	KT949902	KT949902	MH554435	MH554918	Jaklitsch *et al.* (2016), Liu *et al.* (2019)
Amphisphaeria thailandica	MFLU 18-0794	T	MH971225	MH971235	—	MK033640	Samarakoon *et al.* (2019)
Annulohypoxylon michelianum	CBS 119993		KX376320	KY610423	—	KY624234	Kuhnert *et al.* (2016), Wendt *et al.* (2018)
Anthostoma decipiens	CBS 133221		KC774565	KC774565	—	—	Jaklitsch *et al.* (2014)
Anungitiomyces stellenboschiensis	CPC 34726	T	MK876376	MK876415	—	—	Crous *et al.* (2019a)
Arthrinium hysterinum	ICMP 6889		MK014874	MK014841	MK017951	DQ368649	Pintos *et al.* (2019), Tang *et al.* (2007)
Arthrinium pseudoparenchymaticum	SICAUCC 18-0008		MK346319	MK346321	MK359205	MK359207	Wang *et al.* (2018)
Astrosphaeriella erumpens	S.M.H. 1291		—	AF279410	—	AY641073	Bhattacharya *et al.* (2000)
Bactrodesmium abruptum	CBS 145967		—	MN699410	MN704315	MN704290	Réblová *et al.* (2020)
Bactrodesmium diversum	CBS 142448		—	MN699412	MN704317	MN704292	Réblová *et al.* (2020)
Barrmaelia macrospora	CBS 142768	T	KC774566	KC774566	MF489005	MF488995	Jaklitsch *et al.* (2014), Voglmayr *et al.* (2017)
Barrmaelia moravica	CBS 142769	E	MF488987	MF488987	MF489006	MF488996	Voglmayr *et al.* (2017)
Beltrania pseudorhombica	CBS 138003	T	MH554124	KJ869215	MH554558	MH555032	Liu *et al.* (2019)
Beltraniopsis neolitseae	CBS 137974	T	KJ869126	KJ869183	—	—	Crous *et al.* (2014a)
Biscogniauxia nummularia	MUCL 51395	E	KY610382	KY610427	—	KY624236	Wendt *et al.* (2018)
Brachiampulla verticillata	ICMP 15065	P	MW144418	MW144402	MW147322	MW147336	Réblová *et al.* (2021)
Brachiampulla verticillata	ICMP 15993		MW144419	MW144403	MW147323	MW147337	Réblová *et al.* (2021)
Cainia anthoxanthis	MFLUCC 15-0539	T	KR092787	KR092777	—	—	Senanayake *et al.* (2015)
Camillea obularia	ATCC 28093		AF201714	KY610429	—	—	Wendt *et al.* (2018)
Castanediella acaciae	CBS 139896	T	KR476728	MH878661	—	—	Crous *et al.* (2015), Hernández-Restrepo *et al.* (2017)
Castanediella cagnizarii	MUCL 41095		KC775732	KC775707	KJ476985	—	Becerra-Hernández *et al.* (2016)

© 2021 Westerdijk Fungal Biodiversity Institute

Table 1. (Ctd).

Taxon	Specimen/Strain	Type Status	GenBank accession numbers				Reference
			ITS	LSU	*tef1-α*	*rpb2*	
Castanediella ramosa	MUCL 39857		KC775736	KC775711	KJ476989	—	Becerra-Hernández *et al.* (2016)
Clypeophysalospora latitans	CBS 141463	T	KX820250	KX820261	—	—	Giraldo *et al.* (2017)
Collodiscula japonica	CBS 124266		JF440974	JF440974	—	—	Jaklitsch & Voglmayr (2012)
Coniocessia cruciformis	CBS 125769	T	MH863750	MH875218	—	—	Vu *et al.* (2019)
Coniocessia minima	CBS 125765	T	MH863746	MH875214	—	—	Vu *et al.* (2019)
Cryptosphaeria eunomia var. *fraxini*	CBS 223.87		KT425231	KT425295	—	KT425361	Trouillas *et al.* (2015)
Cryptovalsa rabenhorstii	CBS 125574		KC774567	KC774567	—	—	Jaklitsch *et al.* (2014)
Cylindrium elongatum	CBS 115974		KM231853	KM231733	KM231989	KM232429	Lombard *et al.* (2015)
Cylindrium grande	CBS 145578		MK876385	MK876426	MK876496	MK876482	Crous *et al.* (2019a)
Daldinia concentrica	CBS 113277		AY616683	KY610434	—	KY624243	Triebel *et al.* (2005), Wend *et al.* (2018)
Delonicicola siamense	MFLUCC 15-0670	T	MF167586	MF158345	—	MF158346	Perera *et al.* (2017)
Diatrype disciformis	CBS 197.49		—	DQ470964	DQ471085	DQ470915	Spatafora *et al.* (2007)
Diatrypella vulgaris	CBS 128329		MH864880	MH876328	—	—	Vu *et al.* (2019)
Entosordaria perfidiosa	CBS 142773	E	MF488993	MF488993	MF489012	MF489003	Voglmayr *et al.* (2017)
Fasciatispora arengae	MFLUCC 15-0326a		MK120275	MK120300	MK890790	MK890794	Doilom *et al.* (2018)
Fasciatispora cocoes	MFLUCC 18-1445		MN482680	MN482675	MN481516	MN481517	Hyde *et al.* (2020)
Furfurella luteostiolata	CBS 143620	T	MK527842	MK527842	MK523302	MK523273	Voglmayr *et al.* (2019)
Graphostroma platystoma	CBS 270.87		JX658535	DQ836906	DQ836915	KY624296	Zhang *et al.* (2006), Stadler *et al.* (2014), Wendt *et al.* (2018)
Helicoascotaiwania lacustris	CBS 145963	T	—	MN699430	MN704329	MN704304	Réblová *et al.* (2020)
Hypocopra rostrata	NRRL 66178		KM067909	KM067909	—	—	Jayanetti *et al.* (2014)
Hyponectria buxi	UME 31430		—	AY083834	—	—	Unpublished
Hypoxylon fragiforme	MUCL 51264	E	KC477229	KM186295	—	KM186296	Stadler *et al.* (2013)
Idriella lunata	CBS 204.56	T	KP859044	KP858981	—	—	Hernández-Restrepo *et al.* (2016)
Induratia thailandica	MFLUCC 17-2669	T	MK762707	MK762714	—	MK791283	Samarakoon *et al.* (2020)
Iodosphaeria foliicola	NBM-F-07096	T	MZ509148	MZ509160	—	—	This study
Iodosphaeria honghensis	MFLU 19-0719	T	MK737501	MK722172	—	MK791287	Marasinghe *et al.* (2019)
Iodosphaeria phyllophila	PDD 56626		MZ509149	MZ509149	—	—	This study
Iodosphaeria phyllophila	FC 5099-2d		MZ509150	—	—	—	This study

© 2021 Westerdijk Fungal Biodiversity Institute

Table 1. (Ctd).

Taxon	Specimen/Strain	Type Status	GenBank accession numbers				Reference
			ITS	LSU	*tef1-α*	*rpb2*	
Iodosphaeria phyllophila	ILLS00121493	E	MZ509151	—	—	—	This study
Iodosphaeria ripogoni	PDD 103350		MZ509152	MZ509152	—	—	This study
Iodosphaeria tongrenensis	MFLU 15-0393	T	KR095282	KR095283	—	—	Li *et al.* (2015)
Kretzschmaria deusta	CBS 163.93		KC477237	KY610458	—	KY624227	Stadler *et al.* (2013), Wendt *et al.* (2018)
Leiosphaerella praeclara	CBS 125586		JF440976	JF440976	—	—	Jaklitsch & Voglmayr (2012)
Leptosillia acerina	CBS 143939	E	MK527849	MK527849	MK523310	MK523282	Voglmayr *et al.* (2019)
Leptosillia macrospora	CBS 143627	E	MK527853	MK527853	MK523314	MK523286	Voglmayr *et al.* (2019)
Lopadostoma gastrinum	CBS 134632	N	KC774584	KC774584	—	—	Jaklitsch *et al.* (2014)
Lopadostoma turgidum	CBS 133207	E	KC774618	KC774618	—	KC774563	Jaklitsch *et al.* (2014)
Melogramma campylosporum	CBS 141086		JF440978	JF440978	—	—	Jaklitsch & Voglmayr (2012)
Microdochium lycopodinum	CBS 125585	T	JF440979	JF440979	—	KP859125	Jaklitsch & Voglmayr (2012), Hernández-Restrepo *et al.* (2016)
Muscodor yunnanensis	WS38		MG866046	MG866038	—	MG866059	Chen *et al.* (2019)
Neophysalospora eucalypti	CBS 138864	T	KP004462	KP004490	—	—	Crous *et al.* (2014b)
Nothodactylaria nephrolepidis	CBS 146078	T	MN562132	MN567639	—	MN556809	Crous *et al.* (2019b)
Oxydothis metroxylonicola	MFLUCC 15-0281	T	KY206774	KY206763	KY206778	KY206781	Konta *et al.* (2016)
Oxydothis palmicola	MFLUCC 15-0806	T	KY206776	KY206765	KY206780	KY206782	Konta *et al.* (2016)
Phlogicylindrium eucalypti	CBS 120080	T	DQ923534	DQ923534	—	MH554893	Summerell *et al.* (2006), Liu *et al.* (2019)
Phlogicylindrium uniforme	CBS 131312	T	JQ044426	JQ044445	—	—	Crous *et al.* (2011)
Pleurotheciella erumpens	CBS 142447	T	—	MN699435	MN704334	MN704311	Réblová *et al.* (2020)
Pseudapiospora corni	CBS 140736	N	KT949907	KT949907	—	—	Jaklitsch *et al.* (2016)
Pseudomassaria chondrospora	CBS 125600		JF440981	JF440981	—	—	Jaklitsch & Voglmayr (2012)
Pseudosporidesmium lambertiae	CBS 143169	T	MG386034	MG386087	—	—	Crous *et al.* (2017)
Pseudotruncatella arezzoensis	MFLUCC 14-0988	T	MG192320	MG192317	—	—	Perera *et al.* (2018)
Pseudotruncatella bolusanthi	CBS 145532	T	MK876407	MK876448	—	—	Crous *et al.* (2019a)
Requienella seminuda	CBS 140502		KT949912	KT949912	MK523328	MK523300	Jaklitsch *et al.* (2016), Voglmayr *et al.* (2019)
Robillarda sessilis	CBS 114312	E	KR873256	KR873284	—	—	Crous *et al.* (2015)
Seiridium marginatum	CBS 140403	E	KT949914	KT949914	MK523329	MK523301	Jaklitsch *et al.* (2016), Voglmayr *et al.* (2019)

© 2021 Westerdijk Fungal Biodiversity Institute

Table 1. (Ctd).

Taxon	Specimen/Strain	Type Status	GenBank accession numbers				Reference
			ITS	LSU	*tef1-α*	*rpb2*	
Selenodriella cubensis	CBS 683.96	T	KP859053	KP858990	—	—	Hernández-Restrepo *et al.* (2016)
Selenodriella fertilis	CBS 772.83		KP859055	KP858992	—	—	Hernández-Restrepo *et al.* (2016)
Sporidesmium knawiae	CBS 123529	T	FJ349609	FJ349610	—	—	Crous *et al.* (2008)
Strelitziomyces knysnanus	CBS 146056	T	MN562135	MN567642	—	MN556810	Crous *et al.* (2019b)
Subsessila turbinata	MFLUCC 15-0831	T	KX762288	KX762289	KX762291	—	Lin *et al.* (2017)
Vialaea insculpta	DAOM 240257		JX139726	JX139726	—	—	Shoemaker *et al.* (2013)
Vialaea minutella	BRIP 56959		KC181926	KC181924	—	—	McTaggart *et al.* (2013)
Xyladictyochaeta lusitanica	CBS 142290	T	KY853479	KY853543	—	—	Hernández-Restrepo *et al.* (2017)
Xylaria hypoxylon	CBS 122620		KY610407	KY610495	—	KY624231	Wendt *et al.* (2018)
Zygosporium mycophilum	CBS 894.69		MH859474	MH871255	—	—	Vu *et al.* (2019)
Zygosporium pseudomasonii	CBS 146059	T	MN562147	MN567654	—	MN556815	Crous *et al.* (2019b)

rpb2 = 1107, *tef1-α* = 1258) and 2 366 unique character sites (RAxML). This combined four-loci alignment generated a tree with backbone support for familial relationships and correctly placed the new species in the *Iodosphaeria* clade. Therefore, this ML tree is shown in Fig. 1 and includes 34 well-supported families of the *Xylariales*. Five *Iodosphaeria* species form a moderately-supported monophyletic group (78 % BS, 1.0 PP), which is well-supported (100 % BS, 1.0 PP) as a sister clade to the *Pseudosporidesmiaceae*. *Iodosphaeriaceae* are not closely related to the *Amphisphaeriaceae* as previously suggested by Samuels *et al.* (1987), but rather occupies its own position as a distinct family in the *Xylariales*. The three representatives of *I. phyllophila* cluster with moderate support (83 % BS, 1.0 PP) and their ITS sequences, which are 611 bp in length, are 98.2–99.3 % similar with only a single gap. As expected, the specimens from Belgium (ILLS00121493) and France (FC5099-2d) are more closely-related to eachother than they are to the specimen from New Zealand (PDD 56626). The new species occupies a basal position in the *Iodosphaeria* clade.

Taxonomy

Iodosphaeria Samuels *et al.*, *Mycotaxon* **28**: 486. 1987.

Sexual morph: *Ascomata* perithecial, solitary to gregarious, non-stromatic, superficial and easily removed from the substrate, subglobose to globose, black, covered with long, brown, flexuous hairs that project from the ascomata in a stellate fashion, coarse, brown, repent hyphae extending from the base of the ascomata, apex flattened or obtusely rounded, ostiolate, periphysate. *Ascomal wall* two-layered, outer layer of brown, angular cells, inner layer of hyaline, flattened cells. *Paraphyses* hyaline, septate, inflated at the base, tapering towards the tip. *Asci* unitunicate, cylindrical to clavate, with an amyloid ring or ring lacking, 8-spored. *Ascospores* uniseriate to biseriate, ellipsoidal, ellipsoidal-fusiform or allantoid, aseptate, hyaline, smooth-walled, with or without a mucilaginous sheath. *Synasexual morphs*: selenosporella-like conidiophores and conidia and/or ceratosporium-like conidia have been observed in culture, on the surface of ascomata and on the repent hyphae. Selenosporella-like. *Conidiophores* macronematous, mononematous, pigmented, branched, septate. *Conidiogenous cells* integrated, terminal and discrete, lateral, polyblastic, single or in verticilli, with minute denticles along a short apical rachis; conidiogenesis holoblastic-denticulate. *Conidia* subcylindrical, slightly curved or straight, hyaline, aseptate. Ceratosporium-like. *Conidia* arising from aerial hyphae, pigmented, septate, staurosporous with two or more arms.

Taxa included in Iodosphaeria

Iodosphaeria foliicola A.N. Mill. & Réblová, ***sp. nov.***, MycoBank MB 840507. Fig. 2A–G.

Etymology: Epithet derived from *folium* (L) leaf, and *incola* (L) dweller, referring to the substrate on which this species was found.

Typus: **Canada**, Prince Edward Island, Queens County, Port-la-Joye-Fort, Amherst National Historic Site, 46.1958N, -63.1342W, on overwintered leaves of *Alnus* sp., 5 Jun. 2011, *A. Carter* 1555 (**holotype** NBM-F-07096, isotype ILLS00121496), associated with a selenosporella-like asexual morph; GenBank ITS MZ509148, GenBank LSU MZ509160.

© 2021 Westerdijk Fungal Biodiversity Institute

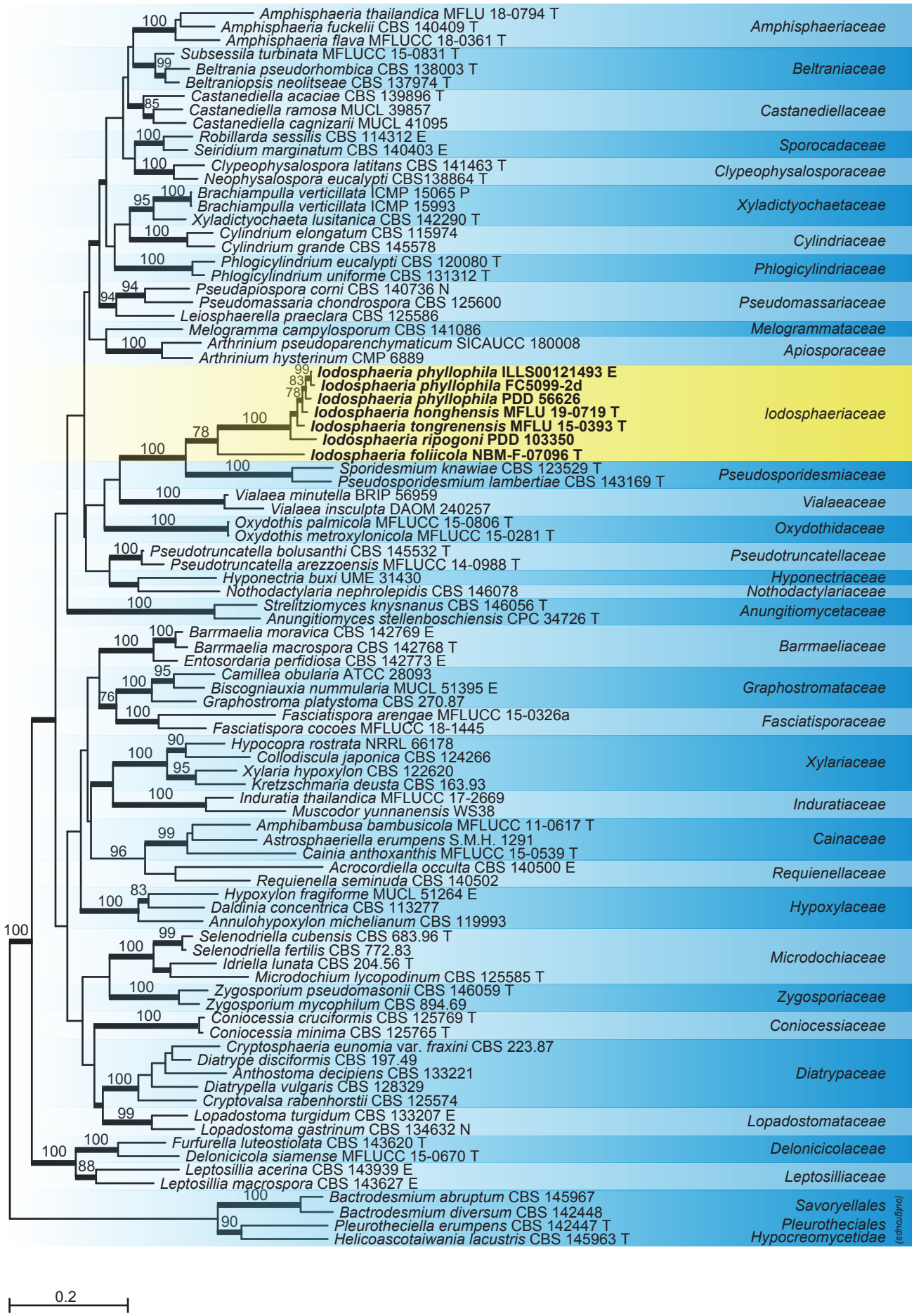

Fig. 1. Maximum likelihood tree generated from a RAxML analysis of combined ITS, LSU, *rpb2* and *tef1-α* sequences of selected members of the *Xylariales*. Members of *Iodosphaeria* are given in bold; T, E, N and P indicate ex-type, ex-epitype, ex-neotype and ex-paratype strains. Maximum likelihood bootstrap branch supports ≥ 75 % are shown above or below nodes and thickened branches indicate Bayesian posterior probabilities ≥ 95 %.

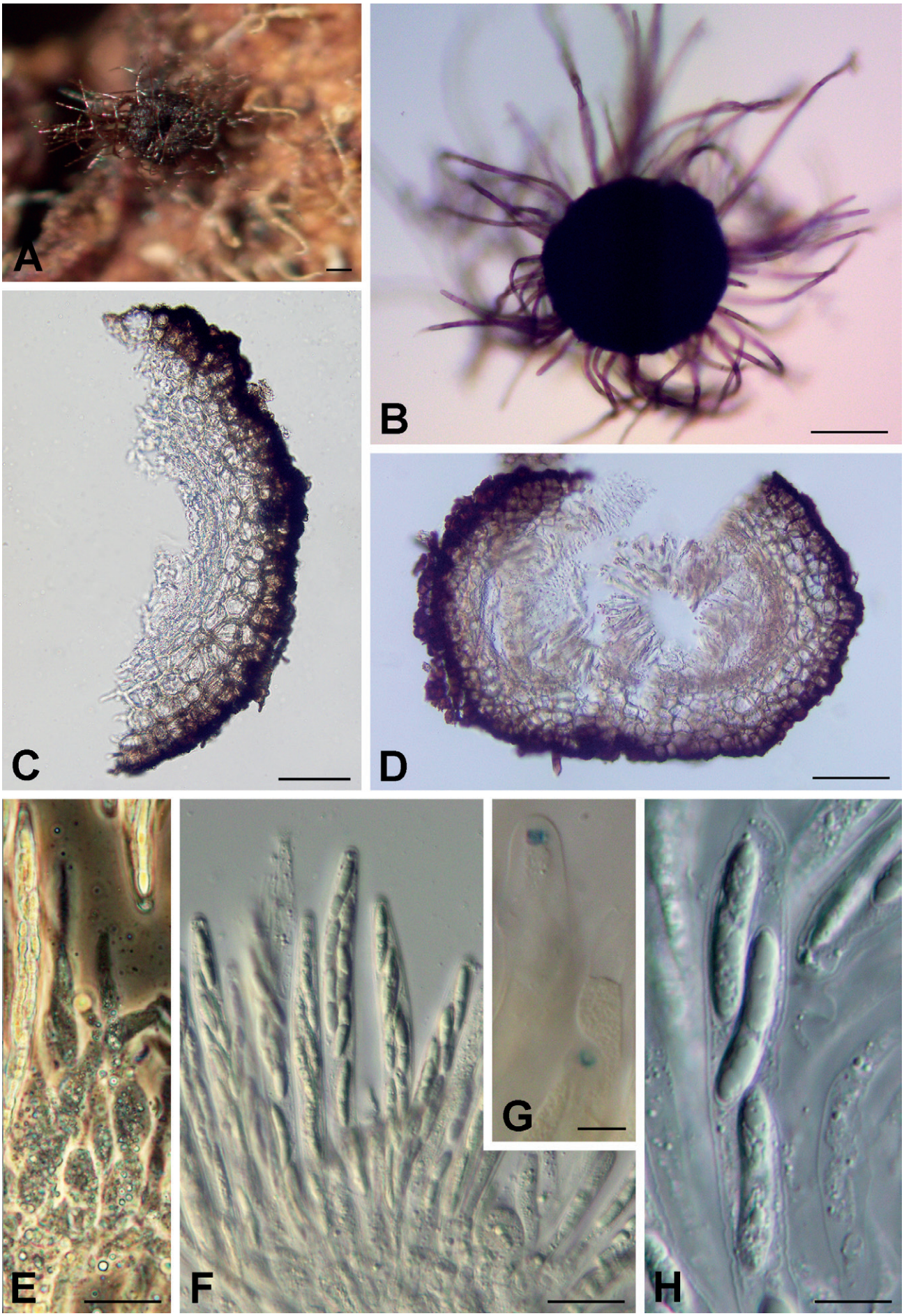

Fig. 2. *Iodosphaeria foliicola* NBM-F-07096. **A.** Ascoma on natural substrate. **B.** Ascoma mounted in water. **C, D.** Vertical sections of the ascomal wall. **E.** Paraphyses. **F.** Asci. **G.** Ascus apical apices with amyloid rings. **H.** Ascospores. Scale bars: A, B = 100 µm; C, D = 50 µm; E, F = 20 µm; H = 10 µm; G = 5 µm.

© 2021 Westerdijk Fungal Biodiversity Institute

Description: *Ascomata* globose to subglobose, 220–400 µm diam., superficial, solitary, black, covered with numerous, brown, septate, flexuous, rarely branched hairs, 145–320 × 6–9 µm, thick-walled (walls 1.5–2.5 µm thick), with rounded ends, singly or in fascicles; apex flattened, ostiolate, periphysate. Ascomal wall 50–70 µm wide, two-layered, outer layer composed of pseudoparenchymatous cells forming a *textura angularis*, composed of 5–8 layers of thin-walled cells, inner cell layers hyaline, outer cell layers becoming smaller and darker brown, outermost layer of thick-walled, melanized, dark brown cells, inner layer composed of 2–3 layers of thin-walled, hyaline, flattened, pseudoparenchymatous cells. *Paraphyses* sparse, hyaline, septate, of similar length as asci, basal cells inflated, tapering to 3–6 µm wide at apex, disintegrating at maturity. *Asci* cylindrical, 94–136 × 7.5–10 µm (120 ± 11.0 × 8.5 ± 0.5), 8-spored, apex rounded, short-stipitate, with a wedge-shaped, amyloid apical ring, 1.5–2.3 × 1–1.2 µm. *Ascospores* oblong to slightly allantoid, ends obtuse, aseptate, eguttulate, hyaline, smooth, 16.5–19.5 × 2.9–4 µm (18 ± 0.8 × 3.5 ± 0.4), without a mucilaginous sheath, uniseriate to biseriate in the ascus.

Habitat and distribution: Found in Canada on mostly the abaxial side of overwintered leaves of *Alnus* sp.

Additional specimens examined: **Canada**, Prince Edward Island, Queens County, Port-la-Joye-Fort, Amherst National Historic Site, 46.1958N, -63.1342W, on overwintered leaves of *Alnus* sp., 21 Jul. 2011, *A. Carter* 1554 (NBM-F-07095), associated with a selenosporella-like asexual morph.

Notes: *Iodosphaeria foliicola* is only known from two specimens growing on overwintered *Alnus* sp. leaves from Prince Edward Island, Canada. It is distinguished from other members of *Iodosphaeria* by its shorter asci (Fig. 2F) with an amyloid ascal ring (Fig. 2G) and oblong to allantoid, shorter ascospores (Fig. 2H) that lack guttules and a mucilaginous sheath. It closely resembles *I. honghensis,* but differs in its shorter, eguttulate ascospores (Table 2). *Iodosphaeria foliicola*, *I. phyllophila* and *I. tarda* can occur on dead fallen leaves, but *I. foliicola* can be separated by its longer asci and shorter, allantoid ascospores. The collector noted a selenosporella-like asexual morph was associated with both collections of *I. foliicola*, but was not found during our examinations.

Iodosphaeria honghensis Marasinghe *et al.* [as '*honghense*'], *Phytotaxa* **420**: 276. 2019.

This species is only known from the type specimen (MFLU 19-0719), which was found growing on dead twigs of an unidentified host from Yunnan Province in China (Marasinghe *et al.* 2019). It is distinguished from other species in the genus by its cylindrical to allantoid, guttulate ascospores that lack a mucilaginous sheath. A ceratosporium-like asexual morph was found growing on the host surface.

The unpublished *tef1-α* sequence (GenBank accession MK776957) from MFLU 19-0719, labeled as *Iodosphaeria* sp., was submitted to GenBank by D.S. Marasinghe & K.D. Hyde. Since the BLASTn search suggests closest relatives in the *Hypocreomycetidae* it is likely a contaminate; it should be removed from GenBank. However, four other sequences (SSU, ITS, LSU and *rpb2*) from this same voucher specimen under the original name, *I. honghense,* published by Marasinghe *et al.* (2019) appear correct, but the taxonomic name should be updated to '*honghensis*'.

Iodosphaeria hongkongensis J.E. Taylor & K.D. Hyde, *Sydowia* **51**: 128. 1999.

This species is only known from four collections, all described as growing on either a dead petiole (holotype) or a dead rachis of a palm, *Archontophoenix alexandrae*, from Hong Kong (Taylor & Hyde 1999). It is separated from other species of *Iodosphaeria* by its smaller asci lacking an ascal ring and smaller, ellipsoidal to fusiform ascospores lacking a mucilaginous sheath. The only other species that lacks an apical ring is *I. ripogoni*, which possesses a mucilaginous sheath surrounding the ascospores. No asexual morph was observed on the host material.

Iodosphaeria phyllophila (Mouton) Samuels *et al.*, *Mycotaxon* **28**: 486. 1987.
Basionym: *Lasiosphaeria phyllophila* Mouton, *Bull. Soc. R. Bot. Belg.* **39**: 48, 1900.

This species is the most commonly collected in the genus, known from at least 20 collections (Dennis 1974, Samuels *et al.* 1987, MyCoPortal 2021). It was originally described as *Lasiosphaeria phyllophila* growing on rotten leaves of *Betula alba* and *Corylus* from Belgium (Mouton 1900). It has a wide distribution and is also known from Brazil, French Guiana, Great Britain, and New Zealand. It has been found growing on a variety of substrates on numerous hosts including leaves of *B. alba*, (Mouton 1900), *Alnus* (Kirchstein 1911) and *Corylus avellana* (Declercq 2008), dead twigs and fallen debris of *Alnus*, *Populus* and *Salix* (Ellis & Ellis 1985), dead stems of *Chamaenerion angustifolium* (Dennis 1974) and *Rubus idaeus* (Declercq 2008), cone scales (Dennis 1974), and on the rachis of *Cyathea dealbata*, *Gahnia* sp., and *Ripogonum scandens* (Samuels *et al.* 1987). *Iodosphaeria phyllophila* is distinguished by its amyloid ascal ring and longer, allantoid, non-guttulate ascospores. Selenosporella- and ceratosporium-like synasexual morphs were reported on field collected material (Bell & Mahoney 2016) and in cultures of *I. phyllophila* (Samuels *et al.* 1987). *Iodosphaeria phyllophila* and its synasexual morphs have previously been illustrated (Ellis & Ellis 1985, Samuels *et al.* 1987, Declercq 2008, Senanayake *et al.* 2015, Bell & Mahoney 2016).

Senanayake *et al.* (2015) revised a collection of *I. phyllophila* originating from New Zealand (PDD 32622, Samuels *et al.* 1987) and incorrectly referred to it as a holotype. The type material is preserved at BR, but since it is over 120 years old, attempts were not made to obtain molecular data directly from this specimen. Instead, a more recent specimen with numerous, fertile ascomata from Belgium was sequenced and chosen as epitype. The ascomata and ascospores of this newly designated epitype specimen have been previously illustrated (Declercq 2008; figs 3C, 4C). Both selenosporella- and ceratosporium-like synasexual morphs were found on and around ascomata of the epitype of *I. phyllophila*.

Typification: **Belgium**, Wachtebeke, Reepkes, IFBL C3.35, on stem of *Rubus idaeus*, 28 Jul. 2007, *B. Declercq* 07/068 (**epitype** designated here ILLS00121493; MBT 10002029; GenBank ITS MZ509151, **isoepitype** GENT), with selenosporella- and ceratosporium-like synasexual morphs, epitype designated for the **holotype**: *Lasiosphaeria phyllophila* Mouton, Bull. Soc. Rot. Bot. Belg. **39**: 48. 1900. (BR).

© 2021 Westerdijk Fungal Biodiversity Institute

Table 2. Morphological characteristics, hosts, geographical distribution and references for species of *Iodosphaeria*.

Species	Length of asci (µm)	Ascal ring	Ascal ring amyloid	Shape of ascospores	Length of ascospores (µm)	Guttules in ascospores	Asexual morph(s)	Host(s)	Geographical distribution	Reference
Iodosphaeria foliicola	94–136	Present	Yes	Allantoid	16.5–19.5	Absent	Selenosporella-like	*Alnus* sp.	Canada	This study
I. honghensis	90–130	Present	Yes	Allantoid	18.5–22.5	Present	Ceratosporium-like	Unidentified	China	Marasinghe *et al.* (2019)
I. hongkongensis	80–102	Absent	n/a	Ellipsoidal	14–22	Absent	Unknown	*Archontophoenix alexandrae*	Hong Kong	Taylor & Hyde (1999)
I. phyllophila	105–138	Present	Yes	Allantoid	21–26.7	Absent	Selenosporella-like and ceratosporium-like	*Alnus* sp., *Betula alba*, *Chamaenerion angustifolium*, *Corylus avellana*, *Cyathea dealbata*, *Gahnia* sp., *Populus* sp. *Ripogonum scandens*, *Rubus idaeus*, *Salix* sp.	Belgium, Brazil, French Guiana, Great Britain, New Zealand	Samuels *et al.* (1987)
I. podocarpi	97–120	Present	Yes	Ellipsoidal	19–20	Absent	Selenosporella-like	*Podocarpus parlatorei*	Argentina	Catania & Romero (2012)
I. polygoni	150–180	Present	Yes	Ellipsoidal	18–23	Present	Ceratosporium-like	*Polygonum chinese*	Taiwan	Hsieh *et al.* (1997)
I. ripogoni	140–185	Absent	n/a	Ellipsoidal	21.5–26	Absent	Selenosporella-like and ceratosporium-like	*Ripogonum scandens*	New Zealand	Samuels *et al.* (1987)
I. tarda	70–85	Present	Yes	Ellipsoidal-fusiform	14–20	Absent	Unknown	*Corylus* sp., *Phyllostachys* sp.	France, Germany	Candoussau *et al.* (1996)
I. tongrenensis	150–210	Present	Yes	Ellipsoidal	18.5–22.5	Absent	Ceratosporium-like	Unidentified	China	Li *et al.* (2015)

© 2021 Westerdijk Fungal Biodiversity Institute

Additional specimens examined: **France,** Las Muros, on scales of *Picea* cone, 24 Sep. 1997, *J. Fournier* FC 5099-2a (CUP); *Ibid*., Sainte-Ogeu, on branch of *Vaccinum myrtillus*?, 1 Mar. 1992, *F. Candoussau* FC 5099-2c (CUP), *Ibid*., Pyrénées Atlantiques, Oloron, Bugangue, 10 Jul. 1994, *F. Candoussau* FC 5099-2d (CUP). **New Zealand**, North Island, Auckland, Hūnua Ranges Regional Park, vic. Mangatangi Dam, -37.1158S, 175.2119E, on *Cyathea dealbata*, 1 Feb. 1989, *P.R. Johnson* (PDD 56626); *Ibid*., Swanson, on rachis of *Cyathea dealbata*, 6 May 1981, *G.J. Samuels* 81-80 (PDD 45501); *Ibid*., Waitemata City, Waitakere Range, Marguerite Track, on rachis of *Cyathea dealbata*, 15 May 1975, *G.J. Samuels* 75-289 (PDD 36844); Erua Forest, near National Park, on dead wood, 6 Apr. 2005, *A. Bell* 919 (PDD 83080), with selenosporella-like asexual morph. **Spain**, Basque region, Gipuzkoa Province, Tolosa, on twig of unidentified shrub, 14 Jan. 1995, *F. Candoussau* FC 5099-2b (CUP), with ceratosporium-like asexual morph.

Iodosphaeria podocarpi Catania & A.I. Romero, *Mycosphere* **3['2']**: 40. 2012.

This species is only known from the type specimen, which was found growing on a branch of *Podocarpus parlatorei* in Argentina (Catania & Romero 2012). It is unique in having shorter asci with an amyloid apical ring and ellipsoid to navicular or slightly allantoid, shorter ascospores. A selenosporella-like asexual morph was found growing near or among the ascomata.

Iodosphaeria polygoni W.H. Hsieh *et al*., *Mycol. Res*. **101**: 841. 1997.

This species is only known from the type specimen found on stems of *Polygonum chinese* in Taiwan (Hsieh *et al.* 1997). It is unique in having longer asci and ellipsoidal, guttulate ascospores. A ceratosporium-like asexual morph was found associated with the repent network of brown hyphae occurring at the base of the ascomata.

Iodosphaeria ripogoni Samuels *et al.*, *Mycotaxon* **28**: 490. 1987.

This species is known from eight collections, all growing on the woody, vine-like stems of *Ripogonum scandens* from New Zealand (Samuels *et al.* 1987, Bell & Mahoney 2016, MyCoPortal 2021). It is distinguished by its lack of an ascal apical ring and its ellipsoidal ascospores that possess a mucilaginous sheath while still in the ascus. The only other species that lacks an apical ring is *I. hongkongensis*, which also lacks a mucilaginous sheath surrounding the ascospores. Although *I. tongrenensis* also has ascospores with a sheath, its asci possess an amyloid ascus ring. Selenosporella- and ceratosporium-like synasexual morphs were reported on the coarse, brown, repent hyphae that radiate from the ascomata and cover the surface of the substrate in field collected material of *I. ripogoni* (Samuels *et al.* 1987).

Additional specimen examined: **New Zealand**, North Island, Mt. Egmont National Park, Stratford, Dawson Falls Road, on dead stems of *Ripogonum scandens*, 18 Jan. 2013, *A. Bell* 1205 (PDD 103350), associated with selenosporella-like asexual morph.

Iodosphaeria tarda (Fuckel) A.N. Mill. & Réblová, ***comb. nov.***, MycoBank MB 840508. Fig. 3A–J.
Basionym: Sphaeria tarda Fuckel*, Fungi Rhen. Exs., Suppl. Fasc*. 6: no. 2021, 1867 [*Bot. Zeitung* **27**(6): 97. 1869].
Synonyms: *Trichosphaeria tarda* (Fuckel) Fuckel, *Jahrb. Nassauischen Vereins Naturk*. **23–24**: 145 (1869–1870) 1870.
Pyrenochaeta tarda (Fuckel) Sacc., *Syll. fung*. **3**: 221. 1884.
Iodosphaeria tarda (Fuckel) M.E. Barr, *Mycol. Helv*. **8**: 14. 1996, *Nom. inval*. (Art. 41.4., Melbourne).

This species was published in the *exsiccatae* series *Fungi Rhen. Exs.* no. 2021 (Fuckel 1870) and is only known from two collections. The isotype has been found on *Corylus* in Germany, whereas the second specimen (FC 319, Candoussau *et al.* 1996) was collected on *Phyllostachys* from France. The isotype at FH was unavailable for study, but another specimen (M-0312560) of the *Fungi Rhen. Exs*. No 2021 at M was available. The latter specimen contains a decaying leaf of *Corylus* sp. with several ascomata arranged mainly along the leaf veins (Fig. 3A). The setae appears at first slightly rigid and erect, covering ascomata (Fig. 3C). Later, setae become decumbent, flexuous and project from the ascomal wall in a stellate fashion (Fig. 3B) leaving the top glabrous. The ascomata are subglobose, without a papilla but do not have the flattened apex that is typical of other species. Instead, the top is obtusely rounded. *Iodosphaeria tarda* is distinguished by its smaller asci and ascospores that are ellipsoidal-fusiform with a smooth wall. Ascospores in the French collection (FC 319) were reported oblong to nearly allantoid; for description and additional illustrations, see Candoussau *et al.* (1996). Candoussau *et al.* (1996) examined the specimen *Fungi Rhen. Exs*. No 2021 (FH), which originated from the Caroline Barbey-Boissier herbarium, labelled Barbey-Boissier 672. Although Candoussau *et al.* (1996) reported that *I. tarda* had a non-amyloid ascal ring, the specimen at M clearly shows an amyloid ring (Fig. 3I, J). The authors also reported no asexual morph or synasexual morph were found associated with either specimen, which agrees with our observations. Candoussau's collections were sent to CUP in 2019, but FC 319 was not found there. The illustrations in Candoussau *et al.* (1996) appear to be drawn by Margaret Barr, who proposed the (invalid) transfer to *Iodosphaeria*. It is possible that she sent FC 319 to MASS, which has been transferred to NY. However, this specimen does not exist at NY (B. Thiers, pers. comm.).

The transfer of the name to *Iodosphaeria* was invalidly published since Candoussau *et al.* (1996) did not reference the date of the basionym (Art. 41.4, Melbourne; McNeill *et al.* 2012). This is now corrected herein and we choose to maintain the same specific epithet.

Additional specimen examined: **Germany**, Johannisberg, on decaying leaf of *Corylus* sp., spring, Fuckel, *Fungi Rhen. Exs*. no. 2021 (**isotype**, M-0312560).

Iodosphaeria tongrenensis Q.R. Li *et al.*, *Phytotaxa* **234**: 125. 2015.

This species is only known from the type specimen, which was collected on dead twigs in the Guizhou Province in China (Li *et al.* 2015). It is separated from all other species in the genus by its amyloid apical ascal ring and ellipsoidal ascospores that are surrounded by a mucilaginous sheath. *Iodosphaeria ripogonii* is the only other species known to have ascospores with a sheath, but it lacks an apical ascus ring. A ceratosporium-like asexual morph was observed on the surface of ascomata in *I. tongrenensis*.

© 2021 Westerdijk Fungal Biodiversity Institute

Fig. 3. *Iodosphaeria tarda Fungi Rhen. Exs.*, Suppl., 2021. **A.** Ascomata on decaying leaf. **B, C.** Ascomata on natural substrate. **D.** Ascoma mounted in water. **E.** Vertical section of the ascomal wall. **F, G.** Setae **H.** Paraphyses. **I, J.** Ascus apical apices with amyloid rings. **K.** Ascospores. Scale bars: A = 1 cm; B, C = 500 µm; D = 100 µm; E, F, H = 20 µm; G = 50 µm; I–K = 5 µm.

© 2021 Westerdijk Fungal Biodiversity Institute

Excluded and doubtful species

Iodosphaeria aquatica K.D. Hyde, *Nova Hedwigia* **61**: 129. 1995.

This species is only known from the type specimen, which was collected on submerged wood in Queensland, Australia. The placement of *I. aquatica* in the genus was questioned by Hyde (1995) when he described it, others have suggested its taxonomic placement is unclear (Kang *et al.* 1999, Taylor & Hyde 1999), and Hsieh *et al.* (1997) excluded it based on the glabrous, pyriform, erumpent ascomata often with lateral necks and its aquatic habitat. The LSU sequence of *I. aquatica* from Jeewon *et al.* (2003), but listed as dothideomycete sp. in GenBank clearly does not belong in the genus. Its LSU sequence is ~98 % similar to *Lentistoma* spp. in the *Dothideomycetes*, but the erumpent, pyriform ascomata and aseptate ascospores of *I. aquatica* are significantly different from the immersed, subglobose ascomata and 1-septate ascospores with a narrow, bipolar sheath found in *Lentistoma* (Hashimoto *et al.* 2018). Additional material of *I. aquatica* should be collected and sequenced to properly place this species in the *Lophiostomataceae*. Likewise, the LSU sequence of *Iodosphaeria* sp. (AF452045) from voucher specimen HKUCC 3154 (Jeewon *et al.* 2003), but listed as dothideomycete sp. in GenBank is 94 % similar to *I. aquatica* and most likely a member of the *Pleosporales*.

Iodosphaeria arundinariae (Ellis & Everh.) M.E. Barr, *Mycotaxon* **46**: 47. 1993.
Basionym: Trichosphaeria arundinariae Ellis & Everh., *N. Amer. Pyrenomyc*. **153**. 1892.

This species is only known from the type specimen, which was originally described as *Trichosphaeria arundinariae* growing on an old culm of *Arundinaria* in Louisiana, USA (Ellis & Everhart 1892). It was transferred to *Iodosphaeria* by Barr (1993). It can be separated from other species in the genus based on its papillate ascomata, non-amyloid ascal ring, and ellipsoidal to fusiform, verruculose ascospores. Barr (1993) did not observe an asexual morph on the holotype. *Iodosphaeria arundinaria* deviates from the generic concept based on *I. phyllophila* in the diagnostic characteristics of ascomata, apical ring and ascospores suggesting certain heterogeneity. Therefore, it is argued that it should be treated as a doubtful species until it is recollected and its relationships are assessed with DNA sequence data.

DISCUSSION

Members of *Iodosphaeria* possess ascomata that are macroscopically nearly identical in shape, size and overall appearance being subglobose to globose, superficial, and black with long, flexuous brown setae. Species are delimited by a combination of limited microscopic characters including: 1) the length of the asci, particularly whether they are longer or shorter than 150 µm, 2) whether or not the asci possess an apical ring, which is always amyloid if present, 3) the shape (ellipsoidal, ellipsoidal-fusiform or allantoid) and length of the ascospores, and 4) whether or not the ascospores have guttules. Although lengths of asci and ascospores and the presence or absence of an apical ascal ring are definitive, objective characters, the shape of the ascospores and the presence or absence of guttules are more ambiguous, subjective characters. Six of the nine accepted members of *Iodosphaeria*, exceptions being *I. hongkongensis, I. phyllophila* and *I. ripogoni*, are known from only one or two collections. Additional material of these six species needs to be recollected so that intraspecific variation, both molecular and morphological, can be examined to determine the significance of these characters in delimiting species.

Either selenosporella- and/or ceratosporium-like synasexual morphs were found in seven of the nine accepted species of *Iodosphaeria*. Both appear to be produced directly from the repent hyphae that radiate from ascomata over the surface of the substrate. Although the selenosporella-like synasexual morph produces conidiophores, the ceratosporium-like synasexual morph does not and conidia arise directly from the repent hyphae. Samuels *et al.* (1987) discovered both synasexual morphs in the only species of *Iodosphaeria* to be obtained in culture, *I. phyllophila*. These synasexual morphs are dematiaceous hyphomycetes with holoblastic conidiogenesis. Molecular data of *Ceratosporium* are unavailable and its systematic placement is unknown. Interestingly, species of *Ceratosporium* form selenosporella-like conidiophores directly on conidia (*e.g*. Hughes 1964), thus the occurrence of both synasexual morphs in the life cycle of *Iodosphaeria* is not surprising. A similar phenomenon, when selenosporella-like conidiophores are formed either on conidia or conidiophores of the respective asexual morph, was described for example in *Teratosperma* (Hughes 1951, Matsushima 1975), *Diplococcium* (Wang & Sutton 1998, Hernández-Restrepo *et al*. 2012) and *Endophragmiella* (*e.g.* Hughes 1979). The selenosporella-like morphotype appears polyphyletic in the *Ascomycota*. The genus *Selenosporella* (Arnaud 1953, MacGarvie 1968), typified with *S. curvispora*, was confirmed with molecular data to belong to the *Helminthosphaeriaceae* (Réblová *et al.* 2021). The family is rich in selenosporella-like asexual morphs and synasexual morphs, which have been linked with *Endophragmiella*, *Echinosphaeria, Hilberina* and *Ruzenia* (Awao & Udagawa 1974, Matsushima 1975, Hughes 1979, Sivanesan 1983, Gams 1973, Miller & Huhndorf 2004). The selenosporella-like synasexual morph was described as part of the life cycle of several hyphomycetes such as *Acrodictys bambusicola* (*Diaporthales*) (Matsushima 1975), *Spadicoides* (*Xenosphadicoidales*) (Kuthubutheen & Nawawi 1991, Castañeda-Ruíz *et al*. 1997, Réblová *et al*. 2018), and also *Arachnophora excentrica* (Hughes 1979), *Polytretophora calcarata* (= *Spadicoides calcarata*, Kuthubutheen & Nawawi 1991) and *Quadracaea mediterranea* (Lunghini *et al*. 1996), whose systematic placements are unknown. In the *Xylariales*, selenosporella-like fungi have been linked with *Oxydothis* (Samuels & Rossman 1987) and were also classified in *Selenodriella* (Castañeda-Ruíz & Kendrick 1990, Hernández-Restrepo *et al*. 2016). However, these genera are unrelated to *Iodosphaeria* (Fig. 1).

Species of *Iodosphaeria* have been reported from Argentina, Belgium, Brazil, China, French Guiana, Great Britain, Hong Kong, New Zealand, Taiwan and the USA (Samuels *et al.* 1987, Barr 1993, Hyde 1995, Candoussau *et al.* 1996, Hsieh *et al.* 1997, Taylor & Hyde 1999, Catania & Romero 2012, Li *et al.* 2015, Table 2). Only 27 collections of *Iodosphaeria* occur in the MyCoPortal (MyCoPortal 2021), 19 of which are either *I. phyllophila* or *I. ripogoni* from New Zealand. One collection of *Iodosphaeria cf. ripogoni* (NY03380508), which Samuels *et al.* (1987) reported as immature and may be a new species, is reported from Hawaii on mistletoe; two previously unidentified specimens from Canada are

© 2021 Westerdijk Fungal Biodiversity Institute

now described as *I. foliicola*, and the remaining five specimens are unidentified *Iodosphaeria* species from Costa Rica and Venezuela. *Iodosphaeria* occurs on many different hosts including *Alnus* sp., *Archontophoenix alexandrae*, *Betula alba*, *Chamaenerion angustifolium, Corylus avellana*, *Cyathea dealbata*, *Phyllostachys* sp., *Podocarpus parlatorei*, *Polygonum chinense*, *Populus* sp., *Ripogonum scandens*, *Rubus idaeus*, and *Salix* sp.

Several species of *Iodosphaeria* lack DNA data; only five of the nine species have been sequenced. Molecular data should be obtained from either voucher specimens or freshly-collected material for the remaining four species: *I. hongkongensis*, *I. podocarpi*, *I. polygoni*, and *I. tarda*, and for the doubtful species, *I. arundinariae*. This will enable a better understanding of the relationships, distributions, host associations and ecology of members of *Iodosphaeria*.

ACKNOWLEDGMENTS

The authors thank Ann Bell, Adrian Carter, Jacques Fournier, Dan Mahoney and Bernard DeClercq for the collection and loan of specimens. We thank the curators of CUP (Teresa Iturriaga), M (Dagmar Triebel), NBM (Alfredo Justo), and PDD (Eric McKenzie) for loan of herbarium specimens. The Roy J. Carver Biotechnology Center at the University of Illinois Urbana-Champaign is thanked for providing sequencing services. This work has been supported by the Institute of Botany, Czech Academy of Sciences (RVO 67985939) (M.R.).

Conflict of interest: The authors declare that there is no conflict of interest.

REFERENCES

Alfaro ME, Zoller S, Lutzoni F (2003). Bayes or bootstrap. A simulation study comparing the performance of Bayesian Markov chain Monte Carlo sampling and bootstrapping in assessing phylogenetic confidence. *Molecular Biology and Evolution* **20**: 255–266.

Arnaud G (1953). Mycologie concrète: Genera II. *Bulletin de la Société mycologique de France* **69**: 265–306.

Awao T, Udagawa SI (1974). *Endophragmia dimorphospora*, a new hyphomycete. *Transactions of the Mycological Society of Japan* **15**: 99–10.

Barr ME (1990). Prodromus to non-lichenized pyrenomycetous members of the class Hymenoascomycetes. *Mycotaxon* **39**: 43–184.

Barr ME (1993). Redisposition of some taxa described by J. B. Ellis. *Mycotaxon* **46**: 45–76.

Becerra-Hernández CI, González I, De Luna E, *et al*. (2016). First report of pleoanamorphy in *Gyrothrix verticiclada* with an Idriella-like synanamorph. *Cryptogamie Mycologie* **37**: 241–252.

Bell A, Mahoney DP (2016). *Field Studies in the* Lasiosphaeriaceae *and* Helminthosphaeriaceae *Sensu Lato*. CBS Biodiversity Series, No. 15. Utrecht, The Netherlands: CBS-KNAW Fungal Biodiversity Centre.

Bhattacharya D, Lutzoni F, Reeb V, *et al*. (2000). Widespread occurrence of spliceosomal introns in the rDNA genes of ascomycetes. *Molecular Biology & Evolution* **17**: 1971–1984.

Candoussau F, Magni J-F, Petrini LE, *et al*. (1996). Bambusicolous fungi collected in southwestern France: an annotated list. *Mycologia Helveltica* **8**: 11–20.

Castañeda-Ruíz RF, Guarro J, Cano J (1997). Notes on conidial fungi. XII. New or interesting hyphomycetes from Cuba. *Mycotaxon* **63**: 169–181.

Castañeda-Ruíz RF, Kendrick B (1991). Conidial fungi from Cuba: II. *University of Waterloo Biology Series* **33**: 1–62

Catania M del V, Romero AI (2012). *Crassoascus monocaudatus* and *Iodosphaeria podocarpi*, two new species on *Podocarpus parlatorei* from "Las Yungas", Argentina. *Mycosphere* **3**(1): 37–44.

Chen JJ, Feng XX, Xia CY, *et al*. (2019). Confirming the phylogenetic position of the genus *Muscodor* and the description of a new *Muscodor* species. *Mycosphere* **10**: 187–201

Crous PW, Groenewald JZ, Wood AR (2008). *Sporidesmium knawiae*. Fungal Planet, no. 29.

Crous PW, Summerell BA, Shivas RG, *et al*. (2011). Fungal Planet description sheets: 92–106. *Persoonia* **27**:130–162.

Crous PW, Shivas RG, Quaedvlieg W, *et al*. (2014a). Fungal Planet description sheets: 214–280. *Persoonia* **32**: 184–306.

Crous PW, Wingfield MJ, Schumacher RK, *et al*. (2014b). Fungal Planet description sheets: 281–319. *Persoonia* **33**: 212–289.

Crous PW, Carris LM, Giraldo A, *et al*. (2015). The Genera of Fungi - fixing the application of the type species of generic names - G 2: *Allantophomopsis*, *Latorua*, *Macrodiplodiopsis*, *Macrohilum*, *Milospium*, *Protostegia*, *Pyricularia*, *Robillarda*, *Rotula*, *Septoriella*, *Torula*, and *Wojnowicia*. *IMA Fungus* **6**(1): 163–198.

Crous PW, Wingfield MJ, Burgess TI, *et al*. (2017). Fungal Planet description sheets: 625–715. *Persoonia* **39**: 270–467.

Crous P, Carnegie A, Wingfield M, *et al*. (2019a). Fungal Planet description sheets: 868–950. *Persoonia* **42**: 291–473.

Crous PW, Wingfield MJ, Lombard L, *et al*. (2019b). Fungal Planet description sheets: 951–1041. *Persoonia* **43**: 223–425.

Declercq B (2008). Omtrent *Lasiosphaeria* S.L. *Sterbeeckia* **28**: 35–41.

Dennis RWG (1974). New or interesting British microfungi. II. *Kew Bulletin* **29(**1): 157–179.

Doilom M, Hyde KD, Phookamsak R, *et al*. (2018). Mycosphere Notes 225–274: types and other specimens of some genera of Ascomycota. *Mycosphere* **9**(4): 647–754.

Edgar RC (2004). MUSCLE: a multiple sequence alignment method with reduced time and space complexity. *BMC Bioinformatics* **5**: 113.

Ellis MB, Ellis JP (1985). *Microfungi on Land Plants. An Identification Handbook*. Macmillan, New York.

Ellis JB, Everhart BM (1892). *The North American* Pyrenomycetes. Self-published, Newfield, New Jersey, USA.

Gams W (1973). Phialides with solitary conidia? Remarks on conidium ontogeny in some hyphomycetes. *Persoonia* **7**: 161–169.

Giraldo A, Crous PW, Schumacher RK, *et al*. (2017). The Genera of Fungi - G3: *Aleurocystis*, *Blastacervulus*, *Clypeophysalospora*, *Licrostroma*, *Neohendersonia* and *Spumatoria*. *Mycological Progress* **16**: 325–348.

Hashimoto A, Hirayama K, Takahashi H, *et al*. (2018). Resolving the *Lophiostoma bipolare* complex: Generic delimitations within *Lophiostomataceae*. *Studies in Mycology* **90**: 161–189.

Hernández-Restrepo M, Silvera-Simón C, Mena-Portales J, *et al*. (2012). Three new species and a new record of *Diplococcium* from plant debris in Spain. *Mycological Progress* **11**: 191–199.

Hernández-Restrepo M, Groenewald JZ, Crous PW (2016). Taxonomic and phylogenetic re-evaluation of *Microdochium*, *Monographella* and *Idriella*. *Persoonia* **36**: 57–82.

Hernández-Restrepo M, Gene J, Castaneda-Ruiz RF, *et al*. (2017). Phylogeny of saprobic microfungi from Southern Europe. *Studies in Mycology* **86**: 53–97.

Hilber R, Hilber O (2002). *The genus* Lasiosphaeria *and allied taxa*. Self-published, publication 9. Germany.

Hillis DM, Bull JJ (1993). An Empirical Test of Bootstrapping as a Method for Assessing Confidence in Phylogenetic Analysis. *Systematic Biology* **42**: 182–192.

© 2021 Westerdijk Fungal Biodiversity Institute

Hsieh WH, Chen CY, Sivanesan A (1997). *Iodosphaeria polygoni sp. nov.*, a new pyrenomycete from Taiwan. *Mycological Research* **101**: 841–842.

Huelsenbeck JP, Ronquist FR (2001). MrBayes: Bayesian inference of phylogenetic trees. *Bioinformatics* **17**: 754–755.

Huelsenbeck JP, Ronquist FR (2005). Bayesian analysis of molecular evolution using MrBayes. In: *Statistical Methods in Molecular Ecology* (Nielsen R, ed). Springer Publishing Company, New York, USA: 186–226.

Hughes SJ (1951). Studies on micro-fungi. III. *Mastigosporium*, *Camposporium*, and *Ceratophorum*. *Mycological Papers* **36**: 1–44.

Hughes SJ (1964). New Zealand fungi 1. *Ceratosporium* Schw., *New Zealand Journal of Botany* **2**: 305–309.

Hughes SJ (1979). Relocation of species of *Endophragmia* auct. with notes on relevant generic names. *New Zealand Journal of Botany* **17**: 139–188.

Hyde KD (1995). Tropical Australian freshwater fungi. VII. New genera and species of Ascomycetes. *Nova Hedwigia* **61**: 119–140.

Hyde KD, Dong Y, Phookamsak R, *et al*. (2020). Fungal diversity notes 1151–1276: taxonomic and phylogenetic contributions on genera and species of fungal taxa. *Fungal Diversity* **100**: 5–277.

Jaklitsch WM, Voglmayr H (2012). Phylogenetic relationships of five genera of *Xylariales* and *Rosasphaeria gen. nov*. (*Hypocreales*). *Fungal Diversity* **52**(1): 75–98.

Jaklitsch WM, Fournier J, Rogers JD, *et al*. (2014). Phylogenetic and taxonomic revision of *Lopadostoma*. *Persoonia* **32**: 52–82.

Jaklitsch WM, Gardiennet A, Voglmayr H (2016). Resolution of morphology-based taxonomic delusions: *Acrocordiella*, *Basiseptospora*, *Blogiascospora*, *Clypeosphaeria*, *Hymenopleella*, *Lepteutypa*, *Pseudapiospora*, *Requienella*, *Seiridium* and *Strickeria*. *Persoonia* **37**: 82–105.

Jayanetti DR, Yue Q, Bills GF, *et al*. (2014). Hypocoprins A–C: New sesquiterpenoids from the coprophilous fungus *Hypocopra rostrata*. *Journal of Natural Products* **78**: 396–401.

Jeewon R, Liew EC, Hyde, KD (2003). Molecular systematics of the *Amphisphaeriaceae* based on cladistic analyses of partial LSU rDNA gene sequences. *Mycological Research* **107**: 1392–1402.

Kang JC, Hyde KD, Kong RYC (1999). Studies on *Amphisphaeriaceae*: the genera excluded from the *Amphisphaeriaceae*, *Cainaceae* and *Clypeosphaeriaceae*. *Fungal Diversity* **2**: 135–151.

Kirschstein W (1911). Sphaeriales. *Kryptogamenflora der Mark Brandenburg* **7**(2): 164–304.

Konta S, Hongsanan S, Tibpromma S, *et al*. (2016). An advance in the endophyte story: *Oxydothidaceae fam. nov*. with six new species of *Oxydothis*. *Mycosphere* **7**: 1425–1446.

Kuhnert E, Sir EB, Lambert C, *et al*. (2016). Phylogenetic and chemotaxonomic resolution of the genus *Annulohypoxylon* (*Xylariaceae*) including four new species. *Fungal Diversity* **85**:1–43.

Kuthubutheen AJ, Nawawi A (1991). Two new species of *Spadicoides* from Malaysia. *Mycological Research* **95**: 163–168.

Lanfear R, Frandsen PB, Wright AM, *et al.* (2017). PartitionFinder 2: new methods for selecting partitioned models of evolution for molecular and morphological phylogenetic analyses. *Molecular Biology and Evolution* **34**: 772–773.

Larget B, DL Simon (1999). Markov Chain Monte Carlo algorithms for the bayesian analysis of phylogenetic trees. *Molecular Biology and Evolution* **16**: 750–759.

Li Q, Kang JC, Hyde KD (2015). A multiple gene genealogy reveals the phylogenetic placement of *Iodosphaeria tongrenensis sp. nov.* in *Iodosphaeriaceae* (*Xylariales*). *Phytotaxa* **234**: 121–132.

Lin CG, Dai DQ, Bhat DJ, *et al.* (2017). *Subsessila turbinata gen. et. sp. nov.* (*Beltraniaceae*), a Beltrania-like fungus from Thailand. *Mycological Progress* **16**: 393–401.

Liu JK, Hyde KD, Jones EBG, *et al.* (2015). Fungal Diversity Notes 1-100: Taxonomic and phylogenetic contributions to fungal species. *Fungal Diversity* **72**:1–197.

Liu F, Bonthond G, Groenewald JZ, *et al.* (2019). *Sporocadaceae*, a family of coelomycetous fungi with appendage-bearing conidia. *Studies in Mycology* **92**: 287–415.

Lombard L, van der Merwe NA, Groenewald JZ, *et al.* (2015). Generic concepts in *Nectriaceae*. *Studies in Mycology* **80**: 189–245.

Lunghini D, Pinzari F, Zucconi L (1996). Studies on Mediterranean hyphomycetes. III. *Quadracaea mediterranea anam.-gen.* and *sp. nov. Mycotaxon* **60**: 103−110.

MacGarvie QD (1968). Hyphomycetes on *Juncus effusus* L. *Scientific Proceedings of the Royal Dublin Society* **2**: 153–161.

Marasinghe DS, Samarakoon MC, Hongsana S, *et al.* (2019). *Iodosphaeria honghense sp. nov.* (*Iodosphaeriaceae, Xylariales*) from Yunnan Province, China. *Phytotaxa* **420**: 273–282.

Matsushima T (1975). *Icones Microfungorum a Matsushima lectorum*. The Nippon Printing & Publishing Co., Osaka, Japan.

McNeill J, Barrie FF, Buck WR, *et al*. (eds) (2012). *International Code of Nomenclature for algae, fungi, and plants (Melbourne Code).* [Regnum vegetabile no. 154.]. Koeltz Scientific Books, Königstein.

McTaggart AR, Grice KR, Shivas RG (2013). First report of *Vialaea minutella* in Australia, its association with mango branch dieback and systematic placement of *Vialaea* in the *Xylariales*. *Australasian Plant Disease Notes* **8**: 63–66.

Miller AN, Huhndorf SM (2004b). A natural classification of *Lasiosphaeria* based on nuclear LSU rDNA sequences. *Mycological Research* **108**: 26−34.

Miller MA, Pfeiffer W, Schwartz T (2010). "Creating the CIPRES Science Gateway for inference of large phylogenetic trees" in Proceedings of the Gateway Computing Environments Workshop (GCE), 14 Nov. 2010, New Orleans, LA: 1–8.

Mouton V (1900). 4ème notice sur des Ascomycetes nouveaux ou peu connus. *Bulletin de la Société Royale de Botanique de Belgique* **39**: 37–53.

MycoBank (2021). http://mycobank.org. Accessed on April 1.

MyCoPortal (2021). http://mycoportal.org/portal/index.php. Accessed on April 7.

Perera RH, Maharachchikumbura SSN, Jones EBG, *et al.* (2017). *Delonicicola siamense gen.* & *sp. nov.* (*Delonicicolaceae fam. nov., Delonicicolales ord. nov*.), a saprobic species from *Delonix* regia seed pods. *Cryptogamie Mycologie* **38**: 321–340.

Perera RH, Maharachchikumbura SSN, Hyde KD, *et al.* (2018). An appendage-bearing coelomycete *Pseudotruncatella arezzoensis gen.* and *sp. nov.* (*Amphisphaeriales genera incertae sedis*) from Italy, with notes on *Monochaetinula*. *Phytotaxa* **338**: 177–188.

Pintos A, Alvarado P, Planas J, *et al.* (2019). Six new species of *Arthrinium* from Europe and notes about *A. caricicola* and other species found in *Carex* spp. hosts. *MycoKeys* **49**: 15–48.

Réblová M (1999). Studies in *Chaetosphaeria* sensu lato IV. *Crassochaeta gen. nov*., a new lignicolous genus of the *Trichosphaeriaceae*. *Mycotaxon* **71**: 45–67.

Réblová M, Hernández-Restrepo M, Fournier, *et al.* (2020). New insights into the systematics of *Bactrodesmium* and its allies and introducing new genera, species and morphological patterns in the *Pleurotheciales* and *Savoryellales* (*Sordariomycetes*). *Studies in Mycology* **95**: 415–466.

Réblová M, Miller AN, Réblová K, *et al.* (2018) Phylogenetic classification and generic delineation of *Calyptosphaeria gen. nov*., *Lentomitella*, *Spadicoides* and *Torrentispora* (*Sordariomycetes*). *Studies in Mycology* **89**: 1–62.

© 2021 Westerdijk Fungal Biodiversity Institute

Réblová M, Kolařík M, Nekvindová J, *et al.* (2021). Phylogeny, global biogeography and pleomorphism of *Zanclospora*. *Microorganisms* **9**: 706.

Rehner SA, Samuels GJ (1995). Molecular systematics of the *Hypocreales*: a teleomorph gene phylogeny and the status of their anamorphs. *Canadian Journal of Botany* **73** (Suppl 1): S816–S823.

Samarakoon MC, Liu JK, Hyde KD, *et al.* 2019. Two new species of *Amphisphaeria* (*Amphisphaeriaceae*) from northern Thailand. *Phytotaxa* **391**: 207–217.

Samarakoon MC, Thongbai B, Hyde KD, *et al.* 2020. Elucidation of the life cycle of the endophytic genus *Muscodor* and its transfer to *Induratia* in *Induratiaceae fam. nov*., based on a polyphasic taxonomic approach. *Fungal Diversity* **101**: 177–210.

Samuels GJ, Müller E, Petrini O (1987). Studies in the *Amphisphaeriaceae* (*sensu lato*) 3. New species of *Monographella* and *Pestalosphaeria* and two new genera. *Mycotaxon* **28**: 473–499.

Samuels GJ, Rossmann AY (1987). Studies in the *Amphisphaeriaceae* (*sensu lato*) 2. *Leiosphaerella cocoës* and two new species of *Oxydothis* on palms. *Mycotaxon* **28**: 461−471.

Senanayake IC, Maharachchikumbura SSN, Hyde KD *et al.* (2015). Towards unraveling relationships in *Xylariomycetidae* (*Sordariomycetes*). *Fungal Diversity* **73**: 73–144.

Shoemaker RA, Hambleton S, Liu M (2013). *Vialaea insculpta* revisited. *North American Fungi* **8**: 1–13.

Spatafora JW, Sung GH, Johnson D, *et al.* (2006). A five-gene phylogeny of *Pezizomycotina*. *Mycologia* **98**: 1018–1028.

Stadler M, Kuhnert E, Peršoh D, *et al.* (2013). The *Xylariaceae* as model example for a unified nomenclature following the "One Fungus-One Name" (1F1N) concept. *Mycology* **4**: 5–21.

Stadler M, Laessoe T, Fournier J, *et al.* (2014). A polyphasic taxonomy of *Daldinia* (*Xylariaceae*). *Studies in Mycology* **77**: 1–143.

Stamatakis A (2014). RAxML Version 8: A tool for Phylogenetic Analysis and Post-Analysis of Large Phylogenies. *Bioinformatics* **30**: 1312–1313.

Stamatakis A, Hoover P, Rougemont J (2008). A fast bootstrapping algorithm for the RAxML web-Servers. *Systematic Biology* **57**: 758–771.

Summerell BA, Groenewald JZ, Carnegie AJ, *et al.* (2006). Eucalyptus microfungi known from culture. 2. *Alysidiella*, *Fusculina* and *Phlogicylindrium genera nova*, with notes on some other poorly known taxa. *Fungal Diversity* **23**: 323–350.

Tang AM, Jeewon R, Hyde KD (2007). Phylogenetic utility of protein (RPB2, beta-tubulin) and ribosomal (LSU, SSU) gene sequences in the systematics of *Sordariomycetes* (*Ascomycota, Fungi*). *Antonie Van Leeuwenhoek* **91**: 327–349.

Taylor JE, Hyde KD (1999). Fungi from palms. XL. *Iodosphaeria*. *Sydowia* **51**: 127–132.

Triebel D, Peršoh D, Wollweber H, *et al.* (2005). Phylogenetic relationships among *Daldinia*, *Entonaema*, and *Hypoxylon* as inferred from ITS nrDNA analyses of *Xylariales*. *Nova Hedwigia* **80**(1): 25–43.

Trouillas FP, Peduto-Hand F, Inderbitzin P *et al.* (2015). The genus *Cryptosphaeria* in the western United States: taxonomy, multi-locus phylogeny and a new species, *C. multicontinentalis*. *Mycologia* **107**: 1304–1313.

Vilgalys R, Hester M (1990). Rapid identification and mapping of enzymatically amplified ribosomal DNA from several *Cryptococcus* species. *Journal of Bacteriology* **172**: 4238–4246.

Voglmayr H, Friebes G, Gardiennet A, *et al.* (2017). *Barrmaelia* and *Entosordaria* in *Barrmaeliaceae* (*fam. nov., Xylariales*) and critical notes on *Anthostomella*-like genera based on multigene phylogenies. *Mycological Progress* **17**: 155–177.

Voglmayr H, Aguirre-Hudson MB, Wagner HG, *et al.* (2019). Lichens or endophytes? The enigmatic genus *Leptosillia* in the *Leptosilliaceae fam. nov.* (*Xylariales*), and *Furfurella gen. nov.* (*Delonicicolaceae*). *Persoonia* **42**: 228–260.

Vu D, Groenewald M, de Vries M, *et al.* (2019). Large-scale generation and analysis of filamentous fungal DNA barcodes boosts coverage for kingdom fungi and reveals thresholds for fungal species and higher taxon delimitation. *Studies in Mycology* **92**: 135–154.

Wang CJK, Sutton BC (1998). *Diplococcium hughesii sp. nov*. with a *Selenosporella* synanamorph. *Canadian Journal of Botany* **76**: 1608–1613.

Wang M, Tan XM, Liu F, *et al.* (2018). Eight new *Arthrinium* species from China. *MycoKeys* **34**: 1–24.

Wendt L, Sir EB, Kuhnert E, *et al.* (2018). Resurrection and emendation of the *Hypoxylaceae*, recognised from a multigene phylogeny of the *Xylariales*. *Mycological Progress* **17**: 115–154.

White TJ, Bruns T, Lee S, *et al.* (1990). Amplification and direct sequencing of fungal ribosomal RNA genes for phylogenetics. In: *PCR Protocols: A Guide to Methods and Applications* (Innis MA, ed). Academic Press, San Diego, USA: 315–322.

Zhang N, Castlebury LA, Miller AN, *et al.* (2006). An overview of the systematics of the *Sordariomycetes* based on a four-gene phylogeny. *Mycologia* **98**: 1076–1087.

© 2021 Westerdijk Fungal Biodiversity Institute

FUSE

Fungal Systematics and Evolution

VOLUME 8
DECEMBER 2021
PAGES 65–80

doi.org/10.3114/fuse.2021.08.06

Hysterangiales revisited: expanded phylogeny reveals new genera and two new suborders

N. Davoodian[1*], T. Lebel[1,2], M.A. Castellano[3], K. Hosaka[4]

[1]Royal Botanic Gardens Victoria, South Yarra, VIC 3141, Australia
[2]Botanic Gardens and State Herbarium of South Australia, Adelaide, SA 5001, Australia; Royal Botanic Gardens Victoria, South Yarra, VIC 3141, Australia
[3]US Department of Agriculture Forest Service, Northern Research Station, Corvallis, OR 97331, USA
[4]National Museum of Nature and Science, Tsukuba, Ibaraki 305-0005, Japan (ORCID: 0000-0002-4469-8303)

*Corresponding author: Naveed.Davoodian@rbg.vic.gov.au

Key words:
atp6
Phallogaster
phylogenetics
tef1
Trappea

Abstract: *Hysterangiales* (*Phallomycetidae*, *Agaricomycetes, Basidiomycota*) is a diverse, nearly cosmopolitan order of predominantly hypogeous, sequestrate, ectomycorrhizal fungi. Expanding on previously published phylogenies, we significantly increased sampling of *Hysterangiales* specimens, emphasizing representatives from Australia. Using protein-coding genes *atp6* (adenosine triphosphate synthase subunit 6) and *tef1* (translation elongation factor 1-α), we recovered 26 provisional novel genera, and corroborated existing genera and families. Further, two new suborders (*Phallogastrineae subord. nov*. and *Hysterangineae subord. nov*.) and a new family (*Phallogastraceae fam. nov*.) are described, and three new combinations made to *Phallogaster*. Aspects of classification and biogeography are presented.

Citation: Davoodian N, Lebel T, Castellano MA, Hosaka K (2021). *Hysterangiales* revisited: expanded phylogeny reveals new genera and two new suborders. *Fungal Systematics and Evolution* **8**: 65–80. doi: 10.3114/fuse.2021.08.06
Received: 22 January 2021; **Accepted:** 9July 2021; **Effectively published online:** 29 July 2021
Corresponding editor: P.W. Crous

INTRODUCTION

Hysterangiales (*Phallomycetidae*, *Agaricomycetes, Basidiomycota*) was established in 2006 to accommodate a phylogenetically refined *Hysterangiaceae* and relatives (Hosaka *et al.* 2006). *Hysterangiales* comprises a wide array of predominantly hypogeous, sequestrate, ectomycorrhizal fungi, but some taxa in the basal lineage (*Phallogastraceae*) are epigeous and non-mycorrhizal. *Hysterangiales* possess a range of unusual morphologies (Fig. 1), such as basidiomes with a powdery spore mass (and often with a sterile core) in the *Mesophelliaceae* (Trappe *et al.* 1996), the gelatinized or cartilaginous gleba with translucent columella in *Gallaceaceae* and *Hysterangiaceae*, or the utricle-encased spores of many *Mesophelliaceae* and *Hysterangiaceae* (Castellano & Beever 1994; Fig. 2). Like many truffle-like fungi, *Hysterangiales* often have distinct odours, which attract small animals for spore dispersal via mycophagy (*e.g*. Fogel & Trappe 1978, Claridge & May 1994). The characteristics of being mostly hypogeous and nearly universally dependent on other organisms for dispersal, combined with their worldwide (excluding Antarctica) distribution and diversity, have led to the consideration of multiple biogeographic scenarios for *Hysterangiales*, ranging from ancient Pangaean vicariance to recent long-distance dispersal (Hosaka *et al.* 2008).

Hysterangiales taxa are remarkably abundant and highly diverse in Australia (a major impetus for the present study), particularly the endemic family *Mesophelliaceae*. Ectomycorrhizal *Myrtaceae* and *Nothofagaceae* species are the primary symbionts of *Hysterangiales* in Australasia. Another impetus for the present study is that numerous novel Australasian *Hysterangiales* taxa yet to be formally described have been known for over a decade but generic boundaries were not strongly supported (Hosaka 2005, Hosaka *et al.* 2006, 2008). We expanded on previous work initiated by Hosaka *et al.* (2006, 2008) by sampling extensively from Australian specimens, which corroborated known genera (both formally described and provisional) and families, and elucidated additional provisional novel genera.

MATERIALS AND METHODS

Collections referred to in this study are housed at various fungaria including AD, ATH, BRI, OSC, and MEL. Collections were initially sorted into morphotaxa based on macro- and micro-characters, and a broad selection of material encompassing as many genera as possible were then sampled for molecular analyses. This included some material from non-Australasian taxa that had not previously been sampled, to better support previous taxonomic hypotheses. Thin sections of fungal tissue were mounted in KOH, Melzers' reagent and occasionally Congo Red + KOH to examine peridium and glebal structure, and spore size, shape, presence of a utricle, and ornamentation. Imaging was completed using either an Olympus BX-52 microscope with DP-73 camera and measurement tools using Olympus cellSens standard (v. 1.16) or a Zeiss/Moticam 10 camera system.

Adenosine triphosphate synthase subunit 6 (*atp6*; mitochondrial) and translation elongation factor 1-α (*tef1*;

Fungal Systematics and Evolution is licensed under a Creative Commons Attribution-NonCommercial-ShareAlike 4.0 International License

© 2021 Westerdijk Fungal Biodiversity Institute

Fig. 1. Examples of a range of basidiome morphologies in *Hysterangiales*. **A–C**. *Phallogastraceae* **A.** "*Gen. prov*. 1" (AU, photo credit M. Castellano). **B.** *Phallogaster* (*Trappea*) *phillipsii* (photo credit N. Siegel). **C.** *Phallogaster saccatus* (photo credit D. Mitchell/B. Roody); **D–F.** *Gallaceaceae.* **D.** *Austrogautieria* sp. (NZ, photo credit K. Hosaka). **E.** *Gallacea eburnea* (photo credit N. Siegel). **F.** *Gallacea scleroderma* (photo credit N. Siegel); **G–I.** *Hysterangiaceae.* **G.** *Aroramyces* sp. (AU, photo credit M. Castellano). **H.** *Hysterangium* sp. (AU, photo credit Castellano). **I.** *Hysterangium* sp. (NZ, photo credit K. Hosaka); **J–L.** *Mesophelliaceae.* **J.** *Chondrogaster* sp. (photo credit M. Castellano). **K.** "*Gen. prov*. 3" (photo credit M. Castellano). **L.** *Mesophellia* sp. (photo credit D. Catcheside); **M–O.** *Mesophelliaceae.* **M.** *Nothocastoreum cretaceum* (photo credit D. Catcheside). **N.** *Castoreum radicatum* (photo credit M. Castellano). **O.** *Gummiglobus pachythrix* (photo credit M. Castellano). Scale bars = 10 mm.

© 2021 Westerdijk Fungal Biodiversity Institute

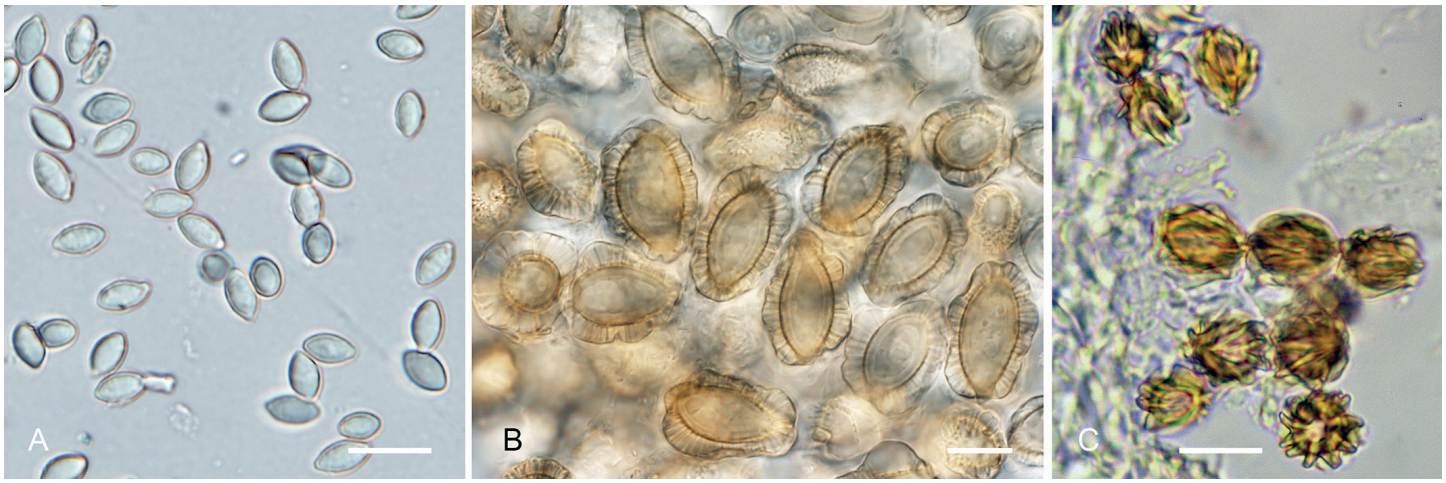

Fig. 2. Three spore types observed in *Hysterangiales*. **A.** *Mesophellia brevispora* (photo credit M. Castellano): smooth, no utricle. **B.** "*Genus prov.* 7" (photo credit N. Davoodian): ornamented, utricle present. **C.** *Austrogautieria* (photo credit T. Lebel): ribbed, no utricle. Scale bars = 10 µm.

nuclear) nucleotide sequence data for *Hysterangiales* available on GenBank were downloaded. Further, new *atp6* and *tef1* sequences were generated for 99 *Hysterangiales* specimens, as well as one specimen of *Phallales* and one specimen of *Cantharellales* to use as outgroup (Table 1). For these newly sequenced specimens, DNA was extracted from dried herbarium material with the E.Z.N.A. Forensic DNA Kit (Omega Bio-tek). A portion of the mitochondrial protein-coding gene *atp6* was PCR amplified with ATP6-3 and ATP6-2 primers (Kretzer & Bruns 1999) using the following cycling protocol: 95 °C for 5 min; 8 cycles of 94 °C for 35 s, 37 °C for 55 s, 72 °C for 60 s; 35 cycles of 72 °C for 60 s, 94 °C for 35 s, 45 °C for 55 s; 72 °C for 2 min. A portion of the nuclear protein-coding gene *tef1* was PCR amplified with *EF1*-983F and *EF1*-1567R, or *EF1*-1953R, primers (Rehner & Buckley 2005) using the following cycling protocol: 95 °C for 5 min; 10 cycles of 94 °C for 30 s, 65 °C for 60 s, 72 °C for 90 s; 30 cycles of 94 °C for 45 s, 55 °C for 60 s, 72 °C for 70 s; 72 °C for 5 min. Sanger sequencing was conducted in forward and reverse directions at the Australian Genome Research Facility (Melbourne, Victoria, Australia). Sequences are deposited in GenBank (Table 1).

Each gene was aligned using MAFFT online (Katoh *et al.* 2017), visually inspected, and manually adjusted as required. Phylogenetic analyses of each individual gene were conducted using the methods outlined in the next paragraph. Dendrograms from these analyses were then compared using PHYLO.IO (Robinson *et al.* 2016) to assess concordance. The topologies between each gene were found to be almost completely concordant at the generic level and below, corroborating all genera and species (with the exception of specimen H381 which appeared in different positions). Also, many relationships between genera were corroborated between *atp6* and *tef1*. In the individual gene analyses, higher taxonomic levels (e.g. family, suborder) were either not recovered or recovered with low support.

After the assessment of the individual gene phylogenies, *atp6* and *tef1* were concatenated, resulting in an alignment of 1 464 sites long with 223 terminals. MrBayesS v. 3.2.7a (Ronquist *et al*. 2012) was used via the CIPRES REST API (Miller *et al.* 2015) for Bayesian inference (BI) analysis. An analysis using default priors and the following parameters was run for 20 000 000 generations; nstopts: 6, nucmodelopts: 4by4, rateopts: gamma, nrunsval: 2, nchainsval: 4, tempval: 0.200, swapfreqval: 1, nswapsval: 1, samplefreqval: 1 000, burninfracval: 0.5, vparam.stopval: 0.003, sump_burninfrac: 0.5, sumpnruns: 2, sumt_burninfrac: 0.5, sumtnruns: 2, sumtntrees: 1. The average potential scale reduction factor reported for all parameters was 1.038. The alignment and resultant consensus phylogram is deposited in TreeBASE under study number 27527. To corroborate our topology and support values, we conducted additional separate analyses using different outgroup taxa (*Geastrales*), extended generations (ranging from 22 000 000 to 59 000 000), different models of rate variation among sites, and different partitions *i.e.* one partition, two partition (each gene), or multi-partition (codon positions for each gene, as well as introns for *tef1*) analyses. We also conducted maximum likelihood (ML) analysis using RAxML software (Stamatakis *et al*. 2008) via the CIPRES REST API with the following options; dna_gtrcat: GTRGAMMA, select_analysis: fa, choose_bootstrap: x, bootstrap_value: 1 000. Taxon names at individual terminals in the phylogram are field-based, verbatim identifications, from various mycologists.

RESULTS

The BI analysis recovered *Hysterangiales* (Bayesian posterior probability, bpp = 1) with the four constituent families *Gallaceaceae*, *Hysterangiaceae*, *Mesophelliaceae*, and *Phallogastraceae fam. nov*. (all bpp = 1), containing numerous described and undescribed genera (Supplementary Fig. S1, Fig. 3 - Parts 1,2,3). In total, 26 provisional undescribed genera were inferred (25 *Hysterangiales* and 1 *Phallales*). The results of the additional BI analyses and ML analysis were not substantively different from our primary BI analysis, corroborating all taxa indicated in Fig. 3 and Table 1. *Phallogastraceae* is accommodated by a newly established suborder, *Phallogastrineae* (described below, Fig. 3 - Part 1), and the families *Mesophelliaceae* (Fig. 3 - Part 1), *Hysterangiaceae* (Fig. 3 - Part 2) and *Gallaceae* (Fig. 3 - Part 3) are accommodated in the new suborder *Hysterangineae*. *Trappeaceae* is not in *Hysterangiales*, since the type species of *Trappea*, *T. darkeri*, is inferred to be in *Phallales* based on this and previous analyses (Hosaka *et al.* 2006, Sulzbacher *et al.* 2016; Fig. 3 - Part 3, Table 1). Neither *Trappea pinyonensis* nor *T. phillipsii* belong in *Trappea* given their position within *Phallogastraceae* (Xu & Luo 2003, Hosaka *et al.* 2006; Fig. 3 - Part 1); the combination to

© 2021 Westerdijk Fungal Biodiversity Institute

Phallogaster is made here. It should be noted that true *Protubera* lies outside of *Hysterangiales*, since the type (*P. maracuja*) and related species belong in *Protophallaceae*, *Phallales* (Trierveiler-Pereira *et al.* 2014). Thus, *Protubera hautuensis*, *P. nothofagi*, and all other taxa appearing in Fig. 3 - Part 3) labelled as *Protubera* are not true members of the genus (this includes *P. canescens*, which is a synonym of *Ileodictyon gracile* in *Phallaceae*, *Phallales*).

Taxonomy

Order *Hysterangiales* K. Hosaka & Castellano

Phallogastrineae Castellano, T. Lebel, Davoodian & K. Hosaka, ***subord. nov.*** MycoBank MB 838485.

Basidiomes sequestrate, small (0.2 cm wide) to larger (up to 5 cm long and 3 cm wide), subglobose to irregularly subovoid, with a tapered to irregularly shaped base, single or caespitose, with white rhizomorphs (rhizomorphs sometimes discolouring pinkish). Basidiome surface smooth to velvety to finely tomentose, white to clay white (discolouring pinkish to salmon buff to reddish or faint lilac). *Peridium* 160–2 000 µm thick. *Columella* branched, whitish to semi-translucent, gelatinized. *Gleba* varies from green, olivaceous green, greyish olive to pale olive; gelatinized, loculate, locules small. *Basidia* clavate to narrowly clavate to irregularly cylindrical, thin-walled, hyaline, 6–8-spored. *Sterigmata* small to indistinct. *Spores* smooth, elongate-ellipsoid to oblong, thin-walled, utricle absent, hyaline singly, olive buff to honey yellow or pale green in mass. *Clamp connections* present.

Phylogenetic taxon definition of the suborder: The largest crown clade containing *Phallogaster saccatus* Morgan 1893, but not *Hysterangium clathroides* Vittad. 1831, *Mesophellia arenaria* Berk. 1857, and *Gallacea scleroderma* (Cooke) Lloyd 1905. This is a maximum crown-clade definition (Hibbett *et al.* 2018).

Type family: Phallogastraceae Castellano, T. Lebel, Davoodian & K. Hosaka *non Phallogastraceae* Locq., *De Taxia Fungorum*: *I. Syllabus* **1A**: 56. 1974.

Phallogastraceae Castellano, T. Lebel, Davoodian & K. Hosaka, ***fam. nov.*** MycoBank MB 838484.

Basidiomes sequestrate, small (0.2 cm wide) to larger (up to 5 cm long and 3 cm wide), subglobose to irregularly subovoid, with a tapered to irregularly shaped base, single or caespitose, with white rhizomorphs (rhizomorphs sometimes discolouring pinkish). Basidiome surface smooth to velvety to finely tomentose, white to clay white (discolouring pinkish to salmon buff to reddish or faint lilac). *Peridium* 160–2 000 µm thick. *Columella* branched, whitish to semi-translucent, gelatinized. *Gleba* varies from green, olivaceous green, greyish olive to pale olive; gelatinized, loculate, locules small. *Basidia* clavate to narrowly clavate to irregularly cylindrical, thin-walled, hyaline, 6–8-spored. *Sterigmata* small to indistinct. *Spores* smooth, elongate-ellipsoid to oblong, thin-walled, utricle absent, hyaline singly, olive buff to honey yellow or pale green in mass. *Clamp connections* present. *Odour* sometimes fetid. Species apparently saprotrophic, occurring on decaying wood or leaves, or partially buried in litter.

Type genus: *Phallogaster* Morgan, *J. Cincinnati Soc. Nat. Hist.* **15**: 171. 1893.

Notes: *Phallogastraceae* Locq. (1974) is invalid in accordance with Art. 39:1 of the Shenzen code. This is the only clade in *Hysterangiales* with an apparently non-mycorrhizal habit. Although the number of taxa is thus far very limited, the phylogenetic relationships within the family/suborder strongly indicate reciprocal monophyly of the Northern Hemisphere ("*Phallogaster* clade") and Southern Hemisphere clades ("*Gen. prov*. 1") (Fig. 3 - Part 1).

In addition to a traditional morphology-based description for the corresponding suborder (*Phallogastrineae subord. nov.*), we have also applied a phylogenetic taxon definition for the suborder (see Hibbett *et al.* 2018). More taxon sampling in the future may require further amendment of the morphological definition of the suborder, whereas our phylogenetic taxon definition of *Phallogastrinae* will remain stable.

Phallogaster pinyonensis (States) K. Hosaka, Castellano, Davoodian & T. Lebel, ***comb. nov.*** MycoBank MB 838487.
Basionym: *Trappea pinyonensis* States, *Mycotaxon* **41**: 128. 1991. MycoBank MB 129849.

Typus: **USA**, Arizona, Walnut Canyon National Monument, Coconino County, on sandy soil under *Pinus edulis*, 10 Oct. 1986, *J. States* AHF-530 (**holotype** ASC).

Phallogaster phillipsii (Harkn.) K. Hosaka, Castellano, Davoodian & T. Lebel, ***comb. nov.*** MycoBank MB 840085.
Basionym: *Hysterangium phillipsii* Harkn., *Proceedings of the California Academy of Sciences* **1**(8): 255. 1899. MycoBank MB 187085.
Synonym: *Trappea phillipsii* (Harkn.) Castellano, *Mycotaxon* **38**: 7. 1990. MycoBank MB 127551.

Typus: **USA**, California, Wire Bridge, Placer County, in soil, associated with *Quercus*, Jan. 1899, *C.L. Phillips* (Harkness 234, **holotype** BPI)

Notes: Although the species was not included in the phylogenetic analysis in this study, it has clearly been demonstrated to be the sister taxon to *Phallogaster* (*Trappea) pinyonensis* by Hosaka *et al.* (2006). Its basidiome surfaces stain pinkish when bruised, which is also a common characteristic with other species in the genus *Phallogaster*.

Excluded taxa

Trappea cinnamomea A-S. Xu & D.Q. Luo, *Mycosystema* **22**: 192. 2003. MycoBank MB 489004.

Notes: Based on the original description of *T. cinnamomea* (Xu & Luo 2003), its basidiome surfaces have the staining reaction to pink, which is similar to *Trappea phillipsii* and *T. pinyonensis*. However, we so far have no access to the specimens and no DNA data from the species are currently available. Until more definitive evidence becomes available, we keep this taxon in the genus *Trappea*.

Hysterangineae Castellano, T. Lebel, Davoodian & K. Hosaka, ***subord. nov.*** MycoBank MB 838486.

Basidiomes sequestrate, hypogeous or epigeous, and can be small (0.1 cm wide) to larger (up to 10 cm wide), subglobose to

© 2021 Westerdijk Fungal Biodiversity Institute

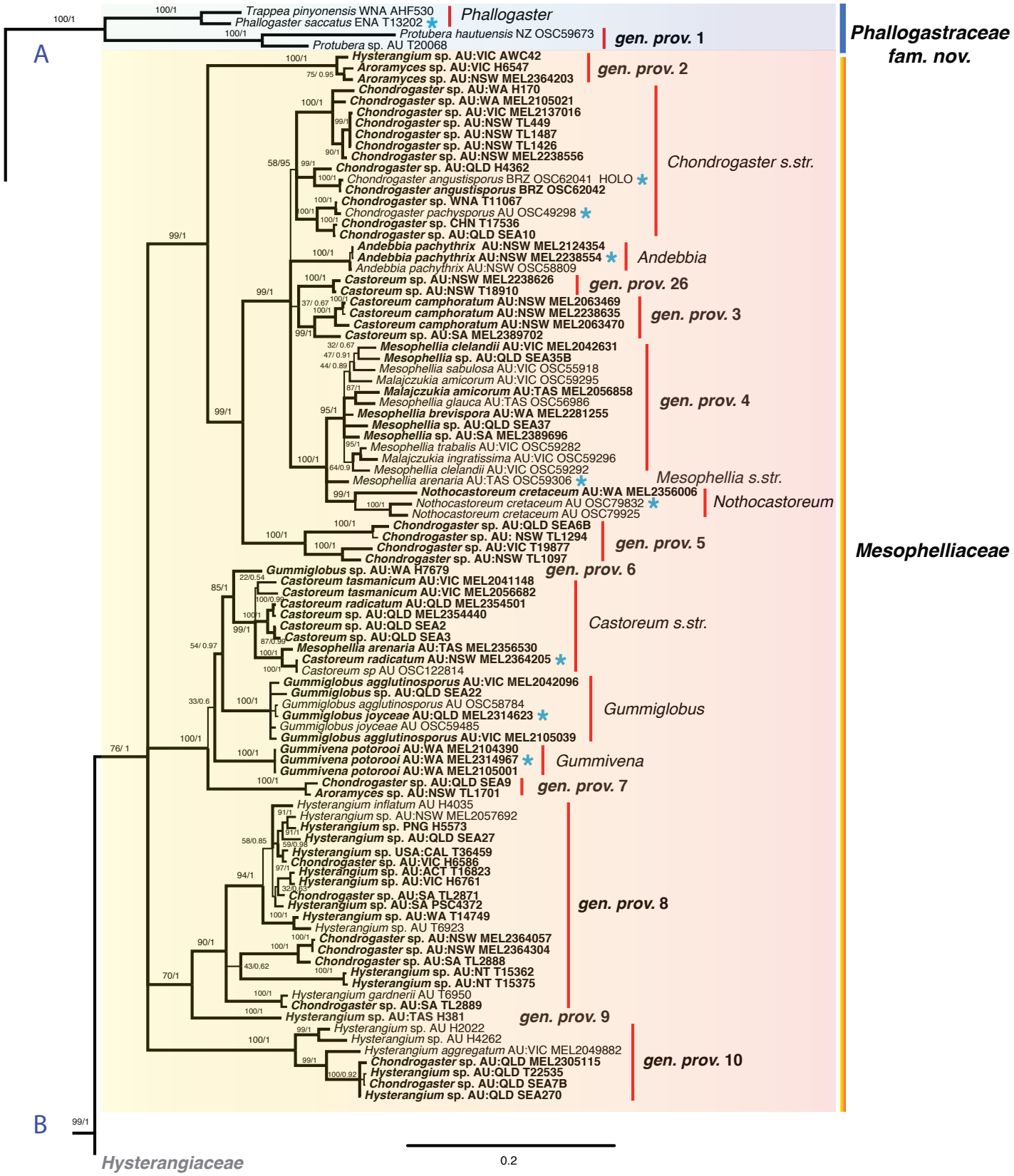

Fig. 3. Part 1. Phylogram from Bayesian analysis showing families and genera within *Hysterangiales*. Node A indicates *Phallogastrineae subord. nov.*; node B indicates *Hysterangineae subord. nov*. Maximum likelihood (ML) bootstrap values / Bayesian posterior probabilities (bpp) are shown at the nodes. The scale bar shows substitutions per site. Where bpp ≥ 0.95 and ML bootstrap ≥ 70%, branches are thickened. Type species indicated by a blue asterisk *. The asterisk in parentheses (*) denotes *Ileodictyon,* the currently accepted genus for *Protubera canescens*. Australian (AU) States and Territories indicated by: WA (Western Australia), NT (Northern Territory), QLD (Queensland), NSW (New South Wales), VIC (Victoria), TAS (Tasmania), SA (South Australia). United States (USA) states indicated by: ARIZ (Arizona), CAL (California), COL (Colorado), ID (Idaho), OR (Oregon). Other geographic areas indicated as follows: NZ (New Zealand), NewCal (New Caledonia), PNG (Papua New Guinea), BRZ (Brazil), MEX (Mexico), WNA (western North America), ENA (eastern North America), CHN (China), Guyana (Guyana), SSA (southern South America), NSA (northern South America), ASIA (Asia), SEASIA (southeast Asia), SING (Singapore), THAI (Thailand), IND (India), EUR (Europe), COSTA (Costa Rica), ZIMB (Zimbabwe).

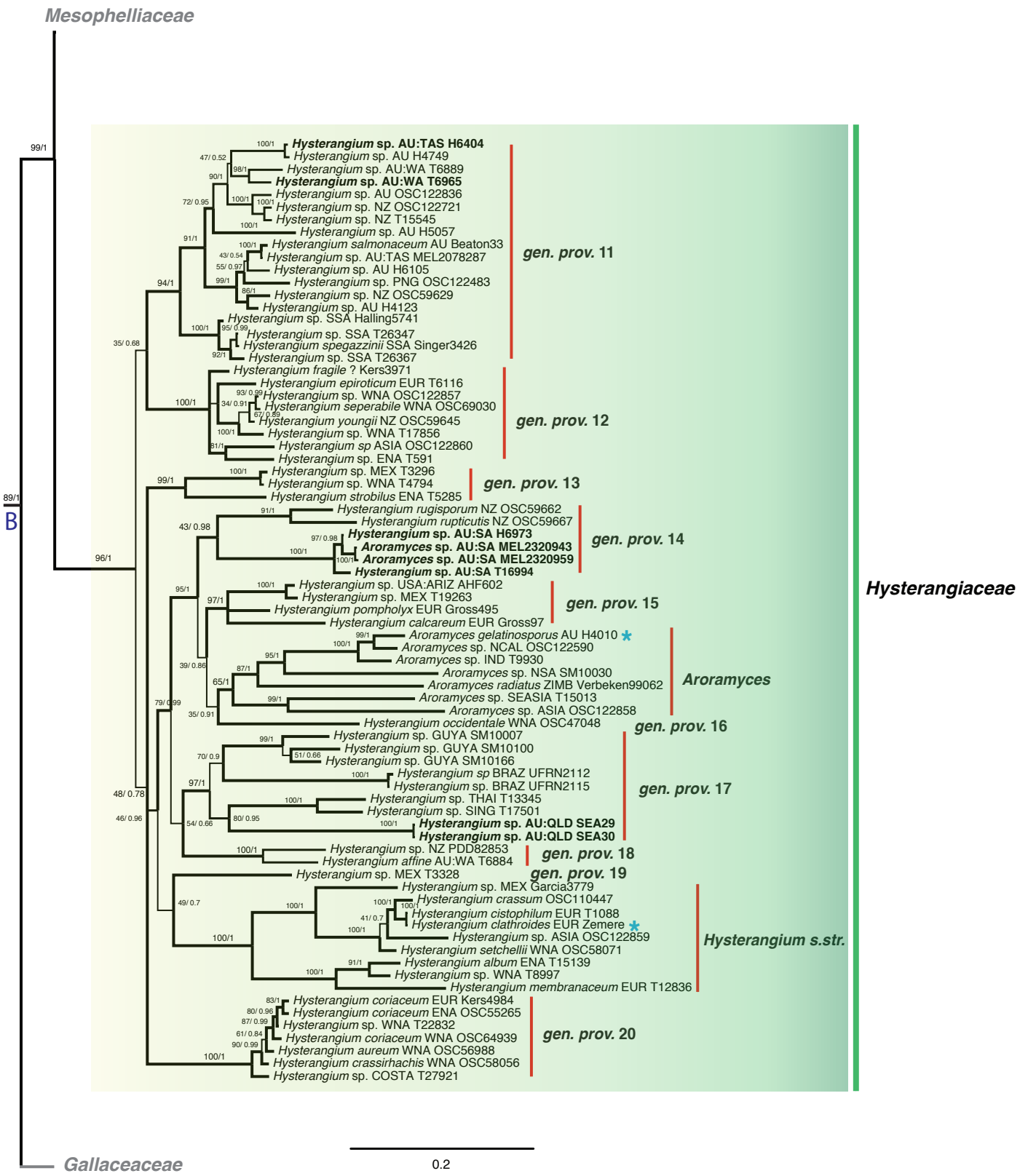

Fig. 3. (Continued) - Part 2.

irregularly subovoid without tapered base, single or gregarious, often covered with adhering sand and soil or encased in debris and rootlets, usually with conspicuous white to off-white rhizomorphs at base or along sides of basidiomata. Basidiome surface smooth to velvety to finely tomentose, often white to off-white in colour and often discolouring pinkish, reddish, yellowish or brownish, but purple to violet in some species. Peridium adherent to often readily separable from gleba, elastic, glutinous or hard and brittle, 1–4-layered, sometimes incorporating mycorrhizae. *Columella* branched, whitish to semi-translucent and gelatinized or a soft to corky or rubbery central core or lacking such structures. *Gleba* varies from green, olivaceous green, greyish olive, brown to ochraceous or pinkish; gelatinous to cartilaginous or with a powdery spore mass at maturity, often with labyrinthine to elongated to circular locules. *Basidia* clavate to narrowly clavate to irregularly cylindrical,

© 2021 Westerdijk Fungal Biodiversity Institute

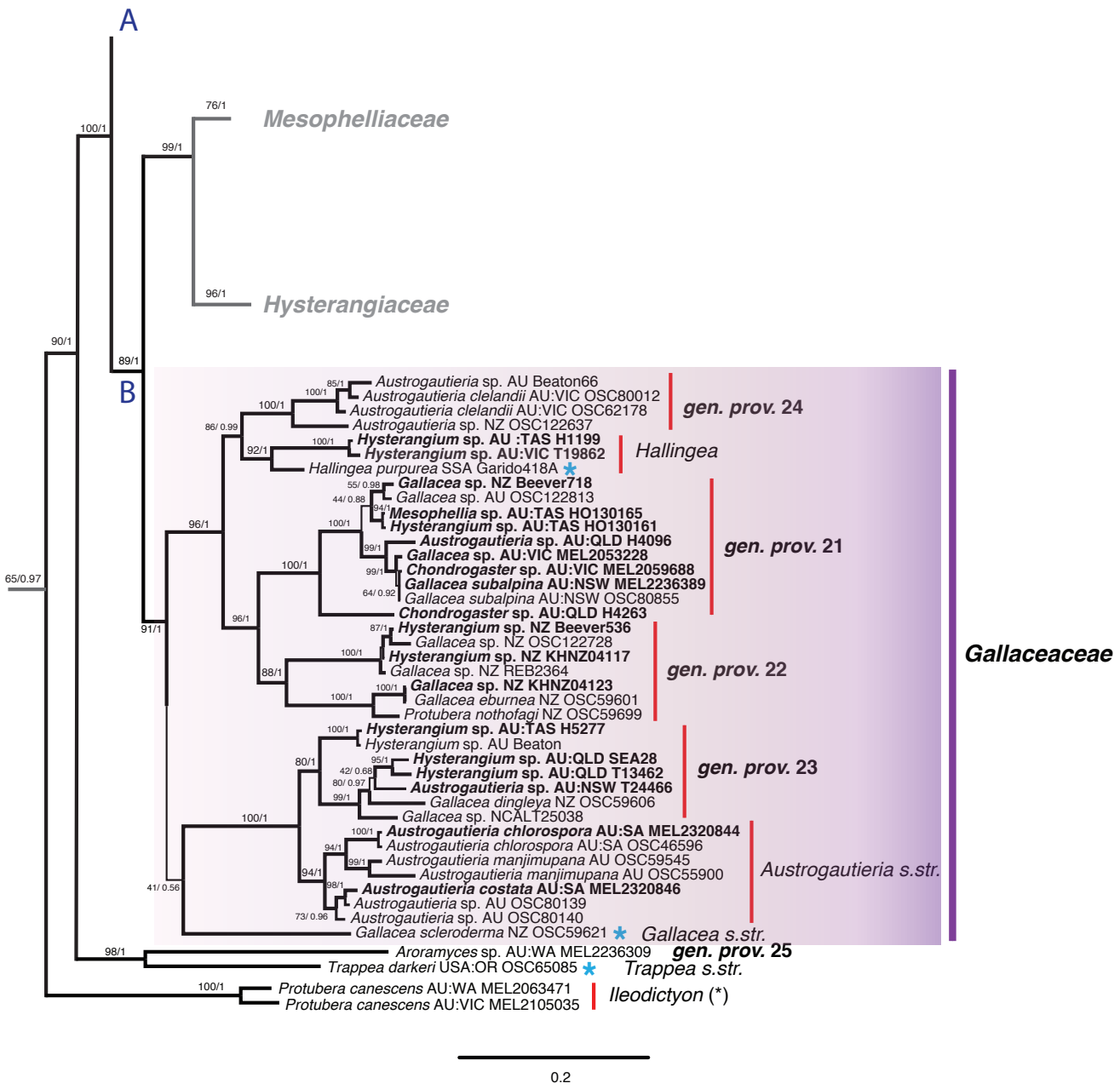

Fig. 3. (Continued) - Part 3.

thin-walled, hyaline, mostly 4-spored. *Spores* ellipsoid to oblong to fusoid, smooth to minutely verrucose or with long spines beneath a utricle, or sometimes with longitudinal ridges, thin- to thick-walled, often covered with a wrinkled to inflated or ephemeral utricle, hyaline, pale green, or brown in KOH, inamyloid, sometimes weakly dextrinoid. *Odour* faint, fetid, or sometimes sweet. *Clamp connections* present or absent. All species are presumably ectomycorrhizal with various vascular plants including *Dipterocarpaceae, Fagaceae, Myrtaceae, Nothofagaceae*, and *Pinaceae*.

Phylogenetic taxon definition of the suborder: The largest crown clade containing *Hysterangium clathroides* Vittad. 1831, but not *Phallogaster saccatus* Morgan 1893. This is a maximum crown-clade definition (Hibbett *et al*. 2018).

Type family: Hysterangiaceae E. Fisch., in Engler & Prantl, *Nat. Pflanzenfam.*, Teil. I (Leipzig): 304. 1899. [1900]

Notes: The *Hysterangineae* is exclusively composed of sequestrate taxa which are ectomycorrhizal with various vascular plants insofar as inferred from available studies. Most species in *Hysterangineae* have rather specific ectomycorrhizal hosts, usually restricted to a single plant family. For example, species distributed in the Southern Hemisphere are associated with *Myrtaceae* (mostly with *Eucalyptus* spp. and/or *Kunzea/ Leptospermum* spp.) or *Nothofagaceae* (Castellano & Beever 1994, Hosaka *et al*. 2008).

This suborder is much more speciose than *Phallogastrineae* and many more new species, especially from Australia, remain to be described for all three families, *i.e.*, *Hysterangiaceae, Mesophelliaceae* and *Gallaceaceae*. We believe that the family-level phylogeny is robust (Fig. 3, Supplementary Fig. S1), but more taxon sampling in the future may require further amendment of the morphological definition of the suborder. Therefore, as is the case for *Phallogastrineae*, we have also applied a phylogenetic taxon definition approach as summarized by Hibbett *et al.* (2018).

© 2021 Westerdijk Fungal Biodiversity Institute

Table 1. Tabulation of specimens and sequences used in this study. Clade names are from Fig. 3. Generic names (genus verbatim determination) without a species name (species verbatim determination) are based on field identification; collections with species names (species verbatim determination) were examined micromorphologically. Australian (AUS) States and Territories indicated by: WA (Western Australia), NT (Northern Territory), QLD (Queensland), NSW (New South Wales), VIC (Victoria), TAS (Tasmania), SA (South Australia). United States (USA) states indicated by: AZ (Arizona), CA (California), CO (Colorado), ID (Idaho), OR (Oregon). Other geographic areas indicated as follows: NZ (New Zealand), NEWCAL (New Caledonia), PNG (Papua New Guinea), BRZ (Brazil), MEX (Mexico), WNA (western North America), ENA (eastern North America), CHN (China), GUYANA (Guyana), SSA (southern South America), NSA (northern South America), ASIA (Asia), SEASIA (southeast Asia), SING (Singapore), THAI (Thailand), IND (India), EUR (Europe), COSTA (Costa Rica), ZIMB (Zimbabwe). Novel DNA sequences generated for this study are indicated by GenBank accessions in **bold**.

Clade	Genus verbatim determination	Species verbatim determination	Collector or Herbarium ID	Geography	ATP6	TEF1	Family	Suborder (Order)
Cantharellaceae	*Cantharellus*	sp.	TL2893	SA	**MT828543**	**MW302303**	*Cantharellaceae*	(*Cantharellales*)
Geastrum	*Geastrum*	*fimbriatum*	OSC60730	USA - OR	DQ218887	DQ219226	*Geastraceae*	(*Geastrales*)
	Geastrum	*floriforme*	OSC29328	USA - CO	DQ218769	DQ219227	*Geastraceae*	(*Geastrales*)
	Geastrum	*fornicatum*	MEL2087743	NSW	DQ218888	DQ219228	*Geastraceae*	(*Geastrales*)
	Geastrum	*pectinatum*	MEL2096557	VIC	DQ218889	DQ219229	*Geastraceae*	(*Geastrales*)
	Geastrum	*recolligens*	OSC41996	USA - ID	DQ218770	DQ219230	*Geastraceae*	(*Geastrales*)
Geastrum (*Radiigera*)	*Radiigera*	*fuscogleba*	OSC58979	—	DQ218896	DQ219234	*Geastraceae*	(*Geastrales*)
Gen. prov. 25 Lebel & Davoodian	*Aroramyces*	sp.	MEL2236309	WA	**MW438321**	**MW302302**	*Trappeaceae*	(*Phallales*)
Trappea	*Trappea*	*darkeri*	OSC65085	USA - OR	DQ218938	DQ219292	*Trappeaceae*	(*Phallales*)
Ileodictyon	*Protubera* [*Ileodictyon*]	*canescens* [*gracile*]	MEL2063471	WA	DQ218931	DQ219283	*Clathraceae*	(*Phallales*)
	Protubera [*Ileodictyon*]	*canescens* [*gracile*]	MEL2105035	VIC	DQ218932	DQ219284	*Clathraceae*	(*Phallales*)
Phallogaster	*Trappea*	*pinyonensis*	AHF530	WNA	DQ218884	DQ219221	*Phallogastraceae*	*Phallogastrineae* (*Hysterangiales*)
	Phallogaster	*saccatus*	T13202	ENA	DQ218882	DQ219217	*Phallogastraceae*	*Phallogastrineae* (*Hysterangiales*)
Gen. prov. 1 Hosaka	*Protubera*	sp.	T20068	AUS	DQ218883	DQ219220	*Phallogastraceae*	*Phallogastrineae* (*Hysterangiales*)
	Protubera	*hautuensis*	OSC59673	NZ	DQ218801	DQ219218	*Phallogastraceae*	*Phallogastrineae* (*Hysterangiales*)
Gen. prov. 24 Castellano & Hosaka	*Austrogautieria*	sp.	Beaton66	AUS	DQ218820	DQ219133	*Gallaceaceae*	*Hysterangineae* (*Hysterangiales*)
	Austrogautieria	sp.	OSC122637	NZ	DQ218819	DQ219132	*Gallaceaceae*	*Hysterangineae* (*Hysterangiales*)
	Austrogautieria	*clelandii*	OSC62178	VIC	DQ218816	DQ219126	*Gallaceaceae*	*Hysterangineae* (*Hysterangiales*)
	Austrogautieria	*clelandii*	OSC80012	VIC	DQ218817	DQ219127	*Gallaceaceae*	*Hysterangineae* (*Hysterangiales*)
Hallingea	*Hallingea*	*purpurea*	Garido418A	SSA	n/a	DQ219145	*Gallaceaceae*	*Hysterangineae* (*Hysterangiales*)
	Hysterangium	sp.	H1199	TAS	**MW449866**	**MW302288**	*Gallaceaceae*	*Hysterangineae* (*Hysterangiales*)
	indet.		T19862	VIC	**MW048610**	**MW302289**	*Gallaceaceae*	*Hysterangineae* (*Hysterangiales*)
Gen. prov. 21 Hosaka	*Austrogautieria*	sp.	H4096	QLD	**MW417403**	**MW302309**	*Gallaceaceae*	*Hysterangineae* (*Hysterangiales*)
	Chondrogaster	sp.	MEL2059688	VIC	**MW048613**	**MW302306**	*Gallaceaceae*	*Hysterangineae* (*Hysterangiales*)
	Chondrogaster	sp.	H4263	QLD	**MW048615**	**MW302290**	*Gallaceaceae*	*Hysterangineae* (*Hysterangiales*)
	Gallacea	sp.	Beever718	NZ	**MW449882**	**MW302308**	*Gallaceaceae*	*Hysterangineae* (*Hysterangiales*)
	Gallacea	sp.	OSC122813	AUS	DQ218829	DQ219144	*Gallaceaceae*	*Hysterangineae* (*Hysterangiales*)
	Gallacea	sp.	MEL2053228	VIC	**MW048612**	**MW264846**	*Gallaceaceae*	*Hysterangineae* (*Hysterangiales*)

© 2021 Westerdijk Fungal Biodiversity Institute

Table 1. (Continued).

Clade	Genus verbatim determination	Species verbatim determination	Collector or Herbarium ID	Geography	ATP6	TEF1	Family	Suborder (Order)
	Gallacea	*subalpina*	MEL2236389	NSW	**MW048614**	**MW302307**	*Gallaceaceae*	*Hysterangineae* (*Hysterangiales*)
	Gallacea	*subalpina*	OSC80855	NSW	DQ218827	DQ219142	*Gallaceaceae*	*Hysterangineae* (*Hysterangiales*)
	Hysterangium	sp.	HO130161	TAS	**MW438331**	**MW302304**	*Gallaceaceae*	*Hysterangineae* (*Hysterangiales*)
	Mesophellia	sp.	HO130165	TAS	**MW048611**	**MW302305**	*Gallaceaceae*	*Hysterangineae* (*Hysterangiales*)
Gen. prov. 22 Castellano	*Gallacea*	sp.	OSC122728	NZ	DQ218828	DQ219143	*Gallaceaceae*	*Hysterangineae* (*Hysterangiales*)
	Gallacea	sp.	REB2364	NZ	DQ218825	DQ219140	*Gallaceaceae*	*Hysterangineae* (*Hysterangiales*)
	Gallacea	sp.	KHNZ04123	NZ	**MW449865**	**MW302293**	*Gallaceaceae*	*Hysterangineae* (*Hysterangiales*)
	Gallacea	*eburnea*	OSC59601	NZ	DQ218766	DQ219138	*Gallaceaceae*	*Hysterangineae* (*Hysterangiales*)
	Hysterangium	sp.	Beever536	NZ	**MW417402**	**MW302291**	*Gallaceaceae*	*Hysterangineae* (*Hysterangiales*)
	Hysterangium	sp.	KHNZ04117	NZ	**MW438330**	**MW302292**	*Gallaceaceae*	*Hysterangineae* (*Hysterangiales*)
	Protubera	*nothofagi*	OSC59699	NZ	AY574786	DQ219219	*Gallaceaceae*	*Hysterangineae* (*Hysterangiales*)
Gen. prov. 23 Hosaka	*Austrogauteria*	sp.	T24466	NSW	**MW438326**	**MW302299**	*Gallaceaceae*	*Hysterangineae* (*Hysterangiales*)
	Gallacea	sp.	T25038	NEWCAL	DQ218826	DQ219141	*Gallaceaceae*	*Hysterangineae* (*Hysterangiales*)
	Gallacea	*dingleyae*	OSC59606	NZ	DQ218824	DQ219137	*Gallaceaceae*	*Hysterangineae* (*Hysterangiales*)
	Hysterangium	sp.	H5277	TAS	**MW048616**	**MW302294**	*Gallaceaceae*	*Hysterangineae* (*Hysterangiales*)
	Hysterangium	sp.	SEA28	QLD	**MW438329**	**MW302297**	*Gallaceaceae*	*Hysterangineae* (*Hysterangiales*)
	Hysterangium	sp.	T13462	QLD	**MW048617**	**MW302298**	*Gallaceaceae*	*Hysterangineae* (*Hysterangiales*)
	Hysterangium	sp.	KandGBeaton	AUS	DQ218790	DQ219174	*Gallaceaceae*	*Hysterangineae* (*Hysterangiales*)
Austrogautieria	*Austrogautieria*	sp.	OSC80139	AUS	DQ218763	DQ219130	*Gallaceaceae*	*Hysterangineae* (*Hysterangiales*)
	Austrogautieria	sp.	OSC80140	AUS	DQ218764	DQ219131	*Gallaceaceae*	*Hysterangineae* (*Hysterangiales*)
	Austrogautieria	*chlorospora*	MEL2320844	SA	**MW048618**	**MW302295**	*Gallaceaceae*	*Hysterangineae* (*Hysterangiales*)
	Austrogautieria	*chlorospora*	OSC46596	AUS	DQ218761	DQ219125	*Gallaceaceae*	*Hysterangineae* (*Hysterangiales*)
	Austrogautieria	*costata*	MEL2320846	SA	**MW438327**	**MW302296**	*Gallaceaceae*	*Hysterangineae* (*Hysterangiales*)
	Austrogautieria	*manjimupana*	OSC55900	AUS	DQ218818	DQ219128	*Gallaceaceae*	*Hysterangineae* (*Hysterangiales*)
	Austrogautieria	*manjimupana*	OSC59545	AUS	DQ218762	DQ219129	*Gallaceaceae*	*Hysterangineae* (*Hysterangiales*)
Gallacea	*Gallacea*	*scleroderma*	OSC59621	NZ	AY574787	DQ219139	*Gallaceaceae*	*Hysterangineae* (*Hysterangiales*)
Gen. prov. 11 Hosaka	*Hysterangium*	sp.	H6404	TAS	**MW417406**	**MW302282**	*Hysterangiaceae*	*Hysterangineae* (*Hysterangiales*)
Gen. prov. 11 Hosaka	*Hysterangium*	sp.	Halling5741	SSA	DQ218781	DQ219158	*Hysterangiaceae*	*Hysterangineae* (*Hysterangiales*)
Gen. prov. 11 Hosaka	*Hysterangium*	sp.	T26347	SSA	DQ218873	DQ219204	*Hysterangiaceae*	*Hysterangineae* (*Hysterangiales*)
	Hysterangium	sp.	T26367	SSA	DQ218874	DQ219205	*Hysterangiaceae*	*Hysterangineae* (*Hysterangiales*)
	Hysterangium	sp.	OSC122836	AUS	DQ218865	DQ219196	*Hysterangiaceae*	*Hysterangineae* (*Hysterangiales*)

Table 1. (Continued).

Clade	Genus verbatim determination	Species verbatim determination	Collector or Herbarium ID	Geography	ATP6	TEF1	Family	Suborder (Order)
	Hysterangium	sp.	T15545	NZ	DQ218837	DQ219161	*Hysterangiaceae*	*Hysterangineae* (*Hysterangiales*)
	Hysterangium	sp.	H4123	AUS	DQ218845	DQ219176	*Hysterangiaceae*	*Hysterangineae* (*Hysterangiales*)
	Hysterangium	sp.	H4749	AUS	DQ218861	DQ219192	*Hysterangiaceae*	*Hysterangineae* (*Hysterangiales*)
	Hysterangium	sp.	H5057	AUS	DQ218862	DQ219193	*Hysterangiaceae*	*Hysterangineae* (*Hysterangiales*)
	Hysterangium	sp.	H6105	AUS	DQ218864	DQ219195	*Hysterangiaceae*	*Hysterangineae* (*Hysterangiales*)
	Hysterangium	sp.	MEL2078287	TAS	DQ218843	DQ219173	*Hysterangiaceae*	*Hysterangineae* (*Hysterangiales*)
	Hysterangium	sp.	OSC122483	PNG	DQ218867	DQ219198	*Hysterangiaceae*	*Hysterangineae* (*Hysterangiales*)
	Hysterangium	sp.	OSC122721	NZ	DQ218866	DQ219197	*Hysterangiaceae*	*Hysterangineae* (*Hysterangiales*)
	Hysterangium	sp.	OSC59629	NZ	DQ218853	DQ219184	*Hysterangiaceae*	*Hysterangineae* (*Hysterangiales*)
	Hysterangium	"irregular"	T6965	WA	**MW438322**	**MW302283**	*Hysterangiaceae*	*Hysterangineae* (*Hysterangiales*)
	Hysterangium	"*rhodocarpum*"	T6889	WA	DQ218858	DQ219189	*Hysterangiaceae*	*Hysterangineae* (*Hysterangiales*)
	Hysterangium	*salmonaceum*	Beaton33	AUS	DQ218785	DQ219165	*Hysterangiaceae*	*Hysterangineae* (*Hysterangiales*)
	Hysterangium	*spegazzinii*	Singer3426	SSA	DQ218787	n/a	*Hysterangiaceae*	*Hysterangineae* (*Hysterangiales*)
Gen. prov. 12 Castellano	*Hysterangium*	sp.	OSC122857	WNA	DQ218851	DQ219182	*Hysterangiaceae*	*Hysterangineae* (*Hysterangiales*)
	Hysterangium	sp.	OSC122860	ASIA	DQ218860	DQ219191	*Hysterangiaceae*	*Hysterangineae* (*Hysterangiales*)
	Hysterangium	sp.	T17856	WNA	DQ218857	DQ219188	*Hysterangiaceae*	*Hysterangineae* (*Hysterangiales*)
	Hysterangium	sp.	T591	ENA	DQ218840	DQ219170	*Hysterangiaceae*	*Hysterangineae* (*Hysterangiales*)
	Hysterangium	*epiroticum*	T6116	EUR	DQ218779	DQ219155	*Hysterangiaceae*	*Hysterangineae* (*Hysterangiales*)
	Hysterangium	*fragile*	Kers3971	—	DQ218780	DQ219156	*Hysterangiaceae*	*Hysterangineae* (*Hysterangiales*)
	Hysterangium	*separabile*	OSC69030	WNA	DQ218786	DQ219166	*Hysterangiaceae*	*Hysterangineae* (*Hysterangiales*)
	Hysterangium	*youngii*	OSC59645	NZ	DQ218789	DQ219169	*Hysterangiaceae*	*Hysterangineae* (*Hysterangiales*)
Gen. prov. 13 Castellano	*Hysterangium*	sp.	T3296	MEX	DQ218842	DQ219172	*Hysterangiaceae*	*Hysterangineae* (*Hysterangiales*)
	Hysterangium	sp.	T4794	WNA	DQ218846	DQ219177	*Hysterangiaceae*	*Hysterangineae* (*Hysterangiales*)
	Hysterangium	*strobilus*	T5285	ENA	DQ218788	DQ219168	*Hysterangiaceae*	*Hysterangineae* (*Hysterangiales*)
Gen. prov. 14 Lebel	*Aroramyces*	sp.	MEL2320943	SA	**MW218374**	**MW302286**	*Hysterangiaceae*	*Hysterangineae* (*Hysterangiales*)
	Aroramyces	sp.	MEL2320959	SA	**MW218375**	**MW302287**	*Hysterangiaceae*	*Hysterangineae* (*Hysterangiales*)
	Hysterangium	*rugisporum*	OSC59662	NZ	DQ218784	DQ219164	*Hysterangiaceae*	*Hysterangineae* (*Hysterangiales*)
	Hysterangium	*rupticutis*	OSC59667	NZ	DQ218838	n/a	*Hysterangiaceae*	*Hysterangineae* (*Hysterangiales*)
	Hysterogaster	sp.	H6973	SA	**MW218372**	**MW302284**	*Hysterangiaceae*	*Hysterangineae* (*Hysterangiales*)
	Hysterogaster	sp.	T16994	VIC	**MW218373**	**MW302285**	*Hysterangiaceae*	*Hysterangineae* (*Hysterangiales*)
Gen. prov. 15 Castellano	*Hysterangium*	sp.	AHF602	USA - AZ	DQ218854	DQ219185	*Hysterangiaceae*	*Hysterangineae* (*Hysterangiales*)

© 2021 Westerdijk Fungal Biodiversity Institute

Table 1. (Continued).

Clade	Genus verbatim determination	Species verbatim determination	Collector or Herbarium ID	Geography	ATP6	TEF1	Family	Suborder (Order)
	Hysterangium	sp.	T19263	MEX	DQ218849	DQ219180	*Hysterangiaceae*	*Hysterangineae* (*Hysterangiales*)
	Hysterangium	*calcareum*	Gross97	EUR	DQ218776	DQ219149	*Hysterangiaceae*	*Hysterangineae* (*Hysterangiales*)
	Hysterangium	*pompholyx*	Gross495	EUR	DQ218783	DQ219163	*Hysterangiaceae*	*Hysterangineae* (*Hysterangiales*)
Aroramyces	*Aroramyces*	*gelatinosporus*	H4010	AUS	DQ218809	DQ219118	*Hysterangiaceae*	*Hysterangineae* (*Hysterangiales*)
	Aroramyces	*radiatus*	Verbeken99062	ZIMB	DQ218810	DQ219119	*Hysterangiaceae*	*Hysterangineae* (*Hysterangiales*)
	Aroramyces	sp.	OSC122590	NEWCAL	DQ218814	DQ219123	*Hysterangiaceae*	*Hysterangineae* (*Hysterangiales*)
	Aroramyces	sp.	OSC122858	ASIA	DQ218813	DQ219122	*Hysterangiaceae*	*Hysterangineae* (*Hysterangiales*)
	Aroramyces	sp.	SM10030	NSA	DQ218815	DQ219124	*Hysterangiaceae*	*Hysterangineae* (*Hysterangiales*)
	Aroramyces	sp.	T15013	SEASIA	DQ218811	DQ219120	*Hysterangiaceae*	*Hysterangineae* (*Hysterangiales*)
	Aroramyces	sp.	T9930	IND	DQ218812	DQ219121	*Hysterangiaceae*	*Hysterangineae* (*Hysterangiales*)
Gen. prov. 16 Lebel & Castellano	*Hysterangium*	*occidentale*	OSC47048	WNA	AY574825	DQ219162	*Hysterangiaceae*	*Hysterangineae* (*Hysterangiales*)
Gen. prov. 17 Lebel & Castellano	*Hysterangium*	sp.	SEA29	QLD	**MW438328**	**MW302300**	*Hysterangiaceae*	*Hysterangineae* (*Hysterangiales*)
	Hysterangium	sp.	SEA30	QLD	**MW438323**	**MW302301**	*Hysterangiaceae*	*Hysterangineae* (*Hysterangiales*)
	Hysterangium	sp.	SM10007	GUYANA	DQ218869	DQ219200	*Hysterangiaceae*	*Hysterangineae* (*Hysterangiales*)
	Hysterangium	sp.	SM10100	GUYANA	DQ218870	DQ219201	*Hysterangiaceae*	*Hysterangineae* (*Hysterangiales*)
	Hysterangium	sp.	SM10166	GUYANA	DQ218871	DQ219202	*Hysterangiaceae*	*Hysterangineae* (*Hysterangiales*)
	Hysterangium	sp.	T13345	THAI	DQ218872	DQ219203	*Hysterangiaceae*	*Hysterangineae* (*Hysterangiales*)
	Hysterangium	sp.	T17501	SING	DQ218841	DQ219171	*Hysterangiaceae*	*Hysterangineae* (*Hysterangiales*)
	Hysterangium	sp.	UFRN2112	BRZ	LT635647	LT635645	*Hysterangiaceae*	*Hysterangineae* (*Hysterangiales*)
	Hysterangium	sp.	UFRN2115	BRZ	LT635648	LT635646	*Hysterangiaceae*	*Hysterangineae* (*Hysterangiales*)
Gen. prov. 18 Castellano & Lebel	*Hysterangium*	sp.	PDD82853	NZ	DQ218868	DQ219199	*Hysterangiaceae*	*Hysterangineae* (*Hysterangiales*)
	Hysterangium	*affine*	T6884	AUS	DQ218831	n/a	*Hysterangiaceae*	*Hysterangineae* (*Hysterangiales*)
Gen. prov. 19 Castellano	*Hysterangium*	sp.	T3328	MEX	DQ218852	DQ219183	*Hysterangiaceae*	*Hysterangineae* (*Hysterangiales*)
Hysterangium	*Hysterangium*	sp.	Garcia3779	MEX	DQ218847	DQ219178	*Hysterangiaceae*	*Hysterangineae* (*Hysterangiales*)
	Hysterangium	sp.	OSC122859	ASIA	DQ218859	DQ219190	*Hysterangiaceae*	*Hysterangineae* (*Hysterangiales*)
	Hysterangium	sp.	T8997	WNA	DQ218876	DQ219207	*Hysterangiaceae*	*Hysterangineae* (*Hysterangiales*)
	Hysterangium	*album*	T15139	ENA	DQ218774	DQ219147	*Hysterangiaceae*	*Hysterangineae* (*Hysterangiales*)
	Hysterangium	*cistophilum*	T1088	EUR	DQ218777	DQ219150	*Hysterangiaceae*	*Hysterangineae* (*Hysterangiales*)
	Hysterangium	*clathroides*	Zemere	EUR	DQ218832	DQ219151	*Hysterangiaceae*	*Hysterangineae* (*Hysterangiales*)
	Hysterangium	*crassum*	OSC110447	—	AY574827	DQ219154	*Hysterangiaceae*	*Hysterangineae* (*Hysterangiales*)
	Hysterangium	*membranaceum*	T12836	EUR	DQ218782	DQ219160	*Hysterangiaceae*	*Hysterangineae* (*Hysterangiales*)

Table 1. (Continued).

Clade	Genus verbatim determination	Species verbatim determination	Collector or Herbarium ID	Geography	ATP6	TEF1	Family	Suborder (Order)
	Hysterangium	*setchellii*	OSC58071	WNA	DQ218839	DQ219167	*Hysterangiaceae*	*Hysterangineae* (*Hysterangiales*)
Gen. prov. 20 Castellano	*Hysterangium*	sp.	T22832	WNA	DQ218850	DQ219181	*Hysterangiaceae*	*Hysterangineae* (*Hysterangiales*)
	Hysterangium	sp.	T27921	COSTA	DQ218875	DQ219206	*Hysterangiaceae*	*Hysterangineae* (*Hysterangiales*)
	Hysterangium	*aureum*	OSC56988	WNA	DQ218775	DQ219148	*Hysterangiaceae*	*Hysterangineae* (*Hysterangiales*)
	Hysterangium	*coriaceum*	Kers4984	EUR	DQ218833	n/a	*Hysterangiaceae*	*Hysterangineae* (*Hysterangiales*)
	Hysterangium	*coriaceum*	OSC55265	ENA	DQ218834	n/a	*Hysterangiaceae*	*Hysterangineae* (*Hysterangiales*)
	Hysterangium	*coriaceum*	OSC64939	WNA	AY574826	DQ219152	*Hysterangiaceae*	*Hysterangineae* (*Hysterangiales*)
	Hysterangium	*crassirhachis*	OSC58056	WNA	DQ218778	DQ219153	*Hysterangiaceae*	*Hysterangineae* (*Hysterangiales*)
Gen. prov. 2 Lebel	*Aroramyces*	sp.	H6547	VIC	**MW417410**	**MW302213**	*Mesophelliaceae*	*Hysterangineae* (*Hysterangiales*)
	Aroramyces	sp.	MEL2364203	NSW	**MW417417**	**MW302214**	*Mesophelliaceae*	*Hysterangineae* (*Hysterangiales*)
	Hysterangium	sp.	AWC42	VIC	**MW417411**	**MW302212**	*Mesophelliaceae*	*Hysterangineae* (*Hysterangiales*)
Chondrogaster	*Chondrogaster*	sp.	H170	WA	**MW438325**	**MW302215**	*Mesophelliaceae*	*Hysterangineae* (*Hysterangiales*)
	Chondrogaster	sp.	H4362	QLD	**MW449881**	**MW302217**	*Mesophelliaceae*	*Hysterangineae* (*Hysterangiales*)
	Chondrogaster	sp.	MEL2137016	VIC	**MW417412**	**MW302218**	*Mesophelliaceae*	*Hysterangineae* (*Hysterangiales*)
	Chondrogaster	sp.	TL449	NSW	**MW417415**	**MW302219**	*Mesophelliaceae*	*Hysterangineae* (*Hysterangiales*)
	Chondrogaster	sp.	TL1487	NSW	**MW417414**	**MW302220**	*Mesophelliaceae*	*Hysterangineae* (*Hysterangiales*)
	Chondrogaster	sp.	TL1426	NSW	**MW417413**	**MW302221**	*Mesophelliaceae*	*Hysterangineae* (*Hysterangiales*)
	Chondrogaster	sp.	T17536	CHN	**MW449874**	**MW302224**	*Mesophelliaceae*	*Hysterangineae* (*Hysterangiales*)
	Chondrogaster	sp.	SEA10	QLD	**MW449868**	**MW302225**	*Mesophelliaceae*	*Hysterangineae* (*Hysterangiales*)
	Chondrogaster	sp.	T11067	WNA	**MW438324**	**MW302223**	*Mesophelliaceae*	*Hysterangineae* (*Hysterangiales*)
	Chondrogaster	sp.	MEL2238556	NSW	**MW417405**	**MW302226**	*Mesophelliaceae*	*Hysterangineae* (*Hysterangiales*)
	Chondrogaster	*angustisporus*	MEL2105021	WA	**MW417407**	**MW302216**	*Mesophelliaceae*	*Hysterangineae* (*Hysterangiales*)
	Chondrogaster	*angustisporus*	OSC62041	BRZ	DQ218822	DQ219135	*Mesophelliaceae*	*Hysterangineae* (*Hysterangiales*)
	Chondrogaster	*angustisporus*	OSC62042	BRZ	**MW449876**	**MW302222**	*Mesophelliaceae*	*Hysterangineae* (*Hysterangiales*)
	Chondrogaster	*pachysporus*	OSC49298	AUS	DQ218823	DQ219136	*Mesophelliaceae*	*Hysterangineae* (*Hysterangiales*)
Andebbia	*Andebbia*	*pachythrix*	MEL2124354	NSW	**MW449879**	**MW302227**	*Mesophelliaceae*	*Hysterangineae* (*Hysterangiales*)
	Andebbia	*pachythrix*	MEL2238554	NSW	**MW449880**	**MW302228**	*Mesophelliaceae*	*Hysterangineae* (*Hysterangiales*)
	Andebbia	*pachythrix*	OSC58809	NSW	DQ218808	DQ219117	*Mesophelliaceae*	*Hysterangineae* (*Hysterangiales*)
Gen. prov. 26 Castellano	*Castoreum*	sp.	MEL2238626	NSW	**MW449869**	**MW302229**	*Mesophelliaceae*	*Hysterangineae* (*Hysterangiales*)
	Castoreum	sp.	T18910	NSW	**MW417409**	**MW302230**	*Mesophelliaceae*	*Hysterangineae* (*Hysterangiales*)
Gen. prov. 3 Castellano	*Castoreum*	sp.	MEL2389702	SA	**MW417408**	**MW302241**	*Mesophelliaceae*	*Hysterangineae* (*Hysterangiales*)

© 2021 Westerdijk Fungal Biodiversity Institute

Table 1. (Continued).

Clade	Genus verbatim determination	Species verbatim determination	Collector or Herbarium ID	Geography	ATP6	TEF1	Family	Suborder (Order)
	Castoreum	*camphoratum*	MEL2063469	NSW	**MW417404**	**MW302231**	*Mesophelliaceae*	*Hysterangineae* (*Hysterangiales*)
	Castoreum	*camphoratum*	MEL2238635	NSW	**MW417416**	**MW302232**	*Mesophelliaceae*	*Hysterangineae* (*Hysterangiales*)
	Castoreum	*camphoratum*	MEL2063470	NSW	**MW449877**	**MW302233**	*Mesophelliaceae*	*Hysterangineae* (*Hysterangiales*)
Gen. prov. 4 Castellano & Lebel	*Malajczukia*	*amicorum*	MEL2056858	TAS	**MW449867**	**MW302235**	*Mesophelliaceae*	*Hysterangineae* (*Hysterangiales*)
	Malajczukia	*amicorum*	OSC59295	VIC	DQ218792	DQ219208	*Mesophelliaceae*	*Hysterangineae* (*Hysterangiales*)
	Malajczukia	*ingratissima*	OSC59296	VIC	DQ218793	DQ219209	*Mesophelliaceae*	*Hysterangineae* (*Hysterangiales*)
	Mesophellia	sp.	SEA37	QLD	**MW449875**	**MW302237**	*Mesophelliaceae*	*Hysterangineae* (*Hysterangiales*)
	Mesophellia	sp.	MEL2389696	SA	**MW449870**	**MW302238**	*Mesophelliaceae*	*Hysterangineae* (*Hysterangiales*)
	Mesophellia	sp.	SEA35B	QLD	**MW438333**	**MW302239**	*Mesophelliaceae*	*Hysterangineae* (*Hysterangiales*)
	Mesophellia	*brevispora*	MEL2281255	WA	**MW449872**	**MW302236**	*Mesophelliaceae*	*Hysterangineae* (*Hysterangiales*)
	Mesophellia	*clelandii*	MEL2042631	VIC	**MW449878**	**MW302234**	*Mesophelliaceae*	*Hysterangineae* (*Hysterangiales*)
	Mesophellia	*clelandii*	OSC59292	VIC	DQ218795	DQ219211	*Mesophelliaceae*	*Hysterangineae* (*Hysterangiales*)
	Mesophellia	*glauca*	OSC56986	TAS	DQ218878	DQ219212	*Mesophelliaceae*	*Hysterangineae* (*Hysterangiales*)
	Mesophellia	*sabulosa*	OSC55918	VIC	DQ218879	DQ219213	*Mesophelliaceae*	*Hysterangineae* (*Hysterangiales*)
	Mesophelllia	*trabalis*	OSC59282	VIC	DQ218880	DQ219214	*Mesophelliaceae*	*Hysterangineae* (*Hysterangiales*)
Mesophellia	*Mesophellia*	*arenaria*	OSC59306	TAS	DQ218877	DQ219210	*Mesophelliaceae*	*Hysterangineae* (*Hysterangiales*)
Nothocastoreum	*Nothocastoreum*	*cretaceum*	MEL2356006	WA	**MW246680**	**MW302240**	*Mesophelliaceae*	*Hysterangineae* (*Hysterangiales*)
	Nothocastoreum	*cretaceum*	OSC79832	AUS	DQ218881	DQ219215	*Mesophelliaceae*	*Hysterangineae* (*Hysterangiales*)
	Nothocastoreum	*cretaceum*	OSC79925	AUS	n/a	DQ219216	*Mesophelliaceae*	*Hysterangineae* (*Hysterangiales*)
Gen. prov. 5 Lebel	*Chondrogaster*	sp.	SEA6B	QLD	**MW246665**	**MW302273**	*Mesophelliaceae*	*Hysterangineae* (*Hysterangiales*)
	Chondrogaster	sp.	TL1294	NSW	**MW246677**	**MW302274**	*Mesophelliaceae*	*Hysterangineae* (*Hysterangiales*)
	Chondrogaster	sp.	T19877	VIC	**MW246684**	**MW302275**	*Mesophelliaceae*	*Hysterangineae* (*Hysterangiales*)
	Chondrogaster	sp.	TL1097	NSW	**MW246685**	**MW302276**	*Mesophelliaceae*	*Hysterangineae* (*Hysterangiales*)
Gen. prov. 6 Lebel & Davoodian	*Gummiglobus*	sp.	H7679	WA	**MW449873**	**MW302242**	*Mesophelliaceae*	*Hysterangineae* (*Hysterangiales*)
Castoreum	*Castoreum*	sp.	SEA2	QLD	**MW246674**	**MW302246**	*Mesophelliaceae*	*Hysterangineae* (*Hysterangiales*)
	Castoreum	sp.	SEA3	QLD	**MW246668**	**MW302247**	*Mesophelliaceae*	*Hysterangineae* (*Hysterangiales*)
	Castoreum	sp.	OSC122814	AUS	DQ218821	DQ219134	*Mesophelliaceae*	*Hysterangineae* (*Hysterangiales*)
	Castoreum	*radicatum*	MEL2354501	QLD	**MW246672**	**MW302244**	*Mesophelliaceae*	*Hysterangineae* (*Hysterangiales*)
	Castoreum	*radicatum*	MEL2364205	NSW	**MW246690**	**MW302250**	*Mesophelliaceae*	*Hysterangineae* (*Hysterangiales*)
	Castoreum	*tasmanicum*	MEL2041148	VIC	**MW246695**	**MW302243**	*Mesophelliaceae*	*Hysterangineae* (*Hysterangiales*)
	Castoreum	*tasmanicum*	MEL2056682	VIC	**MW246683**	**MW302248**	*Mesophelliaceae*	*Hysterangineae* (*Hysterangiales*)

© 2021 Westerdijk Fungal Biodiversity Institute

Table 1. (Continued).

Clade	Genus verbatim determination	Species verbatim determination	Collector or Herbarium ID	Geography	ATP6	TEF1	Family	Suborder (Order)
	Fusicastoreum	sp.	MEL2354440	QLD	**MW246667**	**MW302245**	*Mesophelliaceae*	*Hysterangineae* (*Hysterangiales*)
	Mesophellia	*arenaria*	MEL2356530	TAS	**MW246688**	**MW302249**	*Mesophelliaceae*	*Hysterangineae* (*Hysterangiales*)
Gummiglobus	*Gummiglobus*	sp.	SEA22	QLD	**MW246691**	**MW302252**	*Mesophelliaceae*	*Hysterangineae* (*Hysterangiales*)
	Gummiglobus	*agglutinosporus*	OSC58784	AUS	DQ218830	n/a	*Mesophelliaceae*	*Hysterangineae* (*Hysterangiales*)
	Gummiglobus	*agglutinosporus*	MEL2042096	VIC	**MW246693**	**MW302251**	*Mesophelliaceae*	*Hysterangineae* (*Hysterangiales*)
	Gummiglobus	*agglutinosporus*	MEL2105039	VIC	**MW246670**	**MW302254**	*Mesophelliaceae*	*Hysterangineae* (*Hysterangiales*)
	Gummiglobus	*joyceae*	MEL2314623	QLD	**MW438332**	**MW302253**	*Mesophelliaceae*	*Hysterangineae* (*Hysterangiales*)
	Gummiglobus	*joyceae*	OSC59485	AUS	DQ218772	n/a	*Mesophelliaceae*	*Hysterangineae* (*Hysterangiales*)
Gummivena	*Gummivena*	*potorooi*	MEL2104390	WA	**MW246678**	**MW302255**	*Mesophelliaceae*	*Hysterangineae* (*Hysterangiales*)
	Gummivena	*potorooi*	MEL2314967	WA	**MW246696**	**MW302256**	*Mesophelliaceae*	*Hysterangineae* (*Hysterangiales*)
	Gummivena	*potorooi*	MEL2105001	WA	**MW246673**	**MW302257**	*Mesophelliaceae*	*Hysterangineae* (*Hysterangiales*)
Gen. prov. 7 Davoodian, Lebel & Castellano	*Aroramyces*	sp.	TL1701	NSW	**MT947437**	**MT947438**	*Mesophelliaceae*	*Hysterangineae* (*Hysterangiales*)
	Chondrogaster	sp.	SEA9	QLD	**MT947436**	**MW264847**	*Mesophelliaceae*	*Hysterangineae* (*Hysterangiales*)
Gen. prov. 8 Hosaka	*Chondrogaster*	sp.	H6586	VIC	**MW246682**	**MW302260**	*Mesophelliaceae*	*Hysterangineae* (*Hysterangiales*)
	Chondrogaster	sp.	TL2871	SA	**MW246692**	**MW302262**	*Mesophelliaceae*	*Hysterangineae* (*Hysterangiales*)
	Chondrogaster	sp.	MEL2364057	NSW	**MW246671**	**MW302267**	*Mesophelliaceae*	*Hysterangineae* (*Hysterangiales*)
	Chondrogaster	sp.	MEL2364304	NSW	**MW246697**	**MW302268**	*Mesophelliaceae*	*Hysterangineae* (*Hysterangiales*)
	Chondrogaster	sp.	TL2888	SA	**MW246689**	**MW302269**	*Mesophelliaceae*	*Hysterangineae* (*Hysterangiales*)
	Chondrogaster	sp.	TL2889	SA	**MW246687**	**MW302270**	*Mesophelliaceae*	*Hysterangineae* (*Hysterangiales*)
	Hysterangium	sp.	T16823	ACT	**MW246686**	**MW302258**	*Mesophelliaceae*	*Hysterangineae* (*Hysterangiales*)
	Hysterangium	sp.	T36459	USA - CA	**MW246694**	**MW302259**	*Mesophelliaceae*	*Hysterangineae* (*Hysterangiales*)
	Hysterangium	sp.	PSC4372	SA	**MW246679**	**MW302261**	*Mesophelliaceae*	*Hysterangineae* (*Hysterangiales*)
	Hysterangium	sp.	H6761	VIC	**MW246666**	**MW302263**	*Mesophelliaceae*	*Hysterangineae* (*Hysterangiales*)
	Hysterangium	sp.	SEA27	QLD	**MW246681**	**MW302265**	*Mesophelliaceae*	*Hysterangineae* (*Hysterangiales*)
	Hysterangium	sp.	H5573	PNG	**MW246669**	**MW302264**	*Mesophelliaceae*	*Hysterangineae* (*Hysterangiales*)
	Hysterangium	sp.	T14749	WA	**MW246698**	**MW302266**	*Mesophelliaceae*	*Hysterangineae* (*Hysterangiales*)
	Hysterangium	sp.	T6923	AUS	DQ218855	DQ219186	*Mesophelliaceae*	*Hysterangineae* (*Hysterangiales*)
	Hysterangium	sp.	T15362	NT	**MW246675**	**MW302271**	*Mesophelliaceae*	*Hysterangineae* (*Hysterangiales*)
	Hysterangium	sp.	T15375	NT	**MW246676**	**MW302272**	*Mesophelliaceae*	*Hysterangineae* (*Hysterangiales*)
	Hysterangium	sp.	MEL2057692	NSW	DQ218848	DQ219179	*Mesophelliaceae*	*Hysterangineae* (*Hysterangiales*)

© 2021 Westerdijk Fungal Biodiversity Institute

Table 1. (Continued).

Clade	Genus verbatim determination	Species verbatim determination	Collector or Herbarium ID	Geography	ATP6	TEF1	Family	Suborder (Order)
	Hysterangium	*gardnerii*	T6950	AUS	DQ218835	DQ219157	*Mesophelliaceae*	*Hysteranginеae* (*Hysterangiales*)
	Hysterangium	*inflatum*	H4035	AUS	DQ218836	DQ219159	*Mesophelliaceae*	*Hysteranginеae* (*Hysterangiales*)
Gen. prov. 9 Davoodian	*Hysterangium*	sp.	H381	TAS	**MW449871**	**MW302281**	*Mesophelliaceae*	*Hysteranginеae* (*Hysterangiales*)
Gen. prov. 10 Hosaka	*Chondrogaster*	sp.	MEL2305115	QLD	**MW449861**	**MW302277**	*Mesophelliaceae*	*Hysteranginеae* (*Hysterangiales*)
	Chondrogaster	sp.	SEA7B	QLD	**MW449864**	**MW302280**	*Mesophelliaceae*	*Hysteranginеae* (*Hysterangiales*)
	Hysterangium	sp.	H2022	AUS	DQ218856	DQ219187	*Mesophelliaceae*	*Hysteranginеae* (*Hysterangiales*)
	Hysterangium	sp.	H4262	AUS	DQ218773	DQ219146	*Mesophelliaceae*	*Hysteranginеae* (*Hysterangiales*)
	Hysterangium	sp.	T22535	QLD	**MW449862**	**MW302278**	*Mesophelliaceae*	*Hysteranginеae* (*Hysterangiales*)
	Hysterangium	sp.	SEA270	QLD	**MW449863**	**MW302279**	*Mesophelliaceae*	*Hysteranginеae* (*Hysterangiales*)
	Hysterangium	*aggregatum*	MEL2049882	VIC	DQ218844	DQ219175	*Mesophelliaceae*	*Hysteranginеae* (*Hysterangiales*)

DISCUSSION

In addition to revealing new taxa, our analysis highlights prominent biogeographic patterns in *Hysterangiales*. Trans-Tasman distributions are numerous throughout *Hysterangiales*; almost every New Zealand lineage inferred in our phylogram is sister to an Australian lineage, at various taxonomic scales. Gondwanan disjunctions are also represented, for example "*Gen. prov.* 17" (Fig. 3 - Part 2) contains an Australian and paleotropical clade sister to a northeastern South American clade. Some human-mediated introduction events are apparent as well *e.g. Chondrogaster angustisporus* (OSC62041 - holotype) is from planted *Eucalyptus* in Brazil (Giachini *et al*. 2000). Hosaka *et al*. (2008) postulated that the *Hysterangiales* originated in Australia or Eastern Gondwana and expanded in range over time, possibly through long-distance dispersal. Sheedy *et al.* (2016) inferred that *Hysterangiales* was the first group of *Agaricomycetes* to become sequestrate in Australia (*ca.* 83 million years ago). The rate of sequestration of *Agaricomycetes* was inferred to have increased in Australia after separation from Antarctica, the timing of which overlaps with the radiation of potential mycorrhizal plant associates as well as the emergence of specialized mycophagous marsupials. Although periods of aridification were evidently not the sole driver of sequestration, they likely had a major influence on the diversity of sequestrate fungi in Australia, including *Hysterangiales* (Sheedy *et al.* 2016).

Our analysis indicates phylogenetic signals for some prominent macroscopic features. In the *Mesophelliaceae*, the clade unifying *Gummivena*, *Gummiglobus*, and *Castoreum* is comprised of species that have gummy-like mycelium and/or outer glebal tissue (Fig. 1N, O). Species in the clade containing *Chondrogaster*, *Andebbia*, *Mesophellia*, *Nothocastoreum*, and related provisional genera have a powdery spore mass at maturity and also incorporate roots and soil in a multi-layered mycelial crust surrounding the basidiome (in *Nothocastoreum* this falls off easily and remains in the soil) (Fig. 1J–M). In provisional genera 8 through 10, the basidiomes are typically encased in a mycelial soil crust, and the glebal tissue is gelatinized. Macroscopic characters of *Hysterangiaceae* overlap somewhat with various clades in the *Mesophelliaceae* and *Gallaceaceae*, including having a gelatinized gleba and varying degrees of rhizomorph development across the surface of basidiomes (Fig. 1G–I). In *Gallaceaceae*, most lineages have a firm, cartilaginous peridium surrounding a gelatinized gleba (Fig. 1D–F), and spores lacking an utricle (Fig. 2A). The condition of having ridged spores (Fig. 2C) is not monophyletic in *Hysterangiales*; this character was previously thought to be diagnostic for the genus *Austrogautieria* (Stewart & Trappe 1985) but now appears in two well-supported, distinct clades in *Gallaceaceae* (*Austrogautieria* and "*Gen. prov*. 24"; Fig. 3 - Part 3).

Numerous provisional genera and species have been revealed in this study, which will be described by the respective authors of this paper and other collaborators in upcoming publications. We believe our current approach of recognising numerous provisional genera is a more accurate and conservative estimate of diversity than to lump them into fewer, larger genera. In addition to strong phylogenetic signals, each provisional genus is readily distinguishable by macroscopic and microscopic characters, but species level differentiation within genera requires more sampling in many of these taxa. Moreover, our phylogenetic analyses show that some existing genera, such as *Castoreum* and *Gummiglobus* in *Mesophelliaceae*, are closely related to each other within their respective families, but our provisional genera are more distantly related to these existing genera (Fig. 3, Supplementary Fig. S1). More sampling throughout Australasia and South America will likely uncover additional clades and aid in further refining generic and specific boundaries.

ACKNOWLEDGEMENTS

A special thanks to Dr S. Abell (James Cook University and Australian Tropical Herbarium) for access to *Hysterangiales* collections and early collaboration on this diverse lineage. This project was completed with funding and support from the Australian Biological Resources Study (grant RF217-63: Truffle-like fungi [*Basidiomycetes*]: taxonomy, systematics and a revised classification for all Australian taxa), BioPlatforms Australia, the Friends of the Botanic Gardens Victoria, and the Royal Botanic Gardens Victoria. Dr M. Castellano was also supported in part by the ABRS grant RF217. Dr M. Smith at the University of Florida is thanked for helpful comments to this manuscript. Much appreciation also to the curation staff at the National Herbarium of Victoria (MEL), Queensland State Herbarium (BRI), and State Herbarium of South Australia (AD) for assistance with loans and processing of material. Assistance with processing material and sequencing was provided by technical staff at MEL: R. Jordan, Dr M. Hirst and A. Boxshall. This study was financed in part by JSPS KAKENHI Grants 24680085 and 20K06805 to Dr K. Hosaka.

Conflict of interest: The authors declare that there is no conflict of interest.

REFERENCES

Castellano MA, Beever RE (1994). Truffle-like *Basidiomycotina* of New Zealand: *Gallacea*, *Hysterangium*, *Phallobata*, and *Protubera*. *New Zealand Journal of Botany* **32**: 305–328.

Claridge AW, May TW (1994). Mycophagy among Australian mammals. *Australian Journal of Ecology* **19**: 251–275.

Fogel R, Trappe JM (1978). Fungus consumption (mycophagy) by small animals. *Northwest Science* **52**: 1–31.

Giachini A, Castellano MA, Trappe JM (2000). Ectomycorrhizal fungi in *Eucalyptus* and *Pinus* plantations in southern Brazil. *Mycologia* **92**: 1166–1177.

Hibbett DS, Blackwell M, James TY, *et al.* (2018). Phylogenetic taxon definitions for *Fungi*, *Dikarya*, *Ascomycota* and *Basidiomycota*. *IMA Fungus* **9**: 291–298.

Hosaka K (2005). *Systematics, phylogeny, and biogeography of the Hysterangiales and related taxa (Phallomycetidae, Homobasidiomycetes)*. PhD dissertation. Botany Department, Oregon State University, Oregon, USA.

Hosaka K, Bates ST, Beever RE, *et al.* (2006). Molecular phylogenetics of the gomphoid-phalloid fungi with an establishment of the new subclass *Phallomycetidae* and two new orders. *Mycologia* **98**: 949–959.

Hosaka K, Castellano MA, Spatafora JW (2008). Biogeography of *Hysterangiales* (*Phallomycetidae, Basidiomycota*). *Mycological Research* **112**: 448–462.

Katoh K, Rozewicki J, Yamada KD (2017). MAFFT online service: multiple sequence alignment, interactive sequence choice and visualization. *Briefings in Bioinformatics* **20**: 1160–1166.

Kretzer AM, Bruns TD (1999). Use of *atp6* in fungal phylogenetics: an example from the *Boletales*. *Molecular Phylogenetics and Evolution* **13**: 483–492.

Miller MA, Schwartz T, Pickett BE, *et al.* (2015). A RESTful API for access to phylogenetic tools via the CIPRES science gateway. *Evolutionary Bioinformatics* **11**: EBO–S21501.

Rehner SA, Buckley E (2005). A *Beauveria* phylogeny inferred from nuclear ITS and *EF1-α* sequences: evidence for cryptic diversification and links to *Cordyceps* teleomorphs. *Mycologia* **97**: 84–98.

Robinson O, Dylus D, Dessimoz C (2016). *Phylo.io*: interactive viewing and comparison of large phylogenetic trees on the web. *Molecular Biology and Evolution* **33**: 2163–2166.

Ronquist F, Teslenko M, Van Der Mark P, *et al.* (2012). MrBayes 3.2: efficient Bayesian phylogenetic inference and model choice across a large model space. *Systematic Biology* **61**: 539–542.

Sheedy EM, Martin AF, Ryberg M, *et al.* (2016). Dating the emergence of truffle-like fungi in Australia, by using an augmented meta-analysis. *Australian Systematic Botany* **29**: 284–302.

Stamatakis A, Hoover P, Rougemont J (2008). A rapid bootstrap algorithm for the RAxML web servers. *Systematic Biology* **57**: 758–771.

Stewart EL, Trappe JM (1985). The new genus *Austrogautieria* (*Basidiomycotina*), segregate from *Gautieria*. *Mycologia* **77**: 674–687.

Sulzbacher MA, Grebenc T, Cabral TS, *et al.* (2016). *Restingomyces*, a new sequestrate genus from the Brazilian Atlantic rainforest that is phylogenetically related to early-diverging taxa in *Trappeaceae* (*Phallales*). *Mycologia* **108**: 954–966.

Trappe JM, Castellano MA, Malajczuk N (1996). Australasia truffle-like fungi. VII. *Mesophellia* (*Basidiomycotina, Mesophelliaceae*). *Australian Systematic Botany* **9**: 773–802.

Trierveiler-Pereira L, Meijer AA, Hosaka K, *et al.* (2014). Updates on *Protubera* (*Protophallaceae, Phallales*) and additional notes on *P. maracuja*. *Mycoscience* **55**: 35–42.

Xu A-S, Luo D-Q (2003). A new species in the genus *Trappea*. *Mycosystema* **22**: 191–194.

Supplementary Material: http://fuse-journal.org/

Fig. S1. Overview Phylogram from Bayesian analysis showing relationship between *Hysterangiales*, some *Phallales* and outgroups (OG). Node A indicates *Phallogastrineae subord. nov.*; node B indicates *Hysterangineae subord. nov.* Maximum likelihood (ML) bootstrap values / Bayesian posterior probabilities (bpp) are shown at the nodes. Where bpp ≥ 0.95 and ML bootstrap ≥ 70 %, branches are thickened. Type species indicated by a blue asterisk *. The asterisk in parentheses (*) denotes the currently accepted genus for *Protubera canescens*, *Ileodictyon*. Countries and States indicated with same acronyms as Fig. 3. Terminals representing new DNA sequences generated for this study are in **bold**.

© 2021 Westerdijk Fungal Biodiversity Institute

FUSE

Fungal Systematics and Evolution

VOLUME 8
DECEMBER 2021
PAGES 81–89

doi.org/10.3114/fuse.2021.08.07

Aspergillus diversity from the Gcwihaba Cave in Botswana and description of one new species

C.M. Visagie[1], M. Goodwell[2], D.O. Nkwe[2]

[1]Department of Biochemistry, Genetics and Microbiology, Forestry and Agricultural Biotechnology Institute (FABI), University of Pretoria, Pretoria, South Africa
[2]Department of Biological Sciences and Biotechnology, Botswana International University of Science and Technology, Private Bag 16, Plot 10071, Khurumela Ward, Palapye, Botswana

*Corresponding author: cobus.visagie@fabi.up.ac.za

Key words:
fungal diversity
new taxon
series *Flavipedes*
Southern Africa

Abstract: A fungal survey of the Gcwihaba Cave from Botswana found *Aspergillus* to be one of the more common fungal genera isolated. The 81 *Aspergillus* strains were identified using *CaM* sequences and comparing these to a curated reference dataset. Nineteen species were identified representing eight sections (sections *Candidi, Circumdati, Flavi, Flavipedes, Nidulantes, Nigri, Terrei* and *Usti*). One strain could not be identified. Morphological characterisation and multigene phylogenetic analyses confirmed it as a new species in section *Flavipedes* and we introduce it below as *A. okavangoensis.* The new species is most similar to *A. iizukae*, both producing conidiophores with vesicles typically wider than 20 µm. The new species, however, does not produce Hülle cells and its colonies grow slower than those of *A. iizukae* on CYA at 37 °C (14–15 *vs* 18–21 mm) and CREA (15–16 *vs* 23–41mm).

Citation: Visagie CM, Goodwell M, Nkwe DO (2021). *Aspergillus* diversity from the Gcwihaba Cave in Botswana and description of one new species. *Fungal Systematics and Evolution* **8**: 81–89. doi: 10.3114/fuse.2021.08.07
Received: 23 June 2021; **Accepted:** 10 September 2021; **Effectively published online:** 13 September 2021
Corresponding editor: P.W. Crous

INTRODUCTION

The Gcwihaba Cave is a Botswana national monument and is being considered for UNESCO World Heritage site nomination. It is a spectacular geographical formation located in the Okavango basin, to the north-western edge of Botswana (coordinates: -20.025056, 21.357639) (Mbaiwa & Sakuze 2009, Dandurand *et al.* 2019, Mazebedi & Hesselberg 2020). The cave was formed from rocks primarily composed of calcium magnesium carbonate or dolomite. Some parts of the dolomite cave roof and walls are adorned with tens of thousands of three insectivorous bat species, namely *Hipposideros vittatus* (Striped leaf-nosed bat), *Nycteris thebaica* (Egyptian slit-faced bat) and *Rhinolophus denti* (Dent's horseshoe bat) (Dandurand *et al.* 2019). Bat guano provides a carbon source for the growth of various microorganisms, while bat urine can cause biogenic corrosion of the cave roof and walls (Dandurand *et al.* 2019). This corrosion ultimately compromise the integrity of the dolomite, causing it to chip away and fall onto the ground (Kolo *et al.* 2007). This dolomite, bats excrement, dead vertebrates and invertebrates provide organic matter that supports the growth of various microorganisms. The decomposition of this organic matter is typically carried out by fungi and bacteria (Man *et al.* 2015, Pusz *et al.* 2015).

Several surveys from especially North America and Europe have focused on microbial diversity of caves, mainly driven by the outbreak of White-nose Syndrome (WNS; caused by *Pseudogymnoascus destructans*) in bats and subsequent research that aimed to understand the disease (Blehert *et al.* 2009, Johnson *et al.* 2013, Vanderwolf *et al.* 2013, Zhang *et al.* 2017, Cunha *et al.* 2020, Visagie *et al.* 2020). These studies often found caves to be species rich. Even though WNS has not been reported in Southern Africa, caves are an underexplored biota. The region is one of the worlds biodiversity hotspots (Myers *et al.* 2000). The microbiology of the Gcwihaba Cave has never been studied. The perpetual darkness of the cave, relatively constant temperature (25 °C), high humidity (60–70 %) (Dandurand *et al.* 2019) and location in the heart of the Kalahari Desert present a unique ecological niche that is expected to contain many undescribed fungi. Therefore, the Gcwihaba Cave was considered to represent an untapped potential biotechnological resource and has become the focus of a long-term project looking to discover novel compounds from the region.

The aim of this study was to present results from a preliminarily survey exploring fungal diversity in the Gcwihaba Cave, of which *Aspergillus* was found to be one of the predominate genera. Here we report on the species recovered from bat guano covered soil and, in the process, introduce the new species *A. okavangoensis*.

Fungal Systematics and Evolution is licensed under a Creative Commons Attribution-NonCommercial-ShareAlike 4.0 International License

© 2021 Westerdijk Fungal Biodiversity Institute

MATERIALS AND METHODS

Strains, sampling and isolation

Bat guano-contaminated soil samples were collected in sterile plastic bags from the Gcwihaba Caves situated in the Okavango basin, Botswana. A total of 18 samples were collected from six locations in the cave.

Isolations from soil samples were made using a dilution series by suspending 10 g soil in 90 mL sterile 0.1 % peptone dH_2O and diluting this to 10^{-4}. For each dilution, 100 µL was spread-plated in duplicate onto Potato Dextrose Agar (PDA), Dichloran-Glycerol agar (DG18) and Dichloran Rose Bengal Chloramphenicol Agar (DRBCA) (Samson *et al.* 2014). These were incubated at 30 °C for 7 d, after which colonies of interest were transferred into pure culture onto Malt Extract Agar (MEA) and Sabouraud Dextrose Agar (SDA) plates (Samson *et al.* 2014), and then incubated a further 7 d. Strains were identified to genus level based on colony and microscopic observations. Strains were preserved in 10 % glycerol and stored at -80 °C and accessioned into the working collection of David Nkwe housed at the Botswana International University of Science and Technology, Palapye, Botswana.. The strain of the new species was accessioned into Cobus Visagie's working collection (CN) housed at FABI (Forestry and Agricultural Biotechnology Institute, University of Pretoria, South Africa) and preserved as spore suspensions in 10 % glycerol at -80 °C. It was also deposited into the CMW (FABI, University of Pretoria, Pretoria, South Africa) and CBS (Westerdijk Fungal Biodiversity Institute, Utrecht, the Netherlands) culture collections. A dried specimen representing the holotype of the new species was deposited in PREM, the fungarium of the South African National Collection of Fungi housed at the Agricultural Research Council (ARC; Plant Health and Protection, Roodeplaat, South Africa). Table 1 summarises strains used for the phylogenetic analysis of section *Flavipedes*, including their GenBank and culture collection accession numbers and other metadata.

DNA extraction, sequencing and phylogenetic analysis

DNA was extracted from 7-d-old colonies grown on PDA using the Quick-DNA™ Fungal/Bacterial Miniprep Kit (Zymo Research, CA, USA) following the manufacturer's instructions. DNA extracts were stored at -20 °C. PCR primers and amplification conditions followed protocols defined by Samson *et al.* (2014) and Houbraken *et al.* (2020). Briefly, all *Aspergillus* strains were identified using partial calmodulin (*CaM*) gene region sequences. For new species, the internal transcribed spacer and 5.8S rDNA regions (ITS), partial beta-tubulin (*BenA*) and partial RNA polymerase II second largest subunit (*RPB2*) were also sequenced. Genes were amplified using primer pairs V9G & LS266 (ITS; de Hoog & Gerrits van den Ende 1998, Masclaux *et al* 1995), Bt2a & Bt2b (*BenA*; Glass & Donaldson 1995), cmd5 & cmd6 (*CaM*; Hong *et al*. 2006) and RPB2-RPB2F1 & RPB27CRa (*RPB2*; Houbraken *et al*. 2020). PCRs were prepared in 25 µL volumes containing 0.15 µL MyTaq™ DNA polymerase (Bioline, Meridian Bioscience, USA), 5 µL 5× MyTaq™ Reaction Buffer (BioLine), 0.5 µL of each primer (10 µM), 1 µL template DNA and 17.85 µL MilliQ H_2O. Bidirectional sequencing was done at Inqaba Biotechnical Industries (Pty) Ltd (Pretoria, South Africa) using the same primers used for PCR amplification. Contig sequences were generated in Geneious Prime v. 2021.0.3 (BioMatters Ltd., Auckland, New Zealand).

Strains were identified by comparing *CaM* sequences with a locally curated reference sequence database mainly based on Samson *et al.* (2014) and Houbraken *et al.* (2020). Subsequent phylogenies were calculated for the new species based on its close relatives on a series level. Each dataset was aligned in MAFFT v. 7.453 (Katoh & Standley 2013) using the G-INS-I option and then trimmed and adjusted in Geneious where needed. Datasets were partitioned based on the gene region, as well as introns and exons. For each partition, the appropriate nucleotide substitution model was selected using PartitionFinder v. 2.1 (Lanfear *et al.* 2017) based on the Akaike information criterion (Akaike 1974). Phylogenies were performed using Maximum Likelihood (ML) and Bayesian tree Inference (BI). The ML analysis was performed using IQ-TREE v. 2.1.2 (Nguyen *et al.* 2015) with regular bootstrapping performed using 1 000 replicates. BI analyses were performed in MrBayes v. 3.2.7 (Ronquist *et al.* 2012) using three sets of four chains (1 cold and three heated) and were stopped using the stoprule option at an average standard deviation for split frequencies of 0.01. Trees were visualised using the Interactive tree of life (iTOL) v. 6 (Letunic & Bork 2016) and edited in Affinity Publisher v. 1.9.3 (Serif (Europe) Ltd, Nottingham, UK). The ML trees were used to present phylogenetic results with both bootstrap values (bs) and posterior probabilities (pp) shown for branches.

Morphology

The new species was characterised and described following methods described in Samson *et al.* (2014). Briefly, morphological features were recorded on Czapek Yeast Autolysate agar (CYA), CYA with 5 % NaCl (CYAS), MEA (Oxoid CM0059), DG18 (Oxoid CM0729), Yeast Extract Sucrose agar (YES), Oatmeal agar (OA) and Creatine Sucrose agar (CREA). Media were prepared in 90 mm Petri-dishes. Equidistant three-point inoculations were made and incubated for 7 d at 25 °C, with additional CYA plates incubated at 5, 10, 15, 20, 30 and 37 °C. Colour names and codes used in descriptions follow Kornerup & Wanscher (1967). Colonies were captured within a lightbox equipped with a Sony a6400 camera. A Zeiss AxioImager.A2 compound and Zeiss AXIO dissecting Discovery.V8 microscopes equipped with an AxioCaM 512 colour camera driven by Zen Blue v. 3.2 software (Carl Zeiss CMP GmbH, Göttingen, Germany) were used for all microscopic observations. Extended Depth of Field stacking of colony texture micrographs was performed in Helicon Focus v. 7.5.4 (HeliconSoft, Kharkiv, Ukraine). Microphotographs were edited for aesthetic purposes using the "inpainting brush tool" without altering areas of scientific significance. Photo plates were prepared in Affinity Photo v. 1.9.3 (Serif (Europe) Ltd, Nottingham, UK).

RESULTS

Isolations and Identifications

Isolations from bat guano-contaminated soil samples resulted in 81 *Aspergillus* strains. *CaM* sequences were generated and deposited in GenBank under accessions MW480706–MW480787. Strains were found to represent eight sections and 19 species, including *A. alabamensis* (one strain), *A. 'alboluteus'* (in press) (one strain), *A. allahabadii* (one strain), *A. aureolatus* (two strains), *A. aculeatus* (two strains), *A. flavus* (one strain),

© 2021 Westerdijk Fungal Biodiversity Institute

Table 1. *Aspergillus* section *Flavipedes* strains used for phylogenetic comparisons.

			GenBank Accessions			
Species	**Strains**	**Series**	**ITS**	***BenA***	***CaM***	***RPB2***
Aspergillus alboluteus	CBS 147421 = CMW 56637 = CN 073A5 = DN 84	*Spelaei*	MW480880	MW480788	MW480706	MW480790
	CBS 145854 = CCF 4916 = EMSL 2311 = IFM 66816	*Spelaei*	MW448664	MW478498	MW478512	MW478533
	CBS 145855 = CCF 5695 = EMSL 2420 = IFM 66815 (ex-type)	*Spelaei*	MW448663	MW478497	MW478511	MW478532
	CBS 145859 = CCF 6201 = EMSL 3060	*Spelaei*	MW448662	MW478496	MW478510	MW478531
	CBS 147065 = CCF 6551 = DTO 410-I8	*Spelaei*	MW448666	MW478500	MW478514	MW478535
	CCF 5849 = EMSL 2446 = IFM 66817	*Spelaei*	MW448665	MW478499	MW478513	MW478534
Aspergillus alboviridis	CBS 142665 = FMR 15175 = CCF 6049 = IFM 66819 (ex-type)	*Spelaei*	LT798909	LT798936	LT798937	LT798938
Aspergillus ardalensis	CCF 4031 = CCF 4426 = CMF ISB 1688 = CBS 134372 = NRRL 62824 (ex-type)	*Flavipedes*	FR733808	HG916683	HG916725	HG916704
Aspergillus flavipes	NRRL 302 = ATCC 24487 = IMI 171885 = QM 9566 = Thom 4640.474 = WB 302 (ex-type)	*Flavipedes*	EF669591	EU014085	EF669549	EF669633
Aspergillus iizukae	CBS 541.69 = NRRL 3750 = IMI 141552 = QM 9325 (ex-type)	*Flavipedes*	EF669597	EU014086	EF669555	EF669639
	CCF 4032 = CMF ISB 1245	*Flavipedes*	HG915894	HG916687	HG916730	HG916708
	CBS 138188 = DTO 179-E6 (ex-type of *P. capensis*)	*Flavipedes*	KJ775550	KJ775072	KJ775279	KP987020
	CCF 4845 = S 746	*Flavipedes*	LM999906	LM644270	LM644243	MW478540
Aspergillus inusitatus	CBS 147044 = CCF 6552 = DTO 121-G5 (ex-type)	*Spelaei*	MW448669	MW478502	MW478517	MW478542
Aspergillus lanuginosus	NRRL 4610 = IMI 350352 = CCF 4551 = IFM 66818 (ex-type)	*Spelaei*	EF669604	EU014080	EF669562	EF669646
Aspergillus luppiae	NRRL 6326 = CBS 653.74 = CCF 4545 (ex-type)	*Spelaei*	EF669617	EU014079	EF669575	EF669659
Aspergillus micronesiensis	CBS 138183 = DTO 267-D5 (ex-type)	*Flavipedes*	KJ775548	KJ775085	KJ775355	KP987023
	IMI 357699 = DTO 305-B6 = IBT 23707 (ex-type of *A. sunderbanii nom. inval.*)	*Flavipedes*	KP987084	KP987052	KP987069	KP987026
	NRRL 4263 = CCF 4556	*Flavipedes*	EF669600	EU014083	EF669558	EF669642
Aspergillus movilensis	NRRL 4610 = IMI 350352 = CCF 4551	*Spelaei*	EF669604	EU014080	EF669562	EF669646
	CBS 134395 = PRM 923449 = CCF 4410 = CMF ISB 2614 = NRRL 62819 = DTO 316-C6 (ex-type)	*Spelaei*	KP987089	HG916697	HG916740	HG916718
	DTO 203-C9	*Spelaei*	KP987075	KP987043	KP987058	KP987032
	DTO 203-H3	*Spelaei*	KP987078	KP987046	KP987061	KP987035
	S 1040	*Spelaei*	MW448674	MW478503	MW478522	MW478551
Aspergillus neoflavipes	CBS 260.73 = NNRL 5504 = ATCC 24484 = IMI 171883 = IFM 40894 = CCF 4552 (ex-type)	*Flavipedes*	EF669614	EU014084	EF669572	EF669656
Aspergillus neoniveus	CBS 261.73 = NRRL 5299 = ATCC 24482 = IMI 171878 (ex-type)	*Neonivei*	EF669612	EU014098	EF669570	KP987024
Aspergillus okavangoensis	**CBS 147420 = CMW 56636 = CN 073A3 = DN 24 (ex-type)**	***Flavipedes***	**MW480881**	**MW480789**	**MW480707**	**MW480791**
Aspergillus olivimuriae	NRRL 66783 = CCF 6208 (ex-type)	*Olivimuriarum*	MH298877	MH492010	MH492011	MH492012
Aspergillus polyporicola	NRRL 32683 = CCF 4553 (ex-type)	*Spelaei*	EF669595	EU014088	EF669553	EF669637
	CCF 5427 = EMSL 2612	*Spelaei*	MW448675	MW478504	MW478523	MW478552
	CCF 6262 = EMSL 3169	*Spelaei*	MW448676	MW478505	MW478524	MW478553
	NRRL 58570 = CCF 4828	*Spelaei*	HQ288052	LM644274	LM644252	LM644254

© 2021 Westerdijk Fungal Biodiversity Institute

Table 1. (Continued).

Species	Strains	Series	GenBank Accessions			
			ITS	*BenA*	*CaM*	*RPB2*
Aspergillus spelaeus	CCF 4425 = CMF ISB 2615 = CBS 134371 = NRRL 62826 (ex-type)	*Spelaei*	HG915905	HG916698	HG916741	HG916719
	CCF 4886 = S 716	*Spelaei*	LM999908	LM644272	HG916748	LM644259
	EMSL 4874	*Spelaei*	MW448677	MW478506	MW478525	MW478554
	FMR 14606	*Spelaei*	LT899488	LT899537	LT899590	LT899645
Aspergillus suttoniae	CBS 143866 = UTHSCSA DI14-215 = FMR 13523 (ex-type)	*Flavipedes*	LT899487	LT899536	LT899589	LT899644
Aspergillus templicola	CBS 138181 = DTO 270-C6 (ex-type)	*Flavipedes*	KJ775545	KJ775092	KJ775394	KP987038
	CCF 4698 = CMF ISB 2662 = NRRL 62825 (ex-type of *A. mangaliensis*)	*Flavipedes*	HG915902	HG916695	HG916738	HG916716
	NRRL 4893 = IMI 343701 = CCF 4846	*Flavipedes*	LM999907	LM644271	LM644242	LM644256
Aspergillus terreus	CBS 601.65 = NRRL 255 = ATCC 10071 = ATCC 1012 = IFO 33026 = IMI 017294ii = IMI 17294 = JCM 10257 = LSHBA c .24 = MUCL 38640 = NCTC 981 = NRRL 543 = QM 1 = QM 1991 = Thom 144 = VKMF-67 = WB 255 (ex-type)	*Terrei*	EF669586	EF669519	EF669544	EF669628
Aspergillus urmiensis	CBS 139558 = CCTU 742 = IBT 32593 = DTO 203-C2 (ex-type)	*Flavipedes*	KP987073	KP987041	KP987056	KP987030
	CBS 139557 = CCTU 734 = DTO 203-B3 = IBT 32597	*Flavipedes*	KP987072	KP987039	KP987055	KP987029
	CBS 139766 = CCTU 743 = DTO 203-C3 = IBT 32598	*Flavipedes*	KP987074	KP987042	KP987057	KP987031

Table 2. *Aspergillus* isolated from Botswana during this study.

Species	Strains	Subgenus	Section	Series	GenBank Accession(s): *CaM*
Aspergillus aculeatus	DN78, DN81	*Circumdati*	*Nigri*	*Japonici*	MW480779, MW480782
Aspergillus alabamensis	DN14	*Circumdati*	*Terrei*	*Terrei*	MW480720
Aspergillus alboluteus	CBS 147421 = CMW 56637 = CN 073A5 = DN84	*Circumdati*	*Flavipedes*	*Spelaei*	MW480706
Aspergillus allahabadii	DN23	*Circumdati*	*Terrei*	*Nivei*	MW480727
Aspergillus aureolatus	DN01, DN61	*Nidulantes*	*Nidulantes*	*Speluncei*	MW480708, MW480763
Aspergillus flavus	DN27	*Circumdati*	*Flavi*	*Flavi*	MW480729
Aspergillus fructus	DN02	*Nidulantes*	*Nidulantes*	*Versicolores*	MW480709
Aspergillus germanicus	DN04, DN29, DN43	*Nidulantes*	*Usti*	*Calidousti*	MW480711, MW480731, MW480731
Aspergillus griseoaurantiacus	DN40	*Nidulantes*	*Nidulantes*	*Versicolores*	MW480742
Aspergillus hongkongensis	DN52	*Nidulantes*	*Nidulantes*	*Versicolores*	MW480754
Aspergillus hortae	DN55	*Circumdati*	*Terrei*	*Terrei*	MW480757
Aspergillus neoniger	DN66	*Circumdati*	*Nigri*	*Nigri*	MW480768
Aspergillus ochraceus	DN64, DN65, DN71, DN87	*Circumdati*	*Circumdati*	*Circumdati*	MW480766, MW480767, MW480773, MW480787
Aspergillus okavangoensis	CBS 147420 = CMW 56636 = CN 073A3 = DN24	*Circumdati*	*Flavipedes*	*Flavipedes*	MW480707
Aspergillus parasiticus	DN54	*Circumdati*	*Flavi*	*Flavi*	MW480756
Aspergillus subalbidus	DN12, DN13, DN62, DN63, DN67, DN68, DN69, DN70, DN75, DN76, DN80, DN82, DN85	*Circumdati*	*Candidi*	*Candidi*	MW480718, MW480719, MW480764, MW480765, MW480769, MW480770, MW480771, MW480772, MW480777, MW480778, MW480781, MW480783, MW480785

© 2021 Westerdijk Fungal Biodiversity Institute

Table 2. (Continued).

Species	Strains	Subgenus	Section	Series	GenBank Accession(s): *CaM*
Aspergillus subramanianii	DN72, DN73	*Circumdati*	*Circumdati*	*Sclerotiorum*	MW480774, MW480775
Aspergillus sydowii	DN03, DN05, DN06, DN08, DN09, DN10, DN15, DN18, DN19, DN20, DN21, DN22, DN25, DN28, DN30, DN31, DN32, DN33, DN34, DN35, DN36, DN37, DN38, DN39, DN41, DN42, DN44, DN46, DN47, DN48, DN49, DN50, DN51, DN53, DN56, DN57, DN58, DN59, DN60, DN74, DN79, DN83, DN86	*Nidulantes*	*Nidulantes*	*Versicolores*	MW480710, MW480712, MW480713, MW480715, MW480716, MW480717, MW480721, MW480722, MW480723, MW480724, MW480725, MW480726, MW480728, MW480730, MW480732, MW480733, MW480734, MW480735, MW480736, MW480737, MW480738, MW480739, MW480740, MW480741, MW480743, MW480744, MW480746, MW480748, MW480749, MW480750, MW480751, MW480752, MW480753, MW480755, MW480758, MW480759, MW480760, MW480761, MW480762, MW480776, MW480780, MW480784, MW480786
Aspergillus taichungensis	DN07	*Circumdati*	*Candidi*	*Candidi*	MW480714

A. fructus (one strain), *A. germanicus* (three strains), *A. griseoaurantiacus* (one strain), *A. hongkongensis* (one strain), *A. hortae* (one strain), *A. neoniger* (one strain), *A. ochraceus* (four strains), *A. parasiticus* (one strain), *A. subalbidus* (13 strains), *A. subramanianii* (two strains), *A. sydowii* (43 strains) and *A. taichungensis* (one strain). A summary of these can be found in Table 2. One strain could not be identified using *CaM* sequences. Based on subsequent multigene phylogenies and morphological observations, this strain was shown to represent a new species described below in the Taxonomy section.

Phylogeny

Each gene region was aligned, resulting in alignment lengths of 555, 472, 998, and 532 bp for *BenA*, *CaM, RPB2* and ITS, respectively. The concatenated dataset consisted of these four gene regions that were further partitioned based on intron and exon regions. The most appropriate nucleotide substitution models for each partition were as follows: TRN+I+G for *BenA*_codon1, *BenA*_codon3 and ITS; JC+I for *BenA*_codon2, *CaM*_codon1 and *RPB2*_codon3; TRNEF+I+G for *BenA*_introns and *CaM*_introns; HKY+G for *CaM*_codon2 and *RPB2*_codon1; and TRN+I for *RPB2*_codon2 and *CaM*_codon3. Alignments were submitted to TreeBASE under accession number 27870 (https://www.treebase.org/).

Sequence data resolved the new species in *Aspergillus* section *Flavipedes* (Fig. 1). *Aspergillus okavangoensis* belongs to series *Flavipedes* and resolves on a distinct branch, but deep nodes had low support and its exact relationship with other species is unresolved. The new species had unique sequences for all gene regions considered in this study. Based on BLAST searches against a curated reference database, the closest hits using ITS had highest similarity to *A. iizukae* (strain CBS 541.69^{T}, GenBank EF669597; Identities = 506/512 (98.8 %), no gaps), *A. urmiensis* (strain CBS 139558^{T}, GenBank KP987073; Identities = 504/512 (98.4 %), no gaps), and *A. ardalensis* (strain CCF4031^{T}, GenBank FR733808; Identities = 505/514 (98.4 %), 5 gaps). The closest hits using *BenA* had highest similarity to *A. urmiensis* (strain CBS 139558^{T}, GenBank KP987041; Identities = 474/507 (93.5 %), 3 gaps), *A. templicola* (strain CBS 138180, GenBank KJ775087; Identities = 471/507 (92.9 %), 2 gaps) and *A. suttoniae* (strain CBS 143866^{T}, GenBank LT899536; Identities = 428/463 (92.4 %), 4 gaps). The closest hits using *CaM* had highest similarity to *A. templicola* (strain NRRL4893, GenBank LM644242; Identities = 507/558 (90.9 %), 8 gaps), *A. urmiensis* (strain CBS 139558^{T}, GenBank KP987056; Identities = 502/554 (90.6 %), 4 gaps) and *A. suttoniae* (strain CBS 143866^{T}, GenBank LT899589; Identities = 500/556 (89.9 %), 5 gaps). The closest hits using *RPB2* had highest similarity to *A. suttoniae* (strain CBS 143866^{T}, GenBank LT899644; Identities = 828/855 (96.8 %), no gaps), *A. templicola* (strain CCF4698, GenBank HG916716; Identities = 824/857 (96.1 %), no gaps) and *A. urmiensis* (strain CBS 139558^{T}, GenBank KP987030; Identities = 818/857 (95.4 %), no gaps).

TAXONOMY

Aspergillus okavangoensis Visagie & Nkwe, ***sp. nov.*** MycoBank MB 840269. Fig. 2.

In: subgenus *Circumdati* section *Flavipedes* series *Flavipedes*.

Etymology: Latin, *okavangoensis,* named after the Okavango Delta of Botswana, the origin of this species.

Typus: **Botswana**, Gcwihaba Cave (-20.023000, 21.355200), from bat guano-contaminated soil collected in the cave, Jun. 2019, coll. *D. Nkwe & R. Mazebedi*, isol. *G. Modise & D. Nkwe*

© 2021 Westerdijk Fungal Biodiversity Institute

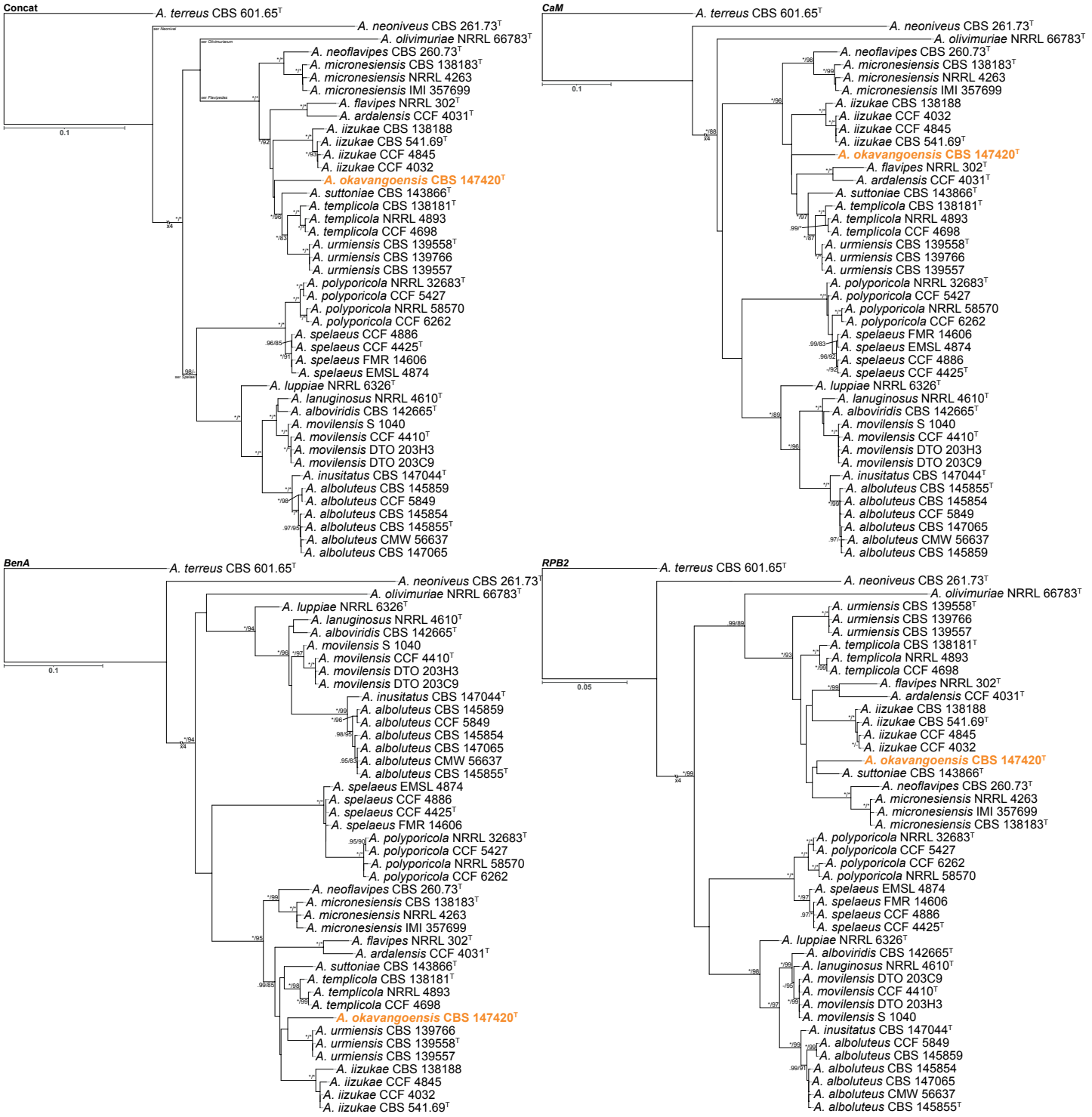

Fig. 1. Phylogenetic trees of *Aspergillus* section *Flavipedes* based on a concatenated dataset of four loci (*BenA*, *CaM*, ITS and *RPB2*) and single-gene phylogenies of *BenA*, *CaM* and *RPB2*. Strains of the new species are shown in bold coloured text. Branch support in nodes higher than 80 % bs and/or 0.95 pp are indicated at relevant branches (T = ex-type; * = 100 % bs or 1.00 pp; - = support lower than 80 % bs and/or 0.95 pp). Trees are rooted to *A. terreus*. Some branches were shortened four times to facilitate layout.

(**holotype** PREM 63212 dried specimen, culture ex-type CBS 147420 = CMW 56636 = CN073A3 = DN24).

ITS barcode: MW480880. Alternative identification markers: *BenA* = MW480788, *CaM* = MW480706, *RPB2* = MW480790.

Diagnosis: Colonies growing moderately fast, on CYA 37 °C 14–15 mm, on CREA 15–16 mm, Hülle cells not produced; Conidiophore vesicles 10–26 µm, conidial colour *en masse* greenish grey.

Colony diam (7 d, in mm): CYA 24–25; CYA 10 °C no growth; CYA 15 °C 10–11; CYA 20 °C 19–20; CYA 30 °C 28–30; CYA 37 °C 14–15; CYAS 24–26; MEA 20–22; DG18 22–23; YES 43–45; OA 16–17; CREA 15–16.

Colony characters CYA 25 °C, 7 d: Colonies surface floccose; mycelial areas cream; sporulation moderately dense, greenish grey to yellowish grey (1A2, 2A2); soluble pigment brownish orange; exudate brownish orange; reverse pigmentation dark

© 2021 Westerdijk Fungal Biodiversity Institute

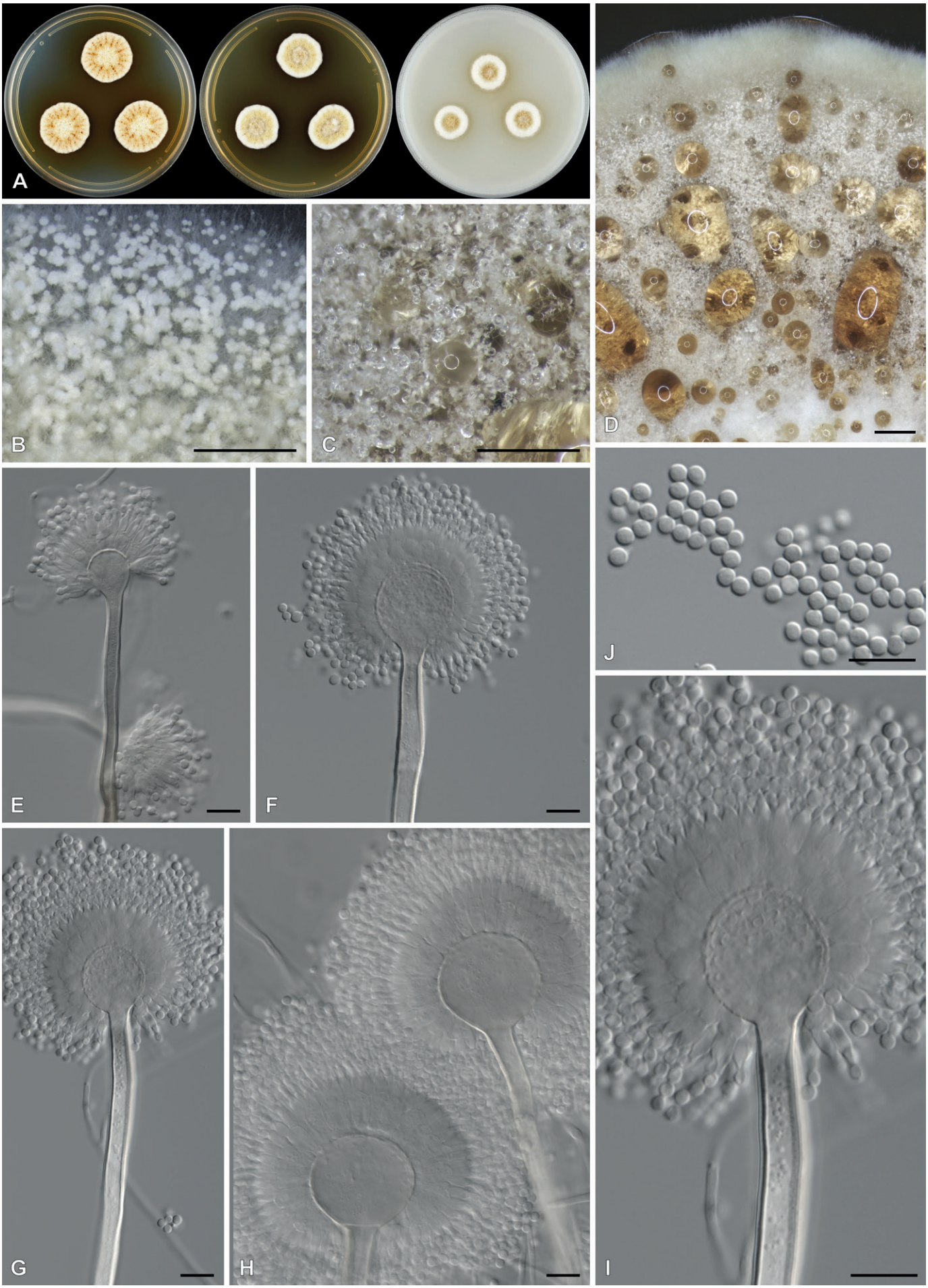

Fig. 2. Morphological characters of *Aspergillus okavangoensis* (CBS 147420[T]). **A.** Colonies from left to right on CYA, MEA and OA. **B.** Texture on DG18. **C.** Texture on MEA. **D.** Texture on CYA. **E–I.** Conidiophores. **J.** Conidia. Scale bars: B–D = 1 mm, E–J = 10 µm.

© 2021 Westerdijk Fungal Biodiversity Institute

brown (6F8–7F8). MEA 25 °C, 7 d: Colonies surface floccose; mycelial areas cream; sporulation moderately dense, greenish grey to yellowish grey (1A2, 2A2); soluble pigment brownish orange; exudate brownish orange, inconspicuous; reverse pigmentation dark brown (6F8–7F8). YES 25 °C, 7 d: Colonies surface floccose; mycelial areas yellow to cream; sporulation absent; soluble pigment absent; exudate absent; reverse pigmentation light brown, brown to dark brown (6D7–7D8, 7E8–8E8). DG18 25 °C, 7 d: Colonies surface floccose; mycelial areas cream to yellow; sporulation moderately dense, yellowish white to dull yellow (2A2–3B4); soluble pigment brownish orange; exudate absent; reverse pigmentation brownish orange to brown (6D7–E8). OA 25 °C, 7 d: Colonies surface floccose; mycelial areas white; sporulation moderately dense, greyish yellow to olive brown (4C5–D5); soluble pigment brown, inconspicuous; exudate absent. CREA 25 °C, 7 d: Colonies dense, acid not produced.

Conidial heads radiate. *Conidiophores* biseriate. *Stipes* hyaline, sometimes lightly pigmented, smooth, 230–510 × 4.5–8 µm. *Vesicles* globose, metulae cover 100 % of vesicle surface, 10–26 µm wide. *Metulae* 5.5–8(–10) × 3.5–6 µm. *Phialides* ampulliform, 5.5–7(–8) × 2–3 µm. *Conidia* globose to subglobose, smooth, 2.5–3 × 2–3 µm, (2.95 ± 0.11 × 2.82 ± 0.12, n = 51) µm, length/width 0.96 ± 0.04. *Hülle cells* and *accessory conidia* were not observed.

DISCUSSION

This study reports on *Aspergillus* species isolated from bat guano-contaminated soil collected from the historic Gcwihaba Cave in Botswana. Even though this was only a preliminary survey, the 81 strains isolated, represented eight sections and 19 species and included the new species described above as *A. okavangoensis*. *Aspergillus okavangoensis* is a distinct species in series *Flavipedes*, but its relationship with others in the series is not fully resolved (Fig. 1). Morphologically, it most closely resembles *A. iizukae*, especially considering their conidiophore vesicles often being wider than 20 µm (Hubka *et al.* 2014). However, they can be distinguished based on the new species' lack of Hülle cells and slightly slower growth observed on CYA 37 °C (14–15 *vs* 18–21 mm) and CREA (15–16 *vs* 23–41mm) (Hubka *et al.* 2014). The Gcwihaba Cave was found to be species-rich with most species isolated in low numbers, except for *A. sydowii* (43 strains) and *A. subalbidus* (13 strains) that dominated communities. Fungal surveys from caves often find *Aspergillus* and *Penicillium* to be very common (Johnson *et al.* 2013, Man *et al.* 2015, , Zhang *et al.* 2017, Zhang *et al.* 2020, Jurado *et al.* 2021, Sanchez-Moral *et al.* 2021). Unfortunately, most of these surveys identified strains based on the ITS barcode which is not reliable on a species level in both of these genera (Houbraken *et al.* 2020). To our knowledge, only a handful of studies used the preferred approach of sequencing either *BenA* or *CaM* for making robust identifications (Novakova *et al.* 2014, Nováková *et al.* 2018, Cunha *et al.* 2020). These studies all showed caves are species-rich with a diverse range of *Aspergillus* recorded, making it difficult to determine a core mycobiota. However, it does seem that especially *Aspergillus* series *Versicolores* species that includes for example *A. sydowii* were common to all these surveys.

Considering recent revisions of *Aspergillus* that released comprehensive reference data (Samson *et al.* 2014, Houbraken *et al.* 2020), exploring species diversity in *Aspergillus* has never been easier. This is evident considering the number of accepted species increasing in the last six years from 339 (Samson *et al.* 2014) to 446 (Houbraken *et al.* 2020). One problem observed is the many monotypic species currently accepted, as infraspecies variation within species are not captured. It is usually not a concern to introduce new species based on a single specimen, as done here, when they are phylogenetically very distinct from all other species. However, often species boundaries are not as clear as in the case of *A. okavangoensis*. An example is *A. capensis* that was introduced as a close relative of *A. iizukae* (Visagie *et al.* 2014). However, in a recently published review of section *Flavipedes* using extensive phylogenetic analyses and species delimitation techniques with a broader range of strains, the authors showed that *A. capensis* should be considered a synonym of *A. iizukae* (Sklenář *et al.* 2021). Even though we try to minimise the number of name changes, this is generally not problematic in a genus like *Aspergillus* for which accepted species lists are updated regularly. It does however illustrate the importance of fungal surveys that isolate, preserve, and generate DNA sequences to help capture infra- and interspecies variations. These data help to better resolve species boundaries and thus also makes future identifications easier.

Botswana as a region is greatly neglected in terms of microbial surveys. The current study aimed to complete a preliminary survey on species diversity associated with bat guano in Botswana caves and will lay the foundations for future work looking to explore Botswana as an untapped source of biological diversity related to potential novel product discovery.

ACKNOWLEDGEMENTS

We acknowledge funding for this work from the Botswana International University of Science and Technology to David Nkwe; and the Department of Tertiary Education Financing (Botswana) that supported Modise Goodwell's BSc studies. Additional funding was provided to Cobus M. Visagie by the Future Leaders - African Independent Research fellowship programme (FLAIR, FLR\R1\201831). The FLAIR Fellowship Programme is a partnership between the African Academy of Sciences and the Royal Society funded by the UK Government's Global Challenges Research Fund. We appreciate the fieldwork assistance of Richard Mazebedi, as well as Jobe Marenga and his colleagues who guided us through the Gcwihaba Cave network during sampling. We are also grateful to David Nsibo who assisted with initial PCR's.

Conflict of interest: The authors declare that there is no conflict of interest.

REFERENCES

Akaike H (1974). A new look at the statistical model identification. *IEEE Transations on Automatic Control* **19**: 716–723.

Blehert DS, Hicks AC, Behr M, *et al.* (2009). Bat White-Nose Syndrome: An Emerging Fungal Pathogen? *Science* **323**: 227–227.

Cunha AOB, Bezerra JDP, Oliveira TGL, *et al.* (2020). Living in the dark: Bat caves as hotspots of fungal diversity. *PLoS ONE* **15**: e0243494.

Dandurand G, Duranthon F, Jarry M, *et al.* (2019). Biogenic corrosion caused by bats in Drotsky's Cave (the Gcwihaba Hills, NW Botswana). *Geomorphology* **327**: 284–296.

© 2021 Westerdijk Fungal Biodiversity Institute

de Hoog GS, Gerrits van den Ende AH (1998). Molecular diagnostics of clinical strains of filamentous *Basidiomycetes*. *Mycoses* **41**: 183–189.

Glass NL, Donaldson GC (1995). Development of premier sets designed for use with the PCR to amplify conserved genes from filamentous *Ascomycetes*. *Applied and Environmental Microbiology* **61**: 1323–1330.

Hong S-B, Cho H-S, Shin H-D*, et al.* (2006). Novel *Neosartorya* species isolated from soil in Korea. *International Journal of Systematic and Evolutionary Microbiology* **56**: 477–486.

Houbraken J, Kocsube S, Visagie CM*, et al.* (2020). Classification of *Aspergillus*, *Penicillium*, *Talaromyces* and related genera (*Eurotiales*): an overview of families, genera, subgenera, sections, series and species. *Studies in Mycology* **95**: 5–169.

Hubka V, Nováková A, Kolarik M*, et al.* (2014). Revision of *Aspergillus* section *Flavipedes*: seven new species and proposal of section *Jani sect. nov*. *Mycologia* **107**: 169–208.

Johnson LJAN, Miller AN, McCleery RA*, et al.* (2013). Psychrophilic and psychrotolerant fungi on bats and the presence of *Geomyces* spp. on bat wings prior to the arrival of white nose syndrome. *Applied and Environmental Microbiology* **79**: 5465–5471.

Jurado V, Del Rosal Y, Liñan C*, et al.* (2021). Diversity and seasonal dynamics of airborne fungi in Nerja Cave, Spain. *Applied Sciences* **11**: 6236.

Katoh K, Standley DM (2013). MAFFT multiple sequence alignment software version 7: improvements in performance and usability. *Molecular Biology and Evolution* **30**: 772–780.

Kolo K, Keppens E, Préat A*, et al.* (2007). Experimental observations on fungal diagenesis of carbonate substrates. *Journal of Geophysical Research* **112**: G01007.

Kornerup A, Wanscher JH (1967). *Methuen Handbook of Colour*. 2nd edn. Methuen & Co Ltd, London, England.

Lanfear R, Frandsen PB, Wright AM*, et al.* (2017). PartitionFinder 2: new methods for selecting partitioned models of evolution for molecular and morphological phylogenetic analyses. *Molecular Biology and Evolution* **34**: 772–773.

Letunic I, Bork P (2016). Interactive tree of life (iTOL) v3: an online tool for the display and annotation of phylogenetic and other trees. *Nucleic Acids Research* **44**: W242–245.

Man B, Wang H, Xiang X*, et al.* (2015). Phylogenetic diversity of culturable fungi in the Heshang Cave, central China. *Frontiers in Microbiology* **6**: 1158.

Masclaux F, Guého E, de Hoog GS*, et al.* (1995). Phylogenetic relationships of human-pathogenic *Cladosporium* (*Xylohypha*) species inferred from partial LS rRNA sequences. *Journal of Medical and Veterinary Mycology* **33**: 327–338.

Mazebedi R, Hesselberg T (2020). A preliminary survey of the abundance, diversity and distribution of terrestrial macroinvertebrates of Gcwihaba cave, northwest Botswana. *Subterranean Biology* **35**: 49–63.

Mbaiwa JE, Sakuze LK (2009). Cultural tourism and livelihood diversification: The case of Gcwihaba Caves and XaiXai village in the Okavango Delta, Botswana. *Journal of Tourism and Cultural Change* **7**: 61–75.

Myers N, Mittermeier RA, Mittermeier CG*, et al.* (2000). Biodiversity hotspots for conservation priorities. *Nature* **403**: 853–858.

Nguyen LT, Schmidt HA, Von Haeseler A*, et al.* (2015). IQ-TREE: A fast and effective stochastic algorithm for estimating maximum-likelihood phylogenies. *Molecular Biology and Evolution* **32**: 268–274.

Novakova A, Hubka V, Saiz-Jimenez C (2014). Microscopic fungi isolated from cave air and sediments in the Nerja Cave – preliminary results. In: *The Conservation of Subterranean Cultural Heritage* (Saiz-Jimenez C. ed.). CRC Press/Balkema: Leiden, The Netherlands: 239–246.

Nováková A, Hubka V, Valinová Š*, et al.* (2018). Cultivable microscopic fungi from an underground chemosynthesis-based ecosystem: a preliminary study. *Folia Microbiologica* **63**: 43–55.

Pusz W, Ogórek R, Knapik R*, et al.* (2015). The occurrence of fungi in the recently discovered Jarkowicka Cave in the Karkonosze Mts. (Poland). *Geomicrobiology Journal* **32**: 59–67.

Ronquist F, Teslenko M, van der Mark P*, et al.* (2012). MrBayes 3.2: Efficient Bayesian phylogenetic inference and model choice across a large model space. *Systematic Biology* **61**: 539–542.

Samson RA, Visagie CM, Houbraken J*, et al.* (2014). Phylogeny, identification and nomenclature of the genus *Aspergillus*. *Studies in Mycology* **78**: 141–173.

Sanchez-Moral S, Jurado V, Fernandez-Cortes A*, et al.* (2021). Environment-driven control of fungi in subterranean ecosystems: the case of La Garma Cave (northern Spain). *International Microbiology*: https://doi.org/10.1007/s10123-021-00193-x

Sklenář F, Jurjević Ž, Houbraken J*, et al.* (2021). Re-examination of species limits in *Aspergillus* section *Flavipedes* using advanced species delimitation methods and proposal of four new species. *Studies in Mycology*: in press.

Vanderwolf KJ, Malloch D, Mcalpine DF*, et al.* (2013). A world review of fungi, yeasts, and slime molds in caves. *International Journal of Speleology* **42**: 77–96.

Visagie CM, Hirooka Y, Tanney JB*, et al.* (2014). *Aspergillus*, *Penicillium* and *Talaromyces* isolated from house dust samples collected around the world. *Studies in Mycology* **78**: 63–139.

Visagie CM, Yilmaz N, Vanderwolf K*, et al.* (2020). *Penicillium* diversity in Canadian bat caves, including a new species*, P. speluncae*. *Fungal Systematics and Evolution* **5**: 1–15.

Zhang Z-F, Zhou S-Y, Eurwilaichitr L, *et al*. (2020). Culturable mycobiota from Karst caves in China II, with descriptions of 33 new species. *Fungal Diversity* **106**: 29–136.

Zhang ZF, Liu F, Zhou X, *et al*. (2017). Culturable mycobiota from Karst caves in China, with descriptions of 20 new species. *Persoonia* **39**: 1–31.

© 2021 Westerdijk Fungal Biodiversity Institute

© 2021 Westerdijk Fungal Biodiversity Institute

FUSE

Fungal Systematics and Evolution

VOLUME 8
DECEMBER 2021
PAGES 91–100

doi.org/10.3114/fuse.2021.08.08

Asperosporus subterraneus, a new genus and species of sequestrate *Agaricaceae* found in Florida nursery production

E. Karlsen-Ayala[1,2*], R. Gazis[1,2], M.E. Smith[2]

[1]University of Florida, Department of Plant Pathology, Tropical Research and Education Center, Homestead, FL 33031, USA
[2]University of Florida, Department of Plant Pathology, Gainesville, FL 32608, USA

*Corresponding author: ekarlsenayala@gmail.com

Key words:
Hydrophobic
new taxa
ornamental plant production
potting soil
saprotrophic fungi
truffle

Abstract: We describe a novel sequestrate genus and species, *Asperosporus subterraneus gen. et sp. nov.,* found associated with nursery production of ferns in south Florida. This truffle species has a unique combination of morphological characters among described *Agaricaceae* in that it lacks a stipe or columella, has large, ornamented spores, the fresh sporocarps rapidly stain pink-red when cut or bruised, and they have a rancid smell. Although this fungus does not appear to be a direct plant pathogen, the hyphae of *A. subterraneus* produce a thick hydrophobic mycelial mat that binds the organic matter and therefore prevents water and fertilizer from being absorbed by plants, consequently causing wilting and chlorosis. Using morphological characteristics and phylogenetic reconstruction based on the internal transcribed spacer (ITS), partial large subunit nuclear ribosomal DNA (LSU), second largest subunit of RNA polymerase II (*rpb2*) and translation elongation factor 1-alpha (*tef1*) regions, we describe this taxon as a new genus and species in *Agaricaceae*.

Citation: Karlsen-Ayala E, Gazis R, Smith ME (2021). *Asperosporus subterraneus*, a new genus and species of sequestrate *Agaricaceae* found in Florida nursery production. *Fungal Systematics and Evolution* **8**: 91–100. doi: 10.3114/fuse.2021.08.09
Received: 9 June 2021; **Accepted:** 19 September 2021; **Effectively published online:** 7 October 2021
Corresponding editor: P.W. Crous

INTRODUCTION

Agaricaceae is a large family of fungi containing species with diverse morphological characteristics, from spore color (white, green, dark brown, black, blue, pale-pink and pale-yellow) to sporocarp type (agaricoid, secotioid, gasteroid) (Lebel *et al.* 2004, Vellinga 2004b). While sporocarps from many genera in *Agaricaceae* bruise or stain red when fresh, this feature can be critical for species level identification in some taxa (Ge *et al*. 2018, Vellinga *et al.* 2010b). Here we refer to *Agaricaceae* as defined in Vellinga *et al.* (2011) but recently a more constrained delimitation of genera in *Agaricaceae s.l.* has been proposed which narrows the number of accepted taxa (Kalichman *et al.* 2020). Recently, several studies have revealed that sequestration is more prolific throughout the family than previously thought and that many of these sequestrate fungi are found in genera with mostly agaricoid fruiting forms (Lebel *et al.* 2004, Kropp *et al*. 2012, Lebel & Syme 2012, Ge *et al*. 2018). Since fungi with gasteroid sporocarp forms are generally hypogeous, finding sufficient collections to describe new taxa is challenging and has resulted in multiple monotypic genera and descriptions based on few collections (Ge & Smith 2013). For instance, genera such as *Amogaster* (gasteroid, now considered in the genus *Lepiota*), and *Barcheria* (gasteroid) are only known from a small number of collections (Lebel *et al.* 2004, Ge & Smith 2013).

In 2017 and 2018, potted Boston fern (*Nephrolepis exaltata*) samples were submitted for disease diagnosis to the University of Florida Plant Diagnostic Clinic (Homestead, Florida). The potting soil contained sequestrate, truffle-like basidiomata that had an unpleasant odor and rapidly stained pink-red when bruised or cut (Fig. 1C). The specimens had highly ornamented brown spores and could not be identified to the genus or species level based on available publications or taxonomic keys of brown-spored truffle-like fungi (Dodge & Zeller 1934, Miller 1999). Preliminary ribosomal sequence data placed the specimens in *Agaricaceae* but with no reliable matches to known species. Based on the unique combination of morphological and molecular characteristics of this truffle we describe this taxon as *Asperosporus subterraneus,* a new genus and species in the *Agaricaceae*. We provide a full description and include sequence data from the internal transcribed spacer (ITS), partial large subunit nuclear ribosomal DNA (LSU), second largest subunit of RNA polymerase II (*rpb2*) and translation elongation factor 1-alpha (*tef1*) regions.

MATERIALS AND METHODS

In 2017 and 2018 potted Boston fern (*N. exaltata*) samples were submitted for disease diagnosis at the University of Florida Plant Diagnostic Clinic (Homestead, Florida) (Fig. 1A). The specimens from 2018 were not dried properly and therefore specimens were not kept nor were DNA sequences obtained. However, photos and notes taken at the time of submission confirm

Fungal Systematics and Evolution is licensed under a Creative Commons Attribution-NonCommercial-ShareAlike 4.0 International License

© 2021 Westerdijk Fungal Biodiversity Institute

that the specimens correspond to the same fungus as the ones submitted in 2017. For both the 2017 and 2018 samples, the plants were excavated for root examination and several gasteroid basidiomata were observed (Fig. 1B). Tissues were examined under a light microscope using H_2O, 5 % KOH, and Melzer's reagent. Spore dimensions are given in the following order length, width, and spore Q (length to width ratio) and spore measurements excluded spore ornaments, which were measured separately. All other morphological examinations (such as color and ornamentation) were based on 20–40 individual structures. Dried specimens were deposited at the University of Florida Fungal Herbarium under the accession number FLAS-F-68001.

Small pieces of basidiomata were ground in liquid nitrogen in 1.5 mL Eppendorf tubes and DNA was extracted using the CTAB extraction method (Doyle & Doyle 1987). PCR amplification was completed with the following primer pairs and thermocycler conditions according to each reference: the internal transcribed spacer (ITS) ITS1F/4 (White *et al*. 1990, Gardes & Bruns 1993), large subunit nuclear ribosomal DNA (LSU) LROR/LR6 (Vilgalys & Hester 1990), RNA polymerase II subunit 2 (*rpb2*) bRPB2-6F and bRPB2-7.1R (Matheny 2005), and the translation elongation factor 1-α locus (*tef1*) EF-983F/EF1-1567R (Rehner & Buckley 2005). PCR products were run on a 1.5 % agarose gel using SYBR Green and sequenced at MCLab (San Francisco, CA). Bi-directional reads were trimmed, assembled, and checked for quality using Geneious v. 2020.1.2. Sequences were aligned with MAFFT v. 7.450 (Katoh *et al*. 2002, Katoh & Standley 2013) using default settings.

Three datasets were assembled to infer the phylogenetic position of the unknown fungus. First, an ITS dataset containing 36 sequences was assembled following the taxon sampling in Vellinga *et al.* (2011) as a framework. Additional sequences were added, focusing on taxa with morphological similarities such as the reddening reaction and gasteroid basidiomata. Because some taxa are only represented by their ITS sequence, the objective of this first analysis was to confirm the uniqueness of the new taxon with respect to previously described gasteroid taxa in the *Agaricaceae* (Kropp *et al*. 2012, Lebel & Vellinga 2013, Zhao *et al.* 2016, Ge *et al*. 2018). Second, an LSU dataset containing 47 sequences was assembled based on the family level taxon sampling used in Vellinga *et al.* (2011) and included a wide range of taxa, many of which lack the regions used in the multilocus analysis. This dataset included representatives of many closely related accepted genera in the family. Finally, a combined LSU, *rpb2*, and *tef1* dataset was assembled by mining the NCBI nucleotide database guided by relevant published studies on the family *Agaricaceae* (Kropp *et al*. 2012, Lebel & Syme 2012, Zhao *et al*. 2016). All taxa in the multilocus alignment contained at least LSU and *rpb2* sequences whereas *tef-1* was present in 62 % of the taxa. The ITS region was excluded from the multilocus analysis because incomplete sequence availability across the selected loci resulted in a data matrix with a high percentage of missing data. Three *Limacella* species (*L. glioderma*, *L. guttata*, and *L. delicata*) were used as outgroups for all datasets. Ambiguously aligned regions were excluded from the alignments using Gblocks v. 0.91b (Talavera & Castresana 2007) with reduced stringency settings by allowing gaps within final blocks and less strict flanking positions. Phylogenies were reconstructed using matrices with and without ambiguously aligned regions. Topologies were compared and inspected for conflict. Conflict was assumed to be significant if a group of taxa was supported at 70 % as monophyletic with one locus but supported as nonmonophyletic by another locus [reciprocal 70 % ML bootstrap support criterion (Reeb *et al.* 2004)].

Maximum Likelihood (ML) phylogenies based on the ITS and LSU regions, and on the concatenated LSU + *rpb2* + *tef1* dataset were constructed using RaxML v. 8.2.10 (Stamatakis 2014) under the GTRGAMMA evolutionary model. Branch support values were estimated using 1 000 bootstrap (BS) replicates. The same alignments were used to infer phylogenies using Bayesian analysis with MrBayes v. 3.2.6 x64 (Huelsenbeck 2004). jModeltest v. 2.1.10 (Darriba *et al*. 2012) was used to estimate the model of evolution for each region and the GTR+I+G model of evolution was assigned to the LSU and *rpb2* regions and the GTR+G model of evolution to the *tef1*. The concatenated matrix was partitioned by locus prior to phylogeny inference. Posterior probabilities (PP) were determined using 10^6 generations with sampling every 1 000 generations. The first 25 % of trees were discarded as the burn in. Sequence data was deposited in NCBI (Table 1), and alignments and trees were deposited on the Open Science Framework (OSF) at https://osf.io/7gn85/?view_only=08df5d71e46b4c08b12388fc775a9c7e.

RESULTS

The ITS and LSU sequences generated from specimens were compared to the NCBI and UNITE (Abarenkov *et al*. 2010) nucleotide databases, using different BLAST strategies (including/excluding environmental sequences and restricting the search to sequences generated from type specimens). Results based on the ITS sequence (701 bp) yielded top BLAST hits to members of the genus *Coniolepiota* (*e.g.*, HM488757, KC625531, and HM488755) but only with approximately 87 % similarity. Results based on the LSU sequence (868 bp) yielded top BLAST hits to *Chlorophyllum molybdites* (KU049687, KU049686, and KU049684) with approximately 98 % similarity. Since BLAST matches provided limited resolution on the identity and taxonomic placement of this novel truffle, we performed a preliminary phylogenetic analysis based on the ITS and LSU regions.

Phylogenetic reconstruction using the ITS region (909 characters / 36 taxa) placed the novel fungus within the *Agaricus*+satellite clade (*sensu* Vellinga *et al.* 2011), which includes *Agaricus* and several other closely related genera such as *Clarkeinda, Coniolepiota, Eriocybe*, *Heinemannomyces*, and *Hymenagaricus* (BS: 75 %; PP: 0.98). Overall, the resulting topologies from the ML and BI analyses were similar and differences in relationships among taxa were unsupported by BS or PP statistics (Supplementary Fig. S1). The ML analysis placed the novel taxon as sister to *Eriocybe chionea* and the BI placed it sister to *Lepiota* cf. *fuscovinacea*, in both cases with no support.

The phylogenetic tree based on the LSU region (861 characters / 44 taxa) resolved the novel fungus as an unsupported lineage sister to *Agaricus* (Supplementary Fig. S2). The analysis based on LSU provided weak support for most relationships across the family. No conflict was found between the ML and BI analysis. The novel lineage was not recovered as closely related to any of the known sequestrate *Agaricaceae* taxa in either the ITS or LSU analyses.

The concatenated alignment based on LSU, *rpb2* and *tef1* consisted of 2 215 characters and comprised 29 taxa. This dataset included 902 bp for LSU, 766 bp for *rpb2* and 547 bp for *tef1*. ML and BI analyses generated phylogenies with non-conflicting

© 2021 Westerdijk Fungal Biodiversity Institute

Table 1. GenBank accession numbers for taxa analyzed in this study. Bold taxa are sequences generated in this study.

Taxon	Collection	Location	ITS	LSU	*rpb2*	*tef1*
Agaricaceae sp.	ecv3807	Thailand	n/a	HM488770	n/a	n/a
Agaricus biberi	LAPAG687	Hungary	KM657919	KR006614	KT951548	KR006642
Agaricus bisporus	AFTOL-ID 448	USA	n/a	MH867670	AF107785	n/a
	n/a	n/a	n/a	MH867670	n/a	n/a
Agaricus campestris	LAPAG370	n/a	KM657927	KR006607	KT951556	KR006636
	n/a	Germany	n/a	AY207134	n/a	n/a
Agaricus comtulus	LAPAG724	Spain	n/a	KT951448	KT951532	KT951593
Agaricus erythosarx	H7638	n/a	JF495069	JF495024	n/a	n/a
	MURU6080	n/a	JF495068	JF495025	n/a	n/a
Agaricus inapertus	ecv2339	USA:California	AF482834	AF482878	n/a	HM488878
Agaricus kerriganii	LAPAG808	Spain	n/a	KT951442	KT951528	KT951589
Agaricus linzhiensis	ZRL2012618	China	KT951378	KT951503	KT951553	KT951582
Agaricus melanosporus	AD9763	n/a	JF495042	JF495027	n/a	n/a
	AD9767	n/a	n/a	JF495026	n/a	n/a
Agaricus subrutilescens	ZRLWXH3276	China	KT951392	KT951522	KT951554	KT951585
Agaricus warritodes	TWM1589	n/a	JF495052	JF495030	n/a	n/a
Asperosporus subterraneus	**FLAS-F-68001**	**USA: Florida**	**SUB9037367**	**SUB9307387**	**MW816922**	**MW816921**
Barcheria willisiana	BA1307	Australia	n/a	AY372212	n/a	n/a
	MEL2177563	Australia	JF495036	AY372216	n/a	n/a
	MEL269353	Australia	JF495035	n/a	n/a	n/a
Chlorophyllum agaricoides	HMAS 71678	China: Nei Mongol	MG742004	MG742021	MG742051	MG742079
Chlorophyllum globosum	PREM 62147	South Africa	MG742002	MG742024	MG742053	MG742081
	n/a	n/a	n/a	MG742023	n/a	n/a
Chlorophyllum molybdites	Z.W.Ge 3377	USA: Florida	MG741992	MG742033	MG742062	MG742090
Clarkeinda trachodes	ecv3550	Thailand	HM488751	KY418837	HM488802	n/a
	ecv3838	Thailand	HM488750	HM488771	n/a	n/a
Coniolepiota sponges	HKAS:60246	China	n/a	KC871015	n/a	n/a
Coniolepiota spongodes	png012	Thailand	HM488756	HM488774	HM488796	HM488796
Coprinus comatus	AFTOL626	n/a	n/a	AF041529	AY780934	AY881026
Coprinus sterquilinus	n/a	n/a	n/a	AF041530	n/a	n/a
Cryptolepiota americana	UTC00143916	n/a	HQ020412	EU130550	n/a	n/a
Cryptolepiota mengei	Trappe 7311	n/a	HQ020413	HQ020417	n/a	n/a
Cryptolepiota microspora	Trappe 17584	n/a	HQ020410	HQ020420	n/a	n/a
Eriocybe chionea	ecv3616	Thailand	HM488753	HM488772	HM488801	n/a
	ecv3560	Thailand	HM488752	HM488773	HM488800	n/a
Heinemannomyces splendidissima	SFSU zrl 3062	n/a	n/a	HM436608	n/a	n/a
	ecv3586	Thailand	HM488760	HM488769	HM488793	KT951657
Hymenagaricus taiwanensis	C.M. Chen 3636	China	n/a	DQ006270	n/a	n/a
Lepiota aff. *fuscovinacea*	mflu 09-0129	Thailand	HM488758	HM488775	n/a	n/a
Lepiota cf. fuscovinacea	ecv3556	Thailand	HM488759	HM488776	n/a	n/a
Lepiota omninoflava	KUN-HKAS 106734	China	MN810157	MN810092	MN820951	MN820924

© 2021 Westerdijk Fungal Biodiversity Institute

Table 1. (Continued).

Taxon	Collection	Location	ITS	LSU	*rpb2*	*tef1*
Leucoagaricus americanus	ecv2454	USA	AY176407	AF482891	n/a	n/a
Leucoagaricus meleagris	n/a	Netherlands	AY176419	AF482890	n/a	n/a
Leucoagaricus sp.	ecv3745	USA: Hawaii	n/a	HM488780	HM488854	n/a
Leucocoprinus cepistipes	ecv3741	USA: Hawaii	n/a	HM488779	HM488844	n/a
Limacella delicata	ZTMyc55818	Switzerland	n/a	KT833807	KT833822	KT833835
Limacella glioderma	MB102389	Germany	n/a	KT833810	KT833825	KT833838
	n/a	Netherlands	n/a	AY176452	n/a	n/a
	HBAU15533	n/a	MZ145070	n/a	n/a	n/a
	GLM:GLM-F51951	Germany	MK412398	n/a	n/a	n/a
	n/a	USA: Michigan	n/a	AY176454	n/a	n/a
Limacella guttata	MB 100157	Germany	n/a	KT833813	KT833828	KT833841
Lycoperdon pyriforme	DSH 96-054	n/a	n/a	AF287873	AY218495	AY883426
Lycoperdon sp.	ecv3825	Thailand	n/a	HM488790	HM488876	n/a
Macrolepiota dolichaula	AFTOL-ID 481	China	DQ221111	DQ411537	DQ385886	n/a
Macrolepiota gasteroidea	H0052	Australia	n/a	JF495031	n/a	n/a
Macrolepiota mastoidea	HKAS 11207	n/a	n/a	JN940272	JN993698	n/a
Macrolepiota procera	KUN: HKAS 8108	China	n/a	AY207233	JN993697	n/a
Macrolepiota turbinata	H0219	Australia	JF495076	JF495032	n/a	n/a
Micropsalliota sp.	Laessoe 6025	Malaysia	n/a	AF482879	n/a	n/a
	ecv3638	Thailand	n/a	HM488768	n/a	n/a
Podaxis pistillaris	n/a	n/a	n/a	AF041539	n/a	n/a
Psuedolepiota zangmui	Z.W.Ge 2175	China: Yunnan	n/a	MG742049	n/a	n/a
Tulostoma kotlabae	n/a	Hungary	n/a	DQ112629	n/a	n/a
Tulostoma squamosum	Mrazek1300	Northern Europe	DQ415732	n/a	n/a	n/a
Xanthagaricus siamensis	MLFU 19-0576	Thailand	MN176993	MN176983	n/a	n/a
Xanthagaricus taiwanensis	n/a	Taiwan	DQ006271	n/a	n/a	n/a

topologies. Bootstrap support values and posterior probabilities were congruent for major nodes and recovered currently accepted phylogenetic relationships among genera within the *Agaricaceae* [for taxonomic revisions of the family see Vellinga (2004b), Vellinga *et al.* (2011), and Kalichman *et al.* (2020)]. The Bayesian analysis recovered (PP: 0.97) the novel taxon as an independent lineage within the *Agaricus*+satellite clade (Fig. 2). Phylogenies based on matrices with and without ambiguously aligned regions resulted in similar topologies. The multilocus phylogeny based on the concatenated alignment with ambiguously aligned regions excluded is shown in Supplementary Fig. S3.

Taxonomy

Asperosporus Karl.-Ayala, Gazis & M.E. Sm., ***gen. nov.*** MycoBank MB 838905.

Etymology: From the Latin "*asper*" (rough) and "*sporus*" (spores), for the highly ornamented spores.
Distinguished from other genera in *Agaricaceae* by a combination of the following characters: *Basidiomata* hypogeous and sequestrate, globose to subglobose, astipitate, and friable when dry. *Gleba* loculate, brownish, turning pink-red when freshly cut or bruised, hydrophobic, drying powdery and friable. *Basidiospores* subglobose to ellipsoid, pale yellow-orange when young but turning brown with age, thick-walled, ornamented, sterigmal remnants attached, and strongly dextrinoid in Melzer's reagent. *Basidiomata* producing a rancid odor when fresh. *Clamp connections* absent.

Type species: *Asperosporus subterraneus* Karl.-Ayala, Gazis & M.E. Sm.

Asperosporus subterraneus, Karl.-Ayala, Gazis & M.E. Sm., ***sp. nov.*** MycoBank MB 838906. Figs 1, 3A–F.

Etymology: From the Latin "*sub*" (below) and "*terra*" (earth), for the habit of fruiting below the soil

Diagnosis: *Basidiomata* 5–30 mm diam, globose to irregular,

© 2021 Westerdijk Fungal Biodiversity Institute

Fig. 1. *Asperosporus subterraneus* specimen FLAS-F-68001 (holotype) **A.** White hydrophobic mycelial mat binding organic matter in one of the potted Boston Fern plants (*Nephrolepsis exaltata*) submitted to the University of Florida Plant Diagnostic Clinic. **B.** Gasteroid basidiomata found in the potting soil. **C.** Red-staining gleba when freshly cut. **D.** Dry powdery gleba in a dried specimen, showing locules and the thin friable peridium. Scale bars: C–D = 1 cm.

astipitate, light tan but drying dark brown and staining pink-red when handled, producing a rancid odor when fresh. *Peridium* thin and friable when dry. *Gleba* loculate, staining pink-red when exposed to air, friable and hydrophobic when dried. *Basidia* 1–3 spored in fresh specimens, collapsing upon drying. *Spores* 16–22 × 12–18 µm, subglobose or ellipsoid, ornamented with warts, thick walled, strongly dextrinoid, often with sterigma remnants remaining attached. The genus is presently monotypic.

Macroscopic features: *Basidiomata* 5–30 mm diam, globose to irregular, lacking a stipe, surface smooth, at first white or light tan but becoming brownish with age, staining pink-red where handled or bruised (Fig. 1C), drying darker brown, particularly where bruised. *Peridium* irregular, friable when dry (Fig. 1D), sometimes sloughing off completely where handled, staining dark brown to black in Melzer's reagent. No response in KOH when dried. *Gleba* compressed, irregular, loculate (Fig. 3A), lacking a columella, light tan at first with occasional veins of white trama tissue and pockets of darker brown spores, staining pinkish or red when cut and exposed to air, reddish staining more notable in younger specimens, turning dark brown, powdery, delicate and hydrophobic upon drying. *Odor* rancid when fresh, indistinctly fungal when dry. *Taste* not determined.

Microscopic features: Basidiospores 16–22 × 12–18 µm (av. 18 × 15 µm) at maturity, globose, subglobose or ellipsoid (Q = 1–1.47 µm, mean Q = 1.21 µm); walls 1–3.5 µm thick (av. =1.8 µm); restricted at the sterigmal attachment point and apiculate, notably ornamented with larger pyramidal to irregular warts, up to 1 µm tall and 1 µm wide. Immature spores are notably smaller, mostly 12–15 × 10–12 µm, and with smaller spines that are 0.5 × 0.5 µm and clearly separated from one another.

© 2021 Westerdijk Fungal Biodiversity Institute

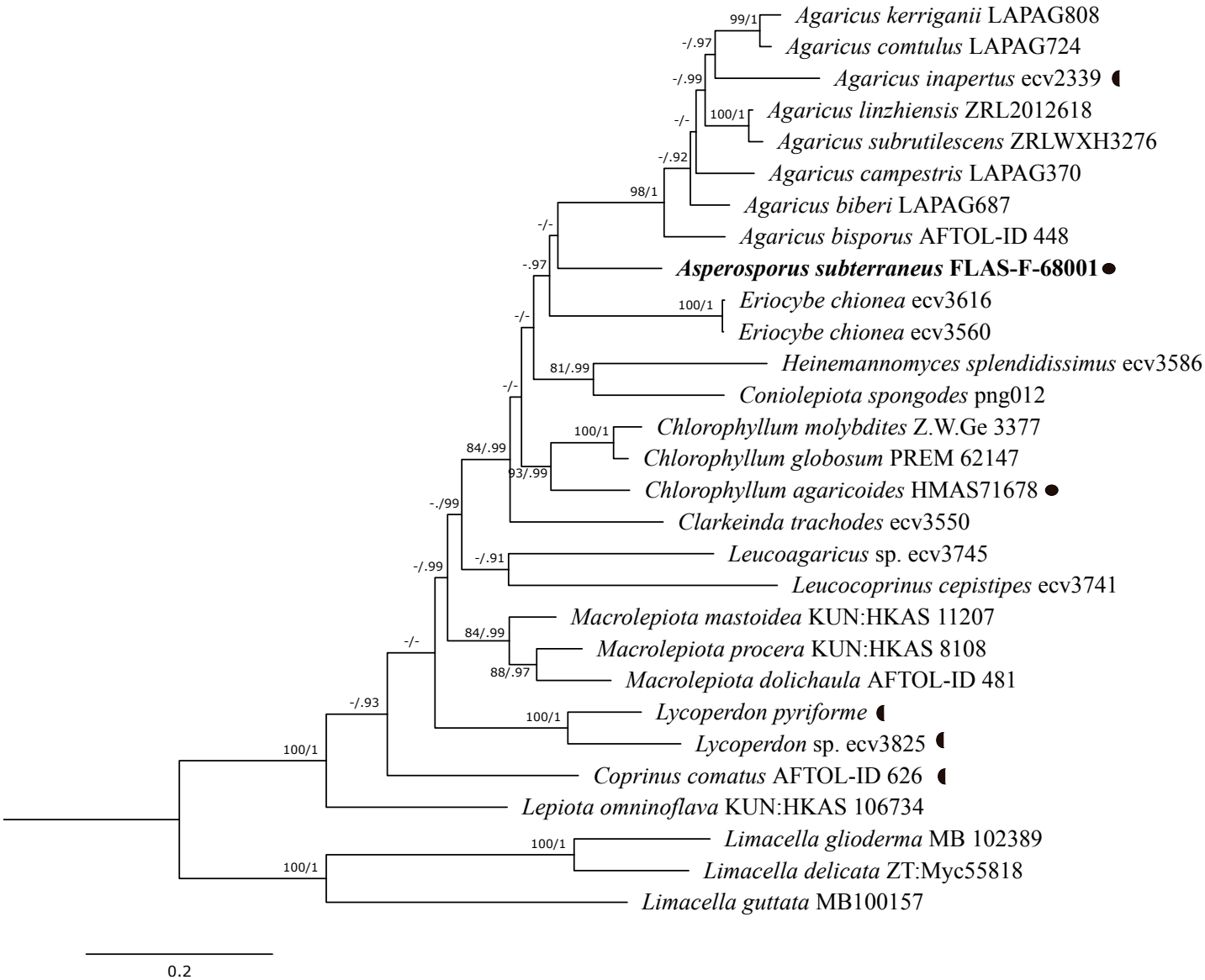

Fig. 2. Maximum likelihood phylogeny based on the combined LSU, *rpb2*, and *tef1* dataset. Branch bootstrap support values >75 % and Bayesian posterior probabilities > 0.90 are indicated. Symbols with closed circles represent gasteroid taxa, symbols with half circles represent secotoid taxa, and all other taxa are agaricoid.

Sterigma remnants often remaining attached and clearly visible in many spores (Fig. 3E) but more common in young spores, most 4–5 µm × 1–2 µm but sometimes up to 9 µm long. Pale yellow-orange when young but becoming darker orange-brown at maturity when observed using KOH or water, strongly dextrinoid in Melzer's reagent with mature spores turning notably darker than younger spores, highly variable in size and shape. *Basidia* 1–3 spored, difficult to find and see, collapsing in mature dried specimens (Fig. 3F). *Cystidia* not observed. *Peridium* (100–)150–250(–350) µm thick, composed of loosely interwoven (Fig. 3B) and irregularly branched and septate, single layered, hyphae 3–5 µm diam, occasionally swelling up to 10 µm; arrangement of hyphae mostly tangled and irregular but occasional bands of hyphae parallel to the exterior near the peridial surface, light yellow-brown, some hyphae strongly dextrinoid. *Trama* tissue 75–200 µm thick, composed of irregularly shaped, elongated and inflated hyaline hyphae, 10–26 µm diam. *Subhymenium* approximately 10–40 µm thick, comprised of densely packed interwoven hyphae with cells 12–14 µm diam that are brown to orange-brown. *Clamp connections* absent on all hyphae. No response to KOH.

Habitat and distribution: Found in south Florida growing in soil of potted nursery plants with poor drainage. Specimens thus far found only in association with Boston Fern (*N. exaltata*) which was planted in a Canadian peat moss and Florida pine bark mixed potting soil during the winter months.

Typus: **USA**, Florida, Tropical Research and Education Center Plant Diagnostic Clinic, Homestead, Miami-Dade Co., 21 Dec. 2017, *R. Gazis*, MES-3094 (**holotype** FLAS-F-68001).

Additional collection examined: **USA**, Florida, Tropical Research and Education Center Diagnostic Clinic, Homestead, Miami-Dade Co., 4 Dec. 2018, *R. Gazis,* 180871 (Photos deposited in MycoBank, but specimens not dried properly and therefore discarded).

© 2021 Westerdijk Fungal Biodiversity Institute

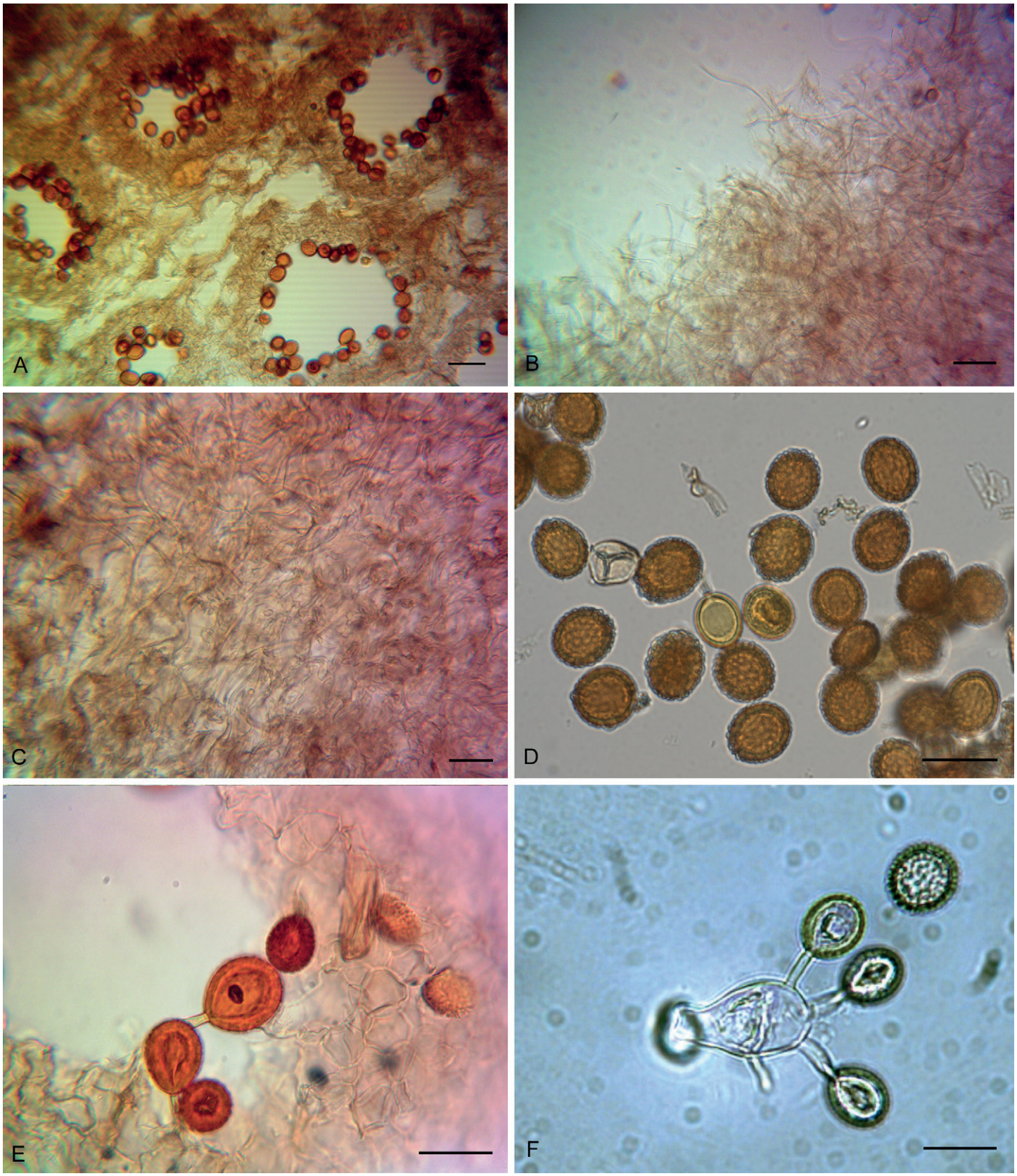

Fig. 3. Microscopic features of *Asperosporus subterraneus* specimen FLAS-F-68001 (holotype) **A.** Loculate gleba **B.** Peridium hyphae. **C.** Tangled peridium hyphae. **D.** Ornamented spores with thick spore walls. **E.** Subhymenium with basidiospores, some of which have retained sterigma remnants (indicated with arrows). **F.** Basidium with basidiospores. Scale bars: A–C = 60 µm, D–F = 20 µm.

© 2021 Westerdijk Fungal Biodiversity Institute

DISCUSSION

Morphology

Several puffballs in *Agaricaceae s.l.* (*i.e.*, *Bovista, Calvatia*, *Lycoperdon*) have features that are similar to those of *A. subterraneus*, such as the highly ornamented, powdery brown spores and a hydrophobic surface. However, these puffballs do not stain red when handled and typically produce aboveground basidiomata (Vellinga, 2004b, Larsson & Jeppson 2008, Jeppson *et al.* 2012). Furthermore, most of these puffball species have spores that are relatively small (*e.g*. less than 10 µm diam) whereas the spores of *A. subterraneus* are much larger (av. 18 × 15 µm) (Miller & Miller 1988). A pink-red staining reaction of the basidiomata is prominent in many genera of the *Agaricaceae*, including in species of *Agaricus, Barcheria, Chlorophyllum, Cystolepiota, Lepiota, Leucoagaricus, Leucocoprinus, Macropsalliota,* and *Melanophyllum* (Pegler 1985, Vellinga 2010, Vellinga *et al.* 2010, 2011, Zhao *et al*., 2010, 2016, Ge *et al*. 2018). However, the combination of red staining basidiomata and ornamented spores is unique to *A. subterraneus* within *Agaricaceae*. *Leucoagaricus* (*Agaricaceae*) also contains red staining taxa without clamp connections (Vellinga *et al.* 2010a, Dutta *et al*. 2021) but these taxa are all agaricoid. Morphologically, *A. subterraneus* could be mistaken for *Barcheria willisiana* (*Agaricaceae*) which is a fragile, astipitate, sequestrate fungus that contains an enclosed, loculate gleba, stains red when bruised, lacks clamp connections, and contains thick-walled globose spores that are strongly dextrinoid in Melzer's reagent (Lebel *et al.* 2004). However, *Barcheria* is currently known only from Australia and this taxon is easily differentiated from *A. subterraneus* by its smooth spores, scaly peridium, and basidia that remain intact upon drying.

Initial molecular and morphological similarities suggested that *A. subterraneus* was closely related to *Chlorophyllum* (*Agaricaceae*). *Chlorophyllum* is a diverse genus that contains several taxa that are sequestrate and stain upon handling as well as taxa that are associated with disturbed, nutrient-rich landscapes (Vellinga 2004a, Ge *et al.* 2018). Recently, more species of sequestrate *Chlorophyllum* have been discovered, such as *C. lusitanicum* (Carlavilla *et al.* 2018) and *C. levantinum* (Loizides *et al*. 2020). However, sequestrate fungi in this genus typically have smooth spores and a well-defined columella or stipe. Kropp *et al.* (2012) described three new species of sequestrate taxa from western North America and erected a new genus, *Cryptolepiota*, that were later transferred to *Lepiota* (*Agaricaceae*) (Lebel & Vellinga 2013). All of these taxa are subglobose, astipitate, sequestrate fungi that are fragile when dry. *Asperosporus* can be differentiated from species of "*Cryptolepiota"* by the pink-red staining reactions, rancid odor when fresh, ornamented spores and basidia that collapse upon drying. While spore ornamentation can be used to differentiate *Asperosporus* from most *Lepiota* species, there are some sequestrate *Lepiota* species with ornamented spores. However, all of these these taxa (*e.g. L. iberica, L. olbia, L. smurfiorum*, and *L. tulostomoides*) are secotioid and retain their stipe at maturity (Vidal *et al*. 2015). The sequestrate fungus *Neosecotium macrosporum* (*Agaricaceae*) also has ornamented spores and a powdery gleba (Lizárraga *et al*. 2012). While there are currently no publicly available sequence data for *Neosecotium macrosporum*, this sequestrate fungus differs from *A. subterraneus* in that *N. macrosporum* has a columella, a thick peridium, smaller and more globose spores, and flatter ornamentation that give the spores a cracked appearance. *Agaricus* (*Agaricaceae*) is a large genus of saprotrophic fungi containing more than 400 species in six subgenera and 21 sections (Zhao *et al.* 2016, Chen *et al.* 2017). This genus has species with diverse basidiomata types, including many different agaricoid, secotoid, and gasteroid taxa. Newly described sequestrate taxa (Lebel & Syme 2012, Lebel 2013) as well as species that were more recently transferred from other obsolete genera (*e.g. Longula texensis* = *Agaricus deserticola*) have expanded the diversity of this genus. Many taxa in *Agaricus* also stain or bruise red when fresh and all lack clamp connections (Zhao *et al.* 2016). However, species of *Agaricus* can be differentiated from *Asperosporus* by their smooth spores that lack the ornamentation seen in *A. subterraneus*.

Asperosporus subterraneus is characterized by a unique combination of morphological features that also differentiates it from other known sequestrate fungi outside *Agaricaceae*. Sequestrate fungi with fully enclosed basidiomata typically lose their ability to forcibly discharge their spores. Evidence of this can be seen in fungi that have poorly reviving basidia when dried and have spores with sterigma remnants (Trappe *et al*. 2009). Sterigma attachments was seen in *Asperosporus subterraneus* and in other sequestrate fungi such as *Guyanagaster necrorhiza* (*Physalacriaceae*) (Henkel *et al.* 2010). *Guyanagaster necrorhiza* is similar to *A. subterraneus* in that both taxa have strongly dextrinoid, thick-walled, ornamented spores and a well-defined gleba. However, the spores of *G. necrorhiza* are spiny, globose and light tan with pink tones and the peridium is highly warted (Henkel *et al.* 2010). Another genus with similarities to *Asperosporus* is *Octaviania* (*Boletaceae*). *Octaviania* basidiomata have sporocarps that often bruise when handled (blue, green, or black but occasionally red) and have globose to subglobose spores with pyramidal ornamentation and dextrinoid reactions (Orihara *et al*. 2012). However, species of *Octaviania* generally have smaller spores with more conspicuous ornaments and a gleba that never becomes powdery at maturity. The truffle *Xerocomellus macmurphyi* (*Boletaceae*) is also similar to *A. subterraneus* in its powdery gleba and in the dextrinoid spores that are similar in size and ornamentation (Smith *et al.* 2018). However, both *Octaviania* and *Xerocomellus* belong to the *Boletales* and are ectomycorrhizal whereas *A. subterraneus* belongs to the *Agaricaceae* and is likely saprotrophic. Many previously described truffle-like fungi with ornamented brown spores were originally placed within the genus *Hymenogaster.* However, morphological and molecular analyses have shown that *Hymenogaster sensu lato* contains many different unrelated taxa (Bougher & Castellano 1993, Smith *et al.* 2018). We have reviewed the descriptions of taxa in *Hymenogaster sensu lato* (Dodge & Zeller 1934) and were unable to locate any species that match the description of *A. subterraneus*.

Phylogenetic placement

Several challenges arise when attempting to place *A. subterraneus* into a phylogenetic context. No close matches (above 90 %) were found in nucleotide databases (NCBI and UNITE) between ITS sequences of *A. subterraneus* and previously collected specimens or environmental sequences generated through metabarcoding studies. Maximum Likelihood and Bayesian analyses based on the LSU and multilocus datasets placed *Asperosporus subterraneus* as sister to *Agaricus* within the *Agaricus*+satellite genera clade (*sensu* Vellinga *et al.* 2011) without support (Fig. 2, Supplementary Fig.

© 2021 Westerdijk Fungal Biodiversity Institute

S2). The phylogenetic tree based on the ITS region also recovered *A. subterraneus* within the *Agaricus*+satellite genera clade, but as an unsupported sister lineage sister to *Eriocybe chionea* in the ML and sister to *Lepiota cf. fuscovinaceae* in the BI analyses (Supplementary Fig. S1). Many of the satellite taxa in the *Agaricus* clade, such as *Coniolepiota*, *Eriocybe*, and *Heinemannomyces* and *Psuedolepiota* are monotypic genera, with limited collections and sequence data, and some of them have been described from a single locality in Asia. *Heinemannomyces* is a monotypic genus but recently has been shown to fall within *Hymenagaricus* (Hussain *et al*. 2018). Moreover, phylogenetic relationships among members of this clade remain unresolved (Watling 1998, Vellinga *et al.* 2011, Ge & Yang 2017) and unsupported nodes may be a reflection of incomplete taxon sampling. Therefore, future efforts to increase taxon sampling may be an important component to improve our accurate phylogenetic placement and understanding of relationships within this group (Som 2015). This includes increasing sequence availability of additional loci from known taxa in this clade together with the description of more unknown taxa.

Ecology of *Asperosporus subterraneus*

Asperosporus subterraneus has thus far only been found in association with potted Boston Fern plants submitted to the University of Florida Plant Diagnostic Clinic in Homestead, Florida in 2017 and 2018. The hyphae of *A. subterraneus* extensively colonize the substrate, thereby generating a hydrophobic mat which binds the organic matter and prevents the plant's roots from accessing water and nutrients. There is no evidence to suggest that *A. subterraneus* is a plant pathogen because there was no obvious root contact with the fungus. However, *A. subterraneus* can cause plants to develop wilting and chlorosis that make them unmarketable. The dense hyphal mats and ample basidiomata found within the substrate suggest that this fungus can become prolific in nursery settings and that the source of inoculum is likely the potting soil. Thus far basidiomata have not been found in soil or pots without plants. The south Florida ornamental industry generally grows plants in outdoor shade houses that allow ambient rainfall, temperature, and humidity to impact the growth of plants. The planting containers likely create suitable conditions for this fungus to fruit during plant production. *Asperosporus subterraneus* has been a recurrent problem in ornamental nurseries in south Florida and is thought to be associated with potting soil containing a mix of peat moss and pine bark (R. Gazis, pers. obs.). A robust understanding of the lifestyle, growth requirements, and dispersal of this fungus will help develop effective management recommendations for nurseries to prevent financial losses due to unmarketable plants. There are several fungi in the *Agaricaceae* that are common in nursery settings or in indoor potted plants. For example, *Leucocoprinus birnbaumii*, commonly called the "yellow house plant mushroom" is frequently found in indoor potted houseplants (Vellinga 2004a). Some disturbance-adapted *Agaricaceae* species have been found far outside their known natural distributions. For example, *Smithiomyces mexicanus,* known from tropical regions in Florida and Brazil, was found growing in Belgium around swimming pools with a sub-tropical landscape (Vellinga 1999). The nutritional mode for *Asperosporus subterraneus* remains unknown but we can infer it as being saprotrophic because it falls within the *Agaricaceae*, close to the *Agaricus* clade, which only contains saprotrophic species (Vellinga 2004b). Although this newly described fungus was not found in a natural environment and we do not know the geographic origin of this fungus, we still introduce this taxon as novel based on morphological characteristics and molecular evidence. Furthermore, the morphological characteristics and molecular placement of this truffle highlight the high diversity and unique combinations of morphological characteristics of sequestrate fungi within the *Agaricaceae*.

ACKNOWLEDGEMENTS

We thank Nattapol Kraisitudomsook, Claudia Paez, and Dr. Pedro Pablo Parra for their advice in the phylogenetic and taxonomic work. We thank Dr. Rosanne A. Healy and Dr. Nicole Reynolds for help with curation at the Florida Museum of Natural History fungal collection (FLAS-F). A fellowship from the University of Florida for graduate studies to E.K.A. is gratefully acknowledged. Participation of M.E.S. was supported by the NIFA-USDA Mcintire-Stennis project 1011527 and FLA-PLP-005289 award.

Conflict of interest: The authors declare that there is no conflict of interest.

REFERENCES

Abarenkov K, Nilsson RH, Larsson KH, *et al*. (2010). The UNITE database for molecular identification of fungi-recent updates and future perspectives. *New Phytologist* **186**: 281–285.

Bougher NL, Castellano MA (1993). Delimitation of *Hymenogaster sensu stricto* and four new segregate genera. *Mycologia* **85**: 273–293.

Carlavilla JR, Moreno G, Mohedano JM (2018). *Chlorophyllum lusitanicum*, a rare species from the Iberian Peninsulla. *Boletín de la Sociedad Micológica de Madrid* **42**: 99–105.

Darriba D, Taboada GL, Doallo R, *et al*. (2012). jModelTest 2: more models, new heuristics and parallel computing. *Nature Methods* **9**: 772–772.

Dodge CW, Zeller SM (1934). *Hymenogaster* and related genera. *Annals of the Missouri Botanical Garden* **21**: 625–708.

Doyle JJ, Doyle JL (1987). A rapid DNA isolation procedure for small quantities of fresh leaf tissue. *Phytochemical Bulletin* **19**: 11–15.

Dutta AK, Stallman JK, Bera S, *et al*. (2021). Lepiotaceous fungi of West Bengal, India: two new species of *Leucoagaricus*. *Mycological Progress* **20**: 493–507.

Gardes M, Bruns TD (1993). ITS primers with enhanced specificity for basidiomycetes-application to the identification of mycorrhizae and rusts. *Molecular Ecology* **2**: 113–118.

Ge ZW, Jacobs A, Vellinga EC, *et al.* (2018). A multi-gene phylogeny of *Chlorophyllum* (*Agaricaceae*, *Basidiomycota*): new species, new combination and infrageneric classification. *MycoKeys* **32**: 65–90.

Ge ZW, Smith ME (2013). Phylogenetic analysis of rDNA sequences indicates that the sequestrate *Amogaster viridiglebus* is derived from within the agaricoid genus *Lepiota* (*Agaricaceae*). *Mycological Progress* **12**: 151–155.

Henkel TW, Smith ME, Aime MC (2010). *Guyanagaster*, a new wood-decaying sequestrate fungal genus related to *Armillaria* (*Physalacriaceae, Agaricales, Basidiomycota*). *American Journal of Botany* **97**: 1474–1484.

Huelsenbeck JP, Larget B, Alfaro ME (2004). Bayesian phylogenetic model selection using reversible jump Markov chain Monte Carlo. *Molecular Biology and Evolution* **21**: 1123–1133.

© 2021 Westerdijk Fungal Biodiversity Institute

Hussain S, Ahmad H, Sher H, *et al*. (2018). *Xanthagaricus pakistanicus sp. nov.* (*Agaricaceae*): first report of the genus from Pakistan. *Turkish Journal of Botany* **42**: 123–133.

Jeppson M, Larsson E, Martín MP (2012). *Lycoperdon rupicola* and *L. subumbrinum*: two new puffballs from Europe. *Mycological Progress* **11**: 887–897.

Katoh K, Standley DM (2013). MAFFT multiple sequence alignment software version 7: improvements in performance and usability. *Molecular Biology and Evolution* **30**: 772–780.

Katoh K, Misawa K, Kuma, *et al*. (2002). MAFFT: a novel method for rapid multiple sequence alignment based on fast Fourier transform. *Nucleic Acids Research* **30***:* 3059–3066.

Kropp BR, Albee-Scott S, Castellano MA, *et al*. (2012). *Cryptolepiota*, a new sequestrate genus in the *Agaricaceae* with evidence for adaptive radiation in western North America. *Mycologia* **104**: 164–174.

Larsson E, Jeppson M (2008). Phylogenetic relationships among species and genera of Lycoperdaceae based on ITS and LSU sequence data from north European taxa. *Mycological Research* **112**: 4–22.

Lebel T (2013). Two new species of sequestrate *Agaricus* (section Minores) from Australia. *Mycological Progress* **12**: 699–707.

Lebel T, Syme A (2012). Sequestrate species of *Agaricus* and *Macrolepiota* from Australia: new species and combinations and their position in a calibrated phylogeny. *Mycologia* **104**: 496–520.

Lebel T, Thompson DK, Udovicic F (2004). Description and affinities of a new sequestrate fungus, *Barcheria willisiana gen. et sp. nov*. (*Agaricales*) from Australia. *Mycological Research* **108**: 206–213.

Lebel T, Vellinga EC (2013). Description and affinities of a sequestrate *Lepiota* (*Agaricaceae*) from Australia. *Mycological Progress* **12**: 525–532.

Lizárraga M, Esqueda M, Vargas-Luna M, *et al.* (2012). First record of the sequestrate fungus *Neosecotium macrosporum* (*Agaricales, Lepiotaceae*) from Mexico. *Mycotaxon* **120**: 437–441.

Loizides M, Alvarado P, Polemis E, *et al*. (2020). Multiple evolutionary origins of sequestrate species in the agaricoid genus *Chlorophyllum*. *Mycologia* **112**: 400–422.

Matheny PB (2005). Improving phylogenetic inference of mushrooms with *RPB1* and *RPB2* nucleotide sequences (*Inocybe*; *Agaricales*). *Molecular Phylogenetics and Evolution* **35**: 1–20.

Miller SL (1999). Field key to common genera of hypogeous and gasteroid basidiomycetes of North America. *McIlvainea* **14**: 8–29.

Miller OK, Miller H (1988). *Gasteromycetes: morphological and developmental features, with keys to the orders, families, and genera*. Mad River Press, Eureka, CA, USA.

Orihara T, Smith ME, Shimomura N, *et al*. (2012). Diversity and systematics of the sequestrate genus *Octaviania* in Japan: two new subgenera and eleven new species. *Persoonia* **28**: 85–112.

Pegler DN (1985). The genus *Clarkeinda* (*Basidiomycotina*: *Agaricaceae*). *Botanical Journal of the Linnean Society* **91**: 245–252.

Reeb V, Lutzoni F, Roux C (2004). Contribution of *RPB2* to multilocus phylogenetic studies of the euascomycetes (*Pezizomycotina, Fungi*) with special emphasis on the lichen-forming *Acarosporaceae* and evolution of polyspory. *Molecular Phylogenetics and Evolution* **32**: 1036–1060.

Rehner SA, Buckley E (2005). A *Beauveria* phylogeny inferred from nuclear ITS and *EF1-α* sequences: evidence for cryptic diversification and links to *Cordyceps* teleomorphs. *Mycologia* **97**: 84–98.

Smith ME, Castellano MA, Frank JL (2018). *Hymenogaster macmurphyi* and *Splanchnomyces behrii* are sequestrate species of *Xerocomellus* from the western United States. *Mycologia* **110**: 605–617.

Som A (2015). Causes, consequences and solutions of phylogenetic incongruence. *Briefings in Bioinformatics* **16**: 536–548.

Stamatakis A (2014). RAxML version 8: a tool for phylogenetic analysis and post-analysis of large phylogenies. *Bioinformatics* **30**: 1312–1313.

Talavera G, Castresana J (2007). Improvement of phylogenies after removing divergent and ambiguously aligned blocks from protein sequence alignments. *Systematic Biology* **56**: 564–577.

Trappe JM (2009). *Diversity, ecology, and conservation of truffle fungi in forests of the Pacific Northwest* (Vol. 772). US Department of Agriculture, Forest Service, Pacific Northwest Research Station.

Vellinga EC (1999). An American in a Belgian swimming pool. *Mycologist* **2**: 50–53.

Vellinga EC (2004). Ecology and distribution of lepiotaceous fungi (*Agaricaceae*) – A review. *Nova Hedwigia* **78**: 273–300.

Vellinga EC (2004). Genera in the family *Agaricaceae*: evidence from nrITS and nrLSU sequences. *Mycological Research* **108**: 354–377.

Vellinga, EC (2010). Lepiotaceous fungi in California, USA *Leucoagaricus* sect. *Piloselli*. *Mycotaxon* **112**: 393–444.

Vellinga EC, Contu M, Vizzini A (2010). *Leucoagaricus decipiens* and *La. erythrophaeus*, a new species pair in sect. *Piloselli*. *Mycologia* **102**: 447–454.

Vellinga EC, Sysouphanthong P, Hyde KD (2011). The family *Agaricaceae*: phylogenies and two new white-spored genera. *Mycologia* **103**: 494–509.

Vidal JM, Juste P, García F, *et al*. (2015). Hongos secotioides del género *Lepiota*: dos nuevas especies, dos nuevas combinaciones y reevaluación del género *Cribrospora*. *Boletín Micológico de FAMCAL* **10**: 47–71.

Vilgalys R, Hester M (1990). Rapid genetic identification and mapping of enzymatically amplified ribosomal DNA from several *Cryptococcus* species. *Journal of Bacteriology* **172**: 4238–4246.

Watling R (1998). *Heinemannomyces*: a new lazuline-spored agaric genus from South-East Asia. *Belgian Journal of Botany*, 133–138.

White TJ, Bruns T, Lee S, *et al*. (1990). Amplification and direct sequencing of fungal ribosomal RNA genes for phylogenetics In: Innis MA, Gelfand DH, Sninsky JJ and White JW (eds): *A Guide to Molecular Methods and Applications*. Academic Press, New York: 315–322.

Zhao R, Karunarathna S, Raspé O, *et al*. (2011). Major clades in tropical *Agaricus*. *Fungal Diversity* **51**: 279–296.

Zhao RL, Desjardin DE, Soytong K, *et al*. (2010). A monograph of *Micropsalliota* in Northern Thailand based on morphological and molecular data. *Fungal Diversity* **45**: 33–79.

Zhao RL, Zhou JL, Chen J, *et al*. (2016). Towards standardizing taxonomic ranks using divergence times–a case study for reconstruction of the *Agaricus* taxonomic system. *Fungal Diversity* **78**: 239–292.

Supplementary Material: http://fuse-journal.org/

Fig. S1. Maximum likelihood tree based on ITS dataset. Branch support values >75 % and Bayesian posterior probabilities > 0.90 are indicated. Symbols with closed circles represent gasteroid taxa, symbols with half circles represent secotoid taxa, and all other taxa are agaricoid. *Limacella glioderma* was used as an outgroup.

Fig. S2. Maximum likelihood tree based on LSU dataset. Branch support values >75 % and Bayesian posterior probabilities > 0.90 are indicated. Symbols with closed circles represent gasteroid taxa, symbols with half circles represent secotoid taxa, and all other taxa are agaricoid. *Limacella glioderma* was used as an outgroup.

Fig. S3. Maximum likelihood tree based on concatenated LSU, *rpb2*, and *tef1* dataset with ambiguously aligned regions excluded. Branch bootstrap support values >75 % and Bayesian posterior probabilities > 0.90 are indicated. *Limacella delicata, Limacella glioderma* and *Limacella guttata* were used as an outgroup

© 2021 Westerdijk Fungal Biodiversity Institute

FUSE

Fungal Systematics and Evolution

VOLUME 8
DECEMBER 2021
PAGES 101–127

doi.org/10.3114/fuse.2021.08.09

Citizen science project reveals novel fusarioid fungi (*Nectriaceae, Sordariomycetes*) from urban soils

P.W. Crous[1,2*], M. Hernández-Restrepo[1], A.L. van Iperen[1], M. Starink-Willemse[1], M. Sandoval-Denis[1], J.Z. Groenewald[1]

[1]Westerdijk Fungal Biodiversity Institute, Uppsalalaan 8, 3584CT Utrecht, The Netherlands
[2]Wageningen University and Research Centre (WUR), Laboratory of Phytopathology, Droevendaalsesteeg 1, 6708 PB Wageningen, The Netherlands

*Corresponding author: p.crous@wi.knaw.nl

Key words:
biodiversity
Fusarium
multi-gene phylogeny
new taxa
systematics

Abstract: Soil fungi play a crucial role in soil quality and fertility in being able to break down organic matter but are frequently also observed to play a role as important plant pathogens. As part of a Citizen Science Project initiated by the Westerdijk Fungal Biodiversity Institute and the Utrecht University Museum, which aimed to describe novel fungal species from Dutch garden soil, the diversity of fusarioid fungi (*Fusarium* and other fusarioid genera), which are members of *Nectriaceae* (*Hypocreales*) was investigated. Preliminary analyses of ITS and LSU sequences from more than 4 750 isolates obtained indicated that 109 strains belong to this generic complex. Based on multi-locus phylogenies of combinations of *cmdA*, *tef1*, *rpb1*, *rpb2* and *tub2* alignments, and morphological characteristics, 25 species were identified, namely 22 in *Fusarium* and three in *Neocosmospora.* Furthermore, two species were described as new namely *F. vanleeuwenii* from the *Fusarium oxysporum* species complex (FOSC), and *F. wereldwijsianum* from the *Fusarium incarnatum-equiseti* species complex (FIESC). Other species encountered in this study include in the FOSC: *F. curvatum, F. nirenbergiae, F. oxysporum* and three undescribed *Fusarium* spp.; in the FIESC: *F. clavus, F. croceum, F. equiseti, F. flagelliforme* and *F. toxicum*; *Fusarium tricinctum* species complex: *F. flocciferum* and *F. torulosum*; the *Fusarium sambucinum* species complex: *F. culmorum* and *F. graminearum*; the *Fusarium redolens* species complex: *F. redolens*; and the *Fusarium fujikuroi* species complex: *F. verticillioides.* Three species of *Neocosmospora* were encountered, namely *N. solani*, *N. stercicola* and *N. tonkinensis.* Although soil fungal diversity has been well studied in the Netherlands, this study revealed two new species, and eight new records: *F. clavus, F. croceum, F. flagelliforme, F. odoratissimum, F. tardicrescens*, *F. toxicum, F. triseptatum* and *N. stercicola*.

Citation: Crous PW, Hernández-Restrepo M, van Iperen AL, Starink-Willemse M, Sandoval-Denis M, Groenewald JZ (2021). Citizen science project reveals novel fusarioid fungi (*Nectriaceae*, *Sordariomycetes*) from urban soils. *Fungal Systematics and Evolution* **8**: 101–127. doi: 10.3114/fuse.2021.08.09
Received: 13 August 2021; **Accepted:** 28 September 2021; **Effectively published online:** 12 October 2021
Corresponding editor: L. Cai

INTRODUCTION

Fusarium and allied fusarioid genera in *Nectriaceae* are highly diverse in morphology and ecology, and have a worldwide distribution, commonly occurring on plants and plant products, in air, water and soil. Macroconidia are typically borne in sporodochia, and taxa have in the past been identified as *Fusarium* if their macroconidia were curved, septate, had a pointed apex, and basal cell with a foot-like notch near the attachment point (Wollenweber & Reinking 1935, Snyder & Hansen 1940, Geiser *et al*. 2021). However, recent studies have shown that this morphology has evolved several times within *Sordariomycetes*, and that within *Nectriaceae* alone up to 20 genera share the fusarioid macromorphology. These genera are distinct phylogenetically and biologically, and have sexual morphs other than *Gibberella*, which is restricted to *Fusarium s. str*. (Gräfenhan *et al.* 2011, Rossman & Seifert 2011, Schroers *et al.* 2011, Rossman *et al*. 2013, Lombard *et al.* 2015, Sandoval-Denis *et al.* 2019, Crous *et al.* 2021a).

Species of fusarioid fungi can produce several different spore types, namely macro-, meso- and microconidia, ascospores and chlamydospores (Crous *et al.* 2021b). Chlamydospores can occur singly or in clusters, forming microsclerotia that have thick, pigmented, smooth to rough walls. They form in hyphae or conidia, either terminally or intercalary, and are the resting spores that make fusarioid taxa highly adapted to survive in soils for extended periods of time. In agricultural soils, chlamydospores commonly occur in plant debris of previous crops, awaiting fresh nutrients and favourable conditions to reactivate (Couteaudier & Alabouvette 1990).

The genus *Fusarium s. str*. contains 17 species complexes that correlate to different phylogenetic lineages (Crous *et al.* 2021b). Common soil-borne fusarioid fungi include the *Fusarium oxysporum* species complex (FOSC; Lombard *et al*. 2019) and species of *Neocosmospora* (formerly known as the *Fusarium solani* species complex; Sandoval-Denis *et al*. 2018, 2019). The FOSC contains many plant pathogenic taxa, several of which are host specific, which paved the way for "special forms" to be recognised as "*formae speciales*", and "races" to help distinguish them (Snyder & Hansen 1940). Such *formae speciales*, however, are frequently seen to represent distinct phylogenetic species

Fungal Systematics and Evolution is licensed under a Creative Commons Attribution-NonCommercial-ShareAlike 4.0 International License

© 2021 Westerdijk Fungal Biodiversity Institute

(Lombard *et al*. 2019, Maryani *et al.* 2019a, b). Despite this terminology being a dated approach to dealing with the diversity in *Fusarium*, plant pathologists still use it to help distinguish the diversity they encounter in the field, and more than 144 *f. spp.* have been named in the FOSC to date (Lombard *et al.* 2019), with additional subspecific classifications including haplotypes, races and vegetative compatibility groups also being used.

Species of *Fusarium* produce a range of trichothecenes (mycotoxins) in different ecological niches, that are of concern to animal and human health when such contaminated products are consumed (O'Donnell *et al.* 2018). These compounds are common throughout *Fusarium s*. *str*. and are observed in well-known plant pathogenic species such as *F. culmorum*, *F. graminearum*, *F. sporotrichioides* and *F. tricinctum* (Bamburg *et al.* 1968, Tatsuno *et al*. 1968, Yoshizawa & Morooka 1973, Jiménez *et al*. 1997), but again absent from species of *Neocosmospora* (Crous *et al.* 2021b). Because of the threat and great losses caused by soilborne fusarioid fungi in plant, human and animal health, it is imperative that we gain knowledge of the diversity of fusarioid fungi in soil to better understand their function and impact in different terrestrial ecosystems.

The present Citizen Science Project was initiated by the Westerdijk Fungal Biodiversity Institute (WI) and the Utrecht University Museum, aiming to investigate the diversity of fungi in Dutch garden soil collected by children in their home gardens and schoolgrounds from different regions in the Netherlands (Crous *et al.* 2017, 2018, 2021a; Groenewald *et al.* 2018, Giraldo *et al*. 2019, Hernández-Restrepo *et al.* 2020, Hou *et al*. 2020). During this project thousands of isolates were obtained from 404 soil samples. Of these, 109 isolates were found to represent fusarioid fungi, and selected for this study. The aim of the present study was to investigate the diversity of fusarioid fungi from Dutch garden soil, describe and illustrate novel species, and compare them with known taxa.

MATERIALS AND METHODS

Isolates

Soil samples collected from garden soils in the urban environment followed the methods of Groenewald *et al.* (2018) and Giraldo *et al*. (2019). Colonies were sub-cultured on 2 % potato-dextrose agar (PDA), oatmeal agar (OA), malt extract agar (MEA) (Crous *et al*. 2019b), synthetic nutrient-poor agar (SNA; Nirenberg 1976), carnation leaf agar (CLA; Fisher *et al*. 1982), and incubated at 25 °C under continuous near-ultraviolet light to promote sporulation. Reference strains and specimens of the studied fungi are maintained in the culture collection (CBS) of the Westerdijk Fungal Biodiversity Institute (WI), Utrecht, the Netherlands.

DNA extraction, amplification (PCR) and phylogeny

Protocols for genomic DNA isolation, PCR amplification of partial calmodulin (*cmdA*) gene, internal transcribed spacer regions with intervening 5.8S nrRNA gene (ITS), partial 28S nrRNA gene (LSU), DNA-directed RNA polymerase II largest (*rpb1*) and second largest subunit (*rpb2*) genes, and translation elongation factor 1-alpha (*tef1*) gene, and sequencing of the novel strains (Table 1) followed Crous *et al.* (2021b). The two parts of *rpb2* listed in Table 1 corresponded to the sequences generated using primer pairs RPB2-5f2 / fRPB2-7cR and fRPB2-7cf / RPB2-11ar (see Crous *et al.* (2021b) for primer details). Partial beta-tubulin (*tub2*) gene sequences were not generated during the course of this study.

Initial identifications to genus level were made using megablast searches (Zhang *et al*. 2000) of the ITS sequences against NCBI's GenBank nucleotide database, after which *tef1* sequences were used to further identify the *Fusarium* species complexes. Reference sequences (Supplementary Table S1) from Crous *et al.* (2021b) and based on megablast searches were then used to construct single-gene and multi-gene alignments for *Neocosmospora* and the different *Fusarium* species complexes. Phylogenetic analyses using RAxML Blackbox v. 1.0.0 (https://raxml-ng.vital-it.ch/#/; Kozlov *et al.* 2019), IQ-TREE v. 2.1.3 (Nguyen *et al*. 2015, Minh *et al*. 2020) and MrBayes v. 3.2.7 (Ronquist & Huelsenbeck 2003) followed Crous *et al.* (2021b), with the exception that trees were saved every 10 or 100 generations (Table 2). All resulting trees were printed with Geneious v. 11.1.5 and the layout of the trees was done in Adobe Illustrator v. CC 2018.

Morphology

Slide preparations were mounted in water, from colonies sporulating on CLA, following the protocols described by Crous *et al*. (2021b). Observations were made with a Nikon SMZ25 dissection-microscope, and with a Zeiss Axio Imager 2 light microscope using differential interference contrast (DIC) illumination and images recorded on a Nikon DS-Ri2 camera with associated software. Colony characters and pigment production were noted after 7 d of growth on MEA, PDA and OA incubated at 25 °C. Colony colours (surface and reverse) were scored using the colour charts of Rayner (1970).

RESULTS

Phylogeny

Six multigene alignments were generated in the present study and subjected to the three phylogenetic analyses described above. Statistical values for the alignments and phylogenetic trees are summarised in Table 2. Sequences derived in this study were deposited in GenBank (Table 1), the alignments in TreeBASE (www.treebase.org; study number 28680), and taxonomic novelties in MycoBank (www.MycoBank.org; Crous *et al*. 2004).

Fusarium citricola and *F. tricinctum* species complexes (Fig. 1): Novel isolates from Dutch soils clustered with three known species, namely *F. acuminatum*, *F. flocciferum* and *F. torulosum* (all three in the *F. tricinctum* species complex). The three phylogenetic analyses (RAxML, IQ-TREE, and MrBayes) overall displayed the same species clades and mainly differed with regards to the backbone relationships between species clades/lineages [data not shown, trees available in TreeBASE and support and posterior probability (PP) values are superimposed on the presented figure]. The loci *cmdA* and *rpb1* are not well-represented in the dataset, with roughly half of the strains having a sequence present (Tables 1, 2, Supplementary Table S1).

Fusarium incarnatum-equiseti species complex (Fig. 2): Novel isolates from Dutch soils clustered with five known species, namely *F. clavus*, *F. croceum*, *F. equiseti*, *F. flagelliforme* and *F. toxicum*, as

© 2021 Westerdijk Fungal Biodiversity Institute

Table 1. Collection details and GenBank accession numbers of isolates treated in this study, and associated ex-type strains where applicable. Species names in bold highlight taxonomic novelties. The ITS and LSU sequences were not used in analyses but are provided for completeness.

Species complex and Species	Culture or working collection number(s)	Country and Substrate	Collector(s) and Collection date	School or educational institution	GenBank accession number(s)[1]						
					tef1	*rpb2* part 1	*rpb2* part 2	*cmdA*	*rpb1*	ITS	LSU
Fusarium fujikuroi species complex											
Fusarium verticillioides	JW 145017	Netherlands: Soil	A.E. Jansen; 2017	–	MZ921825	MZ921693	–	MZ921513	MZ921624	–	MZ890483
Fusarium incarnatum-equiseti species complex											
Fusarium clavus	JW 288002	Netherlands: Soil	Group 8, OBS de Toonladder; 2017	–	MZ921826	MZ921694	–	MZ921514	MZ921625	–	MZ890484
	NL19-041003	Netherlands: Soil	L. Oegema, R. van Stee & D. Kwast; 2019	RSG Simon Vestdijk	MZ921827	MZ921695	–	MZ921515	–	MZ890340	MZ890485
	NL19-048011	Netherlands: Soil	S. Goinga & J. de Groot; 10 Oct. 2019	RSG Simon Vestdijk	MZ921828	MZ921696	–	MZ921516	–	MZ890341	MZ890486
	NL19-056012	Netherlands: Soil	S. Verhage, S. Moens & K. Basting; 29 Oct. 2019	Zwin college	MZ921829	MZ921697	–	MZ921517	–	MZ890342	MZ890487
	NL19-056013	Netherlands: Soil	S. Verhage, S. Moens & K. Basting; 29 Oct. 2019	Zwin college	MZ921830	MZ921698	–	MZ921518	–	MZ890343	MZ890488
Fusarium croceum	NL19-059006	Netherlands: Soil	A. van Strien, I. Beemsterboer & S. Groosman; 23 Oct. 2019	Zwin college	MZ921831	MZ921699	–	MZ921519	–	MZ890344	MZ890489
	NL19-060011	Netherlands: Soil	T. Vercruisse; 27 Oct. 2019	Zwin college	MZ921832	MZ921700	–	MZ921520	–	MZ890345	MZ890490
Fusarium equiseti	CBS 148218 = NL19-25004	Netherlands: Soil	C. Dijkstra & L. Kruit; 6 Jun. 2019	Het Hogeland College Warffum	MZ921833	MZ921701	–	MZ921521	–	MZ890346	MZ890491
	CBS 148383 = NL19-008004	Netherlands: Soil	S. de Boer; 17 Dec. 2019	GSG 't Schylger Jouw	MZ921834	MZ921702	–	MZ921522	–	MZ890347	MZ890492
	NL19-045005	Netherlands: Soil	E.-A. Duinstra, R. Jagersma & M. Postmus; 9 Oct. 2019	RSG Simon Vestdijk	MZ921835	MZ921703	–	MZ921523	MZ921626	MZ890348	MZ890493
	NL19-047003	Netherlands: Soil	S. Kuiper, N. Zijlstra & E. Schot; 10 Oct. 2019	RSG Simon Vestdijk	MZ921836	MZ921704	–	MZ921524	MZ921627	MZ890349	–
	NL19-059004	Netherlands: Soil	A. van Strien, I. Beemsterboer & S. Groosman; 23 Oct. 2019	Zwin college	MZ921837	MZ921705	–	MZ921525	–	MZ890350	MZ890494
	NL19-97009	Netherlands: Soil	S. Frederikze, J. Mes & S. El Maghnouji; 31 Jul. 2019	ACB Wereldwijs	MZ921838	MZ921706	–	MZ921526	MZ921628	MZ890351	MZ890495
Fusarium flagelliforme	NL19-041004	Netherlands: Soil	L. Oegema, R. van Stee & D. Kwast; 2019	RSG Simon Vestdijk	MZ921839	MZ921707	–	MZ921527	MZ921629	MZ890352	MZ890496

Table 1. (Continued).

Species complex and Species	Culture or working collection number(s)	Country and Substrate	Collector(s) and Collection date	School or educational institution	GenBank accession number(s)[1]						
					tef1	*rpb2* part 1	*rpb2* part 2	*cmdA*	*rpb1*	ITS	LSU
	NL19-047004	Netherlands: Soil	S. Kuiper, N. Zijlstra & E. Schot; 10 Oct. 2019	RSG Simon Vestdijk	MZ921840	MZ921708	–	MZ921528	–	MZ890353	MZ890497
	NL19-050003	Netherlands: Soil	T. van der Schoot & J. Koel; 10 Oct. 2019	RSG Simon Vestdijk	MZ921841	MZ921709	–	MZ921529	–	MZ890354	MZ890498
	NL19-052002	Netherlands: Soil	M. Stellemans, L. de Winde & N. Quist; 21 Oct. 2019	Zwin college	MZ921842	MZ921710	–	MZ921530	–	MZ890355	MZ890499
	NL19-068002	Netherlands: Soil	S. Walraven & M. Bekooy; 28 Oct. 2019	Zwin college	MZ921843	MZ921711	–	MZ921531	–	MZ890356	MZ890500
	NL19-97010	Netherlands: Soil	S. Frederikze, J. Mes & S. El Maghnouji; 31 Jul. 2019	ACB Wereldwijs	MZ921844	MZ921712	–	MZ921532	MZ921630	MZ890357	MZ890501
Fusarium toxicum	NL19-041005	Netherlands: Soil	L. Oegema, R. van Stee & D. Kwast; 2019	RSG Simon Vestdijk	MZ921845	MZ921713	–	MZ921533	MZ921631	MZ890358	MZ890502
	NL19-041006	Netherlands: Soil	L. Oegema, R. van Stee & D. Kwast; 2019	RSG Simon Vestdijk	MZ921846	MZ921714	–	MZ921534	MZ921632	MZ890359	MZ890503
	NL19-050001	Netherlands: Soil	T. van der Schoot & J. Koel; 10 Oct. 2019	RSG Simon Vestdijk	MZ921847	MZ921715	–	MZ921535	MZ921633	MZ890360	MZ890504
Fusarium wereldwijsianum sp. nov.	CBS 148219 = NL19-99002	Netherlands: Soil	S. Frederikze, J. Mes & S. El Maghnouji; 31 Jul. 2019	ACB Wereldwijs	MZ921848	MZ921716	–	MZ921536	MZ921634	MZ890361	MZ890505
	CBS 148220 = NL19-99003	Netherlands: Soil	S. Frederikze, J. Mes & S. El Maghnouji; 31 Jul. 2019	ACB Wereldwijs	MZ921849	MZ921717	–	MZ921537	MZ921635	MZ890362	MZ890506
	CBS 148244 = NL19-94009, ex-type	Netherlands: Soil	S. Frederikze, J. Mes & S. El Maghnouji; 31 Jul. 2019	ACB Wereldwijs	MZ921850	MZ921718	–	MZ921538	MZ921636	MZ890363	MZ890507
	CBS 148385 = NL19-057012	Netherlands: Soil	F. Guilliet, T. Bron & I. Geernaert; Oct. 2019	Zwin college	MZ921851	MZ921719	–	MZ921539	–	MZ890364	MZ890508
	CBS 148386 = NL19-059003	Netherlands: Soil	A. van Strien, I. Beemsterboer & S. Groosman; 23 Oct. 2019	Zwin college	MZ921852	MZ921720	–	MZ921540	–	MZ890365	MZ890509
Fusarium oxysporum species complex											
Fusarium curvatum	JW 39001	Netherlands: Soil	R. Ramanand; 2017	–	MZ921853	MZ921721	–	MZ921541	–	MZ890366	MZ890510
Fusarium nirenbergiae	CBS 148373 = JW 5042	Netherlands: Soil	F. & R. Niemeijer; 2017	–	MZ921867	MZ921735	–	MZ921555	MZ921646	MZ890378	MZ890522
	CBS 148379 = JW 124027	Netherlands: Soil	S. Vermeulen; 2017	–	MZ921868	MZ921736	–	MZ921556	MZ921647	–	MZ890523
	CBS 148381 = JW 288013	Netherlands: Soil	Group 8, OBS de Toonladder; 2017	–	MZ921870	MZ921738	–	MZ921558	–	–	MZ890525

© 2021 Westerdijk Fungal Biodiversity Institute

Table 1. (Continued).

Species complex and Species	Culture or working collection number(s)	Country and Substrate	Collector(s) and Collection date	School or educational institution	GenBank accession number(s)[1]						
					tef1	*rpb2* part 1	*rpb2* part 2	*cmdA*	*rpb1*	ITS	LSU
	CBS 148382 = JW 289011	Netherlands: Soil	KMN Spelerij; 2017	–	MZ921871	MZ921739	–	MZ921559	–	–	MZ890526
	CBS 148384 = NL19-048010	Netherlands: Soil	S. Goinga & J. de Groot; 10 Oct. 2019	RSG Simon Vestdijk	MZ921873	MZ921741	–	MZ921561	–	MZ890381	MZ890528
	CBS 148387 = NL19-100010	Netherlands: Soil	S. Frederikze, J. Mes & S. El Maghnouji; 31 Jul. 2019	ACB Wereldwijs	MZ921875	MZ921744	–	MZ921564	–	MZ890384	MZ890531
	CBS 148388 = BE19-004016	Belgium: Soil	T. Antheunis; 2019	Viso Cor Mariae	MZ921866	MZ921734	–	MZ921554	–	MZ890377	MZ890521
	JW 192006	Netherlands: Soil	L. Borsboom; 2017	–	MZ921869	MZ921737	–	MZ921557	–	MZ890379	MZ890524
	NL19-045004	Netherlands: Soil	E.-A. Duinstra, R. Jagersma & M. Postmus; 9 Oct. 2019	RSG Simon Vestdijk	MZ921872	MZ921740	–	MZ921560	MZ921648	MZ890380	MZ890527
	NL19-053002	Netherlands: Soil	L. van Eetveldt, G. Jones & F. Walraven; 25 Oct. 2019	Zwin college	MZ921874	MZ921742	–	MZ921562	–	MZ890382	MZ890529
	NL19-053003	Netherlands: Soil	L. van Eetveldt, G. Jones & F. Walraven; 25 Oct. 2019	Zwin college	–	MZ921743	–	MZ921563	MZ921649	MZ890383	MZ890530
	NL19-28011	Netherlands: Soil	H. Meertens & D. Zaagman; 6 Jun. 2019	Het Hogeland College Warffum	MZ921876	MZ921745	–	MZ921565	MZ921650	MZ890385	MZ890532
	NL19-91009	Netherlands: Soil	S. Frederikze, J. Mes & S. El Maghnouji; 31 Jul. 2019	ACB Wereldwijs	MZ921877	MZ921746	–	MZ921566	MZ921651	MZ890386	MZ890533
	NL19-91010	Netherlands: Soil	S. Frederikze, J. Mes & S. El Maghnouji; 31 Jul. 2019	ACB Wereldwijs	MZ921878	MZ921747	–	MZ921567	MZ921652	MZ890387	MZ890534
	NL19-99011	Netherlands: Soil	S. Frederikze, J. Mes & S. El Maghnouji; 31 Jul. 2019	ACB Wereldwijs	MZ921879	MZ921748	–	MZ921568	MZ921653	MZ890388	MZ890535
Fusarium odoratissimum	JW 54001	Netherlands: Soil	I., M. & L. Zoert; 2017	–	MZ921880	MZ921749	–	MZ921569	MZ921654	–	–
Fusarium oxysporum	JW 11005	Netherlands: Soil	M. Francisca; 2017	–	MZ921881	MZ921750	–	MZ921570	MZ921655	MZ890389	MZ890536
	JW 231014	Netherlands: Soil	D. Pol, R. Verf, J. Wilks & M. de Ruiter; 2017	–	MZ921882	MZ921751	–	MZ921571	MZ921656	MZ890390	–
	JW 257006	Netherlands: Soil	KSU de Achtbaan; 2017	–	MZ921883	MZ921752	–	MZ921572	MZ921657	–	MZ890537
	NL19-94002	Netherlands: Soil	S. Frederikze, J. Mes & S. El Maghnouji; 31 Jul. 2019	ACB Wereldwijs	MZ921884	MZ921753	–	MZ921573	MZ921658	MZ890391	MZ890538
	NL19-94008	Netherlands: Soil	S. Frederikze, J. Mes & S. El Maghnouji; 31 Jul. 2019	ACB Wereldwijs	MZ921885	MZ921754	–	MZ921574	MZ921659	MZ890392	MZ890539

Table 1. (Continued).

Species complex and Species	Culture or working collection number(s)	Country and Substrate	Collector(s) and Collection date	School or educational institution	GenBank accession number(s)[1]						
					tef1	*rpb2* part 1	*rpb2* part 2	*cmdA*	*rpb1*	ITS	LSU
Fusarium sp. 1	CBS 148204 = JW 191014	Netherlands: Soil	T. & K. Wesselink; 2017	–	MZ921858	MZ921726	–	MZ921546	MZ921641	MZ890371	MZ890514
	CBS 148216 = JW 53002	Netherlands: Soil	K. Brennand; 2017	–	MZ921863	MZ921731	–	MZ921551	MZ921645	–	–
	CBS 148217 = NL19-25001	Netherlands: Soil	C. Dijkstra & L. Kruit; 6 Jun. 2019	Het Hogeland College Warffum	MZ921864	MZ921732	–	MZ921552	–	MZ890375	MZ890519
Fusarium sp. 2	CBS 130323 = NRRL 26677	Australia: Subungual debris of 40-year-old female with nail infection	Unknown	–	MH485018	MH484927	–	MH484745	–	–	–
	CBS 148185 = JW 1072	Netherlands: Soil	J. van Dijk; 2017	–	MZ921854	MZ921722	–	MZ921542	MZ921637	MZ890367	MZ890511
	CBS 128.81 = BBA 63925 = NRRL 36233	USA: *Chrysanthemum* sp.	Unknown		MH484975	MH484884	–	MH484702	–	–	–
	CBS 680.89 = IPO 11179 = NRRL 26221	Netherlands: *Cucumis sativus*, in greenhouse on rockwool	N. Hubbeling; –	–	MH484980	MH484889	–	MH484707	–	–	–
Fusarium sp. 3	CBS 148198 = JW 4030	Netherlands: Soil	F. Wiegerinck; 2017	–	MZ921855	MZ921723	–	MZ921543	MZ921638	MZ890368	MZ890512
	CBS 148199 = JW 9002	Netherlands: Soil	A.-S. den Boer; 2017	–	MZ921856	MZ921724	–	MZ921544	MZ921639	MZ890369	MZ890513
	CBS 148200 = JW 10005	Netherlands: Soil	M.J. van Leeuwen; 2017	–	MZ921857	MZ921725	–	MZ921545	MZ921640	MZ890370	–
	CBS 148205 = JW 204009	Netherlands: Soil	I. Kleij; 2017	–	MZ921859	MZ921727	–	MZ921547	MZ921642	–	MZ890515
	CBS 148206 = JW 210014	Netherlands: Soil	N. Keij; 2017	–	MZ921860	MZ921728	–	MZ921548	MZ921643	MZ890372	MZ890516
	CBS 148207 = JW 210019	Netherlands: Soil	N. Keij; 2017	–	MZ921861	MZ921729	–	MZ921549	MZ921644	MZ890373	MZ890517
	CBS 148208 = JW 231016	Netherlands: Soil	D. Pol, R. Verf, J. Wilks & M. de Ruiter; 2017	–	MZ921862	MZ921730	–	MZ921550	–	MZ890374	MZ890518
	CBS 148222 = BE19-004006	Belgium: Soil	T. Antheunis; 2019	Viso Cor Mariae	MZ921865	MZ921733	–	MZ921553	–	MZ890376	MZ890520
Fusarium tardicrescens	JW 6021	Netherlands: Soil	H.W. Vos; 2017	–	MZ921886	MZ921755	–	MZ921575	MZ921660	MZ890393	MZ890540
	JW 6043	Netherlands: Soil	H.W. Vos; 2017	–	MZ921887	MZ921756	–	MZ921576	MZ921661	MZ890394	–
Fusarium triseptatum	CBS 148380 = JW 277008	Netherlands: Soil	Lukasschool; 2017	–	MZ921888	MZ921757	–	MZ921577	MZ921662	–	MZ890541
	JW 277009	Netherlands: Soil	Lukasschool; 2017	–	MZ921889	MZ921758	–	MZ921578	–	–	MZ890542

© 2021 Westerdijk Fungal Biodiversity Institute

Table 1. (Continued).

Species complex and Species	Culture or working collection number(s)	Country and Substrate	Collector(s) and Collection date	School or educational institution	GenBank accession number(s)[1]						
					tef1	*rpb2* part 1	*rpb2* part 2	*cmdA*	*rpb1*	ITS	LSU
Fusarium vanleeuwenii sp. nov.	CBS 148372 = JW 10008, ex-type	Netherlands: Soil	M.J. van Leeuwen; 2017	–	MZ921896	MZ921765	–	MZ921585	MZ921669	MZ890401	–
	CBS 148374 = JW 10001	Netherlands: Soil	M.J. van Leeuwen; 2017	–	MZ921890	MZ921759	–	MZ921579	MZ921663	MZ890395	MZ890543
	CBS 148375 = JW 10003	Netherlands: Soil	M.J. van Leeuwen; 2017	–	MZ921892	MZ921761	–	MZ921581	MZ921665	MZ890397	–
	CBS 148376 = JW 10004	Netherlands: Soil	M.J. van Leeuwen; 2017	–	MZ921893	MZ921762	–	MZ921582	MZ921666	MZ890398	–
	CBS 148377 = JW 10006	Netherlands: Soil	M.J. van Leeuwen; 2017	–	MZ921894	MZ921763	–	MZ921583	MZ921667	MZ890399	–
	CBS 148378 = JW 10007	Netherlands: Soil	M.J. van Leeuwen; 2017	–	MZ921895	MZ921764	–	MZ921584	MZ921668	MZ890400	–
	JW 10002	Netherlands: Soil	M.J. van Leeuwen; 2017	–	MZ921891	MZ921760	–	MZ921580	MZ921664	MZ890396	MZ890544
	JW 10009	Netherlands: Soil	M.J. van Leeuwen; 2017	–	MZ921897	MZ921766	–	MZ921586	MZ921670	MZ890402	–
Fusarium redolens species complex											
Fusarium redolens	NL19-003007	Netherlands: Soil	B. Wulp; 17 Dec. 2019	GSG 't Schylger Jouw	MZ921898	MZ921767		–	MZ921671	MZ890403	MZ890545
Fusarium sambucinum species complex											
Fusarium culmorum	BE19-002002	Belgium: Soil	S. Vanopbroeke; 2019	Viso Cor Mariae	MZ921899	MZ921768	MZ921802	MZ921587	–	MZ890404	MZ890546
	BE19-009002	Belgium: Soil	N. Caen; 2019	Viso Cor Mariae	MZ921900	MZ921769	MZ921803	MZ921588	–	MZ890405	MZ890547
	NL19-047005	Netherlands: Soil	S. Kuiper, N. Zijlstra & E. Schot; 10 Oct. 2019	RSG Simon Vestdijk	MZ921901	MZ921770	MZ921804	MZ921589	–	MZ890406	MZ890548
	NL19-060003	Netherlands: Soil	T. Vercruisse; 27 Oct. 2019	Zwin college	MZ921902	MZ921771	MZ921805	MZ921590	–	MZ890407	MZ890549
	NL19-076001	Netherlands: Soil	W. Vercouteren, S. Meas & R. Verhije; 6 Nov. 2019	Zwin college	MZ921903	MZ921772	MZ921806	MZ921591	–	MZ890408	MZ890550
	NL19-25005	Netherlands: Soil	C. Dijkstra & L. Kruit; 6 Jun. 2019	Het Hogeland College Warffum	MZ921904	MZ921773	MZ921807	–	–	MZ890409	MZ890551
	NL19-93013	Netherlands: Soil	S. Frederikze, J. Mes & S. El Maghnouji; 31 Jul. 2019	ACB Wereldwijs	MZ921905	MZ921774	MZ921808	MZ921592	MZ921672	MZ890410	MZ890552
Fusarium graminearum	NL19-100008	Netherlands: Soil	S. Frederikze, J. Mes & S. El Maghnouji; 31 Jul. 2019	ACB Wereldwijs	MZ921906	MZ921775	MZ921809	MZ921593	MZ921673	MZ890411	MZ890553

© 2021 Westerdijk Fungal Biodiversity Institute

Table 1. (Continued).

Species complex and Species	Culture or working collection number(s)	Country and Substrate	Collector(s) and Collection date	School or educational institution	GenBank accession number(s)[1]						
					tef1	*rpb2* part 1	*rpb2* part 2	*cmdA*	*rpb1*	ITS	LSU
Fusarium tricinctum species complex											
Fusarium acuminatum	JW 288021	Netherlands: Soil	Group 8, OBS de Toonladder; 2017	–	MZ921907	MZ921776	MZ921810	MZ921594	MZ921674	–	MZ890554
	JW 289003	Netherlands: Soil	KMN Spelerij; 2017	–	MZ921908	MZ921777	MZ921811	MZ921595	MZ921675	–	MZ890555
	NL19-048014	Netherlands: Soil	S. Goinga & J. de Groot; 10 Oct. 2019	RSG Simon Vestdijk	MZ921909	MZ921778	MZ921812	MZ921596	–	MZ890412	MZ890556
	NL19-077002	Netherlands: Soil	R. van der Wel & T. Wolfret; 5 Nov. 2019	Zwin college	MZ921910	MZ921779	MZ921813	MZ921597	–	MZ890413	MZ890557
Fusarium flocciferum	CBS 143231 = JW 14004	Netherlands: Soil	D. Peters; 2017	–	MG386159	MG386149	MG386149	MZ921598	MG386138	MG386078	MG386131
	CBS 143667 = JW 14005, ex-type of *F. petersiae*	Netherlands: Soil	D. Peters; 2017	–	MG386160	MG386150	MG386150	MZ921599	MG386139	MG386079	MG386132
	CBS 147837 = NL19-100011	Netherlands: Soil	S. Frederikze, J. Mes & S. El Maghnouji; 31 Jul. 2019	ACB Wereldwijs	–	MZ921780	MZ921814	MZ921600	–	MZ890416	MZ890558
	CBS 821.68 = NRRL 28450, ex-epitype	Germany: Greenhouse soil	D. Bredemeier; 1966	–	MW928837	MW928824	MW928824	–	MW928807	–	–
	JW 5026	Netherlands: Soil	F. & R. Niemeijer; 2017	–	MZ921911	MZ921781	MZ921815	MZ921601	MZ921676	MZ890417	MZ890559
	JW 18005	Netherlands: Soil	W. van der Heijden; 2017	–	MZ921912	MZ921782	MZ921816	MZ921602	MZ921677	MZ890418	–
	JW 248008	Netherlands: Soil	J.-W. Koolen; 2017	–	MZ921913	MZ921783	MZ921817	MZ921603	MZ921678	MZ890419	MZ890560
	JW 267001	Netherlands: Soil	Basisschool de Baanbreker; 2017	–	MZ921914	MZ921784	MZ921818	MZ921604	–	–	MZ890561
	NL19-048012	Netherlands: Soil	S. Goinga & J. de Groot; 10 Oct. 2019	RSG Simon Vestdijk	MZ921915	MZ921785	MZ921819	MZ921605	–	MZ890420	MZ890562
	NL19-048013	Netherlands: Soil	S. Goinga & J. de Groot; 10 Oct. 2019	RSG Simon Vestdijk	MZ921916	MZ921786	MZ921820	MZ921606	–	MZ890421	MZ890563
	NL19-97008	Netherlands: Soil	S. Frederikze, J. Mes & S. El Maghnouji; 31 Jul. 2019	ACB Wereldwijs	MZ921917	MZ921787	MZ921821	MZ921607	MZ921679	MZ890422	MZ890564
Fusarium torulosum	JW 24001	Netherlands: Soil	J. van der Stel; 2017	–	MZ921918	MZ921788	MZ921822	MZ921608	MZ921680	MZ890423	MZ890565
Neocosmospora											
Neocosmospora solani	JW 1075	Netherlands: Soil	J. van Dijk; 2017	–	MZ921919	MZ921789	–	MZ921609	MZ921681	MZ890424	MZ890566
	JW 14011	Netherlands: Soil	D. Peters; 2017	–	MZ921920	MZ921790	–	MZ921610	–	MZ890425	MZ890567
	JW 191039	Netherlands: Soil	T. & K. Wesselink; 2017	–	MZ921921	MZ921791	–	MZ921611	MZ921682	MZ890426	MZ890568

© 2021 Westerdijk Fungal Biodiversity Institute

Table 1. (Continued).

Species complex and Species	Culture or working collection number(s)	Country and Substrate	Collector(s) and Collection date	School or educational institution	GenBank accession number(s)[1]						
					tef1	*rpb2* part 1	*rpb2* part 2	*cmdA*	*rpb1*	ITS	LSU
	JW 232018	Netherlands: Soil	M. van Meijl; 2017	–	MZ921922	MZ921792	–	MZ921612	–	MZ890427	MZ890569
	JW 288011	Netherlands: Soil	Group 8, OBS de Toonladder; 2017	–	MZ921923	MZ921793	–	MZ921613	MZ921683	–	MZ890570
Neocosmospora stercicola	JW 1093	Netherlands: Soil	J. van Dijk; 2017	–	MZ921924	MZ921794	–	MZ921614	MZ921684	MZ890428	MZ890571
	JW 75001	Netherlands: Soil	O. Terpstra; 2017	–	MZ921925	MZ921795	–	MZ921615	MZ921685	MZ890429	MZ890572
	JW 235004	Netherlands: Soil	T. Tuinier; 2017	–	MZ921926	MZ921796	–	MZ921616	MZ921686	MZ890430	MZ890573
	JW 235009	Netherlands: Soil	T. Tuinier; 2017	–	MZ921927	MZ921797	–	MZ921617	MZ921687	MZ890431	MZ890574
Neocosmospora tonkinensis	JW 234010	Netherlands: Soil	T. Vanmeulebrouk; 2017	–	MZ921928	MZ921798	–	MZ921618	MZ921688	–	MZ890575
	JW 236012	Netherlands: Soil	A. Vanmeulebrouk; 2017	–	–	MZ921799	–	MZ921619	–	–	MZ890576

[1] *cmdA*: partial calmodulin gene; ITS: internal transcribed spacer regions with intervening 5.8S nrRNA gene; *rpb1*: partial DNA-directed RNA polymerase II largest subunit gene; *rpb2*: partial DNA-directed RNA polymerase II second largest subunit gene; *tef1*: partial translation elongation factor 1-alpha gene; *tub2*: partial beta-tubulin gene.

Table 2. Summary of phylogenetic information for the different analyses in this study[1].

Analysis	Locus[2]	Number of strains (incl. outgroup)	Length incl. gaps	BI unique site patterns	Model (AIC)	Model (BIC)	BI sample frequency	Number of sampled trees (BI)	ML -lnL (R)	ML -lnL (IQ-TREE)
Fusarium citricola & *F. tricinctum* species complexes	*cmdA*	23	669	118	SYM+G	K2P+G4	–	–	–	-1717.014
	rpb1	27	1 787	370	GTR+I	TNe+G4	–	–	–	-4717.229
	rpb2 (part 1)	42	910	226	SYM+G	TNe+G4	–	–	–	-2795.892
	rpb2 (part 2)	34	628	104	GTR+G	TNe+G4	–	–	–	-1747.846
	tef1	41	756	256	GTR+I	TIM2e+G4	–	–	–	-2469.915
	Combined	45	4 750	1 074	–	–	10	78 002	-13596.815643	-13617.725
Fusarium incarnatum-equiseti species complex	*cmdA*	72	661	157	SYM+G	TNe+R3	–	–	–	-2121.606
	rpb1	29	1 729	226	SYM+I	TNe+R2	–	–		-4384.505
	rpb2 (part 1)	73	886	174	GTR+I	TNe+G4	–	–		-2770.072
	tef1	73	743	262	GTR+G	TNe+R3	–	–		-3166.37
	Combined	73	4 019	819	–	–	10	1 285 502	-13545.426546	-13066.849

© 2021 Westerdijk Fungal Biodiversity Institute

Table 2. (Continued).

Analysis	Locus[2]	Number of strains (incl. outgroup)	Length incl. gaps	BI unique site patterns	Model (AIC)	Model (BIC)	BI sample frequency	Number of sampled trees (BI)	ML -lnL (R)	ML -lnL (IQ-TREE)
Fusarium oxysporum species complex	*cmdA*	117	608	53	K80	K2P	–	–	–	-1074.196
	rpb1	73	1451	216	SYM+I+G	TNe+R2	–	–	–	-3381.188
	rpb2 (part 1)	154	882	111	HKY+G	K2P+I	–	–	–	-2070.032
	tef1	154	584	158	HKY+G	TNe+G4	–	–	–	-1733.616
	tub2	74	577	141	SYM+G	TIMe+R2	–	–	–	-1812.746
	Combined	155	4 102	679	–	–	100	80 178	-10424.792230	-10.414.344
Fusarium redolens & F. fujikuroi species complexes	*cmdA*	17	690	149	SYM+I	TIM3e+G4	–	–	–	-1842.997
	rpb1	29	1 788	329	SYM+I	TNe+G4	–	–	–	-5168.810
	rpb2 (part 1)	34	904	297	SYM+I+G	TIM2e+I+G4	–	–	–	-4009.430
	tef1	33	763	323	GTR+G	TIM2e+G4	–	–	–	-3494.236
	Combined	34	4 145	1 098	–	–	10	64 502	-15323.869379	-15336.259
Fusarium sambucinum species complex	*cmdA*	14	661	71	SYM	TNe+I	–	–	–	-1499.250
	rpb1	33	1 793	240	SYM+I	TNe+G4	–	–	–	-4257.654
	rpb2 (part 1)	38	905	212	SYM+G	TIM2e+I	–	–	–	-2940.257
	rpb2 (part 2)	38	629	133	GTR+G	TNe+I	–	–	–	-2089.607
	tef1	38	755	197	GTR+G	TIM2e+R2	–	–	–	-2285.191
	Combined	39	4 743	853	–	–	10	30 752	-13596.206653	-13604.873
Neocosmospora	*cmdA*	42	674	221	SYM+I+G	K2P+G4	–	–	–	-2585.283
	rpb1	42	1 687	524	GTR+I+G	TIM3e+I+G4	–	–	–	-6296.579
	rpb2 (part 1)	69	866	241	SYM+G	TNe+G4	–	–	–	-2990.034
	tef1	76	752	300	GTR+G	TN+F+G4	–	–	–	-3000.621
	Combined	77	3 979	1 286	–	–	10	859 502	-15410.126704	-15411.266

[1] BI: Bayesian inference; Model (AIC): Evolutionary model selected by MrModeltest under the Akaike Information Criterion; Model (BIC): Evolutionary model selected by ModelFinder in IQ-TREE; BI sample frequency: Number of nth generations sampled; ML -lnL (R): Log-likelihood of final tree in RAxML; ML -lnL(IQ-TREE): Log-likelihood of consensus tree in IQ-TREE.

[2] *cmdA*: partial calmodulin gene, *tef1*: partial translation elongation factor 1-alpha gene; *rpb1*: partial DNA-directed RNA polymerase II largest subunit gene; *rpb2*: partial DNA-directed RNA polymerase II second largest subunit gene; *tub2*: partial beta-tubulin gene.

© 2021 Westerdijk Fungal Biodiversity Institute

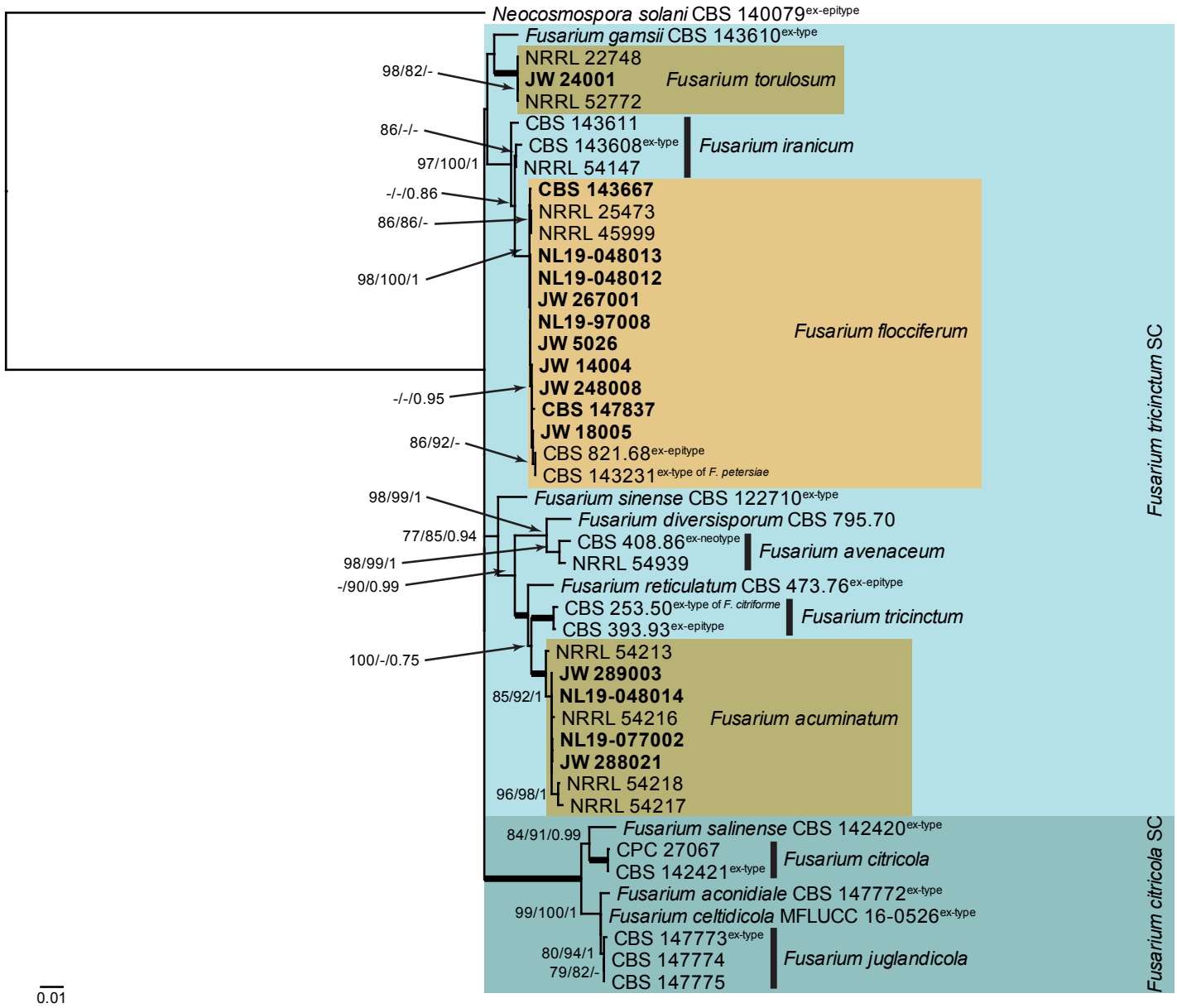

Fig 1. The RAxML consensus tree inferred from the combined *F. citricola*/*tricinctum* species complexes *tef1*, *rpb2* (parts 1 and 2), *rpb1* and *cmdA* sequence alignment. Thickened lines indicate branches with full support (RAxML & IQ-TREE bootstrap = 100 %; PP = 1.0) with support values of other branches indicated at the branches (RAxML > 74 % / IQ-TREE > 84 % / PP > 0.74). The tree is rooted to *Neocosmospora solani* (CBS 140079, ex-epitype culture). The scale bar indicates the number of expected changes per site. Species complexes are indicated on the right and highlighted with coloured blocks. Species clades containing the novel citizen science strains (in bold) are highlighted with coloured blocks.

well as a species clade not associated with any known species. The three phylogenetic analyses (RAxML, IQ-TREE and MrBayes) overall displayed the same species clades and mainly differed with regards to the backbone relationships between species clades/lineages (data not shown, trees available in TreeBASE and support and PP values are superimposed on the presented figure). The locus *rpb1* is not well-represented in the dataset, with less than half of the strains having a sequence present (Tables 1, 2, Supplementary Table S1).

Fusarium oxysporum species complex (Fig. 3): Novel isolates from Dutch soils clustered with six known species, namely *F. curvatum*, *F. nirenbergiae*, *F. odoratissimum*, *F. oxysporum* and *F. triseptatum*, as well as four species clades not associated with any known species. The three phylogenetic analyses (RAxML, IQ-TREE and MrBayes) overall displayed the same species clades and mainly differed with regards to the backbone relationships between species clades/lineages (data not shown, trees available in TreeBASE and support and PP values are superimposed on the presented figure). The loci *rpb1* and *tub2* are not well-represented in the dataset, with roughly half of the strains having a sequence present (Tables 1, 2, Supplementary Table S1).

Fusarium fujikuroi and *F. redolens* species complexes (Fig. 4): Novel isolates from Dutch soils clustered with two known species, namely *F. redolens* (*F. redolens* species complex) and *F. verticillioides* (*F. fujikuroi* species complex). The three phylogenetic analyses (RAxML, IQ-TREE and MrBayes) had the same overall topology and same species clades/lineages (data not shown, trees available in TreeBASE and support and PP values are superimposed on the presented figure). The locus *cmdA* is not well-represented in the dataset, with roughly half of the strains having a sequence present (Tables 1, 2, Supplementary Table S1).

© 2021 Westerdijk Fungal Biodiversity Institute

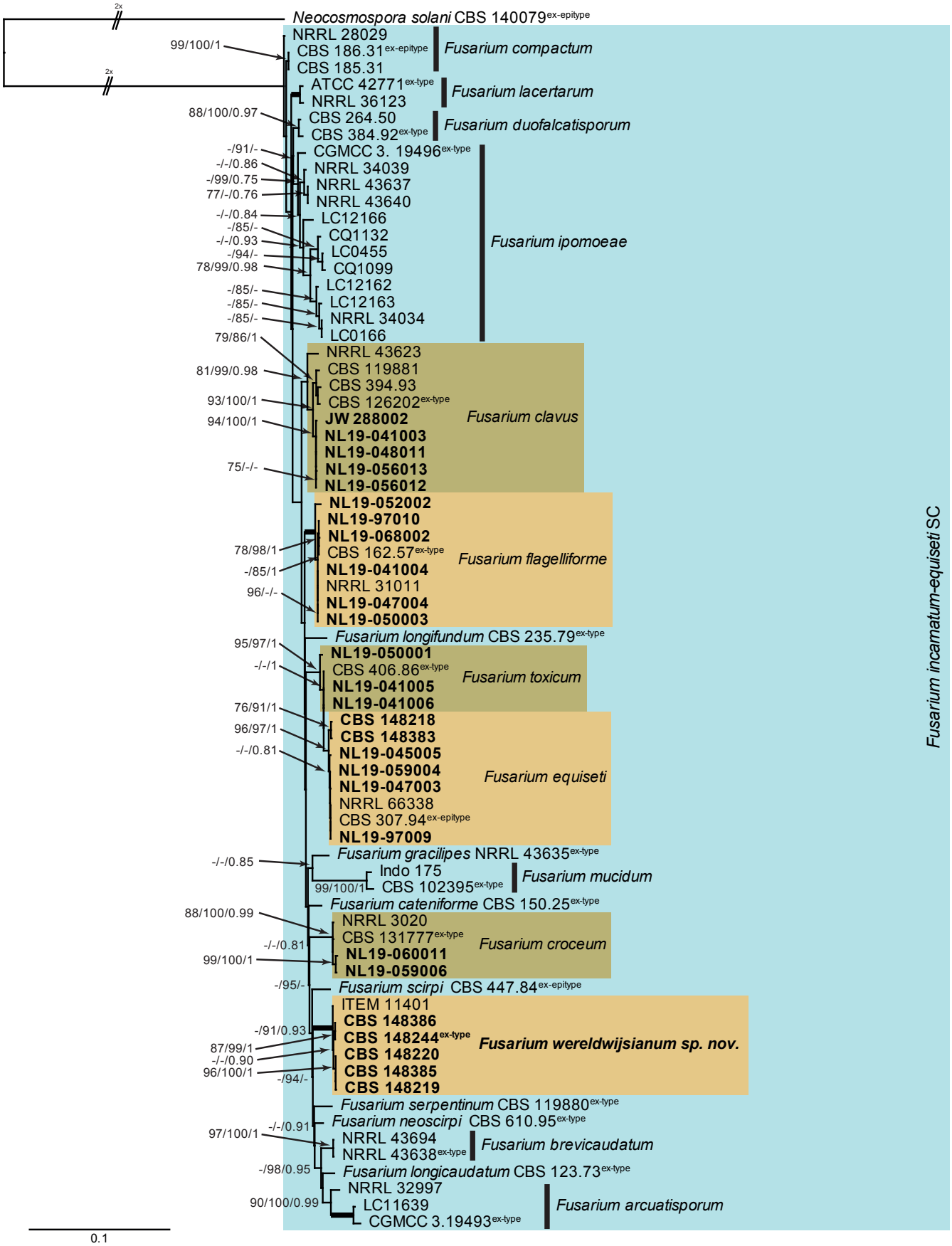

Fig 2. The RAxML consensus tree inferred from the combined *F. incarnatum-equiseti* species complex *tef1*, *rpb2* (first part), *cmdA* and *rpb1* sequence alignment. Thickened lines indicate branches with full support (RAxML & IQ-TREE bootstrap = 100 %; PP = 1.0) with support values of other branches indicated at the branches (RAxML > 74 % / IQ-TREE > 84 % / PP > 0.74). The tree is rooted to *Neocosmospora solani* (CBS 140079, ex-epitype culture) and the two basal branches were halved to facilitate layout. The scale bar indicates the number of expected changes per site. The *F. incarnatum-equiseti* species complex is indicated on the right and highlighted with a coloured block. Species clades containing the novel citizen science strains (in bold) are highlighted with coloured blocks and the novelty described in the present study is printed in bold font.

© 2021 Westerdijk Fungal Biodiversity Institute

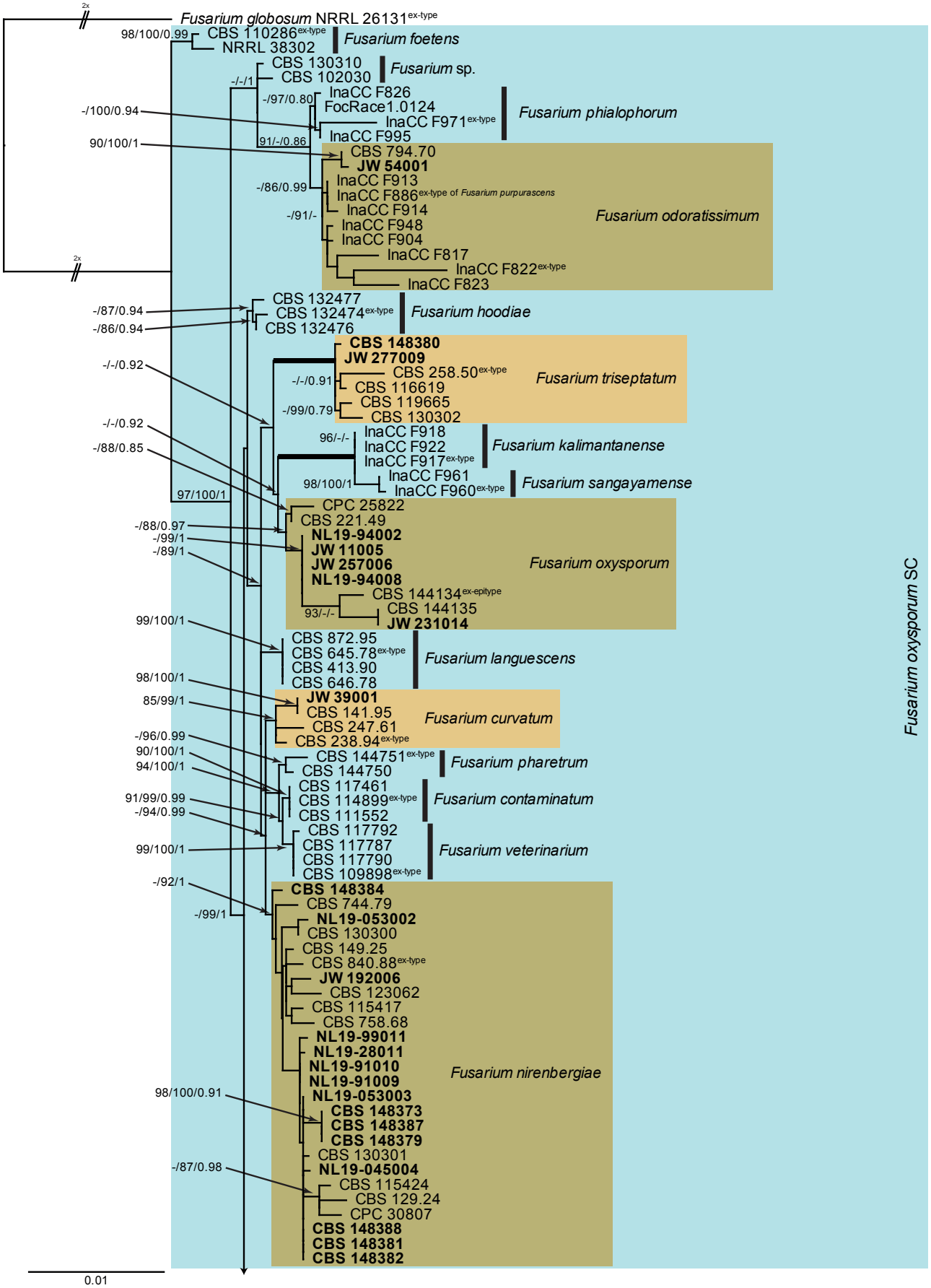

Fig 3. The RAxML consensus tree inferred from the combined *F. oxysporum* species complex *tef1*, *rpb2* (first part), *tub2*, *cmdA* and *rpb1* sequence alignment. Thickened lines indicate branches with full support (RAxML & IQ-TREE bootstrap = 100 %; PP = 1.0) with support values of other branches indicated at the branches (RAxML > 74 % / IQ-TREE > 84 % / PP > 0.74). The tree is rooted to *Fusarium globosum* (NRRL 26131) and the two basal branches were halved to facilitate layout. The scale bar indicates the number of expected changes per site. The *F. oxysporum* species complex is indicated on the right and highlighted with a coloured block. Species clades containing the novel citizen science strains (in bold) are highlighted with coloured blocks and the novelty described in the present study is printed in bold font.

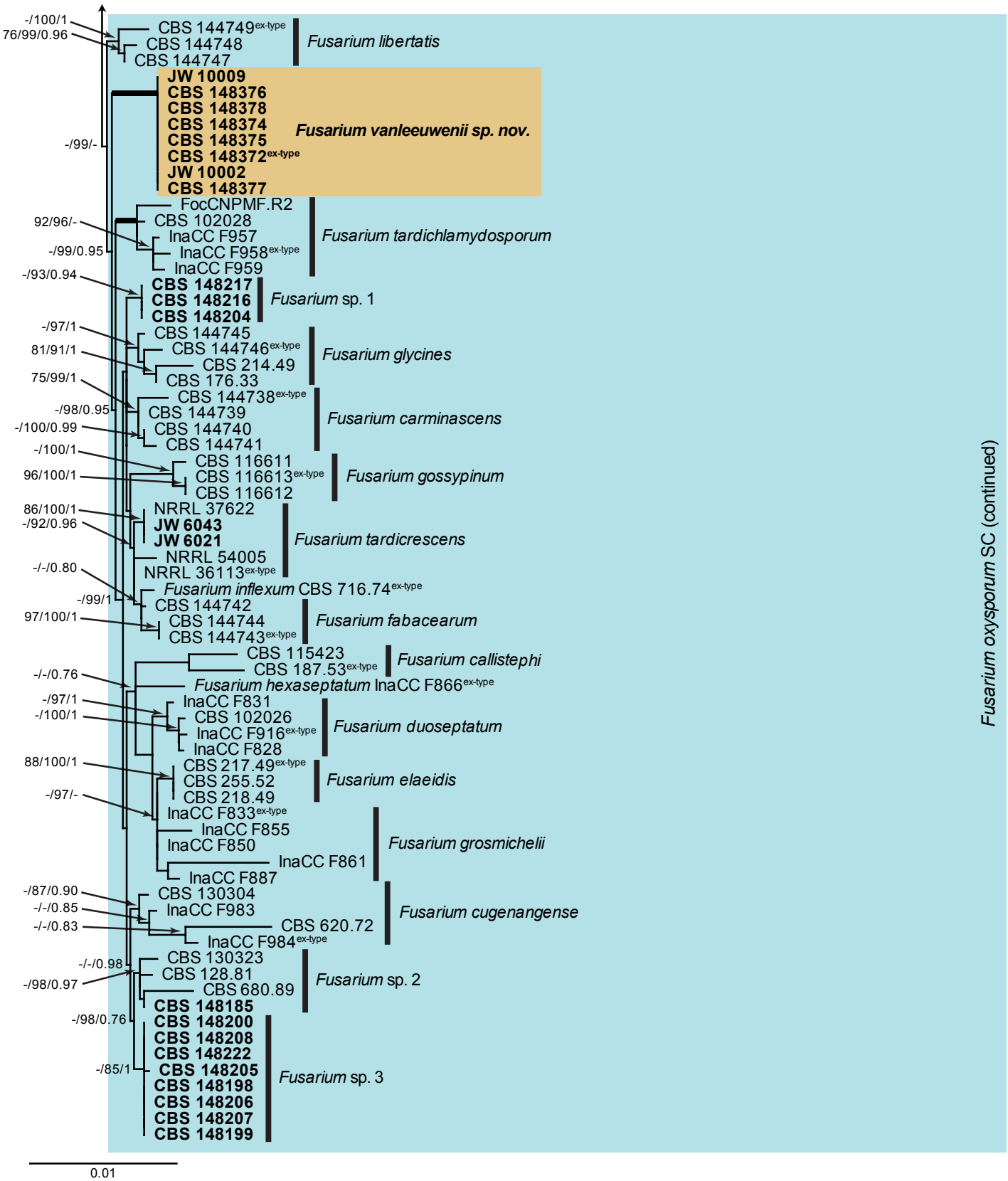

Fig 3. (Continued).

Fusarium sambucinum species complex (Fig. 5): Novel isolates from Dutch soils clustered with two known species, namely *F. culmorum* and *F. graminearum*. The three phylogenetic analyses (RAxML, IQ-TREE and MrBayes) overall displayed the same species clades and the Bayesian phylogeny mainly differed with regards to the backbone relationships between species clades/lineages in the lower half of the tree (data not shown, trees available in TreeBASE and support and PP values are superimposed on the presented figure). The locus *cmdA* is not well-represented in the dataset, with less than half of the strains having a sequence present (Tables 1, 2, Supplementary Table S1).

Neocosmospora (Fig. 6): Novel isolates from Dutch soils clustered with three known species, namely *N. solani*, *N. stercicola* and *N. tonkinensis*. The three phylogenetic analyses

© 2021 Westerdijk Fungal Biodiversity Institute

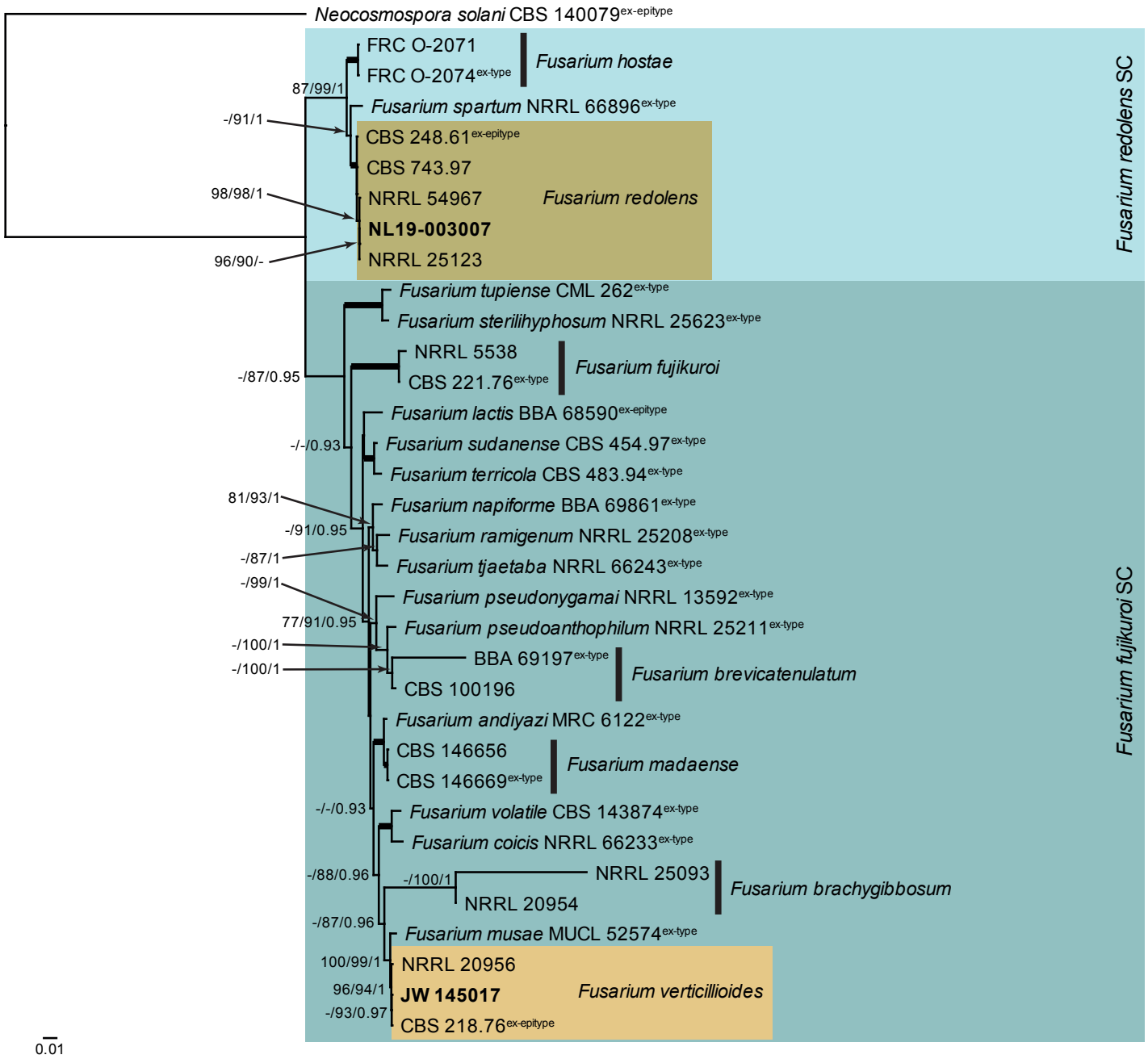

Fig 4. The RAxML consensus tree inferred from the combined *F. redolens*/*fujikuroi* species complexes *tef1*, *rpb2* (first part), *rpb1* and *cmdA* sequence alignment. Thickened lines indicate branches with full support (RAxML & IQ-TREE bootstrap = 100 %; PP = 1.0) with support values of other branches indicated at the branches (RAxML > 74 % / IQ-TREE > 84 % / PP > 0.74). The tree is rooted to *Neocosmospora solani* (CBS 140079, ex-epitype culture). The scale bar indicates the number of expected changes per site. Species complexes are indicated on the right and highlighted with coloured blocks. Species clades containing the novel citizen science strains (in bold) are highlighted with coloured blocks.

(RAxML, IQ-TREE and MrBayes) had the same overall topology, except for swapping around between *N. rectiphora* and *N. vasinfecta* as being the most basal species, and had the same species clades/lineages (data not shown, trees available in TreeBASE and support and PP values are superimposed on the presented figure). The loci *cmdA* and *rpb1* are not well-represented in the dataset, with roughly half of the strains having a sequence present (Tables 1, 2, Supplementary Table S1).

Based on these phylogenetic trees, several taxonomic decisions were made, and the individual and combined trees are discussed under the Notes in the Taxonomy section below, where applicable.

Taxonomy

Fusarium flocciferum Corda, in Sturm, Deutschl. Fl., Abt. 3, Pilze Deutschl. 2: 17. 1828.

New synonym: *Fusarium petersiae* L. Lombard, Persoonia 39: 457. 2017.

Additional synonyms see Crous *et al.* (2021b)

Material examined: **Germany**, from greenhouse soil, 1966, *D. Bredemeier*, ex-epitype culture of *F. flocciferum* CBS 821.68 = NRRL 28450. **Netherlands**, Friesland Province, Harlingen, from soil, 10 Oct. 2019, *S. Goinga & J. de Groot*, cultures NL19-048012, NL19-048013; Gelderland Province, Arnhem, from soil, Mar. 2017, *D. Peters* (holotype of *F. petersiae* CBS

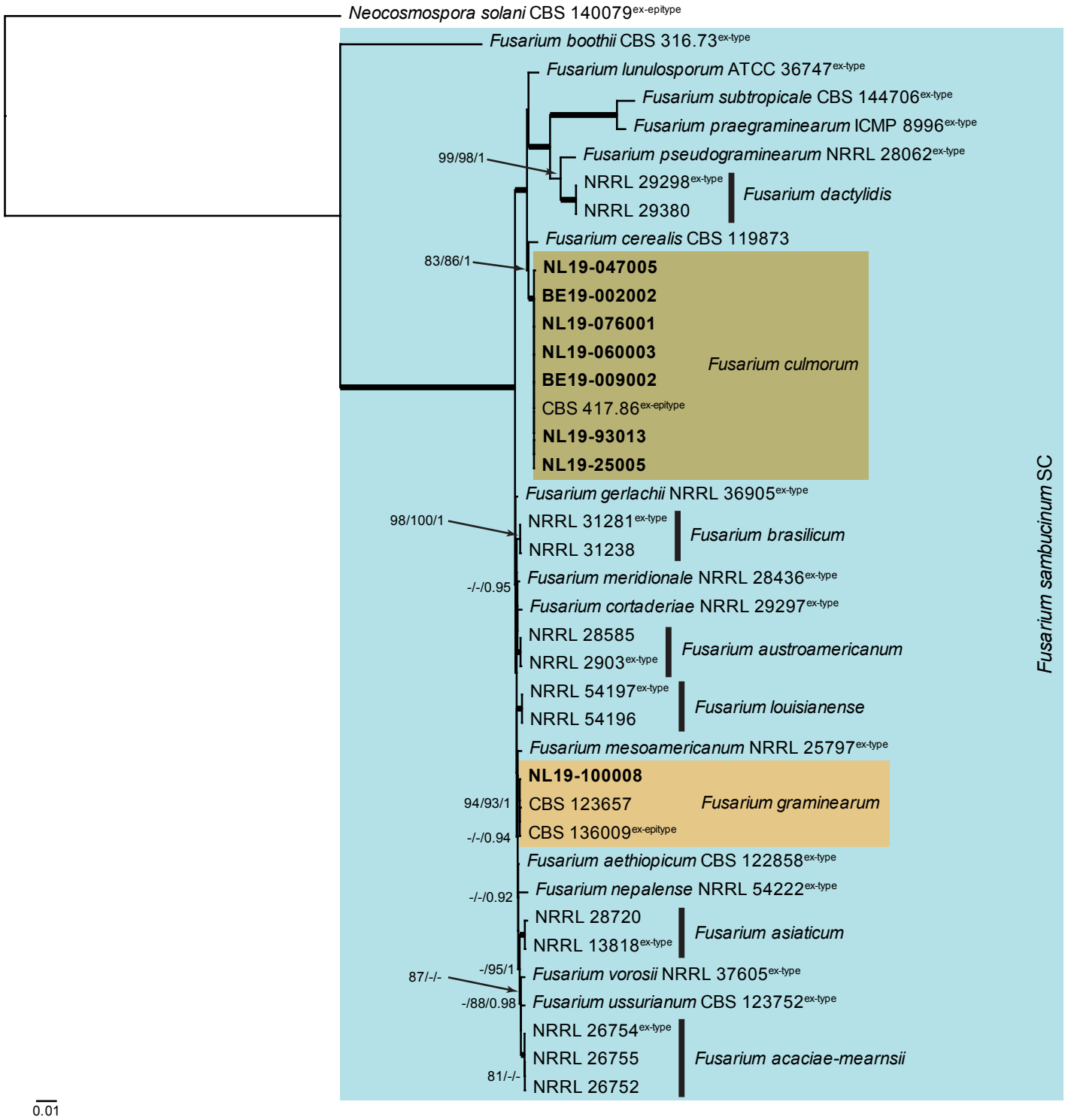

Fig 5. The RAxML consensus tree inferred from the combined *F. sambucinum* species complex *tef1*, *rpb2* (parts 1 and 2), *rpb1* and *cmdA* sequence alignment. Thickened lines indicate branches with full support (RAxML & IQ-TREE bootstrap = 100 %; PP = 1.0) with support values of other branches indicated at the branches (RAxML > 74 % / IQ-TREE > 84 % / PP > 0.74). The tree is rooted to *Neocosmospora solani* (CBS 140079, ex-epitype culture). The scale bar indicates the number of expected changes per site. The *Fusarium sambucinum* species complex is indicated on the right and highlighted with a coloured block. Species clades containing the novel citizen science strains (in bold) are highlighted with coloured blocks.

H-23233, culture ex-type CBS 143231 = JW 14004); *ibid*., culture JW 14005 = CBS 143667; Nijmegen, from soil, 2017, *J.W. Koolen*, culture JW 248008; North Brabant Province, Valkenswaard, from soil, 2017, *W. van der Heijden*, culture JW 18005; Utrecht Province, Utrecht, from soil, 2017, students of Basisschool de Baanbreker, culture JW267001; Bilthoven, Planetenplein, from garden soil, 31 Jul. 2019, *S. Frederikze, J. Mes & S. Maghnouji*, cultures NL19-97008, NL19-100011 = CBS 147837; Nieuwegein, from soil, 2017, *F. & R. Niemeijer*, culture JW 5026.

Notes: *Fusarium petersiae* was described from soil collected in this citizen science project (Crous *et al.* 2017). In the original publication, it was distinguished from *F. flocciferum* by the formation of sporodochia, up to 5-septate macroconidia, and the lack of conidiophores in aerial mycelium. *Fusarium flocciferum* was originally circumscribed as lacking sporodochia in culture and producing abundant 1–3-septate macroconidia on aerial conidiophores (Booth 1971). As we have shown here (Fig. 1),

© 2021 Westerdijk Fungal Biodiversity Institute

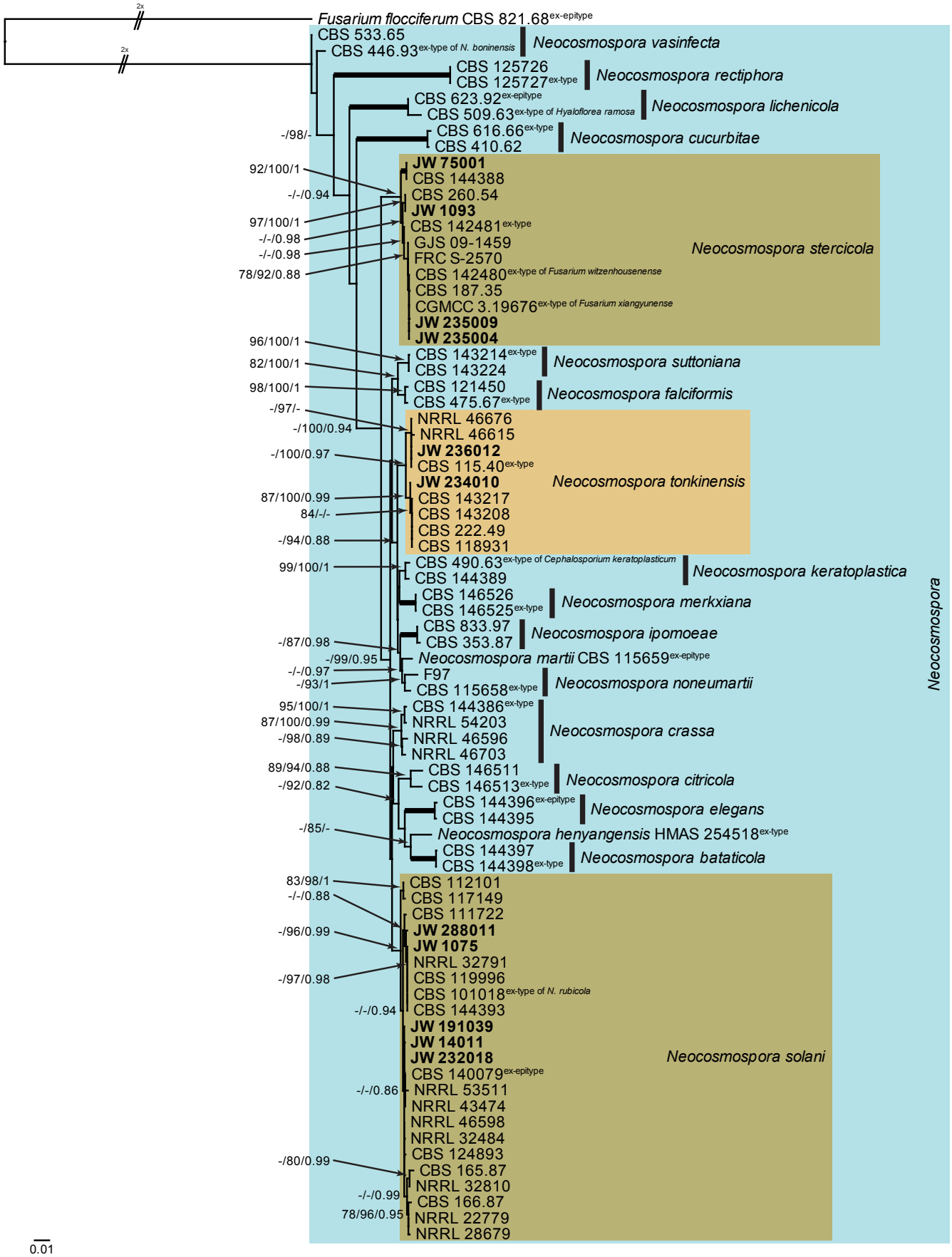

Fig 6. The RAxML consensus tree inferred from the combined *Neocosmospora tef1*, *rpb2* (first part), *rpb1* and *cmdA* sequence alignment. Thickened lines indicate branches with full support (RAxML & IQ-TREE bootstrap = 100 %; PP = 1.0) with support values of other branches indicated at the branches (RAxML > 74 % / IQ-TREE > 84 % / PP > 0.74). The tree is rooted to *Fusarium flocciferum* (CBS 821.68, ex-epitype culture) and the two basal branches were halved to facilitate layout. The scale bar indicates the number of expected changes per site. The genus *Neocosmospora* is indicated on the right and highlighted with a coloured block. Species clades containing the novel citizen science strains (in bold) are highlighted with coloured blocks.

however, *F. petersiae* (CBS 143231) is phylogenetically identical to *F. flocciferum* (ex-type CBS 821.68) and is therefore reduced to synonymy.

***Fusarium* sp. 1.** Fig. 7.

CBS 148217 (= NL19-25001): *Aerial conidiophores* sparingly branched, with terminal or intercalary conidiogenous cells, giving rise to macro- and microconidia; *aerial conidiogenous cells* monophialidic, subulate to subcylindrical, smooth and thin-walled, 5–30 × 2–3.5 µm, with flared collarette and minute periclinal thickening at apex. *Microconidia* aggregating in false heads, ellipsoid to subcylindrical, falcate, 0–1-septate, 5–20 × 3–4 µm. *Sporodochia* pale luteous to orange, abundant on CLA. *Sporodochial conidiophores* densely aggregated, verticillately branched, consisting of a short stipe bearing whorls of 2–3 monophialides; *sporodochial conidiogenous cells* monophialidic, subulate to subcylindrical, 10–15 × 4–5 µm, smooth- and thin-walled, with periclinal thickening at apex and minute, flared collarette. *Sporodochial conidia* falcate, curved dorsiventrally, sides almost parallel, tapering towards both ends; apical cell papillate and curved; basal cell foot-shaped, notch poorly developed, 3(–5)-septate, hyaline, smooth-walled, guttulate; 3-septate conidia (33–)43–45(–48) × (3.5–)4(–5) µm, 5-septate conidia rare, up to 60 µm long. *Chlamydospores* not observed.

Culture characteristics: Colonies spreading, with cottony aerial mycelium. On PDA surface and reverse pale vinaceous. On OA surface pale vinaceous, reverse rosy buff.

Isolates examined: **Netherlands**, Groningen Province, Warffum, from garden soil, 6 Jun. 2019, *C. Dijkstra & L. Kruit*, culture NL19-25001 = CBS 148217; Limburg Province, Ell, 2017, *K. Brennand*, culture JW 53002 = CBS 148216; Utrecht Province, Amersfoort, 2017, *T. & K. Wesselink*, culture JW 191014 = CBS 148204.

Notes: *Fusarium* sp. 1 (CBS 148217) is related (Fig. 3) to *F. tardichlamydosporum* [macroconidia (36–)37–43(–45) × (4–)5–6(–7) µm (av. 40 × 5 µm), 3–5-septate; Maryani *et al.* 2019a], *F. carminascens* [3-septate macroconidia: (21–)26–36(–40) × 3–5 µm (av. 31 × 4 µm); 4-septate macroconidia: (31–)33–43(–44) × 4–5 µm (av. 38 × 4 µm); Lombard et al. 2019]; and *F. vanleeuwenii* [3-septate macroconidia (32–)45–50(–52) × (3.5–)4(–4.5) µm, 4–5-septate conidia 52–60 × 4.5–5 µm, 7–8-septate conidia rare, 65–75 × 5–6 µm] in the FOSC (see elsewhere in this paper). It is morphologically distinct from these species based on the dimensions of its macroconidia. The species is undisguisable from other included species on *cmdA* (intermingled with numerous species), *rpb1* (intermingled with *F. keijii* and *F. joseae*), *rpb2* (intermingled with numerous species), and *tef1* (intermingled with *F. cugenangense*), and can best be identified using a multi-gene phylogenetic analysis. No *tub2* sequences were available for comparison. The species clade is well-supported in two of the analyses (IQ-TREE bootstrap support value = 99 %; Bayesian PP = 0.95). This species is unnamed at present, pending further data.

***Fusarium* sp. 2.** Fig. 8.

CBS 148185 (= JW 1072): *Aerial conidiophores* sparingly branched, 2–20 µm tall, mostly reduced to conidiogenous cells on hyphae; *aerial conidiogenous cells* monophialidic, subulate to subcylindrical, smooth and thin-walled, 2–20 × 2–6 µm, with flared collarette and minute periclinal thickening at apex. *Microconidia* aggregating in false heads, falcate, subcylindrical to reniform, (0–)1(–2)-septate, (10–)13–15(–20) × (3–)3.5–4 µm. *Sporodochia* pale luteous, abundant on CLA. *Sporodochial conidiophores* densely aggregated, verticillately branched, consisting of a short stipe bearing whorls of 2–3 monophialides; *sporodochial conidiogenous cells* monophialidic, subulate to subcylindrical, 9–22 × 3–5 µm, smooth- and thin-walled, with periclinal thickening at apex and minute, flared collarette. *Sporodochial conidia* falcate, moderately curved dorsiventrally, sides almost parallel, tapering towards both ends; apical cell blunt to papillate and curved; basal cell foot-shaped, notch poorly developed, 3(–6)-septate, hyaline, smooth-walled, guttulate; 3-septate conidia (30–)38–43(–47) × 4–5(–6) µm, 4-septate conidia 45–47 × 4.5–5 µm, 5-septate conidia 50–65 × 5 µm. *Chlamydospores* not observed.

Culture characteristics: Colonies flat, spreading, with cottony aerial mycelium. On PDA surface rosy vinaceous, reverse greyish rose. On OA surface and reverse greyish rose.

Isolates examined: **Australia**, Subungual debris of 40-year-old female with nail infection, collection date unknown, collector unknown, culture CBS 130323 =NRRL 26677. **Netherlands**, North Holland Province, Amsterdam, from garden soil, Mar. 2017, *J.F.T.M. van Dijk,* culture CBS 148185 = JW 1072; Zuid-Holland Province, Nootdorp*, Cucumis sativus*, in greenhouse on rockwool, No. 1979, collection date unknown, *N. Hubbeling*, culture CBS 680.89 = IPO 11179 = NRRL 26221. **USA**, on *Chrysantemum* sp., collection date unknown, collector unknown, culture CBS 128.81 =NRRL 36233 = BBA63925.

Notes: *Fusarium s*p. 2. (CBS 148185) is related (Fig. 3) to *F. cugenangense* (FOSC; associated with banana, but non-pathogenic on Gros Michel (AAA) and Cavendish (AAA); Maryani *et al.* 2019a) and *Fusarium* sp. 3 (see below). It is distinguished morphologically from *F. cugenangense* which has smaller micro- (av. 12 × 5 µm), and larger macroconidia (44–)47–54(–57) × (5–)6–7(–8) µm (av. 53 × 7 µm), 3–6-septate (Maryani *et al.* 2019a). *Fusarium* sp. 3 is similar to *Fusarium* sp. 2, but has larger macroconidia, *e.g.* 3-septate macroconidia (33–)43–50(–55) × (3.5–)4(–4.5) µm, 5-septate macroconidia 65–75 × 4–5 µm, and produces chlamydospores. This species can readily be distinguished from other included species based on *tef1*, but is undisguisable from other included species on *cmdA*, *rpb1*, *rpb2* and *tub2*. This species clade is supported in two of the analyses (IQ-TREE bootstrap support value = 94 %; Bayesian PP = 0.98), but is left unnamed, pending further data.

***Fusarium* sp. 3.** Fig. 9.

CBS 148207 (= JW 210019): *Aerial conidiophores* sparingly branched, mostly reduced to monophialides; *aerial conidiogenous cells* monophialidic, subcylindrical, smooth and thin-walled, 2–15 × 3–4 µm, with minute collarette at apex. *Microconidia* aggregating in false heads, ellipsoid to subcylindrical, falcate, 0–1-septate, (8–)10–17(–28) × (2.5–)3(–3.5) µm. *Sporodochia* pale white, sparse on CLA. *Sporodochial conidiophores* densely aggregated, verticillately branched, consisting of a short stipe bearing whorls of 2–3 monophialides; *sporodochial conidiogenous cells* monophialidic, subulate to subcylindrical, 5–15 × 3–5 µm, smooth- and thin-walled, with

© 2021 Westerdijk Fungal Biodiversity Institute

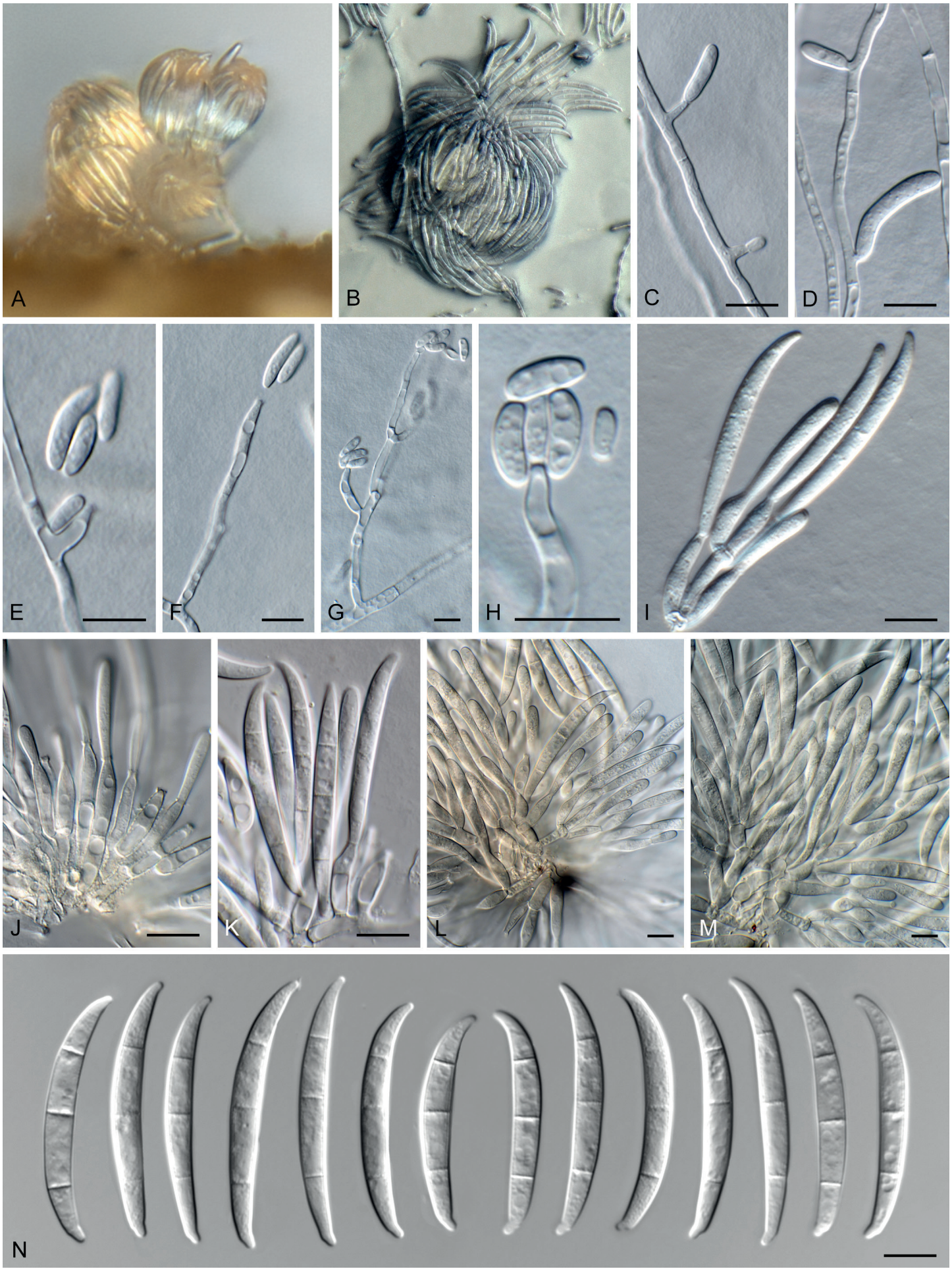

Fig. 7. *Fusarium* sp. 1 (CBS 148217). **A.** Sporodochium on CLA. **B.** Sporodochium on SNA. **C–H.** Aerial conidiophores with microconidia. **I–M.** Sporodochial conidiophores. **N.** Macroconidia. Scale bars = 10 µm.

© 2021 Westerdijk Fungal Biodiversity Institute

Fig. 8. *Fusarium* sp. 2 (CBS 148185). **A.** Sporodochia on CLA. **B–H.** Aerial conidiophores with microconidia. **I, J.** Aerial conidiophores with macroconidia. **K, L.** Sporodochial conidiophores. **M.** Macroconidia. Scale bars = 10 µm.

© 2021 Westerdijk Fungal Biodiversity Institute

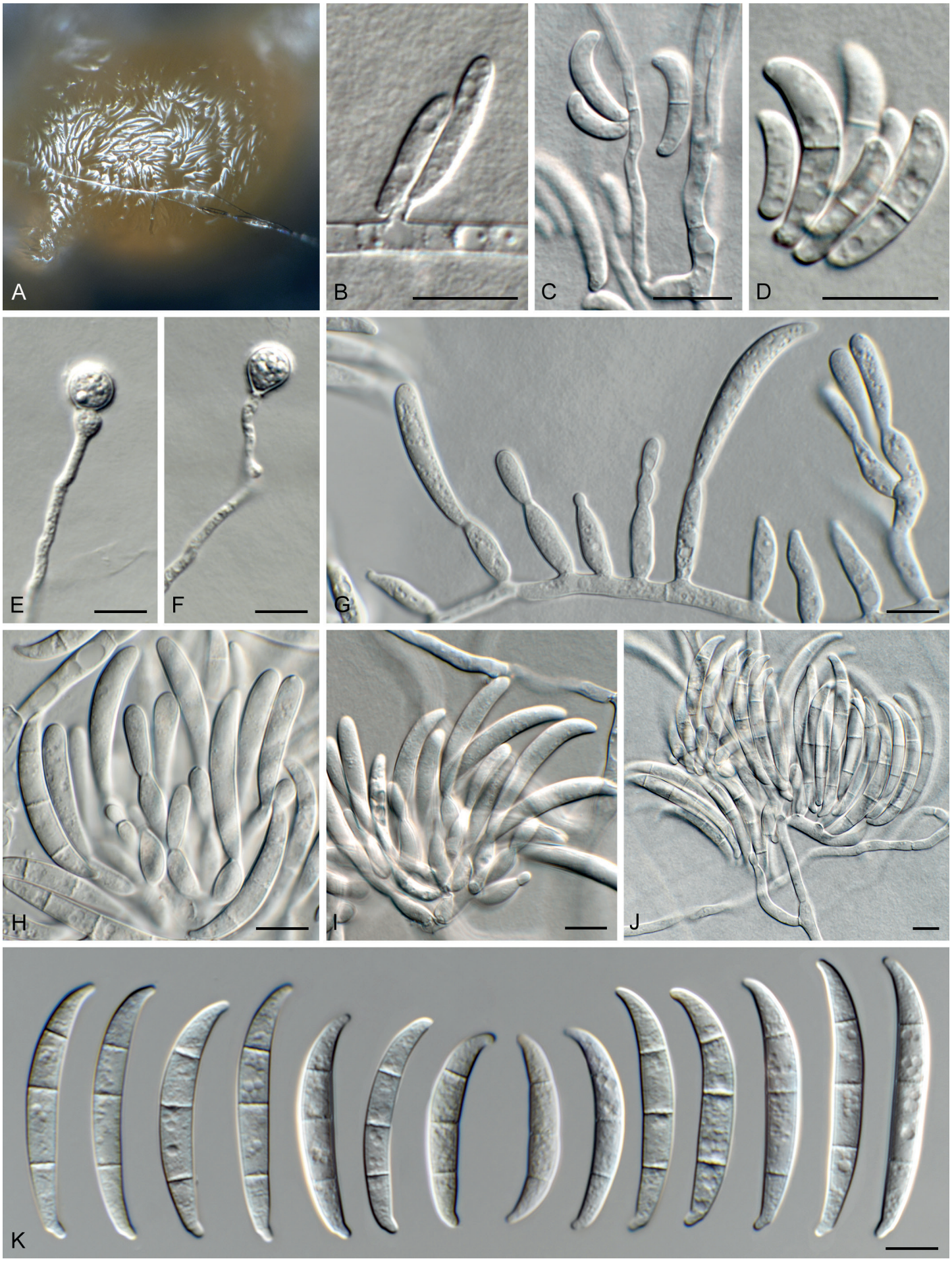

Fig. 9. *Fusarium* sp. 3 (CBS 148207). **A.** Sporodochium on CLA. **B, C, G.** Aerial conidiophores with conidia. **D.** Microconidia. **E, F.** Chlamydospores. **H–J.** Sporodochial conidiophores. **K.** Macroconidia. Scale bars = 10 µm.

© 2021 Westerdijk Fungal Biodiversity Institute

periclinal thickening at apex and minute, flared collarette. *Sporodochial conidia* straight to falcate, curved dorsiventrally, sides almost parallel, tapering towards both ends; apical cell blunt or papillate and curved; basal cell foot-shaped, notch poorly developed, 3(–5)-septate, hyaline, smooth-walled, guttulate; 3-septate conidia (33–)43–50(–55) × (3.5–)4(–4.5) µm, 5-septate conidia rare, 65–75 × 4–5 µm. *Chlamydospores* sparingly formed on CLA, subglobose to globose, pale brown, thick-walled, terminal or intercalary, 6–8 µm diam.

Culture characteristics: Colonies flat, spreading, with sparse aerial mycelium. On PDA surface and reverse pale vinaceous. On OA surface and reverse livid vinaceous.

Isolates examined: **Belgium**, East Flanders, Brakel, from garden soil, 2019, *T. Antheunis*, culture BE 19_004006 = CBS 148222. **Netherlands**, Friesland Province, Heerenveen, from garden soil, 2017, *N. Keij*, culture JW 210019 = CBS 148207; Friesland Province, Heerenveen, from garden soil, 2017, *N. Keij*, culture JW 210014 = CBS 148206; Friesland Province, Leeuwarden, from garden soil, 2017, *D. Pol, R. Verf, J. Wilks & M. de Ruiter*, culture JW 231016 = CBS 148208; Gelderland Province, Geldermalsen, from garden soil, 2017, *A.-S. den Boer,* culture JW 9002 = CBS 148199; Gelderland Province, Culemborg, from garden soil, 2017, *I. Kleij*, culture JW 204009 = CBS 148205; Utrecht Province, Amersfoort, from garden soil, 2017, *F. Wiegerinck*, culture JW 4030 = CBS 148198; Utrecht Province, Utrecht, from garden soil, 2017, *M.J. van Leeuwen*, culture JW 10005 = CBS 148200.

Notes: *Fusarium* sp. 3 (CBS 148207) is closely related (Fig. 3) to *Fusarium* sp. 2 [3-septate macroconidia (30–)38–43(–47) × 4–5(–6) µm] in the FOSC, and can be distinguished morphologically in having larger 3-septate macroconidia, and in producing chlamydospores, which were not observed in *Fusarium* sp. 2. This species can readily be distinguished from other included species based on *cmdA* and *tef1*, but is undisguisable from other included species on *rpb1* and *rpb2*. No *tub2* sequences were available for comparison. The species clade is poorly to fully supported in two of the analyses (IQ-TREE bootstrap support value = 85 %; Bayesian PP = 1), but is left unnamed, pending further data.

Fusarium vanleeuwenii Crous & Sand.-Den., ***sp. nov.*** MycoBank MB 840894. Fig. 10.

Etymology: Named after the collector, Maurits Jesse van Leeuwen. This sample was collected during a Citizen Science project of the Westerdijk Fungal Biodiversity Institute.

Typus: **Netherlands**, Utrecht Province, Utrecht, from garden soil, 2017, *M.J. van Leeuwen*, (**holotype** CBS H-24786, culture ex-type CBS 148372 = JW 10008).

Aerial conidiophores irregularly branched, up to 70 µm tall, or reduced to conidiogenous cells on hyphae; conidiogenous cells monophialidic, subulate to subcylindrical, smooth and thin-walled in branched clusters, 10–25 × 4–5 µm; at times reduced to conidiogenous pegs on hyphae, erect, 2–10 × 1.5–2.5 µm, with flared collarette and minute periclinal thickening at apex. *Microconidia* aggregating in mucoid droplets, 0(–2)-septate, ellipsoid to subcylindrical, reniform to somewhat falcate, apical cell becoming hooked, guttulate, (7–)10–14(–18) × 2.5–4 µm. *Sporodochial conidiophores* in moderate numbers on CLA, pale yellow, densely aggregated, irregularly branched, typically in whorls of 2–4 phialides; *sporodochial conidiogenous cells* monophialidic, subulate to subcylindrical, 9–18 × 3–4.5 µm, with periclinal thickening at apex and inconspicuous collarette. *Sporodochial conidia* falcate, moderately curved, more so on outer than inner plane, widest in middle; apical cell papillate to hooked; basal cell foot-shaped, notch poorly developed, (1–)3(–8)-septate, hyaline, smooth-walled, guttulate; 1-septate conidia 15–20 × 3–4 µm, 2-septate conidia 20–25 × 3–4 µm, 3-septate conidia (32–)45–50(–52) × (3.5–)4(–4.5) µm, 4–5-septate conidia 52–60 × 4.5–5 µm, 7–8-septate conidia rare, 65–75 × 5–6 µm. *Chlamydospores* sparse after 1 wk, globose to subglobose, 7–8 µm diam, formed terminally or intercalary, single, smooth-walled, subhyaline.

Culture characteristics: Colonies erumpent, spreading, covering dish in 7 d, with moderate aerial mycelium. On PDA surface vinaceous, reverse rosy vinaceous. On OA surface livid red, reverse greyish rose. On MEA surface and reverse dark vinaceous.

Additional isolates examined: **Netherlands**, Utrecht Province, Utrecht, from garden soil, 2017, *M.J. van Leeuwen*, cultures CBS 148374 = JW 10001, JW 10002, CBS 148375 = JW 10003, CBS 148376 = JW 10004, CBS 148377 = JW 10006, CBS 148378 = JW 10007, JW 10009.

Notes: *Fusarium vanleeuwenii* is distantly related (Fig. 3) to *F. tardichlamydosporum*, a species in the FOSC associated with Panama disease of banana, pathogenic on Gros Michel (AAA) (Foc-Race1) (Maryani *et al.* 2019a). Morphologically, the two species are very similar, but *F. tardichlamydosporum* has smaller micro- (3–)5–9(–15) × (2–)5(–9) µm, and macroconidia (36–)37–43(–45) × (4–)5–6(–7) µm (av. 40 × 5 µm), 3–5-septate (Maryani *et al.* 2019a).

Fusarium vanleeuwenii is characteristic in that it has sparse chlamydospores, the aerial conidiophores are reduced to conidiogenous pegs on hyphae, and the reniform microconidia tend to have hooked apical cells. This species can readily be distinguished from other included species based on *cmdA*, *rpb1*, and *rpb2*, but is intermingled with *F. foetens* and *F. oxysporum* on *tef1*. No *tub2* sequences were available for comparison. The species clade is fully supported in all analyses (RAxML bootstrap support value = 100 %; IQ-TREE bootstrap support value = 100 %; Bayesian PP = 1).

Fusarium wereldwijsianum Crous & Sand.-Den., ***sp. nov.*** MycoBank MB 840895. Fig. 11.

Etymology: Named after the school "Wereldwijs" (Bilthoven, the Netherlands) where the sample was collected. This sample was collected during a Citizen Science project of the Westerdijk Fungal Biodiversity Institute.

Typus: **Netherlands**, Utrecht Province, Bilthoven, Planetenplein, from garden soil, 31 Jul. 2019, *S. Frederikze, J. Mes & S. Maghnouji* (holotype CBS H-24787, culture ex-type CBS 148244 = NL19-94009).

Aerial conidiophores sparingly branched, 5–20 µm tall, bearing terminal and lateral monophialides, but mostly reduced to conidiogenous cells on hyphae; *aerial conidiogenous cells* monophialidic, subulate to subcylindrical, smooth and thin-walled, 5–15 × 3.5–4 µm, with flared collarette and minute

© 2021 Westerdijk Fungal Biodiversity Institute

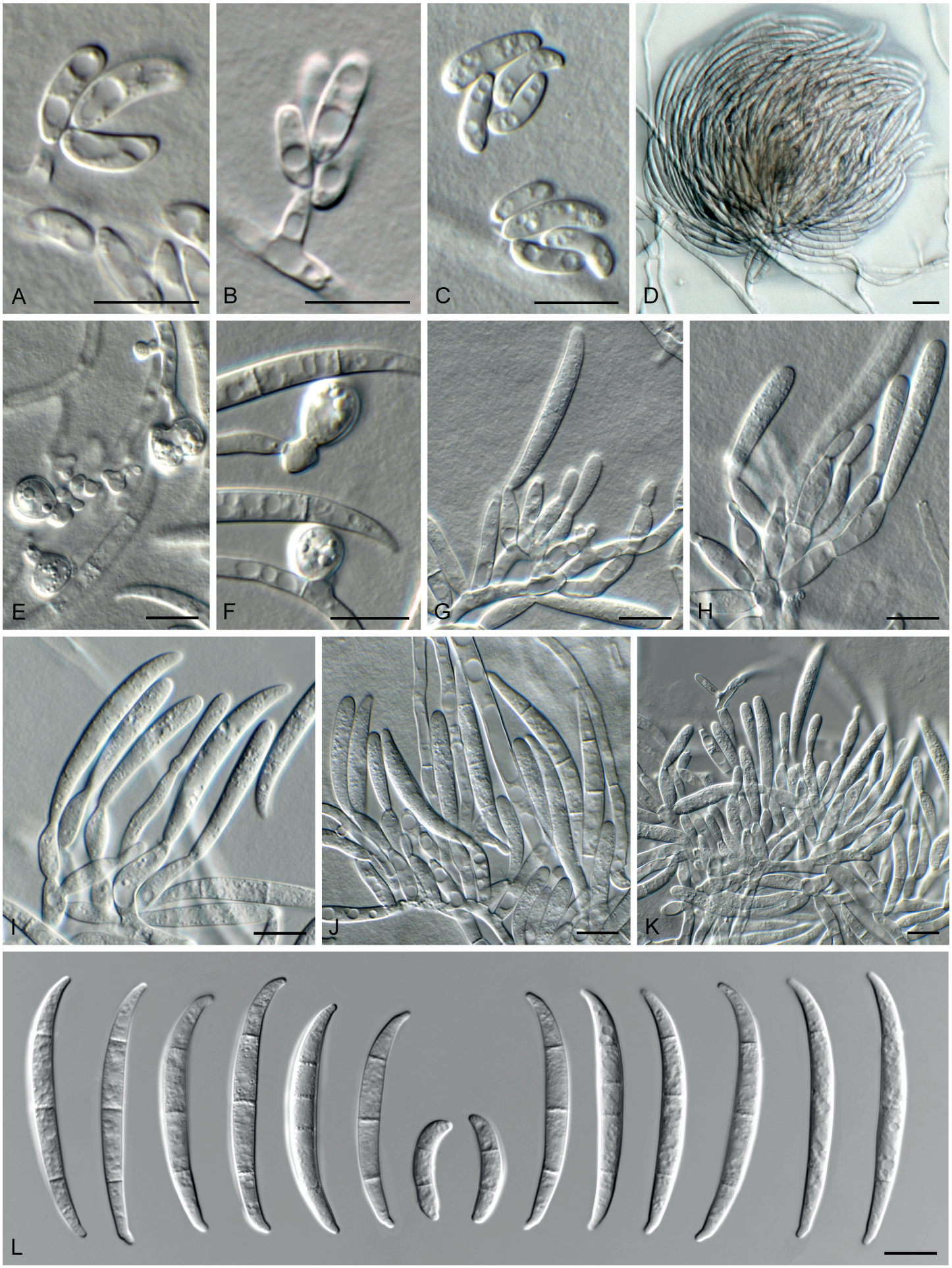

Fig. 10. *Fusarium vanleeuwenii* (CBS 148372). **A–C.** Aerial conidiophores with microconidia. **D.** Sporodochium on SNA. **E, F.** Chlamydospores. **G–K.** Sporodochial conidiophores. **L.** Macroconidia. Scale bars = 10 µm.

© 2021 Westerdijk Fungal Biodiversity Institute

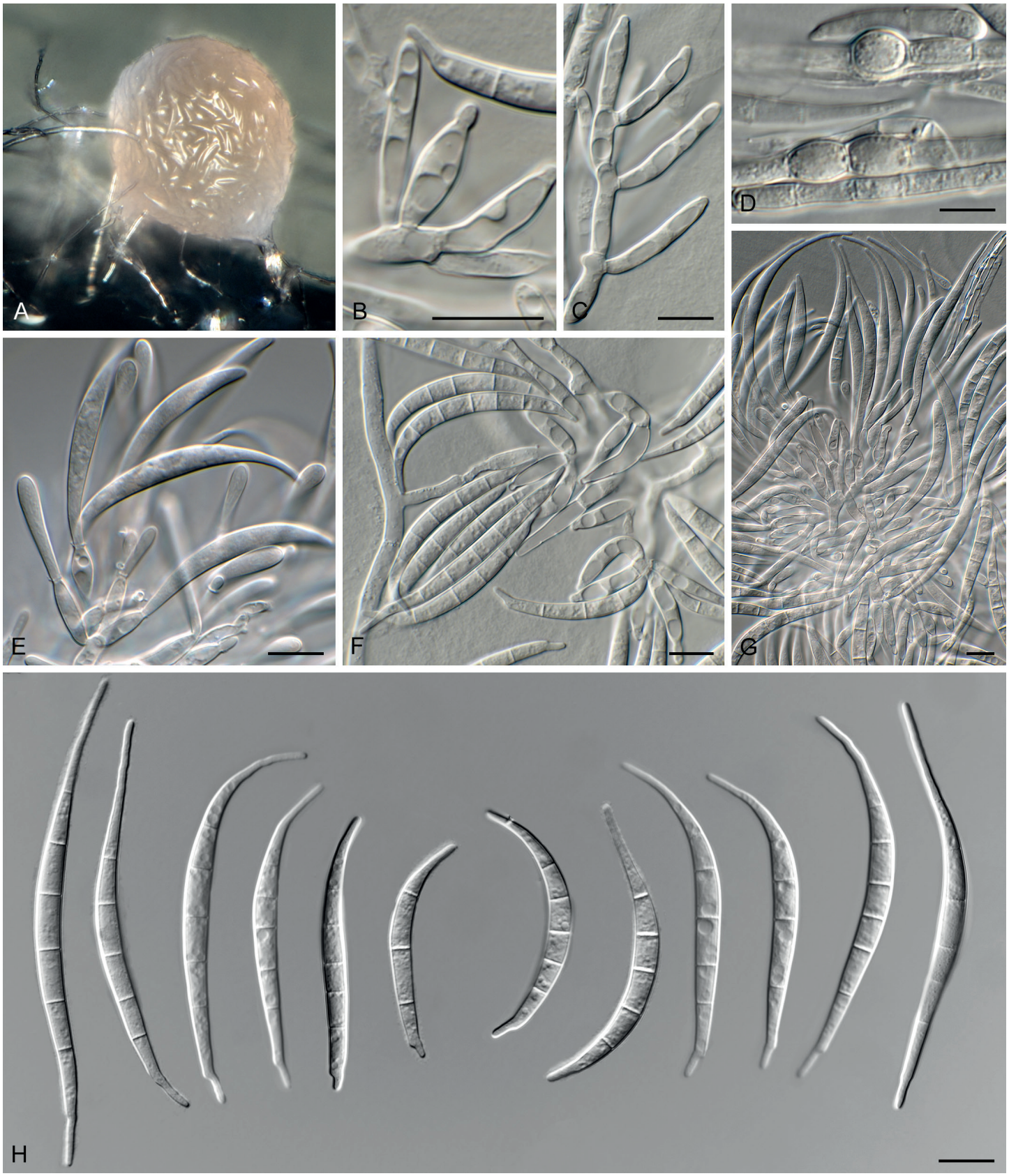

Fig. 11. *Fusarium wereldwijsianum* (CBS 148244). **A.** Sporodochium on CLA. **B, C, E–G.** Sporodochial conidiophores. **D.** Chlamydospores. **H.** Macroconidia. Scale bars = 10 µm.

periclinal thickening at apex. *Aerial conidia* aggregating in false heads, falcate, 1–3-septate, apex obtuse to acutely rounded, base obtuse to notched, (16–)20–22(–25) × 3–3.5(–4) µm. *Sporodochia* orange, abundant on CLA. *Sporodochial conidiophores* densely aggregated, verticillately branched, consisting of a short stipe bearing whorls of 2–4 monophialides; *sporodochial conidiogenous cells* monophialidic, subulate to subcylindrical, 10–20 × 3.5–4 µm, smooth- and thin-walled, with periclinal thickening at apex and minute, flared collarette. *Sporodochial conidia* falcate, curved dorsiventrally, tapering

© 2021 Westerdijk Fungal Biodiversity Institute

towards both ends; apical cell elongated, curved, whip-like; basal cell foot-shaped, notch well developed, 3(–5)-septate, hyaline, smooth-walled, guttulate; 3-septate conidia (40–)45–60(–65) × 4(–5) µm, 5-septate conidia (45–)55–65 × 4–4.5(–5) µm. *Chlamydospores* on SNA after 1 wk sparse, solitary, intercalary or terminal, subglobose, 6–8 µm diam, becoming brown with age.

Culture characteristics: Colonies spreading, with cottony aerial mycelium. On PDA surface and reverse rosy buff. On OA surface buff to rosy buff, reverse rosy buff to rosy vinaceous.

Additional isolates examined: **Netherlands**, Utrecht Province, Bilthoven, Planetenplein, 31 Jul. 2019, *S. Frederikze, J. Mes & S. Maghnouji*, cultures cultures CBS 148219 = NL19-99003, CBS 148220 = NL19-99002; Zeeland Province, Oostburg, 23 Oct. 2019, *A. van Strien, I. Beemsterboer & S. Groosman,* culture CBS 148386 = NL19-059003; Zeeland Province, Oostburg, Oct. 2019, *F. Guilliet, T. Bron & I. Geernaert,* culture CBS 148385 = NL19-057012.

Notes: *Fusarium wereldwijsianum* is a member of the *F. incarnatum-equiseti* species complex (FIESC; Wang *et al.* 2019, Xia *et al.* 2019), clustering among *F. scirpi, F. serpentinum* and *F. neoscirpi* (Fig. 2). It can be distinguished morphologically from *F. scirpi* which commonly has polyphialides, and 6–7-septate macroconidia (Leslie & Summerell 2006). *Fusarium wereldwijsianum* is further distinguished from *F. neoscirpi* which has smaller macroconidia [3-septate conidia: (28–)32–42(–46) × 4–5 µm (av. 37 × 4 µm); 5-septate conidia: (47–)50–58(–64) × 4–6 µm (av. 54 × 5 µm); Xia *et al.* 2019], and lacks chlamydospores. It is also distinct from *F. serpentinum* which has larger, (3–)5–7(–8)-septate macroconidia [3-septate conidia: (42–)43–51(–54) × 4–6 µm; 5-septate conidia: (57–)67–85(–92) × 4–6 µm; Xia *et al.* 2019]. *Fusarium wereldwijsianum* can readily be distinguished from other included species based on *cmdA*, *rpb1*, and *tef1*, but less readily so on *rpb2*. The species clade is fully supported in all analyses (RAxML bootstrap support value = 100 %; IQ-TREE bootstrap support value = 100 %; Bayesian PP = 1).

DISCUSSION

The present study focused on fusarioid fungi that were isolated from soil in the Netherlands during a Citizen Science project, which already has revealed numerous new species of filamentous fungi and yeasts (Crous *et al*. 2017, 2018, Groenewald *et al.* 2018, Giraldo *et al.* 2019, Hou *et al*. 2020, Crous *et al.* 2021a).

Fusarium and allied fusarioid genera are common soil inhabitants, and therefore it should not be seen as surprising that the present study identified 25 taxa, including 22 *Fusarium* spp., and three species of *Neocosmospora*. One new species was described from the FOSC, namely *F. vanleeuwenii,* and one from the FIESC, namely *F. wereldwijsianum.* Furthermore, *F. petersiae* (Crous *et al*. 2017) was also reduced to synonymy under *F. flocciferum*, which was found to be morphologically more variable than suspected when it was first described (Booth 1971).

Although the various soil samples were collected from garden soils in the urban environment, it was somewhat surprising to also encounter a well-known pathogen of banana, such as *F. odoratissimum* (syn. *F. purpurascens sensu* Crous *et al.* 2021b). Some Dutch isolates clustered with named subclades such as *F. callistephi* (CBS 187.53) or *F. tardicrescens* (JW 6021, JW 6043) (Maryani *et al*. 2019a), or appeared to represent new taxa, which we prefer to leave unnamed for now, pending more data to help resolve species boundaries within this clade. The identification of JW 6021 and JW 6043 as *F. tardicrescens* is based on the *rpb1* and *tef1* association with strain NRRL 37622 (see TreeBASE), a strain previously identified as belonging to that species (Maryani *et al*. 2019a).

Other species isolated that belong to the FOSC include: *F. curvatum*, described from *Beaucarnia* sp. and *Hedera helix* in the Netherlands, but also known from *Matthiola incana* in Germany (Lombard *et al.* 2019); *F. nirenbergiae,* described from *Dianthus caryophyllus* and *Solanum lycopersicum* in the Netherlands, but also known from numerous other plant and animal hosts, including humans, in countries such as Brazil, Italy, South Africa and the USA (Lombard *et al.* 2019); *F. oxysporum,* originally described from a rotten tuber of *Solanum tuberosum*, but having a wide host range with a worldwide distribution (Lombard *et al.* 2019), and *F. triseptatum,* known from hosts such as *Ipomoea batatas*, humans (USA), wilted *Gossypium hirsutum* (Ivory Coast), and sago starch (Papua New Guinea) (Lombard *et al.* 2019).

Five species from the FIESC isolated include: *F. clavus,* known from desert soil in Namibia, but also from various plant hosts in Germany, Iran, Russia and the USA (Xia *et al.* 2019); *F. croceum,* described from soil in the Czech Republic, but also known from *Triticum* in Iran (Xia *et al*. 2019); *F. equiseti,* a saprobe or secondary invader, common in cool to temperate or hot and arid climates (Leslie & Summerell 2006); *F. flagelliforme* known from *Pinus nigra* seedlings in Croatia, and various plant hosts in Germany (Xia *et al.* 2019), and *F. toxicum,* known from soil collected in Germany, but also isolated from a dog in the USA (Xia *et al.* 2019).

The *Fusarium tricinctum* species complex (FTSC) was represented by three species: *F. acuminatum,* a soil saprobe associated with roots and crowns of plants in temperate regions (Leslie & Summerell 2006), *F. torulosum,* occurring in soil in temperate regions, and from a number of plant hosts including cereals, tomatoes, beet root and trees (Leslie & Summerell 2006), and *F. flocciferum,* a common species in temperate regions, occurring in soil, and roots, fruits, stems and twigs of various plant hosts in Europe, North America and Iran (Gerlach & Nirenberg 1982, Torbati *et al.* 2018). The *Fusarium sambucinum* species complex (FSAMSC) was represented by two species: *Fusarium culmorum*, a species commonly found in temperate climates, associated with cereal crowns and grain, and plant debris in soil, and *F. graminearum*, a species primarily associated with maize, wheat and barley, but also other plant hosts (Leslie & Summerell 2006). The *Fusarium redolens* species complex (FRSC) was represented by a single species, *F. redolens*, which is a common soilborne fungus found in temperate areas. Likewise, the *Fusarium fujikuroi* species complex (FFSC) was also associated with a single species, *F. verticillioides*, which is a common pathogen of maize with a worldwide distribution (Leslie & Summerell 2006).

Finally, three species of *Neocosmospora* were also encountered in this study. These include *N. solani*, a common soil inhabitant, which is known from several plant species and has a global distribution. Less well-known species include *N. stercicola*, known from soil, and various other plant hosts in Europe (Sandoval-Denis *et al.* 2019), and *N. tonkinensis*, known from *Musa sapientum* in Vietnam, and various plant hosts in Europe, including *Euphorbia fulgens* in the Netherlands, and

© 2021 Westerdijk Fungal Biodiversity Institute

a turtle head lesion and human cornea in the USA (Sandoval-Denis 2019).

These findings underline the fact that fusarioid fungi are common soil inhabitants and are generally widely distributed. The ability of these fungi to produce chlamydospores (resting spores) in hyphae, macroconidia, and plant debris, make them well suited to survive adverse conditions for extended periods of time in the soil environment. Although many are saprobic, they appear to also can switch to an opportunistic or pathogenic lifestyle under more favourable conditions, and once in contact with their ideal host(s). It is therefore probable that several of the species described here as presumed saprobes, will in time be shown to be pathogens under favourable conditions.

In conclusion, this study has revealed a high number of fusarioid taxa in the urban soil environment, underlining the importance of this substrate for the discovery of novel taxa, and for gaining a better understanding of species diversity of fusarioid taxa in soil.

ACKNOWLEDGEMENTS

This study was financially supported by the Utrecht University Museum and the Royal Dutch Academy of Arts and Sciences for promoting the Citizen Science project, and for providing a platform to facilitate interaction with various Dutch primary schools. We are grateful to all the children and parents who participated in this project, collecting samples in their gardens and submitting them to the Westerdijk Institute for analyses. We are thankful to the staff from the Westerdijk Institute: Manon Verweij, Karin Schagen and Mariëtte Oosterwegel, for promoting the project and establishing communication with the collectors and schools. We also thank Marjan Vermaas for assistance with the photographic plates.

Conflict of interest: The authors declare that there is no conflict of interest.

REFERENCES

Bamburg JR, Riggs NV, Strong FM (1968). The structures of toxins from two strains of *Fusarium tricinctum*. *Tetrahedron* **24**: 3329–3336.

Booth C (1971). *The genus Fusarium*. Commonwealth Mycological Institute, Kew, Surrey, England.

Couteaudier Y, Alabouvette C (1990). Survival and inoculum potential of conidia and chlamydospores of *Fusarium oxysporum f.sp. lini* in soil. *Canadian Journal of Microbiology* **36**: 551–556.

Crous PW, Gams W, Stalpers JA, *et al.* (2004). MycoBank: an online initiative to launch mycology into the 21st century. *Studies in Mycology* **50**: 19–22.

Crous PW, Hernández-Restrepo M, Schumacher RK, *et al.* (2021a). New and Interesting Fungi. 4. *Fungal Systematics and Evolution* **7**: 255–343.

Crous PW, Lombard L, Sandoval-Denis M, *et al*. (2021b). *Fusarium*: more than a node or a foot-shaped basal cell. *Studies in Mycology* **98**: 100116.

Crous PW, Luangsa-ard JJ, Wingfield MJ, *et al.* (2018). Fungal Planet description sheets: 785–867. *Persoonia* **41**: 238–417.

Crous PW, Verkleij GJM, Groenewald JZ, *et al.* (2019). Fungal Biodiversity. [Westerdijk Laboratory Manual Series No. 1]. Westerdijk Fungal Biodiversity Institute publishing, Utrecht, Netherlands.

Crous PW, Wingfield MJ, Burgess TI, *et al.* 2017. Fungal Planet description sheets: 625–715. *Persoonia* **39**: 270–467.

Fisher NL, Burgess LW, Toussoun TA, *et al*. (1982). Carnation leaves as a substrate and for preserving cultures of *Fusarium* species. *Phytopathology* **72**: 151–153.

Geiser DM, Al-Hatmi AMS, Aoki T, *et al*. (2021). Phylogenomic analysis of a 55.1 kb 19-gene dataset resolves a monophyletic *Fusarium* that includes the *Fusarium solani* species complex. *Phytopathology* DOI:10.1094/PHYTO-08-20-0330-LE.

Gerlach W, Nirenberg H (1982). The genus *Fusarium* – a pictorial atlas. *Mitteilungen aus der Biologischen Bundesanstalt für Land- und Forstwirtschaft Berlin-Dahlem* **209**: 1–406.

Giraldo A, Hernández-Restrepo M, Crous PW (2019). New plecto-sphaerellaceous species from Dutch garden soil. *Mycological Progress* **18**: 1135–1154.

Gräfenhan T, Schroers H-J, Nirenberg HI, *et al*. (2011). An overview of the taxonomy, phylogeny, and typification of nectriaceous fungi in *Cosmospora*, *Acremonium*, *Fusarium*, *Stilbella* and *Volutella*. *Studies in Mycology* **68**: 79–113.

Groenewald M, Lombard L, de Vries M, *et al.* (2018). Diversity of yeast species from Dutch garden soil and the description of six novel Ascomycetes. *Federation of European Microbiological Societies Yeast Research* **18**: foy076.

Hernández-Restrepo M, Giraldo A, van Doorn R, *et al.* (2020). The Genera of Fungi – G6: *Arthrographis, Kramasamuha, Melnikomyces, Thysanorea,* and *Verruconis. Fungal Systematics and Evolution* **6**: 1–24.

Hou LW, Hernández-Restrepo M, Groenewald JZ, *et al.* (2020). Citizen science project reveals high diversity in *Didymellaceae* (*Pleosporales, Dothideomycetes*). *MycoKeys* **65**: 49–99.

Jiménez M, Huerta T, Mateo R (1997). Mycotoxin production by *Fusarium* species isolated from bananas. *Applied and Environmental Microbiology* **63**: 364–369.

Kozlov AM, Darriba D, Flouri T, *et al.* (2019). RAxML-NG: A fast, scalable, and user-friendly tool for maximum likelihood phylogenetic inference. *Bioinformatics* **35**: 4453–4455.

Leslie JF, Summerell BA (2006). *The Fusarium Laboratory Manual*. Blackwell Publishing Professional, USA.

Lombard L, Sandoval-Denis M, Lamprecht SC, *et al*. (2019). Epitypification of *Fusarium oxysporum* – clearing the taxonomic chaos. *Persoonia* **43**: 1–47.

Lombard L, van der Merwe NA, Groenewald JZ, *et al*. (2015). Generic concepts in *Nectriaceae*. *Studies in Mycology* **80**: 189–245.

Maryani N, Lombard L, Poerba YS, *et al*. (2019a). Phylogeny and genetic diversity of the banana Fusarium wilt pathogen *Fusarium oxysporum f. sp. cubense* in the Indonesian centre of origin. *Studies in Mycology* **92**: 155–194.

Maryani N, Sandoval-Denis M, Lombard L, *et al*. (2019b). New endemic *Fusarium* species hitch-hiking with pathogenic *Fusarium* strains causing Panama disease in small-holder banana plots in Indonesia. *Persoonia* **43**: 48–69.

Minh Q, Schmidt HA, Chernomor O, *et al*. (2020). IQ-TREE2: new models and efficient methods for phylogenetic inference in the genomic era. *Molecular Biology and Evolution* **37**: 1530–1534.

Nguyen LT, Schmidt HA, von Haeseler A, *et al*. (2015). IQ-TREE: a fast and effective stochastic algorithm for estimating maximum-likelihood phylogenies. *Molecular Biology and Evolution* **32**: 268–274.

Nirenberg HI (1976). Untersuchungen über die morphologische und biologische Differenzierung in der *Fusarium*-Sektion *Liseola*. *Mitteilungen aus der Biologischen Bundesanstalt für Land- und Forstwirtschaft Berlin-Dahlem* **169**: 1–117.

O'Donnell K, McCormick SP, Busman M, *et al*. (2018). Marasas *et al*. 1984 "Toxigenic *Fusarium* species: Identity and mycotoxicology" revisited. *Mycologia* **110**: 1058–1080.

© 2021 Westerdijk Fungal Biodiversity Institute

Rayner RW (1970). *A mycological colour chart*. CMI and British Mycological Society, Kew, Surrey, UK.

Ronquist F, Huelsenbeck JP (2003). MrBayes 3: Bayesian phylogenetic inference under mixed models. *Bioinformatics* **19**: 1572–1574.

Rossman AY, Seifert KA, eds (2011). Phylogenetic revision of taxonomic concepts in the *Hypocreales* and other *Ascomycota* - A tribute to Gary J. Samuels. *Studies in Mycology* **68**: 1–256.

Rossman AY, Seifert KA, Samuels GJ, *et al*. (2013). Genera of *Bionectriaceae*, *Hypocreaceae* and *Nectriaceae* (*Hypocreales*) proposed for acceptance and rejection. *IMA Fungus* **4**: 41–51.

Sandoval-Denis M, Guarnaccia V, Polizzi G, *et al*. (2018). Symptomatic *Citrus* trees reveal a new pathogenic lineage in *Fusarium* and two new *Neocosmospora* species. *Persoonia* **40**: 1–25.

Sandoval-Denis M, Lombard L, Crous PW (2019). Back to the roots: a reappraisal of *Neocosmospora*. *Persoonia* **43**: 90–185.

Schroers H-J, Gräfenhan T, Nirenberg HI, *et al*. (2011). A revision of *Cyanonectria* and *Geejayessis gen. nov*., and related species with fusarium-like anamorphs. *Studies in Mycology* **68**: 115–138.

Snyder WC, Hansen HN (1940). The species concept in *Fusarium*. *American Journal of Botany* **27**: 64–67.

Tatsuno T, Saito M, Enomoto M, *et al*. (1968). Nivalenol, a toxic principle of *Fusarium nivale*. *Chemical and Pharmaceutical Bulletin* **16**: 2519–2520.

Torbati M, Arzanlou M, Sandoval-Denis M, *et al*. (2019). Multigene phylogeny reveals new fungicolous species in the *Fusarium tricinctum* species complex and novel hosts in the genus *Fusarium* from Iran. *Mycological Progress* **18**: 119–133.

Wang MM, Chen Q, Diao YZ, *et al*. (2019). *Fusarium incarnatum-equiseti* complex from China. *Persoonia* **43**: 70–89.

Wollenweber HW, Reinking OA (1935). *Die Fusarien*. Verlagsbuchandlung Paul Parey, Berlin, Germany.

Xia JW, Sandoval-Denis M, Crous PW, *et al*. (2019). Numbers to names – reappraisal of the *Fusarium incarnatum-equiseti* species complex. *Persoonia* **43**: 186–221.

Yoshizawa T, Morooka N (1973). Deoxynivalenol and its monoacetate: new mycotoxins from *Fusarium roseum* and moldy barley. *Agricultural and Biological Chemistry* **37**: 2933–2934.

Supplementary Material: http://fuse-journal.org/

Table S1. Collection details and GenBank accession numbers of strains used in the phylogenetic trees.

© 2021 Westerdijk Fungal Biodiversity Institute

© 2021 Westerdijk Fungal Biodiversity Institute

FUSE

Fungal Systematics and Evolution

VOLUME 8
DECEMBER 2021
PAGES 129–142

doi.org/10.3114/fuse.2021.08.10

Wanted on *Agave americana*! *Hymenobolus agaves*, an overlooked introduced pathogen in the western palearctic region

M.A. Ribes[1], V. Escobio[2], R. Negrín[3], H.O. Baral[4], D.H. Pfister[5], L. Quijada[5*]

[1]Avda. Pablo Neruda 120, 28018, Madrid, Spain
[2]Calle Puerto Rico 4, 2° Drcha., 25010, Las Palmas de Gran Canaria, Canary Islands, Spain
[3]Calle Sorondongo 24, 38205, La Laguna, Tenerife, Canary Islands, Spain
[4]Blaihofstr. 42, 72074 Tübingen, Germany
[5]Department of Organismic and Evolutionary Biology, The Farlow Reference Library and Herbarium of Cryptogamic Botany, Harvard University Herbaria, 22 Divinity Avenue, Cambridge, Massachusetts 02138, USA

*Corresponding author: luis_quijada@fas.harvard.edu

Key words:
Ascomycota
Leotiomycetes
molecular systematics
morphology
taxonomy

Abstract: *Hymenobolus agaves* has been reported only in Europe and Africa on the American plant *Agave americana* (*Asparagaceae*). This fungus has never been found in the native range of its host, in arid ecosystems of northern and central Mexico and Texas, USA. It has been suggested to be a pathogen that can kill its host. The fungus grows on succulent leaf bases of the plant. The morphology – black apothecia with a hymenium that disintegrates when asci mature and dark ornamented ascospores – make this species very distinctive, but it has been collected and reported only a few times since its first description. Its systematic position has been unclear, and it has been treated as *incertae sedis,* that is of uncertain placement, in *Leotiomycetes*. With recent collections and additional data on the ecology of *H. agaves*, we use integrative taxonomy (DNA sequences, morphology, ecology) to show its relationships is with *Cenangiaceae*.

Citation: Ribes MA, Escobio V, Negrín R, Baral HO, Pfister DH, Quijada L (2021). Wanted on *Agave americana*! *Hymenobolus agaves*, an overlooked introduced pathogen in the western palearctic region. *Fungal Systematics and Evolution* **8**: 129–142. doi: 10.3114/fuse.2021.08.10
Received: 26 August 2021; **Accepted:** 18 October 2021; **Effectively published online:** 9 November 2021
Corresponding editor: P.W. Crous

INTRODUCTION

The genus *Hymenobolus* Durieu & Mont. was established with a single species, *H. agaves* (Montagne 1845). The type specimen was collected by M.C. Durieu on the underside of dead leaves of *Agave americana* in Algeria in the hills around Bab-el-Oued. Montagne (1845) described the macro- and micro-morphology but gave no measurements and later it was illustrated in Durieu & Bory (1849: pl. 29 fig. 2, in Saccardo 1889 erroneously as pl. 28). Several years later, he added measurements for asci and ascospores (Montagne 1856). *Hymenobolus agaves* was described as an erumpent, cupulate discomycete, 2–4 mm diam, leathery, brownish black, at first closed, opening with a stellate aperture. The hymenium was described as concolorous, waxy, blackish pruinose, and finally smooth. The 8-spored cylindrical asci were 120–160 µm long, and the *pars sporifera* was 100–120 × 8–9 µm. The ascus apex was described as rounded to obtuse, and the base gradually attenuated. The aseptate, oblong-ellipsoid ascospores measured 15–20 × <10 µm, and were noted to be at first hyaline then blackish brown especially at the poles, with 1–2 large guttules. The paraphyses were described as filiform. Montagne (1845) compared *Hymenobolus* with *Ascobolus* mentioning that the asci of both genera disperse their pigmented spores in the same way. He also remarked that *Hymenobolus* differed from all other genera of "*Ordo Patellariacei*" by a unique feature, the destruction or complete disappearance of the hymenium shortly after the apothecia were fully exposed, therefore the asci are difficult to observe (see also Saccardo 1889).

After Montagne's publications, some authors pointed out morphological similarities and relationships with other genera. For example, Boudier (1907) compared *Hymenobolus* with *Velutaria*, probably thinking of *V. rufoolivacea* (now *Velutarina rufoolivacea*), which is leathery, more colorful, not obviously erumpent and lacks a stroma. Both genera have similar ellipsoid, guttulate ascospores that change from hyaline to dark olive brown during development (Boudier 1907). Höhnel (1918) reviewed a collection of *H. agaves* made by O. Jaap and provided additional details about the excipulum which he found to be formed of parallel cells in two layers, an outer layer with yellowish, waxy, incrusted hyphae, and an inner brownish layer. He also mentioned that the asci did not turn blue in iodine. Nannfeldt (1932) compared *Hymenobolus* with *Odontotrema* and *Therrya* because of the carbonaceous consistency of the ascomata and the well-developed excipulum. The most recent detailed description of *Hymenobolus agaves* was that of Rieuf (1962). His description and measurements agree with those of Montagne (1845, 1856), Rieuf provided some interesting additional details.

Fungal Systematics and Evolution is licensed under a Creative Commons Attribution-NonCommercial-ShareAlike 4.0 International License

© 2021 Westerdijk Fungal Biodiversity Institute

He described the ascospores as densely, finely warted and noted four layers of excipular tissues: a hyaline subhymenium, a brownish central medullary excipulum of interwoven hyphae, which is not present at the flanks and margin, and two layers of dark cells that form the ectal excipulum and constitute the layer covering the hymenium when young. The inner of these two layers is composed of paler and slightly thick-walled cells, whereas the cortical layer is of smaller, darker cells with thicker walls. The main difference between Rieuf's (1962) and the original description lies in the ascus size, which is much larger in Rieuf's treatment (190–230 × 12–14 µm). Rieuf did not mention the iodine reaction. He remarked that asci do not mature at the same time, therefore ascospores are successively ejected and sometimes accumulate in old ascomata. Also, he said that in the Montagne herbarium in PC there are eight undated collections, all from the type locality in Algeria.

Index Fungorum (2021) and MycoBank (2021) propose *Coniothyrina agaves* as the current and valid name for *Hymenobolus agaves*. However, this is a confusion: Petrak & Sydow (1927) did not transfer *Hymenobolus agaves* to *Coniothyrina* but rather *Phoma agaves* (see also Petrak 1922–1928). Both species, *Hymenobolus agaves* and *Phoma agaves*, were collected on the same host (*Agave americana*) in the same country (Algeria) but were published in different years. Also, the combinations *Clisosporium agaves* and *Coniothyrium agaves* were based on *Phoma agaves*. These too have been erroneously assigned to *Hymenobolus agaves* in these repositories. Because of this confusion, *Phoma agaves* is listed in Index Fungorum and MycoBank without nomenclatural or taxonomic synonyms. Our study suggests that *Hymenobolus* is an accepted genus, and its type species *H. agaves* has no synonyms.

There has been no agreement on the systematic placement of *Hymenobolus*. Montagne (1845, 1856) placed the genus in the *Discomycetes* in "*Ordo IV Patellariacei*". Twenty-two years later Thümen (1878) reported it in the "*Nectriei*". Saccardo (1889) referred it to *Dermateae-Phaeosporae*, and Boudier (1907) agreed by placing it in the family *Dermateaceae*. Höhnel (1917) placed *Hymenobolus* in *Phacidiaceae*, considering the asci to be inoperculate, but only a year later he revised this view and suggested that it belonged among the operculate *Discomycetes* (Höhnel 1918). In his revision of inoperculate *Discomycetes*, Nannfeldt (1932) agreed with Höhnel's (1917) earlier family placement and included *Hymenobolus* in *Phacidiaceae* (= *Phacidiales s*. Höhnel) within the *Helotiales*. Seaver (1951), Korf (1973), and Dennis (1978) did not include *Hymenobolus* in their treatments of inoperculate *Discomycetes*. Eriksson (1999) and Baral (in Jaklitsch *et al.* 2016) listed the genus in *Helotiales incertae sedis*. At this time *Hymenobolus* lacks a clear affiliation within the *Helotiales* (Wijayawardene *et al.* 2020), mainly because there were no DNA sequences available in repositories (GenBank, UNITE).

Hymenobolus agaves has been found mainly around the Mediterranean Sea in south Europe and north Africa. After the first report from Algeria by Montagne (1845, 1856), it was detected in Europe, first by Thümen (1878) in Coimbra (Portugal), then 22 yr later also in Portugal by Torrend, in Alfeite, on leaves of *Agaves americana* (Torrend, Fungi Selecti Exsiccati n°179, 1910), and later in 1894 in France, Golfe Juan, Château Robert (Roumeguère, Fungi Selecti Exsiccati, n°6838, 1894). Rostrup (1899) observed the species in the hothouses of the botanical garden at Copenhagen. Subsequently it was found in Lesina (now Hvar), Croatia, (Jaap 1915) and Italy, Roma, Villa Pamphili, on leaves of *Agave americana* (Saccardo 1917, "D. Saccardo" Mycotheca italica 878). Finally, Rieuf (1962) reported the species again from northwest Africa in Morocco. It invariably is found on *Agave americana*, a plant native across the arid regions of the southern USA and northern and central Mexico. *Agave americana* has been introduced worldwide (Rojas-Sandoval & Iamonico 2016); it was introduced to Europe, Africa, and the Canary Islands in the sixteenth century. Today it is naturalized in many parts of the world (Rojas-Sandoval & Iamonico 2016).

Agave americana has been traditionally used as natural fences to keep animals confined. Rieuf (1962) explained that parasitism by *Hymenobolus agaves* affects the host's leaves which makes these natural fences useless. Rieuf (1962) hypothesized that the fungus colonizes the leaves through wounds, causing necrosis, and preferentially grows at the leaf axils where water and debris accumulate. Once infected the epidermis of the leaves first changes color from yellow-green to reddish brown to black, then the area swells and is surrounded by blackened areas and then the erumpent ascomata become visible (Rieuf 1962).

Over the last several years, we have found *Hymenobolus agaves* growing on *Agave americana* in the Canary Islands. In this paper we provide new morphological information gained from the study of fresh ascomata. We also have studied collections from the type locality. DNA generated from our collections provided insights into the phylogeny of the genus as well as new ecological information. This work is part of a comprehensive effort to improve the knowledge of the systematics of *Leotiomycetes*.

MATERIAL AND METHODS

Specimens studied

Fresh collections of *Hymenobolus agaves*, as well as two collections of *Hymenobolus agaves* from the type locality deposited in Muséum National d'Histoire Naturelle (PC) from Montagne's herbarium (MC4796, MC4797), and one collection of *Bulgaria agaves* deposited in the Harvard University Herbaria (FH), were used for morphological comparison with previous reports and with fresh collections from the Canary Islands. Specimens were studied in fresh condition, following the methods proposed by Baral (1992), air-dried, and subsequently deposited in AH (Universidad de Alcalá) or LPA (Jardín Botánico Canario Viera y Clavijo) herbarium. Macro- and microscopic techniques follow Ribes *et al.* (2015). Apothecial sections were cut free-hand under a dissecting microscope. Sections were mounted in tap water for observing living cells, CR = Congo red to raise wall contrast, KOH = potassium hydroxide 5–10 % for killing cells or rehydrating dead specimens, IKI = iodine potassium iodide for exploring amyloid or dextrinoid reactions. The living (fresh collection) or dead state (dry collections or KOH-pretreated) of the cells was determined based on Baral (1992), we also followed his terminology to describe guttules inside cells (VBs = refractive vacuolar bodies, LBs = lipid bodies) and symbols * = living state and † = dead state. Color coding refers to Anonymous (1976). Classifications follows Jaklitsch *et al.* (2016) and Johnston *et al.* (2019). Microphotographs were made with a Nikon Eclipse E200 microscope triocular with plan-achromatic objectives corrected to infinity and with a reflex Nikon D70.

© 2021 Westerdijk Fungal Biodiversity Institute

DNA extractions, sequencing, and phylogenetic analyses

Dry apothecia from two fresh collections, AH-44758 and AH-44759, were used for DNA extractions. We sampled one apothecium from each. DNA was extracted using a Qiagen QIAmp DNA Micro Kit according to manufacturer protocols with 12 h of incubation in the lysis buffer at 56 °C. PCR amplification of three DNA regions was performed: the nuclear ribosomal internal transcribed spacer region (ITS) was amplified using primers ITS1f, 5.8SR, 5.8S, and ITS4 described by White *et al.* (1990), partial large subunit of the nuclear ribosomal DNA (LSU) was amplified using primers LR0R and LR5 (Vilgalys & Hester 1990), and translation elongation factor 1-alpha (*TEF1*) gene region using the primer pair EF1-983F and EF1-1567R (Rehner & Buckley 2005). One µL of DNA extract was used with 13.3 µL of Extract-N-Amp PCR ReadyMix (Sigma-Aldrich), 2.5 µL of each primer (10 µM) and 5.7 µL of H_2O. The thermocycler conditions to amplify ITS and LSU rDNA were: 3 min at 94 °C for initial denaturing, 35 cycles of denaturing at 94 °C for 1 min, annealing at 52 °C for 45 s, extension at 72 °C for 90 s, and a final extension for 10 min at 72 °C. Conditions were identical for *TEF1* except for annealing at 54 °C. PCR products were visualized via gel electrophoresis and sequenced by GENEWIZ (Cambridge, Massachusetts) using the same primers.

A BLASTn search was performed to compare our sequences with closely related sequences in GenBank. A phylogenetic analyses of two-gene (ITS and LSU) concatenated data was conducted. Our dataset includes sequences of *Cenangiaceae* (ingroup) and *Rutstroemiaceae/Sclerotiniaceae* (outgroup) obtained after BLASTn comparations and using also sequences included in Pärtel *et al.* (2017), Johnston *et al.* (2019) and Voglmayr *et al.* (2020). Two individual datasets for each gene were aligned using MAFFT v. 7.017 (Katoh *et al.* 2008) and trimmed with Gblocks v. 0.91 (Castresana 2000) before being concatenated. GTR + I + G model was selected to do the Bayesian inference (BI) following Quijada *et al.* (2014, 2019), and GTR for maximum likelihood (ML). Branch support in ML was inferred from 1 000 rounds of bootstrap. Both analyses were done using Geneious v. 6.1.8 and the artwork was prepared in Adobe Illustrator CS5. Information for each specimen included in the analysis with their GenBank numbers are given in Table 1.

RESULTS

Molecular comparison

All the genera currently accepted in *Cenangiaceae* (Jaklitsch *et al.* 2016, Wijayawardene *et al.* 2020) except *Hysterostegiella*, *Korfia* and *Pseudomitrula*, were included in the dataset. These genera were represented by type species where sequences existed. *Pseudomitrula* was not included because the current sequences available in GenBank showed its affiliation in *Helotiaceae* and *Lachnaceae* clades rather than *Cenangiaceae*. One sequence of *Vestigium trifidum* was included based on BLASTn results and comments in Pärtel *et al.* (2017). The combined matrix contained 34 taxa, 28 for the ingroup (*Cenangiaceae*) and six for the outgroup (*Sclerotiniaceae*, *Rutstroemiaceae*) with 1 312 nucleotide positions of which 331 were parsimony-informative, 381 were variable, and 931 were constant. The topology and supported clades for independently analyses of ITS and LSU gave the same results as the concatenated analyses of both genes (Fig. 1). We obtained ITS and LSU for two collections of *Hymenobolus agaves*, and one *TEF1* for one collection. The latter was not used in the analyses because 75 % of targeted species of *Cenangiaceae* used in our analyses do not have this gene available. But our BLASTn comparation using the *TEF1* sequence obtained for *Hymenobolus agaves* has its maximum identity (88–91 %) with genera in *Cenangiaceae* such as *Cenangiopsis*, *Trochila*, *Heyderia*, *Encoelia*, *Mycosphaerangium*, and *Neomelanconium* (unpubl. data). Our results (Fig. 1) showed that *Cenangiaceae* is strongly supported and includes *Hymenobolus*, but the backbone is mostly not supported, therefore we cannot establish generic relationships among *Cenangiaceae* using our molecular result (Fig. 1).

Morphological comparison

Genera in *Cenangiaceae* share morphological features with *Hymenobolus* (Fig. 1). Characters common to the family are: (1) erumpent apothecia; (2) two layers of excipulum: hyaline or pale medullary and dark ectal excipulum with globose-angular cells incrusted with crystals or amorphous resins; (3) surface cells containing refractive vacuolar bodies (*Encoelia*, *Mycosphaerangium*, *Neomelanconium*, *Cenangiopsis*, *Hymenobolus*, *Trochila*, *Chlorencoelia*, *Crumenulopsis*, *Velutarina p.p.*). Species of some genera only have a poorly developed dark-stromatic excipulum as in *Didimascella*, *Rhabdocline*, *Sarcotrochila*, *Trochilla p.p.* and *Fabrella*. Octosporous asci with amyloid *Calycina*-type ring are present in *Hymenobolus*, and also in *Encoelia p.p.*, *Trochila*, *Heyderia*, *Chlorencoelia*, *Sarcotrochila*, and *Velutarina p.p.* Species of some genera have inamyloid asci as in *Cenangium*, *Cenangiopsis*, *Crumenulopsis*, *Mycosphaerangium*, *Neomelanconium*, *Fabrella*. Not all species have octosporus asci, species in four genera have two (*Didymascella*) or four ascospores (*Fabrella*, *Mycosphaerangium*, *Rhabdocline*). Species of most genera have yellow brownish guttules (vacuolar bodies = VBs) in the paraphyses. Often the VBs are large and cylindrical filling most of the apical cell (*Cenangiopsis*, *Chlorencoelia*, *Encoelia*, *Heyderia*, *Hymenobolus*, *Trochila*, *Sarcotrochila*, *Velutarina p.p.*), in other cases they are small, globose, and more or less sparse (*Crumenulopsis*). Furthermore, in other instances there is a pigment around the apical cells of paraphyses which are embedded in gel (*Mycosphaerangium*, *Cenangium*, *Fabrella*). Ascospores of *H. agaves* change from hyaline to dark as they mature. This also happens in species of *Mycosphaerangium*, *Neomelanconium*, *Cenangiopsis*, *Didymascella*, *Velutarina*, and *Fabrella*. In some species the spores turn brown inside the living asci, in others only when overmature. Species of some genera develop ornamented ascospores, for example in species of *Hymenobolus*, *Mycosphaerangium*, and *Neomelanconium*, and commonly the spores are surrounded by a hyaline gelatinous sheath that does not stain with reagents.

We examined two collections from Montagne's herbarium (PC: MC4796, MC4797), both from the type locality in Algeria, and obtained the measurements given in Table 2. Ascospores were observed in both collections, but asci were only seen in one, MC4796. Dead asci of the Canary Islands collections were much longer but also wider than those of MC4796. Measurements of dead ascospores from the Canary Islands specimen agreed well with those from Algeria. They were close to MC4797, whereas those in MC4796 were distinctly wider and also longer (Table 2). We also studied one collection by

© 2021 Westerdijk Fungal Biodiversity Institute

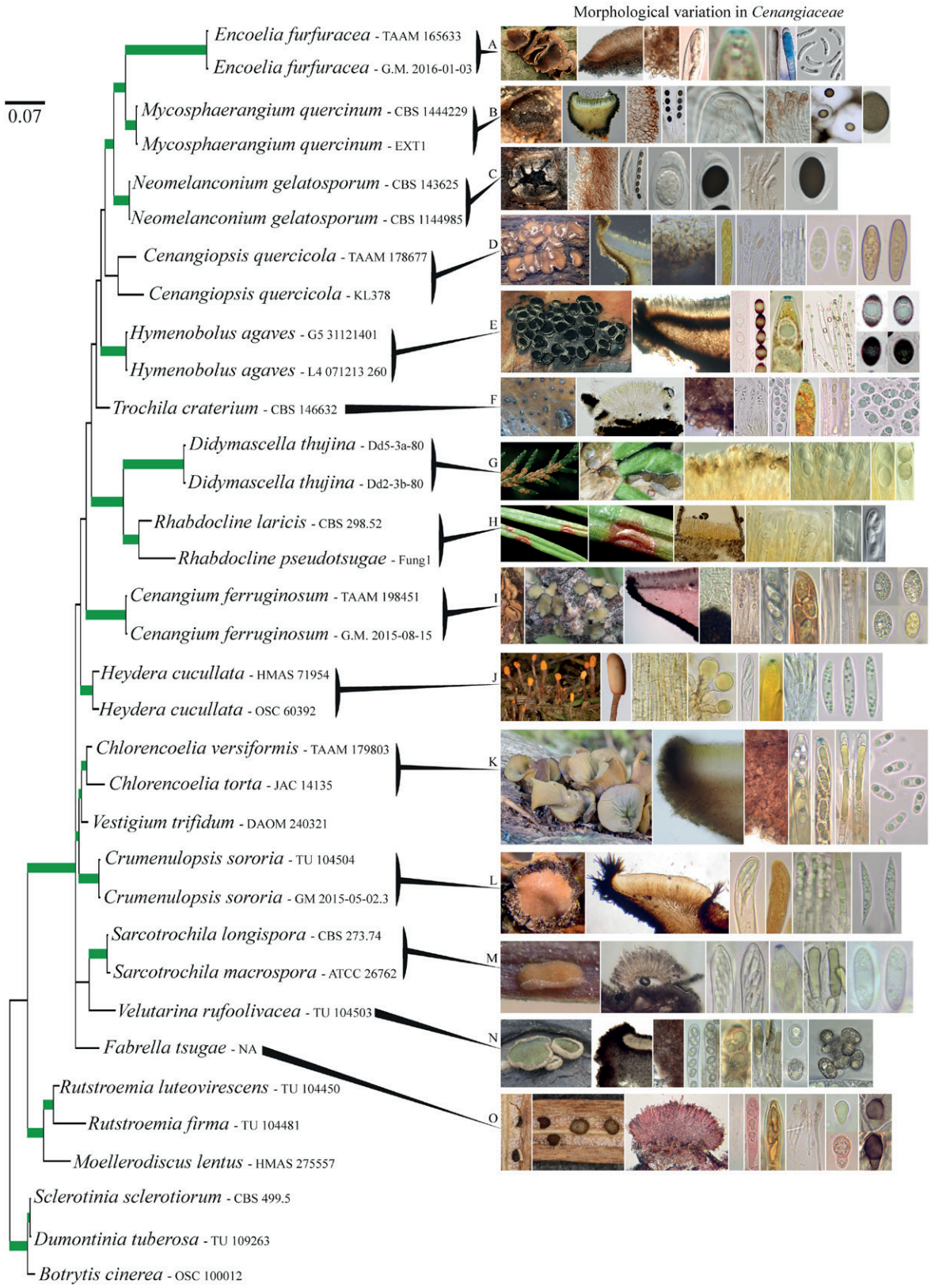

Fig. 1. Bayesian majority-rule consensus tree based on concatenated ITS and LSU sequences. Bold branches are those that were well supported by ML (>95%) and/or BI (>0.95) methods. At the right, details for species of each genus included in the phylogeny for morphological comparison, across the family, of apothecia, excipula, asci, paraphyses and ascospores. **A.** *Encoelia furfuracea* (image by Charles Etienne & Kadri Pärtel). **B.** *Mycosphaerangium tetrasporum*, *M. quercinum* and *M. magnisporum* (images by Hermann Voglmayr & Salvador Tello). **C.** *Neomelanconium gelatosporum* (images by Hermann Voglmayr & Salvador Tello). **D.** *Cenangiopsis alpestris* and *C. raghavanii* (images by Salvador Tello). **E.** *Hymenobolus agaves* (images by Miguel Ángel Ribes). **F.** *Trochila craterium* and *T. bostonensis* (images by Miguel Ángel Ribes & Luis Quijada). **G.** *Didymascella thujina* (images by Bruce Watt). **H.** *Rhabdocline* sp. (images by Bruce Watt). **I.** *Cenangium ferruginosum* (images by Miguel Ángel Ribes & Luis Quijada). **J.** *Heydera cucullata* (images by Dragisa Savić & Matthias Reul). **K.** *Chlorencoelia torta* and *C. versiformis* (images by Miguel Ángel Ribes & Luis Quijada), **L.** *Crumenulopsis* sp. (images by Dragisa Savić, Hans Otto Baral, Juuso Äikäs & Urs Roffler). **M.** *Sarcotrochila alpina* (images by Piotr Perz, Hans Otto Baral & Ingo Wagner). **N.** *Velutarina olivacea* (image by Luis Quijada). **O.** *Fabrella tsugae* (images by Luis Quijada).

© 2021 Westerdijk Fungal Biodiversity Institute

Table 1. Species used in this study with voucher information and GenBank accession numbers. New sequences are indicated in bold.

Taxon	Voucher/culture	ITS	LSU
Botrytis cinerea	OSC100012	DQ491491	AY544651
Cenangiopsis alpestris	KL378	LT158470	KX090839
Cenangiopsis quercicola	TAAM178677	LT158425	KX090811
Cenangium ferruginosum	TAAM198451	LT158471	KX090840
	GM-2015-08-15	KY462796	KY462796
Chlorencoelia torta	JAC14135	MK432802	MK431494
Chlorencoelia versiformis	TAAM 179803	LT158427	KX090795
Crumenulopsis sororia	TU104504	LT158442	KX090826
	GM-2015-05-02.3	KY941133	KY941133
Didymascella thujina	Dd5_3a_800.SCF	KT875767	–
	Dd2_3b_800.SCF	KT875766	–
Dumontinia tuberosa	TU109263	–	KX090843
Encoelia furfuracea	TAAM165633	LT158416	KX090798
	G.M. 2016-01-03.1	MT508552	MT508552
Fabrella tsugae	–	U92304	AF356694
Heyderia abietis	HMAS71954	AY789297	AY789296
	OSC60392	AY789290	AY789289
Hymenobolus agaves	**AH-44758**	**MZ678630**	**MZ700691**
	AH-44759	**MZ678631**	**MZ700692**
Moellerodiscus lentus	HMAS 275557	KU668566	MH729337
Mycosphaerangium quercinum	CBS 144229	MT952893	MT952893
Mycosphaerangium quercinum	EXT1	MT952892	MT952892
Neomelanconium gelatosporum	NG = CBS 143625	MT952889	MT952889
	CBS 144985	MN313810	MN317291
Rhabdocline laricis	CBS 298.52	KT225534	DQ470954
Rhabdocline pseudotsugae	Fung1	KP001552	–
Rustroemia luteovirescens	TU 104450	LT158431	KX090814
Rutstroemia firma	TU104481	LT158450	KX090832
Sarcotrochila longispora	CBS 273.74	KJ663836	KJ663877
Sarcotrochila macrospora	ATCC 26762	AY645900	–
Sclerotinia sclerotiorum	CBS 499.5	MH856725	DQ470965
Trochila craterium	CBS 146632	MT363247	MT363246
Velutarina rufoolivacea	TU104503	–	KX090825
Vestigium trifidum	DAOM240321	KC407777	KC407777

Table 2. Comparison of measurements of dead asci and ascospores of *Hymenobolus agaves* from Canary Islands and Algeria (authentic material of Montagne) and the original description (Montagne 1856), Saccardo (1889), Rieuf's revision (1962), and observations on the invalid *Bulgaria agaves* (*Herbarium vivum mycologicum* Centurie XIII n° 1223).

Hymenobolus agaves	**Asci (µm)**	**Ascospores (µm)**
Montagne (1856)	120–160	15–20 × <10
Saccardo (1889)	100–120 × 8–9 (*Pars sporifera*)	15–17 × 8
Rieuf (1962)	†190–230 × 12–14	†13–17 × 8–11
Canary Islands	†(192–)198–260(–277) × (10–)11–14.5(–16)	†(11.8–)12.5–14(–15) × (6.4–)7–8(–9)
Algerie (MC4796)	†(151–)160–184(–188) × (8.2–)9–12.5(–13.3)	†(13–)13.4–15.3(–15.8) × (8.1–)8.9–10.7(–11.4)
Algerie (MC4797)	n/a	†(11.7–)12.3–13.5(–14.7) × (6.6–)7.2–8.4(–8.8)
Bulgaria agaves	†11–16 width	†11.7–14.3 × 6.9–8.7

© 2021 Westerdijk Fungal Biodiversity Institute

Rabenhort in *Klotzschii Herbarium vivum mycologicum* (1223, fig. 6) preserved at FH under the invalid name *Bulgaria agaves*, the morphology and biometry agreed with that found in our study of the two collections from Montagne's herbarium and our recently collected specimens from the Canary Islands.

Taxonomy

Hymenobolus agaves Durieu & Mont., *Annls Sci. Nat., Bot.,* sér. 3 **4**: 360. 1845. Figs 2–5.
Synonym: *Bulgaria agaves* Rabenh., *Bot. Ztg*. **7**: 293. 1849. *nom. nud.*

Classification: *Cenangiaceae*, *Helotiales*, *Leotiomycetes*, *Pezizomycotina*, *Ascomycota*, *Fungi*.

Description based on our collections: *Apothecia* densely gregarious in clusters of up to 30–40, rarely solitary or in groups of 2–4, (1.5–)2–4(–6) mm diam, 1.1–1.3 mm thick (1.5–2 mm including stroma), emerging from a common stromatic blackened area, erumpent from beneath the epidermis, at first globose and closed (cleistohymenial), opening by irregular clefts when mature, broadly sessile, discoid-urceolate, ± circular or slightly deformed by mutual pressure in dense clusters (Fig. 2). Disc concave to flat with waxy to pulverulent consistency, non-gelatinous, dark grayish brown (62.d.gyBr) to black (267. Black); receptacle leathery, exterior light greyish-yellow-brown (79.l.gy.yBr) to dark gray (266.d.Gray), margin protruding by 0.2-0.27(–0.3) mm, concolorous, smooth, irregularly lacerate, strongly inrolled when dry. *Subhymenium* pale to medium yellow-brown (77.m.yBr) to deep brown (55.s.Br), 60–90 µm thick, of *textura globulosa-angularis* to *intricata*. *Medullary excipulum* hyaline to light olive brown (94.l.OlBr), of vertically oriented *textura globulosa-angular-prismatica*, *(300–)315–365(–400) µm thick in centre, cells *(22.5–)27.5–47.5(–50) × (15.3–)18–26(–35) µm (AH-44757); cell thin-walled and hyaline, close to the subhymenium, but thicker and embedded in deep yellow-brown amorphous substance (75.deepyBR) towards the base and flanks. *Ectal excipulum* brown-orange (54.brO) to dark purplish brown (59.d.Br), of *textura pismatica-angularis* to *epidermoidea*, *(200–)210–275(–325) µm thick, cells *(22.5–)29–41.5(–58.5) × (13–)13.5–20(–21.5) µm (AH-44757); oriented parallel to the outside, thick-walled *(1.1–)1.5–2.7 (–3.1) µm (AH-44757), with dark brown (59.d.Br), amorphous resinous exudate. Excipulum pigmentation does not change when mounted in KOH, no pigment dissolves into medium. *Asci* cylindrical in upper part, with 8 irregularly obliquely biseriate (†uniseriate) ascospores, *(262–)278–302(–305) × (14.1–)15–17.5(–18.8) µm (AH-44758); †(192–)198–260(–277) × (10–)11–14.5(–16) µm (LPA SMGC11106; H.B. 9262), *pars sporifera* *55–65 µm (AH-44758), †110–140 µm (LPA SMGC11106, H.B. 9262), apex hemispherical in living material, thin-walled (~0.6 µm), broadly conical and somewhat truncate above when dead, slightly thick-walled, lateral wall subapically thickened to 1–1.5 µm, apical thickening almost entirely occupied by a euamyloid apical ring staining deep blue in IKI with or without KOH-pretreatment, ring immature 3–3.5 × 3–3.5 µm, mature 3.5–4 × 1.5–2 µm, resembling the *Calycina*-type but also the *Pezicula*- or *Bulgaria*-type (Fig. 4C1–C2), croziers present. *Ascospores* ellipsoid or sometimes slightly fusoid-ovoid, *(13–)13.5–15 (–15.5) × (8–)8.5–9.5(–10.3) µm (LPA SMGC11106; H.B. 9262), †(11.8–)12.5–14(–15) × (6.4–)7–8(–9) µm (AH-44757); hyaline when immature, deep brown (59.d.Br) when mature (prior to ejection), appearing much darker at the poles, thin-walled (wall *ca*. 0.2–0.3 µm); containing one large central lipid body 4–7 µm diam. and some much smaller scattered ones around (rarely two large LBs of different sizes); wall surface ornamented with small warts of *ca.* 0.2–0.5 µm diam, ascospore entirely surrounded by a 2–4 µm thick hyaline gelatinous sheath which does not stain in CRB and later inflates to 5–9 µm (Fig. 4E2–E3); overmature ascospores germinate only on one side (Fig. 4E4). *Paraphyses* cylindrical, slightly enlarged toward the rounded apex, apical cells *(39.5–)46.7–58(–70) × (4–)4.6–6.8(–7.1) µm (LPA SMGC11106, H.B. 9262); †(23–)24.5–37(–46) × (3.4–)3.8–4.9(–5.2) µm (AH-44758), lower cell *(26.5–)35–51(–55) × (2.3–)2.7–4.4(–4.8) µm (LPA SMGC11106, H.B. 9262); unbranched; containing a cylindrical subhyaline, low-refractive VB occupying the entire apical cell in intact mature paraphyses and/or scattered globose, light yellowish olive (106.l.Ol), in damaged paraphyses VB coagulated (precipitation of vacuolar contents forms strongly refractive bodies with more intense color) of 2.5–4 µm diam. in apical cells, about 3–4 per cell, disappearing in dead cells.

Habitat (specimens from Canary Islands): on dead leaves of *Agave americana*.

Drought tolerance: Asci and ascospores are still alive after about 1 mo.

Phenology: November to March, also in July.

Specimens examined (all on leaves of *Agave americana*): **Algeria**, Algiers province, NE of Algiers, Bab-el-Oued hills, 1845, *M.C. Durieu*, MC4796; *idem*., 1845, *M.C. Durieu*, MC4797. **Germany**, undated, without location and collector (Herbarium vivum mycologicum Centurie XIII n° 1223 preserved in FH). **Spain**, Canary Islands, Gran Canaria, Teror, Finca de Osorio, in the monteverde area in north-facing midlands, 28°04'19.2"N, 15°33'02.1"W, 718 m, 17 Mar. 2010, *J. Muñoz & V. Escobio*, LPA SMGC11106, H.B. 9262; *idem*., La Gomera, Valle Gran Rey, Acardece, La Quintana dam, in a humid zone influenced by trade winds, 28°08'28.7"N, 17°18'30.0"W, 900 m, 13 Feb. 2013, *R. Negrín*, AH-44757; *idem*., Valle Gran Rey, Arure, general highway, 28°07'58.0"N, 17°19'18.1"W, 806 m, 7 Dec. 2013, *R. Negrín*, AH-44758; Vallehermoso, Alojera Road, 28°10'05.9"N, 17°18'24.1"W, 610 m, 31 Dec. 2014, *R. Negrín*, AH-44759; *idem*., La Palma, Breña Baja, 28°38'13.66"N, 17°46'34.01"W, 345 m, 22 Nov. 2015, *C.C. Rodríguez, F. Govantes & V. Escobio*, LPA SMGC2015112203; *idem*., Gran Canaria, Guía, 28°03'12.63"N, 15°37'38.33"W, 1 170 m, 16 Dec. 2015, *V. Escobio & C. Lantigua*, LPA SMGC2015121601; Telde, San Roque gorge, 28°00'19.2"N, 15°28'01.0"W, 283 m, 7 Mar. 2018, *V. Escobio*, LPA SMGC2018030702; *idem*., El Hierro, Valverde, Montaña del Hombre Muerto, 27°48'56.8"N, 17°54'57.8"W, 601 m, 17 Mar. 2018, *M. Pérez & V. Escobio*, LPA SMGC2018031702; Valverde, Los Cangrejos airport, 27°48'46.92"N 17°53'19.54"W, 34 m, 23 Jul. 2019, *V. Escobio & C.C. Rodríguez*, LPA SMGC2019072301; *idem*., Fuerteventura, Betancuria, San Buenaventura abbey, 28°25'41.08"N, 14°03'26.88"W, 409 m, 17 Feb. 2019, *C.C. Rodríguez & V. Escobio*, LPA SMGC2019021701; *idem*., Lanzarote, Conil, Tías, Montaña Testeina, 28°59'03.08"N, 13°40'13.15"W, 362 m, 2 Jul. 2019, *V. Escobio, J. Gil & M. Dossena*, LPA SMGC2019070201; Máguez, Haría, 29°09'22.20"N, 13°29'56.80"W, 258 m, 2 Jul. 2019, *V. Escobio & M. Dossena*, LPA SMGC2019070202.

© 2021 Westerdijk Fungal Biodiversity Institute

Fig. 2. Macroscopic features of *Hymenobolus agaves.* **A.** Environment with *Agave americana*. **B.** Base of leaves. **C.** Immature apothecia. **D.** Mature apothecia. **E.** Transversal section of ascomata and basal stroma. Scale bars: B, C = 20 mm; D, E = 10 mm. Photos: A1 = LPA SMGC2019072301; A2 = LPA SMGC2019070202, B, C2–E = LPA SMGC11106, H.B. 9262; C1 = LPA SMGC2015112203.

© 2021 Westerdijk Fungal Biodiversity Institute

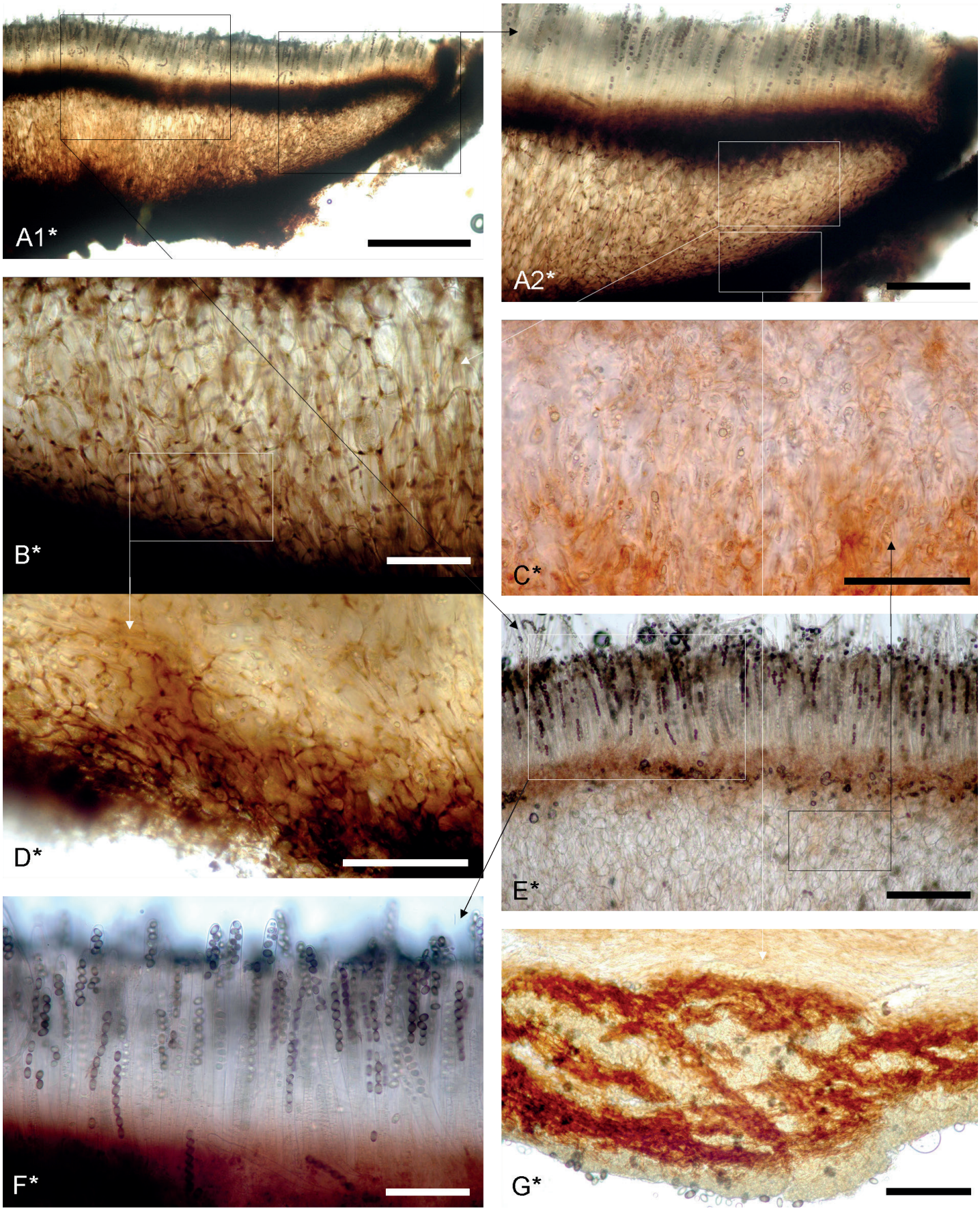

Fig. 3. Excipular characteristics of *Hymenobolus agaves*. **A.** Transverse sections showing layers of the excipulum. **B, D.** Ectal excipulum. **C.** Medullary excipulum. **E–F.** Hymenium, subhymenium and medulla. **G.** Cortical cells of ectal excipulum. Scale bars: A1 = 500 µm; A2, E = 200 µm; B–D, F, G = 100 µm. Reagents: A–G = H_2O. Photos: A, B, F = AH-44758; C, D = AH-44757; E, G = LPA SMGC11106, H.B. 9262.

© 2021 Westerdijk Fungal Biodiversity Institute

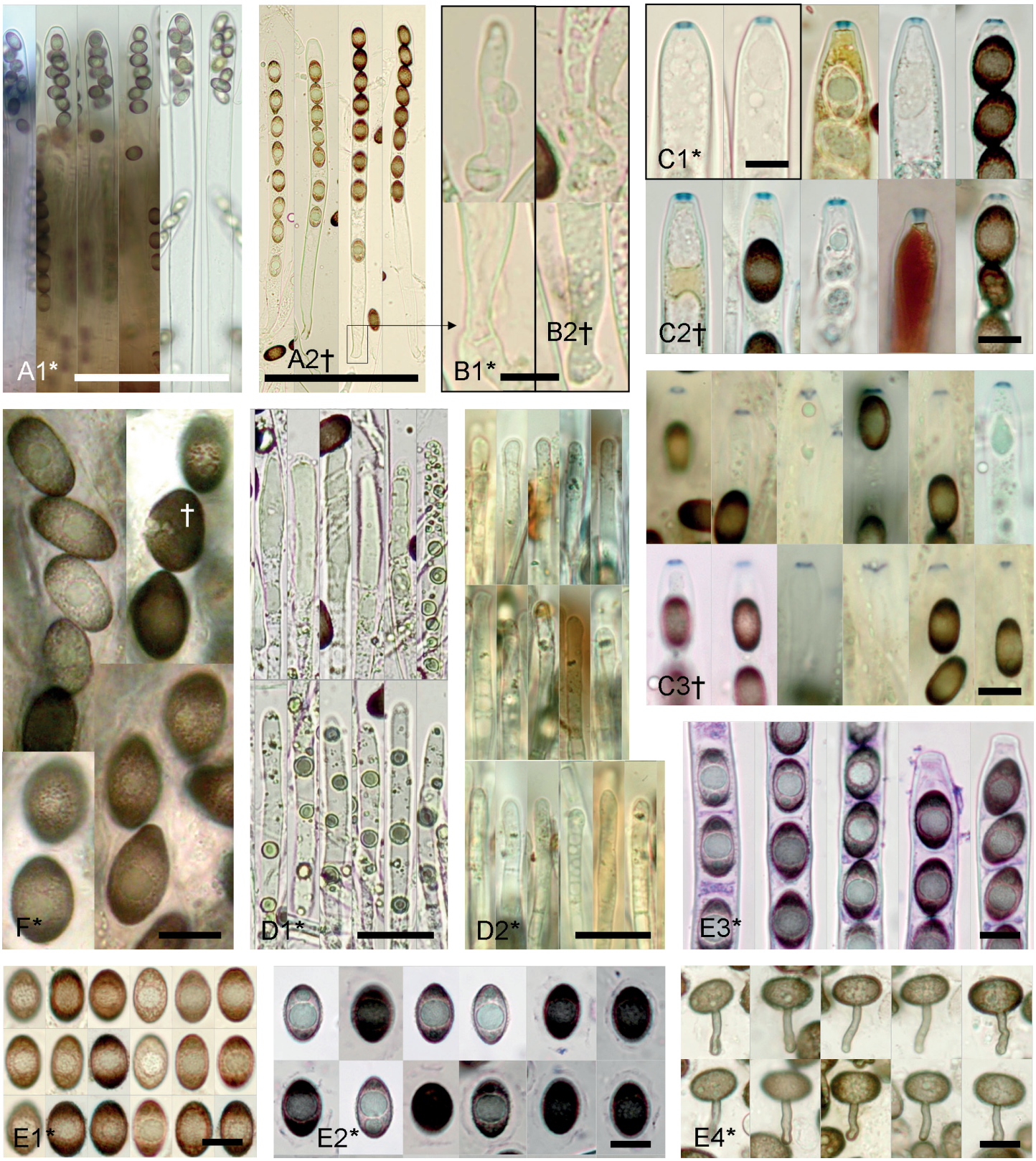

Fig. 4. Asci, paraphyses and ascospores of *Hymenobolus agaves*. **A.** Asci. **A1.** Living asci with mature biseriate ascospores. **A2.** Dead asci with mature uniseriate ascospores. **B.** Ascus base with croziers. **B1.** Living ascus base with croziers. **B2.** Dead ascus base with croziers. **C.** Ascus apical rings in IKI. **C1.** Living apical rings. **C2.** Dead apical rings. **C3.** Dead apical rings with KOH-pretreated, three asci emptied, with everted ring. **D.** Paraphyses. **D1.** Living paraphyses. **D2.** Dead paraphyses. **E.** Ascospores. **E1.** Free ascospores in water after ejection. **E2.** Free ascospores after ejection, in CRB. **E3.** Mature ascospores with gelatinous sheaths inside the asci, in CRB. **E4.** Ascospores with germ tubes, in water. **F.** Ascospore ornamentation in water. Scale bars: A = 100 µm; D = 20 µm; B, C, E, F = 10 µm. Reagent: A, B, D, E1, E4, F = H_2O; C = IKI; E2, E3 = CRB. Photos: A1, D2, E4 = AH-44758; C3 = AH-44757; A2, B, C1, C2, D1, E1–E3, F = LPA SMGC11106, H.B. 9262.

© 2021 Westerdijk Fungal Biodiversity Institute

Fig. 5. Morphological details of Montagne's collections MC4796 and MC4797 of *Hymenobolus agaves* preserved in PC herbarium. **A.** Packets with information about the collections. **A1.** MC4796. **A2.** MC4797. **B.** Apothecia and host substrate for MC4796. **C.** Transverse sections with details of hymenium and subhymenium. **D.** Upper part of asci. **E.** Ascus apical rings in IKI. **F.** Ascospores. **F1.** Ascospores inside asci artificially widened by pressure on cover slip. **F2.** Free ascospores in CRB. **F3.** Free ascospores in water (from MC4794 collection, poorly preserved). Scale bars: B = 20 mm; C = 100 µm; D = 50 µm; E, F = 10 µm. Reagent: C, D1, F1, F3 = H_2O; E = IKI; D2, F2 = CRB. Photos: A1, B–F2 = MC4796; A2, F3 = MC4797.

DISCUSSION

In this study we provided strong morphological and phylogenetic evidence to support the placement of *Hymenobolus* in *Cenangiaceae* (*Helotiales*). Since its erection the genus has been confusingly placed in *Pezizomycotina* even though its morphology is distinctive. The description provided by Montagne (in Montagne 1845, 1856, and Duriey & Bory 1849) was quite precise and lacking only data on excipulum structure and ascus iodine reaction, but there is misinterpretation of some features of the ascospores. Following Montagne several authors provided additional details about the excipulum and provided accurate information about the ascospores (Boudier 1907, Höhnel 1918, Nannfeldt 1932). This was summarized by Rieuf (1962), who made a thorough description that included the number of layers in the excipulum, differences among them, ascus biometric differences, and noted changes in color and ornamentation of the ascospores during maturation. He further pointed out ecological information regarding the development of the apothecia on the host. We agree with all the morphological and ecological details in the various cited papers except for Höhnel's (1918) statement that the asci are inamyloid and operculate (all other authors neglected to report the iodine reaction). We have provided additional information about the

© 2021 Westerdijk Fungal Biodiversity Institute

excipulum, asci, ascospores and paraphyses from the study of living, fresh collections. For example: (1) pigmentation of the excipulum is due to amorphous substances in the walls of the cells and this pigmentation does not change when KOH is added, (2) ascospores are uniseriate in arrangement but only when asci are dead, living mature asci have irregularly biseriate ascospores before their ejection (Fig. 4A1), (3) ascospores are brown when inside the living asci, (4) they consistently germinate laterally by a germ tube (Fig. 4E4), and (5) the paraphyses contain large globose or elongated vacuolar bodies (Fig. 4D1) that can be observed only in fresh material. We also found differences in ascus size among the Canary Islands specimens, the collections examined from Montagne's herbarium, and measurements in the original description of the species. Rieuf's measurements for asci are in good concordance with the measurements from our collections, whereas our measurements from Montagne's specimens and those in the original description of the species (Montagne 1856) were distinctly smaller (Table 2). This led us to conclude that immature and mature asci have been mixed during the examinations made by different authors, and probably most mature asci, the largest ones, cannot be measured well in dried preserved specimens. This explains these differences in biometry.

Only Höhnel (1918) thought *Hymenobolus* could be related to operculate discomycetes. All other authors compared *H. agaves* with various genera in inoperculate discomycetes in "*Patellariacei*", *Dermateae-Phaeosporae* or *Phacidiaceae* (Montagne 1856, Saccardo 1889, Boudier 1907, Nannfeldt 1932, Höhnel 1917). *Hymenobolus agaves* has been placed in different tribes, families or orders throughout its history, but after reviewing our molecular results, which pointed to the placement of *H. agaves* in *Cenangiaceae* (Fig. 1), we can say that only Boudier was correct in comparing *Hymenobolus* with *Velutarina* because both genera are currently in the same family and share several morphological features. Species of most genera in *Cenangiaceae* have erumpent apothecia, and one layer of dark ectal excipulum with globose-angular cells. But, in contrast to species of other genera that develop on leaves (*Didymascella*, *Fabrella*, *Sarcotrochila*, *Rhabdocline* and *Trochila*), *H. agaves* has a well-developed excipulum that is thick and differentiated into more than one layer, it also has incrusted cells with crystals or amorphous resins. This type of excipulum resembles more that of wood-inhabiting species (*Cenangium*, *Cenangiopsis*, *Chlorencoelia*, *Crumenulopsis*, *Encoelia*, *Mycosphaerangium*, *Neomelanconium*, *Velutarina*) than those growing on leaves. Probably this is an adaptation of *H. agaves* to the succulent leaves of *Agave*, which have a consistency, thickness, and decay process clearly different from leaves on which members of typical leaf-inhabiting species grow. Macroscopically, but also microscopically, we can say that the species most similar to *H. agaves* are those in *Mycosphaerangium* and *Neomelanconium* (Fig. 1). They have similar apothecia, excipula, paraphyses, and dark, ornamented ascospores with sheaths. The main differences of *Hymenobolus* are the hosts (wood *vs*. leaves), ascus pore (inamyloid *vs*. amyloid), and the asexual morph (present *vs*. absent). More studies are needed in *Cenangiaceae* to better define generic relationships based on DNA sequence analyses.

Another species was described in *Hymenobolus*, *H. kmetii*, on branches of *Quercus* in Hungary. It was described as having 4-spored asci. The description in Saccardo & Trotter (1913) is reminiscent of the recently described *Mycosphaerangium quercinum* (Voglmayr *et al.* 2020), for which it might provide an earlier name. *Hymenobolus parasiticus* refers to a myxomycete. This was based on *Hymenobolus* Zukal, a later generic homonym, and was later transferred to *Licea* (*Myxogastria*).

Höhnel (1918) mentioned *Bulgaria agaves* (*Botanische Zeitung* **7**: 293 no. 23, 1849), which he considered to be a possible synonym of *Hymenobolus agaves*. However, no published diagnosis of *B. agaves* could be found. Saccardo (1892) only remarked that it was on *Agave* in Germany. The collection was distributed in Klotzsch 1849 (*Herbarium vivum mycologicum, Centurie* **XIII**: N° 1223), but no published description or diagnosis was included in this *exsiccatae*. Braun (2018) considered it a *nomen nudum*. The specimen preserved in FH includes several erumpent apothecia on leaves of *Agave americana*. The larger apothecia had only stroma or excipular tissues but one of the medium-sized apothecia (Fig. 6A1 black arrow) has part of the hymenium preserved. Our morphological study confirmed that *B. agaves* is indeed a synonym of *H. agaves*. We were able to observe all the distinctive features of the species, such as ascus width (†11–16 µm), amyloidity of ascus apical ring, hyaline immature and brown mature ascospores (†11.7–14.3 × 6.9–8.7 µm) with warted surface, lipid guttules within the ascospores, sheaths surrounding the ascospores, cylindrical paraphyses that are slightly enlarged toward apex, and several layers of dark colored excipular cells, some of them with thick walls (Fig. 6).

Hymenobolus agaves has been found so far only on *Agave americana*. This native plant of North America grows in warm and dry ecosystems at sea level or higher altitude in hedges, valleys, slopes, cliffs, stony and sandy places. It has been introduced to Africa, Europe, Asia, Oceania, the Caribbean, and South America (Rojas-Sandoval & Iamonico 2016). It is a monocarpic succulent plant that can attain an age of 10–30 years. After blooming (spring to summer) it dies, but it also reproduces asexually via plantlets, rhizomes and suckers which allow the plant to spread quickly by forming dense colonies over time (Rojas-Sandoval & Iamonico 2016). Curiously, *H. agaves* has not been found in the native range of its host; in the wild reports only exist from around the Mediterranean Sea in South Europe and North Africa (Montagne 1845, Thümen 1878, Saccardo 1917, Rieuf 1962), and now from the Canary Islands. But also, our revision of *Bulgaria agaves* allows us to confirm that this species may occur in other continental areas of Europe such as Germany. However, we cannot confirm if it was collected in the wild or made in a hothouse similar to the one reported by Rostrup (1899) in Copenhagen.

During our collecting trips and explorations of *H. agaves* in the Canary Islands, we found several interesting details about the ecology and association with its host. The fungus was found mainly in places with dense populations of *Agave americana*, from the coast (hyperarid to arid) up to 1 170 m (subhumid) altitude. The plants on which it was found are mostly senescent with seeds and leaves that had started to decay. Rieuf (1962) described *H. agaves* as a parasite that affects healthy plants planted in rows as a fence. He described lesions produced by the fungus and how the fungus developed. We found most of our collections on senescent plants after flowering, not on healthy plants as Rieuf stated. There are reports of other species of *Cenangiaceae* as endophytes, *i.e. Cenangium* (Jurc *et al.* 2000), *Cenangiopsis* (Perić *et al.* 2015), and *Rhabdocline* (Sherwood-Pike *et al.* 1986). Therefore, given our observation and the presence of endophytes in the family, we believe *H. agaves* is an endophyte that can reproduce quickly when its host is about to die.

© 2021 Westerdijk Fungal Biodiversity Institute

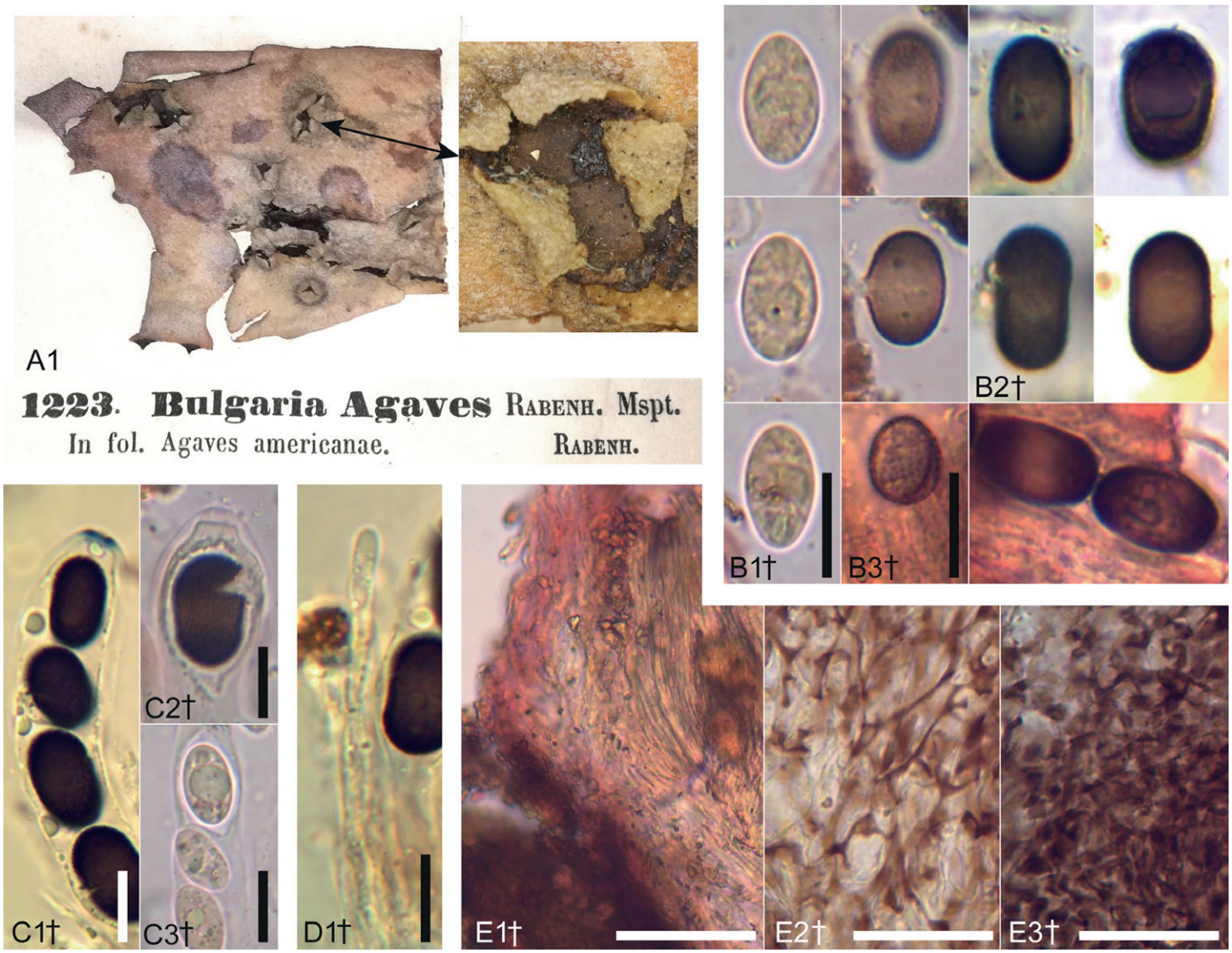

Fig. 6. Morphological details of *Bulgaria agaves* (*Klotzschii Herbarium vivum mycologicum*, Centurie XIII: n ° 1223) preserved in FH herbarium. **A1.** Macrophoto with specimen label. **B1.** Immature ascospores. **B2–3.** Mature ascospores. **C1.** Upper part of ascus with amyloid apical ring and four mature ascospores. **C2.** Ascus apex. **C3.** Immature ascospores inside the ascus. **D1.** Paraphyses. **E1.** Excipulum at margin and upper flank. **E2–3.** Ectal excipular cells. Scale bars: E1–E3 = 50 µm; B1–B3, C1–C3, D1 = 10 µm. Reagents: B1, C2, C3, E2–3 = KOH; B2, C1, D1 = IKI; B3, E1 = CR.

Hymenobolus agaves is clearly adapted to arid environments because of its morphology and the mode of ascomatal development. Ascomata develop mainly in the leaf axils, mostly protected from air currents. They are cupulate, closed when dry by the roof-like apothecial margin that protects the disintegrated hymenium that is ultimately filled with ascospores. Given the placement of the fructification, airflow cannot serve as main source of dispersal, therefore we believe that insects or water plays a critical role. Dark-colored spores have been correlated with species in arid ecosystems to prevent damage by UV exposure (Durrell 1964, Kawamura *et al.* 1999, Coline *et al.* 2020). *Hymenobolus agaves* has dark-colored ascospores that are ornamented and surrounded by a gelatinous sheath (Fig. 4). Spores with these characteristics have been correlated with insect dispersal (Magyar *et al.* 2016). We found that ascospores of *H. agaves* remain alive for 20–30 d or more in the dry state and spores germinate quickly in response to an increase in humidity or under constant humidity (Fig. 4E4). Rieuf (1962) without demonstrating pathogenicity indicated it can kill plants. We believe that *H. agaves* is an endophyte, that sporulates when the host is dying. Insects are probably very important vectors of *H. agaves* ascospores. In arid ecosystems where *Agave americana* develops, it is most likely that insect disperse the spore when they are visiting decayed leaves of *A. americana* during decomposition or fermentation to feed on sugars or yeasts. Ascospores could adhere to their bodies thanks to the roughness of the ascospore surface and the presence of sticky sheaths and be carried to nearby healthy plants. During the transport by the insects, ascospores could survive the harsh condition of exposure to UV radiation and drying because of the melanized spore wall. If they are deposited on a suitable host, they could also survive until better conditions allow them to germinate and infect the new susceptible host perhaps through stomata.

The genus *Hymenobolus* probably has been overlooked in its native range and we assume it could be found worldwide due to the history of introductions of its host, *Agave americana*. We hope this work encourages collectors to detect further occurrences of *H. agaves*, particularly to clarify whether this species is currently present in North America, but also to verify its ecology as an endophyte and its possible adaptation to insect dispersal.

© 2021 Westerdijk Fungal Biodiversity Institute

ACKNOWLEDGEMENTS

Luis Quijada thanks the support of the Farlow Fellowship, Royal T. Moore awards, the Department of Organismic and Evolutionary Biology at Harvard University, and the Harvard University Herbaria. Carlo Agnello, Martin Bemmann, Luis A. Parra, Gernot Friebes, Nicolas Van Vooren and Guy Garcia are thanked for valuable literature data. Antonio Rodríguez, Justo Muñoz, Juan Francisco López-Quintanilla, José Luis Lantigua, Yolanda Toledo, Jacobo Santiago, Cleo Rodríguez, Manuel Pérez-Ramírez, Francisco Govantes, Jaime Gil and Matteo Dossena are thanked for finding collections. Charles Etienne, Kadri Pärtel, Hermann Voglmayr, Salvador Tello, Bruce Watt, Dragisa Savić, Matthias Reul, Juuso Äikäs, Urs Roffler, Piots Perz, Ingo Wagner are thanked for lending images. Finally, we thank Pierre-Arthur Moreau and PC herbarium for helping us to find and study the collections in Montagne's herbarium.

Conflict of interest: The authors declare that there is no conflict of interest.

REFERENCES

Anonymous (1976). *ISCC-NBS Color-name Charts illustrated with centroid colors.* Washington DC: Inter-Society Color Council, National Bureau of Standards.

Baral HO (1992). Vital versus herbarium taxonomy: morphological differences between living and dead cells of *Ascomycetes*, and their taxonomic implications. *Mycotaxon* **44**: 333–390.

Boudier E (1907). *Historie et classification des Discomycètes d'Europe* (BSMPS, reprint 1984). Klingksieck, Paris 221: 158–159.

Braun U (2018). Annotated list of taxonomic novelties published in "*Herbarium Vivum Mycologicum*" issued by J. F. Klotzsch and G. L. Rabenhorst between 1832 and 1855. *Schlechtendalia* **34**: 3–90.

Castresana J (2000). Selection of conserved blocks from multiple alignments for their use in phylogenetic analysis. *Molecular Biology and Evolution* **17**: 540–552.

Coline D, Chieppa J, Nielsen UN, *et al.* (2020). Biogeography of arbuscular mycorrhizal fungal spore traits along an aridity gradient, and responses to experimental rainfall manipulation. *Fungal Ecology* **46**: 100899.

Dennis RWG (1978). *British Ascomycetes*. J. Cramer, Vaduz.

Durieu MC, Bory E (1849). *Exploration scientifique de l'Algérie pendant les années 1840–1842*, Botanique, Atlas [Atlas de la flore de l'Algérie].

Durrell LW (1964). The composition and structure of walls of dark fungus spores. *Mycopathologia* **23**: 339–345.

Eriksson OE (ed.) 1999. *Outline of Ascomycota* - 1999. *Myconet* **3**: 1–88.

Höhnel F von (1917). System der *Phacidiales* v. H. *Berichte Deutschen Botanischen Gesellschaft* **35**: 416–422.

Höhnel F von (1918). Fragmente zur Mykologie. (XXII. Mitteilung, Nr. 1092 bis 1153). Sitzungsberichte Akademie der Wissenschaften in Wien, *Mathematisch-naturwissenschaftliche Klasse, Abteilung* 1, **127** (8–9): 549–634 [1–86].

Jaap O (1915). Siebentes Verzeichnis zu meinem Exsikkatenwerk "Fungi selecti exsiccati". Serien XXV bis XXVIII (Nummern 601-700), nebst Beschreibungen neuer Arten und Bemerkungen. *Verhandlungen des Botanischen Vereins für die Provinz Brandenburg* **57**: 8–25.

Jaklitsch WM, Baral HO, Lücking R *et al.* (2016). *Syllabus of plant families* – A. Engler's Syllabus der Pflanzenfamilien part 1/2: *Ascomycota*, 13th edn. Borntraeger, Stuttgart.

Johnston PR, Quijada L, Smith CA, *et al.* (2019). A multigene phylogeny toward a new phylogenetic classification of *Leotiomycetes*. *IMA Fungus* **10**: 1.

Jurc D, Jurc M, Sieber TN, *et al.* (2000) Endophytic *Cenangium ferruginosum* (*Ascomycota*) as a reservoir for an epidemic of cenangium dieback in Austrian pine. *Phyton-horn* **40**: 103–108.

Katoh K, Toh H (2008). Improved accuracy of multiple ncRNA alignment by incorporating structural information into a MAFFT-based framework. *BMC Bioinformatics* **9**: 212.

Kawamura C, Tsujimoto T, Tsuge T (1999). Targeted disruption of a melanin biosynthesis gene affects conidial development and UV tolerance in the Japanese pear pathotype of *Alternaria alternata*. *Molecular Plant-Microbe Interactions* **12**: 59–63.

Korf RP (1973). *Discomycetes* and *Tuberales.* In: *The Fungi: an advanced treatise*. Vol. IVA. A Taxonomic Review with keys: Ascomycetes and Fungi Imperfecti. Ainsworth GC, Sparrow FK, Sussman AS, (Eds). New York: Academic Press: 249–319.

Magyar D, Vass M, Li D-W (2016). Dispersal Strategies of Microfungi. In: *Biology of Microfungi, Fungal Biology*. De-Wei, L. (Eds). Springer International Publishing Switzerland: 315–371.

Montagne C (1845). Cinquième Centurie des plantes exotiques cellulaires nouvelles. *Annales des Sciences Naturelles, Botanique sér. 3.* **4**: 359–360.

Montagne C (1856). *Sylloge Generum Specierumque Cryptogamarum quas in Variis Operibus Descriptas Iconibusque Illustratas nunc ad Diagnosim Reductas, Nonnullasque Novas Interjectas, Ordine Systematico Exposuit*. France, Paris; Sumptibus J-B Baillière.

Nannfeldt JA (1932). *Studien über die Morphologie und Systematik der nicht-lichenisierten inopeculaten Discomycenten*. Uppsala.

Pärtel K, Baral HO, Tamm H, *et al.* (2017). Evidence for the polyphyly of *Encoelia* and *Encoelioideae* with reconsideration of respective families in *Leotiomycetes*. *Fungal Diversity* **82**:183–219.

Perić B, Baral HO, Pärtel K (2015). *Cenangiopsis raghavanii* and *C. junipericola spp. nov.* (*Cenangiaceae*, *Helotiales*) collected in Montenegro, with redescription of a recent collection of *C. quercicola*. *Mycologia Montenegrina* **18**: 7-40.

Petrak F (1922–1928). List of new species and varieties of fungi, new combinations and new names published, 1922-1928. *Index of Fungi* **1922–1928:** 1–408, 1953. UK, Surrey, Kew; Commonwealth Mycological Institute. [Reprinted from *Just's Botanischer Jahresbericht* **56**: 291–697, 1937].

Petrak F, Sydow H (1927). Die Gattungen der Pyrenomyzeten, Sphaeropsideen und Melanconieen. 1. Die phaeosporen Sphaeropsideen und die Gattung *Macrophoma*. *Repertorium Specierum Novarum Regni Vegetabilis Beihefte* **42**: 1–551.

Quijada L, Baral HO, Jaen-Molina R, *et al.* (2014). Phylogenetic and morphological circumscription of the *Orbilia aurantiorubra* group. *Phytotaxa* **175**: 1–18.

Quijada L, Mitchell JK, Popov E, *et al.* (2019). The Asian-Melanesian bambusicolous genus *Myriodiscus* is related to the genus *Tympanis*, the North American-European tree pathogen. *Forest Pathology* **49**: E12532-N/a.

Rehner SA, Buckley E (2005). A *Beauveria* phylogeny inferred from nuclear ITS and EF1-α sequences: evidence for cryptic diversification and links to *Cordyceps* teleomorphs. *Mycologia* **97**: 84–98.

Ribes MA, Negrín R, Quijada L, *et al.* (2015). Contribución al conocimiento de la micobiota de las Islas Canarias (España) IV. Ascomycetes. *Ascomycete.org* **7**: 375–393.

Rieuf P (1962). Un parasite peu commun de l'Agave *Hymenobolus agaves* Dur. et Mont. *Al Awamia* **4**: 127–134.

Rojas-Sandoval J, Iamonico D (2016). *Agave americana* (century plant). CABI. Invasive Species Compendium. https://www.cabi.org/isc/datasheet/3851 (https://www.cabi.org/isc/datasheet/3851).

Rostrup E (1899). Mykologiske Meddelelser (VIII). Spredte Iagttagelser fra 1897–1898. *Botanisk Tidskrift* **22**: 254–276.

© 2021 Westerdijk Fungal Biodiversity Institute

Saccardo PA (1889). *Sylloge Fungorum* 8: ix–xvii, 1–1143. Italy, Padua; PA Saccardo.

Saccardo PA (1892). *Sylloge Fungorum* 10: i–xxx, 1–964. Italy, Padua; PA Saccardo.

Saccardo PA, Trotter A (1913). *Sylloge Fungorum* 22: i–v, 1–822. Italy, Padua; PA Saccardo.

Saccardo PA (1917). Notae Mycol., XXII, Atti e Memorie della Reale *Accademia di Scienze, Lettere ed Arti in Padova* **33**: 157–195.

Seaver FJ (1951). *The North American Cup-fungi (inoperculates)*. Published by the author, New York.

Sherwood-Pike M, Stone JK, Carroll GC (1986). *Rhabdocline parkeri*, a ubiquitous foliar endophyte of Douglas-fir. *Canadian Journal of Botany* **64**: 1849–1855.

Thümen F von (1878). Contributiones ad floram mycologicam lusitanicam, 138. Mit Vorbemerkung von J. Henriquez. *Jornal de Sciencias Mathematicas Physicas e Naturaes*, *Publicado sob os auspicios da Academia Real das Sciencias de Lisboa*, ser. 1, tome **6** 24 (dez.): 230–253.

Vilgalys R, Hester M (1990). Rapid genetic identification and mapping of enzymatically amplified ribosomal DNA from several *Cryptococcus* species. *Journal of Bacteriology* **172**: 4238–4246.

Voglmayr H, Jaklitsch W, Tello S (2020). *Mycosphaerangium* and *Neomelanconium* (*Cenangiaceae*) are closest relatives: Phylogenetic relationships, morphology and a new species. *Mycological Progress* **19**: 1329–1352.

White TJ, Bruns TD, Lee S *et al.* (1990). Amplification and direct sequencing of fungal ribosomal RNA genes for phylogenetics. In: *PCR Protocols, a Guide to Methods and Applications*. Innis MA, Gelfand DH, Sninsky JJ, White TJ (Eds). Academic Press, San Diego, 315–322.

Wijayawardene NN, Hyde KD, Al-Ani LKT *et al.* (2020). Outline of Fungi and fungus-like taxa. *Mycosphere* **11**: 1060–1456.

© 2021 Westerdijk Fungal Biodiversity Institute

FUSE

Fungal Systematics and Evolution

VOLUME 8
DECEMBER 2021
PAGES 143–154

doi.org/10.3114/fuse.2021.08.11

Polyozellus vs. Pseudotomentella: generic delimitation with a multi-gene dataset

S. Svantesson[1,2,3*], U. Kõljalg[4,5], C. Wurzbacher[1,2,6], I. Saar[5], K.-H. Larsson[2,7], E. Larsson[1,2]

[1]Department of Biological and Environmental Sciences, University of Gothenburg, Box 463, 405 30 Göteborg, Sweden
[2]Gothenburg Global Biodiversity Centre, Box 461, 405 30 Göteborg, Sweden
[3]Royal Botanic Gardens Victoria, Birdwood Ave, Melbourne, Victoria 3004, Australia
[4]Natural History Museum, University of Tartu, 14a Ravila, 50411 Tartu, Estonia
[5]Institute of Ecology and Earth Sciences, University of Tartu, 14a Ravila, 50411 Tartu, Estonia
[6]Chair of Urban Water Systems Engineering, Technical University of Munich, Am Coulombwall 3, 85748 Garching, Germany
[7]Natural History Museum, University of Oslo, P.O. Box 1172, Blindern, 0318 Oslo, Norway

*Corresponding author: sten.svantesson@gmail.com

Key words:
Molecular systematics
new taxa
ribosomal tandem repeat
species tree
STACEY
Thelephorales

Abstract: *Polyozellus* and *Pseudotomentella* are two genera of closely related, ectomycorrhizal fungi in the order *Thelephorales*; the former stipitate and the latter corticioid. Both are widespread in the Northern Hemisphere and many species from both genera seem to be restricted to old growth forest. This study aimed to: a) identify genetic regions useful in inferring the phylogenetic relationship between *Polyozellus* and *Pseudotomentella*, b) infer this relationship with the regions identified and c) make any taxonomic changes warranted by the result. *RPB2*, mtSSU and nearly full-length portions of nrLSU and nrSSU were found to be comparatively easy to sequence and provide a strong phylogenetic signal. A STACEY species tree of these three regions revealed that *Polyozellus* makes *Pseudotomentella* paraphyletic. As a result, nearly all species currently placed in *Pseudotomentella* were recombined to *Polyozellus*. *Pseudotomentella larsenii* was found to be closer to *Tomentellopsis* than *Polyozellus*, but its placement needs further study and it was hence not recombined.

Citation: Svantesson S, , Kõljalg U, Wurzbacher C, Saar I, Larsson K-H, Larsson E (2021). *Polyozellus vs. Pseudotomentella*: generic delimitation with a multi-gene dataset. *Fungal Systematics and Evolution* **8**: 143–154. doi: 10.3114/fuse.2021.08.11
Received: 12 July 2020; **Accepted:** 26 October 2021; **Effectively published online:** 18 November 2021
Corresponding editor: P.W. Crous

INTRODUCTION

Thelephorales is a large order of basidiomycetes with a vast number of undescribed species; according to Kirk *et al.* (2008) 269 described species belong to the order, but following the UNITE ITS sequence database it contains 4 305 Species Hypotheses (SHs), at 1.5 % minimum distance between sister species (Kõljalg *et al.* 2013, Nilsson *et al.* 2018).

Nearly all *Thelephorales* species are ectomycorrhizal, notable exceptions being *Lenzitopsis*, *Odontia* and possibly *Amaurodon* (Miettinen & Kõljalg 2007, He *et al.* 2019). *Thelephorales* often constitutes a large proportion of the ectomycorrhizal symbionts found on root tips in any ecosystem where such are present, and are hence important facilitators of forest and shrub growth in for example tundra, boreal and temperate ecosystems in large parts of the world (*e.g*. Kõljalg *et al.* 2000, Brundrett 2002, Sønstebø 2002, Taylor & Peterson 2005, Mühlmann & Peintner 2008, Ryberg *et al.* 2009, Bücking *et al.* 2012, Botnen *et al.* 2015). Some genera also form orchid mycorrhiza (*e.g*. Bidartondo *et al.* 2004, Jacquemyn *et al.* 2017).

Although most *Thelephorales* species are resupinate (*Amaurodon*, *Odontia*, *Pseudotomentella*, *Tomentella*, *Tomentellopsis*), some are stipitate hydnoid (*Hydnellum*, *Phellodon*, *Sarcodon*), stipitate poroid (*Boletopsis*), stipitate smooth (*Thelephora*) or cantharelloid (*Polyozellus*, *Thelephora*; Stalpers 1993, He *et al.* 2019). A few species are finger-like (*Thelephora*) and two are lamellate (*Lenzitopsis*; Stalpers 1993, He *et al.* 2019). A morphological feature common to all species, except possibly *Amaurodon mustialaensis* (fine ornamentation sometimes visible in SEM), is the verrucose to echinulate spores (Ginns 1989, Stalpers 1993, He *et al.* 2019).

Polyozellus was described by Murrill (1910) to accommodate a blackish, cantharelloid fungus, which up until then had been known as *Cantharellus multiplex*. The genus remained monotypic until Voitk *et al.* (2018) showed that the morphological concept of this species, *Po. multiplex*, comprised five molecularly distinct species, four of which were hence previously undescribed.

All presently described *Polyozellus* species have spathulate to funnel-shaped basidiomata, with a ridged underside, which usually fuse at the base to form irregularly rosette-shaped clumps (Voitk *et al.* 2018; Fig. 1). They overlap in colour and range from brown to blue, purple or black, depending on species and stage of maturity. The pilei of young specimens are woolly or hirsute on top but become smooth with age, while the hymenium has a consistently matte appearance. Their consistency is soft and brittle. Microscopically all *Polyozellus* species are similar and share the features of hyaline, inamyloid spores covered in irregular lobes and nodules, thread-like hyphidia and clamped

Fungal Systematics and Evolution is licensed under a Creative Commons Attribution-NonCommercial-ShareAlike 4.0 International License

© 2021 Westerdijk Fungal Biodiversity Institute

Fig. 1. Basidiomata of species currently placed in *Polyozellus* and *Pseudotomentella*. **A.** *Ps. mucidula*. **B.** *Ps. media*. **C.** *Ps. griseopergamacea*. **D.** *Ps. humicola*. **E.** *Po. multiplex*. **F.** *Po. mariae*. Scale bars = 2 cm. Photos A–D. Urmas Kõljalg; E. Michael Burzynski; F. Andrus Voitk.

hyphae. The hyphae have a bluish black pigment in the walls, which produces a bluish green solution in KOH. As a genus *Polyozellus* is easily recognised in the field and by a combination of macroscopical characters and spore size it is possible to distinguish between species. Two species with smaller spores, *Po. multiplex* and *Po. atrolazulinus* can be separated from three species with larger spores: *Po. mariae*, *Po. marymargaretae* and *Po. purpureoniger* (Voitk *et al.* 2018).

Based on ITS sequences, the small-spored *Polyozellus* species form separate phylogenetic clades, while the large-spored species comprise one clade (Voitk *et al.* 2018). The species have different but overlapping geographical distributions and range from North America to Asia but are not present in Europe (Voitk *et al.* 2018). The conservation statuses of the new species are not known but prior to their description *Po. multiplex* was considered a rare but locally abundant species in North America and a good indicator of old-growth forest (United States Forest Service 1994, Baroni 2017). It is also used in wool-dyeing and as a potential medicine against Alzheimer's disease (Hwang et al. 1997).

Pseudotomentella was described by Svrček (1958), with the pale brown, corticioid species *Ps. mucidula* as type. Svrček (1958, 1960) described and recombined a further eight species into the genus. Larsen (1967a, b, 1968, 1971a, b, 1974, 1983) subsequently described an additional 13 *Pseudotomentella* species. Hjortstam (1970, 1974) recombined three of the species

© 2021 Westerdijk Fungal Biodiversity Institute

described by Svrček into *Tomentellopsis* and Kõljalg & Larsson (Kõljalg 1996) moved two into *Amaurodon*. Kõljalg (1996) also synonymised many of the species described by Larsen, and hence reduced the number of names to eight: *Ps. atrofusca*, *Ps. flavovirens*, *Ps.griseopergamacea*, *Ps. humicola*, *Ps. mucidula*, *Ps. nigra*, *Ps. tristis* and *Ps. vepallidospora*. Four species have later been described by various authors in separate publications: *Ps. armata* (Martini & Hentic 2002), *Ps. larsenii* (Kõljalg & Dunstan 2001), *Ps. ochracea* (Kõljalg & Larsson 1998) and *Ps. rhizopunctata* (Martini & Hentic 2003). Svantesson *et al.* (2019, 2021) described 12 new species from basidiomata previously identified as *Ps. tristis*, de-synonymised *Ps. umbrina* from the same and showed in a multi-gene phylogeny that these species form a clade sister to a clade containing *Ps. rhizopunctata* and *Ps. atrofusca*.

All *Pseudotomentella* species have corticioid, resupinate basidiomata, with a quite dense but soft and felt-like texture (Fig. 1). In similarity to *Polyozellus*, their hymenia have a matt appearance, but vary in colour from white to nearly black, past yellow, green, blue, purple, brown and grey. Microscopically, *Pseudotomentella* species display considerable variation: some species are simple-septate (*e.g*. *Ps. flavovirens*, *Ps. griseopergamacea* and *Ps. mucidula*), whereas others have clamped hyphae (*e.g. Ps. humicola*, the *Ps. tristis* group and *Ps. vepallidospora*); some species are monomitic (*e.g*. the core *Ps. tristis* group) and others are dimitic (*e.g. Ps. humicola*, *Ps. mucidula* and *Ps. rhizopunctata*); some species have dark-coloured spores (the *Ps. tristis group*) and others have hyaline spores (*e.g. Ps. griseopergamacea*, *Ps. mucidula*); a few species have chlamydospores (*Ps. rhizopunctata* and *Ps. vepallidospora*) but the rest do not. All species, however, have spores with bi- or trifurcate verrucae to echinuli. This feature in combination with the texture characteristics of their basidiomata makes *Pseudotomentella* readily recognisable under the microscope and to the trained eye they can be identified to species group already in the field. For identification to the level of species a combination of macro- and microscopical features is often needed (Kõljalg 1996, Kõljalg & Larsson 1998, Kõljalg & Dunstan 2001, Martini & Hentic 2002, 2003, Svantesson *et al.* 2019, 2021).

Pseudotomentella basidiomata are formed on the underside of dead wood, stones and turf, often very close to the ground (Kõljalg 1996, Svantesson *et al.* 2019). The spores of *Tomentella sublilacina* have been shown to be insect-dispersed (Lilleskov & Bruns 2005) and the similarity in spore-shape and growth habit of basidiomata indicate that this is likely the case for *Pseudotomentella* as well.

With the exception of *Ps. larsenii*, *Pseudotomentella* species are only naturally occurring in the Northern Hemisphere (Kõljalg 1996, Kõljalg & Larsson 1998, Kõljalg & Dunstan 2001, Martini & Hentic 2002, 2003, Svantesson *et al.* 2019, 2021). Less is known about their habitat than for *Polyozellus*, but many species are thought to only occur in old-growth forest. Svantesson *et al.* (2019) showed that all species in the *Ps. tristis* group, except the very widespread *Ps. umbrina*, are limited to ground with medium to high pH. Eight *Pseudotomentella* species are Red Listed in Sweden, three in Denmark and two in Estonia (Moeslund *et al.* 2019, Saar *et al.* 2019, SLU Artdatabanken 2020).

Vizzini *et al.* (2016) published an ITS phylogeny of *Thelephorales* indicating that, with the exception of *Ps. ochracea* and *Ps. larsenii*, *Polyozellus* and *Pseudotomentella* form a weakly supported clade together, while the clades of most other *Thelephorales* genera were strongly supported. Preliminary analyses based on ITS and partial LSU sequences for the current study also displayed a close phylogenetic relationship between the genera *Polyozellus* and *Pseudotomentella*. These have, however, in addition shown that the partial LSU region alone has too weak a signal to resolve this part of the *Thelephorales* tree, while the majority of ITS is too variable to be reliably aligned. The purpose of this article is to explore what genetic markers can resolve the relationship between *Polyozellus* and *Pseudotomentella*, establish this relationship with a multi-gene species tree more densely sampled for the taxa of interest and make any nomenclatural changes warranted by the conclusions.

MATERIALS AND METHODS

Taxon sampling

The ingroup consisted of all described species of *Polyozellus* and *Pseudotomentella* or representatives from already known clades of described species where such exist, except *Ps. nigra*, *Ps. tenebrosa* and the heterotypic synonyms of *Ps. flavovirens*, *Ps. griseopergamacea* and *Ps. mucidula*. The latter are so similar to the species with which they are currently synonymised that it is unclear whether they are separate species. This approach was taken in order to minimise costs and keep sequencing efforts within the time-frame set by a PhD project (pursued by the first author). The identities of *Ps. nigra* and its heterotypic synonym *Ps. tenebrosa* are unclear and will be addressed in a separate publication. The sampling hence included one species from each of the *Polyozellus* clades identified by Voitk *et al.* (2018), the eight *Pseudotomentella* species accepted by Kõljalg (1996), except for *Ps. nigra*, the four *Pseudotomentella* species subsequently published by various authors, as well as four species from the *Ps. tristis* group, as delimited by Svantesson *et al.* (2019). In addition, *Tomentella italica* was added to the dataset, since Tedersoo *et al.* (2016) suspected it of belonging to *Pseudotomentella*. Sequencing was attempted for the types of *Ps. mucidula*, and *Ps. griseopergamacea*. In cases (other than for *Ps. nigra*) where the phylogenetic identity of a species was unclear and several genetically different contenders existed for a name, a representative of each was included in the dataset and were referred to as *e.g. Ps. cf. vepallidospora* 1 and 2.

In order to further account for as yet undescribed *Polyozellus* and *Pseudotomentella* species when inferring the relationship between the two genera, the Compound Cluster function of the UNITE database was used (Kõljalg *et al.* 2013, Nilsson *et al.* 2018). Compound Clusters consist of DNA sequences with 80 % or less sequence similarity. The database was queried for sequences belonging to non-singleton Species Hypotheses at the 3 % level. The retrieved sequences were included in the dataset if their taxonomic identity was stated as *Polyozellus* or *Pseudotomentella* in UNITE, INSD or both and they were found to belong to other Compound Clusters than those containing sequences of formally described species (or contenders of such). To reveal the phylogenetic placement of the two focal genera two species (type species and one other) were selected from all other genera within *Thelephorales*. Two specimens of an undescribed species of *Auricularia* were chosen as outgroup, due to their easy sequenceability and inclusion in an earlier dataset (Table 1; see next subsection).

© 2021 Westerdijk Fungal Biodiversity Institute

Molecular data

Seven genetic regions were targeted for DNA sequencing: nrLSU, nrSSU, β-tubulin, mtSSU, *Tef1α, RPB1* and *RPB2*. All are unlinked except nrLSU and nrSSU. A majority of the nrLSU and nrSSU sequences were full-length and generated through Nanopore and PacBio sequencing, as part of Wurzbacher *et al.* (2019; Table 1). These sequences were complemented with sequences derived through Sanger sequencing. Approximately 2 500 bases were amplified from the nrLSU gene with the primers LR0R and LR7, LR7R and LR14 (Hopple & Vilgalys 1999); *ca.* 1 500 bases from the nrSSU gene with NS1 and NS4, NS3 and NS8 (White *et al.* 1990); *ca.* 500 bases from the β-tubulin gene with B36f and B12r (Nagy *et al.* 2011), *ca.* 600 bases from the *Tef1α* gene with EF983F and EF1567R (Rehner & Buckley 2005), *ca.* 700 bases from the mtSSU gene with MS1 and MS2 (White *et al.* 1990) and *ca*. 1 100 bases were amplified from the *RPB2* gene with fRPB2-5F and bRPB2-7.1 (Liu *et al.* 1999, Matheny 2005). *RPB1* sequences were obtained from whole genome sequencing by Tedersoo *et al.* (2016).

The primers used for sequencing were: for nrLSU - Ctb6 (Garbelotto *et al.* 1997) LR3R, LR5, LR7R, LR8R, LR9, LR14R (Hopple & Vilgalys 1999), for nrSSU - NS1, NS2, NS3, NS4 and NS8 (White *et al.* 1990), for β-tubulin - B36f and B12r, for *Tef1α* - EF983F and 1567R, for mtSSU - MS1 and MS2 and for *RPB2* - bRPB2-7R, bRPB-6f and fRPB-5f (Matheny 2005).

The DNA sequences were assembled with Sequencher v. 5.4.6 (Gene Codes, Ann Arbor, MI, USA) and lodged in GenBank (Table 1). Alignments were made in AliView v. 1.18 (Larsson 2014), utilising the L-INS-i strategy, as implemented in MAFFT v. 7.017 (Katoh & Standley 2013). Introns and low-quality ends were manually trimmed from the sequences prior to analysis.

Molecular analyses

Gblocks v. 0.91b (Castresana 2000, Talavera & Castresana 2007) was used to trim the alignments of problematic character regions (*e.g*. missing data, saturated sites and sections with unclear homology). The program has not been evaluated for Bayesian inference (BI), which was employed in this study for generating gene and species trees, but for neighbour joining, parsimony and maximum likelihood (ML) methods. Although they are conceptually very different methods the results of ML and BI tend to be the most similar, and Gblocks was therefore run in the relaxed version of the program, as outlined in Talavera & Castresana (2007), which according to the same study is suitable for ML analysis of alignments created with MAFFT. The resulting alignments were unchanged in length for nrSSU, mtSSU, *Tef1α* and *RPB1*, 2 609 bases long for nrLSU (3 405 before) and 1 042 bases long for *RPB2* (1 056 before).

RDP4 (Martin *et al.* 2015) was used to test for recombination. During a first round of testing the methods RDP, GENECONV, Chimaera and MaxChi were used and the significance level set to 0.01. Sequences with significant signs of recombination were submitted to a second round of testing that made use of all recombination methods. Any sequences with a positive result for more than two methods with p-values ≤ 10^{-5} in the second round were regarded as probable recombinants. Recombined sections of such sequences were removed from the alignments prior to further analysis.

In the phylogenetic analyses the following minimal partitions were assumed: nrLSU, nrSSU, mtSSU and for the protein-encoding genes: first, second and third positions. The automated best-fit tests implemented in PAUP v. 4.0a (Swofford 2002) were used to select optimal substitution models and optimal substitution model partitions. In agreement with the substitution models available in the BI programs used (BEAST v. 2 and STACEY) the tests evaluated models with three substitution schemes and equal or gamma-distributed among-site rate variation, based on BIC score. The partitioning result provided the best fit for keeping all minimal partitions separate, except first and second positions of *Tef1α* and *RPB1*. The substitution model GTR+G was output as the optimal model for all partitions except *Tef1α* and *RPB1* first+second positions and *RPB2* second positions. For these partitions the optimal models were JC+G, JC+G and K80+G, respectively.

To generate gene trees and assess their concordance prior to the species tree analysis BEAST v. 2.6.2 (Bouckaert *et al.* 2014, 2019) was used. The xml-files were prepared in the associated software BEAUti v. 2.6.2 (Bouckaert *et al.* 2014, 2019). The alignments were assigned the optimal partitions and substitution models output by PAUP v.4, but the substitution model was set to HKY+G for *RPB2* second partitions, since it is the most similar model to K80+G available in the program. Test runs revealed that all trees retained the same topology if GTR+G was changed to HKY+G, but convergence was considerably faster. This change in substitution models was hence implemented, in order to ensure consistency with the ensuing species tree analysis, which is often slow to converge even under optimal circumstances and where enhanced speed is thus preferable. The trees of the partitions were set as linked inside each genetic linkage group but a separate clock model was assumed for each. The clock models were set as relaxed, lognormal, since all partitions had a coefficient of variation well above 0.1 (*i.e*. implying a relatively high rate variation among branches) in test runs. The clock rate of each partition was estimated in the run, using a lognormal prior with a mean set to 1 in real space. The growth rate prior was set to lognormal, with a mean of 5 and a standard deviation of 2. These priors were set according to the STACEY package documentation (Jones 2014). The Markov Chain Monte Carlo chains were run until analyses converged well in advance of the 10 % burn-in threshold, had ESS values well above 200 for all parameters, and satisfactory chain mixing, as assessed in Tracer v. 1.6.0 (Rambaut *et al.* 2014). After discarding the burn-in trees, maximum clade credibility trees were identified by TreeAnnotator v. 2.6.2 (Bouckaert *et al.* 2014, 2019).

A species tree inferred under the multispecies coalescent model was estimated in STACEY v. 1.2.5 (Jones 2017). Substitution and clock models as well as clock and growth rate priors were set the same as for the gene tree analyses. All individuals were assumed as minimal clusters. The Collapse Height prior was set to 10^{-5} and a lognormal prior with a mean of -7 and a standard deviation of 2 was set to the PopPriorScale parameter, as per the STACEY package documentation (Jones 2014). The length and result of the analysis was determined and summarized as for the gene trees. The phylograms were visually prepared in FigTree v. 1.4.4 (Rambaut 2012) and Inkscape v. 0.92.3. (https://inkscape.org)

RESULTS

Seven DNA regions were assessed for their functionality in inferring the relationship between the closely related genera

© 2021 Westerdijk Fungal Biodiversity Institute

Table 1. DNA sequences included in the STACEY species tree analysis and their vouchers. GenBank (two-letter combination)/ENA (four-letter combination) numbers in boldface and italics indicate sequences generated for this study and as part of Wurzbacher *et al.* (2019), respectively.

Species	Voucher	nrLSU 1st part	nrLSU 2nd part	nrSSU	*RPB2*	mtSSU
Polyozellus atrolazulinus	TUF117559	**MT737307**	**MT732081**	**MT732090**	**MT724777**	**OK586800**
Polyozellus marymargaretae	TUF117347	**MT737308**	**MT732082**	**MT732089**	**MT724778**	**OK586801**
Polyozellus multiplex	TUF115322	*SAMEA4659525*	*SAMEA4659525*	*SAMEA4659525*	**MT724779**	**OK586802**
Pseudotomentella flavovirens	KHLarsson16727	**OK559566**	**OK559602**	**OK559682**	**OK632648**	**OK586803**
Pseudotomentella griseopergamacea	SSvantesson401	*SAMEA4659512*	*SAMEA4659512*	*SAMEA4659512*	**OK632653**	**OK586810**
Pseudotomentella cf. humicola 1	SSvantesson345	MK290724	**OK559582**	**OK559681**	**OK632649**	MK290650
Pseudotomentella cf. humicola 2	SSvantesson539	**OK559565**	—	**OK559680**	**OK632650**	**OK586804**
Pseudotomentella larsenii	TUF100440	**MT737309**	**MT732084**	**MT732093**	**OK632665**	**OK586811**
Pseudotomentella cf. mucidula 1	SSvantesson132	*SAMEA4659509*	*SAMEA4659509*	*SAMEA4659509*	**OK632654**	**OK586805**
Pseudotomentella cf. mucidula 2	SSvantesson458	**OK559564**	**OK559603**	**OK559679**	**OK632655**	**OK586806**
Pseudotomentella cf. rhizopunctata 1	EMartini 10413	**OK559563**	**OK559601**	**OK559678**	**OK632668**	**OK586807**
Pseudotomentella cf. rhizopunctata 2	SSvantesson129	MK290717	**OK559581**	**OK559677**	**OK632669**	MK290652
Pseudotomentella sciastra	SSvantesson213	*SAMEA4659508*	*SAMEA4659508*	*SAMEA4659508*	**OK632659**	**OK586812**
Pseudotomentella tristis	SSvantesson193	MK290679	**OK559580**	**OK559676**	**OK632658**	MK290662
Pseudotomentella umbrina	SSvantesson351	*SAMEA4659515*	*SAMEA4659515*	*SAMEA4659515*	**OK632667**	MK290659
Pseudotomentella umbrinascens	SSvantesson335	*SAMEA4659496*	*SAMEA4659496*	*SAMEA4659496*	**OK632666**	MK290670
Pseudotomentella cf. vepallidospora 1	SSvantesson456	**OK559562**	**OK559605**	**OK559675**	**OK632651**	**OK586808**
Pseudotomentella cf. vepallidospora 2	SSvantesson493	**OK559561**	**OK559604**	**OK559674**	**OK632652**	**OK586809**
Amaurodon sumatranus	TUF115407	*SAMEA4659524*	*SAMEA4659524*	*SAMEA4659524*	**OK632661**	**OK586789**
Amaurodon viridis	TUF115739	***OK559560***	***OK559555***	***OK559673***	—	**OK586790**
Boletopsis leucomelaena	MKrikorev140912	MK602710	**OK559579**	**OK559672**	**OK632676**	—
Hydnellum ferrugineum	ELarsson312-16	*SAMEA4659497*	*SAMEA4659497*	*SAMEA4659497*	**OK632673**	**OK586794**
Hydnellum suaveolens	ELarsson8-14	*SAMEA4659503*	*SAMEA4659503*	*SAMEA4659503*	**OK632672**	**OK586795**
Lenzitopsis daii	HSYuan2959	JN169795	**MT732078**	**MT732087**	**MT724774**	**OK586796**
Lenzitopsis oxycedri	TUF115268	*SAMEA4659519*	*SAMEA4659519*	*SAMEA4659519*	**MT724775**	**OK586797**
Odontia ferruginea	TUF124098	*SAMEA4659527*	*SAMEA4659527*	*SAMEA4659527*	**MT724776**	**OK586798**
Odontia fibrosa	SSvantesson38	*SAMEA4659510*	*SAMEA4659510*	*SAMEA4659510*	**OK632664**	**OK586799**
Phellodon melaleucus	RGCarlsson160924	*SAMEA4659494*	*SAMEA4659494*	*SAMEA4659494*	**OK632675**	—
Phellodon violascens	RGCarlsson14033	*SAMEA4659505*	*SAMEA4659505*	*SAMEA4659505*	**OK632674**	**OK586793**
Sarcodon imbricatus	ELarsson384-10	*SAMEA4659502*	*SAMEA4659502*	*SAMEA4659502*	**OK632670**	**OK586813**
Sarcodon squamosus	ELarsson248-12	MK602767	**OK559578**	**OK559671**	**OK632671**	—
Thelephora palmata	ATaylor20136	*SAMEA4659526*	*SAMEA4659526*	*SAMEA4659526*	**OK632647**	—
Thelephora terrestris	SSvantesson404	*SAMEA4659516*	*SAMEA4659516*	*SAMEA4659516*	**OK632660**	**OK586814**
Tomentella asperula	SSvantesson392	***OK559559***	**OK559556**	***OK559670***	**OK632662**	**OK586815**
Tomentella ferruginea	SSvantesson367	*SAMEA4659514*	*SAMEA4659514*	*SAMEA4659514*	**OK632663**	**OK586816**
Tomentellopsis echinospora	TUF110333	*SAMEA4659521*	*SAMEA4659521*	*SAMEA4659521*	**MT724780**	**OK586817**
Tomentellopsis zygodesmoides	TUF124075	**MT737311**	—	**MT732091**	**MT724781**	**OK586818**
Auricularia sp.	ELarsson17030	***OK559557***	**OK559606**	***OK559668***	**OK632657**	**OK586791**
	ELarsson17032	***OK559558***	**OK559607**	***OK559669***	**OK632656**	**OK586792**

Polyozellus and *Pseudotomentella*. Out of these four could be readily sequenced and had a serviceable phylogenetic signal: nrLSU, nrSSU, *RPB2* and mtSSU (Table 1). The BEAST v. 2 gene tree analyses for *RPB2*, mtSSU and the combined nrDNA regions were run for 30 M, 10 M and 30 M generations, respectively. The gene trees were concordant for all supported nodes, with the exception of the relative placement of *Odontia* to *Tomentella*/*Thelephora*, and could hence be combined into a species tree analysis. The β-tubulin gene proved to be very hard to sequence and *RPB1* was found to have a very weak phylogenetic signal. Sequencing of these genes was therefore discontinued, and they were not included in the species tree dataset. *Tef1α* was found to be paralogous above genus level and therefore unusable in this study. This result will be presented in full in a separate publication. The sequencing attempts of the types of *Ps. griseopergamacea* and *Ps. mucidula* were unsuccessful,

© 2021 Westerdijk Fungal Biodiversity Institute

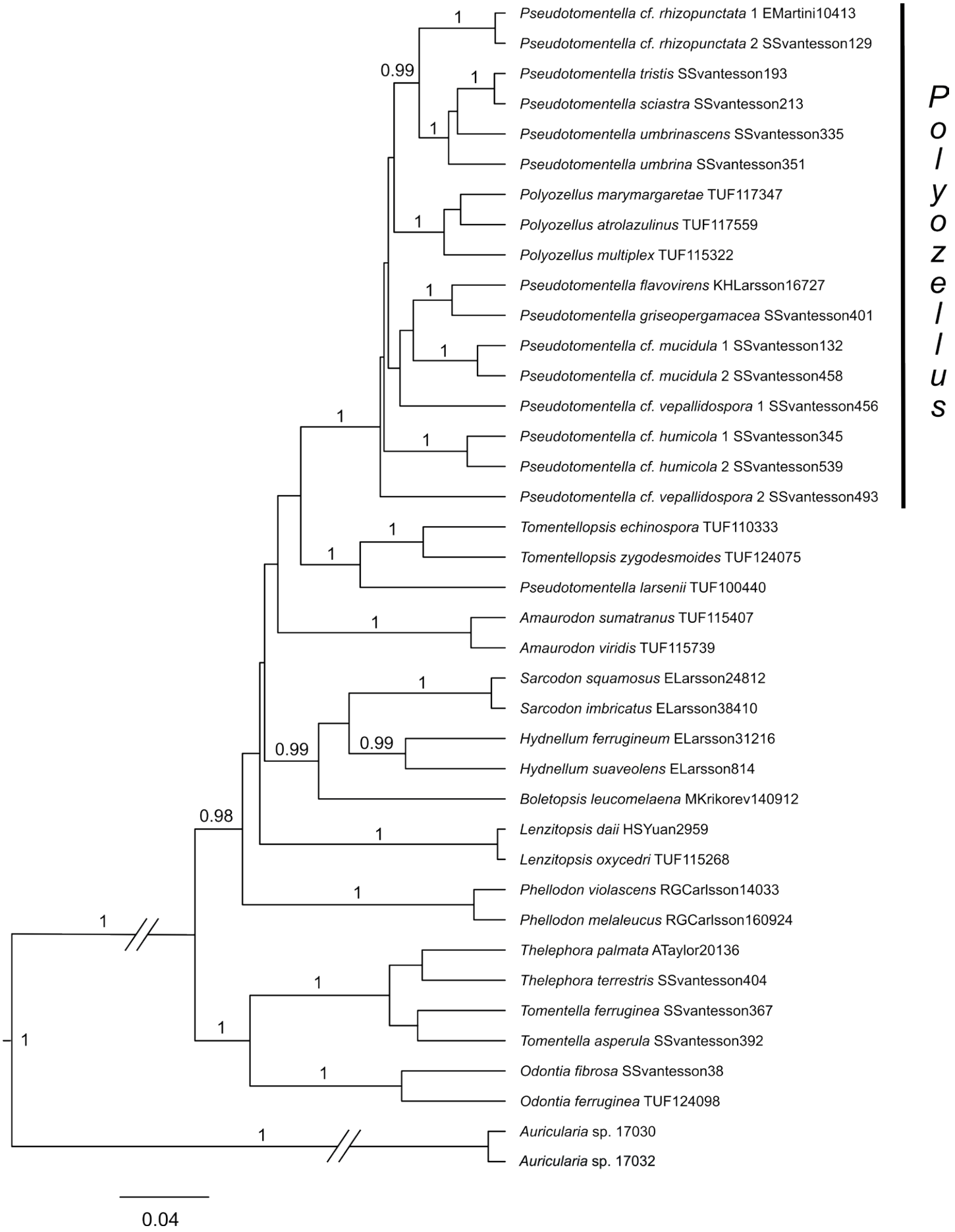

Fig. 2. STACEY species tree of *Thelephorales* with in-depth sampling of *Polyozellus* and *Pseudotomentella*, based on nrLSU, nrSSU, *RPB2* and mtSSU alignments. Only posterior probability values ≥ 0.95 are shown.

© 2021 Westerdijk Fungal Biodiversity Institute

as was the sequencing of most genetic regions for *Ps. armata*, *Ps. ochracea*, *T. italica* and *Boletopsis grisea*. They were hence excluded from the analyses. No sequences were found to be recombinants.

The STACEY species tree analysis was run for 500 M generations. Its resulting phylogram strongly supports *Polyozellus* as a monophyletic genus but not *Pseudotomentella* (Fig. 2). The three species of *Polyozellus* included in the analysis as representatives of three main clades of *Polyozellus* (see *Materials and methods*) were retrieved as a fully supported clade and so was the *Ps. tristis* group. These clades along with all other species of *Pseudotomentella*, except *Ps. larsenii*, were found to reside in a fully supported clade with little additional internal structure, *i.e*. a group corresponding to *Polyozellus* together with the thus paraphyletic *Pseudotomentella*. *Pseudotomentella larsenii* was retrieved as closely related to *Tomentellopsis*. The sequences of *Ps. humicola*, *Ps. mucidula* and *Ps. rhizopunctata* notably keep together in well-supported clades, while the sequences of *Ps. vepallidospora* do not.

The *Polyozellus* and *Pseudotomentella* species included in the analyses were found to belong in eight UNITE Compound Clusters: UCL8_013290, UCL8_012144, UCL8_002955, UCL8_010302, UCL8_012755, UCL8_007778, UCL8_007844, UCL8_008897 and UCL8_018843. Many of these clusters included large numbers of Species Hypotheses with non-singleton DNA-sequences not currently attributed to formally described species. Non-singleton DNA sequences of undescribed species identified as *Polyozellus* or *Pseudotomentella* in UNITE or INSD, belonging to other Compound Clusters than the formally described species were not retrieved.

In order to retain monophyly and uphold nomenclatural priority all *Pseudotomentella* species included in the analysis, except *Ps. larsenii*, are recombined to *Polyozellus*, together with close relatives of them within the *Ps. tristis* group (as shown by Svantesson *et al.* 2019, 2021). The genus description of *Polyozellus* is revised accordingly.

Taxonomy

Polyozellus Murrill, *N. Amer. Fl.* **9**: 171. 1910, ***emend.*** Svantesson & Kõljalg

Type species: *Polyozellus multiplex* (Underw.) Murrill, *N. Amer. Fl.* **9**: 171. 1910.
Basionym: *Cantharellus multiplex* Underw., *Bull. Torrey Bot. Club* **26**: 254. 1899.

Description: *Basidiomata* annual, of two types:

1. Stipitate, multiple, complex, imbricately foliose; single pilei flabelliform to spathulate, sometimes funnel-shaped; terrestrial. *Pileus* surface downy to tomentose in active growth, becoming matt with concentric zonation or longitudinal ribbing; black, blue, purple, or brown; eventually glabrous and often shiny, darker in colour, often black. *Hymenium* composed of irregular, longitudinal, sinuous, anastomosing, decurrent folds, which can vary within basidiomata to be smooth, reticulate or almost poroid; various shades of blue, purple and grey, becoming darker with age. *Stipe* solid, fibrous, tapering downwards; often multiple, fused, converging to a common subterranean base; matt, scaly or shiny; blue, dark blue, dark purple, dark brown or black. *Context* soft, brittle, whitish, yellowish, pale grey, various shades of purple and blue or black. *Odour* faintly pungent, chemical, fruity, mildly sweetish or unremarkable. *Taste* not recorded for most species, one species (*Po. atrolazulinus*) mild. *Spore deposit* white. Basidiomata resistant to decay and often last over a month in the field.

2. Corticioid, resupinate, membranaceous, effused; mature parts continuous, immature parts discontinuous; with a soft, somewhat fibrous and elastic (cottony) texture when fresh and a similar or soft yet compact, fibrous and ± elastic texture when dried; on the underside of wood, stones and debris lying on the ground, common in the roofs of rodent burrows. *Hymenium* smooth, but sometimes strongly undulating; colour ranging from nearly white, past yellow, green, blue, purple, brown and grey to nearly black. *Subiculum* well developed, loose, often fibrous, with whitish, yellow, orange, brown or black colours; often forms the outer edge of basidiomata, extending beyond the hymenium. *Odour* and *taste* not recorded. *Spore deposit* white to brown.

Hyphal system monomitic or dimitic, hyphae simple-septate or clamped. Hyphal cords lacking or present. *Subicular hyphae*, when present, often thick-walled, forming a loose tissue, hyaline or with yellow, orange, brown or black colours. *Subhymenial hyphae* straight to somewhat sinuous, for some species interwoven and nodulose; thin to thick-walled; often forming a rather dense tissue; hyaline or pale green, yellow, orange or brown in KOH; in some species with a pigment in the walls which has a blue-green reaction in the presence of air and produces a similarly coloured solution; in some species amyloid. *Encrustation* present or absent, amorphous to granular; hyaline, or with green, orange, brown, purple or black colours in KOH, in some species sometimes dark blue green in the presence of air; when present occurring on the upper parts of subhymenial hyphae and on the lower parts of basidia. *Basidia* 4-sterigmate, occasionally 2-sterigmate; clavate, narrowly clavate or clavopedunculate, thin-walled, with 1–3 slight constrictions; sterigmata slightly curved; colours and reactions the same as for subhymenial hyphae, but in addition often with granular contents in KOH. *Hyphidia* present in some species; simple, filiform, not extending beyond basidia. *Basidiospores* in frontal face with a subcircular, subellipsoid or triangular basic shape; outline angular, nodulose, triangular, subcircular, subellipsoid, heart-shaped or cross-shaped; unlobed or with 3–7 lobes; lateral face with a subcircular, subellipsoid, ellipsoid or ovoid basic shape; outline evenly rounded, angular, lobed or nodulose; apiculus prominent to prolonged (possibly except for in *Po. mariae*); echinuli in most species long and prominent, bi- or trifurcate, sometimes singularly attached, in some species short and irregularly attached; colours and reactions the same as for subhymenial hyphae but often darker and reactions less frequent. *Chlamydospores* present or absent. Forming ectomycorrhiza.

Polyozellus abundilobus (Svantesson) Svantesson & Kõljalg, ***comb. nov.*** MycoBank MB 836134. UNITE SH: 1152984.08FU.
Basionym: *Pseudotomentella abundiloba* Svantesson, *MycoKeys* **50**: 24. 2019.

Typus: **Norway**, Oslo (county), Oslo (municipality), Bygdøy, Hengsåsen, boreonemoral mixed forest on soil with high pH, 22 Sep. 2010, *S. Svantesson* (**holotype** O F110312).

© 2021 Westerdijk Fungal Biodiversity Institute

Polyozellus alnophilus (Svantesson) Svantesson & Kõljalg, ***comb. nov.*** MycoBank MB 836135. UNITE SH: 1564303.08FU.
Basionym: *Pseudotomentella alnophila* Svantesson, *MycoKeys* **50**: 26. 2019.

Typus: **Norway**, Buskerud, Ringerike, Juveren N, boreonemoral *Alnus incana* forest on soil with intermediate pH, 25 Sep. 2010, *S. Svantesson & N. Svensson* (**holotype** O F110313).

Polyozellus alobatus (Svantesson) Svantesson & Kõljalg, ***comb. nov.*** MycoBank No.: MB 836136. UNITE SH: 1230089.08FU.
Basionym: *Pseudotomentella alobata* Svantesson, *MycoKeys* **50**: 29. 2019.

Typus: **Sweden**, Dalsland, Mellerud, Skållerud, Norgekullen SW, coniferous forest on soil with high pH, 20 Sep. 2017, *S. Svantesson* 425 (**holotype** GB).

Polyozellus atrofuscus (M.J. Larsen) Svantesson & Kõljalg, ***comb. nov.*** MycoBank MB 836137. UNITE SH: 1230079.08FU.
Basionym: *Pseudotomentella atrofusca* M.J. Larsen, *Bull. Torrey Bot. Club* **98**: 39. 1971.

Typus: **USA**, Arizona, Fort Valley, Coconino Co., on *Pinus ponderosa*, 21 Sep. 1967, *R.L. Gilbertson* 7553 (**holotype** ARIZ; **isotype**: SSMF 685–4578).

Polyozellus badjelanndanus (Svantesson) Svantesson & Kõljalg, ***comb. nov.*** MycoBank MB 841511. UNITE SH: 1564288.08FU.
Basionym: *Pseudotomentella badjelanndana* Svantesson, *Phytotaxa* **497**: 69. 2021.

Typus: **Sweden**, Lule Lappmark, Jokkmokk, Oarjep Slahpetjåhkkå, middle alpine *Dryas octopetala* heath on ground with high pH, on underside of stones and *Dryas* twigs, 18 Aug. 2016, *S. Svantesson* 303 (**holotype** GB).

Polyozellus flavovirens (Höhn. & Litsch.) Svantesson & Kõljalg, ***comb. nov.*** MycoBank MB 836138. UNITE SH: 1184825.08FU.
Basionym: *Tomentella flavovirens* Höhn. & Litsch., *Sitzungsber. Kaiserl. Akad. Wiss., Wien. Math.-Naturwiss. Cl., Abt. 1* **116**: 831. 1907.

Typus: **Germany**, Braunlage am Harz, auf nackter Erde [= on bare soil], Lindau, (**holotype** FH [v. Höhnel herb., sheet 1979]).

Polyozellus griseopergamaceus (M.J. Larsen) Svantesson & Kõljalg, ***comb. nov.*** MycoBank MB 836139. UNITE SH: 1184823.08FU.
Basionym: *Pseudotomentella griseopergamacea* M.J. Larsen, *Bull. Torrey Bot. Club* **98**: 38. 1971.

Typus: **USA**, New York, Highland Forest, Fabius P.O., Onondaga Co., on *Pinus resinosa*, 21 Oct. 1961, *R. L. Gilbertson 3096* (**holotype** BPI; **isotype**: SSMF 695–4961).

Polyozellus humicola (M.J. Larsen) Svantesson & Kõljalg, ***comb. nov.*** MycoBank MB 836140. UNITE SH: 1236694.08FU, —.
Basionym: *Pseudotomentella humicola* M.J. Larsen, *Mycologia* **60**: 547. 1968.

Typus: **Canada**, Ontario, Algonquin Park, Opeongo Lake, on *Thuja occidentalis*, 18 Sep. 1939, *R. F. Cain* (**holotype** SSMF 8868; **isotypes**: TRTC 44362 and BPI).

Polyozellus medius (Svantesson & Kõljalg.) Svantesson & Kõljalg, ***comb. nov.*** MycoBank MB 836141. UNITE SH: 1185287.08FU.
Basionym: *Pseudotomentella media* Svantesson & Kõljalg, *MycoKeys* **50**: 33. 2019.

Typus: **Estonia**, Valga, Otepää, Trommi, 12 Sep. 2012, *U. Kõljalg* (**holotype** TUF 115609).

Polyozellus mucidulus (P. Karst.) Svantesson & Kõljalg, ***comb. nov.*** MycoBank MB 836142. UNITE SH: 1234281.08FU, 1234278.08FU.
Basionym: *Hypochnus mucidulus* P. Karst., *Bidrag Kännedom Finlands Natur Folk* **37**: 163. 1882.

Typus: **Finland**, Haarankorpi, in ligno mucido, 09 Oct. 1878, *P. A. Karsten* (**lectotype** H).

Polyozellus pinophilus (Svantesson) Svantesson & Kõljalg, ***comb. nov.*** MycoBank MB 836143. UNITE SH: 1185292.08FU.
Basionym: *Pseudotomentella pinophila* Svantesson, *MycoKeys* **50**: 36. 2019.

Typus: **Sweden**, Småland, Jönköping, Svarttorp, Ramlaklint, boreonemoral, mixed, old-growth forest, on soil with intermediate pH, 12 Sep. 2016, *S. Svantesson* 358 (**holotype** GB).

Polyozellus plurilobus (Svantesson) Svantesson & Kõljalg, ***comb. nov.*** MycoBank MB 836144. UNITE SH: 1185290.08FU.
Basionym: *Pseudotomentella pluriloba* Svantesson, *MycoKeys* **50**: 39. 2019.

Typus: **Finland**, Uusimaa, Loviisa, Rutosinpyhtää, Marinkylä, rotten trunk on the ground (*Picea*), 30 Sep. 2010, *U. Söderholm* 4263 (**holotype** H 6018127).

Polyozellus rhizopunctatus (E.C. Martini & Hentic) Svantesson & Kõljalg, ***comb. nov.*** MycoBank MB 836148. UNITE SH: 1230075.08FU, 1230078.08FU.
Basionym: *Pseudotomentella rhizopunctata* E.C. Martini & Hentic, *Bull. Trimestriel Soc. Mycol. France* **119**: 20. 2003.

Typus: **Switzerland**, canton Tessin, Someo, sur écorce d'une branche de *Pinus sylvestris*, 14 Nov. 1998, *E. Zenone* em-6886 (**holotype** PC; **isotype**: LUG).

Polyozellus rotundisporus (Svantesson) Svantesson & Kõljalg, ***comb. nov.*** MycoBank MB 836149. UNITE SH: 1185296.08FU.
Basionym: *Pseudotomentella rotundispora* Svantesson, *MycoKeys* **50**: 41. 2019.

Typus: **Sweden**, Västergötland, Götene, Medelplana, Eriksberg, boreonemoral, mixed forest on soil with high pH, 17 Oct. 2016, *S. Svantesson* 413 (**holotype** GB).

Polyozellus sciastrus (Svantesson & Kõljalg.) Svantesson & Kõljalg, ***comb. nov.*** MycoBank MB 836150. UNITE SH: 1230076.08FU.

© 2021 Westerdijk Fungal Biodiversity Institute

Basionym: *Pseudotomentella sciastra* Svantesson & Kõljalg, *MycoKeys* **50**: 44. 2019.

Typus: **Sweden**, Småland, Jönköping, Svarttorp, Ramlaklint, boreonemoral, mixed, old-growth forest, on soil with intermediate pH, 12 Sep. 2016, *S. Svantesson* 359 (**holotype** GB).

Polyozellus sorjusensis (Svantesson) Svantesson & Kõljalg, ***comb. nov.*** MycoBank MB 841513. UNITE SH: 1185284.08FU.
Basionym: *Pseudotomentella sorjusensis* Svantesson, *Phytotaxa* **497**: 71. 2021.

Typus: **Sweden**, Lule Lappmark, Jokkmokk, Sårjås N, low alpine heath on ground with intermediate pH, on underside of stone, 17 Aug. 2016, *S. Svantesson* 298 (**holotype** GB).

Polyozellus tristis (P. Karst.) Svantesson & Kõljalg, ***comb. nov.*** MycoBank MB 836151. UNITE SH: 1230077.08FU.
Basionym: *Hypochnus subfuscus* subsp. *tristis* P. Karst., *Meddeland. Soc. Fauna Fl. Fenn.* **9**: 71. 1883.

Typus: **Finland**, *Tavastia australis* [= Etelä-Häme], Tammela, Mustiala, ad Betulam, 19 Aug. 1865, *P. A. Karsten* (**lectotype** H 6018703 [Herbarium P. A. Karsten 3036]); **epitype**: **Sweden**, Västerbotten, Vännäs, Orrböle, boreal, mixed forest on soil with high pH, 28 Aug. 2015, *S. Svantesson* 193 (GB).

Polyozellus tristoides (Svantesson & K.H. Larss.) Svantesson & Kõljalg, ***comb. nov.*** MycoBank MB 836152. UNITE SH: 1230081.08FU.
Basionym: *Pseudotomentella tristoides* Svantesson & K.H. Larss., *MycoKeys* **50**: 52. 2019.

Typus: **Norway**, Nord-Tröndelag, Snåsa, Bergsåsen, boreal, deciduous forest on soil with intermediate pH, 28 Aug. 2012, *K.-H. Larsson* (**holotype** O F110306).

Polyozellus umbrinus (Fr.) Svantesson & Kõljalg, ***comb. nov.*** MycoBank MB 836153. UNITE SH: 1185280.08FU.
Basionym: *Thelephora umbrina* Fr., *Elench. fung.* **1**: 199. 1828, *nom. sanct*.

Typus: **Sweden**, Småland, Femsjö, *E. Fries* (**neotype** UPS F003106 [Herb. Fries]); **epitype**: **Sweden**, Småland, Hylte, Femsjö, Femsjö Church Nature Reserve, boreonemoral, mixed forest on soil with intermediate pH, 7 Sep. 2016, *S. Svantesson* 351 (GB).

Polyozellus umbrinascens (Svantesson) Svantesson & Kõljalg, ***comb. nov.*** MycoBank MB 836154. UNITE SH: 1185297.08FU.
Basionym: *Pseudotomentella umbrinascens* Svantesson, *MycoKeys* **50**: 60. 2019.

Typus: **Sweden**, Bohuslän, Tanum (municipality), Tanum (parish), Greby Kleva, boreonemoral, deciduous forest on soil with high pH, RT90: E1236840, N6518916, 6 Sep. 2016, *S. Svantesson* 335 (**holotype** GB).

Polyozellus vepallidosporus (M.J. Larsen) Svantesson & Kõljalg, ***comb. nov.*** MycoBank MB 836155. UNITE SH: 1191930.08FU, SH1244119.08FU.
Basionym: *Pseudotomentella vepallidospora* M.J. Larsen, *Canad. J. Bot*. **45**: 1299. 1967.

Typus: **USA**, Washington, Quinault, Olympic Peninsula, on rotten conifer log, 15 Oct. 1958, *J. L. Lowe* 10368 (**holotype** BPI; **isotype**: SYRF).

DISCUSSION

Among homobasidiomycetes there is a general evolutionary trend from structurally simple, corticioid basidiomata with flat hymenia to more complex, stipitate forms with gills, tubes, *etc.*, occasionally followed by reversions to simpler forms (Hibbett & Binder 2002, Larsson *et al.* 2004). Most of these transitions occurred early during fungal evolution and the complex forms have since become well separated from the lineages that have retained a simple basidiome morphology. However, in a few cases species with complex basidiome forms occur nested within the same genus as species with simple forms, for example in *Trechispora*, as currently circumscribed (Ryvarden 2002, Meiras-Ottoni *et al.* 2021) and in *Thelephorales* seemingly also in *Tomentella*/*Thelephora* (Vizzini *et al.* 2016). Here it is documented for *Polyozellus*/*Pseudotomentella*.

The authors choose to recombine the type species of *Pseudotomentella* along with most other species previously placed in the genus to *Polyozellus*, thus delimiting the latter as a monophyletic genus including species with both stipitate and resupinate basidiomata. Two other alternatives would have been possible: either retaining *Pseudotomentella*, in the knowledge that is a paraphyletic genus with regards to *Polyozellus* or keeping both monophyletic and describing many small genera. The first option was not viewed as a fitting solution to the present situation, given the evolutionary reality of basidiome transitions among homobasidiomycetes and the fact that paraphyletic genera are inadvisable in general. A more acceptable way would perhaps have been to create many small genera. However, as already implied genera are a subjective, human construct, to ease our understanding of the relationship between species. In this context it is the view of the authors that it is easier to handle a genus with two distinct but readily identifiable morphologies than to deal with seven genera, where many display small and often overlapping morphology (*e.g.* the two different contenders for the name *Po. vepallidospora*). Given additional molecular data from currently undescribed species, this view might change but given that no undescribed species were retrieved from any UNITE Compound Clusters other than those containing the formally described *Polyozellus* and *Pseudotomentella* species included in this study, it does not currently seem likely that major changes to the present phylogeny would arise with the inclusion of such.

Four DNA regions, *RPB2*, mtSSU and the combined nrLSU and nrSSU, were found to be usable in delimiting *Polyozellus vs. Pseudotomentella*. Additional regions would have been preferable to account for *e.g.* incomplete lineage sorting, but given the lack of conflict with respect to the ingroup the current dataset was deemed sufficient for the purpose of this study. The ease of sequencing and high information content of the regions used make them good candidates for further systematic studies within *Thelephorales*. In addition, this result further testifies to the usability of the full tandem repeat as a molecular marker for fungi, especially in cases where the ITS region is too variable to be reliably aligned but the partial LSU region normally used contains too little information to infer a satisfyingly resolved phylogeny (*e.g.* Krehenwinkel *et al.* 2019, Wurzbacher *et al.* 2019, Bradshaw *et al.* 2020).

© 2021 Westerdijk Fungal Biodiversity Institute

The precise phylogenetic identities of *Po. humicola*, *Po. mucidula*, *Po. rhizopunctata* and *Po. vepallidospora* are currently unknown. Given the unsuccessful sequencing efforts of the types of *Po. griseopergamacea* and *Po. mucidula*, epitypification or sequencing with other methods are ways of resolution that should be explored. However, since the several available candidates for these four species were all shown to belong in *Polyozellus*, as here delimited, lack of knowledge about their definite identity does not pose a problem for their recombination.

The phylogenetic meaning of the heterotypic names currently synonymised with *Po. flavovirens*, *Po. griseopergamacea* and *Po. mucidula* is also unclear. Many of these species, *e.g*. *Pseudotomentella fumosa*, *Ps. kaniksuensis*, and *Ps. molybdea*, are very similar to the species currently given nomenclatural priority and are therefore unlikely not to belong in *Polyozellus*. Even so, their possible recombination needs clarification of their status as separate species.

Pseudotomentella larsenii is clearly more closely related to *Tomentellopsis* than to *Polyozellus* and is hence not recombined into the latter. This decision means that *Polyozellus* remains a genus restricted to the Northern Hemisphere. The possible inclusion of *Ps. larsenii* in *Tomentellopsis* needs to be addressed by further taxon sampling.

Pseudotomentella armata, *Ps. ochracea* and *T. italica* could not be included in the analyses, since sequencing of several gene regions failed. Their phylogenetic placement thus remains to be revealed by further studies.

Concerning conservation, *Pseudotomentella* is a larger genus than *Polyozellus* and the recombination of its species into the latter hence warrants more name changes than if the opposite were to be pursued. However, since *Polyozellus* is both older and has a wider usage – as a food source and indicator of old-growth forest, in dyeing *etc*. – this was not pursued.

It is clear that the identities of many members of what was formerly *Pseudotomentella*, and now constitute corticioid *Polyozellus* species, are deficiently known and will need further study in order to be clarified. Many of these species are rare and probably threatened by extinction due to loss of old growth forest. It is therefore the hope of the authors that their phylogenetically merited incorporation in *Polyozellus* will bring renewed interest to them and thereby facilitate the amount of attention and study that they deserve.

ACKNOWLEDGEMENTS

Funding for this study was received from The Swedish Taxonomy Initiative (2014-152 4.3), the Norwegian Biodiversity Information Centre (ADB54-09), Stiftelsen Lars Hiertas Minne, Helge Ax:son Johnsons Stiftelse and Kungl. Vetenskaps- och Vitterhets-Samhället i Göteborg. Urmas Kõljalg and Irja Saar were supported by the European Regional Development Fund (Centre of Excellence EcolChange) and the Estonian Research Council (PRG1170). Andrus Voitk and Michael Burzynski are sincerely thanked for the loan of *Polyozellus* pictures and the curators of herbaria BPI and H for granting and arranging loans.

Conflict of interest: The authors declare that there is no conflict of interest.

REFERENCES

Baroni TJ (2017). *Mushrooms of the Northeastern United States and Eastern Canada*. Timber Press, USA.

Bidartondo MI, Burghardt B, Gebauer G, *et al.* (2004). Changing partners in the dark: isotopic and molecular evidence of ectomycorrhizal liaisons between forest orchids and trees. *Proceedings of the Royal Society B: Biological Sciences* **271**: 1799–1806.

Botnen S, Kauserud H, Carlsen T, *et al.* (2015). Mycorrhizal fungal communities in coastal sand dunes and heaths investigated by pyrosequencing analyses. *Mycorrhiza* **25**: 447–456.

Bouckaert R, Heled J, Kühnert D, *et al.* (2014). BEAST 2: A software platform for Bayesian evolutionary analysis. *PLoS Computational Biology* **10**: e1003537.

Bouckaert R, Vaughan TG, Barido-Sottani J, *et al.* (2019). BEAST 2.5: An advanced software platform for Bayesian evolutionary analysis. *PLoS Computational Biology* **15**: e1006650.

Bradshaw M, Grewe F, Thomas A, *et al.* (2020). Characterizing the ribosomal tandem repeat and its utility as a DNA barcode in lichen-forming fungi. *BMC Evolutionary Biology* **20**: 2.

Brundrett MC (2002). Tansley Review No. 134: Coevolution of Roots and Mycorrhizas of Land Plants. *New Phytologist* **154**: 275–304.

Bücking H, Liepold E, Ambilwade P (2012). The Role of the Mycorrhizal Symbiosis in Nutrient Uptake of Plants and the Regulatory Mechanisms Underlying These Transport Processes. In: *Plant Science* (Dhal NK, Sahu SC, eds.) IntechOpen, Croatia: 107–138.

Castresana J (2000). Selection of conserved blocks from multiple alignments for their use in phylogenetic analysis. *Molecular Biology and Evolution* **17**: 540–552.

Garbelotto MM, Lee HK, Slaughter G, *et al.* (1997). Heterokaryosis is not required for virulence of *Heterobasidion annosum*. *Mycologia* **89**: 92–102.

Ginns J (1989). Descriptions and notes for some unusual North American corticioid fungi (*Aphyllophorales*, *Corticiaceae*). *Memoirs of the New York Botanical Garden* **49**: 129–137.

He MQ, Zhao RL, Hyde KD, *et al.* (2019). Notes, outline and divergence times of *Basidiomycota*. *Fungal Diversity* **99**: 105–367.

Hibbett DS, Binder M (2002). Evolution of complex fruiting-body morphologies in homobasidiomycetes. *Proceedings of the Royal Society B: Biological Sciences* **269**: 1963–1969.

Hjortstam K (1970). Studies in the Swedish species of the genus *Tomentella* (*Thelephoraceae*). II. *Svensk Botanisk Tidskrift* **64**: 421–428.

Hjortstam K (1970). Studies in the Swedish species of the genus *Tomentella* (*Thelephoraceae*). III. The genus *Tomentellopsis*. *Svensk Botanisk Tidskrift* **68**: 51–56.

Hopple Jr JS, Vilgalys R (1999). Phylogenetic relationships in the mushroom genus *Coprinus* and dark spored allies based on sequence data from the nuclear gene coding for the large ribosomal subunit RNA: divergent domains, outgroups, and monophyly. *Molecular Phylogenetics and Evolution* **13**: 1–19.

Hwang J-S, Song K-S, Kim W-O, *et al.* (1997). Polyozellin, a new inhibitor of prolyl endopeptidase from *Polyozellus multiplex*. *The Journal of Antibiotics* **50**: 773–777.

Jacquemyn H, Duffy KJ, Selosse MA (2017). Biogeography of Orchid Mycorrhizas. In: *Biogeography of Mycorrhizal Symbiosis. Ecological Studies (Analysis and Synthesis)*, vol. 230 (Tedersoo L, ed.). Springer, Switzerland: 159–177.

Jones G (2014). STACEY package documentation: species delimitation and species tree estimation with BEAST2. http://www.indriid.com/software.html

© 2021 Westerdijk Fungal Biodiversity Institute

Jones G (2017). Algorithmic improvements to species delimitation and phylogeny estimation under the multispecies coalescent. *Journal of Mathematical Biology* **74**: 447–467.

Katoh K, Standley DM (2013). MAFFT multiple sequence alignment software version 7, improvements in performance and usability. *Molecular Biology and Evolution* **30**: 772–80.

Kirk PM, Cannon PF, Minter DW, *et al.* (2008). *Ainsworth & Bisby's Dictionary of the Fungi*. 10th edn. CABI Europe, UK.

Kõljalg U (1996). *Tomentella* (*Basidiomycota*) and related genera in Temperate Eurasia. *Synopsis Fungorum* **9**: 1–213.

Kõljalg U, Larsson E (1998). *Pseudotomentella ochracea sp. nov.*, based on morphological and molecular data. *Folia Cryptogamica Estonica* **33**: 53–56.

Kõljalg U, Dahlberg A, Taylor AF, *et al.* (2000). Diversity and abundance of resupinate thelephoroid fungi as ectomycorrhizal symbionts in Swedish boreal forests. *Molecular Ecology* **9**: 1985–1996.

Kõljalg U, Dunstan W (2001). *Pseudotomentella larsenii sp. nov.* (*Thelephorales*), a common ectomycorrhiza former in dry eucalypt woodland and forests of Western Australia. *Harvard Papers in Botany* **6**: 123–130.

Kõljalg U, Nilsson RH, Abarenkov K, *et al.* (2013). Towards a unified paradigm for sequence-based identification of Fungi. *Molecular Ecology* **22**: 5271–5277.

Krehenwinkel H, Pomerantz A, Henderson JB, *et al.* (2019). Nanopore sequencing of long ribosomal DNA amplicons enables portable and simple biodiversity assessments with high phylogenetic resolution across broad taxonomic scale. *GigaScience* **8**: giz006.

Larsen MJ (1967a). *Tomentella* and related genera in North America: III. New species of *Tomentella* and *Pseudotomentella*. *Canadian Journal of Botany* **45**: 1297–1307.

Larsen MJ (1967b). *Tomentella* and related genera in North America V. New North American records of tomentelloid fungi. *Mycopathologia et Mycologia Applicata* **32**: 37–67.

Larsen MJ (1968). A new species of *Pseudotomentella* from North America. *Mycologia* **60**: 547–552.

Larsen MJ (1971a) [1972]. The genus *Pseudotomentella* (*Basidiomycetes*, *Thelephoraceae s. str*.). *Nova Hedwigia* **22**: 599–619.

Larsen MJ (1971b). Notes on tomentelloid fungi III. New species of *Pseudotomentella*. *Bulletin of the Torrey Botanical Club* **98**: 38–41.

Larsen MJ (1974). Some notes on *Pseudotomentella*. *Mycologia* **66**: 165–168.

Larsen MJ (1983). Notes on tomentelloid fungi V. Additional new species of *Pseudotomentella*. *Mycologia* **75**: 556–562.

Larsson A (2014). AliView: a fast and lightweight alignment viewer and editor for large data sets. *Bioinformatics* **30**: 3276–3278.

Larsson KH, Larsson E, Kõljalg U (2004). High phylogenetic diversity among corticioid homobasidiomycetes. *Mycological Research* **108**: 983–1002.

Lilleskov EA, Bruns TD (2005). Spore dispersal of a resupinate ectomycorrhizal fungus, *Tomentella sublilacina*, via soil food webs. *Mycologia* **97**: 762–769.

Liu YL, Whelen S, Hall BD (1999). Phylogenetic relationships among ascomycetes: evidence from an RNA polymerase II subunit. *Molecular Biology and Evolution* **16**: 1799–1808.

Martin DP, Murrell B, Golden M, *et al.* (2015). RDP4: Detection and analysis of recombination patterns in virus genomes. *Virus Evolution* **1**: vev003.

Martini EC, Hentic R (2002). Deux nouvelles espèces de champignons tomentelloides. *Bulletin trimestriel de la Société Mycologique de France* **118**: 79–90.

Martini EC, Hentic R (2003). *Pseudotomentella rhizopunctata sp. nov.*, une nouvelle espèce de champignon tomentelloïde chlamydosporée. *Bulletin trimestriel de la Société Mycologique de France* **119**: 19–29.

Matheny PB (2005). Improving phylogenetic inference of mushrooms with *RPB1* and *RPB2* nucleotide sequence (*Inocybe*, *Agaricales*). *Molecular Phylogenetics and Evolution* **35**: 1–20.

Meiras-Ottoni A, Larsson KH, Gibertoni TB (2021). Additions to *Trechispora* and the status of *Scytinopogon* (*Trechisporales, Basidiomycota*). *Mycological Progress* **20**: 203–222.

Miettinen O, Kõljalg U (2007). *Amaurodon sumatranus* (*Thelephorales*, *Basidiomycota*), a new species from Indonesia. *Mycotaxon* **100**: 51–59.

Moeslund JE, Nygaard B, Ejrnæs R, *et al.* (2019). Rødliste 2019. Aarhus Universitet, DCE – Nationalt Center for Miljø og Energi. www.redlist.au.dk.

Mühlmann O, Peintner U (2008). Mycobionts of *Salix herbacea* on a glacier forefront in the Austrian Alps. *Mycorrhiza* **18**: 171–180.

Murrill WA (1910). *North American Flora, volume 9, (Agaricales*) *Polyporaceae–Agaricaceae*. The New York Botanical Garden, USA.

Nagy LG, Walther G, Házi J, *et al.* (2011). Understanding the evolutionary processes of fungal fruiting bodies: Correlated evolution and divergence time in the *Psathyrellaceae*. *Systematic Biology* **60**: 303–317.

Nilsson RH, Larsson K-H, Taylor AFS, *et al.* (2018). The UNITE database for molecular identification of fungi: handling dark taxa and parallel taxonomic classifications. *Nucleic Acids Research* **47**: D259–D264.

Rambaut A (2012). FigTree 1.4.3. http://tree.bio.ed.ac.uk/software/figtree/

Rambaut A, Suchard MA, Xie D, *et. al* (2014). Tracer 1.6. http://tree.bio.ed.ac.uk/software/tracer/

Rehner SA, Buckley E (2005). A *Beauviera* phylogeny inferred from nuclear ITS and *EF1-α* sequences: evidence for cryptic diversification and links to *Cordyceps* teleomorphs. *Mycologia* **97**: 84–98.

Ryberg M, Larsson E, Molau U (2009). Ectomycorrhizal diversity on *Dryas octopetala* and *Salix reticulata* in an alpine cliff ecosystem. *Arctic, Antarctic, and Alpine Research* **41**: 506–514.

Ryvarden L (2002). A note on the genus *Hydnodon* Banker. *Synopsis Fungorum* **15**: 31–33.

Saar I, Oja J, Põldmaa K, *et al.* (2019). Red List of Estonian Fungi – 2019 update. *Folia Cryptogamica Estonica* **56**: 117–126.

SLU Artdatabanken (2020). *Rödlistade arter i Sverige 2020*. SLU Artdatabanken, Sweden.

Sønstebø JH (2002). *Molecular ecology of ectomycorrhizal fungi on* Bistorta vivipara *(L.) Gray in four alpine tundra communities*. Cand. scient. thesis. Department of Biology, University of Oslo, Norway.

Stalpers JA (1993). The aphyllophoraceous fungi I. Keys to the species of the *Thelephorales*. *Studies in Mycology* **35**: 1–168.

Svantesson S, Larsson K-H, Kõljalg U, *et al.* (2019). Solving the taxonomic identity of *Pseudotomentella tristis s.l.* (*Thelephorales*, *Basidiomycota*) – a multi-gene phylogeny and taxonomic review, integrating ecological and geographical data. *MycoKeys* **50**: 1–77.

Svantesson S, Larsson K-H, Larsson E (2021). *Pseudotomentella badjelanndana*, *Pseudotomentella sorjusensis* and *Tomentella viridibasidia* – three new corticioid *Thelephorales* species from the Scandes Mountains. *Phytotaxa* **497**: 61–78.

Svrček M (1958). Contribution to the taxonomy of the resupinate *Thelephoraceous* Fungi. *Ceská Mykologie* **12**: 66–77.

Svrček M (1960). Tomentelloideae Čechoslovakiae, Genera resupinata familae *Thelephoraceae s.str*. *Sydowia* **14**: 170–245.

Swofford DL (2002). PAUP*. Phylogenetic Analysis Using Parsimony (*and Other Methods) 4.0a, build 167. Sinauer Associates, Sunderland, MA. https://paup.phylosolutions.com/

Talavera G, Castresana J (2007). Improvement of phylogenies after removing divergent and ambiguously aligned blocks from protein sequence alignments. *Systematic Biology* **56**: 564–577.

© 2021 Westerdijk Fungal Biodiversity Institute

Taylor JH, Peterson CA (2005). Ectomycorrhizal impacts on nutrient uptake pathways in woody roots. *New Forests* **30**: 203–214.

Tedersoo L, Liiv I, Kivistik PA, *et al.* (2016). Genomics and metagenomics technologies to recover ribosomal DNA and single-copy genes from old fruit-body and ectomycorrhiza specimens. *MycoKeys* **13**: 1–20.

United States Forest Service (1994). *Record of decision for amendments to Forest Service and Bureau of Land Management planning documents within the range of the Northern Spotted Owl: and, standards and guidelines for management of habitat for late-successional and old-growth forest related species within the range of the Northern Spotted Owl.* US Department of Agriculture, Forest Service, Ecosystem management, USA.

Vizzini A, Angelini C, Losi C, *et al.* (2016). *Thelephora dominicana* (*Basidiomycota*, *Thelephorales*), a new species from the Dominican Republic, and preliminary notes on thelephoroid genera. *Phytotaxa* **265**: 27–38.

Voitk A, Saar I, Trudell S, *et al.* (2017). *Polyozellus multiplex* (*Thelephorales*) is a species complex containing four new species. *Mycologia* **109**: 975–992.

White TJ, Bruns T, Lee L, *et al.* (1990). Amplification and direct sequencing of fungal ribosomal RNA genes for phylogenetics. In: *PCR Protocols, A guide to Methods and Applications* (Innis MA, Gelfand DH, Sininski JJ, *et al.*, eds.). Academic Press, USA: 315–322.

Wurzbacher C, Larsson E, Bengtsson-Palme J, *et al.* (2019). Introducing ribosomal tandem repeat barcoding for fungi. *Molecular Ecology Resources* **19**: 118–127.

© 2021 Westerdijk Fungal Biodiversity Institute

FUSE

Fungal Systematics and Evolution

VOLUME 8
DECEMBER 2021
PAGES 155–161

doi.org/10.3114/fuse.2021.08.12

Ophiostomatoid fungi including a new species associated with Asian larch bark beetle *Ips subelongatus*, in Heilongjiang (Northeast China)

R. Chang[1,2], M.J. Wingfield[1], S. Marincowitz[1], Z.W. de Beer[1], X. Zhou[1], T.A. Duong[1*]

[1]Department of Biochemistry, Genetics and Microbiology, Forestry and Agricultural Biotechnology Institute (FABI), University of Pretoria, Pretoria 0002, South Africa
[2]College of Life Sciences, Shandong Normal University, Jinan 250014, China

*Corresponding author: tuan.duong@fabi.up.ac.za

Key words:
Ophiostomatales
Microascales
new taxon
Scolytinae
vector

Abstract: *Ips subelongatus* (*Coleoptera*, *Scolytinae*) is an important bark beetle species that infests *Larix* spp. in Asia. Individuals of this beetle are vectors of ophiostomatoid fungi, on their exoskeletons, that are transmitted to infested trees. In this study, the symbiotic assemblage of ophiostomatoid fungi associated with *I. subelongatus* in Northeast China was studied. Fungal isolates were identified based on their morphological characters and sequences of ITS, beta-tubulin, elongation factor 1-alpha and calmodulin gene regions. In total, 48 isolates were collected and identified, residing in six taxa. These included a novel species, described here as *Ophiostoma gmelinii sp. nov.*

Citation: Chang R, Wingfield MJ, Marincowitz S, De Beer ZW, Zhou X, Duong TA (2021). Ophiostomatoid fungi including a new species associated with Asian larch bark beetle *Ips subelongatus*, in Heilongjiang (Northeast China). *Fungal Systematics and Evolution* **8**: 155–161. doi: 10.3114/fuse.2021.08.12
Received: 11 August 2021; **Accepted:** 8 November2021; **Effectively published online:** 18 November 2021
Corresponding editor: P.W. Crous

INTRODUCTION

The Asian larch bark beetle, *Ips subelongatus* (*Coleoptera*, *Scolytinae*), is the most important insect pest infesting various *Larix* (larch) species in China (Chen *et al.* 2015). This beetle is also found in other Eurasian countries including Japan, Mongolia, North Korea, Russia, and South Korea (Cognato 2015). *Ips subelongatus* typically infests weakened, wind-thrown, and fire-damaged trees, but it is also able to kill healthy trees when outbreaks result in substantial population growth (Zhang *et al.* 1992).

Ips subelongatus as well as other bark beetles and their associated phoretic mites are well-known vectors of ophiostomatalean and microascalean fungi (Six 2003, Hofstetter & Moser 2014). The best known genera are *Ophiostoma* and *Ceratocystis* respectively (De Beer & Wingfield 2013). Most of these fungi only cause discoloration of the sapwood of infested trees (Six 2003). However, some species such as the Dutch elm disease fungi (*Ophiostoma ulmi* and *O. novo-ulmi*) and species accommodated in *Ceratocystis sensu lato* are important tree pathogens (Brasier 2001, Roux & Wingfield 2009).

There have been several investigations considering the fungal associates of bark beetle *I. subelongatus* in China (Liu *et al.* 2017, Wang *et al.* 2020) and these have revealed 21 species. Specifically, the recent study by Wang *et al*. (2020) was the most extensive and included the description of eight new taxa. The present study arose from a collection of isolates made from the beetles and galleries of *I. subelongatus* infesting *Larix gmelinii* in Heilongjiang, China. Identification of these isolates based on DNA sequence comparisons showed that most were of known taxa. Three of isolates appeared to represent a novel taxon and the aim of this study was to test this hypothesis.

MATERIALS AND METHODS

Fungal collection

Samples for this study were collected in July 2011, during the flight season of *I. subelongatus,* from a natural forest in Heilongjiang (northeast China) where *L. gmelinii* was also present. A total of 44 beetles and 46 galleries were collected and used for fungal isolation. The isolation medium was 2 % malt extract agar [MEA: 20 g Difco agar, 20 g Difco Bacto™ malt extract (Becton, Dickinson & Company), 1 L deionized water] supplemented with 0.05 % streptomycin. Fungal spore drops were picked up directly from the galleries and inoculated onto MEA plates. Living beetles were placed onto the surface of MEA plates and let crawling for several minutes and removed thereafter. Dead beetles were crushed and spread onto MEA plates. The MEA plates were incubated at room temperature (~ 25 °C) until fungal growth was observed. Tips of hyphae were picked and transferred onto new MEA plates. All the isolates collected in this study have been maintained in Culture Collection (CMW) of the Forestry and Agricultural Biotechnology Institute (FABI), University of Pretoria, South Africa. Ex-type cultures of a new species were deposited in the culture collection (CBS) of the Westerdijk Fungal Biodiversity Institute, Utrecht, the Netherlands. Herbarium specimens established as dried cultures were deposited to South African National Collection of Fungi (PREM), Roodeplaat, Pretoria, South Africa.

Fungal Systematics and Evolution is licensed under a Creative Commons Attribution-NonCommercial-ShareAlike 4.0 International License

© 2021 Westerdijk Fungal Biodiversity Institute

DNA extraction and PCR

DNA was extracted from fresh mycelium grown on 2 % MEA following the instructions provided by PrepMan™ Ultra Sample Preparation Reagent (Applied Biosystems, Foster City, CA). The primers ITS1F and ITS4 (White *et al.* 1990; Gardes & Bruns 1993) were used to amplify the internal transcribed spacer region (ITS), the primers BT2a and BT2b (Glass & Donaldson 1995) were used to amplify the beta-tubulin (*BT*) gene, the primers EF2F (Marincowitz *et al.* 2015) and EF2R (Jacobs *et al.* 2004) were used to amplify the translation elongation factor 1-alpha gene (*EF*). The primers CL2F and CL2R (Duong *et al.* 2012) were used to amplify the calmodulin gene (*CAL*). PCR and sequencing were conducted using the methods described by Duong *et al.* (2012). All sequences were assembled and checked by forward and reverse sequence using Geneious v. 7.1.4 (Biomatters, Auckland, New Zealand).

DNA sequence analyses

The ITS sequences of all isolates were subjected to BLASTn searches against the NCBI GeneBank nucleotide database (http://blast.ncbi.nlm.nih.gov) for preliminary identification. Based on the BLAST results, datasets of *BT*, *EF* and *CAL* sequences for different genera and species complexes were compiled and analyzed separately. Sequence alignments were done using an online version of MAFFT v. 7.0 (Katoh & Standley 2013), and were further curated in MEGA v. 6 (Tamura *et al.* 2013). Maximum likelihood (ML) and Bayesian inference (BI) analyses were conducted using RAxML-HPC2 v. 8.2.4 (Stamatakis 2014) and MrBayes v. 3.2.6 (Ronquist *et al.* 2012) respectively; both are available from the CIPRES Science Gateway (Miller *et al.* 2010). For the BI analysis, trees were sampled every 100th generation for 5 M generations and 25 % of trees were discarded as burn-in phase. All alignments have been deposited in TreeBASE (https://treebase.org/) under the study number S28534.

Morphology and culture characteristics

Depending on the number of isolates available, two to three isolates per species were chosen for morphological examination. Fresh mycelium was inoculated onto MEA plates to which sterilized pine twigs (with bark) had been added to induce the production of sexual or asexual structures. Fungal structures were examined using a Nikon Eclipse Ni light microscope (Nikon, Japan) and a Nikon SMZ 18 dissection microscope attached with a Nikon DS-Ri2 camera. Up to 50 measurements were made for characteristic structures whenever available using the NIS Elements BR software. Measurements are presented as "maximum – minimum" except for spores where "average ± standard deviation" was additionally presented.

Growth rates were determined at seven temperatures ranging from 5 to 35 °C at 5 °C intervals. Mycelial plugs (5 mm diam) were transferred from the margins of actively growing cultures to the centers of 90 mm Petri dishes containing 2 % MEA. Two diameter measurements perpendicular to each other were made of the colonies and the daily growth rate was calculated.

RESULTS

A total of 48 ophiostomatoid isolates were obtained. Twenty-one were obtained from the galleries of the beetle and the remaining isolates were from the beetles themselves. BLAST searches of the ITS sequences showed that the isolates collected in this study resided in three genera, *Endoconidiophora*, *Ophiostoma*, and *Sporothrix* (Table 1). Analyses of ITS (Fig. 1), *BT*, *EF* and *CAL* sequences suggested that these isolates resided in six taxa, five of which were known species *i.e.*, *O. hongxingense* (11 isolates) (Fig. S1), *O. peniculi* (two isolates) (Fig. S1), *O. pseudobicolor* (one isolate) (Fig. S2), *Sporothrix cf. abietina* (two isolates) (Fig. S3), and *Endoconidiophora fujiensis* (five isolates) (Fig. S4), and three isolates belonging to a novel species (Fig. 2) which is described below.

Taxonomy

Ophiostoma gmelinii R.L. Chang, Z.W. de Beer & M.J. Wingf., ***sp. nov.*** MycoBank MB 840569. Fig. 3.

Etymology: The epithet *gmelinii* refers to *Larix gmelinii,* a tree that *Ips subelongatus* infests in China.

Diagnosis: Ophiostoma gmelinii differed from its closest phylogenetic relatives, *O. rufum* and *O. xinganense*, in the size of conidia, growth rate, and lack of pesotum-like asexual morph.

Sexual morph not observed. *Asexual morph* sporothrix-like. *Mycelium* mostly submerged, densely compacted, hyaline, sometimes developing brown strings of hyphae with age. *Conidiophores* simple, upright, flexuous, rarely branched, septate, occasionally reduced to conidiogenous cells, 4–290 × 1–2 µm (4–30 µm long when reduced to conidiogenous cells). *Conidiogenous cells* blastic, denticulate, often showing sympodial growth, terminal, sometimes directly borne on vegetative hyphae. *Conidia* hyaline, mostly oblong, aseptate, the apex often slightly inflated, tapering abruptly to the pointed base, 4.5–8 × 2–3 µm (6.4 ± 0.96 × 2 ± 0.22 µm).

Culture characteristics: Colony shiny, smooth, colorless to whitish, developing pigmented zone or patches of hyphal strings when aged or damaged. Optimum growth at 25 °C (2.8 mm / d), followed by 20 °C (2.3 mm / d), 15 °C (1.7 mm / d), 10 °C (1 mm / d), 30 °C (0.9 mm / d), no growth at 5 and 35 °C.

Typus: **China**, Heilongjiang province, from gallery of *Ips subelongatus* on *Larix gmelinii*, 2011, coll. *X.D. Zhou* (**holotype** PREM 61562, culture ex-type CMW 40463 = CBS 141909).

Additional material examined: **China**, Heilongjiang province, from gallery of *Ips subelongatus* on *Larix gmelinii*, 2011, coll. *X.D. Zhou,* PREM 61564, culture CMW 40464 = CBS 141911.

Notes: The newly described *O. gmelinii* resides in the *O. piceae* species complex. Based on the analyses of *BT* sequences, all the isolates of this species formed a single clade together with *O. rufum,* which was recently described from the Czech Republic (Jankowiak *et al.* 2019), and *O. xinganense* described from China (Wang *et al.* 2020). This clade had a strong bootstrap support in the ML analysis but not in the case of the BI analysis (Fig. 2). However, based on the analyses of ITS sequences, *O. gmelinii* formed a well-resolved clade and this formed a sister clade with *O. genhense* and *O. multisynnematum*. *Ophiostoma rufum* grouped with *O. piceae*, *O. micans*, and other species. In the *EF* tree, all isolates of *O. gmelinii* formed a sister clade with *O.*

© 2021 Westerdijk Fungal Biodiversity Institute

Table 1. Isolates of ophiostomatoid fungi obtained from *I. subelongatus* on *Larix gmelinii* in Heilongjiang and used in phylogenetic analyses.

	Isolate number[1,2]			GenBank number[4]			
Species	**CMW**	**CBS**	**B/G[3]**	**ITS**	***BT***	***EF***	***CAL***
Endoconidiophora	40450		B	MW581513	MW579724	MW579746	n/a
fujiensis	40453		B	MW581514	MW579725	MW579747	n/a
	40460		B	MW581515	MW579726	MW579748	n/a
	40465		G	MW581516	MW579727	MW579749	n/a
	40479		B	MW581517	MW579728	MW579750	n/a
Ophiostoma gmelinii sp. nov.	40447		B	MW581494	MW579705	MW579729	n/a
	40463 H	141909	B	MW581495	MW579706	MW579730	n/a
	40464	141911	B	MW581496	MW579707	MW579731	n/a
O. hongxingense	40448		G	MW581498	MW579709	MW579733	n/a
	40455		G	MW581499	MW579710	MW579734	n/a
	40466		B	MW581500	MW579711	MW579735	n/a
	40467		B	MW581501	MW579712	MW579736	n/a
	40469		B	MW581502	MW579713	MW579737	n/a
	40474		B	MW581503	MW579714	MW579738	n/a
	40477		B	MW581504	MW579715	MW579739	n/a
	40483		B	MW581505	MW579716	MW579740	n/a
	40485		B	MW581506	MW579717	n/a	n/a
	40486		B	MW581507	MW579718	MW579741	n/a
	40487		B	MW581508	MW579719	MW579742	n/a
O. peniculi	40444		G	MW581509	MW579720	MW579743	n/a
	40472		B	MW581510	MW579721	MW579744	n/a
O. pseudobicolor	40478		B	MW581497	MW579708	MW579732	n/a
Sporothrix cf. abietina	40475		B	MW581511	MW579722	n/a	MW579751
	40454		G	MW581512	MW579723	MW579745	MW579752

[1] CMW: Culture Collection of the Forestry and Agricultural Biotechnology Institute (FABI), University of Pretoria, Pretoria, South Africa; CBS: Culture Collection of the Westerdijk Fungal Biodiversity Institute, Utrecht, the Netherlands.

[2] H = ex-holotype isolate.

[3] B = beetle; G = gallery.

[4] ITS = internal transcribed spacer regions 1 and 2 of the nuclear ribosomal DNA operon, including the 5.8S region; *BT* = beta-tubulin; *EF* = translation elongation factor 1-alpha; *CAL* = calmodulin.

flexuosum, O. multisynnematum and *O. genhense*. Collectively, these analyses resolved *O. gmelinii* as a distinct species in the *O. piceae* species complex as defined by Yin *et al*. (2016).

Morphological characters of *O. gmelinii* differed from its closest relatives *O. rufum* and *O. xinganense*. The conidia of *O. gmelinii* were larger than those of *O. rufum* (Jankowiak *et al.* 2019) but similar to those of *O. xinganense* (Wang *et al.* 2020). The growth rate of *O. gmelinii* was faster than in *O. rufum,* but much slower than in *O. xinganense*. In addition, *O. gmelinii* and *O. xinganense* are able to grow, albeit slowly at 30 °C, but *O. rufum* is not able to grow at this temperature (Jankowiak *et al.* 2019). Only a sporothrix-like asexual state was found in *O. gmelinii*, which is different to most of the other species in the *O. piceae* complex. These fungi typically produce pesotum-like synnemata as well as a sporothrix-like asexual morph (Yin *et al.* 2016, Wang *et al*. 2020). All the species in this complex, including the newly described *O. gmelinii*, are from conifer hosts (Yin *et al.* 2016, Jankowiak *et al*. 2019).

DISCUSSION

In this study, 48 isolates of ophiostomatoid fungi were obtained from beetles of *I. subelongatus* or its galleries. Six taxa were identified, residing in either the *Microascales* (one species) or the *Ophiostomatales*, including one new species. All the known species had previously been reported from China. *Sporothrix cf. abietina* was isolated from *I. subelongatus* for the first time.

Previous studies have revealed 21 species associated with *I. subelongatus* in China with 14 were new to science (Paciura *et al*. 2010, Wang *et al.* 2016, Liu *et al*. 2017, Wang *et al.* 2020). The present study adds two more species to this list. These results suggest that the fungal symbionts of *I. subelongatus* have now been relatively well sampled. As is true for many other ophiostomatoid fungi associated with conifer-infesting bark beetles, relatively little is known regarding their biology. In this regard, most are thought not to play a role in killing trees (Six & Wingfield, 2011). Although in the case of *Endoconidiophora fujiensis* (Yamaoka *et al.* 1998), which is a sister species to the *E. laricicola* associate of

© 2021 Westerdijk Fungal Biodiversity Institute

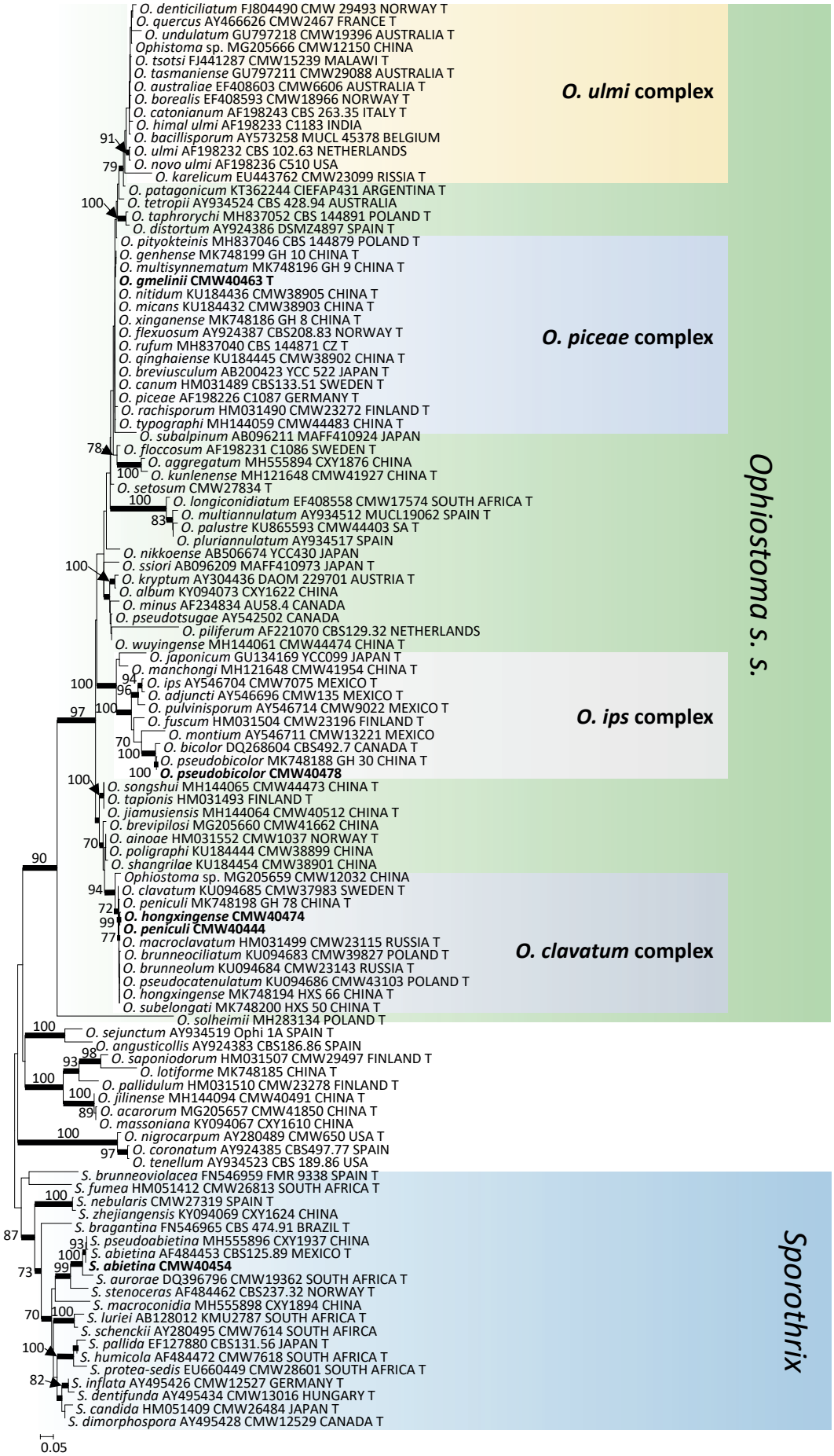

Fig. 1. Phylogram obtained from ML analyses of the ITS region of *Ophiostoma* and *Sporothrix*. Sequences obtained in this study are printed in bold type. Maximum-likelihood bootstrap support values (1 000 replicates) above 70 % are indicated at the nodes. Bayesian inference posterior probabilities (above 0.9) are indicated by bold lines at the relevant branches. T = ex-type cultures.

© 2021 Westerdijk Fungal Biodiversity Institute

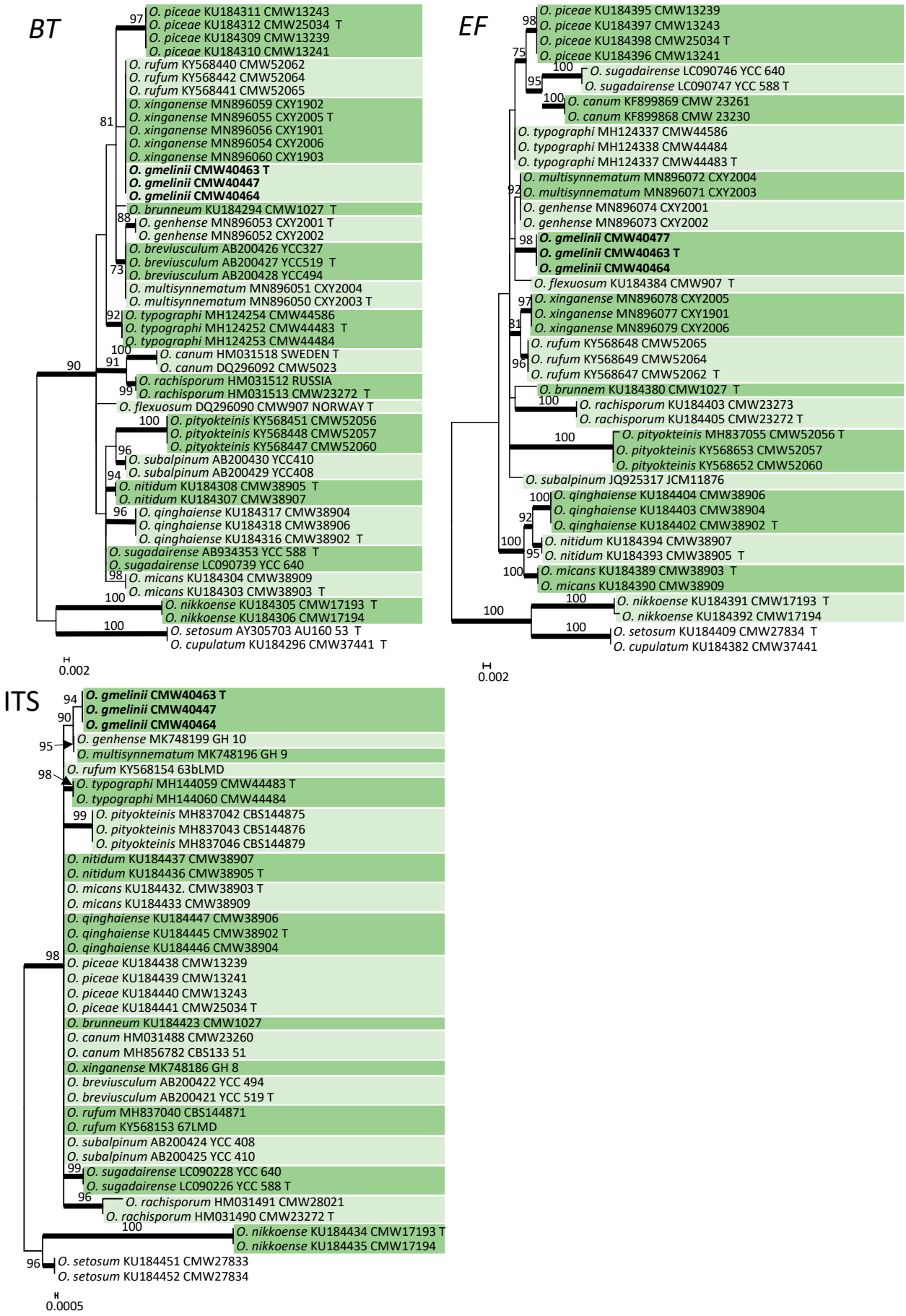

Fig. 2. Phylogrammes obtained from ML analyses of the ITS region, and the partial *BT* and *EF* gene regions of the *O. piceae* species complex. Isolates of the novel species are printed in bold type. Maximum-likelihood bootstrap support values (1 000 replicates) above 70 % are indicated at the nodes. Bayesian inference posterior probabilities (above 0.9) are indicated by bold lines at the relevant branches. T = ex-type cultures.

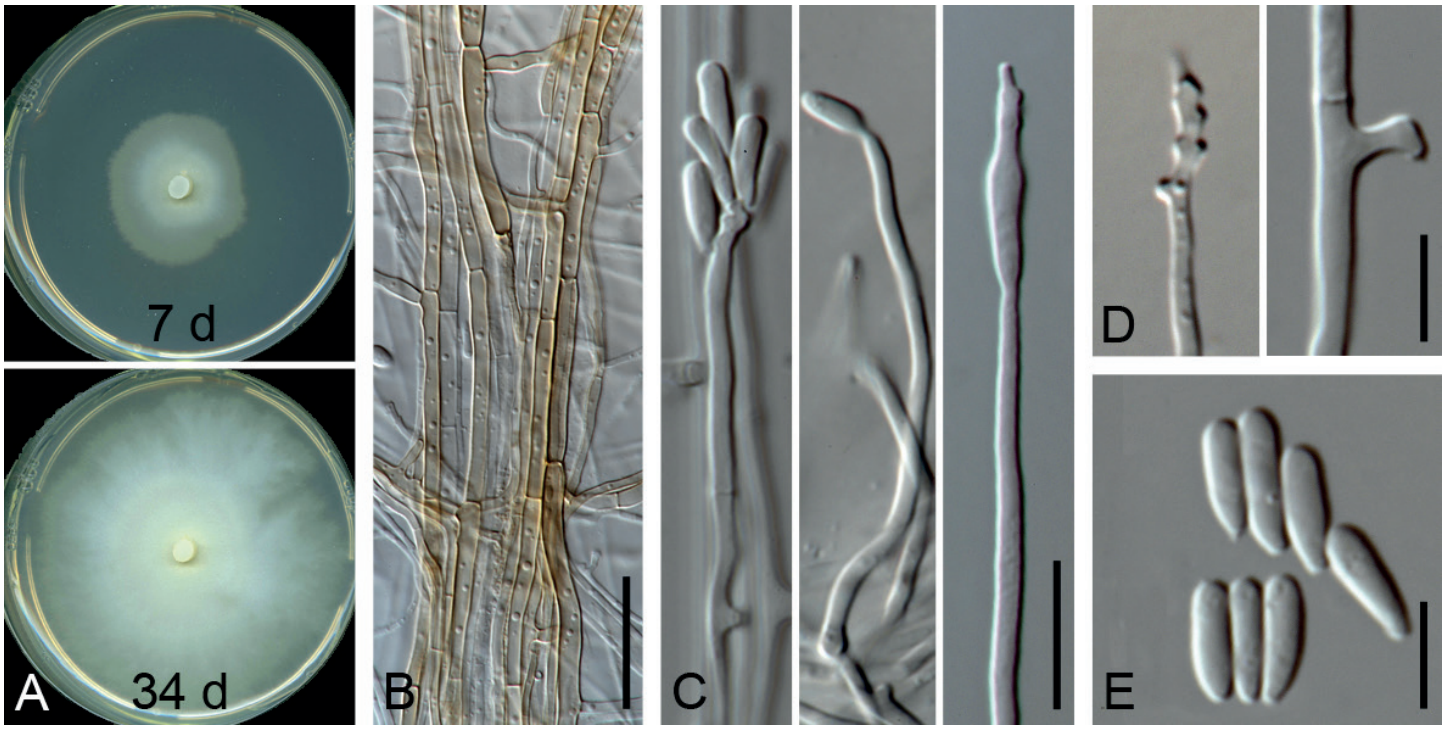

Fig. 3. Microscopic features of *Ophiostoma gmelinii sp. nov.* (ex-holotype, CMW 40463 = CBS 141909). **A.** Colony grown at 25 °C for 7 and 34 d in the dark. **B.** String of pigmented hyphae found in aged culture. **C.** Conidiophore. **D.** Conidiogenous cell. **E.** Conidia. Scale bars: B = 25 µm; C, D = 10 µm; E = 5 µm.

Ips cembrae (Marin *et al.* 2005) and the *E. polonica* associate of *I. typographus* (Krokene & Solheim, 1998), this question remains contentious (Lieutier *et al.* 2009, Biedermann *et al.* 2019)

Ips subelongatus has a wide distribution in China (Yang *et al.* 2007), including Heilongjiang, Jilin, Liaoning, Xinjiang, Gansu, Shandong, Shanxi, Hebei, Beijing, Zhejiang and Yunnan provinces and in other parts of Asia (Cognato 2015). All the studies on the fungal associates of this beetle in China have been in the north eastern parts of this country. It would thus be valuable in future studies to compare the fungal associates of this insect in different parts of China, as well as in other areas of East Asia.

ACKNOWLEDGEMENTS

We thank members of Tree Protection and Cooperation Programme (TPCP), the Department of Science and Technology (DST)-National Research Foundations (NRF), Center of Excellence in Plant Health Biotechnology (CPHB), and University of Pretoria, Pretoria, South Africa for financial support.

Conflict of interest: The authors declare that there is no conflict of interest.

REFERENCES

Biedermann PHW, Müller J, Grégoire J-C, *et al.* (2019). Bark beetle population dynamics in the Anthropocene: challenges and solutions. *Trends in Ecology & Evolution* **34**: 914–924.

Brasier CM (2001). Rapid evolution of introduced plant pathogens via interspecific hybridization: hybridization is leading to rapid evolution of Dutch elm disease and other fungal plant pathogens. *BioScience* **51**: 123–133.

Chen DF, Li YJ, Zhang QH, *et al.* (2015). Population divergence of aggregation pheromone responses in *Ips subelongatus* in northeastern China. *Insect Science* **23**: 728–738.

Cognato AI (2015). Biology, systematics, and evolution of *Ips*. In: *Bark Beetles: Biology and ecology of native and invasive species* (Vega FE, Hofstetter RW, eds). Academic Press, San Diego: 351–370.

De Beer ZW, Wingfield MJ (2013). Emerging lineages in the *Ophiostomatales*. In: *The Ophiostomatoid Fungi: Expanding Frontiers* (Seifert KA, De Beer ZW, Wingfield MJ, eds). CBS, Utrecht, The Netherlands: 21–46.

Duong TA, De Beer ZW, Wingfield BD, *et al.* (2012). Phylogeny and taxonomy of species in the *Grosmannia serpens* complex. *Mycologia* **104**: 715–732.

Gardes M, Bruns TD (1993). ITS primers with enhanced specificity for basidiomycetes-application to the identification of mycorrhizae and rusts. *Molecular Ecology* **2**: 113–118.

Glass NL, Donaldson GC (1995). Development of primer sets designed for use with the PCR to amplify conserved genes from filamentous Ascomycetes. *Applied and Environmental Microbiology* **61**: 1323–1330.

Hofstetter RW, Moser JC (2014). The role of mites in insect-fungus associations. *Annual Review of Entomology* **59**: 537–557.

Jacobs K, Bergdahl DR, Wingfield MJ, *et al.* (2004). *Leptographium wingfieldii* introduced into North America and found associated with exotic *Tomicus piniperda* and native bark beetles. *Mycological Research* **108**: 411–418.

Jankowiak R, Bilański P, Strzałka B, *et al.* (2019). Four new *Ophiostoma* species associated with conifer- and hardwood-infesting bark and ambrosia beetles from the Czech Republic and Poland. *Antonie van Leeuwenhoek* **112**: 1501–1521.

Katoh K, Standley DM (2013). MAFFT multiple sequence alignment software version 7: improvements in performance and usability. *Molecular Biology and Evolution* **30**: 772–780.

Krokene P, Solheim H (1998). Pathogenicity of four blue-stain fungi

© 2021 Westerdijk Fungal Biodiversity Institute

associated with aggressive and non aggressive bark beetles. *Phytopathology* **88**: 39–44.

Lieutier F, Yart A, Salle A (2009). Stimulation of tree defenses by ophiostomatoid fungi can explain attack success of bark beetles on conifers. *Annals of Forest Science* **66**: 801.

Liu XW, Wang HM, Lü Q, *et al.* (2017). Taxonomy and pathogenicity of *Leptographium* species associated with *Ips subelongatus* infestations of *Larix* spp. in northern China, including two new species. *Mycological Progress* **16**: 1–13.

Marin M, Preisig O, Wingfield BD, *et al.* (2005). Phenotypic and DNA sequence data comparisons reveal three discrete species in the *Ceratocystis polonica* species complex. *Mycological Research* **109**: 1137–1148.

Marincowitz S, Duong TA, De Beer ZW, *et al.* (2015). *Cornuvesica*: A little known mycophilic genus with a unique biology and unexpected new species. *Fungal Biology* **119**: 615–630.

Miller MA, Pfeiffer W, Schwartz T (2010). Creating the CIPRES Science Gateway for inference of large phylogenetic trees. Institute of Electrical and Electronics Engineers, New Orleans, LA: 1–8.

Paciura D, De Beer ZW, Jacobs K, *et al.* (2010). Eight new *Leptographium* species associated with tree-infesting bark beetles in China. *Persoonia* **25**: 94–108.

Ronquist F, Teslenko M, van der Mark P, *et al*. (2012) MrBayes 3.2: efficient Bayesian phylogenetic inference and model choice across a large model space. *Systematic Biology* **61**: 539–542.

Roux J, Wingfield MJ (2009). *Ceratocystis* species: emerging pathogens of non-native plantation *Eucalyptus* and *Acacia* species. *South Forests* **71**: 115–120.

Six DL (2003). Bark beetle-fungus symbioses. In: *Insect Symbiosis* (Bourtzis K, Miller T, eds), CRC Press, Boca Raton, Florida USA: 77–114.

Six DL, Wingfield MJ (2011). The role of phytopathogenicity in bark beetle-fungus symbioses: a challenge to the classic paradigm. *Annual Review of Entomology* **56**: 255–272.

Stamatakis A (2014) RAxML version 8: a tool for phylogenetic analysis and post-analysis of large phylogenies. *Bioinformatics* **30**: 1312–1313.

Tamura K, Stecher G, Peterson D, *et al.* (2013). MEGA6: molecular evolutionary genetics analysis version 6.0. *Molecular Biology and Evolution* **30**: 2725–2729.

Wang H, Lu Q, Meng X, *et al.* (2016). *Ophiostoma olgensis*, a new species associated with *Larix* spp . and *Ips subelongatus* in northern China. *Phytotaxa* **282**: 282–290.

Wang Z, Liu Y, Wang H, *et al.* (2020). Ophiostomatoid fungi associated with *Ips subelongatus*, including eight new species from northeastern China. *IMA Fungus* **11**: 3.

White TJ, Bruns T, Lee S, *et al.* (1990). Amplification and direct sequencing of fungal ribosomal RNA genes for phylogenetics. In: *PCR protocols: a guide to methods and applications* (Innis MA, Gelfand DH, Sninsky JJ, White TJ, eds). Academic Press, San Diego (California): 315–322.

Yamaoka Y, Wingfield M, Ohsawa M, *et al.* (1998). Ophiostomatoid fungi associated with *Ips cembrae* in Japan and their pathogenicity of Japanese larch. *Mycoscience* **39**: 367–378.

Yang J, Lin Q, Chen G (2007). Risk analysis of *Ips subelongatus* motschulsky (in Chinese). *Journal of Northeast Forestry University* **35**: 60–63.

Yin ML, Wingfield MJ, Zhou XD, *et al.* (2016). Multigene phylogenies and morphological characterization of five new *Ophiostoma* spp. associated with spruce-infesting bark beetles in China. *Fungal Biology* **120**: 454–470.

Zhang QH, Byers JA, Schlyter F (1992). Optimal attack density in the larch bark beetle, *Ips cembrae* (*Coleoptera*: *Scolytidae*). *Journal of Applied Ecology* **29**: 672–678.

Supplementary Material: http://fuse-journal.org/

Fig. S1. Phylogram obtained from ML analyses of the partial *BT* and *EF* gene sequences of the *O. clavatum* species complex. Sequences obtained in this study are printed in bold type. Maximum-likelihood bootstrap support values (1 000 replicates) above 70 % are indicated at the nodes. Bayesian inference posterior probabilities (above 0.9) are indicated by bold lines at the relevant branches. T = ex-type cultures.

Fig. S2. Phylogram obtained from ML analyses of the ITS region and the partial *BT* gene of the *O. ips* species complex. Sequences obtained in this study are printed in bold type. Maximum-likelihood bootstrap support values (1 000 replicates) above 70 % are indicated at the nodes. The Bayesian inference posterior probabilities (above 0.9) are indicated by bold lines at the relevant branches. T = ex-type cultures.

Fig. S3. Phylogram obtained from ML analyses of the ITS region, and the partial *BT* and *CAL* gene sequences of the *Sporothrix gossypina* species complex. Sequences obtained in this study are printed in bold type. Maximum-likelihood bootstrap support values (1 000 replicates) above 70 % are indicated at the nodes. Bayesian inference posterior probabilities (above 0.9) are indicated by bold lines at the relevant branches. T = ex-type cultures.

Fig. S4. Phylogram obtained from ML analyses of the ITS region, and the partial *BT* and *EF* gene sequences of *Endoconidiophra*. Sequences obtained in this study are printed in bold type. Maximum-likelihood bootstrap support values (1 000 replicates) above 70 % are indicated at the nodes. Bayesian inference posterior probabilities (above 0.9) are indicated by bold lines at the relevant branches. T = ex-type cultures.

© 2021 Westerdijk Fungal Biodiversity Institute

© 2021 Westerdijk Fungal Biodiversity Institute

FUSE

Fungal Systematics and Evolution

VOLUME 8
DECEMBER 2021
PAGES 163–178

doi.org/10.3114/fuse.2021.08.13

On six African species of *Lyomyces* and *Xylodon*

I. Viner[1*], F. Bortnikov[2], L. Ryvarden[3], O. Miettinen[1]

[1]Botanical Museum, Finnish Museum of Natural History, University of Helsinki, P.O. Box 7, 00014, Finland
[2]Faculty of Biology, Lomonosov Moscow State University, Leninskie Gory 1/12, 119234 Moscow, Russia
[3]Institute of Biological Sciences, University of Oslo, P.O. Box 1066, Blindern, N.0316 Oslo, Finland

*Corresponding author: ilya.viner@helsinki.fi

Key words:
Corticioids
new species
phylogeny
taxonomy

Abstract: We studied a number of sub-Saharan collections of corticioid *Xylodon* and *Lyomyces* species, including several types. Morphological descriptions and molecular analyses based on the ribosomal DNA loci nuc rDNA ITS1-5.8S-ITS2 and when possible nuc 28S rDNA, allow us to introduce four new species: *L. densiusculus, X. angustisporus*, *X. dissiliens*, and *X. laxiusculus*. DNA barcodes for *X. submucronatus* and *X. pruniaceus* are published for the first time and *X. pruniaceus* is re-described.

Citation: Viner I, Bortnikov F, Ryvarden L, Miettinen O (2021). On six African species of *Lyomyces* and *Xylodon*. *Fungal Systematics and Evolution* **8**: 163–178. doi: 10.3114/fuse.2021.08.13
Received: 1 October 2021; **Accepted:** 8 November 2021; **Effectively published online:** 24 November 2021
Corresponding editor: P.W. Crous

INTRODUCTION

Sub-Saharan Africa remains poorly explored for fungi due to the lack of taxonomists and scientific infrastructure. Yet, the region is a hotspot for discovering new species (Cheek *et al.* 2020). In this situation, local and global extinction events caused by habitat loss or climate change may occur unnoticed simply because science has not recorded the existence of species (Cheek *et al.* 2018). Consequently, nature conservation strategies cannot consider fungal diversity. Other than fungal inventories based on the morphological identification of sporocarps, an ample source of species records to work with is DNA sequences from environmental samples. Those have an advantage of spotting fungi in stages other than morphologically identifiable sporocarps. Inconveniently, such DNA fragments often cannot be precisely attributed to species names. They may represent already described taxa without DNA barcodes or truly undescribed species known only from environmental sequences. Environmental sequences cannot be given taxonomic names because of the lack of a physical voucher specimen deposited in a fungarium (Lücking & Hawksworth 2018). For these reasons, we find it important to work towards filling the gaps in our knowledge of African mycota.

Lyomyces and *Xylodon* are two closely related genera with unclear molecular and morphological borders. These genera had been treated in *Hyphodontia* for a couple of decades until Hjortstam & Ryvarden (2007, 2009) re-introduced them. Together they are the most species-rich and abundant group in the family *Schizoporaceae* (*Hymenochaetales*, *Basidiomycota*) worldwide. Despite their great abundance, we are aware of only six currently recognised species described from Africa including Réunion. We describe here four new species in this group and provide molecular data for two already existing taxa, which previously lacked DNA barcodes.

MATERIALS AND METHODS

Morphological methods

Type material and specimens from fungaria H, O, and GB were studied. Fungarium abbreviations are given according to Index Herbariorum (Thiers). Microscopic methods were described in Miettinen *et al*. (2006). All measurements were made in Cotton Blue (CB, Merck 1275; Kenilworth, New Jersey) with phase contrast illumination (1 250 ×), which allowed reporting them with 0.1 µm precision. The benefits of phase contrast illumination over bright-field microscopy are explained by Stein (1969). The following abbreviations were used in microscopic descriptions: L – mean spore length; W – mean spore width; Q – mean L/W ratio; n – number of elements (basidiospores, basidia, cystidia, and hyphae) measured, which are followed by the number of specimens studied. We excluded 5 % of measurements from each end of the range representing variation of basidiospores and cystidia. Excluded extreme values were indicated in parentheses when they strongly differed from the lower or higher 95 % percentile.

DNA extraction and sequencing

Total genomic DNA was extracted from herbarium specimens using a CTAB-chloroform extraction protocol (Kutuzova *et al*. 2017). We used standard as well as self-designed primers (Table 1) to amplify complete nuc rDNA ITS1-5.8S-ITS2 (ITS) and in some cases nuc 28S rDNA (28S) for all focal taxa. After amplification PCR products were run on a 1.5 % agarose gel stained with Gel Red staining (Biotium, Fremont, California) and visualized under UV light. PCR products were purified from agarose gels using a Fermentas Genomic DNA Purification Kit (Thermo Fisher

Fungal Systematics and Evolution is licensed under a Creative Commons Attribution-NonCommercial-ShareAlike 4.0 International License

© 2021 Westerdijk Fungal Biodiversity Institute

Table 1. Primers used in this study.

Primer name	Sequence	Target DNA locus	Binding site	Direction	Reference
ITS5	GGAAGTAAAAGTCGTAACAAGG	ITS, ITS1	18S	fwd	White *et al.* (1990)
ITS2	GCTGCGTTCTTCATCGATGC	ITS1	5.8S	fwd	White *et al.* (1990)
58A1F	GCATCGATGAAGAACGC	ITS2	5.8S	fwd	Martin & Rygiewicz (2005)
ITS2.2rXyl	TTATCACACCGCATATATGC	ITS2	ITS2	rev	this study
ITS2.2fXyl	CTTCYCTTGAATGYATTA	ITS2	ITS2	fwd	this study
ALR0.2	GATATGCTTAAGTTCAGCGGG	ITS, ITS2	28S	rev	Riebesehl & Langer (2017)
LR22	CCTCACGGTACTTGTTCGCT	ITS	28S	rev	Vilgalys lab, Duke University (https://sites.duke.edu/vilgalyslab/files/2017/08/rDNA-primers-for-fungi.pdf)
JS1	CGCTGAACTTAAGCATAT	28S	28S	fwd	Landvik (1996)
LR7	TACTACCACCAAGATCT	28S	28S	rev	Hopple & Vilgalys (1994)

Scientific, Waltham, Massachusetts). Sequencing reactions were performed on an ABI 3730XL DNA analyzer (Applied Biosystems) by Macrogen (Amsterdam, the Netherlands).

A number of additional 28S sequences used in the analyses came from partial genomes. The corresponding DNA extractions were sequenced with the aid of NextSeq 550 sequencing using the Nextera kit at Biomedicum Functional Genomics Unit (Helsinki, Finland). The assessment of read quality and their cleaning was performed using the FastQC and FastP tools (Chen *et al.* 2018). For the identification of 28S from the fungal genomes, the cleaned reads were mapped to nrDNA and 28S sequences and then were assembled using the SPADES (Bankevich *et al.* 2012) and MEGAHIT assemblers (Li *et al.* 2015). Additionally, to check the homology of the predicted genes, nrDNA and 28S were aligned to the assembled genomes using LASTz (Harris 2007). Sequences with the identity of at least 50 % and the coverage of 70 % were extracted. All newly produced sequences used in this study have been deposited in GenBank (Table 2).

Phylogenetic analyses

Extremely high diversity of ITS sequences in the focal genera precluded attempts to construct a reliable all-encompassing alignment for this locus, even if *Lyomyces* and *Xylodon* are analysed separately. Phylogenies produced based on such alignments became highly sensitive to the taxon sampling and the selected alignment algorithm. Therefore, we produced a reliably aligned dataset based on more conservative locus 28S (D1–D4) to show the phylogenetic placement of focal taxa with available nuclear LSU sequences. Then we constructed three additional ITS alignments for *L. densiusculus*, *X. laxiusculus*, and *X. submucronatus*, which belonged to lineages abundant in GenBank (Benson *et al.* 2018) as of 1 July 2021. Only sequences that could be reliably aligned were used in the ITS analyses. This corresponded to 89–93 % threshold of pairwise similarity to our newly produced sequences. As ITS of *X. angustisporus*, *X. dessiliens*, and *X. pruniaceus* had no close matches in public databases, these sequences were not used for building the ITS-based phylogenies.

Alignments were calculated through the MAFFT v. 7.429 online server (https://mafft.cbrc.jp/alignment/server/) using the L-INS-I strategy (Katoh *et al.* 2017). After removing unalignable fragments, the length of the alignment and the number of parsimony informative characters were correspondingly 1 280 and 235 bp for the 28S alignment; 570 and 54 bp for the *L. densiusculus* alignment; 660 and 51 bp for the *X. laxiusculus* alignment; 550 and 85 bp for the *X. submucronatus* alignment. The full alignments with annotation of the excluded characters were deposited at TreeBASE (study 28841).

We inferred rooted phylogenetic trees with maximum likelihood (ML) and Bayesian Inference (BI). Nucleotide substitution models for BI were chosen with TOPALI v. 2.5 (Milne *et al.* 2008) based on the Bayesian information criterion (BIC). We performed BI using MrBayes v. 3.2 (Ronquist *et al.* 2012). In these analyses three parallel runs with four chains each and other default parameters were run for one million generations. A burn-in of 25 % was used in the final analyses, ensuring the average standard deviation of split frequencies had reached < 0.01 for all data sets. Support at nodes was indicated when posterior probabilities were ≥ 0.8. For ML analyses, IQ-TREE v. 1.2.2 (Nguyen *et al.* 2015) with the best-fitted model option was used. Bootstrapping was performed using the standard nonparametric bootstrap algorithm with the number of replicates set to 1 000. Support at nodes was indicated with bootstrap values ≥ 70 %.

RESULTS

Bayesian Inference and ML returned similar topologies and relevant support values from these analyses were indicated at nodes in Figs 1–4. The 28S analysis returned a tree with a clade consisting of *Xylodon* and *Lyomyces* distinct from *Hastodontia* and *Fasciodontia* (Fig. 1). All *Lyomyces* taxa were confined to one clade supported only by BI. Basal relationships within the *Xylodon*/*Lyomyces* cluster were not resolved. Newly described *X. angustisporus* occupied a place at the deepest split of the *Xylodon*/*Lyomyces* cluster.

Our ITS analyses showed that *X. submucronatus* occurred as a sister taxon to *X. rimosissimus* (Fig. 2), *L. densiusculus* ended up in the same clade with *L. fimbriatus* (Fig. 3), while *X. laxiusculus* formed a subclade with *X. subclavatus* (Fig. 4). As blasting ITS of newly described *X. angustisporus* and *X. dissiliens* returned no close hits that would have allowed building a reliable ITS alignment, we included these species only in the 28S analysis (Fig. 1). *X. pruniaceus* – sequenced for the first time in this study – turned out to be the single close relative of *X. angustisporus* in our dataset, with a 96.4 % ITS similarity, or only 22 bp difference.

© 2021 Westerdijk Fungal Biodiversity Institute

Table 2. Sequences used in this study. Sequences marked with * were produced for this study.

Species	Specimen	ITS	28S
Fasciodontia bugellensis	Larsson 8195	OK273855*	OK273855*
Fasciodontia sp.	Zhao 6280	–	MZ146327
Hastodontia hastata	Larsson 14646	MH638232	MH638232
Lyomyces aff. *orientalis*	Boidin 383	MH857295	–
Lyomyces bambusinus	Zhao 4831	–	MW264919
Lyomyces crustosus	Spirin 12603	OK273832*	OK273832*
Lyomyces densiusculus	Ryvarden 44818	OK273853*	OK273853*
Lyomyces elaeidicola	He 6360	–	MW507035
	He 6378	–	MW507036
Lyomyces fimbriatus	Wu 910620-7	MK575209	–
	Wu 911204-4	MK575210	–
Lyomyces griseliniae	Larsson 5289	OK273851*	OK273851*
Lyomyces leptocystidiatus	Zhao 20170815-30	MT319427	–
	Zhao 20170815-43	MT319428	–
	Zhao 20170814-14	MT319429	–
	Zhao 20170815-2	MT319430	–
	Zhao 20170818-1	MT319431	–
	Zhao 20170814-8	MT319432	–
	Zhao 20170818-8	MT319433	–
	Zhao 20170908-14	MT319434	–
	Zhao 20170818-9	MT319435	–
Lyomyces macrosporus	He 6179	–	MW507034
	Zhao 4516	–	MW264920
Lyomyces microfasciculatus	He 2651	–	MW507027
	Zhao 5109	–	MW264921
Lyomyces orientalis	He 3616	–	MW507030
	He 3686	–	MW507031
Lyomyces pruni	Spirin 12682	OK273833*	OK273833*
Lyomyces sambuci	Miettinen 11705	OK273852*	OK273852*
	He 6108	–	MW507033
	He 6576	–	MW507037
Lyomyces sp.	Zhao 8188	MW713744	–
	Zhao 17855	MW713745	–
	Burdsall HHB-19410	MW740296	–
	Burdsall HHB-19323	MW740297	–
	Zhao 10474	–	MZ262525
	Zhao 4299	–	MW713731
	Zhao 4352	–	MW713732
	Zhao 4385	–	MZ262521
	Zhao 4394	–	MW713733
	Zhao 4725	–	MZ262522
	Zhao 6224	–	MZ262523
	Zhao 6431	–	MZ262526
	Zhao 6442	–	MZ262527
	Zhao 6474	–	MZ262528
	Zhao 6483	–	MZ262529
	Zhao 6565	–	MZ262531
	Zhao 8188	–	MW713736

© 2021 Westerdijk Fungal Biodiversity Institute

Table 2. (Continued).

Species	Specimen	ITS	28S
	Zhao 9784	–	MW713735
Lyomyces vietnamensis	He 3260	–	MW507028
Lyomyces wuliangshanensis	He 3498	–	MW507029
	He 4765	–	MW507032
Xylodon aff. *borealis*	UC2022850	KP814307	–
Xylodon angustisporus	Ryvarden 50691b	OK273831*	OK273831*
Xylodon apacheriensis	Miettinen 16686	OK273835*	OK273835*
Xylodon asperus	clone BF-OTU19	AM902054	–
	Nilsson 2004b	DQ873606	DQ873607
	Langer 3257	EU583424	–
	NFLI 2000-112/1	JQ358805	–
	UC2023164	KP814364	–
	UC2023169	KP814365	–
	UC2023187	KP814366	–
	Dai 14824	KY290980	–
	NIBIO 2016-0924/1	MF511090	–
	Zhao 1035	MG231619	–
	Zhao 1068	MG231620	–
	Zhao 1070	MG231621	–
	Zhao 1076	MG231622	–
	Zhao 1078	MG231623	–
	Zhao 1154	MG231624	–
	Zhao 1168	MG231625	–
	Zhao 1169	MG231626	–
	Zhao SWFU 006420	MK809500	–
	Zhao 6543	MW940726	–
	Spirin 11923	OK273838*	OK273838*
Xylodon attenuatus	Spirin 8775	MH324476	–
	Spirin 8714	OK273839*	OK273839*
Xylodon bambusinus	Zhao 11211	MW394658	MW394651
	Zhao 11219	MW394659	MW394653
	Zhao 11310	MW394660	MW394655
	Zhao 11215	MW394661	MW394652
	Zhao 11224	MW394662	MW394654
Xylodon borealis	Spirin 10911	OK273846*	OK273846*
Xylodon crystalliger	KUN3347	OK273842*	OK273842*
Xylodon cystidiatus	Savchenko AS171128/1625B	OK273850*	OK273850*
Xylodon detriticus	Miettinen 22106	OK273844*	OK273844*
Xylodon dissiliens	Ryvarden 44817	OK273856*	OK273856*
Xylodon flaviporus	MA Fungi 79440	MH260071	MH260066
Xylodon hyphodontinus	Savchenko AS171124/1235	OK273848*	OK273848*
Xylodon laurentianus	DLL2009-049	JQ673187	–
	DLL2009-082	JQ673188	–
	DLL2009-087	JQ673189	–
	clone CMH177	KF800268	–
	DLL2011-142	KJ140643	–
	HHB_719	KY962845	–
	Zhao 140	MG231647	–

© 2021 Westerdijk Fungal Biodiversity Institute

Table 2. (Continued).

Species	Specimen	ITS	28S
	Russell 8118	MK575271	–
Xylodon laxiusculus	Ryvarden 44877	OK273827*	–
Xylodon nespori	Nordon 030915	DQ873622	DQ873622
	Viner 2019_59	OK273834*	OK273834*
Xylodon niemelaei	Savchenko TU114922	OK273836*	OK273836*
	GC 1508-146	–	KX857816
Xylodon nongravis	Spirin 5615	OK273849*	OK273849*
Xylodon nothofagi	ICMP 13839	AF145582	MH260064
Xylodon ovisporus	ICMP 13835	AF145586	MH260063
	KUC8140	JGI	JGI
Xylodon paradoxus	Oivanen PO109	OK273843*	OK273843*
Xylodon patagonicus	strain P.CH-4	KF562013	–
	MA-Fungi 90705	KY962835	–
	MA-Fungi 90702	KY962836	–
	MA-Fungi 90707	KY962837	–
	MA-Fungi 90704	KY962840	–
	MA-Fungi 90703	KY962841	–
	Smith MES-2446	MH930325	–
Xylodon pruinosus	Viner 2019_21	OK273845*	OK273845*
	Nilsson 990902	DQ677507	DQ677507
Xylodon pruniaceus	Ryvarden 11251	OK273828*	–
Xylodon pseudolanatus	HHB-10703-Sp	OK273847*	OK273847*
Xylodon pseudotropicus	Otto Miettinen 16558.2	OK273854*	OK273854*
Xylodon quercinus	Miettinen 15050.1	KT361632	–
	Larsson 11076	KT361633	–
	Boidin 4014	MH858169	–
	MA-Fungi 91815	MT158722	–
	MA-Fungi 91816	MT158723	–
	clone 4248_520	MT236714	–
	Spirin 12030	OK273841*	OK273841*
Xylodon raduloides	Dai 12631	KT203307	–
	MA-Fungi 12864	KY962820	–
	MA-Fungi 12877	KY962821	–
	MA-Fungi 22499	KY962822	–
	MA-Fungi 22513	KY962823	–
	MA-Fungi 75310	KY962825	–
	MA-Fungi 70457	KY962827	–
	MA-Fungi 78658	KY962828	–
	MA-Fungi 75272	KY962829	–
	MA-Fungi 79314	KY962830	–
	MA-Fungi 35643	KY962831	–
	MA-Fungi 12778	KY962832	–
	MA-Fungi 75244	KY962833	–
	MA-Fungi 608	KY962838	–
	NY s.n.	KY962843	–
	MA-Fungi 90709	KY962844	–
	Riebesehl KAS-JR03	MH880222	–
	Riebesehl KAS-JR09	MH880223	–

© 2021 Westerdijk Fungal Biodiversity Institute

Table 2. (Continued).

Species	Specimen	ITS	28S
	Riebesehl KAS-JR26	MH880225	–
	clone 4248_300	MT236523	–
	Polemis EP.18-A1543	MT458537	–
	Dai 12631	–	KT203328
Xylodon ramicida	Spirin 7664	NR138013	–
Xylodon rimosissimus	Ryberg 021031	DQ873627	–
	plB4D	HM136630	–
	clone 201	KC785580	–
	Lindner 2011-081	KJ140600	–
	UC2023147	KP814193	–
	UC2023148	KP814194	–
	UC2022842	KP814311	–
	UC2023109	KP814414	–
	Zhao 1487	MG231649	–
	Russell 8120	MK575252	–
	Dirks PUL F24614	MW448610	–
	Miettinen 12026.1	OK273840*	OK273840*
Xylodon sp.	Langer 3365	DQ340324	–
	Larsson 12386	DQ873612	DQ873612
	Berglund 1117	DQ873633	DQ873634
	clone F126	JX981881	–
	Larsson 6686	LN714553	–
	Zhao SWFU 006465	MK809410	–
	LWZ 20180904-28	MT319674	–
	Zhao 16090	MW566132	–
	Zhao 18342	–	MW980779
	Zhao 18379	–	MW980780
	Zhao 18394	–	MW980781
	Zhao 210	–	MN654918
	Zhao 214	–	MN654919
	Zhao 215	–	MN654920
Xylodon spathulatus	Spirin 12007	OK273837*	OK273837*
	Wu 1307-42	–	KX857810
Xylodon subclavatus	TUB-FO 42167	MH880232	–
Xylodon submucronatus	Ryvarden 9322b	OK273829*	–
	Renvall 1602	OK273830*	–
Xylodon subtropicus	Wu 1508-2	KX857806	–
	Zhao 20180512-15	MT319539	–
Xylodon verecundus	Larsson 12261	–	DQ873643
Xylodon xinpingensis	Zhao 9125	–	MW394649
	Zhao 9174	–	MW394650
Xylodon yarraensis	LWZ 20180510-4	MT319635	–
	LWZ 20180510-16	MT319637	–
	LWZ 20180510-19	MT319638	–
	LWZ 20180510-5	MT319639	–
	LWZ 20180509-7	MT319640	–
	LWZ 20180512-21	MT319641	–
	LWZ 20180512-22	MT319642	–

© 2021 Westerdijk Fungal Biodiversity Institute

Table 2. (Continued).

Species	Specimen	ITS	28S
	LWZ 20180512-23	MT319643	–
	LWZ 20180512-29	MT319644	–
	LWZ 20180512-19	MT319645	–

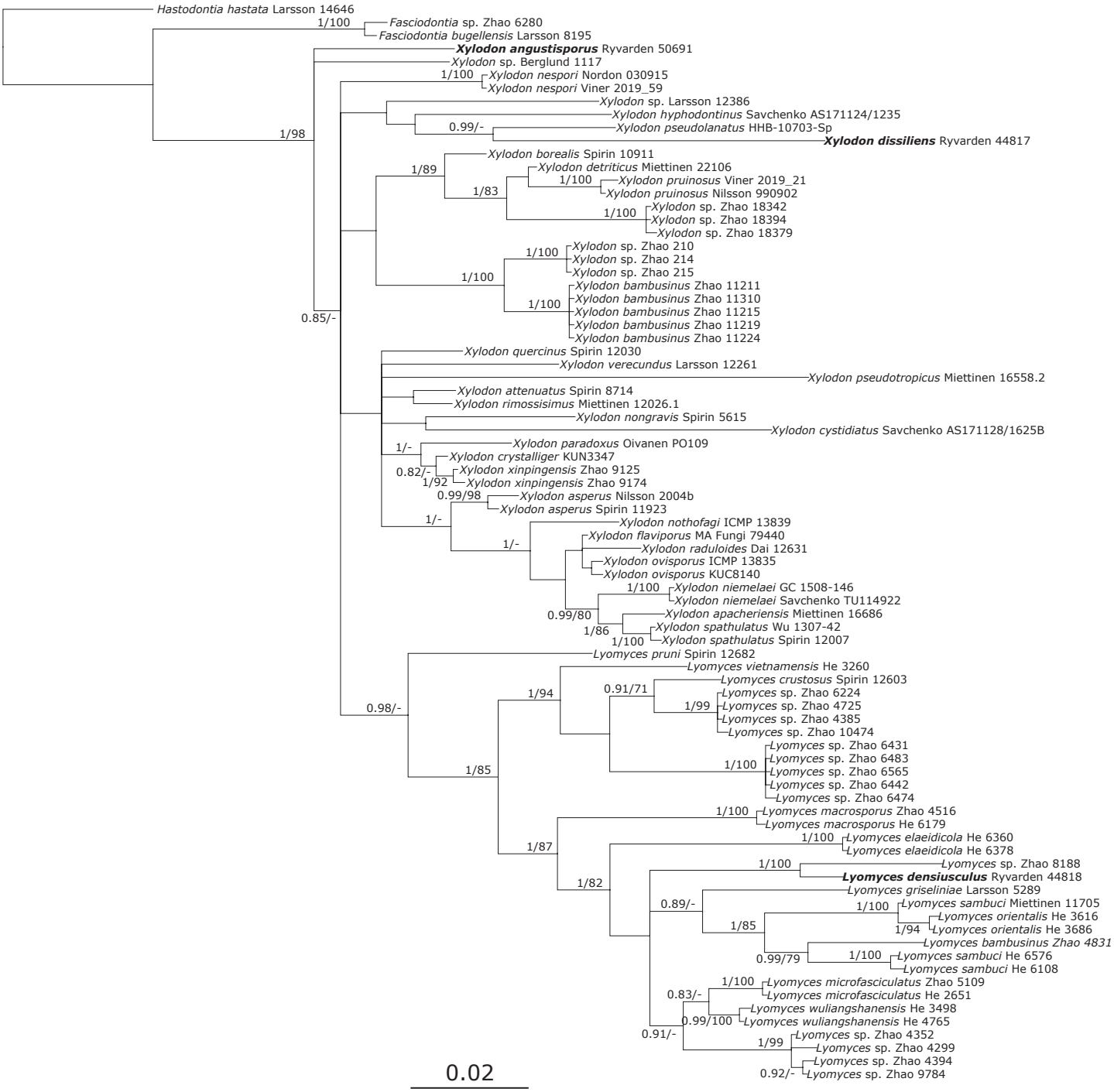

Fig. 1. Phylogenetic relationships of *Xylodon* and *Lyomyces* inferred from 28S sequences using BI analysis. Bayesian posterior probabilities followed by ML bootstrap values are shown at nodes; branch lengths reflect estimated number of changes per site.

© 2021 Westerdijk Fungal Biodiversity Institute

There were three 28S sequences with questionable species assignment. Zhao 210 (GenBank MN654918), Zhao 214 (GenBank MN654919), and Zhao 215 (GenBank MN654920) belong to one of the *Xylodon* clades despite being published as *Trechispora yunnanensis* (*Trechisporales*, *Basidiomycota*). The *X. submucronatus* tree also contained two similarly problematic ITS sequences. MA-Fungi 91816 (GenBank MT158723) and MA-Fungi 91815 (GenBank MT158722) clearly belong to *X. quercinus* despite being published as *X. magallanesii*.

Morphological differences between species in *Xylodon* and *Lyomyces* complex are often small, but we have found reliable characters to separate all newly described species from other African material we are aware of. We introduce four new species supported by the results of our molecular and morphological analyses.

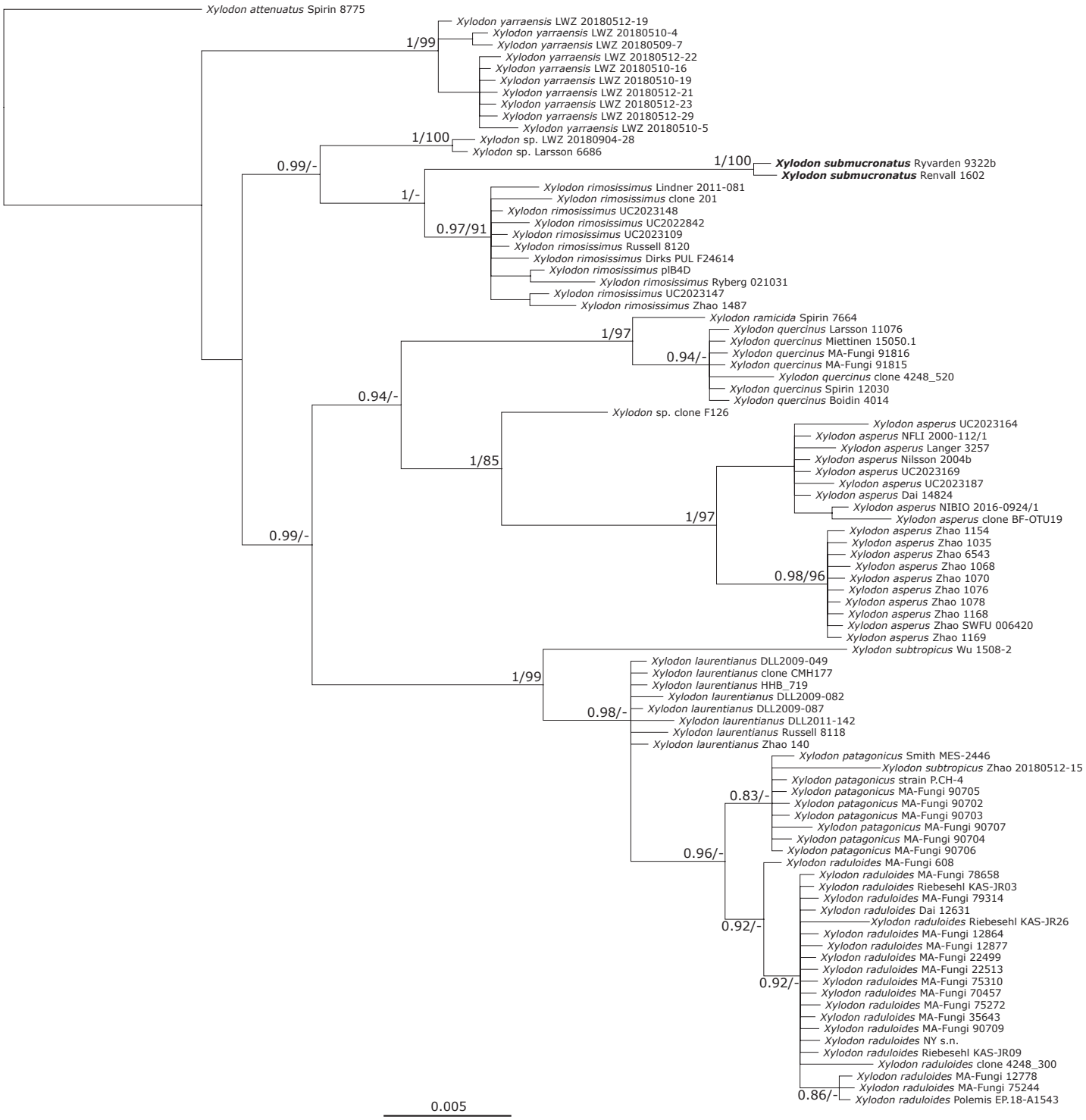

Fig. 2. Phylogenetic relationships of *Xylodon submucronatus* and allied taxa inferred from ITS sequences using BI analysis. Bayesian posterior probabilities followed by ML bootstrap values are shown at nodes; branch lengths reflect estimated number of changes per site.

© 2021 Westerdijk Fungal Biodiversity Institute

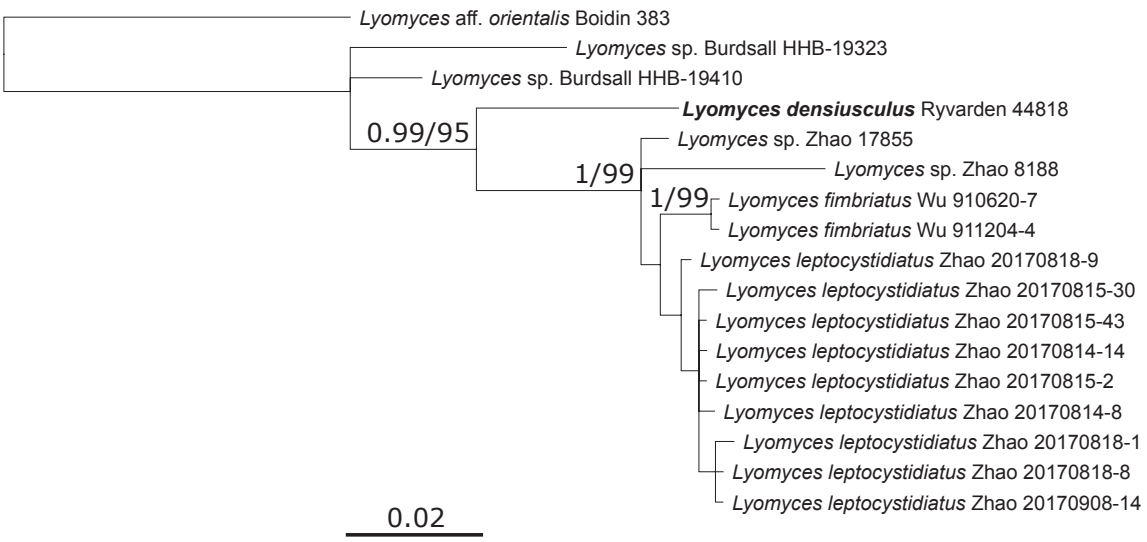

Fig. 3. Phylogenetic relationships of *Lyomyces densiusculus* and allied taxa inferred from ITS sequences using BI analysis. Bayesian posterior probabilities followed by ML bootstrap values are shown at nodes; branch lengths reflect estimated number of changes per site.

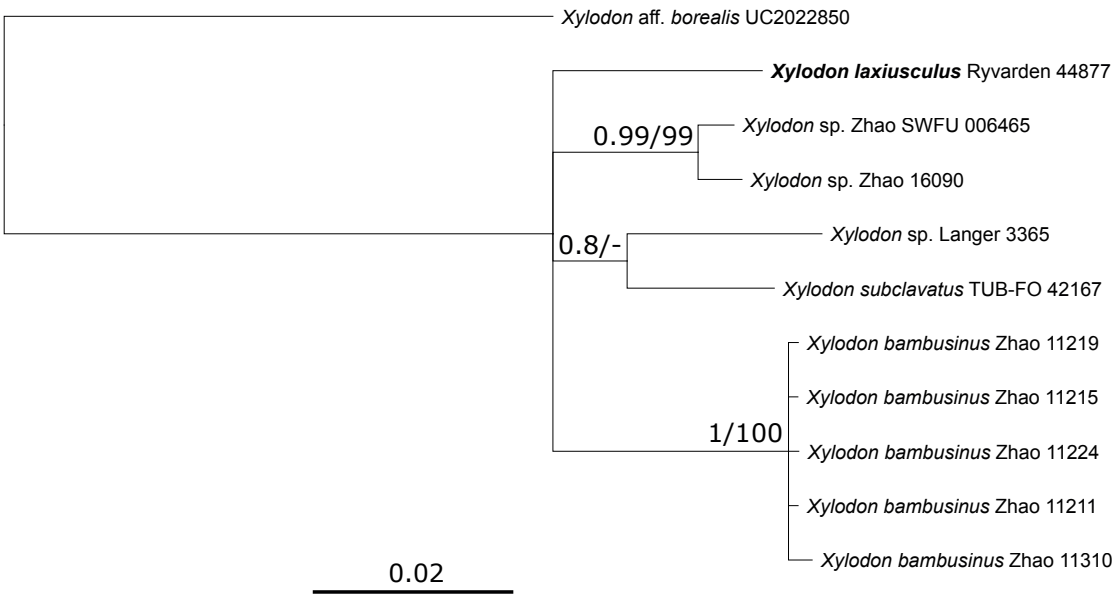

Fig. 4. Phylogenetic relationships of *Xylodon laxiusculus* and allied taxa inferred from ITS sequences using BI analysis. Bayesian posterior probabilities followed by ML bootstrap values are shown at nodes; branch lengths reflect estimated number of changes per site.

TAXONOMY

Lyomyces densiusculus Viner & Ryvarden, ***sp. nov.*** MycoBank MB 841943. Fig. 5.

Etymology: *Densiusculus* (Lat., adj.), a bit dense, refers to the dense and obscure hyphal system.

Basidiocarp effused, up to 6 cm in the widest dimension. Margin indistinct, hymenial surface cream to almost white, smooth to tuberculate; hymenophoral projections barely visible with an unaided eye, up to 70 µm high, 50–80 µm broad at base, 1–3 per mm. *Hyphal system* monomitic; hyphae clamped, thin- to thick-walled especially in subiculum (up to 1 µm). While being mostly obscure and densely packed, hyphal fragments of 4–5 cells may be observed at some places in subiculum and subhymenium. Large clusters of crystalline matter sprinkled throughout the fruit-body obscure the hyphal structure even further. *Subhymenial hyphae* mostly obscure but those which can be seen, slightly cyanophilic, 1.8–3.3(–3.8) µm wide (n = 20/1). *Subicular hyphae* not cyanophilic, branched mostly at right angles, 1.8–4.7 µm wide (n = 19/1). *Cystidial elements* from capitate to tapering, 13–21(–25) × 4–7 µm (n = 23/1), evenly distributed in and between hymenophoral projections. *Basidia* suburniform, 4-spored, 13–20 × 4.2–6 µm (n = 16/1). *Basidiospores* thin-walled, narrowly ellipsoid to subcylindrical, slightly cyanophilic, 5.3–6.9(–7.2) × 3.1–4(–4.2) µm (n = 30/1), L = 6.165, W = 3.62, Q = 1.7.

Distribution and ecology: Western Uganda, on bark of angiosperm branch. So far known only from the type locality.

© 2021 Westerdijk Fungal Biodiversity Institute

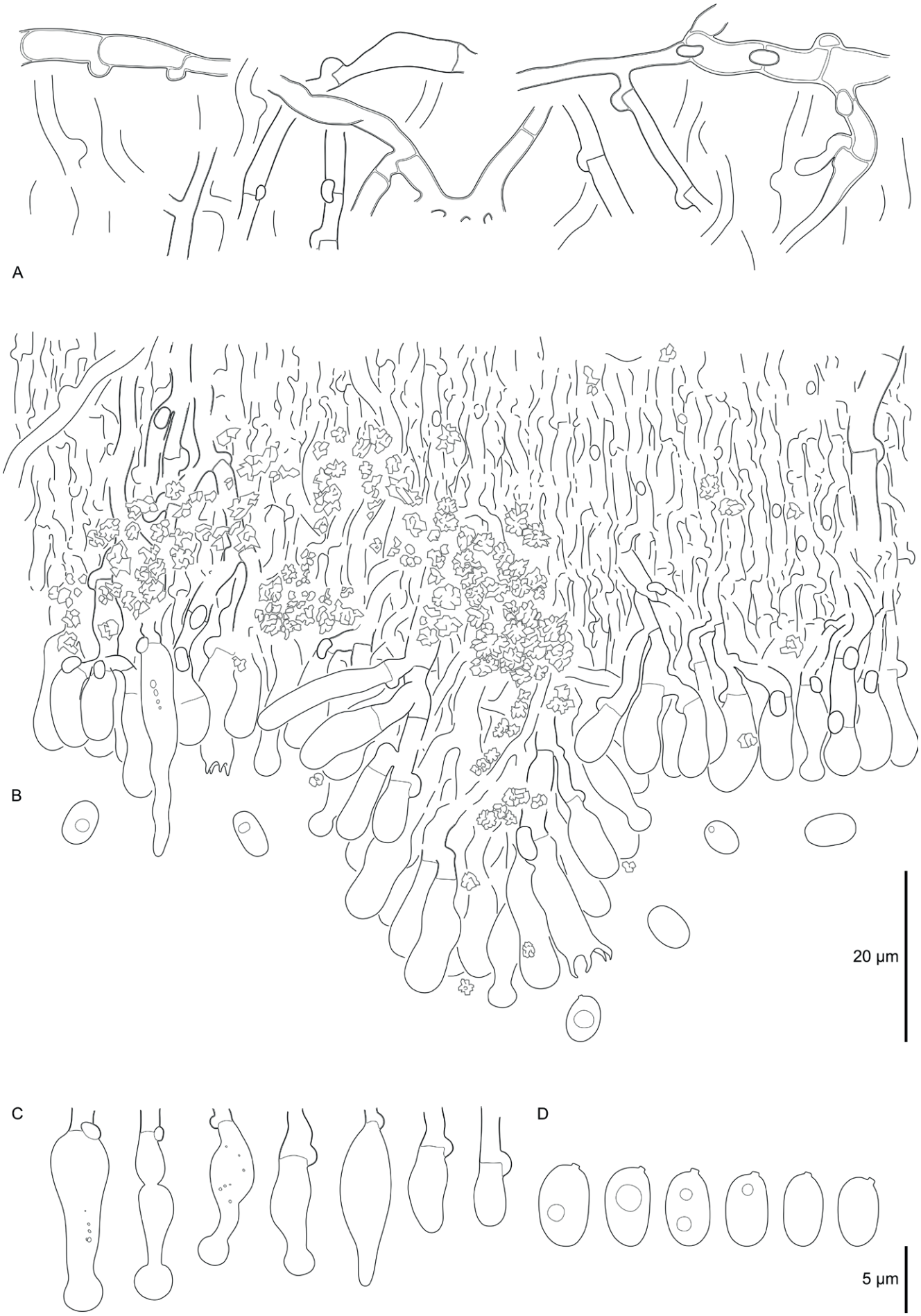

Fig. 5. *Lyomyces densiusculus* (holotype). **A.** Subiculum. **B.** Section of the sporocarp through hymenophoral projection and subhymenium. **C.** Sterile hymenophoral elements including cystidia of different shapes. **D.** Spores.

© 2021 Westerdijk Fungal Biodiversity Institute

Typus: **Uganda**, Western Uganda, Kabarole district, Kibale National Park, Makerere University Field Station, on bark of angiosperm branch, 20 Apr. 2002, *L. Ryvarden*, 44818 (**holotype** O, **isotype** in H) – ITS and 28S sequence, GenBank OK273853.

Notes: *Lyomyces densiusculus* resembles the *L. sambuci* species complex. Despite being recently addressed by Yurchenko *et al.* (2017) and Wang *et al.* (2021), some taxonomic problems in the *L. sambuci* complex still linger. According to the published data and our own observations, it contains several true species – undescribed or with existing old names – separated by DNA, morphology (at least in some cases), and ecological preferences. While making the decision to introduce *L. densiusculus* as a new species, we were guided by the following considerations. Morphologically, the combination of densely packed hyphae and subcylindrical spores allows separating this species from European or African collections of *L. sambuci s.l.* we are aware of. According to our molecular analyses, *L. densiusculus* is distant enough (the closest match is 94.6 %, or 40 bp difference in ITS) from any sequences in public databases, as well as our unpublished sequences, to not belong to some recently described *Lyomyces*. We also studied the type of its closest relative *L. fimbriatus*, Wu 880729-13, described from Taiwan. It has grandinioid basidiocarps with fimbriate projections, more loose hyphal structure, well-differentiated long cystidia, and ellipsoid to broadly ellipsoid spores, altogether making distinguishing these two species easy.

Xylodon angustisporus Viner & Ryvarden, ***sp. nov.*** MycoBank MB 841321. Fig. 6.

Etymology: *Angustisporus* (Lat., adj.), narrow-spored, refers to the narrow spores.

Basidiocarp effused, up to 5 cm in the widest dimension. Margin indistinct, hymenial surface cream to almost light ochraceous, grandinioid; hymenophoral projections up to 200 µm high, 150–200 µm broad at base, 8–11 per mm. *Hyphal system* monomitic; hyphae clamped, distinct, thin- to thick-walled especially in subiculum (up to 1 µm). *Subhymenial hyphae* cyanophilic, 1.5–3.5 µm wide (n = 29/2). *Subicular hyphae* slightly cyanophilic, branched mostly at right angles, (1.2–)2.1–4.6(–5) µm wide (n = 22/2). A few subicular hyphae have large intercalary inflations, 7–10 µm wide. Characteristic rounded crystals scattered through basidiocarp, 3–6 µm in diam. Hymenial elements cyanophilic to strongly cyanophilic. *Cystidia* are of different shapes: from capitate and spathulate to obtuse and moniliform, 12–21.4(–35) × (3.2–)3.5–5.5(–6.2) µm (n = 73/2). Moniliform cystidia are mostly confined to the base of hymenophoral projections. Cystidia of all shapes sometimes have strongly cyanophilic contents and (or) thickened-walls (up to 0.8 µm). Thick- to thin walled hyphidia make up the core of hymenophoral projections. Some thin walled hyphidia moderately to strongly flexuous. *Basidia* suburniform, 4-spored, 13–22 × 3.9–5 µm (n = 21/2). *Basidiospores* thin-walled, narrowly ellipsoid to subcylindrical, slightly cyanophilic, (4.3–)4.8–6.2 × 2.4–3.2 µm (n = 63/2), L = 5.2, W = 2.4, Q = 1.84.

Distribution and ecology: So far known only from Cameroon, on bark of angiosperms.

Typus: **Cameroon**, the East Region, Upper Nyong Division, Dja Biosphere Reserve, NW Dja sector, 3 km south of Somalomo, on bark of angiosperm branch, 12 Sep. 2019, *L. Ryvarden*, 50691B (**holotype** O, **isotype** in H) – ITS and 28S sequence, GenBank OK273831.

Additional materials examined: **Cameroon**, the Southwest Region, Ndian Division, Korup National Park, on trail to transect P, lowland rain forest, on liana hanging down from high canopy, 2 Mar. 1991, *L. Ryvarden*, 22729 (O).

Notes: *Xylodon angustisporus* is a sister taxon of *X. pruniaceus* (see below) described from eastern Africa, which differs only in the spore morphology and slightly more robust basidiocarps. *Xylodon angustisporus* might be confused with *X. nespori*, a species (or probably a species complex) with a wide intercontinental distribution. *Xylodon nespori* specimen Ryvarden 22729 reported from Cameroon (Hjortstam *et al.* 1993), turned out to be *X. angustisporus*, thus further underlining the morphological similarity between the two species. Generally, *X. nespori* differs in spore morphology but, in our experience, some individuals of *X. nespori* from the Holarctic give spore measurements overlapping with *X. angustisporus*. Therefore, spores alone might not be characteristic enough. We find moniliform cystidia, flexuous hyphidia, slightly more dense hyphal structure, and hymenium with abundant strongly cyanophilic elements in *X. angustisporus* to be good distinguishing features between the two species.

Xylodon dissiliens Viner & Ryvarden, ***sp. nov.*** MycoBank MB 841330. Fig. 7.

Etymology: *Dissiliens* (Lat., adj.), bursting, refers to the cystidia, which easily collapse.

Basidiocarp effused, up to 5 cm in the widest dimension. Margin pruinose, grayish, while the rest of hymenial surface white, grandinioid; hymenophoral projections rather irregularly arranged, barely visible for the unaided eye, up to 100 µm high, 80–100 µm broad at base, 9–11(–13) per mm. *Hyphal structure* monomitic, hyphae clamped. *Subhymenial hyphae* thin-walled, slightly cyanophilic, (2.9–)3.4–5 µm wide (n = 20/1). *Subicular hyphae* slightly thick-walled, branched mostly at right angles 2.8–5 µm wide (n = 20/1). Large stellate crystals scattered throughout the basidiocarp. *Cystidia* of two types: a) large, thin-walled leptocystidia of subhymenial origin, from cylindrical to almost globose, sometimes with protuberances close to the apex, 20–43(–50) × 5–20(–25) µm (n = 21/1); b) capitate cystidia in hymenium, often bearing a stellate crystalline cap, 14–26×4–10 µm (n = 20/1). *Basidia* suburniform, 4-spored, 14–17.5 × 4–5.5 µm (n = 11/1). *Basidiospores* thin-walled, ellipsoid, slightly cyanophilic, 5–6.3(–6.7) × 3.7–4.8 µm (n = 30/1), L = 5.5, W = 4.16, Q = 1.32. The whole basidiocarp structure is very delicate: most elements easily collapse if pressed too hard while mounting the slide. This is especially relevant for large leptocystidia, which burst first even when basidia and capitate cystidia are still intact.

Distribution and ecology: Western Uganda, on bark of angiosperm branch. So far known only from the type locality.

Typus: **Uganda**, Western Uganda, Kabarole district, Kibale National Park, Makerere University Field Station, on bark of angiosperm branch, 20 Apr. 2002, *L. Ryvarden*, 44817 (**holotype** O, **isotype** in H) – ITS and 28S sequence, GenBank OK273856.

© 2021 Westerdijk Fungal Biodiversity Institute

Fig. 6. *Xylodon angustisporus* (holotype). **A.** Section of the sporocarp through hymenophoral projection. **B.** Capitate cystidia. **C.** Moniliform cystidia.

© 2021 Westerdijk Fungal Biodiversity Institute

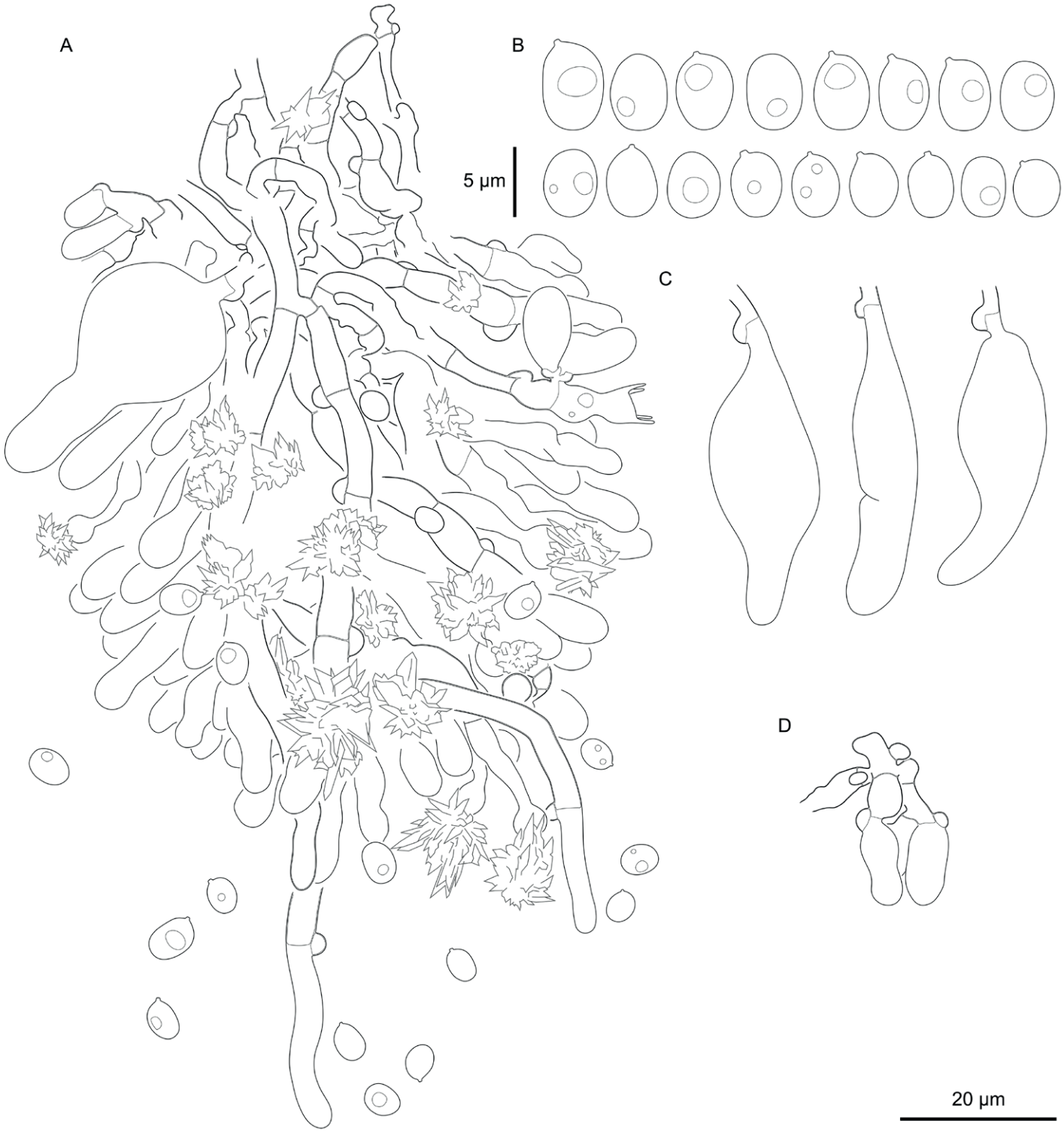

Fig. 7. *Xylodon dissiliens* (holotype). **A.** Section of the sporocarp through hymenophoral projection. **B.** Spores. **C.** Leptocystidia. **D.** Sterile hymenophoral elements.

Notes: Despite that the holotype Ryvarden 44817 was previously identified as *L. sambuci* s.*l.* (Ryvarden & Spirin 2019), the combination of readily collapsing lepto- and capitate cystidia with stellate crystalline cap makes *X. dissiliens* an easily distinguishable element in *Xylodon*. The presence of similar capitate cystidia resembles *X. detriticus*, *X. pruinosus*, and *X. ussuriensis*, another morphologically outlined group in the genus (the former *Lagarobasidium* Jülich).

Xylodon laxiusculus Viner & Ryvarden, ***sp. nov.*** MycoBank MB 841331. Fig. 8.

Etymology: *Laxiusculus* (Lat., adj.), a bit loose, refers to the loose hyphal structure.

Basidiocarp effused, up to 4.5 cm in the widest dimension. Margin pruinose, white, while the rest of hymenial surface cream-coloured, grandinioid; hymenophoral projections rather irregularly arranged, hardly visible with an unaided eye, up to 50

© 2021 Westerdijk Fungal Biodiversity Institute

µm high, 50–70 µm broad at base, 8–11 per mm. *Hyphal structure* monomitic, rather loose, hyphae clamped. *Subhymenial hyphae* thin-walled, slightly cyanophilic, 2.8–4.5 µm wide (n = 21/1). *Subicular hyphae* slightly thick-walled, branched mostly at right angles, (2.2–)2.8–4.5 µm wide (n = 20/1), rarely short-celled. Hyphae mostly naked, but loose clusters of rod-shaped crystals present on some subicular hyphae and more rarely in hymenium. Rare hyphal ends bear globose thin-walled swollen apex up to 6 µm in diam. *Cystidia* irregular in shape, sometimes with several constrictions and (or) swollen apex 9–23.5(–28) × (3–)3.7–6.2) µm (n = 31/1); some cystidia have protuberances close to the apex. A few cystidia have one clamped septum. *Basidia* suburniform, 4-spored, 17–21 × 4.1–5 µm (n = 13/1). *Basidiospores* thin-walled, ellipsoid, slightly cyanophilic, (4.2–) 4.8–5.4 × (3–)3.8–4.3 µm (n = 31/1), L = 5.01, W = 3.95, Q = 1.27.

Distribution and ecology: Western Uganda, on angiosperm wood (fallen decorticated logs). So far known only from the type locality.

Typus: **Uganda**, Western Uganda, Kabarole district, Kibale National Park, Makerere University Field Station, on dead angiosperm wood, 20 Apr. 2002, *L. Ryvarden* 44877, (**holotype** O, **isotype** in H) – ITS sequence, GenBank OK273827.

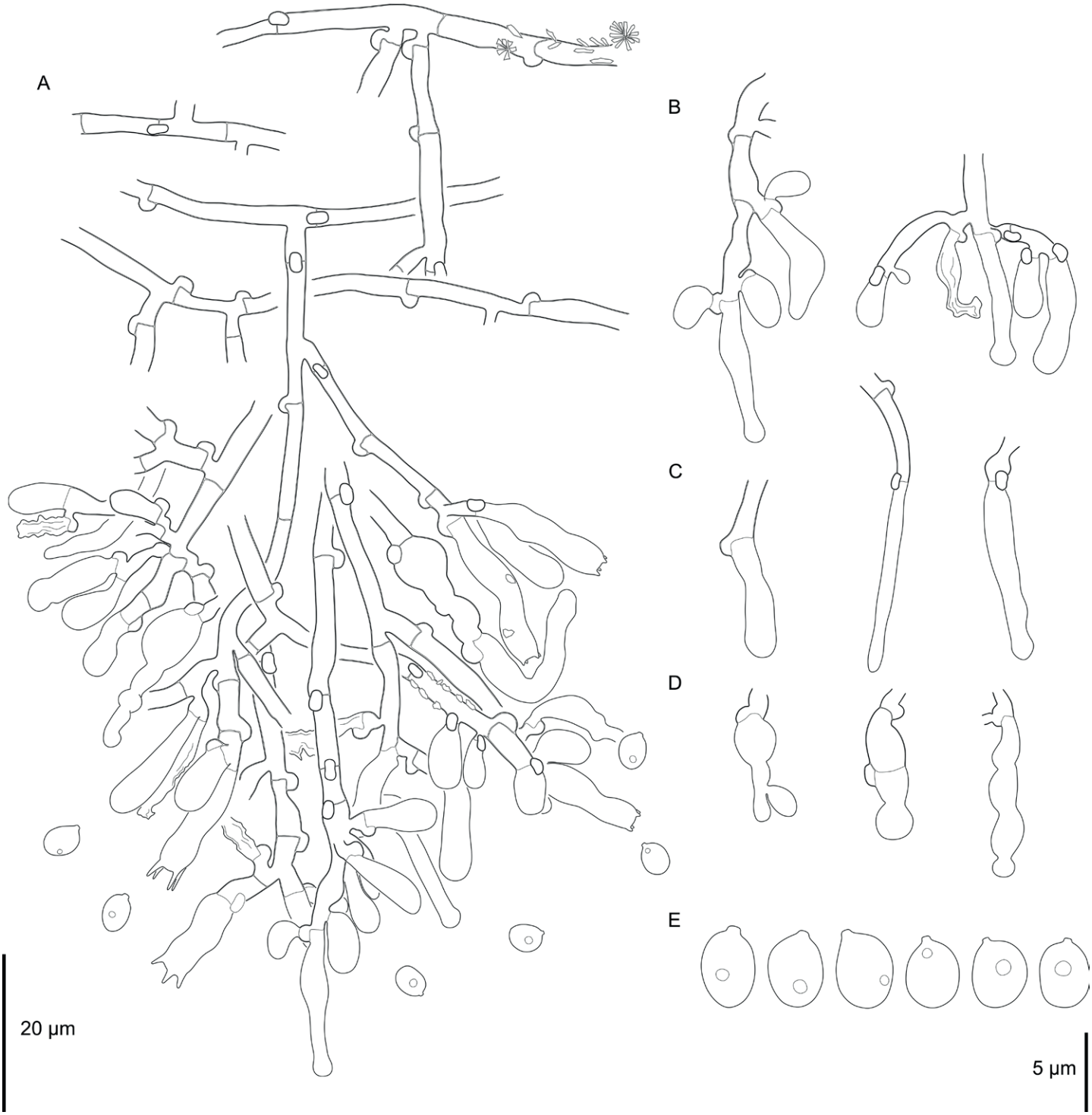

Fig. 8. *Xylodon laxiusculus* (holotype). **A.** Section of the sporocarp through hymenophoral projection. **B.** Clusters of sterile hymenophoral elements. **C.** Sterile hymenophoral elements. **D.** Cystidia. **E.** Spores.

© 2021 Westerdijk Fungal Biodiversity Institute

Notes: We compared *X. laxiusculus* with collections of its closest match (93.8 % similarity or 41 bp difference in ITS), the Taiwanese species *X. subclavatus* (Wu 880310-1, 880510-2, 880516). *Xylodon laxiusculus* lacks most distinguishing features of the former. Those are odontioid hymenium, well-pronounced moniliform cystidia, and capitate hyphal ends with resinous cap. Macroscopically, *X. laxiusculus* is distinguished by loose (at margin almost porulose) fruit-body with hymenial projections visible only under the lens. *Xylodon laxiusculus* slightly resembles the conifer-dwelling *X. brevisetus*, but lacks its characteristic crystals and gloeocystidia. That was the reason why *X. laxiusculus* was initially reported as *X. brevisetus s.l.* (Ryvarden & Spirin 2019).

Xylodon pruniaceus (Hjortstam & Ryvarden) Hjortstam & Ryvarden, *Syn. Fung.* (Oslo) **26**: 39. 2009.
Basionym: *Hyphodontia pruniacea* Hjortstam & Ryvarden, *Syn. Fung.* (Oslo) **18**: 25. 2004.

Basidiocarp effused, up to 5 cm in the widest dimension. Margin indistinct, hymenial surface cream to almost light ochraceous, grandinioid to odontioid; aculei up to 400 µm high, 150–250 µm broad at base, 5–7 per mm. *Hyphal system* monomitic; hyphae clamped, distinct, thin- to thick-walled especially in subiculum (up to 1,5 µm). *Subhymenial hyphae* cyanophilic, 1.7–4(–4.8) µm wide (n = 71/6). *Subicular hyphae*, slightly cyanophilic, branched mostly at right angles, 2–4.9 µm wide (n = 69/6). A few subicular hyphae have large intercalary inflations, 6–9 µm wide. Characteristic rounded crystals are scattered throughout the basidiocarp, 3–6 µm in diam. Hymenial elements cyanophilic to strongly cyanophilic. *Cystidia* are of different shapes: from capitate and spathulate to obtuse and moniliform, 11–25(–30) × 3–6 µm (n = 184/6). Moniliform cystidia are mostly confined to the base of hymenophoral projections. Cystidia of all shapes sometimes have strongly cyanophilic contents and (or) thickened-walls (up to 0.8 µm). Thick- to thin-walled hyphidia make up the core of hymenophoral projections. Some thin-walled hyphidia moderately to strongly flexuous. *Basidia* suburniform, 4-spored, 12–21 × 3.9–6 µm (n = 68/6). *Basidiospores* thin-walled, narrowly ellipsoid to subcylindrical, slightly cyanophilic, (3.5–)4.6–5.8(–6.9) × 2.8–3.8(–4.1) µm (n = 176/6), L = 5.14, W = 3.29, Q = 1.57.

Distribution and ecology: Previously reported only from the type locality in Tanzania, but several additional specimens from Tanzania and Malawi have been identified by us. The species grows on angiosperm wood.

Typus: **Tanzania**, Kilimanjaro Province, Mt. Kilimanjaro west slope, W. Kilimanjaro Forest Sta., alt. *ca*. 1 800 m, on angiosperm wood, 10–11 Feb. 1973, *L. Ryvarden*, 10223 (**holotype** K, **isotype** in O, studied).

Additional materials examined: **Malawi**, Southern Province, Zomba district, Zomba plateau, alt. *ca*. 1 500–1 700 m, on dead angiosperm wood, 7 Mar. 1973, *L. Ryvarden*, 11251 (H, O). **Tanzania**, Kilimanjaro Province, Mt. Kilimanjaro south slope above Mweka, alt. *ca*. 1 800–2 300 m, on angiosperm wood, 12 Feb. 1973, *L. Ryvarden*, 10286 (**paratype** in K, O); *L. Ryvarden*, 10301b (H, O); Mt. Kilimanjaro west slope, W. Kilimanjaro Forest Sta., alt. *ca*. 1 800 m, on angiosperm wood, 10 Feb. 1973, *L. Ryvarden*, 10216 (H, O); 11 Feb. 1973, *L. Ryvarden*, 10283 (H, O).

Notes: The species is very similar in almost all respects to its Western African relative *X. angustisporus* described above and resembles the widely distributed *X. nespori*. The spore morphology of *X. pruniaceus* allows separating it from those two species.

Xylodon submucronatus (Hjortstam & Renvall) Hjortstam & Ryvarden, *Syn. Fung.* (Oslo) **26**: 40. 2009.
Basionym: *Hyphodontia submucronata* Hjortstam & Renvall, *Edinb. J. Bot.* **55**: 481. 1998.

Typus: **Tanzania**, Arusha (Northern) Province, Arusha District, western side of Mt. Meru above Laikinoi, ridge between the streams Engare Olmotonyi and Engare Narok, in *Hagenia abyssinica* forest, alt. 2 800 m, fallen branch of *H. abyssinica*, 14 Dec. 1988, *Renvall*, 1602 (**holotype** H, **isotypi** in K, KUO, GB) – ITS sequence, GenBank OK273830.

Additional materials examined: **Kenya**, Central Province, Trans-Nzoia county, Mt. Elgon, south of the Suam River valley to Kapcalwa Gate, on dead angiosperm wood, 24 Jan. 1973, *Ryvarden*, 9322b (H, O).

Notes: The second collection of *X. submucronatus* reported in this study fits well with the description and illustration given by Niemelä *et al.* (1998). Its identity was further reaffirmed by our ITS analyses. This finding extends the known distribution of this species north up to Eastern Kenya. Despite its morphological similarity to *X. spathulatus* indicated by Niemelä *et al.* (1998), the closest match to *X. submucronatus* is *X. rimosissimus* (96 % similarity or 25 bp difference in ITS; Fig. 2). Thus, *X. submucronatus* appears to be a well-defined morphological species among known taxa allied to *X. rimosissimus*. On the other hand, sequences of *X. spathulatus* did not even pass the similarity threshold of 93 %.

DISCUSSION

All published results suggest that the relationships within *Xylodon* and allied genera (including *Lyomyces*) are not well resolved when the ribosomal DNA loci are the sole source for genetic information. There has been a recent attempt to establish a reliable phylogeny of this group based on a comprehensive taxon sampling and multiple DNA loci by Wang *et al.* (2021). Their analysis of a concatenated dataset consisting of ITS, 28S, and mitochondrial small subunit (mtSSU) resolved *Lyomyces* and *Xylodon* as monophyletic genera. However, the analysis could suffer from a "gappy" alignment approach. Their large collection of partial gene sequences was assembled in a multiple sequence alignment containing a lot of missing data: a number of species were represented by just one or two loci while missing the remaining ones. Such a pattern of missing data could pose a major problem for the phylogenetic analysis (Hartmann & Vision 2008). Considering that Wang *et al.* (2021) have not mentioned any statistical methods compensating for the missing data, the existence of *Xylodon* and *Lyomyces* as two separate genera requires further investigation.

The addition of our four new species brings the number of currently recognized *Xylodon* and *Lyomyces* described from sub-Saharan Africa (including Réunion) to 10. Obviously, that number is not even close to the true diversity of this group on the continent. Considering that tropical Africa remains poorly explored for wood-inhabiting fungi, it is likely that many more *Xylodon* species will be found.

© 2021 Westerdijk Fungal Biodiversity Institute

ACKNOWLEDGEMENTS

We thank the anonymous reviewers of the manuscript for their useful comments. This research was supported by a University of Helsinki three-year research project (OM, IV) and Societas pro Fauna et Flora Fennica (IV). Karl-Henrik Larsson and Ellen Larsson (GB) kindly helped us with organizing a loan. Anton Savchenko (Tartu), Evgeniy Dunayev (Young Naturalist Club of the Zoological Museum, Lomonosov Moscow State University), Karl-Henrik Larsson, and Viacheslav Spirin (Helsinki) provided us with valuable fungal collections. Gaurav Sablok (Helsinki) helped us with the processing of genomic data.

Conflict of interest: The authors declare that there is no conflict of interest.

REFERENCES

Bankevich A, Nurk S, Antipov D, *et al.* (2012). SPAdes: a new genome assembly algorithm and its applications to single-cell sequencing. *Journal of computational biology* **19**: 455–477.

Benson DA, Cavanaugh M, Clark K, *et al.* (2018). GenBank. *Nucleic Acids Research* **46**: D41–D47.

Cheek M, Gosline G, Onana JM (2018). *Vepris bali* (*Rutaceae*), a new critically endangered (possibly extinct) cloud forest tree species from Bali Ngemba. Cameroon. *Willdenowia* **48**: 285–292.

Cheek M, Nic Lughadha E, Kirk P, *et al.* (2020). New scientific discoveries: Plants and fungi. *Plants, People, Planet* **2**: 371–388.

Chen S, Zhou Y, Chen Y, *et al.* (2018). fastp: an ultra-fast all-in-one FASTQ preprocessor. *Bioinformatics* **34**: 884–890.

Katoh K, Rozewicki J, Yamada KD (2017). MAFFT online service: multiple sequence alignment, interactive sequence choice and visualization. *Briefings in Bioinformatics* **20**: 1160–1166.

Landvik S (1996). *Neolecta*, a fruit-body producing genus of the basal ascomycetes, as shown by SSU and LSU rDNA sequences. *Mycological Research* **100**: 199–202.

Li D, Liu CM, Luo R, *et al.* (2015). MEGAHIT: an ultra-fast single-node solution for large and complex metagenomics assembly via succinct de Bruijn graph. *Bioinformatics* **31**: 1674–1676.

Lücking R, Hawksworth DL (2018). Formal description of sequence-based voucherless Fungi: promises and pitfalls, and how to resolve them. *IMA Fungus* **9**: 143–166.

Harris RS (2007). *Improved pairwise alignment of genomic DNA*. Ph.D. dissertation. College of Engineering, the Pennsylvania State University, USA.

Hartmann S, Vision TJ (2008). Using ESTs for phylogenomics: can one accurately infer a phylogenetic tree from a gappy alignment? *BMC Evolutionary Biology* **8**: 1–13.

Hjortstam K, Ryvarden L (2007). Studies in corticioid fungi from Venezuela III (*Basidiomycotina*, *Aphyllophorales*). *Synopsis Fungorum* **23**: 56–107.

Hjortstam K, Ryvarden L (2009). A checklist of names in *Hyphodontia sensu stricto - sensu lato* and *Schizopora* with new combinations in *Lagarobasidium*, *Lyomyces*, *Kneiffiella*, *Schizopora*, and *Xylodon*. *Synopsis Fungorum* **26**: 33–55.

Hjortstam K, Ryvarden L, Watling R (1993). Preliminary checklist of non-agaricoid macromycetes in the Korup National Park, Cameroon and surrounding area. *Edinburgh Journal of Botany* **50**: 105–119.

Hopple JS, Vilgalys R (1994). Phylogenetic relationships among coprinoid taxa and allies based on data from restriction site mapping of nuclear rDNA. *Mycologia* **86**: 96–107.

Kutuzova IA, Kokaeva LY, Pobendinskaya MA, *et al*. (2017). Resistance of *Helminthosporium solani* strains to selected fungicides applied for tuber treatment. *Journal of Plant Pathology* **99**: 635–642.

Martin KJ, Rygiewicz PT (2005). Fungal-specific PCR primers developed for analysis of the ITS region of environmental DNA extracts. *BMC Microbiology* **5**: 1–11.

Miettinen O, Niemela T, Spirin W (2006). Northern *Antrodiella* species: the identity of *A. semisupina*, and type studies of related taxa. *Mycotaxon* **96**: 211–240.

Milne I, Lindner D, Bayer M, *et al.* (2008). TOPALi v2: a rich graphical interface for evolutionary analyses of multiple alignments on HPC clusters and multi-core desktops. *Bioinformatics* **25**: 126–127.

Nguyen L-T, Schmidt HA, Von Haeseler A, *et al.* (2015). IQ-TREE: a fast and effective stochastic algorithm for estimating maximum-likelihood phylogenies. *Molecular Biology and Evolution* **32**: 268–274.

Niemelä T, Renvall P, Hjortstam K (1998). *Hagenia abyssinica* and its fungal decayers in natural stands. *Edinburgh Journal of Botany* **55**: 473–484.

Riebesehl J, Langer E (2017). *Hyphodontia s.l.* (*Hymenochaetales*, *Basidiomycota*): 35 new combinations and new keys to all 120 current species. *Mycological Progress* **16**: 637–666.

Ronquist F, Teslenko M, Van Der Mark P, *et al.* (2012). MrBayes 3.2: efficient Bayesian phylogenetic inference and model choice across a large model space. *Systematic Biology* **61**: 539–542.

Ryvarden L, Spirin V (2019). Studies in *Aphyllophorales* of Africa 39. Some corticoid species from Uganda. *Synopsis Fungorum* **39**: 38–40.

Stein F (1969). Particle size measurements with phase contrast microscopy. *Powder Technology* **2**: 327–334.

Wang XW, May TW, Liu SL, *et al.* (2021). Towards a natural classification of *Hyphodontia sensu lato* and the trait evolution of basidiocarps within *Hymenochaetales* (*Basidiomycota*). *Journal of Fungi* **7**: 478.

White TJ, Bruns T, Lee S, *et al.* (1990). Amplification and direct sequencing of fungal ribosomal RNA genes for phylogenetics. In: *PCR protocols: A guide to the methods and applications* (Innis MA, Gelfand DH, Sninsky JJ, White TJ, eds). Academic Press. New York: 315–322.

Yurchenko E, Riebesehl J, Langer E (2017). Clarification of *Lyomyces sambuci* complex with the descriptions of four new species. *Mycological Progress* **16**: 865–876.

© 2021 Westerdijk Fungal Biodiversity Institute

FUSE

Fungal Systematics and Evolution

VOLUME 8
DECEMBER 2021
PAGES 179–201

doi.org/10.3114/fuse.2021.08.14

Anchoring the species *Rhizophagus intraradices* (formerly *Glomus intraradices*)

C. Walker[1,2*], A. Schüßler[3], B. Vincent[4], S. Cranenbrouck[5], S. Declerck[4]

[1]Royal Botanic Garden Edinburgh, 21A Inverleith Row, Edinburgh EH3 5LR, UK
[2]School of Agriculture and Environment, University of Western Australia, 35 Stirling Highway, Crawley, WA 6009, Australia
[3]SYMPLANTA GmbH & Co. KG, Graupnerweg 42, 64287 Darmstadt, Germany
[4]Université catholique de Louvain, Earth and Life Institute, Mycology, Croix du Sud, 2 box L7.05.06, 1348 Louvain-la-Neuve, Belgium
[5]Université catholique de Louvain, Earth and Life Institute, Mycology, Mycothèque de l'Université catholique de Louvain (MUCL[a]), Croix du Sud, 2 Box L7.05.06, 1348 Louvain-la-Neuve, Belgium

[*]Corresponding author: c.walker@rbge.ac.uk

Key words:
arbuscular mycorrhizal fungi
Glomeromycota
molecular phylogeny
phenotypic plasticity
species definition

Abstract: The nomenclatural type material of *Rhizophagus intraradices* (basionym *Glomus intraradices*) was originally described from a trap pot culture established with root fragments, subcultures of which later became registered in the INVAM culture collection as FL 208. Subcultures of FL 208 (designated as strain ATT 4) and a new strain, independently isolated from the type location (ATT 1102), were established as both pot cultures with soil-like substrate and *in vitro* root organ culture. Long-term sampling of these cultures shows spores of the species to have considerable morphological plasticity, not described in the original description. Size, shape and other features of the spores were much more variable than indicated in the protologue. Phylogenetic analyses confirmed earlier published evidence that sequences from all *R. intraradices* cultures formed a monophyletic clade, well separated from, and not representing a sister clade to, *R. irregularis*. Moreover, new phylogenetic analyses show that *Rhizoglomus venetianum* and *R. irregularis* are synonymous. The morphological characters used to separate these species exemplify the difficulties in species recognition due to the high phenotypic plasticity in the genus *Rhizophagus*. *Rhizophagus intraradices* is morphologically re-described, an epitype is designated from a single-spore isolate derived from ATT 4, and *R. venetianum* is synonymised with *R. irregularis*.

Citation: Walker C, Schüßler A, Vincent B, Cranenbrouck S, Declerck S (2021). Anchoring the species *Rhizophagus intraradices* (formerly *Glomus intraradices*). *Fungal Systematics and Evolution* **8**: 179–201. doi: 10.3114/fuse.2021.08.14
Received: 10 August 2021; **Accepted:** 6 November 2021; **Effectively published online:** 29 November 2021
Corresponding editor: P.W. Crous

INTRODUCTION

Glomus intraradices, described from a citrus plantation in Florida (Schenck & Smith 1982), is an arbuscular mycorrhizal fungus (AMF) that predominantly forms its spores intraradically. After *Glomus* was shown to be well separated at the generic level from this species, *G. intraradices* was renamed *Rhizophagus intraradices* (Schüβler & Walker 2010) following previous use of the genus name for AMF forming their spores in roots (Butler 1939, Gerdemann & Trappe 1974). Sieverding *et al.* (2014) proposed that *Rhizophagus* should be replaced with *Rhizoglomus*, but Walker *et al*. (2017) challenged this and proposed that the generic name *Rhizophagus* should be conserved, but with a change of type species to *R. intraradices*. We follow recommendation 14A.1 of the International Code of Nomenclature for algae, fungi, and plants (ICNafp) (Turland *et al.* 2018) by retaining 'existing usage'. Consequently, the current name, *Rhizophagus intraradices*, will be used throughout this work except where additional clarity will be gained by specifically using previous names.

From examination of published literature and DNA sequence databases, *R. intraradices* would seem to be common and widespread throughout the world, and organisms named *Glomus intraradices* have been used very extensively in mycorrhiza research. On 30 October 2021, a search for the species in the University of Western Australia's library (https://onesearch.library.uwa.edu.au) produced 5 739 peer reviewed references to *Glomus intraradices*, 1 470 to *Rhizophagus intraradices*, and 176 to *Rhizoglomus intraradices*, though in some publications, more than one of these names occur. For many of those published works it is impossible to verify the identity of the fungi used, and in most molecular ecological studies the species has been ascribed to *G. intraradices*, now classified in the genus *Rhizophagus* (Schüßler & Walker 2010). However, several distinct species have been confounded in most of these studies and erroneously named (Stockinger *et al.* 2009). In particular, the fungus formerly known as '*G. intraradices* DAOM197198', a widely used 'model organism' and the first genome-sequenced arbuscular mycorrhizal fungus (AMF) (Martin *et al.* 2008), was later determined to be *R. irregularis* (synonym *G. irregulare*), not *R. intraradices* (Stockinger *et al*. 2009, Sokolski *et al.* 2010). *Rhizophagus intraradices* cultures identifiable through molecular

[a]Part of the Belgian Coordinated Collections of Microorganisms (BCCM).

Fungal Systematics and Evolution is licensed under a Creative Commons Attribution-NonCommercial-ShareAlike 4.0 International License

© 2021 Westerdijk Fungal Biodiversity Institute

sequencing seem to have rarely been collected or isolated since its original description by Schenck & Smith (1982).

Molecular community studies, identifying the fungus based on species-resolving molecular characterisation, have shown the presence of *R. intraradices* in *Zea mays* in Belgium (Alaux *et al.* 2021), *Capsicum annuum* var. *glabriusculum*, *Glycine max* and *Citrus sinensis* in Mexico (Senés-Guerrero *et al*. 2020), *Triticum aestivum* from Switzerland and composite root samples from Ecuador (Schlaeppi *et al.* 2016) but, to date, it appears to have been established in pure culture only from citrus plantations (Schenck & Smith 1982, this study) and the Konza prairie, Kansas, USA (INVAM culture KS906).

The morphological descriptions of some species in the genus *Rhizophagus* overlap considerably (*e.g*., *R. irregularis* (Błaskowski *et al*. 2008), *R. custos* (Cano *et al*. 2009) *R. prolifer* (Declerk *et al.* 2000), *R. venetianum* (Turrini *et al.* 2018), *R. aggregatum* and *R. intraradices* (Schenck & Smith 1982)) and it is very difficult or impossible to distinguish them from spores collected from field soils. Difficulties in interpreting type species, their descriptions and the possibility of cryptic speciation in the genus *Rhizophagus* present serious problems for interpreting and assigning species names with confidence. The paucity of molecular data for accurately identified species in the phylum *Glomeromycota* is a further barrier to interpreting species of AMF, as discussed by Stefani *et al.* (2020).

Glomeromycotan fungi presently cannot be maintained in axenic culture, and are normally grown in pot culture (PC) with a suitable host plant, or monoxenically in root organ culture (ROC) or with tissue-cultured plants or disinfested seedlings on a gel-based substrate in sealed systems (Vestberg & Uosukainen 1992, Fortin *et al.* 2002, Lalaymia & Declerck 2020). *Rhizophagus intraradices* and its close relatives can be established by these methods, so we compared its spore morphology in both PC and ROC from type material, ex-type cultures (including a single-spore isolate), and a new isolate established from samples taken from the original type location approximately 30 yr after the species was first collected. Samples of subcultures of different ages and with different host plants were used to define the taxonomical molecular and morphological characteristics of the species.

Based on spore characteristics and phylogenetic data, the aims of this study were:

- to re-describe the fungus *Rhizophagus intraradices* (synonym *Glomus intraradices*) from an ex-type culture,
- to compare ex-type culture material with a new isolate established from the type locality approximately three decades after the original type was collected,
- to define an epitype from a single spore isolate derived from the original ex-type culture,
- to compare the phenotypic plasticity of spores formed in ROC and PC on different plant hosts, providing a detailed description of *R. intraradices* spore variation.

MATERIALS AND METHODS

Specimens

For convenience, we follow Seifert & Rossman (2010), by referring to type-descendant cultures as 'ex-type'. The nomenclatural code (ICNafp) (Turland *et al.* 2018) recommends, but does not mandate (Recommendation 8B.2), the use of this term for cultures derived from type material that were "… permanently preserved in a metabolically inactive state". The parental cultures of such 'type-descendent cultures' are not metabolically inactive and may have changed or have been contaminated over time. Nevertheless, the term is easily understood and acts as a useful shorthand. The term as applied to *R. intraradices* refers to many culturing generations over almost four decades, most of which lack detailed published records.

The holotype of *R. intraradices* was borrowed from the herbarium at Oregon State University (OSC 40255). Some of the spores from this collection (preserved in lactophenol) were washed in water and placed in a Petri dish of water for initial observations. Some of these were then transferred to microscope slides for observation through the compound microscope.

Cultures

The original 'type culture' appears not to have been given an identifier, but an ex-type culture was designated culture FL 208 upon incorporation in the INVAM culture collection. A sample of substrate, containing roots and spores, was obtained from INVAM, and established in PC and ROC. Cultures were catalogued with an attempt (ATT) number and subculture number (Walker & Vestberg 1998), the former being the unique identifier of the first attempt at establishing a culture, and the latter indicating the particular subculture (Fig. S1). Initial culture attempts are always "number-0" and all subsequent culture attempts derived from it are automatically given their unique subculture number. The original trap culture, established by S. Nemec, at the United States Department of Agriculture, Agricultural Research Service, Orlando, Florida was catalogued as ATT 4-0 and the 'type culture' was labelled ATT 4-1. The full history of subculturing from ATT 4-0 is unknown and Fig. S1 provides all the available information. Where data were not available, some attempt numbers (*e.g*. ATT 4-1 and 4-3) (Fig. S1-1) are 'notional entries' covering several subcultures. Subcultures were established from ATT 4-36 resulting in isolates from single propagules in both PC and ROC (Fig. S1-2). A sample of ATT 4-88 (of single-spore ancestry) was sent to M. Saito (Tohoku and Iwate Universities, Japan) and incorporated in the National Agriculture and Food Research Organisation, Japan (NARO) Genebank as MAFF 520088.

Three decades after the first isolation of ATT 4-0, a new sample collected by S. Nemec, from *Citrus* sp. at the type locality, was used to establish a closed soil-trap PC (ATT 1102-0) with *P. lanceolata* as host. A single spore from this culture was then used to establish a new isolate, ATT 1102-7 as a culture-line independent of the *R. intraradices* type culture and the resultant INVAM FL 208 culture (Fig. S1-3). Further PC and ROC subcultures with various host plants were established, allowing comparison of two independent cultures, established 30 years apart, from the type locality.

The database also controls the identifier given to samples and specimens therefrom, whether from field collections or from cultures. Each such sample receives its unique number, and consequently a culture may produce more than one voucher, *e.g.*, W 5413 and W 5501 from ATT 4-41 (Fig. S1-2) if sampled at different dates. Voucher numbers (usually applied to prepared microscope slides, but sometimes dried PC substrate containing roots and spores) were prefixed by 'W', thus, for example, the voucher from the notional ATT 4-36 (the INVAM culture from which material was supplied to us) is W 5128. Unless otherwise

© 2021 Westerdijk Fungal Biodiversity Institute

stated, all vouchers are part of the C. Walker collection, lodged at the Herbarium of the Royal Botanic Garden Edinburgh (E) (see Index Herbariorum – http://sweetgum.nybg.org/science/ih/). Specimens from these collections and cultures were examined by light microscopy to determine morphological characteristics.

Specimen extraction

For PC, extraradical spores and root fragments containing spores were extracted from the substrate by suspending a sample (approx. 30 mL) in a beaker of water, agitating vigorously with a spatula, stirring to produce a vortex, and decanting through a 53 µm sieve after approx. 10 s of settling ('swirling and decanting'). The resultant sievings were then backwashed into 6-cm-diam Petri dishes for observation under a dissecting microscope with reflected light. The spores and roots from ROC were retrieved with forceps and washed in water to remove any remaining gel before being similarly transferred to a dish of water. Spores were handled with finely sharpened flexible stork bill tweezers (http://vomm.com, item 113 SA, Solingen, Germany) that facilitate the handling of individual spores without causing physical damage.

Phylogenetic analyses

The extended barcode for AMF (Stockinger *et al.* 2010) was used as DNA marker for molecular phylogenetics, consisting of the 3' region small subunit rRNA gene (SSU), the ITS region including the 5.8S rRNA gene, and a 5' region of the large subunit rRNA gene (LSU), usually described as SSU-ITS-LSU fragment or sequence, amplified with AMF-specific primers SSUmCf and LSUmBr (Krüger *et al.* 2009). To improve robustness and resolution of deeper branches, individual SSU-ITS-LSU sequence variants (~1.5 kb) from *R. intraradices*, if available, were concatenated with a SSU consensus sequence (~1.8 kb) of the same isolate (Krüger *et al.* 2012). An analysis excluding this SSU as 'anchor' was consistent and resulted in the same clades, but partly with lower bootstrap support (not shown). Sequences of the highly variable ITS1 and ITS2 regions were excluded from the analyses, because they show a very high intraspecific variability of up to 15 % for *Rhizophagus* species (Stockinger *et al.* 2010), making unambiguous alignment difficult.

For *R. irregularis* DAOM197198, phylogenetic trees including short sequences had been already published (Stockinger *et al.* 2009); here, only near-full-length SSU-ITS-LSU sequences allowing good phylogenetic resolution were used. PCR primer binding sites were excluded from all analyses. Sequences of the closely related genus *Sclerocystis* were used as the outgroup.

A maximum likelihood phylogenetic analysis was computed using the raxmlGUI v. 2.0 (Edler *et al*. 2020). The analysis, based on an alignment of 158 sequences with a length of 2 739 base pairs was computed with RAxML v. 8 (Stamatakis 2014) with 1 000 bootstraps. The GTRGAMMAI substitution model was selected as the best substitution model, using modeltest as implemented in RAxML v. 8.

Morphological analysis

Where possible, specimens were separated into extraradical or intraradical spores which were measured separately. Observations on specimens were made following the established methods, initially, by reflected light, under a dissecting microscope at magnifications of up to 50×, followed by detailed examination of individual spores mounted on microscope slides in polyvinyl alcohol lacto-glycerol with (PVLG-M) or without (PVLG) the addition of Melzer's reagent (Walker *et al.* 1993, Walker & Vestberg 1998).

Images were recorded digitally with a Canon EOS D30, 5D, 60D or 6D camera mounted on a phototube with 80 mm, 5× or 10× projective lens. Spore colour was established by comparing the specimens in a dish of water (BPI watchglass - https://catalog.ndsglass.com/viewitems/all-categories-new-products/bpi-watch-glasses) under a Leica MZ8 microscope with the Royal Botanic Garden Edinburgh (RBGE) colour chart (Anon 1969), the Munsell® Soil colour chart (Anon 1990) or the Methuen Book of Colour (Kornerup & Wanscher 1978). On occasions when it was not possible to make comparisons with a chart, a vernacular colour name was given. Charts were illuminated by the third arm of the split fibre optic illumination source as described in Walker *et al.* (1993) to match colours. The RBGE colours are indicated by a name with a number [*e.g.*, ochre (9)] representing the colour chip on the chart. Munsell numbers are in standard notation (*e.g.*, 10YR 5/8, strong brown) representing the hue, value and chroma and a standard colour name. Methuen colours are designated with the plate number and colour patch number with the associated general colour name (*e.g.*, 5F8, brown).

Spore dimensions were measured by means of a calibrated eyepiece graticule. Most were measured with a graticule division size of 1.6 µm, but those larger than about 160 µm had to be measured at a lower magnification, with graticule divisions of 2 or 2.5 µm. Consequently, though most measurements are accurate to within 0.8 µm, overall accuracy should be assumed to be ± 1.25 µm. Measurements were always length by width, the length being taken as the longest dimension perpendicular to the point of development from the subtending hypha, and the width at right angles to this, hence many specimens are 'broader than long'. Guidance on spore measurements and shape determination is summarised in Fig. 1. Because the size and shape of irregular spores are so variable, these were treated separately.

Statistical analyses

Measurements of spores from the type material and subsequent subcultures (ATT 4) and from the new strain (ATT 1102) were analysed statistically (Tables 1, S1). Not every culture produced both intraradical and extraradical spores. From the type culture material (ATT 4-1), 52 extraradical spores and 100 intraradical spores were measured. All were from a PC of unknown age. From the subsequent 9 PCs sampled, 675 extraradical, and 461 intraradical spores were measured from 10 vouchers aged between 95 and 1 789 d from inoculation. There were seven ROCs from culture line ATT 4, one of which was sampled on two different dates. Together, these produced 654 extraradical spores, but only two within root tissue.

ATT 1102 was sampled from three PCs, one of which was sampled on two different occasions, resulting in 350 extraradical spores and 300 intraradical spores. Three ROCs were sampled resulting in 245 extraradical spores and no intraradical specimens.

Twenty-nine different spore shapes were identified (Table 2) and compared by strain (ATT 4 vs ATT 1102), spore position (extraradical or intraradical), culture type (PC or ROC) (Table 1) and shape of spores (Table 2) The effect of host plant on the main spore shape was also examined (Tables 3, 4).

© 2021 Westerdijk Fungal Biodiversity Institute

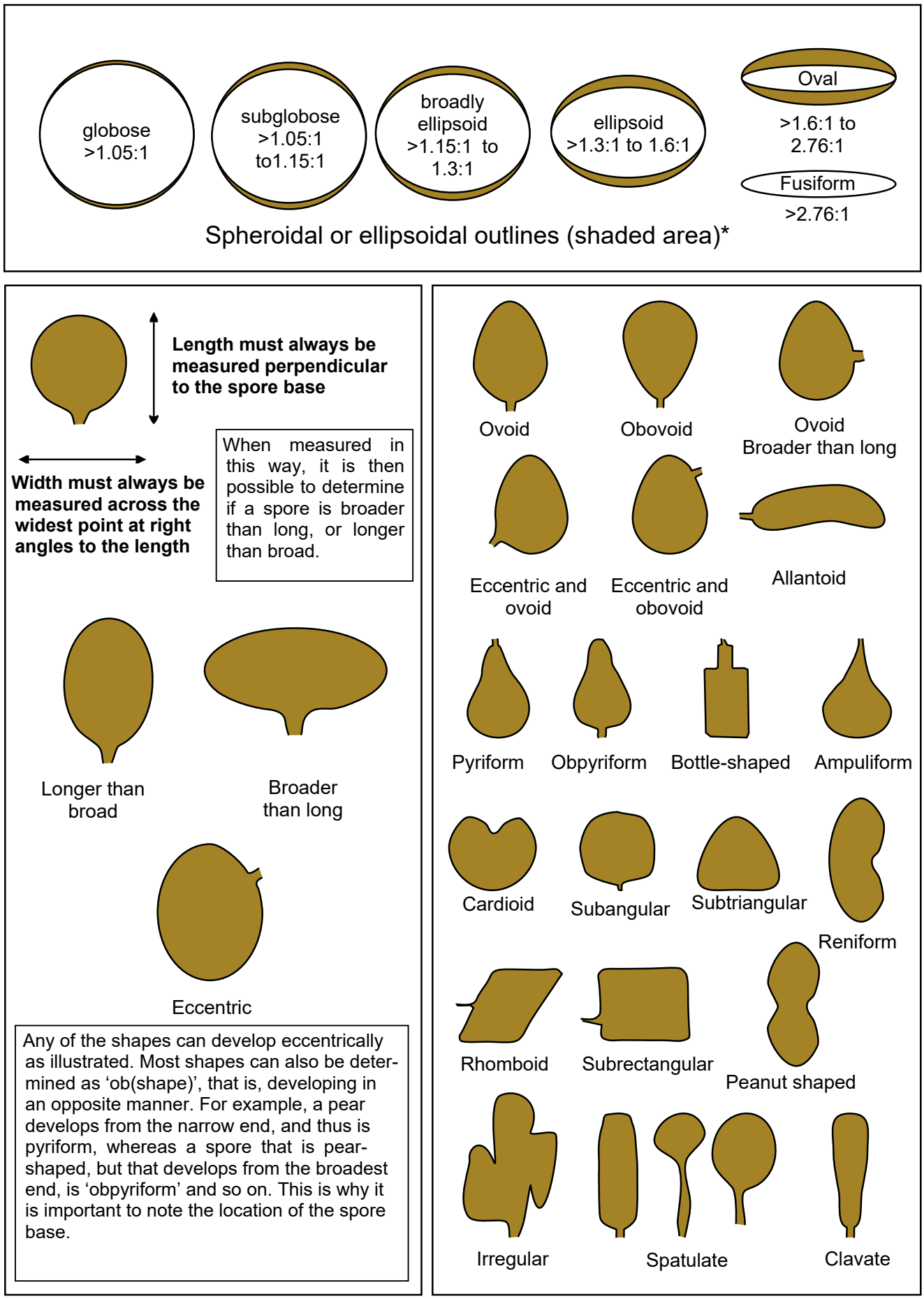

*Adapted partly from Kirk *et al*. (2010)

Fig. 1. Guidance for measuring spores of glomeromycotan fungi, including standard spheroid descriptions (adapted from Kirk *et al*. 2010) and some common different shape outlines.

© 2021 Westerdijk Fungal Biodiversity Institute

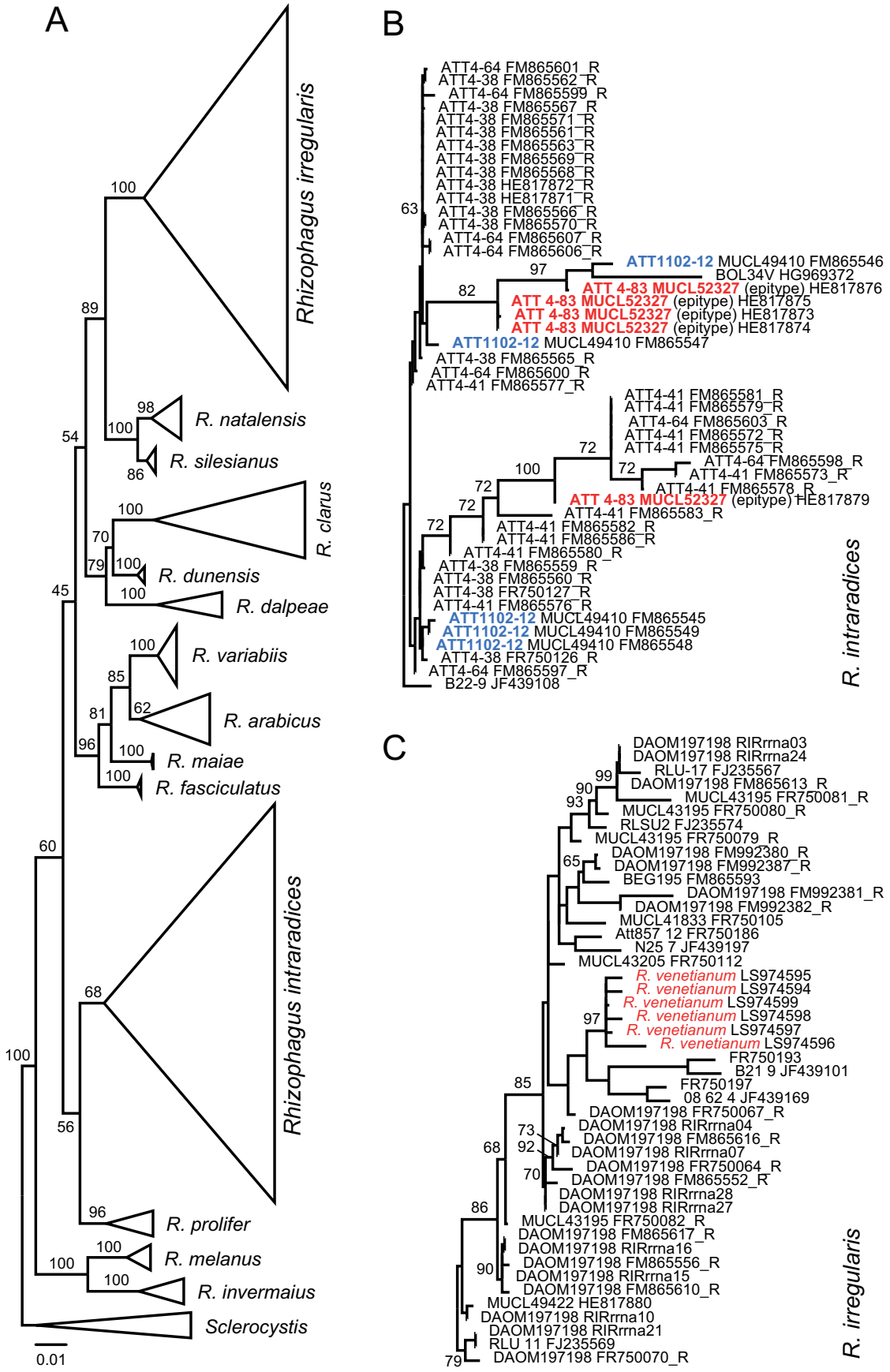

Fig. 2. Phylogenetic maximum likelihood tree of *Rhizophagus* species and isolates ATT 4 (FL 208) and ATT 1102 of *R. intraradices*. For the completely resolved and annotated tree see Fig. S2. **A.** Characterised *Rhizophagus* species, with *Sclerocystis* as outgroup. Size of triangles represent the sequence numbers (vertically) and distances (horizontally). **B.** Details of *R. intraradices*, showing that descendants (ATT 4-38, ATT 4-41, ATT 4-64) of the ex-type culture FL 208, including (red typeface) the culture from which the epitype was taken (MUCL 52327 = ATT 4-83) and (blue typeface) the strain (MUCL 49410 = ATT 1102-12) newly isolated from the type locality cluster in the same monophyletic clade. **C.** Details of *R. irregularis*, showing that "*Rhizoglomus venetianum*" (red typeface) represents one subtype of the DNA sequence variants of *R. irregularis*; sequence variants annotated 'RIRrrna##' are from a genome sequencing project (Maeda *et al.* 2018).

© 2021 Westerdijk Fungal Biodiversity Institute

Table 1. Spore lengths and widths (µm) of *Rhizophagus intraradices* strains (ATT 4 and ATT 1102 and both combined), for pot cultures (PC) and root organ cultures (ROC) by culture type and spore position (intra- or extraradical). For each strain, means were compared to each other. Means with the same letters are not significantly different (P ≤ 0.05). To aid comparison, the protologue measurements (Schenck & Smith 1982) and our own measurements from the holotype material (ATT 4-1) are shown separately.

				Spore length (µm)					Spore width (µm)				
Strain	**Culture type**	**Spore position**	**n**	**min**	**median**	**max**	**mean ± SD**	**CV %**	**min**	**median**	**max**	**mean ± SD**	**CV %**
ATT 4	PC	intraradical	561	18	82	234	84 ± 29 b	34	16	72	152	74 ± 27 b	37
	PC	extraradical	727	29	99	224	98 ± 27 a	28	29	96	165	96 ± 26 a	27
	ROC	extraradical	654	30	97	182	98 ± 24 a	24	30	96	178	96 ± 25 a	26
	PC & ROC	extraradical	1 381	29	98	224	98 ± 26 a	26	29	96	178	96 ± 26 a	27
	PC & ROC	intraradical	561	18	82	234	84 ± 29 b	34	16	72	152	74 ± 27 b	37
	PC & ROC	intra- & extraradical	1 942	18	94	234	94 ± 27	29	16	91	178	90 ± 28	31
ATT 1102	PC	intraradical	300	18	93	218	99 ± 37 a	37	25	80	202	85 ± 31 c	36
	PC	extraradical	350	26	88	383	92 ± 39 b	42	26	88	398	92 ± 40 b	43
	ROC	extraradical	245	48	96	147	96 ± 18 a	19	46	94	146	95 ± 18 a	19
	PC & ROC	extraradical	595	26	91	383	94 ± 32 a	34	26	91	398	93 ± 33 a	35
	PC & ROC	intraradical	300	18	93	218	99 ± 37 a	37	25	80	202	85 ± 31 b	36
	PC & ROC	intra- & extraradical	895	18	93	383	95 ± 34	35	25	88	398	90 ± 32	36
Combined	PC	intraradical	861	18	85	234	89 ± 32 a	36	16	75	202	77 ± 29 a	38
	PC	extraradical	1 077	26	96	383	96 ± 32 b	33	26	94	398	95 ± 31 b	33
	ROC	extraradical	899	30	96	182	97 ± 22 b	23	30	96	178	96 ± 23 b	24
	PC & ROC	extraradical	1 976	26	96	383	96 ± 28 a	29	26	95	398	95 ± 28 a	29
	PC & ROC	intraradical	861	18	85	234	89 ± 32 b	36	16	75	202	77 ± 29 b	38
	PC & ROC	intra- & extraradical	2 837	18	93	383	94 ± 29	31	16	90	398	90 ± 29	32
Isotype	PC	extraradical	52	42	103	224	104 ± 30 a	29	42	98	154	99 ± 23 a	23
	PC	intraradical	100	29	71	186	79 ± 31 b	39	18	61	147	66 ± 29 b	44
	PC	intra- & extraradical	152	29	86	224	87 ± 33	38	18	79	154	77 ± 31	40
protologue	PC	intraradical	n/a	40.5	n/a	191.5	n/a	n/a	93	n/a	131	n/a	n/a

All statistical analyses were conducted in R (R Core team, 2017) with a significance level of p ≤ 0.05. Normality of distribution and homogeneity of variance were checked for spore dimension data, followed, where appropriate, by ANOVA for specific factors (*e.g.*, to determine if number of attempts or type of culture had an impact on the spore dimensions). Significant ANOVA (p ≤ 0.05) tests were followed by a post-hoc Tukey's test for comparisons among means (p ≤ 0.05). The spore shape data were analysed with Chi square tests (p ≤ 0.05) in relation to attempt number, spore position, type of culture, and host plant used for subcultures.

RESULTS

Molecular analysis

Rhizophagus intraradices sequences, including all culture lines studied here (Figs 2, S2), form a monophyletic clade at the species level, separated from other species in the genus. The species is more closely related to *R. prolifer* than to *R. irregularis* (Fig. 2A). Sequences from ATT 1102-12 (the new strain from the type locality) are scattered within this clade (Fig. 2B).

During the studies, it became evident that *Rhizoglomus venetianum* (Turrini *et al.* 2018), was described based on a biased sequence selection. Its molecular phylogenetic position was therefore re-analysed. The analysis showed that the published sequences are phylogenetically embedded within the *R. irregularis* clade (Fig. 2C).

Morphology

Both ATT 4 and ATT 1102 produced spores externally in the substrate and within the root cortex or bursting through the roots (Figs 3A, B, 4A, B, 5G, H, 6G, H, 10B, G, H). Spore morphology, including length, width, shape (Figs 7, 8), colour and characteristics of the subtending hypha (Fig. 9) were much more variable among the ex-type cultures (ATT 4) and the new strain (ATT 1102) than in the type material.

Extraradical spores occurred singly, in loose clusters, in dense clusters (fascicles) in the substrate, loosely or densely around roots, in voids such as empty seed coats (Fig. 10A) or insect and mite integuments, and occasionally in mats on surfaces of soil components such as decaying leaves, but not all from any particular sample. They were similar in both PC and ROC (Figs 5, 6), except for differences in production of irregular spores, although in the latter they were usually much less darkly coloured. Intraradical spore production varied from none or few (particularly in ROC) through occasional individual spores in cortical cells (Fig. 4F), to roots crammed full of spores (Figs 3A, 4A), often bursting through the epidermis (Figs 5C, 6C). Most irregularly-shaped spores (Fig. 8) were identified as having come from root tissue.

© 2021 Westerdijk Fungal Biodiversity Institute

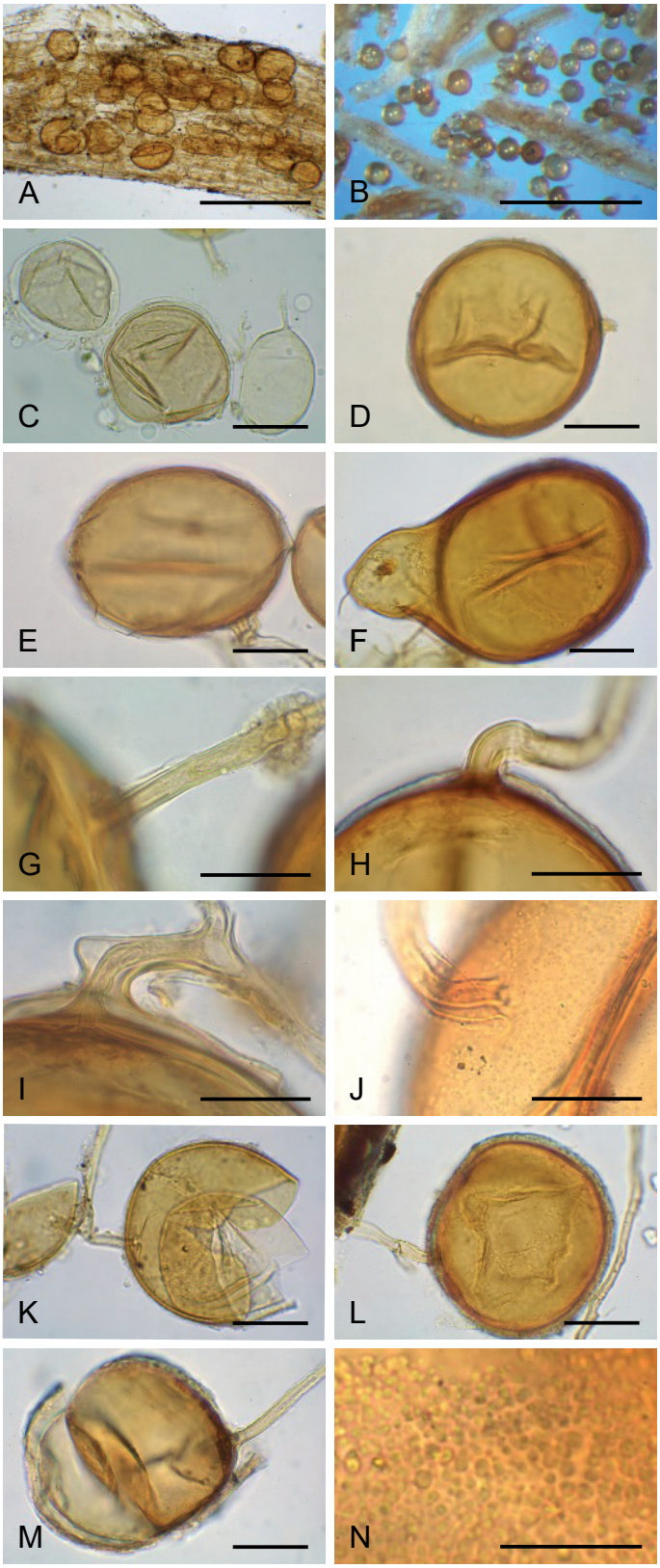

Fig. 3. Micromorphology of the holotype specimen of *Rhizophagus intraradices* (OSC 40255, 5 May 1981). **A.** Intraradical spores. **B.** With extra-radical spores singly and in clusters. **C.** Thin-walled spores extruded from a crushed root. **D.** Globose spore with subtending hypha (SH) detached close to the spore. **E.** Broadly ellipsoid spore. **F.** 'Pip-shaped' spore. **G.** Parallel-sided SH. **H.** Recurved SH. **I.** Recurved angular SH with lateral protrusion. **J.** SH with tubaeform flare. **K.** Crushed spore showing separation of wall components. **L.** Outer wall with thickening by bacterial colonies. **M.** Wall components separating on crushing. **N.** Bacterial colonies giving an impression of ornamentation. Scale bars: A = 250 µm; B = 1 mm; C–F, K–M = 50 µm; G–J, N = 25 µm.

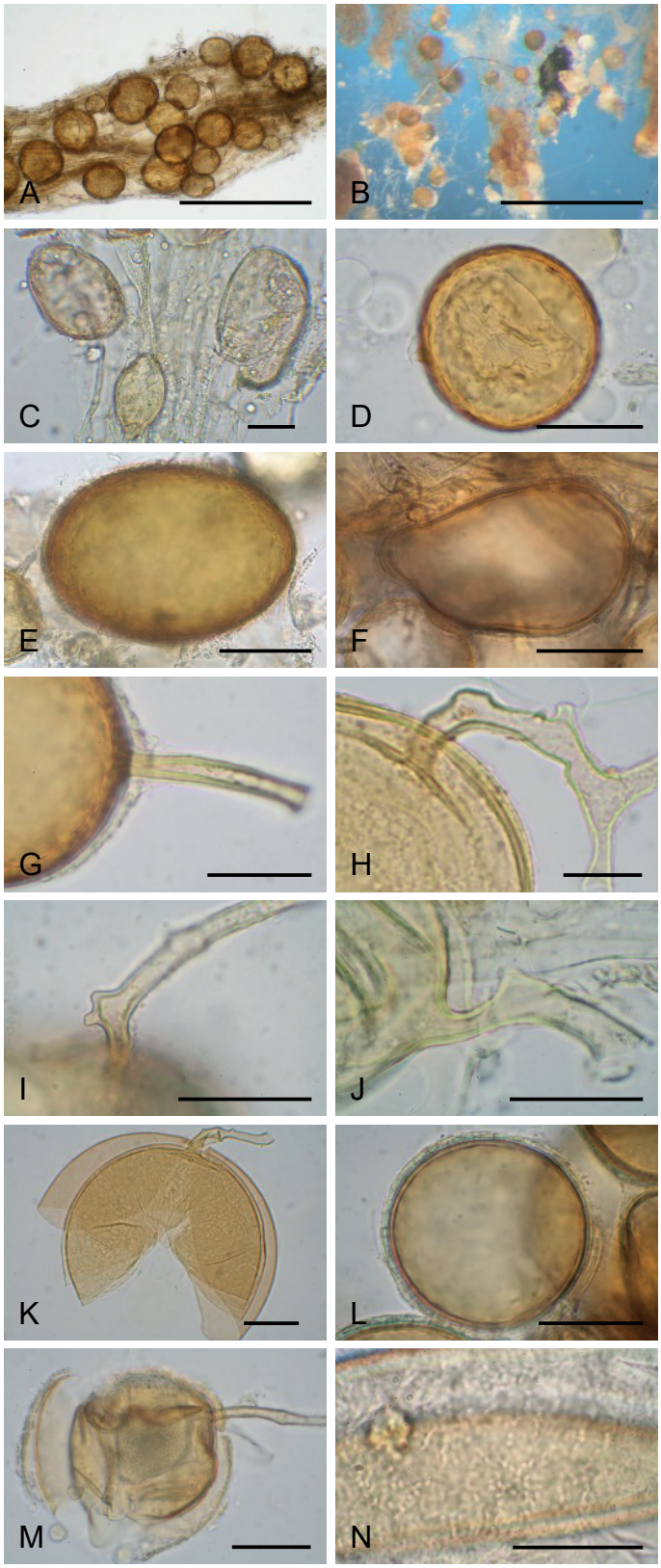

Fig. 4. *Rhizophagus intraradices* strain re-isolated from type locality in 1974. **A.** Intraradical spores. **B.** With extra-radical spores singly and in clusters. **C.** Thin-walled spores extruded from a crushed root. **D.** Globose spore with subtending hypha (SH) detached close to the spore. **E.** Broadly ellipsoid spore. **F.** 'Pip-shaped' spore. **G.** Parallel-sided SH. H. Recurved SH. **I.** Recurved angular SH with lateral protrusion. **J.** SH with tubaeform flare. **K.** Crushed spore showing separation of wall components. **L.** Outer wall with thickening by bacterial colonies. **M.** Wall components separating on crushing. **N.** Bacterial colonies giving an impression of ornamentation. Scale bars: A = 250 µm; B = 1 mm; C–M = 50 µm; N = 25 µm.

© 2021 Westerdijk Fungal Biodiversity Institute

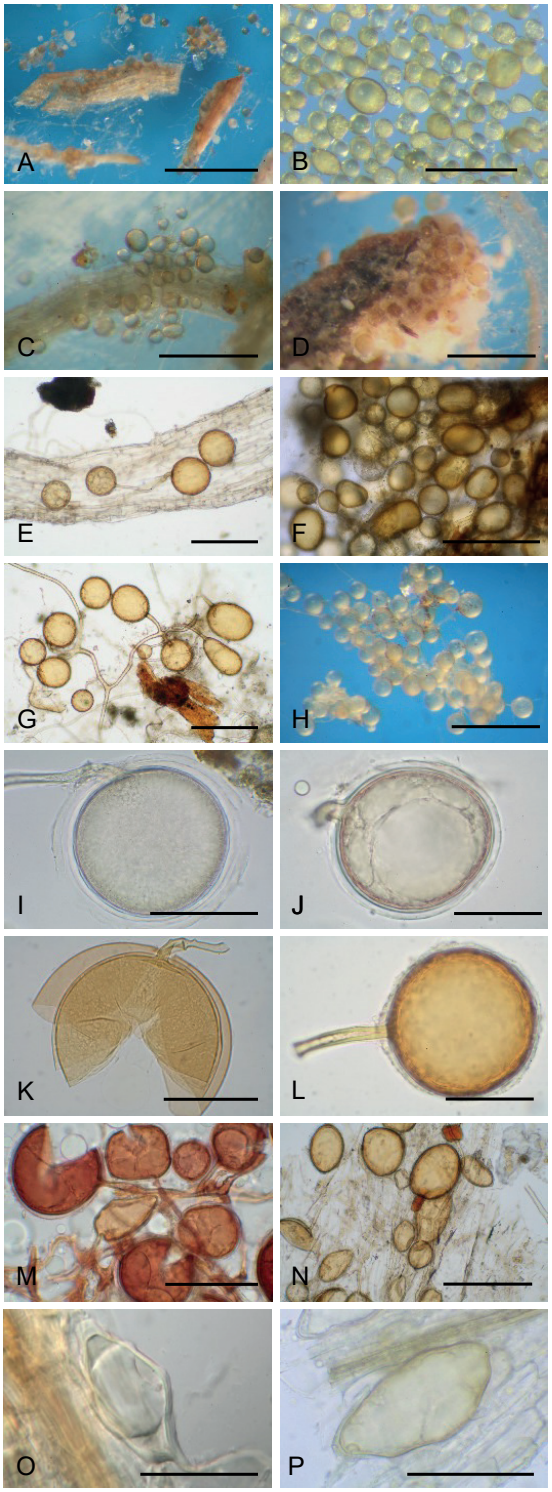

Fig. 5. *Rhizophagus intraradices* from pot cultures. **A.** Intra- and extra-radical spores. **B.** Extracted spores that were formed singly. **C.** Spores bursting through the root cortex and epidermis. **D.** Aggregation (fascicle) of pale extraradical spores. **E.** Spores formed in the root cortex. **F.** Fascicle of darkly coloured spores. **G.** Loose cluster of extraradical spores. **H.** Small, dense clusters of spores. **I.** Almost colourless young spore with expanding outermost wall component. **J.** Older spore developing pigmentation and with colourless outer component. **K.** Crushed spore showing wall components 2 & 3, having lost the evanescent outermost component. **L.** Darkly coloured spore retaining colourless outer component. **M.** Cluster of young spores with red reaction to Melzer's reagent. **N.** Cluster of old spores lacking a reaction to Melzer's reagent. **O.** Intraradical spore showing cap-like distal thickening of wall component 2. **P.** Misshapen (irregular) intraradical spore. Scale bars: A = 1 mm; B–D, H = 500 µm; E, G = 150 µm; F = 250 µm; I, K, M, P = 100 µm; N = 200 µm; J, L, O = 50 µm.

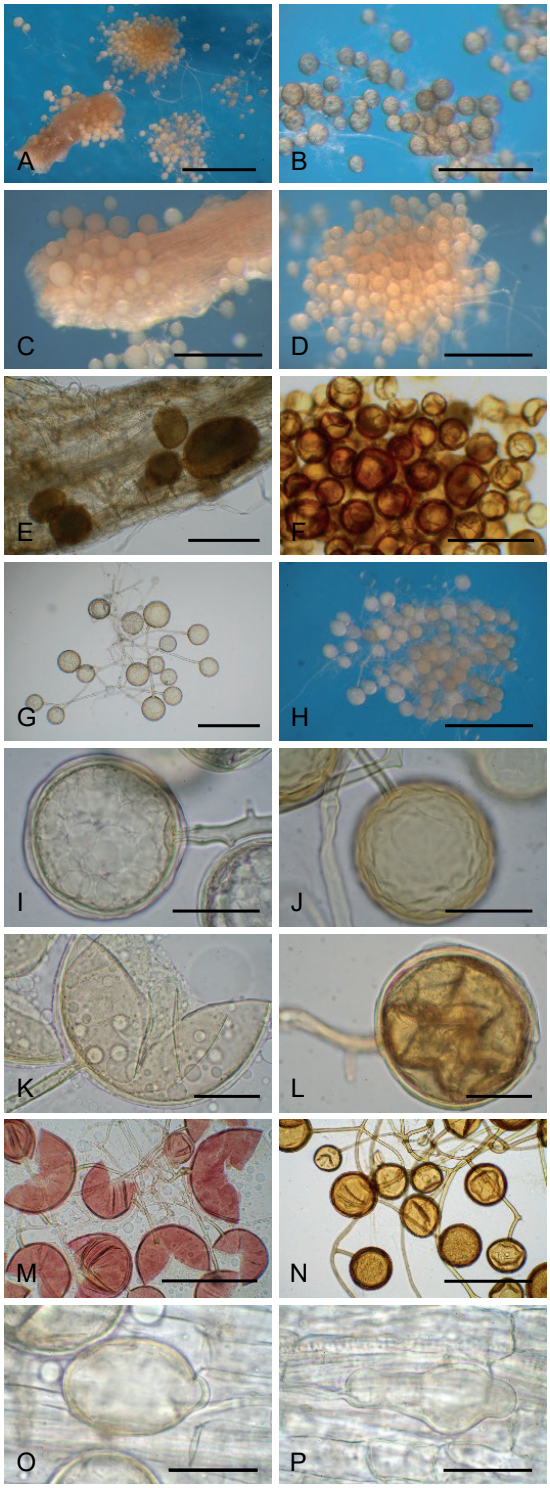

Fig. 6. *Rhizophagus intraradices* from root organ cultures. **A.** Intra- and extra-radical spores. **B.** Extracted spores that were formed singly. **C.** Spores bursting through the root cortex and epidermis. **D.** Aggregation (fascicle) of pale extraradical spores. **E.** Spores formed in the root cortex. **F.** Fascicle of darkly coloured spores. **G.** Loose cluster of extraradical spores. **H.** Small, dense clusters of spores. **I.** Almost colourless young spore with expanding outermost wall component. **J.** Older spore developing pigmentation and with colourless outer component. **K.** Crushed spore showing wall components 2 & 3, having lost the evanescent outermost component. **L.** Darkly coloured spore retaining colourless outer component. **M.** Cluster of young spores with red reaction to Melzer's reagent. **N.** Cluster of old spores lacking a reaction to Melzer's reagent. **O.** Intraradical spore showing cap-like distal thickening of wall component 2. **P.** Misshapen (irregular) intraradical spore. Scale bars: A = 1 mm; B–D, H = 500 µm; E = 150 µm; F, G = 250 µm; I–L, O, P = 50 µm; M, N = 200 µm.

© 2021 Westerdijk Fungal Biodiversity Institute

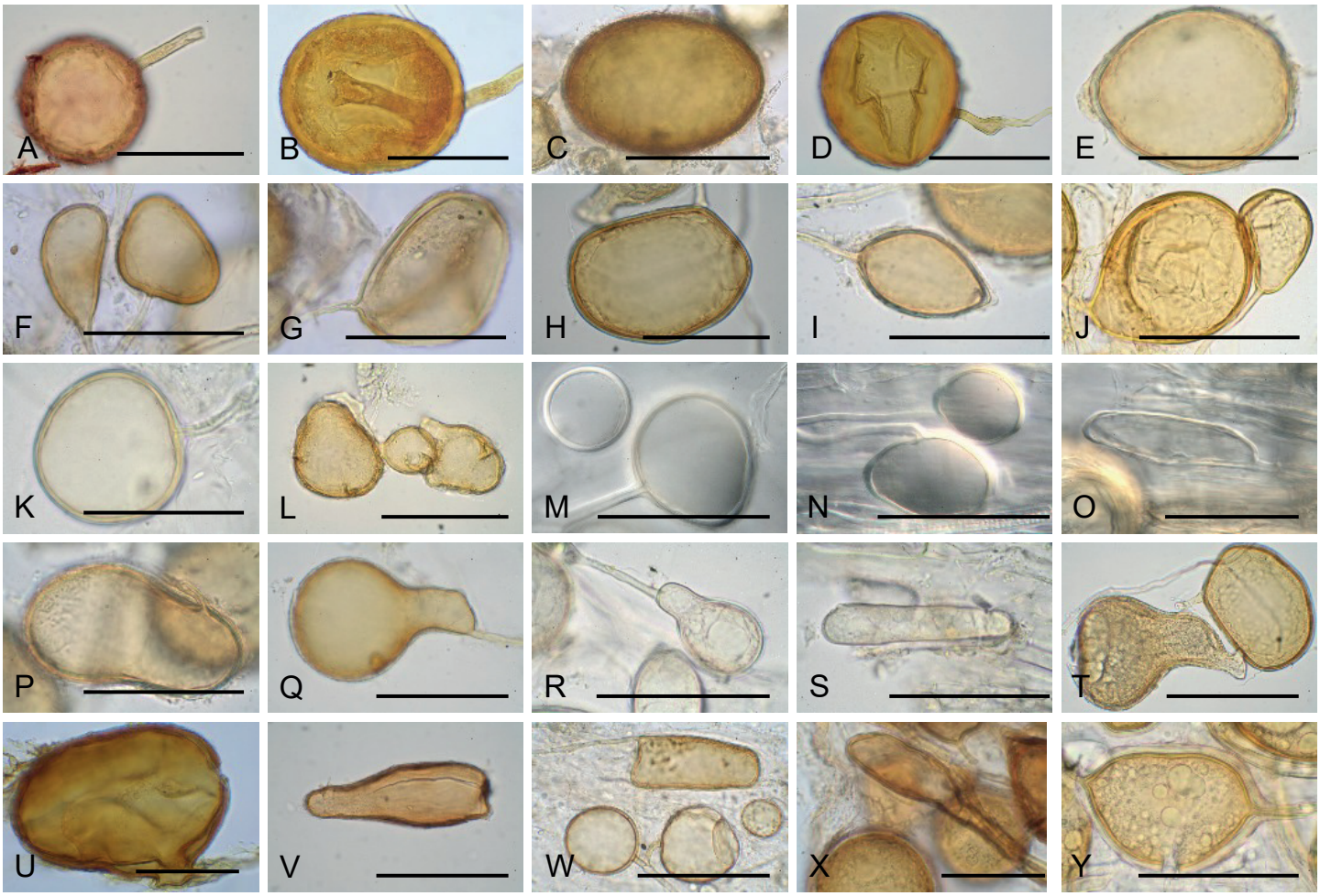

Fig. 7. Some examples of the many sizes, colours and shapes of spores of *Rhizophagus intraradices* (basionym *Glomus intraradices*). Scale bars: A–N, P, R, S, U, Y = 100 µm; O = 50 µm; Q, T, V, W, X = 150 µm.

Fig. 8. Examples of the convoluted and irregular shapes found amongst pot cultures, but rarely in root organ cultures, of *Rhizophagus intraradices* spores. Scale bars: A = 250 µm; B, G = 200 µm; C–F, J = 100 µm; H–I = 150 µm.

Spore colour

The colour (Table S2, Figs 10, 11) of both extraradical and intraradical spores (both ATT 4 and ATT 1102), was very variable, ranging from colourless through shades of yellow to shades of brown. At first spores are thin-walled and very pale in colour (Fig. 11A), but as they develop, the laminated components thicken and darken, and gradually the overall spore colour changes through yellow (Fig. 11B) to yellowish brown, until they may appear quite dark brown (Fig. 11C). Most of the colour change occurs in the second (innermost) laminated component (Fig. 11D).

Spore shape

Combining data from both ATT 4 and ATT 1102 in PC and ROC, from 2 679 spores, the overall distribution of shapes varied considerably. The majority were globose (57.1 %) to subglobose (21.8 %). Other relatively common shapes included broadly ellipsoid (5.7 %), ellipsoid (3.7 %), oval (3.0 %) irregular (2.7 %) or ovoid (2. 4) specimens. Spores of 22 other shapes were observed, each with a frequency of < 2 % (Fig. 12). When comparing the shape of spores produced by ATT 4 and ATT 1102, the former had more different shapes (25:16) than the latter.

© 2021 Westerdijk Fungal Biodiversity Institute

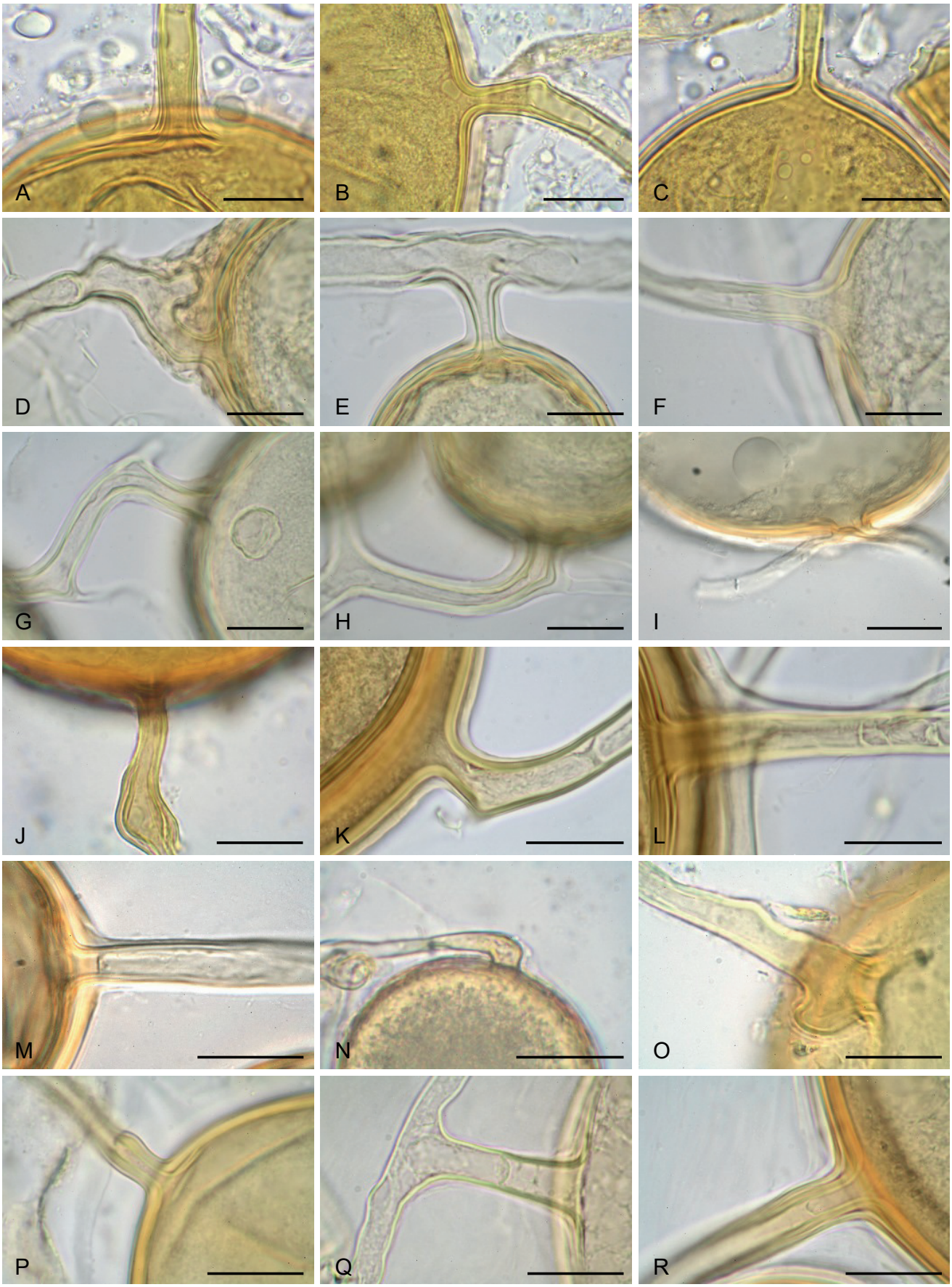

Fig. 9. Some of the variation among subtending hyphae of *Rhizophagus intraradices*. **A.** Parallel-sided, slightly flared proximally. **B.** Slightly recurved and narrowed at spore base. **C.** Gradually narrowing towards spore. **D.** Convoluted, branched. **E.** Short branch, narrowing towards spore. **F.** Funnel-shaped. **G.** Recurved, with tubaeform flare. **H.** Recurved, angular, flared. **I.** Laterally budded (lacking stalk). **J.** Swollen distally, tapering proximally. **K.** Recurved, angular with lateral peg. **L.** Flared, tapering slightly distally. **M.** Flared, tapering slightly proximally. **N.** Sharply recurved, expanded towards the spore base. **O.** Subangular, swollen and flared at the spore base. **P.** Thickened and constricted proximally. **Q.** Short branched, tubaeform. **R.** Tapering proximally, slightly flared, with septal occlusion. Scale bars = 20 µm.

© 2021 Westerdijk Fungal Biodiversity Institute

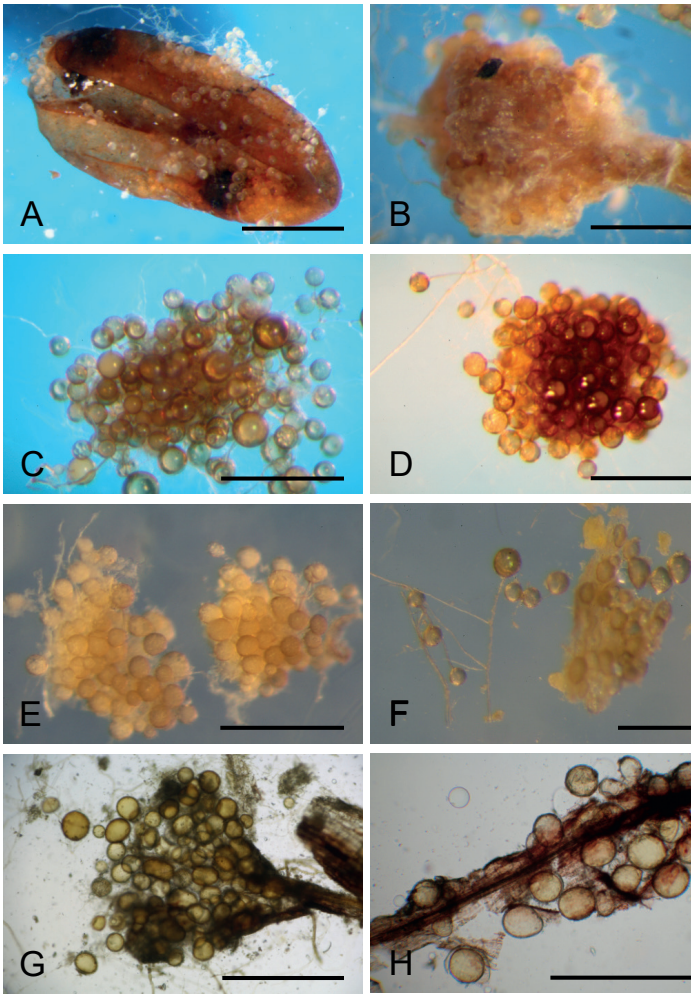

Fig. 10. *Rhizophagus intraradices* clusters of spores. **A.** Spores occupying an empty *Plantago lanceolata* seed. **B.** A dense cluster of spores amongst fine mycelium surrounding a root fragment. **C–F.** Spores in clusters of varying density showing colour variation. **G.** Cluster of spores bursting through the cortex of a decaying root. **H.** Spores clustering around the surface of a decaying root. Scale bars: A = 1 mm; B–H = 500 µm.

In ATT 4, only 1.66 % of spores were irregular, whereas for ATT 1102, the proportion was 5.19 % (Fig. 12). Moreover, this spore shape distribution is significantly different between ATT 4 and ATT 1102 at $p \leq 0.001$ (Table 2).

Several factors, predominantly spore position (whether extraradical or intraradical) (Fig. 13), culture type (Fig. 15) and host plant (Table 3, Fig. 16) significantly influence spore shape. For example, 91 % of extraradical spores were mostly globose (70 %) or subglobose (21 %), whereas 90 % of intraradical spores were globose (26 %), subglobose (23 %), ellipsoid (13 %), broadly ellipsoid (13 %), oval (9 %) or irregular (6 %) (Fig. 14).

Culture type had significant effect on spore shape with the distribution of shapes being significantly different ($p \leq 0.001$) between PC and ROC (Table 2). There were 8 different shapes from ROC (Fig. 15), mainly represented by globose (81 %), subglobose (15 %) and obovoid (2 %) spores, while spore shape in PC was much more variable, producing 27 shapes, mainly represented by globose (47 %), subglobose (25 %), broadly ellipsoid (6 %), ellipsoid (5 %), irregular (5 %), oval (4 %) and obovoid (3 %) spores. Similarly, spore shapes varied significantly among plant hosts (Fig. 16, Table 4), each host plant having its own specific spore shape distribution, except for *P. lanceolata* and *L. japonicus*.

Comparing the two lineages, cultures of ATT 4 and ATT 1102 produced predominantly globose (56.8 and 56.4 %) to subglobose spores (22.9 and 18.4 %). However, the remaining proportion of spores from the two cultures differed (Fig. 16). ATT 4 produced 21 different shapes of spores, including many irregular spores and some angular or asymmetrical in outline, whereas ATT 1102 had only 14, most of which were smooth in outline and bilaterally symmetrical.

For ATT 4, both the holotype collection and ex-type cultures, spores were produced both extra- and intra- radically (Fig. 13). The spores from the holotype were predominantly regular in shape (spheroid to ellipsoid), whereas much greater morphological variation occurred among the ex-type cultures (Figs 3, 7, 8). Although most were regular (globose, subglobose, broadly ellipsoid, ellipsoid or oval, fusiform, obovoid or ovoid), the range of shapes also encompassed bottle-shaped, pyriform, obpyriform, lacrimoid, rhomboid, reniform, subreniform, subcardioid, subtriangular, subangular, clavate, spatulate, lanceolate, flattened on one side through juxtaposition with other developing spores, or misshapen (irregular) (Figs 3–8). There were clear differences between the degree of shape variation among intraradical and extraradical spores. In particular, irregularly shaped spores were found predominantly in the PCs (both origins). However, ATT 4-84, a PC established from the ROC, ATT 4-88, yielded irregular intraradical spores, but no misshapen extraradical specimens.

For type and ex-type specimens (ATT 4) in PC, 27 (~5 %) of the intraradical spores and only 5 (~0.7 %) of the extraradical spores (and two base-unidentified) were irregular in shape. In ROC, there were two misshapen spores. For the new isolate (ATT 1102) in PC, 23 (9.2 %) intraradical spores and 22 (~8.6 %) extraradical spores were misshapen (irregular). All of these came from a subculture (ATT 1102-13) of (ATT 1102-7), a single spore isolate that had not produced misshapen spores. This strain did not produce irregular spores in ROC (extraradical spores only were formed), whereas in PC, there were differences among subcultures. For example, ATT 1102-7 (with *Plantago lanceolata*), the first generation of the single spore isolate, produced very large numbers of mainly extraradical spores (W 4655), whereas intraradical spores were sparse. Of the 100 extraradical and 50 intraradical spores examined, none was irregular, although two of the latter were somewhat flattened (asymmetrical) due to juxtaposition in the root. A later sample from the same pot (W 5576) produced predominantly intraradical spores which were abundant, often bursting through the roots, along with lower numbers of extraradical spores, and of the 97 spores examined, all were spheroid (including two obovoid and two ovoid intraradical spores). In contrast, a first-generation subculture from this, ATT 1102-13 (a PC with a mixture of *P. lanceolata, Allium schoenoprasum* and *Festuca ovina*) produced an abundance of both intraradical and extraradical spores (W 5580) with considerable variation in shape. This culture produced predominantly spheroid spores, but also a few pyriform, subpyriform, subangular, subreniform, and subtriangular spores, along with a high proportion of misshapen specimens (23 % extraradical and 16 % intraradical) (Fig. 6).

Other than the greater variation in spore shape, it was not possible morphologically to distinguish spores of ATT4 (ex-type origin) from those produced by ATT 1102 from the type locality.

© 2021 Westerdijk Fungal Biodiversity Institute

Table 2. *Rhizophagus intraradices*: numbers of specimens of different spore shapes by strain ATT 4 (type and ex-type cultures), and ATT 1102 (new strain from type locality established some 30 years later): listed by ATT, spore position (extra- or intraradical) and nature of culture (pot culture or root organ culture). Data from repeated sampling over almost 40 yr (ATT 4) and 19 yr (ATT 1102).

Spore shape	Attempt number		Spore position		Type of culture	
	ATT 4	ATT 1102	extraradical	intraradical	PC	ROC
globose	1 097	435	1 288	188	729	725
subglobose	441	142	383	170	380	138
broadly ellipsoid	121	32	43	95	96	11
ellipsoid	81	37	18	96	79	2
oval	48	32	11	68	65	0
irregular	32	40	26	45	69	0
obovoid	38	26	43	18	42	19
ovoid	15	6	12	9	19	2
fusiform	16	0	0	15	13	0
subtriangular	9	3	5	6	11	0
subangular	6	6	4	6	10	0
flattened	2	6	0	8	8	0
pyriform	2	1	2	0	2	0
peanut-shaped	2	0	2	0	1	1
subcardioid	2	0	1	1	2	0
bottle-shaped	2	0	0	2	1	0
rhomboid	2	0	0	2	2	0
spatulate	0	2	0	2	2	0
flask-shaped	1	0	0	1	1	0
funneliform	1	0	0	1	1	0
clavate	1	0	0	1	1	0
balloon-shaped	1	0	1	0	0	1
lacrimoid	1	0	0	0	0	0
lanceolate	1	0	0	1	1	0
cardioid	0	1	0	1	1	0
pip-shaped	1	0	1	0	1	0
reniform	1	0	0	0	0	0
subpyriform	0	1	0	1	1	0
subreniform	0	1	1	0	1	0
TOTAL	1 930	771	1 847	737	1 545	899
Chi square test	X^2 = 51.843, df = 7, p-value ≤ 6.269e-09		X^2 = 652.0621, df = 7, p-value ≤ 2.2e-16		X^2 = 284.7482, df = 7, p-value ≤ 2.2e-16	

Table 3. *Rhizophagus intraradices*: differences in the number and proportion of spores of the main (spheroid and ellipsoid) shapes in relation to host plant indicating a possible host-induced effect.

Host plant	Culture type	globose		subglobose		broadly ellipsoid		ellipsoid	
		n	%	n	%	n	%	n	%
Cichorium intybus	ROC	423	78.6	104	2.4	10	1.6	1	0.2
Festuca ovina	PC	23	56.1	9	8.7	2	1.9	7	6.5
Lotus japonicus	PC	27	55.1	17	14.8	4	3.4	1	0.8
Paspalum notatum	PC	46	26.9	46	91.3	42	14.5	37	12.2
Plantago lanceolata	PC	640	58.0	323	12.3	79	6.7	62	5.2
Daucus carota	ROC	302	89.3	34	0.3	1	0.2	1	0.2

© 2021 Westerdijk Fungal Biodiversity Institute

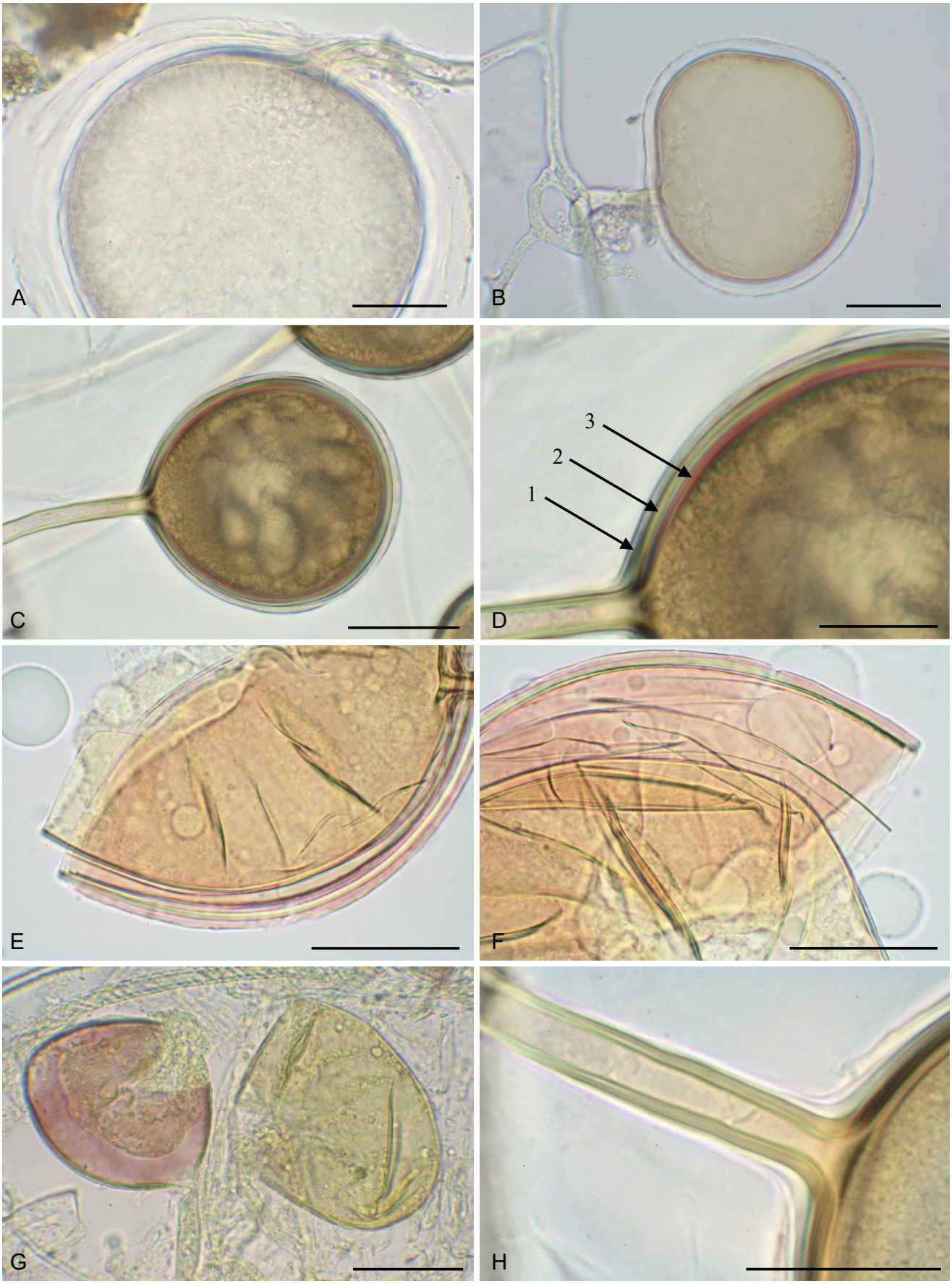

Fig. 11. Main spore characteristics of *Rhizophagus intraradices*. **A.** Immature spore from ROC showing expansion and apparent layering of the outer component. **B.** Semi-mature spore with outer component still intact and pigmentation of main structural wall. **C.** Mature spore from root organ culture (ROC). **D.** Detail of the wall structure of the spore in C, showing three wall components (1–3): 1, evanescent before degradation; 2, yellow, finely laminate pale yellow; 3, coarsely laminated dark brown. **E, F.** Crushed spores in polyvinyl alcohol lacto-glycerol with Melzer's reagent (PVLG-M) showing pale pink reaction of the evanescent wall component. **G.** Different reactions to PVLG-M; right no reaction, left outer component pink. **H.** Parallel-sided subtending hypha with slight tubaeform flare and proximal wall thickening. Scale bars: A, B, G = 50 µm; C, E, F = 100 µm; D, H = 25 µm.

© 2021 Westerdijk Fungal Biodiversity Institute

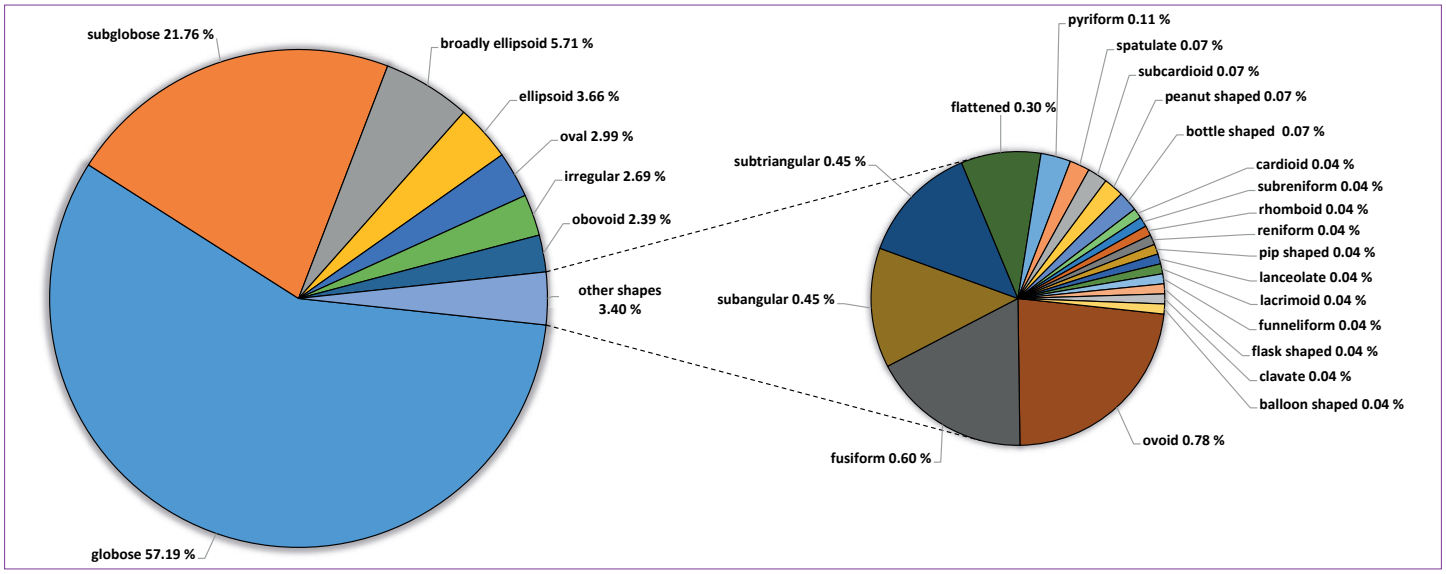

Fig. 12. *Rhizophagus intraradices*: distribution of spore shapes over all treatments (n = 2 673). The 'other shapes' section includes all those occurring with a frequency < 2 %.

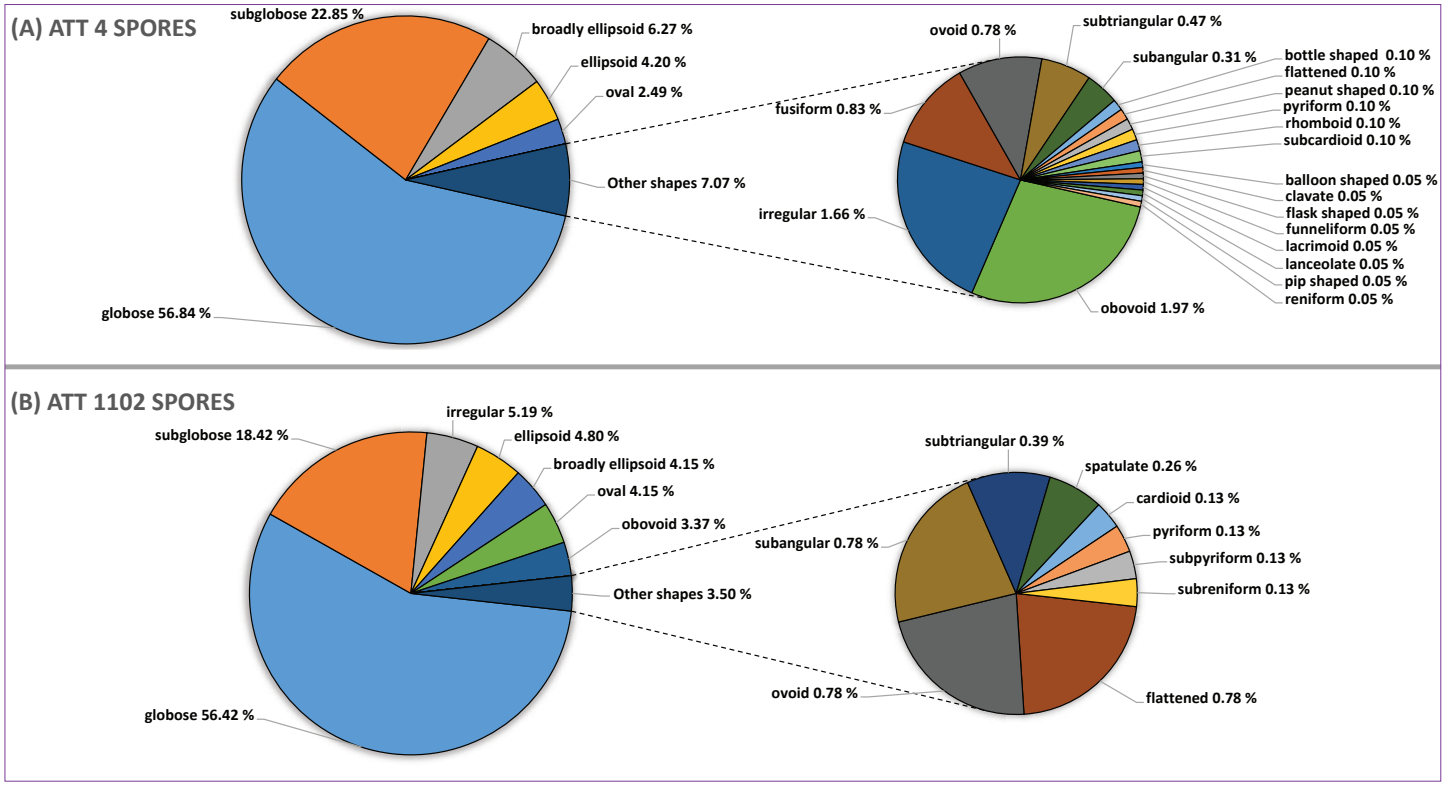

Fig. 13. *Rhizophagus intraradices*: distribution (percentage of measured spores) of the spore shapes between those from ATT 4 (Panel A) (n = 1 924) and ATT 1102 (Panel B) (n = 771). Other shapes include those occurring with a frequency < 2 %.

Table 4. *Rhizophagus intraradices*: matrix comparison of the spore shapes in relation to the host plant used for subcultures (two strains, ATT 4 and ATT 1102, combined). Results of Chi square tests are expressed with the X^2 value, and its significance level (*** when P ≤ 0.001; ** when P ≤ 0.01; * when P ≤ 0.05; NS when P > 0.05).

Host plant	*Cichorium intybus*	*Festuca ovina*	*Lotus japonicus*	*Paspalum notatum*	*Plantago lanceolata*	*Daucus carota*
Cichorium intybus						
Festuca ovina	X^2 = 190 ***					
Lotus japonicus	X^2 = 33 ***	X^2 = 20 **				
Paspalum notatum	X^2 = 306 ***	X^2 = 22 ***	X^2 = 28 ***			
Plantago lanceolata	X^2 = 149 ***	X^2 = 48 ***	X^2 = 8 NS	X^2 = 150 ***		
Daucus carota	X^2 = 20 **	X^2 = 133 ***	X^2 = 56 ***	X^2 = 263 ***	X^2 = 168 ***	

© 2021 Westerdijk Fungal Biodiversity Institute

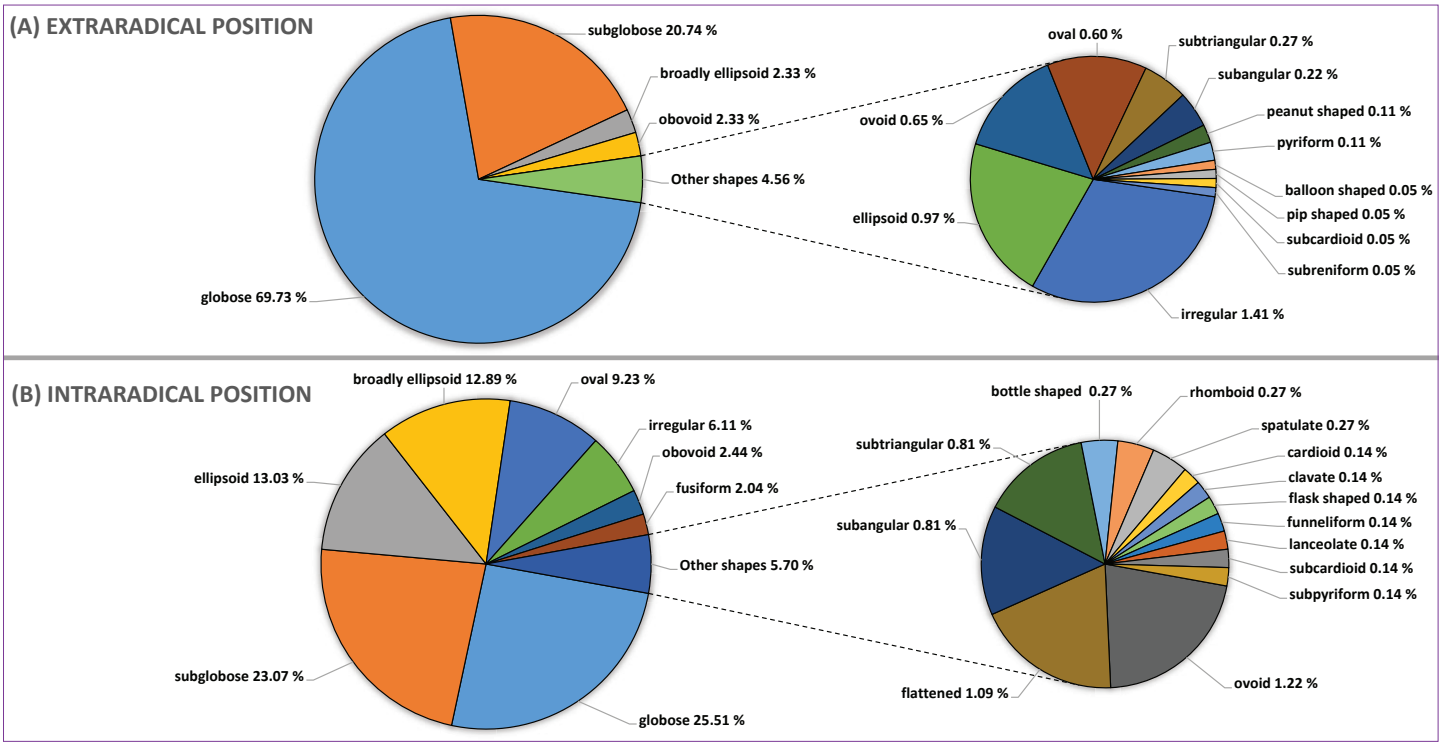

Fig. 14. *Rhizophagus intraradices*; distribution (percentage of measured spores) of the spore shapes between extraradical spores (Panel A) (n = 1 841) and intraradical spores (Panel B) (n = 737). Other shapes include those occurring with a frequency < 2 %.

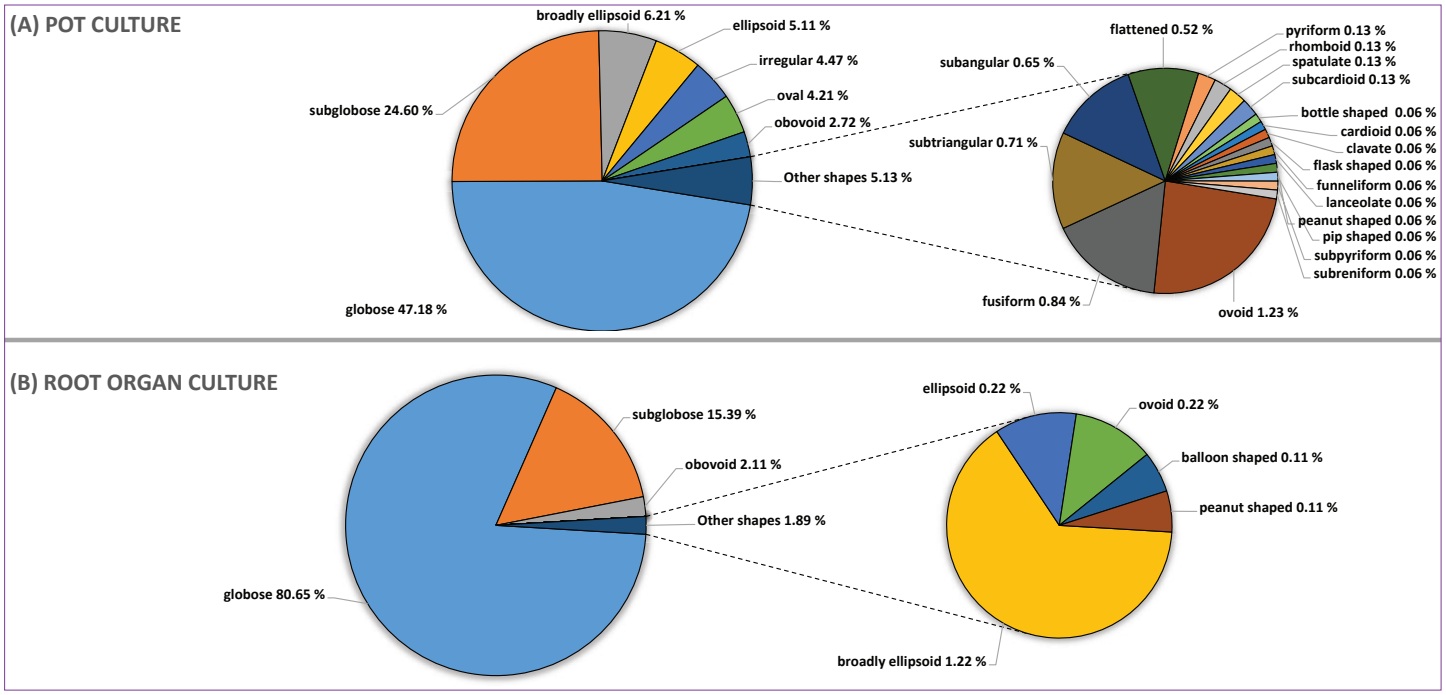

Fig. 15. *Rhizophagus intraradices*: distribution (percentage of measured spores) of the spore shapes between (Panel A) pot cultures (n = 1 559) and (Panel B) root organ cultures (n = 899). Other shapes include those occurring with a frequency < 2 %.

Subtending hypha

The spores develop centrally or eccentrically from a 'subtending hypha' (Figs 3, 4G–I, 9, 11H) that is very variable in size, shape, colour, and wall thickness. In some specimens, it is parallel-sided or tapered distally, with very little expansion at the spore base (Figs 9M, 10H), in others it is flared through expansion (tubaeform) proximally (Figs 3J, 9L–Q). In others it may be swollen asymmetrically (Fig. 9O), or constricted proximally (Fig. 9J). The hypha may be straight, parallel with the major axis of the spore (Fig. 11C), or it may be angled or recurved to varying degrees (Figs 3H, I, 4H, I, 6L, K) or otherwise distorted (*e.g.*, Fig. 9D, O). In most specimens, the spore is open-pored (*e.g.*, Fig. 9C), but it may be occluded by a thickened plug (Fig. 9K) or a proximal or distal septum (Fig. 9L, M, Q) formed from the innermost laminated component. The subtending hyphae can be colourless (*e.g.*, Fig. 7M, N), pale yellow (*e.g.*, Fig. 9H) or brownish yellow (*e.g.*, Fig. 9A, C, K).

© 2021 Westerdijk Fungal Biodiversity Institute

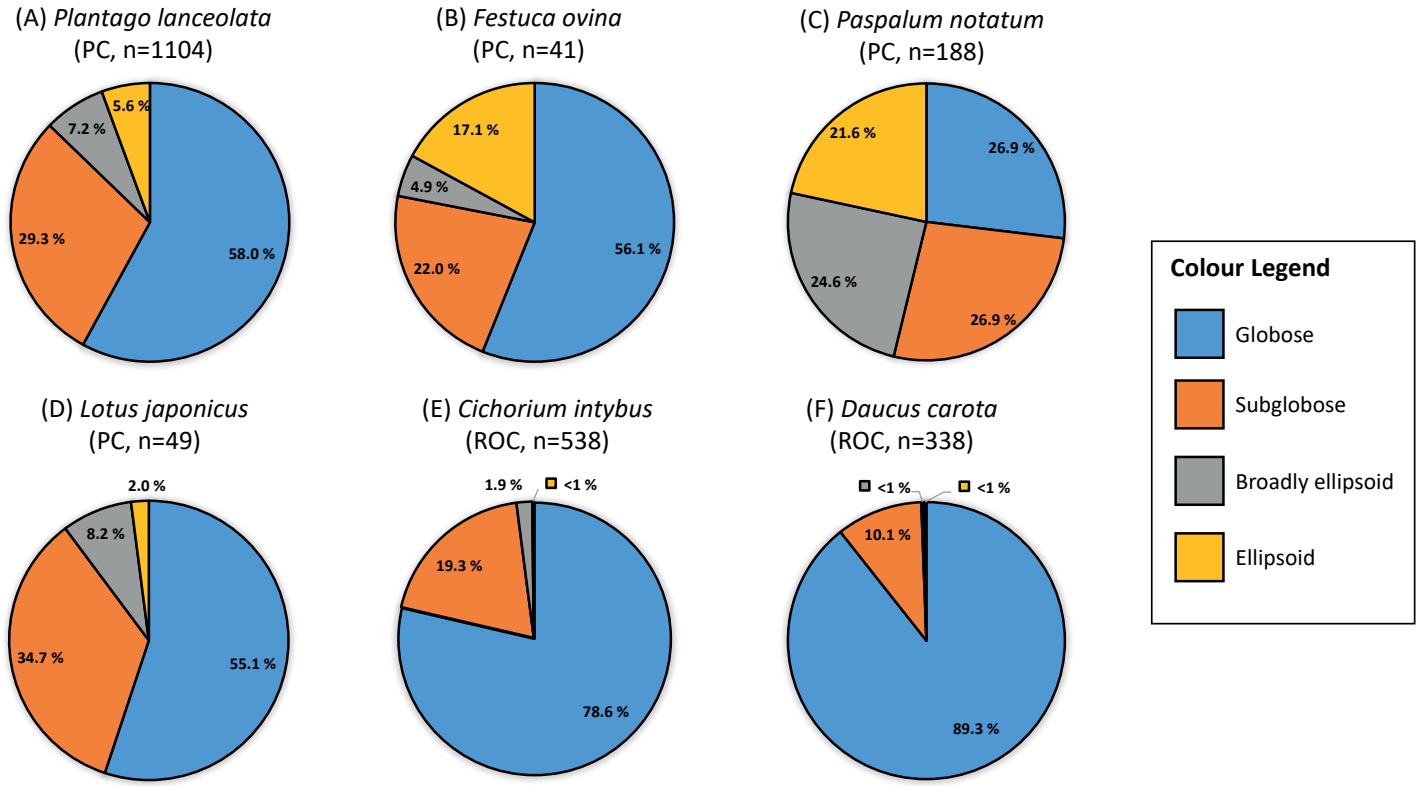

Fig. 16. *Rhizophagus intraradices* distribution of the four most abundant spore shapes (globose, subglobose, broadly ellipsoid, and ellipsoid) in relation to their host plant. For each panel, the culture method (Pot Culture, PC or Root Organ Culture, ROC) and the number of spores measured are given. Values are given as a percentage of the total spores measured. When a percentage is very low and the colour barely visible (*i.e.*, < 1 %), the colour legend is indicated next to the number.

Spore dimensions

It was difficult to decide which parameter to use for analysis of the data. Length, width, longest, widest, volume and the ratio of longest to widest measurement could all be analysed. Volume calculations necessarily assumed an isodiametric shortest dimension, but many spores appear somewhat pulvinate, and the irregular specimens also were much thinner than broad. Consequently, a two-dimensional representation of the longest and widest measurement was chosen. By almost any class variable, there were significant differences among individual samples (Table S1), but overall, the analysis of the two different culture lines (ATT 4 and ATT 1102) did not differ significantly. It should be noted, however, that the sample size and number of repetitions of samples (over time) were grossly different. There were probably too few irregular spores to make a good comparison, and the lack of significance may be the results of the low number of observations. Spores that could not be determined as either extraradical or intraradical were excluded from the measurements, as were those spores with the subtending hypha obscured or broken so that the spore base could not be identified.

For ATT 4 spores, 70 % were extraradical and 30 % were intraradical. For ATT 1102, 72 % were extraradical and 28 % were intraradical. For ATT 4-1, the type culture, measurements of 52 extraradical spores (42–224 × 42–154 µm, mean 104 × 99 µm) and 100 intraradical spores (29–186 × 18–147 µm, mean 79 × 66 µm) gave an overall size range of 29–224 × 18–154 µm, mean 87 × 77 µm. These data together with measurements from ex-type PCs gave dimensions of 29–224 × 29–165 µm, mean 98 × 96 µm for 727 extraradical spores and 18–234 × 16–152 µm, mean 84 × 74 µm for 561 intraradical spores. For ATT4 spores in ROC, 556 extraradical spores were measured (30–182 × 30–178 µm, mean 98 × 97 µm). There were insufficient intraradical spores in ROC to make meaningful measurements. Another 71 spores from PCs were measured (55–141 × 50–179 µm, mean 93 × 91 µm) that could not be assigned with certainty as either intraradical or extraradical spores. Taking all these measurements into account, the overall spore dimensions from 1 915 spores were 18–234 × 16–179 µm, mean 94 × 90 µm.

The new isolate (ATT 1102) in pot culture produced extraradical spores of 26–383 × 26–398 µm mean 94 × 93 µm (n = 250) and intraradical spores of 48–383 × 34–398 µm, mean 112 × 150 µm (n = 150), and in ROC (extraradical only) of 48–123 × 46–122 µm, mean 88 × 88 µm (n = 145), giving an overall size range of 26–383 × 26–398 µm, mean 99 × 97 µm (n = 545).

Spore wall structure

Wall structure comparisons used in descriptions of glomeromycotan spores are primarily based on light microscopy of PVLG-mounted specimens, with occasional observations in water or glycerol. In these mounting media, spores from both PC and ROC were similar, except that in the former, some older specimens developed what appeared to be a new outer wall component, formed by the growth of what appear to be bacterial colonies. These manifested themselves as an apparent ornamentation of rounded surface bumps or scrobicular patterning (Figs 3N, 4N).

Whether in glycerol or water mounts, not subject to the effects of the acidic PVLG-based mounting media, or in PVLG and PVLG-M, the wall structure is of an outer, evanescent component, up to 1 µm thick, overlaying a colourless to pale yellow finely laminated component (1–4 µm thick) that sometimes

© 2021 Westerdijk Fungal Biodiversity Institute

misleadingly appears unitary (*i.e.*, without laminations). A third, darker yellow to brown laminated component then becomes evident, at first appearing as a unit component, but later developing laminae that may be tightly adherent, or loosened to varying degrees. In many specimens, the laminae become very loosely associated, often to the point of seeming to consist of many different unit components (Fig. 11F). This third component is indeterminate in thickness because it lays down new laminae with time. These laminae may be very loosely associated or become separated. Occasionally, when mounted in PVLG, the outer wall component can react, apparently depending on the age and condition of the particular specimen. In very young spores, component 1 sometimes can expand in PVLG to become up to 8 µm thick, and to give the appearance of a doublet (Figs 5I, 10C), but later this may not be observable in the mounting medium. In middle aged spores, it may or may not expand slightly, but it usually reacts with Melzer's reagent (in PVLG-M) to become pink or red. In what seem to be fully mature spores, this component remains evident, but does not always react to Melzer's reagent. In very old spores, this component disappears, hence its designation as evanescent. The reaction to Melzer's reagent is thus variable and seemingly inconsistent. In some specimens, there is no reaction at all. In others, the outer evanescent component reacts rapidly to become pink, whereas in others it turns purple, and in yet others, it does not react at all. The innermost laminated component also can react to become rust red in some specimens, but it did not react at all in most specimens examined. The only consistency seems to be that the first laminated component [which appears as a unit component in some ROC cultures (W6517 & W6158)] does not react at all to Melzer's reagent.

Germination

Spores of *R. intraradices* germinate (Fig. 9R) by hyphae emerging through the broken end of the subtending hypha. New hyphae may also emerge from hyphal fragments in the substrate.

Mycorrhiza

Rhizophagus intraradices forms arbuscular mycorrhizas (Fig. 17), often producing spores in the root cortex. It may form vesicles (thin-walled balloon-shaped structures), but there is a difficulty in defining the latter. Here, we define spores in the roots as having a multiple wall structure, normally with relatively thick walls. Vesicles (temporary storage organs, such as those in the genera *Ambispora, Acaulospora* or *Funneliformis*) lack such thickening. It is not always possible to know for *R. intraradices*, if such thin-walled structures in a root are vesicles (and thus will not proceed in development any further) or immature spores (in which case their wall will thicken and differentiate in the same manner as extraradical spores). Vesicles may occur near penetration points and arbuscules (thus active mycorrhizas), whereas the thick-walled spores in roots are not associated with active structures such as these. Mycorrhizas were not compared systematically, but they are not known to provide species-discriminating characters. Comparisons were not made either with other AMF, or with the same organism under different hosts, conditions and developmental stages: consequently, the images in Fig. 17 should not be considered as typical of the species.

Publications in which structures described as vesicles were recognised and used as inoculum do not indicate why they were referred to as vesicles (*e.g.*, Plenchette & Strullu 2003) and most provide neither description nor illustration. Given the current knowledge of the genus *Rhizophagus*, it seems most likely the authors were actually referring to spores (identified at the time as *G. intraradices*, although possibly not identified correctly). One publication (Diop *et al.* 1994) does, in their fig. 13, illustrate the so-called vesicles, showing thickened walls typical of spores formed by *Rhizophagus* spp. within roots. Similarly, extraradical and intraradical propagules have been distinguished, respectively, as spores and vesicles (Declerck *et al.* 1998), but one illustrated as a 'vesicle of *Glomus intraradices*' (their fig. 3) is a thick-walled intraradical spore.

TAXONOMY

The genus *Rhizophagus* was described with illustrations of arbuscules and spores in roots and it has long been accepted that its assignment as a chytrid-like pathogen of poplar was erroneous. Based on the accumulated wisdom of biologists throughout the 20th century, it has been widely accepted as such (*e.g.*, Petri 1919, Peyronel 1923, Butler 1939, Kelly 1950, Greenall 1963). However, it was later considered a synonym of *Glomus* by Gerdemann & Trappe (1974). Subsequently, when *Glomus* was circumscribed in a narrow sense from molecular analysis (Schüßler & Walker 2010), *Rhizophagus* was resurrected as belonging in a separate clade. It was then assigned to the clade accommodating *R. intraradices inter alia*, a move that has been very widely accepted. There was no requirement for a physical type specimen when the genus, based on *Rhizophagus populinus* was published (Dangeard 1896), and there were no known culture lines representing that species. The lack of a type was rectified by Walker *et al.* (2017) when illustrations by Dangeard (1900) were designated as neotype.

Although no new information had been published since the widespread acceptance of the application of the genus *Rhizophagus* (Schüβler & Walker 2010) for organisms in the clade GlGrAb (as defined in Stockinger *et al.* 2009), Sieverding *et al*. (2014) proposed the name *Rhizoglomus*, reiterating that *R. populinus* was a pathogenic organism. The ICNafp states (Preamble 12) that "The only proper reasons for changing a name are either a more profound knowledge of the facts resulting from adequate taxonomic study or the necessity of giving up a nomenclature that is contrary to the rules." No such profound knowledge, taxonomic study or nomenclatural error was demonstrated with this name change. The genus *Rhizoglomus* is therefore herein formally designated as a later heterotypic synonym of *Rhizophagus.*

Rhizoglomus venetianum

The organism named *Rhizoglomus venetianum* by Turrini *et al.* (2018) shares morphological characters with *R. intraradices* and *R. irregularis*. In the protologue, the species is described as having a wall consisting of four layers. The illustrations provided, however, are not sufficiently detailed to understand how this conclusion was reached, but the ultrastructure of the walls of *R. intraradices* (Maia & Kimbrough 1994; the culture studied in this publication, LITR 208, most likely represents *R. intraradices*) shows that the laminated component can separate into what appear to be separate layers, and it would be easy to misinterpret these, at the light microscopic level, as different components. It

© 2021 Westerdijk Fungal Biodiversity Institute

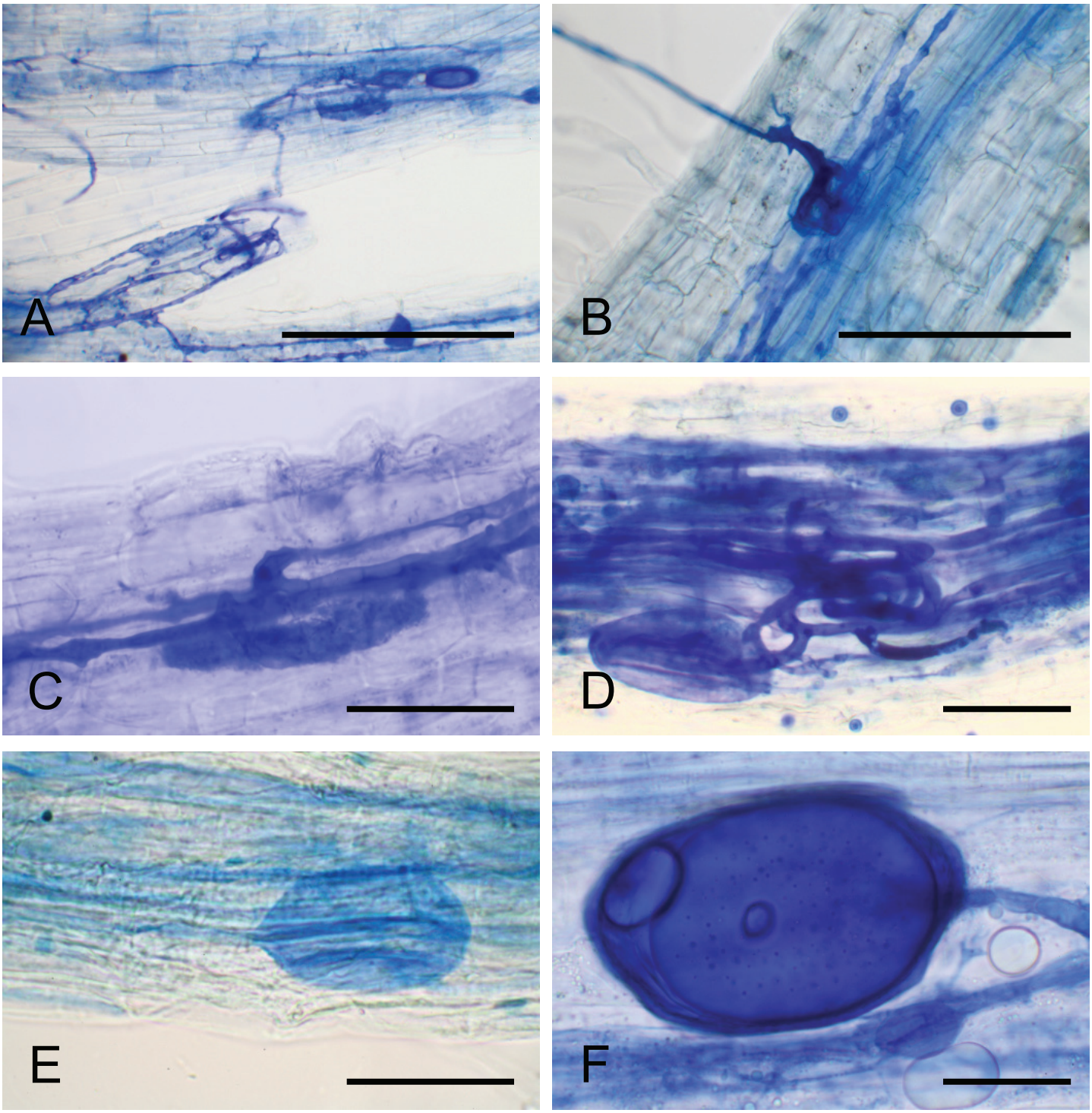

Fig. 17. *Rhizophagus intraradices* mycorrhiza with *Plantago lanceolata* as host, cleared with KOH and stained with 0.02 % methyl blue in 0.1 M HCl. **A.** Crushed fine root showing arbuscular mycorrhiza and intraradical spores. **B.** Appressorium at entry point into root cortex. **C.** Finely branched arbuscule. **D.** Entry point showing hyphal coils in outer cortical cells and a thin-walled structure, either a vesicle or an immature spore. **E.** Thin-walled structure in the cortex which could be interpreted as a vesicle, but may be an intraradical spore in the earliest development stage. **F.** Thick-walled mature intraradical spore. Scale bars: A = 250 µm, B = 125 µm, C–F = 50 µm.

is likely that the fourth wall component, used in the protologue to distinguish *Rhizoglomus venetianum* from both *R. intraradices* and *R. irregularis,* is an innermost loose lamina of the second laminated wall component (see Figs 3K, 10F).

The phylogenetic analysis of *Rhizoglomus venetianum* in the protologue showed a well-supported separate clade when compared with a widely-used Canadian isolate of *R. irregularis* (DAOM 197198, also labelled MUCL 46241). However, when analysed amongst a more comprehensive sequence sampling representing the intraspecific variability of *R. irregularis*, including also sequence variants characterised in a genome sequencing project (Maeda *et al.* 2018), it becomes obvious that the '*Rhizoglomus venetianum*' sequences merely represent a ribotype within the clade representing *R. irregularis* (Fig. 2C). There are, thus, neither substantial morphological, nor molecular phylogenetic characters that separate it from *R. irregularis*, and it therefore is placed as conspecific with that species.

© 2021 Westerdijk Fungal Biodiversity Institute

Rhizophagus P.A. Dang., *Botaniste* **5**: 43 (1896) [1896–1897] *sensu* Schüßler & Walker, *The Glomeromycota*: 19 (2010).
Synonyms: *Rhizoglomus* Sieverd. *et al., Mycotaxon* **129**: 377 (2015) [2014]
Stigeosporium C. West, *Ann. Bot., Lond.* **30**: 357 (1916).

Rhizophagus intraradices (N.C. Schenck & G.S. Sm.) C. Walker & Schüßler, *The Glomeromycota*: 19. 2010. Figs 2–10.
Basionym: *Glomus intraradices* N.C. Schenck & G.S. Sm., *Mycologia* **74**: 78. 1982. (holotype OSC40255).
Synonym: *Rhizoglomus intraradices* (N.C. Schenck & G.S. Sm.) Sieverd. *et al.*, *Mycotaxon* **129**: 378. 2015. (2014).

Chlamydospores (thick-walled one-celled asexual resting spores) produced in the substrate or in root cortical cells: overall length by width 18–383 × 16–398 µm. *Extraradical spores* formed singly, in loose to dense clusters (fascicles), clustered around roots; sometimes occupying voids such as empty seeds or arthropod integuments in soil. Fascicles up to approx. 2 × 2 mm in planar view. *Spores* colourless to white to pale yellow to yellow to brownish yellow to pale yellow-brown to yellow-brown to dark yellowish brown to dark brown. Spore shape globose, subglobose, broadly ellipsoid, ellipsoid, oval, sometimes subangular, pyriform, spatulate, subcardioid, reniform or subreniform, peanut shaped, obovoid, ovoid or often misshapen (irregular); sometimes partly flattened by juxtaposition with other spores in dense clusters; 26–383 × 26–398 µm. *Intraradical spores* very variable in size and shape, formed singly, or in clusters either entirely within the root cortex, or bursting through the cortex to form spore clusters around the roots. Globose, subglobose, broadly ellipsoidal, ellipsoidal, ovoid, obovoid, reniform, peanut shaped, bottle shaped, subrectangular, or irregular; colourless to pale yellow to yellow brown to dark yellowish brown; 18–234 × 16–202 µm.

Subtending hypha very variable in size and shape, often curved or sharply recurved, frequently constricted at the spore base or expanded distally, sometimes straight, parallel sided or funnel shaped. Open-pored, or occluded by a proximal or distal septum. *Spore wall* structure of three components (1–3) in one wall group. Component 1 sometimes appearing unitary, sometimes expanding in acidic mounting media, and sometimes evanescent, and in older spores often covered by bacteria that can produce the impression of an ornamented outermost component. Wall component 2 colourless to very pale yellow, 1–5 µm thick, under light microscopy, sometimes appearing unitary, but mostly finely laminated. Component 3 laminated, sometimes with very easily separable laminae, yellow to brown, increasing in thickness depending on the age of the spore to become up to 5 µm thick. Both intraradical and extraradical spores reacting variably to Melzer's reagent in PVLG-M. In young spores usually rapidly pink (outer component), with the middle component not reacting, and the inner laminated component darkening, sometimes becoming dark rust red. In some spores the reaction absent, or developing slowly over several days. Reaction fading over time with storage in polymerised PVLG-M.

Molecular phylogenetic analyses of the SSU-ITS-LSU sequences (Fig. 2) as the extended DNA barcode for glomeromycotan fungi (Stockinger *et al.* 2010) separate the clade with sequences from *R. intraradices* from any other clade representing other *Rhizophagus* species (Figs 2A, S2) and the culture lines studied here fall into the monophyletic clade that represents *R. intraradices* (Fig. 2C. The closest relative, based on present knowledge, is *Rhizophagus prolifer*. *Rhizophagus irregularis* is clearly separated, despite the absence of any clear morphological characters distinguishing the two species.

Specimens examined: **USA**, Florida, Orlando, Clermont-Mineola (approx. 28°30'31''N 81°46'15''W), *Paspalum notatum*, from a pot culture established with roots of *Citrus* sp. coll. *S. Nemec* (*N.C. Schenck & G.S. Smith*), **holotype** OSC 40255 (5 May 1981) and numerous ex-type cultures PC and ROC) with various hosts in North America and Europe (*C. Walker* ATT 4) (Fig. S1); Florida, Orlando, Clermont-Mineola (approx. 28°30'31''N 81°46'15''W), from a pot culture with *Plantago lanceolata* established with spores from a soil trap culture with *P. lanceolata* (*C. Walker*, UK, New Milton, Hampshire) and numerous ex-type cultures (PC and ROC) with various hosts in Great Britain and mainland Europe (*C. Walker* ATT 1102-0 (established 14 Oct. 2001) and subcultures) (Fig. S1); [**epitype** here designated, W 5719 (E), IF 553332], 30 Mar. 2010, from a ROC, with the ex-type culture in its ancestry, cultivated with *Cichorium intybus* as host (MUCL 52327, M 5F1A4, ATT 4-83), GenBank sequence registration numbers HE817873, HE817874 HE817875 (all from the same gathering).

Synonymisation of *Rhizophagus* spp.

Having synonymised *Rhizoglomus* with *Rhizophagus*, five species named within the former genus must be formally transferred as new combinations:

Rhizophagus dalpeae (Błaszk. *et al.*) C. Walker & Schüβler, ***comb. nov.*** IF 551357.
Basionym: *Rhizoglomus dalpeae* Błaszk. *et al.*, *Mycologia* **111**: 972. 2019.

Rhizophagus dunensis (Błaszk. & Kozłowska) C. Walker & Schüβler, ***comb. nov.*** IF 551358.
Basionym: *Rhizoglomus dunense* Błaszk. & Kozłowska, *Botany* **95**: 636. 2017.

Rhizophagus maiae (Jobim *et al.*) C. Walker & Schüβler ***comb. nov.*** IF 551359.
Basionym: *Rhizoglomus maiae* Jobim *et al*., *Mycologia* **111**: 973. 2019.

Rhizophagus silesianus (Magurno *et al.*) C. Walker & Schüβler, ***comb. nov.*** IF 551360.
Basionym: *Rhizoglomus silesianum* Magurno *et al*., *Mycologia* **111**: 976. 2019.

Rhizophagus variabilis (Corazon-Guivin *et al.*) C. Walker & Schüβler, ***comb. nov.*** IF 551361.
Basionym: *Rhizoglomus variabile* Corazon-Guivin *et al.*, *Sydowia* **71**: 185. 2019.

DISCUSSION

Rhizophagus intraradices and related species

The type material of *G. intraradices* (*R. intraradices*) appears as if it was not made from freshly collected material, but perhaps from material that had been kept after extraction for some time before preservation. It was heavily degraded, and the wall structure was difficult to determine. It was also much darkened

© 2021 Westerdijk Fungal Biodiversity Institute

in colour due to the action of lactophenol. Nevertheless, it was possible to see most of the characteristics used by the original authorities to describe the species, although it was much more varied than the species description and illustrations in the protologue indicated.

In the original protologue (Schenck & Smith 1982), the species was described as forming spores singly or in clusters in roots, and '… rarely formed outside the root …'. Spore shape was said to be '… predominantly globose, but frequently subglobose …', and their dimensions were given as (40.5–)98.5(–190.5) µm diam when globose, and 93–119 × 112–131 µm when subglobose. Our independent new measurements of spores from the type material resulted in spore dimensions of 29–224 × 18–154 µm and our new measurements herein extend the range further to 18–383 × 16–398 µm. The images supporting the description are few, and do not show the degree of variation that the species can manifest. Two uncrushed spores are illustrated, one subglobose, and the other obovoid. There is an image showing the base of one spore with a 'tubaeform flare' formed by the 'walls of the spore extending into the hyphal attachment…' at the junction of the subtending hypha and the spore base. The subtending hypha, however, is described as '9–33 µm wide with a wall thickness of 1.5–2.5 µm at the base … occasionally constricted 2–3 µm' basally. The fourth illustration is of spores densely occupying the cortex of a root. There is no overall description of spore colour, but the spore wall is described as yellow to grey brown, with a greenish brown appearance in transmitted light. The use of transmitted light to assess colour can be misleading, as it depends on the colour temperature of the light source, and, for this reason, is best avoided in species descriptions. The wall structure of spores is described as of '... 1 or 2, occasionally up to 4 laminated walls ...', with '... on young spores an additional, hyaline, ephemeral outer wall (1–2 µm) ...'. It is difficult to interpret the wall structure from this description. The illustrations are of too low a magnification to see any detail, and only show a pale outer component overlaying a series of up to 7 coarse laminae. Observations of *R. irregularis* over many years (C. Walker, unpublished) show a range of spore colour from colourless to white to various shades of yellow to brown.

In a publication by Stürmer & Morton (1997), spore developmental patterns were used in re-description of a fungus identified as '*G. intraradices*'. The ex-type INVAM culture FL 208 was cited in the materials and methods. However, it was not specifically described or illustrated, but another culture, designated KS 906, was illustrated, for which ITS sequences (AF185669-73) were available that provides verification of its species identity. The spore wall was described as being at first of a 'mucilaginous' layer and a 'semiflexible layer', neither of which had any distinguishable structure. Later, a pale-yellow laminated component is described as developing which gradually increases in thickness as new laminae are developed with age. In the murographic illustration (their fig. 1), this is indicated as a second laminated component. The latter is concordant with our interpretation of an evanescent and two distinct laminated structural components.

From our study, we consider that the spore wall has three components at the light microscope level: an ephemeral (evanescent) outer component, a persistent pale-yellow component that initially does not have obvious layers, but later can be seen to be finely laminated, and a multi-layered 'laminated' main structural component that increases in thickness with age by addition of more laminae, some of which may separate by splitting. The outermost of these is colourless, and usually reacts to become pink in PVLG-M. It behaves sometimes as a unitary component, sometimes as an evanescent component, and sometimes as an expanding component, rendering these descriptive terms of considerably less use in species description than was first proposed by Walker (1983). In very young specimens, the outermost component may expand in PVLG to produce the impression of an extra component (Fig. 11 A).

The outer, colourless ephemeral component may be colonised by bacterial clusters which can be so dense, in older spores, that they may appear to form an additional outer wall component. Similar bacterial colonies, attributed predominantly to the genus *Azotobacter* were described for *R. fasciculatus* (as *Glomus fasciculatus*) by Gerdemann & Trappe (1974). Maia & Kimbrough (1994) illustrated them for *R. intraradices* culture LITR208, suggesting that they are responsible for degradation of the wall component, though experimental evidence for this is lacking. We have not observed these amongst *in vitro* cultures and experimental investigation would be required to determine if this is so.

Spore colour in reflected light is extremely variable. The greenish brown tint in transmitted light, referred to (Schenck & Smith 1982) in the protologue, was rarely noted because only observations with reflected light were used for colour determination, but one sample of spores (Fig. 5B) did show a greenish tint.

The original species description does not encompass all the morphological variation present in the type collection. The study of newly collected ex-type material and a second conspecific isolate revealed much more variation than displayed by the type material. Ideally, new species of glomeromycotan fungi should be described from cultures that have been grown sufficiently long to produce spores encompassing, as far as possible, the morphological variation within the species concerned. For many species that are recalcitrant or impossible to culture, this aim cannot be achieved, but it appears that many species in *Rhizophagus* are relatively easy to establish in both PC and ROC, and thus are amenable to being described in this way.

Błaszkowski *et al.* (2008), in the species description of *R. irregularis* (as *Glomus irregulare*), compared two pot cultured fungi from the same geographic area, maritime sand dunes at Bornholm, one given the new name, and the other determined as *G. intraradices*. These authors concluded that the morphological differences between the specimens they examined were sufficient to distinguish the two species from each other. However, these two fungi were both the same species (Stockinger *et al.* 2009), and thus the comparison was between two different cultures of *R. irregularis*. Consequently, the variation in the seven properties that were provided to separate these two species must represent intraspecific differences between the two cultures. Indeed, from our study, *R. intraradices* also shares all seven of these properties, that is: 1) presence of both terminal and intercalary intraradical spores; 2) spore colour varies from almost colourless, through yellow, to brown (the 'greenish tint' used as a character is unreliable); 3) some spores possessing an 'apical cap' caused by thickening of the colourless outer wall component; 4) spores with an outer wall component that disintegrates, and may be rough or smooth, depending on age; 5) a laminated spore-wall component that may be inseparable, or may separate under pressure when mounted on a microscope slide; 6) a variable reaction to Melzer's reagent, to which both outer and inner components can react,

© 2021 Westerdijk Fungal Biodiversity Institute

seemingly dependent on age and condition; 7) spores produced both in roots, and in the substrate. Since, for both species, spore colour, spore wall structure, subtending hyphal form, spore shape, spore size, or reaction to Melzer's reagent are similarly variable, we suggest that molecular evidence is required to separate these, and probably some other species in the genus.

The *Rhizophagus intraradices* sequences of all culture lines studied here, including the newly isolated strain from the type locality, form a monophyletic clade at the species level, clearly separated from other species in the genus, supporting the analyses of Stockinger *et al.* (2009, 2010) and Krüger *et al.* (2012) that the species is not phylogenetically sister to *R. irregularis*.

This survey of *R. intraradices*, in culture over a very long period, shows that several phenotypic characteristics of spores, particularly spore shape and size, can be affected by external factors such as culture type and host plant. The nature of the present survey does not allow explanation of how this can be so, but there are implications for species descriptions. A new species may be described from a single sample, and the rules of nomenclature dictate that the type material must be from 'a single gathering', and thus protologue descriptions are unlikely to cover all the variation that might occur within the species. Over time, this can be rectified if the type culture, and others that can be shown, *e.g.*, by molecular analysis, to be conspecific, are maintained as living cultures. In addition, caution should be exercised when describing new species based solely on morphological comparison with the species description alone, or even after examination of type material. There is considerable scope for experimental studies to examine the effects of such factors on spore morphology.

CONCLUSIONS

Molecular analyses show that sequences of *R. intraradices* culture-lines, derived from the ex-type culture and from a re-isolation from the type locality, occupy a monophyletic clade and represent the same species. The original species description required considerable amendment, and a new description and designation of an epitype is made to provide a sound basis for further studies of this and similar organisms.

We propose that, although not a requirement of the ICNafp, it is most important to have molecular evidence, including characterisation of intraspecific variability, to define many of the *Rhizophagus* species. In several genera in the *Glomeromycota* species are found that form different spore morphs, and for species such as *R. intraradices* spore morphology is extremely plastic and variable.

This paper highlights the need for intermittent redescriptions of species in the *Glomeromycota* as more knowledge of the variation within a species is gathered. The type specimen of a species is often unlikely to encompass the entire degree of variation, hence the specific statement in the ICNafp that the nomenclatural type is not necessarily the most typical or representative element of a taxon. Original species descriptions are likely to encompass only a subset, perhaps a very small subset, of the variation within a species. We offer this re-description, based on precisely defined isolates, as a reliable foundation for further investigations into the taxonomy, systematics, and, eventually, functional diversity of species in *Rhizophagus*.

The variation in anatomical characters within this single species, indeed within single isolates of the species, implies that the following characteristics, particularly if based on a small point sample, cannot be used as reliable characteristics for separating the species of *Rhizophagus* with yellow to yellow-brown to brown spores [some species, such as *R. clarus* are always pale, and others, such as *R. neocaledonius* are described as being dark-coloured with bleaching necessary to visualise spore walls (Crossay *et al.* 2018)]:

- spore dimensions,
- spore shapes,
- production of spores in roots,
- production of spores in fascicles or small 'sporocarps',
- spore colour,
- subtending hypha morphology, including mode of occlusion,
- germination characteristics,
- reaction to Melzer's reagent.

Molecular phylogenetic analyses of the SSU-ITS-LSU marker can robustly differentiate the known *Rhizophagus* species. However, the example of '*Rhizoglomus venetianum*' shows that, beside the morphological plasticity, the intraspecific DNA sequence variability of a species must be considered in the characterisation. There are several recently described species names that are characterised by only one major sequence variant, often with some sub-variants within the range of the PCR error rate. This is very unfortunate (and not congruent with the concept of DNA barcoding) because species can only be reliably identified based on DNA sequences if their intraspecific variability, at least of the major sequence variants, is characterised. Further analysis will be required to examine if it will be necessary to synonymise some of these with existing species.

For future studies, ex-type material of *R. intraradices* will be available as descendant cultures of the original root trap pot culture from INVAM as FL 208, and from GINCO-BEL (ATT 4 above), the Belgian *Glomeromycota in vitro* collection (https://www.mycorrhiza.be/ginco-bel/index.php), hosted within the BCCM/MUCL collection (https://bccm.belspo.be/about-us/bccm-mucl), under two different numbers, MUCL 49413 for cultures directly descended from a multi-spore ROC, and MUCL 52327 for those from the ex-epitype single spore isolate. For operational reasons, the GINCO-BEL cultures are temporarily unavailable (October 2021), but an ex-epitype culture derived from MUCL 52327 is registered with the Microorganisms Section of the National Institute of Agrobiological Sciences, Japan as MAFF 520088 (www.gene.affrc.go.jp/databases-micro_search_en.php). The *R. intraradices* culture (ATT 1102, above), established independently from the type locality of the species, is available from GINCO-BEL as MUCL 49410.

ACKNOWLEDGEMENTS

We thank R. Halse, the curator of OSC for the loan of the type material, S. Nemec for providing the sample from the type locality, J.B. Morton, INVAM for the provision of FL 208, M. IJdo (Louvain-la-Neuve, Belgium), for establishing the original root organ culture, and L. Renard (Louvain-la-Neuve, Belgium) for supplying some of the cultures. We also acknowledge and thank two referees who provided helpful and comprehensive reviews. The Royal Botanic Garden Edinburgh (RBGE) is supported by the Scottish Government's Rural and Environmental Science and Analytical Services Division.

Conflict of interest: The authors declare that there is no conflict of interest.

© 2021 Westerdijk Fungal Biodiversity Institute

REFERENCES

Alaux P-L, Mison C, Senés-Guerrero, *et al.* (2021). Diversity and species composition of arbuscular mycorrhizal fungi across maize fields in the southern part of Belgium. *Mycorrhiza* **31**: 265–272.

Anon (1969). Royal Botanic Garden Edinburgh, *Flora of the British Fungi Colour Identification Chart*. HMSO, Edinburgh, UK.

Anon (1990). *Munsell Soil Color Charts 1990 edition revised*. Munsell Color Macbeth Division of Kollmorgen Instruments Corp., Maryland, USA.

Błaszkowski J, Czerniawska B, Wubet T, *et al.* (2008). *Glomus irregulare*, a new arbuscular mycorrhizal fungus in the *Glomeromycota*. *Mycotaxon* **106**: 247–267.

Butler EJ (1939). The occurrence and systematic position of the vesicular-arbuscular type of mycorrhizal fungi. *Transactions of the British Mycological Society* **22**: 274–301

Cano C, Bago A, Dalpé Y (2009). *Glomus custos sp. nov.*, isolated from a naturally heavy metal-polluted environment in southern Spain. *Mycotaxon* **109**: 499–512.

Crossay T, Cilia A, Cavaloc Y, *et al*. (2018). Four new species of arbuscular mycorrhizal fungi (*Glomeromycota*) associated with endemic plants from ultramafic soils of New Caledonia. *Mycological Progress* **17**: 729–744.

Dangeard P-A (1896). Une maladie du peuplier dans l'ouest de la France. *Le Botaniste* **5**: 38–43.

Dangeard P-A (1900). Le "*Rhizophagus populinus*" Dangeard. *Le Botaniste* **7**: 285–287.

Declerck S, Strullu DG, Plenchette C (1998). Monoxenic culture of the intraradical forms of *Glomus* sp. isolated from a tropical ecosystem: A proposed methodology for germplasm collection. *Mycologia* **90**: 579–585.

Declerck S, Cranenbrouck S, Dalpé Y, *et al.* (2000). *Glomus proliferum sp. nov*.: a description based on morphological, biochemical, molecular and monoxenic cultivation data. Mycologia **92**: 1178–1187.

Diop TA, Plenchette C, Strullu DG (1994). Dual axenic culture of sheared-root inocula of vesicular-arbuscular mycorrhizal fungi associated with tomato roots. *Mycorrhiza* **5**: 17–22.

Edler D, Klein J, Antonelli A, *et al.* (2020). RaxmlGUI 2.0: A graphical interface and toolkit for phylogenetic analyses using RAxML. *Methods in Ecology and Evolution* **12**: 373–377.

Fortin JA, Bécard G, Declerck S, *et al.* (2002). Arbuscular mycorrhiza on root-organ cultures. *Canadian Journal of Botany* **80**: 1–20.

Gerdemann JW, Trappe JM (1974). The *Endogonaceae* in the Pacific Northwest. *Mycologia Memoir* **5**: 1–76. New York Botanical Society and The Mycological Society of America.

Greenall JM (1963). The mycorrhizal endophytes of *Griselinia littoralis (Cornaceae)*. *New Zealand Journal of Botany* **1**: 389–400.

Kelley, AP (1950). *Mycotrophy in plants. Lectures on the biology of mycorrhizae and related structures*. Waltham, USA. Kornerup A, Wanscher JH (1978). *Methuen Handbook of Colour*. 3rd edn. Methuen, London.

Krüger M, Stockinger H, Krüger C, *et al*. (2009). DNA-based species level detection of *Glomeromycota*: one PCR primer set for all arbuscular mycorrhizal fungi. *New Phytologist* **183**: 212–223.

Krüger M, Krüger C, Walker C, *et al.* (2012). Phylogenetic reference data for systematics and phylotaxonomy of arbuscular mycorrhizal fungi from phylum to species level. *New Phytologist* **193**: 970–984.

Lalaymia I, Declerck S (2020). The Mycorrhizal Donor Plant (MDP) *In vitro* culture system for the efficient colonization of whole plants. *Methods in Molecular Biology* **2146**: 19–31.

Maeda T, Kobayashi Y, Kameoka H, *et al.* (2018). Evidence of non-tandemly repeated rDNAs and their intragenomic heterogeneity in *Rhizophagus irregularis*. *Communications Biology* **1**: 87.

Maia LC, Kimbrough JW (1994). Ultrastructural studies on spores of *Rhizophagus intraradices*. *International Journal of Plant Science* **155**: 689–698.

Martin FM, Gianinazzi-Pearson V, Hijri M, *et al.* (2008). The long hard road to a completed *Glomus intraradices* genome. *New Phytologist* **180**: 747–750.

Petri L (1919). Sopra una presunta malattia del pioppo. *Annali del R. Istituto Superiore Forestale Nazionale* **4**: 95–104.

Peyronel B (1923). Prime richerche sulle micorize endotrofiche a arbuscules et a vesicules des mycorrhizes endotrophes. *Revista di biologia* **5**: 463–485.

Plenchette C, Strullu DG (2003). Long-term viability and infectivity of intraradical forms of *Glomus intraradices* vesicles encapsulated in alginate beads. *Mycological Research* **107**: 614–616.

R Core Team (2017). *R: A language and environment for statistical computing.* R Foundation for Statistical Computing, Vienna, Austria: 1–3729.

Schenck NC, Smith GS (1982). Additional new and unreported species of mycorrhizal fungi (*Endogonaceae*) from Florida. *Mycologia* **74**: 77–92.

Schlaeppi K, Franz Bender S, Mascher F, *et al.* (2016). High-resolution community profiling of arbuscular mycorrhizal fungi. *New Phytologist* **212**: 780–791.

Schüβler A, Walker C (2010). *The Glomeromycota*. *A species list with new families and new genera.* Schüßler and Walker, Gloucester, UK: 1–56. (Available at amf-phylogeny.com).

Seifert K, Rossman AY (2010). How to describe a new fungal species. *IMA Fungus* **1**: 109–116.

Senés-Guerrero C, Giménez S, Pacheco A, *et al.* (2020). New MiSeq based strategy exposed plant-preferential arbuscular mycorrhizal fungal communities in arid soils of Mexico. *Symbiosis* **81**: 235–246.

Sieverding E, Alves da Silva G, Berndt R, *et al.* (2014). *Rhizoglomus*, a new genus of the *Glomeraceae*. *Mycotaxon* **129**: 373–386.

Sokolski S, Dalpé Y, Séguin S, Khasa D, *et al.* (2010). Conspecificity of DAOM 197198, the model arbuscular mycorrhizal fungus, with *Glomus irregulare*: molecular evidence with three protein-encoding genes. *Botany* **88**: 829–838.

Stamatakis A (2014). RAxML version 8: a tool for phylogenetic analysis and post-analysis of large phylogenies. *Bioinformatics* **30**: 1312–1313.

Stefani F, Bencherif K, Sabourin S, *et al.* (2020). Taxonomic assignment of arbuscular mycorrhizal fungi in an 18S metagenomic dataset: a case study with saltcedar (*Tamarix aphylla*). *Mycorrhiza* **30**: 243–255.

Stockinger H, Krüger M, Schüßler A (2010). DNA barcoding of arbuscular mycorrhizal fungi. *New Phytologist* **187**: 461–474.

Stockinger H, Walker C, Schüβler A (2009). "*Glomus intraradices* DAOM197198", a model fungus in arbuscular mycorrhiza research, is not *Glomus intraradices*. *New Phytologist* **183**: 1176–87.

Stürmer SL, Morton JB (1997). Developmental patterns defining morphological characters in spores of four species of *Glomus*. *Mycologia* **89**: 72–81.

Turland NJ, Wiersema JH, Barrie, FR, *et al.* (eds.) (2018). *International Code of Nomenclature for algae, fungi, and plants (Shenzhen Code)* adopted by the Nineteenth International Botanical Congress Shenzhen, China, July 2017. *Regnum Vegetabile* **159**: 1–254. Koeltz Botanical Books, Glashütten, Germany.

Turrini A, Saran M, Giovannetti M, *et al.* (2018). *Rhizoglomus venetianum*, a new arbuscular mycorrhizal fungal species from a heavy metal-contaminated site, downtown Venice in Italy. *Mycological Progress* **17**: 1213–1224.

© 2021 Westerdijk Fungal Biodiversity Institute

Vestberg M, Uosukainen M (1992). A new method for producing VA-mycorrhiza inoculum in a soil-free substrate. *Mycologist* **6**: 38.

Walker C (1983). Taxonomic concepts in the *Endogonaceae* - spore wall characteristics in species descriptions. *Mycotaxon* **18**: 443-455.

Walker C, Gianinazzi-Pearson V, Marion-Espinasse H (1993). *Scutellospora castanea*, a newly described arbuscular mycorrhizal fungus. *Cryptogamie, Mycologie* **14**: 279–286.

Walker C, Trappe JM, Schüßler A, *et al.* (2017). (2491) Proposal to conserve the name *Rhizophagus* with a conserved type (*Fungi*: *Glomeromycota*: *Glomeraceae*). *Taxon* **66**: 199–200.

Walker C, Vestberg M (1998). Synonymy amongst the arbuscular mycorrhizal fungi: *Glomus claroideum*, *G. maculosum*, *G. multisubstenum* [*sic*] and *G. fistulosum*. *Annals of Botany* **82**: 601–624.

Supplementary Material: http://fuse-journal.org/

Fig. S1. *Rhizophagus intraradices*: culturing history of the type and successful ex-type culture attempts (ATT 4) and a new isolate (ATT 1102) from the type location established approx. 30 years later. Both pot cultures (PC) and root organ cultures (ROC) are shown with dates of establishment and voucher numbers for samples that yielded specimens for preservation in herbaria. Sun bags are item B7062, Sigma Aldrich (https://www.sigmaaldrich.com). Location of cultures: Forestry Commission Northern Research Station or other localities in UK; Université catholique de Louvain (UCL); Ludwig Maximilian University of Munich (LMU). Gel refers to a small portion of substrate from a parent ROC, with a single spore, several spores, or root fragments (usually with attached mycelium).

Fig. S2. Phylogenetic maximum likelihood phylogenetic tree of *Rhizophagus* species and isolates characterised for the SSU-ITS-LSU rDNA region, with *Sclerocystis* as outgroup. Bootstrap (BS) values below 60 % and BS values of terminal sister relations are not shown. "*Rhizoglomus venetianum*" (= *R. irregularis*) sequences are marked in red, sequence variants characterised in a *Rhizophagus irregularis* genome project are marked in blue. Sequences of *Rhizophagus intraradices* cultures derived from the ex-type culture FL 208, including the epitype (voucher W 5719 from MUCL 52327 = ATT 4-83), are shown in green and sequences of the new isolate collected from the type locality (MUCL 49410 = ATT 1102-12) in brown.

Table S1. *Rhizophagus intraradices*: lengths and widths (µm) of extra- and intraradical spores from two strains, ATT 4 and ATT 1102 spores with inferential statistics (number of spores observed (n), minimum value (Min), first quartile of the data (Q1), median, third quartile of data (Q3), maximum value (Max), mean, standard deviation (SD) and % coefficient of variation (CV %)).

Table S2. *Rhizophagus intraradices*: spore colours from two strains (ATT 4 – type and ex-type) and ATT 1102 (new culture from type locality) from pot cultures (PC) and root organ cultures (ROC). Where possible, colours were matched with charts from Royal Botanic Garden Edinburgh, Munsell, or Methuen Handbook of Colour.

© 2021 Westerdijk Fungal Biodiversity Institute

Fungal Systematics and Evolution (ISSN: 2589-3823, E-ISSN: 2589-3831)

About Fungal Systematics and Evolution

Fungal Systematics and Evolution has an OPEN ACCESS publishing policy. All manuscripts will undergo peer review before acceptance, and will be published as quickly as possible following acceptance. There are no page charges or length restrictions, or fees for colour plates. The official journal language is English. All content submitted to Fungal Systematics and Evolution is checked for plagiarism.

Fungal Systematics and Evolution is licensed under a Creative Commons Attribution-NonCommercial-ShareAlike 4.0 International License

For more information and ordering of other books and publications, see www.fuse-org.com and www.wi.knaw.nl.

About the Westerdijk Fungal Biodiversity Institute

The Westerdijk Fungal Biodiversity Institute is the largest expertise centre for microfungi in the world. Our renowned researchers dedicate themselves to enriching and expanding our Fungal Biobank. We explore the fungal kingdom to gain a better understanding of their fungal characteristics and their potential applications, especially in the fields of industry, agriculture and healthcare.

The Westerdijk Fungal Biodiversity Institute is part of the Royal Netherlands Academy of Arts and Sciences (KNAW).

Explore - study - preserve